Transcriptomic analysis of disease resistance responses using a tobacco-*Botrytis cinerea* pathosystem

by

Carin Elizabeth Basson

Dissertation presented for the degree of

Doctor of Philosophy (Agricultural Science)

at

Stellenbosch University

Institute for Wine Biotechnology, Department of Viticulture and Oenology, Faculty of AgriSciences

Supervisor: Prof MA Vivier

December 2017

Declaration

By submitting this dissertation electronically, I declare that the entirety of the work contained therein is my own, original work, that I am the sole author thereof (save to the extent explicitly otherwise stated) that reproduction and publication thereof by Stellenbosch University will not infringe any third party rights and that I have not previously in its entirety or in part submitted it for obtaining any qualification.

Date: December 2017

Summary

Cultivation of plants for food and raw materials is regularly hampered by phytopathogens that reduce quality and yield. Necrotrophic fungi are among the most damaging pathogens, killing plant cells to complete their lifecycle. Many of these fungi release cell wall degrading enzymes (CWDE) to breach this first defensive barrier of plant cells. Some of the most important CWDE are polygalacturonases (PGs), that degrade the pectin-component of the plant cell wall and often act as virulence factors. To combat PGs, plants have evolved polygalacturonase-inhibiting proteins (PGIPs). In most cases, constitutive expression of PGIPs confer some level of resistance to pathogenic fungi. Two mechanisms have been proposed to explain PGIP-induced resistance. Firstly, they protect the cell wall from degradation through PGIP-PG inhibition interactions and secondly, they assist in activating defence signalling, by prolonging the survival of signalling molecules (oligogalacturonides, OGs) derived from cell wall degradation to activate the salicylic acid (SA) branch of defence signalling.

The defence role of *Vitis vinifera* PGIP1 (VviPGIP1) was established using transgenic tobacco (*Nicotiana tabacum*) plants challenged with *Botrytis cinerea*, a model necrotrophic fungal phytopathogen. VviPGIP1 inhibited the two PGs that are virulence factors for *B. cinerea*, and reduced lesion diameter during infection assays. A subsequent characterisation of uninfected transgenic tobacco revealed wide-ranging changes in gene expression, enhanced lignin deposition and changes in hemicellulose composition, pointing to new and previously unexplored alterative functions of PGIPs in plant defence. Moreover, when the tobacco lines were infected, a more rapid accumulation of the defence hormone jasmonic acid was seen in the transgenic lines. These changes suggested that the constitutive expression of VviPGIP1 induced defence priming, a mechanism whereby plants induce slight metabolic and transcriptomic changes prior to infection, but display an enhanced defence response upon challenge. The work that formed part of this study follows on from these previous studies and had as aim to study the mechanisms that contributed to the defence phenotype observed in the tobacco lines expressing the grapevine PGIP encoding gene. The approach was to profile the molecular response of the host (tobacco) when infected by *B. cinerea*, contrasting the native tobacco response with that of the PGIP tobacco lines.

The disease progression of *B. cinerea* has been extensively studied in *Arabidopsis* and other model host species. The first two days after infection has been established as the critical phase that determines the outcome of the interaction (susceptibility/resistance). Consequently, this period was chosen to profile transcriptional changes following *B. cinerea* infection of wild-type and VviPGIP1-expressing tobacco. A time-course, consisting of five sampling points (0 h, 12 h, 24 h, 36 h and 48 h), was used to profile the localised defence response and the response in distal organs. The time-course represented two day-night cycles, providing the opportunity to investigate diurnal gene expression patterns.

Wild-type tobacco mounted a localised defence response that shared many elements with those of other plant hosts of *B. cinerea*, including the dampening of diurnal patterns and induction of antioxidant mechanisms, jasmonate and ethylene biosynthesis and secondary metabolism. In leaves distal to the infection, the diurnal patterns of gene expression were not disrupted, but genes related to anti-fungal proteins and secondary metabolite synthesis were induced. This suggested partial induced resistance (IR) had been activated by distal

infection, but systemic acquired resistance (SAR) had not yet been established. Profiling of volatile secondary metabolites emphasised a strong ontogenic effect.

The resistant tobacco line (expressing VviPGIP1) displayed enhanced activation of jasmonate/divinyl ether biosynthesis and repression of ethylene-responsive transcription factors. Monolignol biosynthesis was affected, and may have led to altered lignin composition. Several biological processes were affected at 24 hours after infection, reportedly a critical point during *B. cinerea* pathogenesis. These included enhanced activation of pterostilbene synthesis, fungitoxic SAR8.2 proteins, proteinase inhibitors and antimicrobial peptides, while oxidative stress was reduced. In terms of priming, several stress-responsive genes were more rapidly induced in the PGIP line, which also displayed an accelerated transition from source to sink metabolism. With regards to the specific role of VviPGIP1 during infection, this study represented the first untargeted transcriptomic analysis of an infected PGIP-expressing tobacco line. The enhancement of jasmonate synthesis suggested that hormone signalling may differ between VviPGIP1-expressing transgenics and plants expressing cotton or bean PGIPs. In leaves distal to the infection, where signalling molecules derived from cell wall degradation by *B. cinerea* would not be generated, priming- and IR-like responses were observed, further underscoring the connection of VviPGIP1 with defence priming.

The recurring appearance of cell wall modification in responses to *B. cinerea*, and the prior analyses that found changes in hemicellulose composition, prompted a more detailed examination of the xyloglucan endotransglycosylase/hydrolase (XTH) family in tobacco. The catalytic domain and other characteristic features of XTHs were identified for predicted XTH proteins. Functional information from characterised XTHs was mapped onto homologous sequences in order to infer functions for tobacco XTHs, however, the high sequence homology of XTHs in general, and of XTHs with contrasting expression patterns, suggested that promoter analysis would be required to accurately predict functions for specific XTHs. The sequence alignments and transcriptional information generated for the *XTH* gene family during this study provides a useful context for studies into tobacco cell wall metabolism.

This study has generated novel gene expression data for *B. cinerea*-infected tobacco, provided the opportunity to compare the timing and magnitude of transcriptional responses in susceptible and resistant plant lines, and to investigate the basis for PGIP-induced resistance. Further studies should consider utilising *de novo* sequencing to identify processes not represented on the microarray and attempt to distinguish between OG-induced responses and PGIP-induced responses. This study successfully reinforced the proposed defence priming role of VviPGIP1, not only at the site of infection, but in tissues where PGs were not active.

Opsomming

Gehalte- en opbrengste van oesplante word dikwels belemmer deur plant patogene. Nekrotrofiese swamme is van die mees skadelike patogene; hierdie organismes maak plantselle dood terwyl hul lewensiklus voltooi word. Baie van hierdie swamme stel selwand-afbrekende ensieme (SWAE) vry om die selwand, die plant se eerste verdegingslinie, te oorkom. Poligalakturonases (PGs) is van die mees prominente SWAE en is verantwoordelik om die pektien-komponent van die plant selwand af te breek, maar word ook dikwels as virulensiefaktore beskou. Om PGs te beheer het plante poligalakturonase-inhiberende proteïene (PGIPs) ontwikkel. In die meeste gevalle lei konstitutiewe uitdrukking van PGIPs tot 'n mate van weerstand teen patogeniese swamme. Twee meganismes is voorgestel om dié weerstand te verduidelik. Eerstens beskerm hulle die selwand deur middel van PGIP-PG inhibisie interaksies, en tweedens help hulle om verdedigingseine te aktiveer, deurdat hulle aksies die leeftyd verleng van seinmolekules wat hul oorsprong het as afbreekprodukte van selwande. Dié seinmolekules, oligogalakturonides (OGs), aktiveer die salisielsuur (SA)-been van die verdedigingsein-netwerk.

Die verdedigingsrol van *Vitis vinifera* PGIP1 (VviPGIP1) is bevestig met behulp van transgeniese tabak (*Nicotiana tabacum*) plante wat met *Botrytis cinerea*, 'n model-nekrotrofiese plant swampatogeen, infekteer is. VviPGIP1 het die twee PGs wat virulensiefaktore vir *B. cinerea* is geïnhibeer, en die deursnee van infeksieletsels tydens infeksie verminder. In 'n opvolgstudie is bevind dat ongeïnfekteerde transgeniese tabak grootskaalse veranderinge in geen-uitdrukking, verhoogde lignienvorming en veranderinge in hemisellulose-samestelling vertoon het. Dit het gedui op unieke funksies van PGIPs in plantverdediging. Verder, tydens infeksie het die transgeniese tabaklyne vinniger toenames in jasmoonsuur getoon. Hierdie veranderinge het daarop gedui dat die konstitutiewe uitdrukking van VviPGIP1 verdedigingsvoorvoerding (“priming”) veroorsaak het, 'n meganisme waardeur plante slegs klein metaboliese en transkripsionele veranderinge voor infeksie ervaar, maar 'n verbeterde verdedigingsreaksie na infeksie vertoon. Die huidige studie volg dus op die werk van hierdie vorige studies en het ten doel gehad om die meganismes wat bygedra het tot die verdedigingsfenotipe van die VviPGIP1-tabaklyne verder te bestudeer. Die benadering was om die molekulêre reaksies van die gasheer (tabak) te volg tydens ‘n *B. cinerea* infeksie en om die kontrole tabak se reaksie met dié van die PGIP-tabaklyne te vergelyk.

Die siekteverloop van *B. cinerea* is reeds omvattend bestudeer in *Arabidopsis* en ander model gasheer spesies. Die eerste twee dae na infeksie word beskou as die kritieke fase wat die uitkoms van die interaksie sal bepaal (vatbaarheid/weerstand). Gevolglik was hierdie tydperk gekies om transkripsionele veranderinge te volg tydens *B. cinerea*-infeksie van kontrole en ‘n VviPGIP1-uitdrukende tabaklyn in die huidige studie. 'n Tydsverloopstudie, bestaande uit vyf tydpunte (0 h, 12 h, 24 h, 36 h en 48 h), is gebruik om die reaksie op infeksie in weefsel by/naby die letsel (lokale reaksie), sowel as in blare distaal tot die infeksie (distale reaksie) te volg. Die tydsverloop het twee dag-nag siklusse ingesluit, wat die geleentheid gebied het om dag-nag (“diurnal”) uitdrukkingspatrone te ondersoek.

Die resultate het getoon dat die kontrole tabak 'n lokale verdedigingsreaksie geloods het wat baie elemente gedeel het met dié van ander plantgashere van *B. cinerea*, byvoorbeeld die demping van dag-nag-patrone en die induksie van antioksidantmeganismes, jasmoon- en etileenbiosintese, asook sekondêre metabolisme. In

blare distaal aan die infeksie is die dag-nag-patrone van geen-uitdrukking nie ontwrig nie, maar gene wat kodeer vir anti-swam proteïene en sekondêre-metaboliet sintese is geïnduseer. Dit dui daarop dat gedeeltelike geïnduseerde weerstand (IW) geaktiveer word deur distale infeksie, maar sistemiese weerstand ("systemic acquired resistance", SAR) nog nie bereik is nie. Profiele van vlugtige sekondêre metaboliete het ook 'n sterk ontogeniese effek uitgewys.

Die weerstandbiedende tabaklyn (wat *VviPGIP1* uitdruk) het verhoogde aktivering van jasmonaat/ divinieletersintese en onderdrukking van etileen-beheerde transkripsiefaktore getoon. Monolignolsintese is ook geaffekteer, en kon gelei het tot veranderde ligniensamestelling. Verskeie biologiese prosesse was geraak teen 24 uur na die infeksie, wat 'n kritieke punt tydens *B. cinerea*-patogenese is. Dit sluit byvoorbeeld 'n sterker aktivering van pterostilbeensintese, fungitoksiese SAR8.2 proteïene, protease-inhibeerders en antimikrobiese peptiede in, terwyl oksidatiewe stres skynbaar verminder is. In terme van verdedigings-voorbereiding, het die PGIP-lyn verskeie gene wat verband hou met stres-reaksies, vinniger geaktiveer en ook vinniger van bron- na sink-metabolisme oorgeskakel. Hierdie studie beskryf die eerste transkriptomiese analise van 'n geïnfekteerde PGIP-uitdrukkende tabaklyn. Die verbetering van jasmonatesintese wat waargeneem is kan daarop dui dat hormoonregulering van die verdedigingsein-netwerk verskil tussen plante wat VviPGIP1 uitdruk en dié wat katoen- of boontjie-PGIPs uitdruk. In blare distaal aan die infeksie, waar seinmolekules wat afgelei is van selwandafbreking deur *B. cinerea* nie gegenereer sou word nie, is verdedigingsvoorvoerding- en IW-agtige reaksies waargeneem, wat die koppeling van VviPGIP1 met verdedigings-voorbereiding verder onderstreep.

Die herhaalde voorkoms van selwandmodifikasie in reaksies op *B. cinerea*, en die vorige ontledings wat veranderinge in hemisellulose-samestelling aangetref het, het 'n meer gedetailleerde ondersoek van die xiloglukaan-endotransglikosilase/hidrolase (XTH)-familie in tabak gemotiveer. Die katalitiese domein en ander kenmerkende eienskappe van XTHs is geïdentifiseer vir hipotetiese XTH proteïene. Funksionele inligting afkomstig van gekarakteriseerde XTHs is op homoloë proteïenvolgordes toegepas om sodoende moontlike funksies vir tabak XTHs af te lei. Die hoë volgorde-homologie van XTHs in die algemeen en van XTHs met kontrasterende uitdrukkingspatrone het egter daarop gedui dat die analise van geenpromotore sou nodig wees om funksies akkuraat te voorspel vir spesifieke XTHs. Die volgorde-belynings en transkripsionele inligting wat vir die XTH-geenfamilie tydens hierdie studie geskep is, bied egter 'n nuttige konteks vir studies in tabak selwandmetabolisme.

Hierdie studie het nuwe gene-ekspressie data vir *B. cinerea*-geïnfekteerde tabak verkry; die geleentheid gebied om die tydsberekening en omvang van transkripsionele response in vatbare en weerstandige plantlyne te vergelyk; asook om die basis vir PGIP-geïnduseerde weerstand te ondersoek. Verdere studies moet oorweeg om gebruik te maak van *de novo*-volgordebepaling om prosesse wat nie op die mikrorooster ("microarray") voorgestel word nie, te identifiseer en om sodoende te probeer onderskei tussen OG-geïnduseerde en PGIP-geïnduseerde reaksies. Resultate van hierdie studie het die verdedigingsrol van VviPGIP1 verder versterk en toegelig en het aangedui dat dit nie net op die plek van infeksie 'n rol speel nie, maar ook in weefsels waar PGs nie aktief was nie.

This dissertation is dedicated to my “ouma” Myrna, for her unfailing encouragement and prayers.

Biographical sketch

Carin Elizabeth Basson was born in Bellville, South Africa on 9 April 1983 and matriculated from Stellenbosch High School in 2001. She enrolled at Stellenbosch University in 2002 and obtained a BSc degree in Plant Biotechnology in 2004. Subsequently she completed HonsBSc and MSc degrees in Plant Biotechnology at the Institute for Plant Biotechnology, Stellenbosch University in 2005 and 2008. After working at the Institute for Plant Biotechnology to finalise her MSc research for publication, she enrolled for a PhD in Wine Biotechnology at the Institute for Wine Biotechnology. During her doctoral studies, she also acted as lab coordinator for the Grapevine Molecular Biology Group for two years.

Acknowledgements

I wish to express my sincere gratitude and appreciation to the following persons and institutions:

Prof MA Vivier for acting as supervisor, her guidance and advice;

Dr Erik Alexandersson for guidance on experimental design and data analysis;

Cobus Steyn for performing leaf disk infections;

Dr Abré de Beer, **Dr Mukani Moyo Okoba** and **Varsha Premsagar** for their help during sample collection;

Dr Jay Belli Kullan, **Dr Dan Jacobson** and **Debbie Weighill** for bioinformatics support;

Dr Hans Eyeghe-Bikong, **Ms Anke Berry** and **Mr Lucky Mokwena** for assistance with metabolite analyses;

Prof Gerard Tromp for processing of the raw microarray data;

Drs John Moore, **Fanny Buffetto**, **Philip Young**, **Mukani Moyo Okoba**, **Anscha Zietsman**, **Jay Belli Kullan** and **Yu Gao** for advice and constructive criticism;

Ilse, **Karí**, **Helmien** and **Florent** for sharing in my academic highs and lows;

Lab colleagues for fruitful discussions and the occasional laugh;

Technical and administrative staff and assistants for their essential role in keeping the wheels turning;

My family and friends, for their prayers, support, advice and encouragement;

The National Research Foundation, Wine Industry Network for Expertise and Technology (Winetech), Technology and Human Resources for Industry Programme (THRIP), Stellenbosch University and the **Institute for Wine Biotechnology** for financial support.

Preface

Chapter 1	**General Introduction and project aims**
Chapter 2	**Literature review** Plant defence mechanisms in general with a specific emphasis on defence against *Botrytis cinerea*
Chapter 3	**Research results** Obtaining a baseline of the early transcriptional responses of tobacco when infected by *Botrytis cinerea*
Chapter 4	**Research results** In a *Botrytis*-tobacco pathosystem, overexpression of a grapevine PGIP reduced oxidative stress during lesion development and enhanced secondary metabolism in infected leaves and leaves distal to the infection
Chapter 5	**Research results** *In silico* analysis of the *XTH* gene family in tobacco
Chapter 4	**General discussion and conclusions**

I hereby declare that, with the exception of the contributions by others stated below, I was responsible for and performed the whole plant infection assay, tissue extractions for microarray and volatile analysis, data preparation, bioinformatic analyses, interpretation and compilation of the written work presented in this thesis. Microarray analyses (Chapter 3 and 4) were outsourced to commercial enterprises and Prof Gerard Tromp (Department of Biomedical Sciences, Faculty of Medicine and Health Sciences, Stellenbosch University) performed the quality control and normalisation of the raw microarray data. Dr Dan Jacobson performed the initial re-annotation of the array, which was used for gene ontology enrichment. Subsequently, I annotated the differentially expressed transcripts using the newly release *N. tabacum* annotations. Dr Hans Eyeghe-Bikong analysed the volatile organic compounds (Chapter 3 and 4) that I had extracted, integrated the GC-MS traces and provided peak areas for each sample. Dr Jay Belli Kullan identified the *Arabidopsis* homologs of tobacco gene models. Antioxidant capacity (Chapter 4) was analysed by Fanie Rautenbach at the Oxidative Stress Research Centre at the Cape Peninsula University of Technology. Mr Cobus Steyn, an MSc student under the supervision of Prof MA Vivier, performed the leaf disk infection assay (Chapter 4) and associated analyses. Dr Philip Young assisted in conceptual development of the *in silico* analyses of the XTH gene/protein family (Chapter 5). My supervisor Prof MA Vivier was involved in the conceptual development of the study and continuous critical evaluation of the results and research in general.

Table of contents

Abbreviations

4CL	4-coumarate-CoA ligase
ABA	abscisic acid
ACC	1-aminocyclopropane-1-carboxylic acid
ACO	ACC oxidase
ACS	ACC synthase
ADC	arginine decarboxylase
AMP	antimicrobial peptide
AOC	allene oxide cyclase
AOS	allene oxide synthase
AP2	APETALA2
APX	ascorbate peroxidase
Avr	avirulence
BABA	β-aminobutyric acid
BAK1	brassinosteroid insensitive 1-associated kinase 1
BIK1	*Botrytis*-induced kinase 1
BIR1	baculovirus inhibitor of apoptosis repeat protein 1
BR	brassinosteroid
CAT	catalase
CCoAOMT	caffeoyl-CoA O-methyltransferase
CCR	cinnamoyl-CoA reductase
CEBiP	chitin elicitor-binding protein
CERK	chitin elicitor receptor kinase
CHIT	chitinase
CNL	coiled-coil N-terminal domain NLR
COI1	coronatine insensitive1
COMT	caffeic acid 3-O-methyltransferase
Csp	cold shock protein
CWDE	cell wall degrading enzyme
DAB	3,3-diaminobenzidine-HCl
DAMP	damage-associated molecular patterns
DEP	distal expression profile
DES	divinyl ether synthase
DHAR	dehydroascorbate reductase
DORN1	Does not respond to Nucleotides 1
DP	degree of polymerisation
DVB/CAR/PDMS	divinylbenzene/carboxen/polydimethyl-siloxane
DXS	1-deoxy-D-xylulose 5-phosphate synthase
eATP	exogenous ATP
EDS1	enhanced disease susceptibility 1
EIL1	ethylene insensitive3-like1
EIN3	ethylene insensitive3
ER	endoplasmic reticulum
ERF	ethylene response factor
EST	expressed sequence tag
ET	ethylene
ETI	effector-triggered immunity
ETR1	ethylene receptor 1
ETS	effector-triggered susceptibility
FLS2	flagellin sensing 2
GC	gas chromatography
GGPP	geranylgeranyl pyrophosphate
GH16	glycoside hydrolase 16
GLV	green leaf volatile
GO	gene ontology
GST	glutathione S-transferase
HAMP	herbivory-associated molecular patterns
HQT	hydroxycinnamoyl CoA quinate transferase
HR	hypersensitive response
HS	head space
HSP	heat shock protein
HSR	hypersensitive response-related
ICS	isochorismate synthase
IR	induced resistance
IS	internal standard
ISR	induced systemic resistance
JA	jasmonic acid
JA-Ile	jasmonoyl-isoleucine
JAR1	jasmonate resistant 1
JAZ	jasmonate ZIM-domain
LEP	local expression profile
LHY	late-elongating hypocotyl
ligPER	lignin-forming peroxidases
LOX	lipoxygenase
LRE	linear regression of expression
LRR	leucine-rich repeat protein
LYM2	lysin motif domain-containing glycosylphosphatidylinositol-anchored protein 2
MAMP	microbe-associated molecular pattern
MAPK/MPK	mitogen-activated protein kinase
MA-plots	log ratio-mean average plots
MB	mature grape berries
MEP	2-C-methyl-D-erythritol 4-phosphate
MEV	mevalonate
MG	mature green tomato fruit
miRNA	microRNA
MLO	mildew-resistance locus
MS	mass spectrometry
MS	Murashige and Skoog media
MYB	myeloblastosis transcription factor
MYC	myelocytomatosis oncogene
NB-LRR	nucleotide-binding leucine-rich repeat
necrosis	N
Nep1	necrosis and ethylene inducing 1
NLR	nucleotide-binding leucine-rich repeat proteins
NOX	NADPH oxidase
NPR1	NON-EXPRESSOR OF PR1
OG	oligogalacturonide
OPDA	cis-(+)-12-oxophytodienoic acid
OPLS-DA	orthogonal partial least squares discriminate analyses
OPR	OPDA reductase
ORA59	octadecanoid-responsive AP2/ERF 59
ORAC	oxygen radical absorbance capacity
PAD4	phytoalexin-deficient 4
PAL	phenylalanine ammonia lyase
PAMP	pathogen-associated molecular patterns
PBS1	AvrPphB susceptible 1
PCA	principal component analysis
PCD	programmed cell death
PDF1.2	plant defensin 1.2
Pep	danger signal peptide
PER	peroxidases
PG	polygalacturonase
PGIP	polygalacturonase-inhibiting protein
PGPR	plant growth-promoting rhizobacteria
POA	polyamine oxidase
PR	pathogenesis-related

PR-2	β-1,3-glucanase
PR-5	osmotin
PRR	pattern recognition receptor
PTI	pattern-triggered immunity
qRT-PCR	quantitative reverse-transcriptase PCR
R2x	percentage variance
RAP2-3	related to APETALA 2-3
RBOH	respiratory burst oxidase homolog
RBPG1	responsiveness to botrytis polygalacturonases 1
RGA	resistance gene analog
R-genes	*Resistance*-genes
RIN4	RPM1-interacting protein 4
RK	receptor kinase
RLP	receptor-like protein
ROMT	trans-resveratrol di-O-methyltransferase
ROS	reactive oxygen species
RPM1	Resistance to *Pseudomonas syringae* pv maculicola 1
RR	red ripe tomato fruit
SA	salicylic acid
SAM	S-adenosylmethionine
SAMS	SAM synthase
SAR	systemic acquired resistance
SIC	single ion count
SOD	superoxide dismutase
SPDS	spermidine synthase
SPME	solid phase microextraction
sRNA	small RNA
STS	stilbene synthase
SVA	surrogate variable analysis
TAXI	*Triticum aestivum* xylanase inhibitor
TF	transcription factor
TGA	TGACG motif binding factor
TIC	total ion count
TLXI	thaumatin-like xylanase inhibitor
TMV	tobacco mosaic virus
TNL	Toll-interleukin 1 receptor NLR
Trolox	6-hydroxy-2,5,7,8-tetramethylchroman-2-carboxylic acid
VB	véraison grape berries
VIP score	variable importance to the projection score
VOC	volatile organic compounds
WAK1	wall-associated kinase 1
Xcv	Xanthomonas campestris pv. vesicatoria
XEG	xyloglucan-specific endoglucanase
XIP	xylanase inhibitor protein
XTH	xyloglucan endotransglycosylase/hydrolase
Δg	fold change between genotypes at sampling point (relative to WT)
Δt	fold change between sampling points (relative to earlier sampling point)

List of Figures

List of Tables

Chapter 1

General introduction and project aims

General introduction and project aims

Plant diseases are a global problem affecting food security and industries that rely on plant materials (Strange and Scott, 2005). The use of chemical disease control is increasingly unpopular with consumers and environmentalists alike (de Waard, 1993), but since all crop plants are subject to diseases before and after harvest (Strange and Scott, 2005), measures to prevent plant diseases cannot be avoided. An attractive alternative to external control of the disease-causing organisms, is to use the plant defence mechanisms more effectively, without diverting resources away from growth and development (Conrath, 2009). Many plant species are resistant to the pathogens that causes diseases on crop plants, therefore successful mechanisms of defence exist. In some cases, the insertion of a single gene can make previously susceptible plants resistant to pathogens. For example, the *N* (necrosis) gene of a wild tobacco species conferred resistance to tobacco mosaic virus (TMV) in cultivated tobacco (Holmes, 1938) and tomato (Whitham et al., 1996). Since not all phytopathogens can be neutralised in this way (Bent and Mackey, 2007), understanding how effective defence responses differ from ineffectual responses is required to understand the basis of resistance and susceptibility.

1.1 What do we know about plant defence mechanisms?

Plant defence mechanisms can be viewed as a “toolbox” that plants must access when challenged. Resistance against diseases requires that plant cells have the capacity to select and use the correct “tools” for the pathogen and to do so in a timely manner. Microbes are recognised by highly conserved microbe-associated molecular patterns (MAMPs) that are often integral parts of their cell surfaces, or by effector molecules that are generally extremely specific to particular plant-pathogen combinations. MAMPs and effectors (formerly called “virulence factors”) activate pattern-triggered immunity (PTI) and effector-triggered immunity (ETI) respectively. ETI is effectively an enhanced form of PTI, but with unique regulatory mechanisms (Liu et al., 2016) that enable better “tool selection”.

1.1.1 Common features of defence

The universal characteristic of a plant initiating a defence response is the repression of photosynthesis (Bilgin et al., 2010) and the reallocation of primary metabolites (Bolton, 2009) indicating a switch from growth and development to defence. Furthermore, plants use a combination of attacking and defending strategies and, as a last resort, cell suicide of affected cells. A host of pathogenesis-related (PR) proteins are induced by pathogens, with many classes of PR proteins possessing anti-microbial activities (Van Loon, 1985). Additional anti-microbial strategies include the synthesis of toxic metabolites such as phytoalexins (Hammerschmidt, 1999) and reactive oxygen species (ROS, Nanda et al., 2010). Many of these proteins and metabolites are exported to the cell periphery, where they, along with the cell wall, act to limit access to the nutrient-rich interior of the

cell. The cell wall is commonly modified in response to infection, where cross-linking of cell wall proteins, chemical modification of cell wall polymers (to make them less degradable by pathogen enzymes) and deposition of lignin together create a more effective barrier to the invader (Bhuiyan et al., 2009; Brisson et al., 1994; Hückelhoven, 2007). The most dramatic feature of defence response is the hypersensitive response (HR), where a burst of ROS induces programmed cell death (PCD) and attempts to isolate the pathogen in an island of dead tissue (Heath, 2000). Regulation of these responses is primarily mediated by three hormones, namely salicylic acid (SA), jasmonic acid (JA) and ethylene (ET) (Glazebrook, 2005). The classic paradigm states that SA signalling antagonises JA and ET signalling, but exceptions to this highlight that defence signalling is strongly dependent on individual host-pathogen interactions (Liu et al., 2016; Shigenaga and Argueso, 2016).

Plant defence mechanisms against biotrophic pathogens, that invade the living cells of the host, and necrotrophic pathogens, that invade and kill the cells of the host, are intrinsically different (Glazebrook, 2005; Kliebenstein and Rowe, 2008). For example, the most common defence mechanism that plants use against biotrophic pathogens is the HR (Hammond-Kosack and Jones, 1996). While this approach is very effective against pathogens that require living cells, it is often catastrophically self-defeating against necrotrophic pathogens. These may even manipulate the host metabolism to trigger PCD so that they can consume the dead tissue (Govrin and Levine, 2000). Resistance to necrotrophic pathogens has been attributed to timely activation of defence responses such as enhanced callose or lignin deposition, upregulated hormonal signalling compounds and direct attack of the pathogen by the production of toxic compounds (Asselbergh et al., 2007; Charles et al., 2008; Geraats et al., 2003; Langcake and Pryce, 1976; Méndez-Bravo et al., 2011).

1.1.2 Pathogens induce defence responses throughout the whole plant

While the focus of research was initially on the responses of plant cells in contact with or near the invading pathogen, the systemic nature of plant defence has long been known. The characteristic of plants to activate defence responses systemically was initially observed when tobacco infected with TMV became resistant to TMV and other viruses in TMV-free parts of the plant (Ross, 1961). The phenomenon was termed systemic acquired resistance (SAR) and launched many studies into systemic responses. The plant hormone salicylic acid (SA) was traditionally thought to be the key signalling molecule that induces SAR, but although it plays a part, pipecolic acid was in fact shown to play this role (Bernsdorff et al., 2016).

It was initially thought that SAR was always linked to necrotic lesion formation, but MAMPs have since been shown to elicit SAR without any macroscopic symptoms (Mishina and Zeier, 2007). Since the initial discovery of SAR, other types of systemic induced resistance, including induced systemic resistance (ISR), have been described. ISR is induced through root colonisation by non-pathogenic rhizobacteria, using JA and ET signalling (Van Wees et al., 1999). A distinction has been made

between SAR, that is characterised by the systemic activation of defence, and the various forms of priming, the latter being characterised by the potentiation of defence without expression of active defence metabolism (Martinez-Medina et al., 2016).

1.2 The *Nicotiana tabacum-Botrytis cinerea* pathosystem

Many factors influence development of plant disease in the field – the plant species and cultivar, pathogen species and strain, age and developmental stage of the plants, macroclimate and microclimate conditions and the amount of pathogen inoculum in the environment. To effectively study defence mechanisms, and identify specific factors that contribute to the outcome of the interaction, a defined set of experimental parameters is required. In the plant defence context, these parameters are referred to as a pathosystem (Robinson, 1977). Ideally, the plant host (species, variety and developmental stage) and challenging pathogen (species, strain and application method) are defined. Other parameters may also be specified, such as light regime, humidity and temperature. The infection conditions, infection protocol and disease progression are mapped to provide a comprehensively described, predictable (and repeatable) experimental workflow. The status/success of the tobacco-*Botrytis* pathosystem is best contextualised by briefly introducing each of the partners (tobacco and *Botrytis*) before providing a summary of existing data that already originated from the specific pathosystem in recent years.

1.2.1 *Nicotiana tabacum*

Though tobacco was the first plant to be genetically modified (Hoekema et al., 1983), its allotetraploid genetic background reportedly made the tobacco genome assembly challenging (Sierro et al., 2014). This has delayed the development of comprehensive genome tools for tobacco compared to those that exist for other model plants, including other Solanaceous species (i.e. tomato, potato and pepper). Currently, the draft genomes of three commercially important cultivars of *N. tabacum* and the parental species *N. tomentosiformis* and *N. sylvestris* (Edwards et al., 2017; Sierro et al., 2013, 2014) have been included in the Sol Genomics Network database (Mueller et al., 2005) and in the RefSeq database of the National Center for Biotechnology Information (NCBI) (Geer et al., 2010).

Unlike the archetypal model plant *Arabidopsis thaliana*, studies in tobacco are divided into the study of commercially-relevant factors, including nicotine metabolism and nitrogen requirements (Sierro et al., 2014), agronomic concerns (Lei et al., 2014) or aroma-determinants (Lei et al., 2013) and on fundamental scientific questions such as unravelling its evolutionary history (Bombarely et al., 2012) or, indeed, as part of a pathosystem. The latter included the studies of putative defence genes, PR proteins, elicitors, priming and biocontrol agents, as well as pathogen virulence factors. Table 1.1 gives examples of these using *B. cinerea* as challenging pathogen, while a recent review (Alexandersson et al., 2016) highlights the use of tobacco to study induced systemic defence against economically important pathogens blue mould (*Peronospora tabacina*) and TMV. Transcriptomic

studies in tobacco pathosystems include infection by TMV (Jada et al., 2014); a non-host bacterial infection with *Xanthomonas campestris* pv. *vesicatoria* used to study the role of chloroplast redox balance during infection (Zurbriggen et al., 2009); a time-series of a non-host bacterial infection with *X. axonopodis* pv. *citri* (Daurelio et al., 2011); PTI against an avirulent *Pseudomonas syringae* pv. *syringae hrcC*- mutant (Szatmári et al., 2014); and ETI against virulent *P. syringae* pv. *syringae* bacteria (Bozsó et al., 2016).

Table 1.1 Summary of reported research where resistance/susceptibility of *Nicotiana tabacum* to *Botrytis cinerea* was used to evaluate potential defence-related factors

Aspect studied	Other analyses	Reference
Symbiotic interactions		
Arbuscular mycorrhizal fungus	Defence-gene expression	Shaul et al. (1999)
Plant growth-promoting rhizobacteria (PGPR)	Defence-gene expression	Lee et al. (2014)
PGPR with differing secretomes	Oxylipin-related gene expression	Cawoy et al. (2014)
Trichoderma harzianum biocontrol		De Meyer et al. (1998)
Elicitor treatment		
B. cinerea cerato-platanin	SA levels	Frías et al. (2013)
B. cinerea glycoprotein BcGs1	Defence-gene expression	Zhang et al. (2015)
Oligo-carrageenans	PAL activity, phenylpropanoid compounds	Vera et al. (2012)
Role of SA		Murphy et al. (2000)
Characterisation		
N. plumbaginifolia PDR1 ortholog	Expression analysis	Bultreys et al. (2009)
Tobacco cultivars	PR protein and phytoalexin levels	El Oirdi et al. (2010)
Transgenic plants		
Antimicrobial peptide analogue MSI-99		Chakrabarti et al. (2003)
Ascorbate oxidase	Redox-gene expression	Fotopoulos et al. (2006)
Bean PGIP2		Manfredini et al. (2005)
Cryptogein with hsr203J promoter	Defence-gene expression	Keller et al. (1999)
Ethylene insensitive tobacco	Peroxidase activity (uninfected)	Geraats et al. (2003)
Fungal PG	Auxin sensitivity	Ferrari et al. (2008)
IVR-like protein from resistant tobacco	Seed germination, root growth rate	Akad et al. (2005)
Lipid transfer protein homolog		Kiba et al. (2012)
Pathogen-derived harpin	Defence-gene expression	Sohn et al. (2007)
Pathogen-derived harpin	Cell size, growth and development	Jang et al. (2006)
Saccharomyces cerevisiae chitinases		Carstens et al. (2003)
T. hamatum chitinase		Kálai et al. (2006)
V. vinifera PGIP1		Joubert et al. (2006)
V. vinifera WRKY1		Marchive et al. (2007)
SA accumulation mutants		Achuo et al. (2004)
Tomato phospholipid hydroperoxide glutathione peroxidase	Salt and heat stress response	Chen et al. (2004)

1.2.2 *Botrytis cinerea*

B. cinerea is the causal agent for grey mould rot (Williamson et al., 2007). As a necrotrophic fungus with a broad host range that extends over many climatic regions, it is increasingly seen as a model pathogen (Fillinger and Elad, 2016; Mbengue et al., 2016; Van Kan, 2006). Its wide-ranging impact and the prevalence of field isolates that developed resistance against fungicides has spurred research into its infection strategies and virulence factors. In addition, its wide host range makes it an interesting (and important) phytopathogen to study. To date, the genomes of three strains have been sequenced and made publicly available (Amselem et al., 2011; Blanco-Ulate et al., 2013; Staats and Van Kan, 2012, Van Kan et al., 2017) and numerous characterised mutants have been generated (botbioger.versailles.inra.fr/botmut/).

The infection process of *B. cinerea* is generally similar to that of other necrotrophic fungi. After spores germinate on intact plant tissues, *B. cinerea* infection begins by penetrating the host tissue, through the development of an appressorium. The appressorium forms a penetration peg that degrades the surface of the tissue and the anti-clinal cell walls through the release of cell wall degrading enzymes (CWDEs). Polygalacturonases (PGs) are some of the first CWDE to be secreted (D'Ovidio et al., 2004a) and BcPG2 (one of six isoforms) is essential for penetration (Kars et al., 2005). By feeding off the nutrients released by the dead plant cells, the fungus continues to macerate the tissue and typically forms wet necrotic lesions, a process that requires BcPG1 (Ten Have et al., 1998). To complete its lifecycle, the fungus sporulates, generating the characteristic grey-brown branched conidiophores that give the fungus its common and scientific names. The success of *B. cinerea* as pathogen can partly be attributed to its ability to induce the HR (Govrin and Levine, 2000), by releasing, among others, phytotoxic metabolites such as botcinic acid and botrydial (Choquer et al., 2007), and HR-inducing proteins like the glucan 1,4-alpha-glucosidase BcGs1 (Zhang et al., 2015) and cerato-platanin family protein BcSpl1 (Frías et al., 2011). In addition, its anti-apoptotic machinery enables it to survive the initial plant defence responses, including HR-induced PCD (Shlezinger et al., 2011).

Botrytis strains are known to effectively infect tobacco (Elad et al., 2016; El Oirdi et al., 2010), leading to the establishment of several well-defined pathosystems of different tobacco genotypes and *Botrytis* strains. One such established pathosystem is of *N. tabacum* Havana Petit SR1 – *B. cinerea* that has been optimised to perform functional analysis of several defence genes, namely *Saccharomyces cerevisiae* chitinase gene *CTS2-1* (Carstens et al., 2003); *Vitis vinifera antimicrobial peptide 1* (Vv-AMP1, De Beer, 2008); and *V. vinifera polygalacturonase-inhibiting protein 1* (*VviPGIP1*, Alexandersson et al., 2011; Joubert et al., 2006, 2007; Nguema-Ona et al., 2013). Several model species, as well as crop plants have been used to study the PGIP encoding gene families, PGIP characteristics, protein activities, mode of action and defence and/other roles (Table 1.2). Most plant species harbour *pgip* gene families (Kalunke et al., 2015); in tobacco the *NtPGIP* gene, encoding a protein with inhibitory activity against *Phytophthora capsici* PG has been described (Zhang et al., 2016), while another, encoding *N. tabacum* leucine-rich repeat protein 1 (NtLRR1) is homologous to other PGIP-encoding genes, but has not been reported to inhibit PGs (Xu et al., 2009). Although tobacco PGIPs are active against PGs from some pathogens (Becker, 2002; Zhang et al., 2016), wild-type tobacco did not display inhibitory activity against *B. cinerea* PGs (Joubert et al., 2006), making it a suitable host to study PGIPs in the *N. tabacum* Havana Petit SR1 – *B. cinerea* pathosystem.

Table 1.2 Studies using transgenic plants interacting with necrotizing pathogens to study PGIP defence phenotypes.

Host	PGIP source	Gene	Pathogen (and disease)	Reference
Arabidopsis thaliana	Oilseed rape	*BnPGIP1* **BnPGIP2**	*Sclerotinia sclerotiorum* (white mould)	(Bashi et al., 2013)
	Broad bean	**PvPGIP2**	*B. cinerea* (grey mould)	(Manfredini et al., 2005)
	Arabidopsis thaliana	**AtPGIP1+ AtPGIP2***	*Fusarium graminearum* (head blight/ear rot on wheat)	(Ferrari, 2003)
		AtPGIP1* AtPGIP2*		(Ferrari et al., 2012)
Chinese cabbage	Chinese cabbage	**BrPGIP2***	*Pectobacterium carotovorum* (bacterial soft rot)	(Hwang et al., 2010)
Grapevine	European pear	**pPGIP**	*Xylella fastidiosa* (Pierce's disease on grapevine)	(Agüero et al., 2005)
		pPGIP	*B. cinerea*	
	Wild grapevines	PGIP1012 PGIP1038	*B. cinerea*	(Moyo, 2017)
Potato	Apple	*MdPGIP1*	*Verticillium dahliae* (Verticillium wilt)	(Gazendam et al., 2004)
	Potato	**StPGIP1***	*V. dahliae*	(Guo et al., 2014)
Rice	Rice	**OsPGIP1***	*Rhizoctonia solani* (sheath blight on rice)	(Wang et al., 2014)
Tobacco	Broad bean	**PvPGIP2**	*R. solani* *Phytophthora parasitica* (rot/blight) *Peronospora hyoscyami* (blue mould)	(Borras-Hidalgo et al., 2012)
	Chinese cabbage	**BrPGIP2**	*P. carotovorum*	(Hwang et al., 2010)
	Oilseed rape	**BnPGIP2**	*S. sclerotiorum*	(HuangFu et al., 2013)
	Cultivated grapevine	**VviPGIP1**	*B. cinerea*	(Joubert et al., 2006, 2007)
	Wild grapevines	**14 nVViPGIPs**	*B. cinerea*	(Moyo, 2011)
	Broad bean	**PvPGIP2**	*B. cinerea*	(Manfredini et al., 2005)
	Pepper	**CaPGIP1**	*Alternaria alternata* (leaf rot, spot or blight) *Colletotrichum nicotianae* (anthracnose)	(Wang et al., 2013)
Tomato	Broad bean	*PvPGIP1*	*F. oxysporum* (Fusarium wilt) *B. cinerea* *A. solani*	(Desiderio et al., 1997)
	European pear	**pPGIP**	*B. cinerea*	(Powell et al., 2000)
Wheat	Broad bean	**PvPGIP2**	*Bipolaris sorokiniana* (root rot, spot blotch)	(Janni et al., 2008)
			F. graminearum	(Ferrari et al., 2012; Masci et al., 2015; Tundo et al., 2016)
		PvPGIP2	*Claviceps purpurea* (ergot)	(Volpi et al., 2013)
	Soybean	**GmPGIP3**	*Gaeumannomyces graminis* (take-all)	(Wang et al., 2015)
		GmPGIP3	*B. sorokiniana*	

Genes indicated with an asterisk were overexpressed. Genes highlighted in bold induced resistance, italicized genes had no effect and grey blocked genes induced susceptibility. Underlined pathogen species are bacteria, whereas the rest are fungi.

1.3 PGIPs and their roles in plant defence

Plants typically use their PGIPs to counter the PGs that some pathogens use to infect plant hosts (D'Ovidio et al., 2004a). PGIPs have been extensively studied for their role in defence against phytopathogens and have been the subject of numerous reviews (D'Ovidio et al., 2004a; de Lorenzo et al., 2001; Di et al., 2006; Gomathi and Gnanamanickam, 2004; Kalunke et al., 2015; Protsenko et al., 2010). The first evidence of these proteins were observed when protein extracts from plant cell walls inhibited purified PGs from three fungal pathogens (Albersheim & Anderson, 1971). Since then PGIP-encoding genes have been found in all plant species tested and occur as single genes or gene families (Kalunke et al., 2015). The best studied PGIP gene family is that of *Phaseolus vulgaris*, with PvPGIP2 currently known as the PGIP inhibiting the most PG isoforms (D'Ovidio et al., 2004b).

1.3.1 What do we know about the PGIP mode of action

The primary PGIP mode of action relates to their inhibitory activity, as evidenced by their activity against PGs from fungal pathogens representing many important genera, including *Aspergillus*, *Botrytis*, *Colletotrichum*, *Fusarium* and *Verticillium* (Kalunke et al., 2015). PGIPs have been reported to inhibit selected PGs from insects (Doostdar et al., 1997; Frati et al., 2006) and bacteria (Agüero et al., 2005; Hwang et al., 2010; Wang et al., 2014), but these have not been as widely tested as fungal and oomycete PGs. The inhibitory activity against microbial pathogens limits infection directly, by preventing degradation of the cell wall, and indirectly, by generating elicitor-active oligogalacturonides that activate defence responses (Ridley et al., 2001). The latter has long been a hypothesis, but has recently been shown by expressing a chimera of PvPGIP2 and *Fusarium phyllophilum* PG in *Arabidopsis* (Benedetti et al., 2015). Pathogen-induced expression of the chimera by the PR1 promotor led to reduced disease symptoms of *B. cinerea*, *Pectobacterium carotovorum* and *P. syringae*, while ergosterol-inducible expression was associated with chlorosis, callose deposition and substantial SA accumulation. The association of SA with PGIP-induced defence was again shown in *Arabidopsis* expressing the cotton PGIP gene GhPGIP1 (Liu et al., 2017). PGIPs may also protect plant cell walls from degradation by masking pectin (Kalunke et al., 2015; Spadoni et al., 2006).

In addition to defence phenotypes, PGIPs appear to have roles in other biological processes (Kalunke et al., 2015). While most plant-derived PGs appear to lack the structural features required for PGIP inhibition, a few reports suggest that PGIPs may regulate activity of plant PGs, for example during seed germination (Cervone et al., 1990; Kanai et al., 2010). Other studies report induction of PGIPs in response to flooding, abscisic acid (ABA) or auxin treatment and phosphate deficiency (Miura et al., 2011; Yin et al., 2016). Grapevine expressing a pear PGIP showed better regrowth after pruning (Agüero et al., 2005). Seen together, these non-defence phenotypes suggest that PGIP may have some role in cellular elongation, potentially by regulating the activity of endogenous PGs.

1.3.2 Functional analysis of a grapevine PGIP in the *N. tabacum-B. cinerea* pathosystem

The starting point of this study was the functional characterisation of VviPGIP1 in the heterologous tobacco system (Becker, 2002, 2007; De Ascensao, 2001; Joubert et al., 2006, 2007). VviPGIP1 is a grapevine defence gene induced most prominently in berries during véraison (Joubert et al., 2013). Transcripts were also detected in roots and other berry stages. Induction by exogenous application of SA, wounding and *B. cinerea* infection highlighted its role in defence. To further study its role in defence, it was constitutively expressed in *N. tabacum* cv Havana Petit SR1 (Joubert et al., 2006). VviPGIP1 was purified from transgenic tobacco and tested against PGs from *Aspergillus niger* and *B. cinerea*, where it reduced the activity of AnPGA, AnPGB, BcPG1, BcPG3 (very slightly), BcPG4 (at low pH) and BcPG6. Subsequently, no inhibitory activity against BcPG2 was found *in vitro*, but transient co-expression in *N. benthamiana* showed that VviPGIP1 was able to reduce the necrotizing activity of BcPG2 *in planta* (Joubert et al., 2007). Further tests were performed to determine whether VviPGIP1 and BcPG2 interacted *in vitro*. At three different pH levels, no inhibition of PG activity could be detected, and plasmon resonance revealed that the two proteins did not interact. This result provided insight that the PGIP-PG interaction could also require other co-factors *in vivo*, as suggested by similar studies with PvPGIP2, where the presence of polygalacturonic acid changed the affinity of PvPGIP2-PG interactions (Gutierrez-Sanchez et al., 2012) and by the unsuccessful attempts to co-crystallise an *in vitro* PGIP-PG complex (Kalunke et al., 2015).

Transgenic *N. tabacum* plants, constitutively expressing VviPGIP1, were more resistant to *B. cinerea* infection, as evidenced by reduced lesion diameter in whole plant infection assays (Joubert et al., 2006). Phytohormone analysis revealed that transgenic tobacco displayed enhanced JA accumulation during infection, while SA and the auxin indole-acetic acid did not differ significantly during infection, though auxin levels were slightly, but significantly higher in transgenic tobacco prior to infection (Alexandersson et al., 2011). Several analyses were performed on uninfected plants expressing VviPGIP1 (Alexandersson et al., 2011; Nguema-Ona et al., 2013). Since, at the time, no microarray was available for tobacco, a potato cDNA microarray was used to quantify transcript levels of two of the resistant transgenic VviPGIP1-expressing tobacco lines, specifically VvPGIP 37 and VvPGIP 45 as described by Joubert et al. (2006). The gene expression analysis of healthy (unchallenged) PGIP-expressing plants revealed sweeping changes in metabolism, including central carbon metabolism, photosynthesis, energy metabolism and stress defence signalling, as well as changes in cell wall modification, hormone signalling and redox metabolism (Alexandersson et al., 2011). JA regulation and synthesis were altered, suggesting an enhanced sensitivity to JA and primed JA synthesis, while ethylene biosynthesis and regulation were repressed. Transcriptional changes to monolignol biosynthesis and xyloglucan modification prompted the analysis of lignin deposition, xyloglucan endotransglycosylase/hydrolase (XTH) activity and cell wall composition. These additional analyses supported the transcriptional information and revealed the VviPGIP1

induced enhanced lignin deposition, repressed XTH activity and slightly reduced rhamnose levels in the cell walls of the transgenic lines. A subsequent study profiled cell wall composition and found changes in the hemicellulose network indicative of increased cross-linking (Nguema-Ona et al., 2013). A hypothetical cell wall model was proposed whereby VviPGIP1 expression leads to increased lignification and a tighter hemicellulose-cellulose network, that could contribute to a reinforced physical barrier to *Botrytis* infection (Blanco-Ulate et al., 2016; Kalunke et al., 2015; Nguema-Ona et al., 2013).

1.4 Aims and objectives of the study

This study forms part of an ongoing research theme at the Institute for Wine Biotechnology that functionally characterises putative defence genes in tobacco (Basson, 2003; Becker, 2002; 2007; Carstens, 2002; De Beer, 2008; Venter, 2010). The previous analysis of VviPGIP1 function in tobacco suggested wide-spread changes prior to infection. The changes observed in the uninfected state, together with the enhanced (faster) accumulation of JA during infection pointed to a mechanism reminiscent of defence priming (Martinez-Medina et al., 2016). According to the definition of priming, the full effects of priming only becomes visible when the primed plant is challenged with a pathogen (Martinez-Medina et al., 2016; Mauch-Mani et al., 2017). **This study therefore aims to follow the transcriptional response of the VviPGIP1-tobacco when challenged with *B. cinerea*, to understand the transcriptional basis of the known resistance phenotype observed, and to further inform or redefine the hypothesis that VviPGIP1 acts as a priming agent to modulate resistance in the PGIP-tobacco – *Botrytis* pathosystem**.

The resources available to this study were the previously characterised tobacco populations and the well-defined and tested tobacco-*Botrytis* pathosystem we routinely use and reported on (Alexandersson et al., 2011; Carstens et al., 2003; Joubert et al., 2006, 2007). The approach was to use microarray analysis of gene expression in a time-course experiment to follow the early period of the infection and map the host's initial resistance responses. We were interested to explore the transcriptional responses at the infection sites, as well as in leaves distal to the infection. The following objectives were formulated for the study:

1. Establish and maintain a suitable population of tobacco plants (constitutively expressing VviPGIP1 lines as well as wild-type controls) from the seed bank of the IWBT.
2. Perform whole-plant infections according to the reported infection procedure (Joubert et al., 2006; Alexandersson et al., 2011) and obtain samples, in a time-course of the local lesions, as well as samples of leaves distal to the infection.
3. Perform microarray analysis on the samples and implement computational tools to assist in data analysis, identification of gene families and biological interpretation.

4. In locally and distally responding tissue, characterise gene expression and metabolites for the baseline tobacco response.
5. Identify differences in transgenic tobacco that could inform/expand the model for VviPGIP1 mode of action.

The outcomes of the research objectives are presented as follows in the thesis:

Microarray analyses of WT- and VviPGIP1-expressing tobacco were conducted in parallel, but local and distal responses were analysed separately. Expression profiling, based on these microarray data, is presented in two Chapters (Chapter 3 and Chapter 4). In Chapter 3, the transcriptional response of the susceptible WT *Nicotiana tabacum* - *Botrytis cinerea* pathosystem is described, both at the infection spots as well as in leaves distal to the infection. In Chapter 4, this baseline transcriptional response of tobacco was used to compare the response of transgenic tobacco with a resistant phenotype against *B. cinerea* infection and to evaluate the transcriptional impact of the *Vvipgip1* transgene in these populations. In both Chapters 3 and 4, metabolite analyses were used to corroborate the transcriptional changes. Chapter 5 describes the identification and *in silico* analysis of characterised and putative tobacco XTH-encoding genes and proteins.

The research Chapters presented in this thesis follow a literature review (presented in Chapter 2) and the major outcomes, insights and new hypotheses are presented in Chapter 6.

1.5 Literature cited

Achuo EA, Audenaert K, Meziane H, Höfte M (2004). The salicylic acid-dependent defence pathway is effective against different pathogens in tomato and tobacco. *Plant Pathol* 53, 65–72. doi:10.1046/j.1365-3059.2003.00947.x.

Agüero CB, Uratsu SL, Greve LC, Powell ALT, Labavitch JM, Meredith CP, Dandekar AM, Ave OS (2005). Evaluation of tolerance to Pierce's disease and *Botrytis* in transgenic plants of *Vitis vinifera* L. expressing the pear PGIP gene. *Mol Plant Pathol* 6, 43–51. doi:10.1111/J.1364-3703.2004.00262.X.

Akad A, Teverovsky E, Gidoni D, Elad Y, Kirshner B, Rav-David D, Czosnek H, Loebenstein G (2005). Resistance to tobacco mosaic virus and *Botrytis cinerea* in tobacco transformed with complementary DNA encoding an inhibitor of viral replication-like protein. *Ann Appl Biol* 147, 89–100. doi:10.1111/j.1744-7348.2005.00015.x.

Albersheim P, Anderson AJ (1971). Proteins from plant cell walls inhibit polygalacturonases secreted by plant pathogens. *PNAS* 68, 1815–1819.

Alexandersson E, Mulugeta T, Lankinen Å, Liljeroth E, Andreasson E (2016). Plant resistance inducers against pathogens in Solanaceae species-from molecular mechanisms to field application. *Int J Mol Sci* 17, 1673. doi:10.3390/ijms17101673.

Amselem J, Cuomo CA, Van Kan JAL, Viaud M, Benito EP, Couloux A, Coutinho PM, De Vries RP, Dyer PS, Fillinger S, Gout L, Hahn M, Kohn L, Lapalu N, Plummer KM, Sharon A, Simon A, Ten Have A, Que E, et al. (2011). Genomic analysis of the necrotrophic fungal pathogens *Sclerotinia sclerotiorum* and *Botrytis cinerea*. *PLoS Genet* 7, e1002230. doi:10.1371/journal.pgen.1002230.

Asselbergh B, Curvers K, França SC, Audenaert K, Vuylsteke M, Van Breusegem F, Höfte M (2007). Resistance to *Botrytis cinerea* in *sitiens*, an abscisic acid-deficient tomato mutant, involves timely production of hydrogen peroxide and cell wall modifications in the epidermis. *Plant Physiol* 144, 1863–1877. doi:10.1104/pp.107.099226.

Bashi ZD, Rimmer SR, Khachatourians GG, Hegedus DD (2013). *Brassica napus* polygalacturonase inhibitor proteins inhibit *Sclerotinia sclerotiorum* polygalacturonase enzymatic and necrotizing activities and delay symptoms in transgenic plants. *Can J Microbiol* 59, 79–86. doi:10.1139/cjm-2012-0352.

Basson EM (2003). The expression of yeast antifungal genes in tobacco as possible pathogenesis-related proteins. *MSc thesis*, Stellenbosch University, South Africa, 1–67.

Becker JVW (2002). Plant defence genes expressed in tobacco and yeast. *MSc thesis*, Stellenbosch University, South Africa, 1–88.

Becker JVW (2007). Evaluation of the role of PGIPs in plant defense responses. *PhD dissertation*, Stellenbosch University, South Africa, 1–113.

Benedetti M, Pontiggia D, Raggi S, Cheng Z, Scaloni F, Ferrari S, Ausubel FM, Cervone F, De Lorenzo G (2015). Plant immunity triggered by engineered in vivo release of oligogalacturonides, damage-associated molecular patterns. *PNAS* 112, 5533–5538. doi:10.1073/pnas.1504154112.

Bent AF, Mackey D (2007). Elicitors, effectors, and *R* genes: the new paradigm and a lifetime supply of questions. *Annu Rev Phytopathol* 45, 399–436. doi:10.1146/annurev.phyto.45.062806.094427.

Bernsdorff F, Doering A-C, Gruner K, Schuck S, Bräutigam A, Zeier J (2016). Pipecolic acid orchestrates plant systemic acquired resistance and defense priming via salicylic acid-dependent and independent pathways. *Plant Cell* 28, 102–129. doi:10.1105/tpc.15.00496.

Bhuiyan NH, Selvaraj G, Wei Y, King J (2009). Role of lignification in plant defense. *Plant Signal Behav* 4, 158–159. doi:10.1093/jxb/ern290.8.

Bilgin DD, Zavala JA, Zhu J, Clough SJ, Ort DR, DeLucia EH (2010). Biotic stress globally downregulates photosynthesis genes. *Plant, Cell Environ* 33, 1597–1613. doi:10.1111/j.1365-3040.2010.02167.x.

Blanco-Ulate B, Allen G, Powell ALT, Cantu D (2013). Draft genome sequence of *Botrytis cinerea* BcDW1, inoculum for noble rot of grape berries. *Genome Announc* 1, e00252-13. doi:10.1128/genomeA.00252-13.Copyright.

Blanco-Ulate B, Labavitch JM, Vincenti E, Powell ALT, Cantu D (2016). Hitting the wall: Plant cell walls during *Botrytis cinerea* infections. *Botrytis - Fungus, Pathog its Manag Agric Syst*, 361–386. doi:10.1007/978-3-319-23371-0_18.

Bolton MD (2009). Primary metabolism and plant defense--fuel for the fire. *Mol Plant-Microbe Interact* 22, 487–497. doi:10.1094/MPMI-22-5-0487.

Bombarely A, Edwards KD, Sanchez-Tamburrino J, Mueller LA (2012). Deciphering the complex leaf transcriptome of the allotetraploid species *Nicotiana tabacum*: a phylogenomic perspective. *BMC Genomics* 13, 406. doi:10.1186/1471-2164-13-406.

Borras-Hidalgo O, Caprari C, Hernandez-Estevez I, De Lorenzo G, Cervone F (2012). A gene for plant protection: expression of a bean polygalacturonase inhibitor in tobacco confers a strong resistance against *Rhizoctonia solani* and two oomycetes. *Front Plant Sci* 3, 268. doi:10.3389/fpls.2012.00268.

Bozsó Z, Ott PG, Kámán-Tóth E, Bognár GF, Pogány M, Szatmári Á (2016). Overlapping yet response-specific transcriptome alterations characterize the nature of tobacco-*Pseudomonas syringae* interactions. *Front Plant Sci* 7, 251. doi:10.3389/fpls.2016.00251.

Brisson LF, Tenhaken R, Lamb CJ (1994). Function of oxidative cross-linking of cell wall structural proteins in plant disease resistance. *Plant Cell* 6, 1703–1712. doi:10.1105/tpc.6.12.1703.

Bultreys A, Trombik T, Drozak A, Boutry M (2009). *Nicotiana plumbaginifolia* plants silenced for the ATP-binding cassette transporter gene *NpPDR1* show increased susceptibility to a group of fungal and oomycete pathogens. *Mol Plant Pathol* 10, 651–663. doi:10.1111/j.1364-3703.2009.00562.x.

Carstens M, Vivier MA, Pretorius IS (2003). The *Saccharomyces cerevisiae* chitinase, encoded by the *CTS1-2* gene, confers antifungal activity against *Botrytis cinerea* to transgenic tobacco. *Transgenic Res* 12, 497–508. doi:10.1023/A:1024220023057.

Carstens M (2002). The Saccharomyces cerevisiae chitinase, encoded by the CTS1-2 gene, as an antifungal and biocontrol agent. *MSc thesis*, Stellenbosch University, South Africa, 1–101.

Cawoy H, Mariutto M, Henry G, Fisher C, Vasilyeva N, Thonart P, Dommes J, Ongena M (2014). Plant defense stimulation by natural isolates of *Bacillus* depends on efficient surfactin production. *Mol Plant-Microbe Interact* 27, 87–100. doi:10.1094/MPMI-09-13-0262-R.

Cervone F, De Lorenzo G, Pressey R, Darvill AG, Albersheim P (1990). Can *Phaseolus* PGIP inhibit pectic enzymes from microbes and plants? *Phytochemistry* 29, 447–449.

Chakrabarti A, Ganapathi TR, Mukherjee PK, Bapat VA (2003). MSI-99, a magainin analogue, imparts enhanced disease resistance in transgenic tobacco and banana. *Planta* 216, 587–596. doi:10.1007/s00425-002-0918-y.

Charles MT, Makhlouf J, Arul J (2008). Physiological basis of UV-C induced resistance to *Botrytis cinerea* in tomato fruit. II. Modification of fruit surface and changes in fungal colonization. *Postharvest Biol Technol* 47, 21–26. doi:10.1016/j.postharvbio.2007.05.014.

Chen S, Vaghchhipawala Z, Li W, Asard H, Dickman MB (2004). Tomato phospholipid hydroperoxide glutathione peroxidase inhibits cell death induced by Bax and oxidative stresses in yeast and plants. *Plant Physiol* 135, 1630–1641. doi:10.1104/pp.103.038091.

Choquer M, Fournier E, Kunz C, Levis C, Pradier J-M, Simon A, Viaud M (2007). *Botrytis cinerea* virulence factors: new insights into a necrotrophic and polyphageous pathogen. *FEMS Microbiol Lett* 277, 1–10. doi:10.1111/j.1574-6968.2007.00930.x.

Conrath U (2009). Priming of induced plant defense responses. *Adv Bot Res* 51, 361–395. doi:10.1016/S0065-2296(09)51009-9.

Daurelio LD, Petrocelli S, Blanco F, Holuigue L, Ottado J, Orellano EG (2011). Transcriptome analysis reveals novel genes involved in nonhost response to bacterial infection in tobacco. *J Plant Physiol* 168, 382–391. doi:10.1016/j.jplph.2010.07.014.

De Ascensao A (2001). Isolation and characterisation of a polygalacturonase-inhibiting protein (PGIP) and its encoding gene from *Vitis vinifera* L. *PhD dissertation*, Stellenbosch University, South Africa, 1–106.

De Beer A (2002). Overexpression and evaluation of an antimicrobial peptide from *Heuchera sanguinea* (Hs-AFP1) for inhibition of fungal pathogens in transgenic tobacco. *MSc thesis*, Stellenbosch University, South Africa, 1–84.

De Beer A (2008). Isolation and characterization of antifungal peptides from plants. *PhD dissertation*, Stellenbosch University, South Africa, 1–150.

De Lorenzo G, D'Ovidio R, Cervone F (2001). The role of polygalacturonase-inhibiting proteins (PGIPs) in defense against pathogenic fungi. *Annu Rev Phytopathol* 39, 313–335.

De Meyer GB, Bigirimana J, Elad Y, Höfte M (1998). Induced systemic resistance in *Trichoderma harzianum* T39 biocontrol of *Botrytis cinerea*. *Eur J Plant Pathol* 104, 279–286. doi:10.1023/A:1008628806616.

De Waard MA, Georgopoulos SG, Hollomon DW, Ishii H, Leroux P, Ragsdale NN, Schwinn FJ (1993). Chemical control of plant diseases: problems and prospects. *Annu Rev Phytopathol* 31, 403–421. doi:10.1146/annurev.py.31.090193.002155.

Desiderio A, Aracri B, Leckie F, Mattei B, Salvi G, Tigelaar H, Van Roekel JSC, Baulcombe DC, Melchers LS, De Lorenzo G, Cervone F (1997). Polygalacturonase-inhibiting proteins (PGIPs) with different specificities are expressed in *Phaseolus vulgaris*. *Mol Plant-Microbe Interact* 10, 852–860. doi:10.1094/MPMI.1997.10.7.852.

Di C, Zhang M, Xu S, Cheng T, An L (2006). Role of polygalacturonase-inhibiting protein in plant defense. *Crit Rev Microbiol* 32, 91–100. doi:10.1080/10408410600709834.

Doostdar H, McCollum TG, Mayer RT (1997). Purification and characterization of an endo-polygalacturonase from the gut of west indies sugarcane rootstalk borer weevil (*Diaprepes abbreviatus* L.) larvae. *Comp Biochem Physiol - B Biochem Mol Biol* 118, 861–867. doi:10.1016/S0305-0491(97)00285-X.

D'Ovidio R, Mattei B, Roberti S, Bellincampi D (2004a). Polygalacturonases, polygalacturonase-inhibiting proteins and pectic oligomers in plant-pathogen interactions. *Biochim Biophys Acta* 1696, 237–244. doi:10.1016/j.bbapap.2003.08.012.

D'Ovidio R, Raiola A, Capodicasa C, Devoto A, Pontiggia D, Roberti S, Galletti R, Conti E, O'Sullivan DM, De Lorenzo G (2004b). Characterization of the complex locus of bean encoding polygalacturonase-inhibiting proteins reveals subfunctionalization for defense against fungi and insects. *Plant Physiol* 135, 2424–2435. doi:10.1104/pp.104.044644.

Edwards KD, Fernandez-Pozo N, Drake-Stowe K, Humphry M, Evans AD, Bombarely A, Allen F, Hurst R, White B, Kernodle SP, Bromley JR, Sanchez-Tamburrino JP, Lewis RS, Mueller LA (2017). A reference genome for *Nicotiana tabacum* enables map-based cloning of homeologous loci implicated in nitrogen utilization efficiency. *BMC Genomics* 18, 448. doi:10.1186/s12864-017-3791-6.

El Oirdi M, Trapani A, Bouarab K (2010). The nature of tobacco resistance against *Botrytis cinerea* depends on the infection structures of the pathogen. *Environ Microbiol* 12, 239–253. doi:10.1111/j.1462-2920.2009.02063.x.

Elad Y, Pertot I, Cotes Prado AM, Stewart A (2016). Plant hosts of Botrytis spp. In *Botrytis - the Fungus, the Pathogen and its Management in Agricultural Systems*, eds S Fillinger and Y Elad (Switzerland: Springer International Publishing), 413–486. doi:10.1007/978-3-319-23371-0_20.

Ferrari S, Sella L, Janni M, De Lorenzo G, Favaron F, D'Ovidio R (2012). Transgenic expression of polygalacturonase-inhibiting proteins in *Arabidopsis* and wheat increases resistance to the flower pathogen *Fusarium graminearum*. *Plant Biol* 14, 31–38. doi:10.1111/j.1438-8677.2011.00449.x.

Ferrari S, Galletti R, Pontiggia D, Manfredini C, Lionetti V, Bellincampi D, Cervone F, De Lorenzo G (2008). Transgenic expression of a fungal endo-polygalacturonase increases plant resistance to pathogens and reduces auxin sensitivity. *Plant Physiol* 146, 669–681. doi:10.1104/pp.107.109686.

Ferrari S, Vairo D, Ausubel FM, Cervone F, De Lorenzo G (2003). Tandemly duplicated Arabidopsis genes that encode polygalacturonase-inhibiting proteins are regulated coordinately by different signal transduction pathways in response to fungal infection. *Plant Cell* 15, 93–106. doi:10.1105/tpc.005165.

Fillinger S, Elad Y (2016). Botrytis – *the Fungus, the Pathogen and its Management in Agricultural Systems*. Switzerland: Springer International Publishing doi:10.1007/978-3-319-23371-0.

Fotopoulos V, Sanmartin M, Kanellis AK (2006). Effect of ascorbate oxidase over-expression on ascorbate recycling gene expression in response to agents imposing oxidative stress. *J Exp Bot* 57, 3933–3943. doi:10.1093/jxb/erl147.

Frati F, Galletti R, De Lorenzo G, Salerno G, Conti E (2006). Activity of *endo*-polygalacturonases in mirid bugs (Heteroptera: Miridae) and their inhibition by plant cell wall proteins (PGIPs). *Eur J Entomol* 103, 515–522.

Frías M, Brito N, González C (2013). The *Botrytis cinerea* cerato-platanin BcSpl1 is a potent inducer of systemic acquired resistance (SAR) in tobacco and generates a wave of salicylic acid expanding from the site of application. *Mol Plant Pathol* 14, 191–196. doi:10.1111/j.1364-3703.2012.00842.x.

Frías M, González C, Brito N (2011). BcSpl1, a cerato-platanin family protein, contributes to *Botrytis cinerea* virulence and elicits the hypersensitive response in the host. *New Phytol* 192, 483–495. doi:10.1111/j.1469-8137.2011.03802.x.

Gazendam I, Oelofse D, Berger DK (2004). High-level expression of apple PGIP1 is not sufficient to protect transgenic potato against *Verticillium dahliae*. *Physiol Mol Plant Pathol* 65, 145–155. doi:10.1016/j.pmpp.2005.01.002.

Geer LY, Marchler-Bauer A, Geer RC, Han L, He J, He S, Liu C, Shi W, Bryant SH (2010). The NCBI BioSystems database. *Nucleic Acids Res* 38, 492–496. doi:10.1093/nar/gkp858.

Geraats BPJ, Bakker PAHM, Lawrence CB, Achuo EA, Höfte M, Van Loon LC (2003). Ethylene-insensitive tobacco shows differentially altered susceptibility to different pathogens. *Phytopathology* 93, 813–821. doi:10.1094/PHYTO.2003.93.7.813.

Glazebrook J (2005). Contrasting mechanisms of defense against biotrophic and necrotrophic pathogens. *Annu Rev Phytopathol* 43, 205–227. doi:10.1146/annurev.phyto.43.040204.135923.

Gomathi V, Gnanamanickam SS (2004). Polygalacturonase-inhibiting proteins in plant defence. *Curr Sci* 87, 1211–1217.

Govrin EM, Levine A (2000). The hypersensitive response facilitates plant infection by the necrotrophic pathogen *Botrytis cinerea*. *Curr Biol* 10, 751–757. doi:10.1016/S0960-9822(00)00560-1.

Guo J-L, Zhu Y-P, Shi K, Jue D-W, Liu S-P, Hong Y-B, Xie C, Yang Q (2014). Enhanced resistance to *Verticillium dahliae* in potato plants expressing *Solanum torvum* PGIP gene. *Bothalia* 44, 392–404.

Gutierrez-Sanchez G, King D, Kemp G, Bergmann C (2012). SPR and differential proteolysis/MS provide further insight into the interaction between PGIP2 and EPGs. *Fungal Biol* 116, 737–746. doi:10.1016/j.funbio.2012.04.010.

Hammerschmidt R (1999). Phytoalexins: What have we learned after 60 years? *Annu Rev Phytopathol* 37, 285–306.

Hammond-Kosack KE, Jones JDG (1996). Resistance gene-dependent plant defense responses. *Plant Cell* 8, 1773–1791. doi:dx.doi.org/10.2307/3870229.

Heath MC (2000). Hypersensitive response-related death. *Plant Mol Biol* 44, 321–334.

Hoekema A, Hirsch PR, Hooykaas PJJ, Schilperoort RA (1983). A binary plant vector strategy based on separation of *vir*- and T-region of the *Agrobacterium tumefaciens* Ti-plasmid. *Nature* 303, 179–180. doi:10.1038/303179a0.

Holmes FO (1938). Inheritance of resistance to Tobacco-mosaic disease in tobacco. *Phytopathology* 28, 553–561.

Hwang BH, Bae H, Lim HS, Kim KB, Kim SJ, Im MH, Park BS, Kim DS, Kim J (2010). Overexpression of polygalacturonase-inhibiting protein 2 (*PGIP2*) of Chinese cabbage (*Brassica rapa* ssp. *pekinensis*) increased resistance to the bacterial pathogen *Pectobacterium carotovorum* ssp. *carotovorum*. *Plant Cell Tissue Organ Cult* 103, 293–305. doi:10.1007/s11240-010-9779-4.

Jada B, Soitamo AJ, Siddiqui SA, Murukesan G, Aro E-M, Salakoski T, Lehto K (2014). Multiple different defense mechanisms are activated in the young transgenic tobacco plants which express the full length genome of the tobacco mosaic virus, and are resistant against this virus. *PLoS ONE* 9, e107778. doi:10.1371/journal.pone.0107778.

Janni M, Sella L, Favaron F, Blechl AE, De Lorenzo G, D'Ovidio R (2008). The expression of a bean PGIP in transgenic wheat confers increased resistance to the fungal pathogen *Bipolaris sorokiniana*. *Mol Plant-Microbe Interact* 21, 171–177. doi:10.1094/MPMI-21-2-0171.

Joubert DA, De Lorenzo G, Vivier MA (2013). Regulation of the grapevine polygalacturonase-inhibiting protein encoding gene: expression pattern, induction profile and promoter analysis. *J Plant Res* 126, 267–281. doi:10.1007/s10265-012-0515-5.

Joubert DA, Kars I, Wagemakers L, Bergmann CW, Kemp G, Vivier MA, Van Kan JAL (2007). A polygalacturonase-inhibiting protein from grapevine reduces the symptoms of the endopolygalacturonase BcPG2 from *Botrytis cinerea* in *Nicotiana benthamiana* leaves without any evidence for in vitro interaction. *Mol Plant-Microbe Interact* 20, 392–402. doi:10.1094/MPMI-20-4-0392.

Joubert DA, Slaughter AR, Kemp G, Becker JVW, Krooshof GH, Bergmann CW, Benen JAE, Pretorius IS, Vivier MA (2006). The grapevine polygalacturonase-inhibiting protein (VvPGIP1) reduces *Botrytis cinerea* susceptibility in transgenic tobacco and differentially inhibits fungal polygalacturonases. *Transgenic Res* 15, 687–702. doi:10.1007/s11248-006-9019-1.

Kálai K, Giczey G, Mészáros A, Balázs E, Dénes F (2006). *Trichoderma chitinase* gene expression confers mould resistance in tobacco. *Acta Hortic* 725, 783–789. doi:10.17660/ActaHortic.2006.725.108.

Kalunke RM, Tundo S, Benedetti M, Cervone F, De Lorenzo G, D'Ovidio R (2015). An update on polygalacturonase-inhibiting protein (PGIP), a leucine-rich repeat protein that protects crop plants against pathogens. *Front Plant Sci* 6, 146. doi:10.3389/fpls.2015.00146.

Kanai M, Nishimura M, Hayashi M (2010). A peroxisomal ABC transporter promotes seed germination by inducing pectin degradation under the control of *ABI5*. *Plant J* 62, 936–947. doi:10.1111/j.1365-313X.2010.04205.x.

Kars I, Krooshof GH, Wagemakers L, Joosten R, Benen JAE, Van Kan JAL (2005). Necrotizing activity of five *Botrytis cinerea* endopolygalacturonases produced in *Pichia pastoris*. *Plant J* 43, 213–225. doi:10.1111/j.1365-313X.2005.02436.x.

Keller H, Pamboukdjian N, Ponchet M, Poupet A, Delon R, Verrier J, Roby D, Ricci P (1999). Pathogen-induced elicitin production in transgenic tobacco generates a hypersensitive response and nonspecific disease resistance. *Plant Cell* 11, 223–235. doi:10.2307/3870852.

Kiba A, Nakatsuka T, Yamamura S, Nishihara M (2012). Gentian lipid transfer protein homolog with antimicrobial properties confers resistance to *Botrytis cinerea* in transgenic tobacco. *Plant Biotechnol* 29, 95–101. doi:10.5511/plantbiotechnology.11.1114a.

Kliebenstein DJ, Rowe HC (2008). Ecological costs of biotrophic versus necrotrophic pathogen resistance, the hypersensitive response and signal transduction. *Plant Sci* 174, 551–556. doi:10.1016/j.plantsci.2008.03.005.

Langcake P, Pryce RJ (1976). The production of resveratrol by *Vitis vinifera* and other members of the Vitaceae as a response to infection or injury. *Physiol Plant Pathol* 9, 77–86. doi:10.1016/0048-4059(76)90077-1.

Lee SW, Lee SH, Balaraju K, Park KS, Nam KW, Park JW, Park K (2014). Growth promotion and induced disease suppression of four vegetable crops by a selected plant growth-promoting rhizobacteria (PGPR) strain *Bacillus subtilis* 21-1 under two different soil conditions. *Acta Physiol Plant* 36, 1353–1362. doi:10.1007/s11738-014-1514-z.

Lei B, Lu K, Ding F, Zhang K, Chen Y, Zhao H, Zhang L, Ren Z, Qu C, Guo W, Wang J, Pan W (2014). RNA sequencing analysis reveals transcriptomic variations in tobacco (*Nicotiana tabacum*) leaves affected by climate, soil, and tillage factors. *Int J Mol Sci* 15, 6137–6160. doi:10.3390/ijms15046137.

Lei B, Zhao X-H, Zhang K, Zhang J, Ren W, Ren Z, Chen Y, Zhao H-N, Pan W-J, Chen W, Li H-X, Deng W-Y, Ding F, Lu K (2013). Comparative transcriptome analysis of tobacco (*Nicotiana tabacum*) leaves to identify aroma compound-related genes expressed in different cultivated regions. *Mol Biol Rep* 40, 345–357. doi:10.1007/s11033-012-2067-0.

Liu L, Sonbol F-M, Huot B, Gu Y, Withers J, Mwimba M, Yao J, He SY, Dong X (2016). Salicylic acid receptors activate jasmonic acid signalling through a non-canonical pathway to promote effector-triggered immunity. *Nat Commun* 7, 13099. doi:10.1038/ncomms13099.

Liu N, Zhang X, Sun Y, Wang P, Li X, Pei Y, Li F, Hou Y (2017). Molecular evidence for the involvement of a polygalacturonase-inhibiting protein, GhPGIP1, in enhanced resistance to Verticillium and Fusarium wilts in cotton. *Sci Rep* 7, 39840. doi:10.1038/srep39840.

Manfredini C, Sicilia F, Ferrari S, Pontiggia D, Salvi G, Caprari C, Lorito M, De Lorenzo G (2005). Polygalacturonase-inhibiting protein 2 of *Phaseolus vulgaris* inhibits BcPG1, a polygalacturonase of *Botrytis cinerea* important for pathogenicity, and protects transgenic plants from infection. *Physiol Mol Plant Pathol* 67, 108–115. doi:10.1016/j.pmpp.2005.10.002.

Marchive C, Mzid R, Deluc LG, Barrieu F, Pirrello J, Gauthier A, Corio-Costet M-F, Regad F, Cailleteau B, Hamdi S, Lauvergeat V (2007). Isolation and characterization of a *Vitis vinifera* transcription factor, VvWRKY1, and its effect on responses to fungal pathogens in transgenic tobacco plants. *J Exp Bot* 58, 1999–2010. doi:10.1093/jxb/erm062.

Martinez-Medina A, Flors V, Heil M, Mauch-Mani B, Pieterse CMJ, Pozo MJ, Ton J, Van Dam NM, Conrath U (2016). Recognizing plant defense priming. *Trends Plant Sci* 21, 818–822. doi:10.1016/j.tplants.2016.07.009.

Masci S, Laino P, Janni M, Botticella E, Di Carli M, Benvenuto E, Danieli PP, Lilley KS, Lafiandra D, D'Ovidio R (2015). Analysis of quality-related parameters in mature kernels of polygalacturonase inhibiting protein (PGIP) transgenic bread wheat infected with *Fusarium graminearum*. *J Agric Food Chem* 63, 3962–3969. doi:10.1021/jf506003t.

Mauch-Mani B, Baccelli I, Luna E, Flors V (2017). Defense priming: An adaptive part of induced resistance. *Annu Rev Plant Biol* 68, 485–512. doi:10.1146/annurev-arplant-042916-041132.

Mbengue M, Navaud O, Peyraud R, Barascud M, Badet T, Vincent R, Barbacci A, Raffaele S (2016). Emerging trends in molecular interactions between plants and the broad host range fungal pathogens *Botrytis cinerea* and *Sclerotinia sclerotiorum*. *Front Plant Sci* 7, 422. doi:10.3389/fpls.2016.00422.

Mbewana S (2010). Functional analysis of a lignin biosynthetic gene in transgenic tobacco. *MSc thesis*, Stellenbosch University, South Africa, 1–54.

Méndez-Bravo A, Calderón-Vázquez C, Ibarra-Laclette E, Raya-González J, Ramírez-Chávez E, Molina-Torres J, Guevara-García AA, López-Bucio J, Herrera-Estrella L (2011). Alkamides activate jasmonic acid biosynthesis and signaling pathways and confer resistance to *Botrytis cinerea* in *Arabidopsis thaliana*. *PLoS ONE* 6, e27251. doi:10.1371/journal.pone.0027251.

Mishina TE, Zeier J (2007). Pathogen-associated molecular pattern recognition rather than development of tissue necrosis contributes to bacterial induction of systemic acquired resistance in Arabidopsis. *Plant J* 50, 500–513. doi:10.1111/j.1365-313X.2007.03067.x.

Miura K, Lee J, Gong Q, Ma S, Jin JB, Yoo CY, Miura T, Sato A, Bohnert HJ, Hasegawa PM (2011). *SIZ1* Regulation of phosphate starvation-induced root architecture remodeling involves the control of auxin accumulation. *Plant Physiol* 155, 1000–1012. doi:10.1104/pp.110.165191.

Moyo M (2011). Molecular and phenotypic characterisation of grapevines expressing non-vinifera PGIP encoding genes. *MSc thesis*, Stellenbosch University, South Africa, 1–74.

Moyo M (2017). The interaction between Vitis vinifera and fungal pathogens: A molecular approach using characterized grapevine mutants. *PhD dissertation*, Stellenbosch University, South Africa, 1–182.

Mueller LA, Solow TH, Taylor N, Skwarecki B, Buels R, Binns J, Lin C, Wright MH, Ahrens R, Wang Y, Herbst E V, Keyder ER, Menda N, Zamir D, Tanksley SD (2005). The SOL Genomics Network: a comparative resource for Solanaceae biology and beyond. *Plant Physiol* 138, 1310–1317. doi:10.1104/pp.105.060707.

Murphy AM, Holcombe LJ, Carr JP (2000). Characteristics of salicylic acid-induced delay in disease caused by a necrotrophic fungal pathogen in tobacco. *Physiol Mol Plant Pathol* 57, 47–54. doi:10.1006/pmpp.2000.0280.

Nanda AK, Andrio E, Marino D, Pauly N, Dunand C (2010). Reactive oxygen species during plant-microorganism early interactions. *J Integr Plant Biol* 52, 195–204. doi:10.1111/j.1744-7909.2010.00933.x.

Nguema-Ona E, Moore JP, Fagerström AD, Fangel JU, Willats WGT, Hugo A, Vivier MA (2013). Overexpression of the grapevine PGIP1 in tobacco results in compositional changes in the leaf arabinoxyloglucan network in the absence of fungal infection. *BMC Plant Biol* 13, 46. doi:10.1186/1471-2229-13-46.

Powell ALT, Van Kan JAL, Ten Have A, Visser J, Greve LC, Bennett AB, Labavitch JM (2000). Transgenic expression of pear PGIP in tomato limits fungal colonization. *Mol Plant-Microbe Interact* 13, 942–950. doi:10.1094/MPMI.2000.13.9.942.

Protsenko MA, Bulantseva EA, Korableva NP (2010). Polygalacturonase-inhibiting proteins in plant fleshy fruits during their ripening and infections. *Russ J Plant Physiol* 57, 356–362. doi:10.1134/S1021443710030064.

Ridley BL, Neill MAO, Mohnen D (2001). Pectins: structure, biosynthesis, and oligogalacturonide-related signaling. *Phytochemistry* 57, 929–967. doi:10.1016/S0031-9422(01)00113-3.

Robinson RAA (1977). Plant pathosystems. *Ann N Y Acad Sci* 287, 238–242. doi:10.1016/0308-521X(77)90071-3.

Ross AF (1961). Systemic acquired resistance induced by localized virus infections in plants. *Virology* 14, 340–358. doi:10.1016/0042-6822(61)90319-1.

Shaul O, Galili S, Volpin H, Ginzberg I, Elad Y, Chet I, Kapulnik Y (1999). Mycorrhiza-induced changes in disease severity and PR protein expression in tobacco leaves. *Mol Plant-Microbe Interact* 12, 1000–1007. doi:10.1094/MPMI.1999.12.11.1000.

Shigenaga AM, Argueso CT (2016). No hormone to rule them all: Interactions of plant hormones during the responses of plants to pathogens. *Semin Cell Dev Biol* 56, 174–189. doi:10.1016/j.semcdb.2016.06.005.

Shlezinger N, Minz A, Gur Y, Hatam I, Dagdas YF, Talbot NJ, Sharon A (2011). Anti-apoptotic machinery protects the necrotrophic fungus *Botrytis cinerea* from host-induced apoptotic-like cell death during plant infection. *PLoS Pathog* 7, e1002185. doi:10.1371/journal.ppat.1002185.

Sierro N, Battey JND, Ouadi S, Bakaher N, Bovet L, Willig A, Goepfert S, Peitsch MC, Ivanov N V (2014). The tobacco genome sequence and its comparison with those of tomato and potato. *Nat Commun* 5, 3833. doi:10.1038/ncomms4833.

Sierro N, Battey JN, Ouadi S, Bovet L, Goepfert S, Bakaher N, Peitsch MC, Ivanov N V (2013). Reference genomes and transcriptomes of *Nicotiana sylvestris* and *Nicotiana tomentosiformis*. *Genome Biol* 14, R60. doi:10.1186/gb-2013-14-6-r60.

Sohn SI, Kim YH, Kim BR, Lee SY, Lim CK, Hur JH, Lee JY (2007). Transgenic tobacco expressing the *hrpN*$_{EP}$ gene from *Erwinia pyrifoliae* triggers defense responses against *Botrytis cinerea*. *Mol Cells* 24, 232–239. doi:1124 [pii].

Spadoni S, Zabotina O, Di Matteo A, Mikkelsen JD, Cervone F, De Lorenzo G, Mattei B, Bellincampi D (2006). Polygalacturonase-inhibiting protein interacts with pectin through a binding site formed by four clustered residues of arginine and lysine. *Plant Physiol* 141, 557–564. doi:10.1104/pp.106.076950.

Staats M, Van Kan JAL (2012). Genome update of *Botrytis cinerea* strains B05.10 and T4. *Eukaryot Cell* 11, 1413–1414. doi:10.1128/EC.00164-12.

Strange RN, Scott PR (2005). Plant disease: a threat to global food security. *Annu Rev Phytopathol* 43, 83–116. doi:10.1146/annurev.phyto.43.113004.133839.

Szatmári Á, Zvara Á, Móricz ÁM, Besenyei E, Szabó E, Ott PG, Puskás LG, Bozsó Z (2014). Pattern triggered immunity (PTI) in tobacco: Isolation of activated genes suggests role of the phenylpropanoid pathway in inhibition of bacterial pathogens. *PLoS ONE* 9, e102869. doi:10.1371/journal.pone.0102869.

Ten Have A, Mulder W, Visser J, Van Kan JAL (1998). The endopolygalacturonase gene *Bcpg1* is required for full virulence of *Botrytis cinerea*. *Mol Plant-Microbe Interact* 11, 1009–1016. doi:10.1094/MPMI.1998.11.10.1009.

Tundo S, Janni M, Moscetti I, Mandalà G, Savatin D, Blechl A, Favaron F, D'Ovidio R (2016). PvPGIP2 accumulation in specific floral tissues, but not in the endosperm, limits *Fusarium graminearum* infection in wheat. *Mol Plant-Microbe Interact* 29, 815–821. doi:10.1094/MPMI-07-16-0148-R.

Van Kan JAL (2006). Licensed to kill: the lifestyle of a necrotrophic plant pathogen. *Trends Plant Sci* 11, 247–253. doi:10.1016/j.tplants.2006.03.005.

Van Kan JAL, Stassen JHM, Mosbach A, Van Der Lee TAJ, Faino L, Farmer AD, Papasotiriou D, Zhou S, Seidl MF, Cottam E, Edel D, Hahn M, Schwartz DC, Dietrich RA, Widdison S, Scalliet G (2017). A gapless genome sequence of the fungus *Botrytis cinerea*. *Mol Plant Pathol* 8, 75–89. doi:10.1111/mpp.12384.

Van Loon LC (1985). Pathogenesis-related proteins. *Plant Mol Biol* 116, 111–116.

Van Wees SCM, Luijendijk M, Smoorenburg I, Van Loon LC, Pieterse CMJ (1999). Rhizobacteria-mediated induced systemic resistance (ISR) in *Arabidopsis* is not associated with a direct effect on expression of known defense-related genes but stimulates the expression of the jasmonate-inducible gene Atvsp upon challenge. *Plant Mol Biol* 41, 537–549. doi:10.1023/A:1006319216982.

Venter A (2010). The functional analysis of Vitaceae protein (PGIP) encoding genes overexpressed in tobacco. *MSc thesis*, Stellenbosch University, South Africa, 1–67.

Vera J, Castro J, Contreras RA, González A, Moenne A (2012). Oligo-carrageenans induce a long-term and broad-range protection against pathogens in tobacco plants (var. Xanthi). *Physiol Mol Plant Pathol* 79, 31–39. doi:10.1016/j.pmpp.2012.03.005.

Volpi C, Raiola A, Janni M, Gordon A, O'Sullivan DM, Favaron F, D'Ovidio R (2013). *Claviceps purpurea* expressing polygalacturonases escaping PGIP inhibition fully infects PvPGIP2 wheat transgenic plants but its infection is delayed in wheat transgenic plants with increased level of pectin methyl esterification. *Plant Physiol Biochem* 73, 294–301. doi:10.1016/j.plaphy.2013.10.011.

Wang A, Wei X, Rong W, Dang L, Du L-P, Qi L, Xu H-J, Shao Y, Zhang Z (2015). GmPGIP3 enhanced resistance to both take-all and common root rot diseases in transgenic wheat. *Funct Integr Genomics* 15, 375–381. doi:10.1007/s10142-014-0428-6.

Wang R, Lu L, Pan X, Hu Z, Ling F, Yan Y, Liu Y, Lin Y (2014). Functional analysis of OsPGIP1 in rice sheath blight resistance. *Plant Mol Biol* 87, 181–191. doi:10.1007/s11103-014-0269-7.

Wang X, Zhu X, Tooley P, Zhang X (2013). Cloning and functional analysis of three genes encoding polygalacturonase-inhibiting proteins from *Capsicum annuum* and transgenic CaPGIP1 in tobacco in relation to increased resistance to two fungal pathogens. *Plant Mol Biol* 81, 379–400. doi:10.1007/s11103-013-0007-6.

Whitham S, McCormick S, Baker B (1996). The *N* gene of tobacco confers resistance to tobacco mosaic virus in transgenic tomato. *PNAS* 93, 8776–8781. doi:10.1073/pnas.93.16.8776.

Williamson B, Tudzynski B, Tudzynski P, Van Kan JAL (2007). *Botrytis cinerea*: the cause of grey mould disease. *Mol Plant Pathol* 8, 561–580. doi:10.1111/J.1364-3703.2007.00417.X.

Xu ZS, Xiong TF, Ni ZY, Chen XP, Chen M, Li LC, Gao DY, Yu XD, Liu P, Ma YZ (2009). Isolation and identification of two genes encoding leucine-rich repeat (LRR) proteins differentially responsive to pathogen attack and salt stress in tobacco. *Plant Sci* 176, 38–45. doi:10.1016/j.plantsci.2008.09.004.

Yin X, Nishimura M, Hajika M, Komatsu S (2016). Quantitative proteomics reveals the flooding-tolerance mechanism in mutant and abscisic acid-treated soybean. *J Proteome Res* 15, 2008–2025. doi:10.1021/acs.jproteome.6b00196.

Zhang C, Feng C, Wang J, Kong F, Sun W, Wang F (2016). Cloning, expression analysis and recombinant expression of a gene encoding a polygalacturonase-inhibiting protein from tobacco, *Nicotiana tabacum*. *Heliyon* 2, e00110. doi:10.1016/j.heliyon.2016.e00110.

Zhang Y, Zhang Y, Qiu D, Zeng H, Guo L, Yang X (2015). BcGs1, a glycoprotein from *Botrytis cinerea*, elicits defence response and improves disease resistance in host plants. *Biochem Biophys Res Commun* 457, 627–634. doi:10.1016/j.bbrc.2015.01.038.

Zurbriggen MD, Carrillo N, Tognetti VB, Melzer M, Peisker M, Hause B, Hajirezaei M-R (2009). Chloroplast-generated reactive oxygen species play a major role in localized cell death during the non-host interaction between tobacco and *Xanthomonas campestris* pv. *vesicatoria*. *Plant J* 60, 962–973. doi:10.1111/j.1365-313X.2009.04010.x.

Chapter 2

Plant defence mechanisms in general with a specific emphasis on defence against *Botrytis cinerea*

Plant defence mechanisms in general with a specific emphasis on defence against *Botrytis cinerea*

Plant-pathogen interactions have been intensively studied for many years, using a plethora of tools to observe and quantify plant responses to pathogens. Similarly, the epidemiology of the pathogens, their fitness and virulence traits and well as their infections strategies have been well covered (Dean et al., 2012; de Waard, 1993; Horbach et al., 2011; Knogge, 1996; Nakajima and Akutsu, 2013; Sacristán and García-Arenal, 2008; Williamson et al., 2007). Since the key elements of plant defence (Figure 2.1) have been the subject of comprehensive reviews in recent years (Asai and Shirasu, 2015; Choi and Klessig, 2016; Liu et al., 2015b; Mauch-Mani et al., 2017; Seo and Choi, 2015; Shigenaga and Argueso, 2016), this review will present a brief overview of these aspects to provide context for the review of information gleaned from studies of host-*Botrytis* interactions.

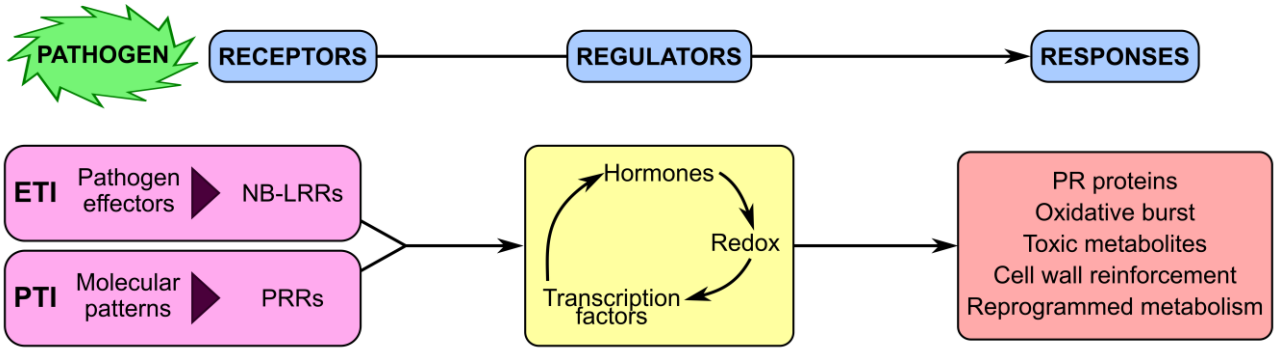

Figure 2.1 Simplified diagram of plant defence, showing the general process in blue blocks and more specific elements of each process in the different colour blocks. The general process (blue) is initiated by the pathogen (green) that bind to RECEPTORS, that in turn induce changes in REGULATORS controlling defence RESPONSES. Two classical types of immunity (purple), effector-triggered immunity (ETI) and pattern-triggered immunity (PTI), have been defined based on the type of elicitor and receptor, but the subsequent regulatory mechanisms (yellow) and characteristic responses (red) are common to both. NB-LRR: Nucleotide-binding Leucine-rich repeat proteins; PRR: Pattern recognition receptors; PR: Pathogenesis-related.

2.1 Overview of plant defence mechanisms

2.1.1 Recognising the presence of a pathogen

Plant-pathogen interaction studies initially identified two classes of elicitors of plant defence, namely pathogen-associated molecular patterns (PAMPs) and effectors (formerly virulence factors), which induce PAMP-triggered immunity (PTI, also basal resistance) and effector-triggered immunity (ETI, formerly gene-for-gene resistance) respectively (Boller and Felix, 2009; Jones and Dangl, 2006). The discovery of PAMPs in non-pathogens has led to the adoption of microbe-associated molecular patterns (MAMPs) instead, as a more appropriate term, while the abbreviation PTI has been amended to represent pattern recognition receptor (PRR) triggered immunity, after the MAMP-binding receptors (Macho and Zipfel, 2015). The distinction between MAMPs and effectors had been defined related to the functionality of the elicitor in the pathogen, with MAMPs being essential

components for microbial fitness, whereas effectors are essential for virulence, but not general fitness (Bent and Mackey, 2007). This binary model has since expanded to also include herbivory-associated molecular patterns (HAMPs) and damage-associated molecular patterns (DAMPs), that recognize compounds specific to insect oral secretions, saliva and oviposition (Mithöfer and Boland, 2008), and molecules indicative of damage, such as enzymatic degradation products of the plant cell wall (Aziz et al., 2004; Boller and Felix, 2009) respectively. The recognition of molecular patterns that derive from pathogens (MAMPs and HAMPs) and from the actions of these pathogens (DAMPs) emphasises the robust surveillance network that plants use to detect when defence is required.

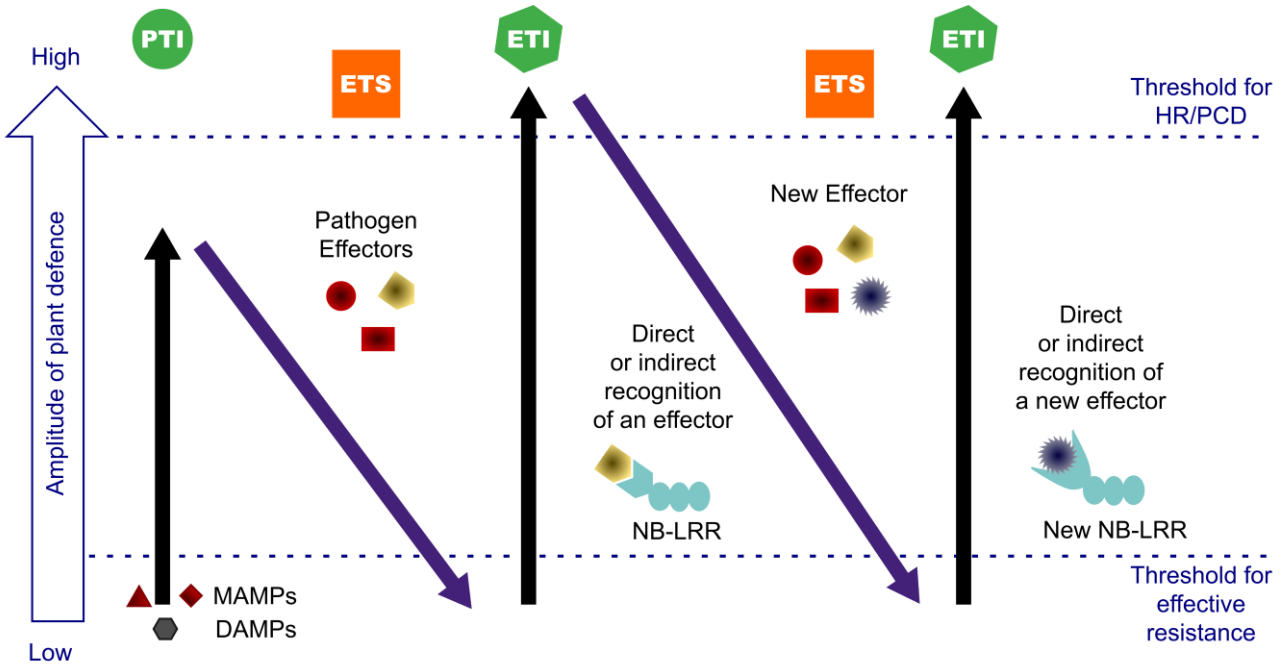

Figure 2.2 The zig-zag model of plant immunity/pathogen effector evolution, originally illustrated by Jones and Dangl (2006). Pattern-triggered immunity (PTI, green circle) first occurs when microbe-associated molecular patterns (MAMPs) or damage-associated molecular patterns (DAMPs) are recognised. Pathogens evolve effectors that induce effector-triggered susceptibility (ETS, orange square). Effector-triggered immunity (ETI, green hexagon) requires recognition of the effector through evolution of nucleotide-binding leucine-rich repeat (NB-LRR) proteins. ETI induces a stronger response, causing the hypersensitive response (HR) and programmed cell death (PCD). A second round of ETS follows the pathogen's evolution of a new effector, which is overcome by the plant's evolution of a new NB-LRR. Adapted from Zvereva and Pooggin (2012).

Though PTI and ETI are not the only modes of the plant immune system, they still provide crucial insights into the processes plants use to defend themselves. These modes have been described in a four-part or zigzag model of evolved resistance (Figure 2.2; Bent and Mackey, 2007; Chisholm et al., 2006; Jones and Dangl, 2006). Critically, in this model ETI relies on pathogens requiring living tissue to access nutrients, and is therefore only suitable for biotrophic and hemibiotrophic pathogens, that are absolutely or partially restricted to colonisation of living tissue (Glazebrook, 2005). Despite this limitation, ETI has been successfully employed to enhance or establish resistance to many commercially relevant diseases (Bent and Mackey, 2007). The zig-zag model proposes that hypersensitive programmed cell death (PCD) is the marker for ETI, since it is commonly seen in many pathosystems (Bent and Mackey, 2007; Jones and Dangl, 2006), however some forms of ETI appear to be independent of hypersensitivity, and instead rely on cell wall reinforcement and

phytoalexin synthesis (Bulgarelli et al., 2010; Cui et al., 2015). In general, ETI and PTI share the same characteristic defence mechanisms, but the factors are typically more robustly and/or enduringly activated during ETI (Cui et al., 2015; Tsuda and Katagiri, 2010).

As per the original definitions, MAMPs are patterns found in a wide range of microbes, and are perceived by a wide range of plant species, with highly conserved PRRs evolving before species differentiation occurred, while effectors are molecules specific to a specific host-pathogen interaction that are under constant evolutionary pressure (Boller and Felix, 2009). Classifying elicitors into effectors or MAMPs has become problematic because continued research has revealed that ETI and PTI form part of a continuum of plant immune responses (Thomma et al., 2011). A helpful definition may be the type of receptor that perceives them, and the rate of evolutionary differentiation forms the basis for classification (De Lorenzo et al., 2011; Jones and Dangl, 2006; Mithöfer and Boland, 2008; Yamaguchi et al., 2006; Zipfel and Robatzek, 2010). Rapidly-evolving effectors would be commonly recognised by intracellular proteins and slowly-evolving MAMPs recognised by plasma membrane-localised receptors, with the caveat that not all elicitors will strictly fall in either category. Much progress has been made in identifying receptors for pathogen effectors, MAMPs and DAMPs, and in identifying downstream regulatory elements.

Molecular patterns and their receptors

PTI is triggered by the recognition of “non-self” molecules and by molecules that indicate cellular damage (Choi and Klessig, 2016). Where microbial pathogens are concerned, these molecules are MAMPs and DAMPs, which have been more extensively studied than HAMPs, their insect-derived counterparts (Boller and Felix, 2009; Mithöfer and Boland, 2008). Classical MAMPs are found on or near the surface of the pathogen, such as flagellin, the primary protein constituent of bacterial flagella (Gómez-Gómez and Boller, 2002), ergosterol, the main sterol in fungal membranes (Granado et al., 1995) and chitin, an important component of fungal cell walls (Miya et al., 2007). Other MAMPs are the intracellular bacterial cold shock protein (Csp), which is a MAMP for Solanaceae (Wang et al., 2016) and *Botrytis cinerea* polygalacturonases (BcPGs), that are secreted during the earliest phases of infection (D’Ovidio et al., 2004).

Though Zhang et al. (2014) showed that BcPGs act as MAMPs in a manner that is independent of the hydrolytic activities of these enzymes, their pectin-degrading activities produce oligogalacturonide (OG) fragments from the plant cell walls they act on, that can act also as DAMPs (Benedetti et al., 2015). Other ubiquitous DAMPs have been identified, namely monomers of cutin, derived from degradation of the cuticle (Schweizer et al., 1996) and exogenous ATP (eATP), that is released by cell damage (Tanaka et al., 2014). Intriguingly, peptide DAMPs that derive from proteolytic cleavage of precursor proteins are specific to certain plant families, such as systemin in Solanaceous species (Ryan and Pearce, 1998) and danger signal peptide 1 (AtPep1) in *Arabidopsis*

(Krol et al., 2010), that derive from cleavage of prosystemin and PROPEP1 respectively. PROPEP orthologs have been identified in many plant families, but individual peptides appear to be biologically active only in closely related species (Lori et al., 2015).

Most MAMP receptors share the characteristic leucin-rich repeat (LRR) domains that are common in their intracellular counterparts (Boller and Felix, 2009; Trdá et al., 2015; Zipfel, 2014). The best studied MAMP receptor is *Arabidopsis* FLAGELLIN SENSING 2 (FLS2) that binds flagellin. This receptor is a membrane-spanning LRR receptor kinase (RK), with the extracellular LRR-motif recognising the flg22 epitope and the intracellular kinase domain forming a complex with BRASSINOSTEROID INSENSITIVE 1-ASSOCIATED KINASE 1 (BAK1). FLS2 is evolutionarily ancient and is found in all major groups of higher plants (Boller and Felix, 2009; Trdá et al., 2015). In the presence of flagellin, FLS2 and BAK1 are phosphorylated by BOTRYTIS-INDUCED KINASE 1 (BIK1; Lu et al., 2010). The most common fungal MAMP is chitin, that triggers defence responses in a wide range of higher plants (Boller and Felix, 2009). In rice, the chitin-binding PRR (chitin elicitor-binding protein; CEBiP) forms a complex with a transmembrane RK (chitin elicitor receptor kinase 1; CERK1) to induce defence responses, while in *Arabidopsis* CERK1 directly binds chitin (Shinya et al., 2012). The chitin-binding homolog of OsCEBiP in *Arabidopsis*, LYSIN MOTIF DOMAIN-CONTAINING GLYCOSYLPHOSPHATIDYLINOSITOL-ANCHORED PROTEIN 2 (LYM2) binds chitin *in vitro* but is not required for chitin-triggered phosphorylation cascades (Narusaka et al., 2013), but rather reduces flux through plasmodesmata to restrict cell-to-cell movement by the pathogen (Faulkner et al., 2013). Four BcPGs (BcPG2, BcPG3, BcPG4 and BcPG6) are perceived by an *Arabidopsis* LRR receptor-like protein (RLP) AtRLP42 (Zhang et al., 2014). Here too, the receptor formed a complex with another LRR-RLP after binding to its MAMP.

The identification of DAMP receptors is still at a very early stage; however, RKs critical for DAMP perception have been identified in *Arabidopsis* for OGs, eATP and AtPep1 (Zipfel, 2014). The receptor for eATP was identified as Does not respond to Nucleotides 1 (DORN1), a transmembrane lectin RK (Choi et al., 2014), while wall-associated kinase 1 (WAK1) is required for OG perception (Brutus et al., 2010) and AtPep1 perception involves PEP receptor 1 (PEPR1), an LRR-RK (Yamaguchi et al., 2006).

Pathogen effectors and their receptors

Effectors form part of a system that enables pathogens to evade basal immune responses by preventing or manipulating the plant defence metabolism (Asai and Shirasu, 2015). Effector-triggered susceptibility (ETS) arises when effectors act in different subcellular compartments and target various defence mechanisms, such as inhibiting MAMP recognition, activating unsuitable hormone signalling, interrupting defence signalling or disarming hostile plant enzymes. Although many effectors identified to date originate from biotrophic or hemibiotrophic pathogens (Wang et al.,

2014), some examples of necrotroph-derived effectors have been identified, such as the necrosis and ethylene inducing 1 (Nep1) protein originally identified in *Fusarium oxysporum* (Bailey, 1995) that has since been found in many biotrophic and necrotrophic pathogens (Gijzen and Nürnberger, 2006). In some cases, processes activated by pathogen effectors are not involved in immune responses, but rather manipulate plant metabolism to facilitate infection. For example, the sugar transporter SWEET4 in *Vitis vinifera* is induced by *B. cinerea* Nep1-like protein effectors to facilitate sugar acquisition by the fungus (Chong et al., 2014; Schouten et al., 2008) and *Xanthomonas campestris* pv *vesicatoria* expresses a Type III effector protein that activates cell expansion by stimulating transcription of auxin-responsive and expansin-encoding genes (Marois et al., 2002). Intriguingly, plants possess "susceptibility factors" which can be viewed as pathogen effectors encoded in the plant genome (Eckardt, 2002), the most well-known being the *mildew-resistance locus* (*MLO*) genes first described in barley (Kusch and Panstruga, 2017). Some effectors act as transcription factors (TFs) that activate transcription of host genes, including susceptibility factors (Schornack et al., 2013). In addition to proteinaceous effectors, pathogens also use small RNA (sRNA) to interfere with plant metabolism and promote disease progression (Wang et al., 2014; 2015a; Weiberg et al., 2013).

ETI depends on the perception or circumvention of pathogen effectors (Cui et al., 2015). Most effector receptors are intracellular nucleotide-binding leucine-rich repeat proteins (NLRs) with either Toll-interleukin 1 receptor or coiled-coil N-terminal domains, abbreviated as TNL and CNL respectively (Chisholm et al., 2006; Cui et al., 2015). CNLs are generally associated with the plasma membrane, while TNLs are nuclear or nucleocytoplasmic. The N-terminal domain recognises effectors or effector-activity and allows the exchange of ADP and ATP to switch the receptor from inactive to active (Takken and Goverse, 2012).

The simplest form of NLR-mediated defence activation is the direct interaction of one or more NLRs with the effectors, encoded by *avirulence* (*Avr*) genes (Cui et al., 2015). For example, flax resistance to *Melampsora lini* follows the binding of two TNLs, L5 and L6, with AvrL567 (Ravensdale et al., 2012). This direct recognition of effectors results in high evolutionary pressure, which can be ameliorated by utilising a "surveillance NLR", that detects interference with the effector target, as in *Arabidopsis*, where ETI is triggered when Resistance to *Pseudomonas syringae* pv *maculicola* 1 (RPM1) and Resistance to *Pseudomonas syringae* 2 detect the cleavage of RPM1-interacting protein 4 (RIN4) by AvrB, AvrRpm1 and AvrRpt2 from *P. syringae* (Kim et al., 2005).

Another approach to reduce evolutionary pressure is to use a pair of NLRs, with one acting as the sensor and the other initiating defence responses, as employed by *Oryza sativa* Resistance gene analog 4 (RGA4) and RGA5 against *Magnaporthe oryzae* Avr-Pia and Avr-Co39 (Césari et al., 2014). Alternatively, sensing changes in stress signalling can be used to identify ETS by, for example,

detecting incorrect protein phosphorylation patterns due to the disruption of a specific mitogen-activated protein kinase (MAPK) that responds to MAMP perception (Zhang et al., 2012).

In some cases, ETI is accomplished by using decoy targets that direct effectors away from their intended targets. One example of this in *Arabidopsis*, where AvrPphB susceptible 1 (PBS1) and BIK1, among others, are targeted by a protease encoded by *AvrPphB* from *P. syringae* (Ade et al., 2007; Zhang et al., 2010). PBS1 is associated with Resistance to *P. syringae* protein 5 (RPS5), that triggers ETI when the protease cleaves PBS1. A second example of decoy targets directs TF effectors that target susceptibility factor genes to also activate resistance factors. In *Capsicum annuum* AvrBs3 from *Xanthomonas campestris* pv *vesicatoria* activates transcription of a flavin-dependent monooxygenase that induces the hypersensitive response (HR), whereas the intended targets include auxin-induced and expansin-like genes that induce cell enlargement (Marois et al., 2002; Römer et al., 2007).

2.1.2 Activating defence responses

Once a plant cell has detected the presence of a pathogen, a signalling mechanism is required to transmit the signal to the nucleus, where changes in gene expression typically shifts the metabolism towards defence (Katagiri, 2004). The signalling machinery used during PTI and ETI is largely the same, but activation of the signal is prolonged in ETI (Tsuda and Katagiri, 2010). Three mechanisms function within the signalling machinery, namely MAPK phosphorylation cascades; reactive oxygen species (ROS); and phytohormones, primarily ethylene (ET), salicylic acid (SA) and jasmonic acid (JA). Since activation of MAPK signalling and treatment of plants with ROS and phytohormones generally induces changes in gene expression (Shulaev et al., 1997; Vandenabeele et al., 2003; Wasternack and Parthier, 1997; Zhang and Klessig, 2001), it follows that TFs would be targets for defence signalling.

Transcription factors

The importance of TFs in defence is highlighted by the observation that they can be targets for pathogen effectors (Marois et al., 2002). As with many regulatory factors, TFs can have positive and negative impacts on defence, in some cases related to the specific pathogen, or possibly balancing defence metabolism with growth and development (Seo and Choi, 2015). Some TFs regulate basal defence in a diurnal pattern, to prime defence signalling during more vulnerable times of the day (Ingle et al., 2015; Shin et al., 2012). In addition to the TFs directly involved with hormone signalling, which will be discussed below, many other TFs are known to function in plant defence. The WRKY family, though not the largest TF family, is widely involved with defence responses and can play key roles in PTI and ETI (Seo and Choi, 2015). For example, two-thirds of *Arabidopsis* WRKYs are transcriptionally activated by SA treatment or bacterial infection (Dong et al., 2003). WRKY33 is a target of the flg22-triggered MAPK cascade, enhances phytoalexin and ET synthesis and influences,

directly and indirectly the expression of a large array of genes (Birkenbihl et al., 2012). WRKYs from rice and barley have been shown to interact with NLRs to overcome ETS (Seo and Choi, 2015). The Ethylene Response Factor (ERF) subgroup of the APETALA2 (AP2)/ERF family is also strongly associated with defence. AtERF6, like AtWRKY33, is activated following flg22 perception (Meng et al., 2013). Myelocytomatosis oncogenes (MYCs) play important roles in regulating the different branches of JA signalling (Boter et al., 2004; Fernández-Calvo et l., 2011; Lorenzo et al., 2004). The myeloblastosis (MYB) TF superfamily has diverse functions and MYBs from various species have been shown to activate defence-related processes and pathogenesis-response (PR) proteins (Ambawat et al., 2013; Gao et al., 2016; Liu et al., 2016).

MAPK cascades

As noted above, many PRRs have, or are associated with, protein kinase domains, that activate MAPK cascades following elicitation (Asai et al., 2002; Brutus et al., 2010; Choi et al., 2014; Yamaguchi et al., 2006; Zhang et al., 2014). The first complete signalling cascade was identified in *Arabidopsis*, linking the transmembrane flagellin receptor FLS2 with WRKY TFs in the nucleus (Asai et al., 2002). In addition to activating WRKY TFs (Asai et al., 2002), they can activate ET and phytoalexin biosynthesis (Ren et al., 2008; Xu et al., 2008). MAPK cascades are considered the “highways” that relays signals from diverse stress inputs through overlapping phosphorylation cascades (Zhang and Klessig, 2001).

Hormone signalling

Signalling in plant defence is dominated by ET, SA and JA, while abscisic acid (ABA), auxin, gibberellin, cytokinins and brassinosteroids typically balance defence metabolism with growth, development and other stress responses (Alvarez, 2000; Bari and Jones, 2009; Broekgaarden et al., 2015; Reymond and Farmer, 1998; Wasternack, 2007). Interestingly, although ABA is not generally considered a defence hormone, it appears to play a role in defence against herbivores (Bodenhausen and Reymond, 2007). In this review, the perception and important TF targets of the three “defence hormones”, will be briefly outlined, beginning with what is known about their biosynthesis.

Biosynthesis of jasmonate, salicylic acid and ethylene

JA biosynthesis occurs in the chloroplast and peroxisome (Wasternack, 2007). α-linolenic acid is oxygenated in the C-13 position by a 13S-lipoxygenase (13-LOX). Allene oxide synthase (AOS) and allene oxide cyclase (AOC) complete the chloroplast-localised section to form cis-(+)-12-oxophytodienoic acid (OPDA). In the peroxisome, OPDA reductase (OPR) and three rounds of β-oxidation complete the synthesis of JA. The bioactive form of JA, jasmonoyl-isoleucine (JA-Ile; Fonseca et al., 2009; Staswick and Tiryaki, 2004) is formed by the JA-isoleucine conjugase JASMONATE RESISTANT 1 (JAR1; Staswick et al., 1992). A cytosolic branch of the LOX pathway

oxygenates α-linolenic acid at the C-9 position, thereafter divinyl ether synthase (DES) converts the 9-hydroperoxides into divinyl ether fatty acids (Fammartino et al., 2007). Unlike the signalling molecules produced in the 13-LOX branch, oxylipin products of the 9-LOX pathway are antimicrobial, and can be considered phytoalexins (Weber et al., 1999).

Despite its central role in plant defence, and particularly in systemic acquired resistance (SAR), the biosynthetic pathways of SA in plants have not been fully resolved (Liu et al., 2015b; Shah, 2003). Two pathways appear to be important for pathogen-induced SA synthesis, originating with isochorismate, synthesised by isochorismate synthase (ICS), and cinnamic acid, synthesised by phenylalanine ammonia-lyase (PAL), however, the downstream components of these pathways have not been identified.

ET is a modulator of defence signalling, and is one of the first phytohormones to be induced after MAMP perception (Broekgaarden et al., 2015). 1-aminocyclopropane-1-carboxylic acid (ACC) synthase (ACS) catalyses the rate limiting step of ET biosynthesis, while ACC oxidase (ACO) fine-tunes ET production (Kende, 1993). In *Arabidopsis*, two ACS isoforms are activated through phosphorylation by MAPKs MPK3 and MPK6, which were in turn activated by FLS2 after binding flg22 (Asai et al., 2002; Xu et al., 2008).

Receptors and transcriptional activation of hormone responses

Two branches of defence signalling (Figure 2.3) rely on SA on the one hand, and JA/ET on the other (Glazebrook, 2005). SA-dependent signalling was traditionally associated with defence against biotrophic pathogens and the JA/ET-dependent pathways with necrotrophic pathogens, but this appears to be specific to only *Arabidopsis* (AbuQamar et al., 2017; Bari and Jones, 2009). The crosstalk between ET, JA, SA and ABA is interpreted to fine-tune the immune response for the appropriate pathogen/pest, be it necrotrophic, biotrophic or herbivorous (Broekgaarden et al., 2015). Elegant models of hormone interactions have been presented for JA-, ET- and ABA cross-talk (Wasternack and Hause, 2013) and for JA-, ET- and SA cross-talk (Broekgaarden et al., 2015). The JA-ET-ABA model illustrates the regulatory mechanisms that dictate a response against herbivorous insects or necrotrophic pathogens, while the JA-ET-SA model explains the molecular machinery that trigger responses by necrotrophic and biotrophic pathogens.

The receptors of the three hormones, namely the jasmonate receptor JASMONATE ZIM-DOMAIN (JAZ; Chini et al., 2007), ethylene receptor ETHYLENE RECEPTOR 1 (ETR1, Bleecker et al., 1988) and salicylic acid receptor NON-EXPRESSOR OF PR1 (NPR1; Shah, 2003) do not directly act as TFs, but rather interact with TFs that modulate gene expression (Figure 2.3, Broekgaarden et al., 2015; Wasternack and Hause, 2013). JAZ functions as a master switch that, in the absence of its ligand, can be bound to ETHYLENE INSENSITIVE3 (EIN3), ETHYLENE INSENSITIVE3-LIKE1 (EIL1) and MYCs, inhibiting their activation of JA/ET and JA/ABA responsive genes. When JA-Ile

binds to JAZ, it triggers the binding of JAZ to CORONATINE INSENSITIVE1 (COI1), which targets the complex for degradation. In the presence of ET, EIN3 and EIL1 in turn inhibit MYC TFs from inducing JA/ABA responsive genes, while simultaneously inducing the expression of JA/ET responsive genes, including ERF1. OCTADECANOID-RESPONSIVE AP2/ERF 59 (ORA59) expression is activated by ERF1, and in turn activates expression of PLANT DEFENSIN 1.2 (PDF1.2).

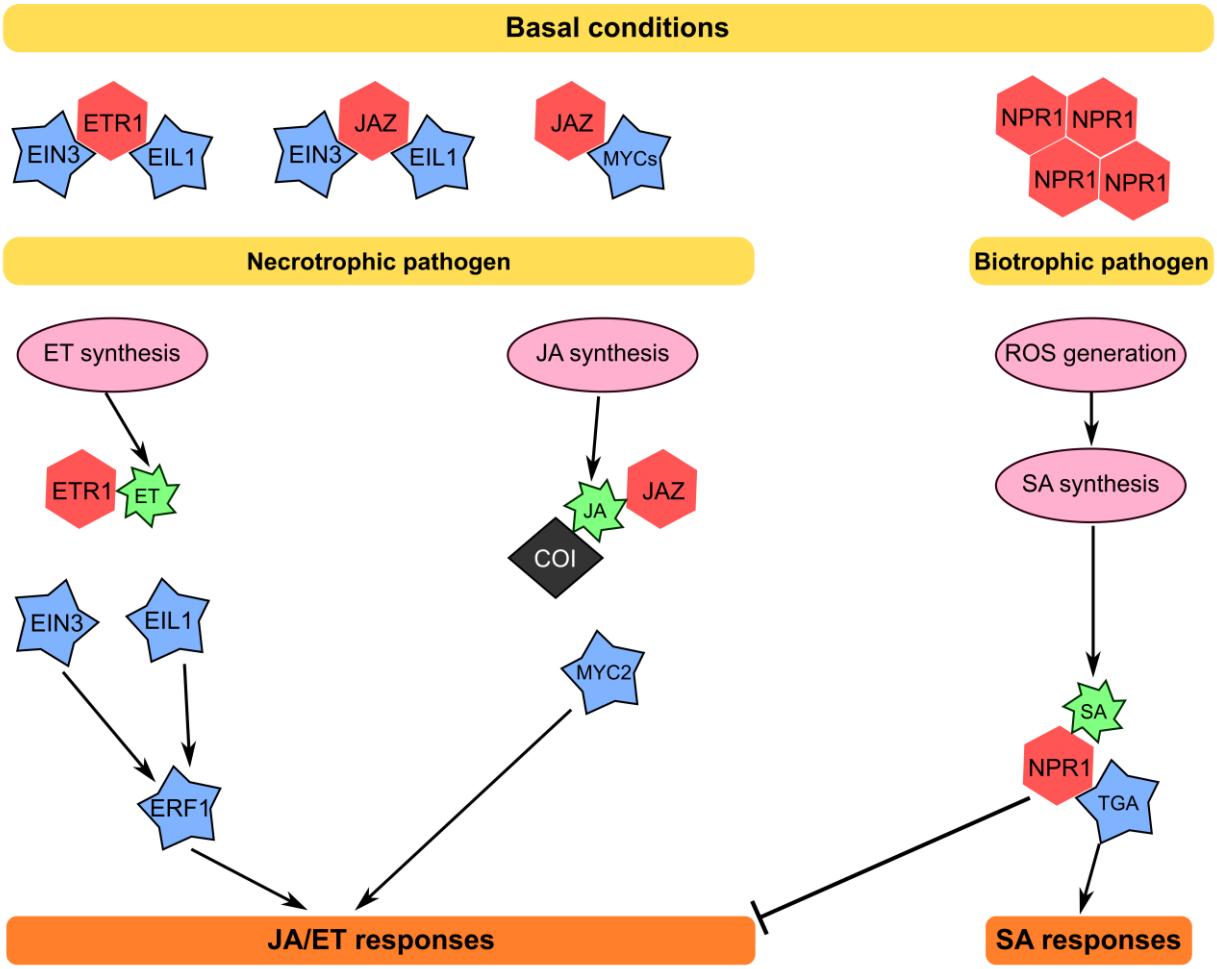

Figure 2.3 Simplified schematic of hormone regulation in response to microbial pathogens from Broekgaarden et al. (2015). Under basal conditions the receptors (hexagons) of ethylene (ET), jasmonoyl-isoleucine (JA) and salicylic acid (SA) are inactive. The ET and JA receptors Ethylene receptor 1 (ETR1) and JA ZIM-domain proteins (JAZ) are bound to transcription factors (TFs; stars), while NON-EXPRESSOR OF PR1 (NPR1) forms an inactive oligomer. Following perception of a necrotrophic pathogen, ET and JA are synthesized and bind to their respective receptors, releasing the bound TFs. JAZ proteins are targeted for degradation by CORONATINE INSENSITIVE 1 (COI1). The TFs Ethylene insensitive 3 (EIN3) and EIN3-like 1 (EIL1) activate transcription of Ethylene Response Factor 1 (ERF1). Myelocytomatosis oncogene 2 (MYC2) and ERF1 activate JA/ET-dependent responses. Perception of a biotrophic pathogen triggers reactive oxygen species (ROS) synthesis, that induces SA synthesis. NPR1-monomers are released and associate with TGACG motif binding factor (TGA) TFs to induce SA-responses that include inhibition of JA/ET-responsive transcription.

During herbivory, the synthesis of ABA leads to the inhibition of ERF1 and ORA59 expression and the activation of MYC-dependent signalling. NPR1-dependent signalling is initiated when SA-induced redox changes induces the de-oligomerisation of NPR1 (Tada et al., 2008), allowing it to bind to SA (Wu et al., 2012), move to the nucleus, associate with a TGACG motif binding factor

(TGA)-element binding protein and activate PR genes (Shah, 2003). This activation is followed by the repression of JA/ET signalling, through degradation and potential transcriptional repression of ORA59. NPR1 induces expression of eight WRKYs linked to stress responses (Wang et al., 2006).

Reactive oxygen species during defence

The early events of defence responses have been extensively studied using systems where elicitors can be homogeneously applied to plant cells (Boller and Felix, 2009). These studies revealed the alkalinisation of the growth medium and protein phosphorylation, including activation of MAPK cascades as early as two minutes after elicitation. Subsequently, an increase in ROS can be observed, signifying an oxidative burst. The oxidative burst is a critical element in the plant's immune response (O'Brien et al., 2012). Two systems are associated with the rapid increase in hydrogen peroxide following pathogen perception, utilising the flavoprotein NADPH oxidase, encoded by respiratory burst oxidase homologs (RBOHs), and heme-containing class III peroxidases (PER). Some plant species require both systems, while others rely on only one. Once generated, ROS act as an intra- and intercellular signal to facilitate the induction of gene expression, cross-linking of cell wall proteins, and organelle re-location (Lamb and Dixon, 1997; O'Brien et al., 2012; Vandenabeele et al., 2003; Wojtaszek, 1997). The most closely associated process to the increase of ROS is, however, the development of the HR, which eventually leads to PCD. Moreover, hydrogen peroxide can be directly toxic to fungal pathogens, and some fungal detoxification mechanisms therefore function as virulence factors (Cessna et al., 2000; Shlezinger et al., 2011b).

2.1.3 Active defence responses

Alongside ROS, several other plant defence responses could also be described as attack strategies. The most effective of these, particularly against necrotrophic pathogens, is likely the synthesis of phytoalexins, antimicrobial secondary metabolites that are newly synthesized after MAMP elicitation (VanEtten et al., 1994), and antimicrobial PR proteins (Ferreira et al., 2007). Phytoalexins and phytoanticipins (phytoalexin-like compounds that are pre-formed but inactive before elicitation) are chemically diverse and can be derived from the phenylpropanoid, isoprenoid, alkaloid or polyketide pathways (Dixon, 2001). PR proteins like chitinases and β-1,3-glucanases target fungal cell walls, while thaumatin-like proteins and osmotins disrupt fungal plasma membranes (Ferreira et al., 2007).

Cell wall reinforcement is perhaps the most clearly defensive of the responses to pathogens and occurs through the combined action of several previously mentioned processes. The phenylpropanoid pathway that can generate phytoalexins also provides the monolignols needed to form lignin and other phenolic compounds, while ROS catalyse the incorporation of monolignols into lignin and cross-linking of cell wall proteins (O'Brien et al., 2012; Weng and Chapple, 2010). Since most phytopathogens need to access the interior of plant cells, they secrete cell wall degrading enzymes (CWDE). Biotrophic pathogens are far more specific in the timing of this secretion than

necrotrophs, since they need to prevent complete maceration of the host tissue (Mendgen and Hahn, 2002). Necrotrophic pathogens, on the other hand, secrete a wide range of CWDE that target, among others, all the main structural components of plant cell walls, namely cellulose, hemicellulose and pectin (Annis and Goodwin, 1997). It is therefore not surprising that plants have developed inhibiting enzymes to counter cell wall degradation (Juge, 2006; Lagaert et al., 2009). The best characterised of these are polygalacturonase-inhibiting proteins (PGIPs), that inhibit pectin-degrading PGs (Kalunke et al., 2015). Another pectin-degrading enzyme, pectate lyase, is not inhibited by a protein, but by epicatechin, a flavonoid secondary metabolite (Lagaert et al., 2009). Xylanases target the main component of hemicellulose and are inhibited by *Triticum aestivum* xylanase inhibitors (TAXIs), xylanase inhibitor proteins (XIPs) and thaumatin-like xylanase inhibitors (TLXIs), while inhibitors for xyloglucan-specific endoglucanases (XEGs) have also been identified (Lagaert et al., 2009).

2.1.4 Induced resistance: Enhancing resistance to pathogens

Despite a plethora of defence mechanisms, many plants are still susceptible to pathogens, in part because the most effective defence mechanisms are only induced following infection, rather than being constitutively active (Heil and Baldwin, 2002). However, activated defence responses carry a fitness penalty in terms of biomass and seed production (Bolton, 2009), explaining why plants do not constitutively activate these mechanisms. In the tissues in contact with or near the infecting pathogen, the cellular system's only priority is to arrest the spread of the infection. The "fitness cost" of defence is explained by the response of primary metabolism following elicitation. The repression of photosynthesis is a near-universal feature of plant immune responses (Bilgin et al., 2010), while carbon skeletons and energy are provided by increased cell wall invertase activity and respiration (Berger et al., 2007; Bolton, 2009). Amino acid metabolism is also harnessed to provide alternate sources of energy, and some plants export nitrogen from the infected tissue to limit nutrient-availability to the pathogen.

Instead of costly constitutive activation, plants have evolved mechanisms that prime their defence machinery to respond more rapidly, or effectively, to the perception of pathogens (Mauch-Mani et al., 2017). Induced resistance (IR), or priming, incorporates systemic resistance that is accomplished by fully active defence, provoking a fitness penalty, or by potentiated defence, that enhances defence without incurring a measurable fitness cost. Defence can be primed to respond faster, earlier, stronger or with greater sensitivity (Figure 2.4; Hilker et al., 2016).

Active induced systemic defence

SAR, the first IR mechanism that was observed (Ross, 1961), is a form of active defence induced throughout the plant after exposure to a necrotising pathogen or MAMP and is effective against secondary challenge by bacterial, fungal and viral pathogens (Durrant and Dong, 2004). Enhanced defence responses were first observed in uninfected leaves of tobacco plants infected with tobacco

mosaic virus (TMV) (Ross, 1961). The observed resistance was not only active against TMV, but also against other viral pathogens. SAR is characterised by the accumulation of PR proteins, particularly the acidic form of PR1 and can be induced by SA and several SA-mimicking compounds (Ryals et al., 1996), but requires the synthesis and systemic transport of pipecolic acid in locally infected tissue to be fully induced (Bernsdorff et al., 2016). Consistent with the energy-intensive nature of active defence, activating a SAR response reduces biomass production (Heil et al., 2000).

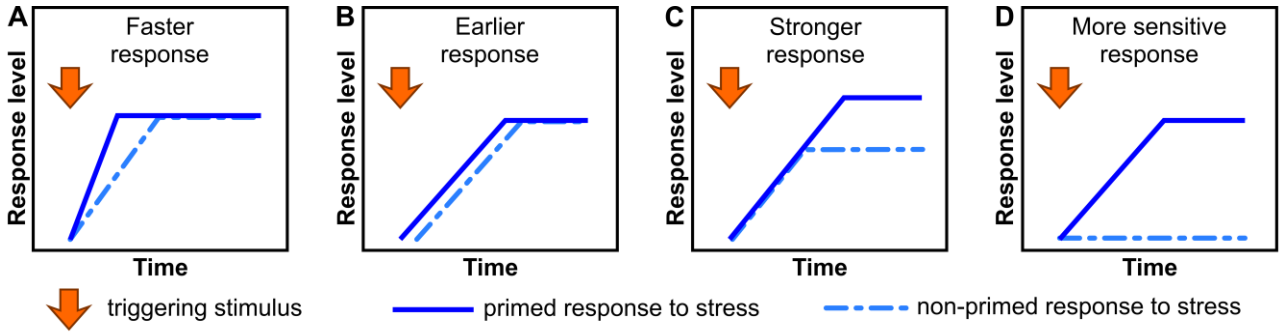

Figure 2.4 Schematic response patterns of primed and non-primed plants to an infection by a pathogenic microorganism (arrow). A prior priming stimulus may alter the velocity (A), onset (B), strength (C) and sensitivity (D) of the response. The responses described by these patterns (e.g. an oxidative burst), will depend on a complex network of signalling and regulatory factors that may be induced or repressed and/or activated or blocked. Figure and legend were adapted from Hilker et al., (2016).

Potentiated induced systemic defence

In addition to SAR, other forms of priming have been identified, that do not fully activate defence responses until they are challenged by a pathogen (Mauch-Mani et al., 2017). Interestingly, the same compounds that induce SAR can also induce potentiated defence when applied at lower concentrations (Conrath, 2009; Wang et al., 2015c). As can be seen by the diversity of priming stimuli listed by Mauch-Mani et al. (2017), primed defence can be induced by different treatments and organisms. Induced systemic resistance (ISR) refers to systemic defence elicited by beneficial microbes, such as plant-growth-promoting rhizobacteria (Van Wees et al., 2008), or plant-growth-promoting fungi. Other elicitors of priming include MAMPs, HAMPs, wounding and mild abiotic stresses.

Priming induces broad spectrum resistance

The specific characteristics of the post-challenge state differ depending on the host-pathogen-priming agent, but are typified by enhanced activation of key defence pathways, including antimicrobial secondary metabolites and PR proteins, cell wall strengthening by callose and lignin deposition, hormone synthesis, ROS accumulation and TFs involved in defence activation (summarised by Mauch-Mani et al. 2017). A common feature of priming is the more rapid repression of photosynthesis (Mathys et al., 2012; Schenk et al., 2014), likely representing a potentiated shift to defence metabolism. In some cases, gene expression can be repressed, as was observed in β-aminobutyric acid (BABA)-primed *Arabidopsis*, that decreased expression of the ROS-scavenging

enzyme ascorbate peroxidase 1 (APX1) following *Plectosphaerella cucumerina* infection (Pastor et al., 2013).

During the priming phase (prior to challenge) and/or the post-challenge state, primed plants generally display transcriptional and metabolic changes across a wide range of potential defence mechanisms (Coolen et al., 2016; Finiti et al., 2014; Mathys et al., 2012; Mauch-Mani et al., 2017). The diversity of mechanisms influenced by priming may explain why a defining feature of priming is proposed to be its broad-spectrum resistance, against necrotrophic and biotrophic fungal and bacterial pathogens and against viral pathogens (Martinez-Medina et al., 2016).

2.1.5 The next level: plant-pathogen interaction

An understanding of the mechanisms that plants use to defend themselves, though an important scientific question on its own, is part of the continued effort to solve the challenges that plant pathogens pose to agriculture (Strange and Scott, 2005). Until relatively recently, in depth study of plant-pathogen interactions was mainly viewed in one component of the pathosystem, since monitoring both plant host and pathogen was logistically difficult and/or expensive. As the overview above attests, this approach has been fruitful in elucidating plant defence components, but since it is clear that plant immune responses and pathogen infection processes are interdependent (Dodds and Rathjen, 2010; Stahl and Bishop, 2000), interaction studies are becoming the new “state of the art” in plant-pathogen studies. The advent of high-throughput sequencing technologies, coupled with genome sequencing and annotation of important crop plants and pathogens, has facilitated the growth in this area since it is possible, in a single sequencing run, to analyse all extracted transcripts whatever their origin. As more of these datasets become available, analysing the interplay of plant- and pathogen-responses will further our understanding of how these processes affect one another.

2.2 Plant defence against *Botrytis cinerea*

The genus *Botrytis* represents a collection of at least 30 pathogen species that cause disease of a range of cultivated species (Fillinger and Elad, 2016). Although most *Botrytis* species have a limited host range, one notable exception is *B. cinerea*, causing disease on at least 1400 plant species, representing 586 genera. In addition, *B. cinerea* is successful over a wide geographic range and also causes disease on economically important crop species, including staple and fruit crops, trees and ornamental plants. *B. cinerea* is a necrotrophic fungus, producing macerating enzymes and a range of toxins that lead to host invasion and cell death on its hosts respectively (Amselem et al., 2011; Blanco-Ulate et al., 2014; Frías et al., 2011; Rossi et al., 2011; Zhang et al., 2015). Research on *B. cinerea* in general, and specifically the infection mechanisms and virulence factors of this important pathogen, has been aided by the publication of genome sequences of various *B. cinerea* strains (Amselem et al., 2011; Blanco-Ulate et al., 2013a; Staats and Van Kan, 2012; Van Kan et al., 2017) as well as the availability of characterised mutants (botbioger.versailles.inra.fr/botmut/).

Though *B. cinerea* is in itself an interesting organism to study, its necrotrophic lifestyle and broad host range has led to its use as challenger in many studies into plant defence (Mbengue et al., 2016).

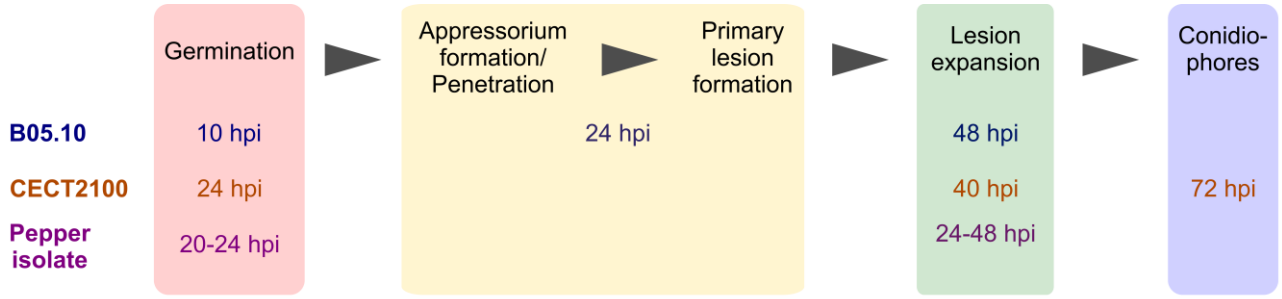

Figure 2.5 Timing of infection progress on wild-type *A. thaliana* with three strains of *B. cinerea*. Infection progression of strains B05.10 (Stefanato et al., 2009) and CECT2100 (Birkenbihl et al., 2012) were followed on whole plants, disease progression from an isolate from pepper (*Capsicum annuum*) was on detached leaves (Windram et al., 2012). *B. cinerea* infection stages were sourced from Van Kan (2006).

In addition to analysing the host responses to infection, the infection process of *B. cinerea* has been established as generally the same on multiple hosts (Eizner et al., 2017; Van Kan, 2006), but the timing of these processes is somewhat variable, and depends on the plant host organ and the *B. cinerea* strain. In *Arabidopsis*, timing of conidial attachment and germination, primary lesion formation and lesion expansion varied depending on the strains used (Figure 2.5; AbuQamar et al., 2006; Birkenbihl et al., 2012; Stefanato et al., 2009; Windram et al., 2012). A detailed examination of infection progression of *B. cinerea* strain B05.10 on *Arabidopsis*, bean and pea leaves showed that the timing of initial events was similar on all three hosts (Shlezinger et al., 2011b). B05.10 induces primary lesion formation after 24 h in *Arabidopsis* leaf during whole plant infection (Stefanato et al., 2009), but only after 48 h in *Vitis vinifera* berries (Kelloniemi et al., 2015). The disease progression is also delayed on detached leaves, because the wound response activates defence mechanisms prior to inoculation (Eizner et al., 2017).

The recent development of a continuous monitoring system (Eizner et al., 2017) has refined the initial events of lesion formation and expansion, characterising four stages of lesion development and expansion. During the “early stage”, small lesions develop within the inoculation spot and eventually coalesce. The “break stage” represents the point where the lesion extends past the inoculation spot and is followed by an “intermediate phase” where the lesion expands at an increasing rate, before the “late stage” where lesion expansion is constant. This system has not yet been used to study disease development on *Arabidopsis*, or with strains other than B05.10, but analysis on bean and *N. benthamiana* revealed quantitative differences between hosts (Eizner et al., 2017).

2.2.1 *B. cinerea* both overcomes and takes advantage of plant defence mechanisms

Initial studies of plant-pathogen interactions described biotrophic pathogens as master manipulators of plant defence mechanisms, while necrotrophic pathogens employed a “brute force” approach (Doehlemann et al., 2017). However, as research progressed, it became clear that necrotrophic

pathogens utilise common plant defence mechanisms, like the HR and PCD to their advantage. *B. cinerea* is a classic example of this, and secretes a battery of effector proteins and toxins that induce necrosis in the host tissue (Frías et al., 2011, 2016; Rossi et al., 2011; Zhang et al., 2015), or activate inappropriate SA signalling pathways that antagonises JA signalling (El Oirdi et al., 2011). Furthermore, *B. cinerea* sRNA suppress expression of target genes involved in cell wall modification, oxidative stress response and several branches of defence signalling, including MAPKs and RKs (Wang et al., 2017; Weiberg et al., 2013).

A classic example of *B. cinerea* "hijacking" plant defence was first described in *Arabidopsis*, where it induces HR (Govrin and Levine, 2000), in part by producing NADPH oxidases to generate ROS (Segmüller et al., 2008). However, this approach comes at a cost, since the burst of hydrogen peroxide that induces cell death in the host also affects the pathogen, which experiences PCD in the early stages of infection (Shlezinger et al., 2011a). BACULOVIRUS INHIBITOR OF APOPTOSIS REPEAT PROTEIN 1 (BIR1) is an anti-apoptotic protein that enables the fungus to survive the initial stage of plant HR-induced PCD (Shlezinger et al., 2011b). Integrating the high-resolution lesion monitoring data (Eizner et al., 2017) with the PCD survival model proposed by Shlezinger et al. (2011b) then suggests that the "early stage" involves the secretion of necrosis-inducing effectors that cause small lesions to form and coalesce as plant cells and the majority of fungal hyphae initiate PCD. The BIR1-dependent anti-apoptotic mechanism protects isolated fungal cells, that proliferate during the "break" and "intermediate" stages. The necrotic tissue protects the viable cells that continue to secrete PCD-inducing factors during lesion expansion. The ability of *B. cinerea* to survive PCD can be overwhelmed, provided the oxidative burst is early enough and strong enough to ensure that the anti-apoptotic mechanisms cannot compensate (Bindschedler et al., 2006; Małolepsza, 2005; Wang et al., 2015b), but in most cases, resistance to *B. cinerea* is associated with other defence mechanisms.

2.2.2 Gene expression studies of host-*Botrytis* interactions

To achieve successful plant defence against *B. cinerea*, many studies have aimed to identify which defence mechanisms plants activate, how they are regulated, and which mechanisms are associated with resistance or susceptibility. Transgenic or mutant plants have been useful in elucidating important aspects of defence and have revealed that functional JA signalling is key for resistance in *Arabidopsis* (Méndez-Bravo et al., 2011; Thomma et al., 1998) and tomato (Diaz et al., 2002; Mehari et al., 2015; Vicedo et al., 2009) and is important in regulating diurnal changes in resistance/susceptibility (Ingle et al., 2015), while SA signalling occasionally functions in induced resistance (Segarra et al., 2013). Ethylene perception has also been reported to play an important role (Diaz et al., 2002). Fungitoxic metabolites and enzymes play a central role in resistance against *B. cinerea*, with resistance associated with increased phytoalexin levels (Aziz et al., 2006), as well as chitinase and β-1,3-glucanase activity (Aziz et al., 2006; Carstens et al., 2003; Zheng et al., 2011)

being observed in multiple hosts. The use of gene expression analysis (Table 2.1) has provided confirmation of these aspects and has been used to identify more mechanisms used by hosts in response to *B. cinerea*.

Table 2.1 Summary of studies where gene expression analysis was performed on *B. cinerea* infected plant tissue.

Treatment	Host	Focus	Reference
Stilbene synthase gene	Nta	Phytoalexins	Hain et al. (1993)
ASCORBATE OXIDASE GENE	Nta	Apoplast ascorbate redox state	Fotopoulos et al. (2006)
ABA-deficient mutant	Sly	ROS, cell wall cross-linking	Asselbergh et al. (2007)
***S.pimpinellifolium* MYB transgene**	Nta	Functional characterisation of SpMYB	Liu et al. (2016)
Resistant cultivar	Pla	Global response	Gong et al. (2015)
Wild species	Sld	Global response	Smith et al. (2014)
WRKY33 MUTANT	Ata	Global response: ABA role examined	Liu et al. (2015a)
JA, ET, SA mutants	Ata	Global response: signalling networks	AbuQamar et al. (2006)
Ethylene	Sly	Importance of ethylene sensitivity	Diaz et al. (2002)
SPERMIDINE SYNTHASE GENE	Sly	Importance of ethylene synthesis	Nambeesan et al. (2012)
Hexanoic acid	Ata	JA-dependence	Kravchuk et al. (2011)
Inoculation time (day/NIGHT)	Ata	JA-dependence	Ingle et al. (2015)
Low red/far-red ratio	Ata	JA-dependence	Cerrudo et al. (2012)
B. CINEREA EXOPOLYSACCHARIDE	Sly	SA/JA antagonism by pathogen	El Oirdi et al. (2011)
β-aminobutyric acid	Ata	SA-dependence (not JA/ET)	Zimmerli et al. (2001)
GLOMUS INTRARADICES	Nta	Susceptibility in mycorrhizal plants	Shaul et al. (1999)
Oligogalacturonides	Ata	Hormone signalling not required	Ferrari et al. (2007)
Oligogalacturonides	Ata	Oxidative burst not required	Galletti et al. (2008)
Oligogalacturonides/ *Aspergillus niger PG* gene	Ata/ Nta	Decreased auxin sensitivity	Ferrari et al. (2008)
Oligogalacturonides	Vvi	Oxidative burst and protein kinase role	Aziz et al. (2004)
Electrostated water	Sly	Priming – Active IR	Imada et al. (2015)
Hexanoic acid	Sly	Priming – Active/Potentiated IR	Finiti et al. (2014)
Oligandrin	Sly	Priming – Active/Potentiated IR	Lou et al. (2011)
Oligandrin/ *Pythium oligandrum*	Vvi	Priming – Active/Potentiated IR	Mohamed et al. (2007)
Bacillus amyloliquefaciens	Bna	Priming – Potentiated IR	Sarosh et al. (2009)
***Micromonospora* strains**	Sly	Priming – Potentiated IR	Martínez-Hidalgo et al. (2015)
Pseudomonas fluorescens	Vvi	Priming – Potentiated IR	Gruau et al. (2015)
***Trichoderma hamatum* T382**	Ata	Priming – Potentiated IR	Mathys et al. (2012)

Treatments in **bold** induced resistance, in SMALL CAPS induced susceptibility. Abbreviations: Ata, *Arabidopsis thaliana*; Bna, *Brassica napus*; Lsa, *Lacucta sativa*; Nta, *Nicotiana tabacum*; Pla, *Paeonia lactiflora*; Sld, *Solanum lycopersicoides*; Sly, *Solanum lycopersicum*; Vvi, *Vitis vinifera*.

By far the most common focus in host-*Botrytis* studies has been the role of hormones. The first transcriptomic study of a host-*B. cinerea* interaction was performed on *Arabidopsis* wild-type and mutants in JA, SA and ET responses (AbuQamar et al., 2006) and highlighted the importance of functional JA and ET signalling in the response to *B. cinerea*. These mutants were also used to better understand the role of hormones in the resistance-response induced by OGs (Ferrari et al., 2007). The sophistication of *B. cinerea* infection strategies was emphasised when it was found to antagonise the JA/ET branch of defence signalling by secreting an exopolysaccharide that activated the SA branch (El Oirdi et al., 2011). Several treatments induce resistance to *B. cinerea* and act though JA-mediated signalling, including BABA (Zimmerli et al., 2001), hexanoic acid (Finiti et al., 2014; Kravchuk et al., 2011) and non-pathogenic soil bacteria (Martínez-Hidalgo et al., 2015; Sarosh

et al., 2009), although SA is occasionally associated with resistance (Agudelo-Romero et al., 2015; Imada et al., 2015).

In addition to hormone regulation, the responses of ROS in host-*B. cinerea* interactions are often found to be important in resistant/susceptible phenotypes. Their importance is such that transcriptomic studies almost always report on the enzymes that generate and detoxify ROS (Blanco-Ulate et al., 2015; De Cremer et al., 2013; Finiti et al., 2014; Gong et al., 2015; Kelloniemi et al., 2015; Kong et al., 2015). Resistance to *B. cinerea* is generally associated with enhanced detoxification of ROS (Finiti et al., 2014; Fotopoulos et al., 2006; Liu et al., 2016), but occasionally enhanced ROS production is observed in resistant plants, most commonly associated with enhanced cell wall strengthening or defence signalling (Asselbergh et al., 2007; Galletti et al., 2008). Besides a reinforced cell wall, accumulation of secondary metabolites is commonly associated with response to *B. cinerea*.

Intriguingly, *B. cinerea* induces anthocyanin formation in white grapes during noble rot, along with several other ripening-related parameters (Blanco-Ulate et al., 2015), while anthocyanin accumulation is associated with ISR in *Arabidopsis* (Mathys et al., 2012). Reduced phytoalexin accumulation (Liu et al., 2015a) is associated with susceptibility, whereas enhanced activation of secondary metabolism, particularly phytoalexin accumulation, is typically associated with resistance (Ferrari et al., 2007; Gong et al., 2015; Gruau et al., 2015; Hain et al., 1993; Mathys et al., 2012; Wang et al., 2009). In addition to fungitoxic metabolites, several fungitoxic PR proteins are associated with resistance. The importance of PR proteins, and other defence genes, has been confirmed using gene expression studies. Susceptibility is induced when PR protein expression is supressed (Shaul et al., 1999), while resistance is associated with accelerated induction or higher expression of defence genes (Finiti et al., 2014; Gong et al., 2015; Lou et al., 2011; Smith et al., 2014; Wang et al., 2009).

The emergence of large-scale gene expression profiling technologies emphasised the massive scope of gene expression during pathogen interactions (Table 2.2), sparking interest in the “reprogramming” of metabolism and the TFs and other mechanisms that regulate gene expression. The role of WRKY33 has been extensively studied (Birkenbihl et al., 2012; Liu et al., 2015a), but transcriptional profiling has provided datasets to mine for co-regulating genes and the TFs that affect key defence mechanisms (AbuQamar et al., 2006; Liu et al., 2016; Villegas-Fernández et al., 2014; Windram et al., 2012). Other studies have aimed to profile sRNA, that are believed to play a role in the host-*B. cinerea* interaction (Jin et al., 2012; Zhao et al., 2015) and *B. cinerea* sRNAs have been identified that silence plant defence genes (Weiberg et al., 2013). The effect of drought- and insect herbivory-reprogrammed metabolism on transcriptional responses to *B. cinerea* has also recently been explored (Coolen et al., 2016).

Table 2.2 Transcriptome studies analysing response to *B. cinerea*.

Host	Strain	Samples	Citation
Arabidopsis thaliana	B05.10	24, 48h	Mathys et al. (2012)
		72h	Sela et al. (2013)
		3, 6, 12, 24, 48h	Wang et al. (2015b)
		6, 12, 18,24h	Coolen et al. (2016)
	CECT2100	14h	Birkenbihl et al. (2012)
		14h	Liu et al. (2015a)
	Pepper	12, 24h	Mulema and Denby (2012)
		18, 24h	Ingle et al. (2015)
	Unspecified	24, 36, 60h	AbuQamar et al. (2006)
		72h	Segarra et al. (2013)
		18h	Sham et al. (2014)
	Pepper	2h intervals – detached leaf	Windram et al. (2012)
Cucumber leaf	B05.10	96h	Kong et al. (2015)
Grape berries (detached)	B05.10	24, 48h (véraison stage)	Kelloniemi et al. (2015)
	B05.10	24, 48h (mature stage)	
Grape berries	DW1	Three stages of disease severity at same harvest date (field study)	Blanco-Ulate et al. (2015)
Grape berries	Grape isolate	Green, véraison – field study	Agudelo-Romero et al. (2015)
Herbaceous peony	Peony isolate	Three stages of disease severity progression in resistant and susceptible cultivars	Gong et al. (2015)
		Combined above stages per cultivar	Zhao et al. (2015)
Lettuce	B05.10	12, 24, 48h	De Cremer et al. (2013)
Medicago truncatula	CA-06	48h	Villegas-Fernández et al. (2014)
Solanum lycopersicoides	B05.10	24, 48h	Smith et al. (2014)
Tomato fruit	B05.10	24h (mature green stage)	Cantu et al. (2009)
		24h (red ripe stage)	
		24h (mature green stage)	Blanco-Ulate et al. (2013b)
		24h (red ripe stage)	
Tomato leaf	B05.10	Time not specified	Vega et al. (2015)
	CECT2100	24h	Finiti et al. (2014)
	R16	8h	Asselbergh et al. (2007)
	Unspecified	7 days	Jin et al. (2012)

2.2.3 Insights from transcriptomic studies of model hosts

The development of high-throughput RNA sequencing (RNA-Seq) technologies has led to an increase of gene expression analyses of *B. cinerea*-infected tissues in many plants, especially those without an assembled and annotated genome sequence (e.g. De Cremer et al., 2013; Kong et al., 2015; Smith et al., 2014). While these resources are useful, and can be mined more efficiently when genome annotations become available, (genetically) well-characterised plant hosts provide more detailed information. For this reason, this review will focus on the model plant *Arabidopsis*, as a typical example of *B. cinerea* infection on leaf tissue, whereas *Vitis vinifera* (grapevine) will be used as an example for fruit (berry) infections, as well as an economically important host for *B. cinerea*. The seminal work on tomato fruit will be compared with what has been reported in grapevine berries. This review utilised gene ontology (GO) enrichments presented by the cited papers, since this

facilitates cross-comparison of analyses performed using different platforms (e.g. different microarray designs and/or RNA sequencing on difference species). For a more exact comparison, meta-analysis of gene expression data, as was performed by Sham et al. (2014) for *Arabidopsis*, would minimise differences due to changes in GO annotation.

A. thaliana leaf – *B. cinerea* interaction

As mentioned above, the timing of *B. cinerea* infection processes differs depending on the host and strain used. To construct a timeline of transcriptomic responses to infection, we therefore use the pathosystem where a whole plant infection assay was performed on *Arabidopsis* using *B. cinerea* strain B05.10 (Figure 2.6), as reported by Coolen et al. (2016) and Mathys et al. (2012). These studies used GO enrichment to describe the response and overlapped at a single time point (24 h). A third of the GO categories reported by Mathys et al. (2012) showed an opposite response at this time point, highlighting that even with the same host and strain some variability in response occurs, depending on other parameters of the pathosystem. When excluding the ambiguous terms, the general response of *Arabidopsis* to B05.10 was revealed. The oxidative burst was induced during the earliest stage of infection (6-24 h), but not during the lesion expansion phase, while defence response, HR, chitinase activity, ethylene and salicylic acid responses and jasmonate and lignin biosynthesis were induced at 48 h as well. Camalexin biosynthesis and toxin catabolism were delayed by six and twelve hours respectively, and the characteristic repression of photosynthesis coincided with primary lesion formation. Considering the work of Shlezinger et al. (2011b), it is likely that the massive reprogramming of metabolism occurs during the time the majority of fungal hyphae have experienced PCD, but, in wild-type *Arabidopsis* (ecotype Columbia), these changes are not sufficient to halt the pathogen expansion.

In other hosts infected with the B05.10 strain, these processes are likely conserved, but the less comprehensively annotated genomes of lettuce (De Cremer et al., 2013) and cucumber (Kong et al., 2015) limit the amount of GO terms that can be assessed. Challenges of *Arabidopsis* with another *B. cinerea* strain (Mulema and Denby, 2012; Windram et al., 2012) highlighted the induction of toxin catabolism, response to jasmonate and ethylene and repression of photosynthesis as typical features, independent of the challenging strain. When *Arabidopsis* plants are maintained at high humidity, *B. cinerea* can complete its infection, as evidenced by the emergence of conidiophores, within 3 days (Birkenbihl et al., 2012). In field conditions, these favourable conditions (extremely high spore load combined with 100% relative humidity) are rarely, if ever, seen and *B. cinerea* infections progress much more slowly. Despite this difference, the typical features of the response were largely conserved in *Paeonia lactiflora* (herbaceous peony, Gong et al., 2015).

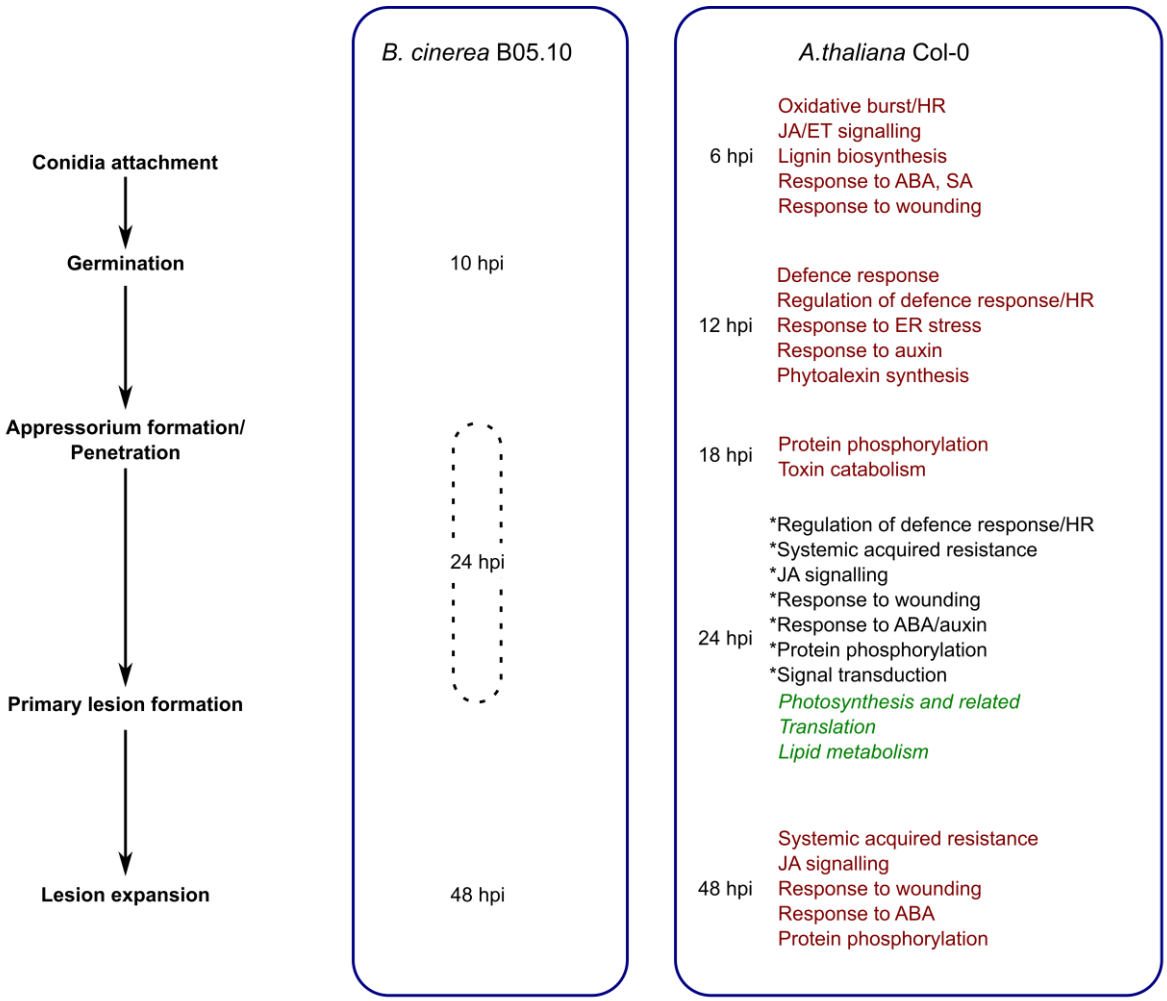

Figure 2.6 The interaction of *A. thaliana* and *B. cinerea* strain B05.10 - time course of infection progress (Stefanato et al., 2009) and transcriptomic responses (Coolen et al., 2016; Mathys et al., 2012). Red text: induced; green italicised text: repressed; *divergent responses: induced in Mathys et al. (2012), repressed in Coolen et al. (2016). *B. cinerea* Infection stages were sourced from Van Kan (2006). The dotted line indicates that the indicated time occurred between two distinct stages. Abbreviations: ABA, abscisic acid; ER, endoplasmic reticulum; ET, ethylene; HR, hypersensitive response; JA, jasmonate; SA, salicylic acid.

V. vinifera berry – *B. cinerea* interaction

B. cinerea is somewhat unique among phytopathogens, since the same strain can cause unwanted grey mould rot and desirable noble rot on grapevine, depending on microclimatic conditions (Fournier et al., 2013). While grey mould rot reduces yield and wine quality, noble rotted grapes are used to make high-value sweet wines. The transcriptomes and metabolomes of *B. cinerea* and Sémillon grapes was recently profiled in noble rotted grapes (Blanco-Ulate et al., 2015), and the same approach was used to study the development of grey mould rot in Marselan berries (Figure 2.7, Kelloniemi et al., 2015). The two analysis methods neatly complemented one another, and revealed that the infection program of *B. cinerea* relies on the same key processes during noble and grey mould rot, namely release of CWDE and toxins and activation of ROS synthesis and detoxification. During noble rot infection however, *B. cinerea* induced additional detoxification mechanisms, including laccases and multi-drug resistance transporters, activated autophagy-related mechanisms (that likely act to counter PCD) and released isochorismatases that may inactivate SA-dependent signalling in the hosts (Blanco-Ulate et al., 2015). Berries experiencing noble rot activated many

defence mechanisms, including the HR, JA/ET signalling and JA synthesis, and glutathione S-transferases (GSTs), thought to act as detoxification agents (Blanco-Ulate et al., 2015). They also induced expression of PRRs and *Resistance*-genes (*R*-genes), MAPKs and WRKY transcription factors. Many of these were observed in infected Trincadeira berries as well, but since Kelloniemi et al. (2015) used microarray analysis and Blanco-Ulate et al. (2015) used RNA-Seq, the “missing” features may simply have remained undetected.

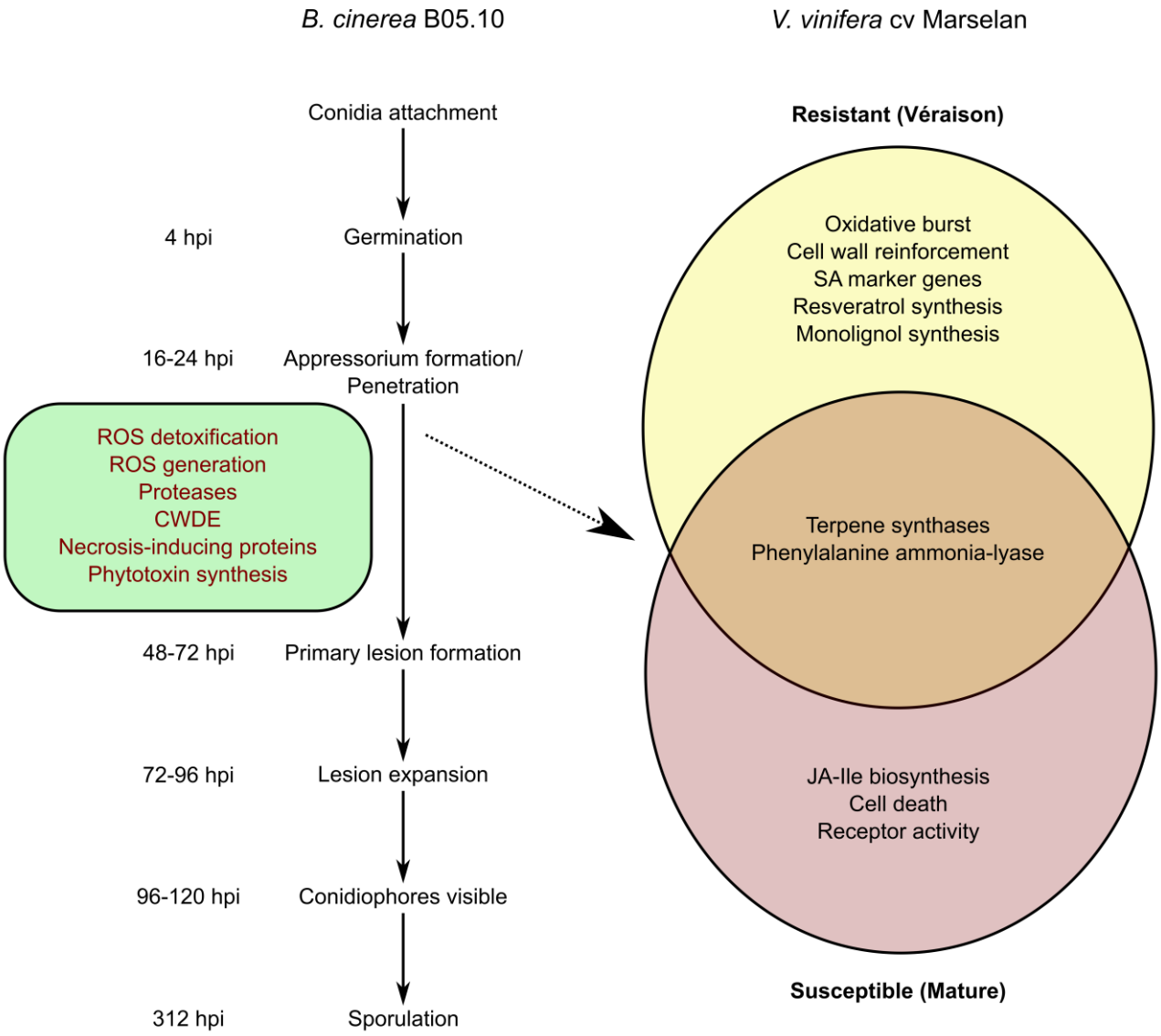

Figure 2.7 Transcriptomic study of resistant (véraison) and susceptible (mature) *V. vinifera* berries cv Marselan inoculated with *B. cinerea* strain B05.10 (Kelloniemi et al., 2015) - time course of infection progress on mature grape berries (MB), induced processes of *B. cinerea* on MB (green) and of véraison (yellow) and mature (red) berries during infection. *B. cinerea* infection stages were sourced from Van Kan (2006). Abbreviations: CWDE, cell wall degrading enzymes; JA-Ile, jasmonoyl-isoleucine; ROS, reactive oxygen species; SA, salicylic acid.

In general, grape berries are resistant to *B. cinerea* grey mould rot until véraison, subsequently becoming more susceptible as the berries mature (Deytieux-Belleau et al., 2009). Intriguingly, grape berries from the Trincadeira cultivar, however, were susceptible to a grapevine isolate of *B. cinerea* even before véraison (Figure 2.8; Agudelo-Romero et al., 2015), while berries from the Marselan cultivar were resistant at véraison (Figure 2.7; Kelloniemi et al., 2015) suggesting that the host cultivar can influence the outcome of the interaction. These experiments were conducted with different *B. cinerea* strains, and one (Agudelo-Romero et al., 2015) was field-based using intact plants, while the other used detached berries under controlled conditions (Kelloniemi et al., 2015). Some interesting contrasts could be observed on the transcriptomic level between these two studies: Resistance appeared to be linked to SA-mediated defence pathways in Marselan, while susceptibility was associated with JA and/or ET-mediated defence pathways in mature Marselan, as well as in green and véraison Trincadeira berries. This somewhat unexpected connection between SA-mediated defence pathways and resistance to *B. cinerea* has also been reported in *Arabidopsis* (Benedetti et al., 2015), and further muddles the delineation of SA- and JA/ET-mediated defences as primary regulation for biotrophic and necrotrophic pathogens respectively.

Fruit ripening and *B. cinerea*

Just as different plant species have unique transcriptional responses to *B. cinerea* infection, so too do tissues at different developmental stages. In fruit, increased ripeness generally coincides with increased susceptibility to infection (Cantu et al., 2009; Kelloniemi et al., 2015), and *B. cinerea* has been shown to in fact activate/enhance ripening mechanisms to facilitate infection (Blanco-Ulate et al., 2015; Cantu et al., 2009). The role of fruit developmental stage on the transcriptional response to *B. cinerea* has been reported in tomato (Blanco-Ulate et al., 2013b; Cantu et al., 2009) and *V. vinifera* berries (Agudelo-Romero et al., 2015; Kelloniemi et al., 2015). The most common approach to studying the influence of ripeness on infection is to use fruit detached from the plant at a specific developmental stage (Blanco-Ulate et al., 2013b; Cantu et al., 2009; Kelloniemi et al., 2015). Comparing expression profiles of infected mature green (MG) and red ripe (RR) tomatoes, revealed that resistant MG fruit reduced expression of TGA transcription factors involved in SA signalling, ET biosynthesis via ACO, JA biosynthesis via AOS and ABA signalling (Blanco-Ulate et al., 2013b; Cantu et al., 2009). MAPK activation was induced, while antimicrobial compound biosynthesis via hydroxycinnamoyl-CoA:tyramine N-(hydroxy-cinnamoyl) transferases and DES was more strongly induced in MG than in RR. Susceptible RR fruit, in contrast, induced ET synthesis, SA signalling, ABA synthesis and signalling, while having higher basal expression of several PR proteins.

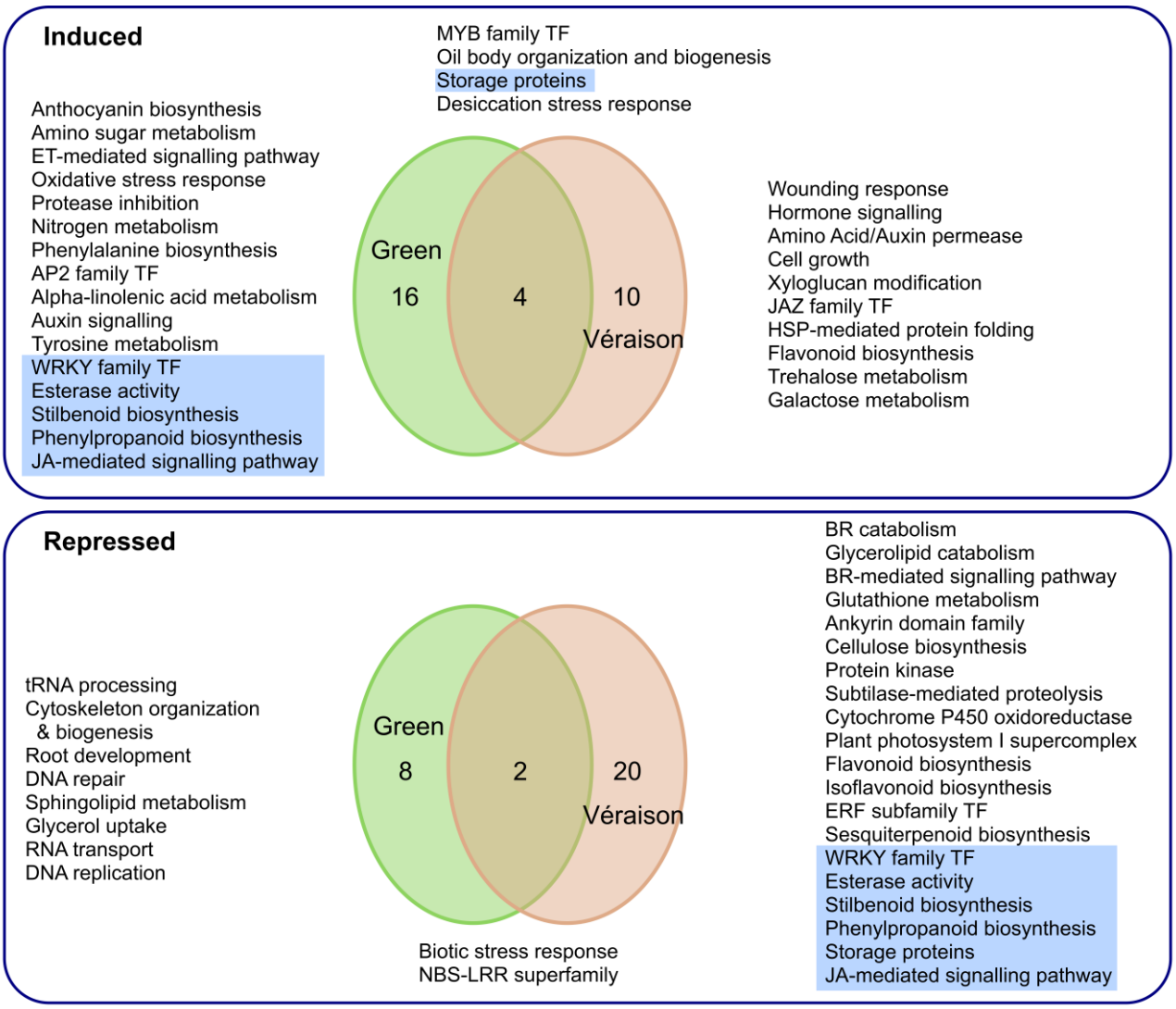

Figure 2.8 The analysis of the transcriptional interaction of *V. vinifera* cv Trincadeira infected by a *B. cinerea* strain isolated from grapevine (Agudelo-Romero et al. 2015). The infection progress in the field was analysed at two berry developmental stages. Both stages were susceptible to infection. Functional enrichment of the genes, was compared for induced and repressed genes. To emphasise the effect of developmental stages, terms that are counter-regulated in the two stages are highlighted in blue. Abbreviations: AP2, APETALA2; BR, brassinosteroid; ERF, ethylene response factor; ET, ethylene; HSP, heat shock protein; JA, jasmonate; JAZ, jasmonate ZIM-domain; MYB, myeloblastosis transcription factor; NBS-LRR, nucleotide-binding site-leucine-rich repeat; TF, transcription factor.

It is perhaps not surprising that the characteristics of ripening-induced susceptibility of grape berries differ from those of tomato, given that tomato fruits are climacteric and grape berries non-climacteric. The similarities between them are the association with increased JA-Ile levels in susceptible ripe fruit, and cell wall strengthening in resistant unripe fruit (Blanco-Ulate et al., 2013b; Kelloniemi et al., 2015). In véraison berries (VB) that are resistant to *B. cinerea* infection, several extracellular anti-microbial PR proteins were induced, along with PGIP and extensins (Kelloniemi et al., 2015). VB displayed enhanced induction of stilbene synthase (STS) and PAL, accelerated accumulation of ROS and higher basal SA levels. Susceptible mature berries (MB) showed delayed terpene synthase induction, and induced JA biosynthesis, cysteine-rich receptor kinases and extracellular laccase and peroxidase.

2.2.4 Induced resistance against *B. cinerea*

Engineering effective resistance to *B. cinerea* has increasingly turned to priming as a viable alternative to application of costly fungicides. Though many instances of priming to *B. cinerea* have been reported, few reports have investigated the mechanisms of the observed resistance. These mechanisms vary, but a common feature is enhanced antioxidant levels in primed tissues (Finiti et al., 2014; Małolepsza and Urbanek, 2000; Mathys et al., 2012; Pane et al., 2011). Higher levels of WRKY TFs have been reported, which may enable an accelerated response following infection (Finiti et al., 2014; Mathys et al., 2012). Hexanoic acid-induced resistance of tomato to *B. cinerea* additionally potentiated oxylipin and ethylene synthesis (Finiti et al., 2014). Application of *Trichoderma hamatum* T382, a biocontrol fungus, to *Arabidopsis* roots induced a systemic response that was similar to a *B. cinerea* induced defence response, but without the repression of photosynthesis and growth that usually accompanies an active defence response (Mathys et al., 2012). *T. hamatum*-induced ISR potentiated JA synthesis and responses, including a wound response. The phenylpropanoid branch of secondary metabolism was enhanced instead of camalexin synthesis and many of the *B. cinerea* induced defence responses were suppressed during infection. Interestingly, SA inducible genes were induced prior to infection before being repressed, while JA-regulated genes were transiently induced before being repressed. At the time of writing, transcriptome studies of tomato and *Arabidopsis* primed with other agents had not been reported. Comparing the mechanisms of different priming agents would likely give further insight into the varied tactics plants employ to induce resistance against *B. cinerea*.

2.2.5 The future of *B. cinerea* interaction studies

Multiple “omics” technologies would provide a more comprehensive view

Transcriptome analyses provide a snapshot of the transcriptional control mechanism used by living cells to respond to stimuli, however, other control mechanisms cannot be ignored (Östlund and Sonnhammer, 2012). For this reason, many transcriptomic studies reviewed here included corroborating analyses of the key processes identified. The use of mutants has been especially helpful in confirming the roles of plant hormones and TFs (AbuQamar et al., 2006; Asselbergh et al., 2007; Birkenbihl et al., 2012; Blanco-Ulate et al., 2013b; Cantu et al., 2009; Dobón et al., 2015; Ingle et al., 2015; Liu et al., 2015a; Mathys et al., 2012). Histochemical analysis of ROS and targeted metabolite quantification have been used to bolster conclusions drawn from gene expression data (Asselbergh et al., 2007; Cantu et al., 2009; Finiti et al., 2014; Kelloniemi et al., 2015; Mathys et al., 2012). However, in order to provide additional dimensions to transcriptomic data, untargeted metabolite and protein profiling techniques need to be employed (AbuQamar et al., 2016). Studies integrating transcriptomic and metabolomic analyses are rare, though transcript and metabolite profiling has been performed during *B. cinerea* infection in tomato leaves (Camañes et al., 2015; Finiti et al., 2014) and grape berries (Agudelo-Romero et al., 2015). Parallel profiling of transcripts

and proteins has not been reported for *B. cinerea* infected tissues, however, proteomic studies have been reported from grape berry cell cultures (Dadakova et al., 2015) and ripening tomato (Shah et al., 2012). Since profiling of metabolites and proteins is more challenging than transcript profiling, it may be some time before multi-omics approaches are commonplace, but they promise to provide rich sources of information. Transcriptomic analyses too have the potential to provide deeper insights into control mechanisms, since we now know that some non-coding RNAs, such as microRNA (miRNA), also play an important role in modulating defence responses. Few studies have been reported to date, but miRNA profiles during infection of tomato leaf (Jin et al., 2012) and *P. lactiflora* (Zhao et al., 2015) have been determined using microarray and RNA-Seq respectively.

Observing the interaction between host and pathogen

The interaction between *B. cinerea* and its hosts, once considered to be somewhat primitive compared to the highly specific interactions of biotrophs, has since been revealed to be far more complex than previously thought (Fillinger and Elad, 2016; Van Kan, 2006). Parallel analyses of host and *B. cinerea* transcriptomes have recently been reported (Blanco-Ulate et al., 2015; Kelloniemi et al., 2015; Kong et al., 2015; Smith et al., 2014). These studies have largely confirmed what previous analyses have reported, but it is particularly interesting to compare *B. cinerea* gene expression on resistant and susceptible hosts. The new continuous monitoring system developed by Eizner et al. (2017) could provide a valuable tool to refine our understanding of disease progression. The importance of the oxidative burst, as well as host and pathogen PCD in susceptibility/virulence is also well established (Govrin and Levine, 2000; Segmüller et al., 2008; Shlezinger et al., 2011b). With respect to ROS, two contrasting resistance mechanisms have been observed, with some mechanisms involving alleviation of oxidative stress (Finiti et al., 2014; Fotopoulos et al., 2006; Liu et al., 2016), while others display enhanced ROS accumulation (Asselbergh et al., 2007; Galletti et al., 2008). Employing the Bcbir1 mutant to study these phenotypes in greater detail may shed some light on the function of elevated ROS, which has been linked to cell wall modification, rather than PCD (Asselbergh et al., 2007; Kelloniemi et al. 2015). This link was built on parallel analysis of host and *B. cinerea* gene expression and histochemistry of infected tissues, further highlighting the advantages of employing multiple layers of analysis.

Facilitating cross-comparison

The *Arabidopsis-P. syringae* pathosystem is arguably the most comprehensively used pathosystem. A cursory examination of the publications reporting the use of this pathosystem reveals that two pathovars (maculicola ES4326 and tomato DC3000) are typically used and infected tissues are mostly collected two or three days post infection. This standardisation of the pathosystem greatly facilitates comparison of phenotypes, gene functions and many other investigated aspects. In contrast, in the publications reporting transcriptomic changes of *Arabidopsis* following *B. cinerea* infection (Table 2.5), three specified isolates and five unspecified isolates were used, with differing

timing in infection progress (Figure 2.5). The sequenced B05.10 strain is, however, by far the most reported strain. In other host species, the isolates and harvest time points are even more diverse. For example, tomato microRNA profiling was performed seven days after infection by an unspecified isolate of *B. cinerea* (Jin et al. 2012). To facilitate a similar level of cross-comparison to that possible in the *Arabidopsis-P. syringae* pathosystem, it would be of great benefit to define a basic model pathosystem with regards to the infection stage analysed, perhaps by determining the lesion development stages described by Eizner et al. (2017) for common hosts and *B. cinerea* strains. Since *B. cinerea* is a pathogen of many fruit crops, it would be very useful to also establish such basic pathosystems for fruit crops such as tomato and grapevine. Transcriptomic analyses of plant tissues infected with *B. cinerea* have revealed the complexity of the response of plant and pathogen in this life-or-death interaction. As sequencing technologies become more affordable, and genome annotation progresses, we have a great opportunity to tease apart the mechanisms used by plant and pathogen during their interactions.

2.3 Literature cited

AbuQamar SF, Moustafa K, Tran L-SP (2016). “Omics” and plant responses to *Botrytis cinerea*. *Front Plant Sci* 7, 1658. doi:10.3389/fpls.2016.01658.

AbuQamar S, Chen X, Dhawan R, Bluhm B, Salmeron J, Lam S, Dietrich RA, Mengiste T (2006). Expression profiling and mutant analysis reveals complex regulatory networks involved in Arabidopsis response to *Botrytis* infection. *Plant J* 48, 28–44. doi:10.1111/j.1365-313X.2006.02849.x.

AbuQamar S, Moustafa K, Tran L-SP (2017). Mechanisms and strategies of plant defense against *Botrytis cinerea*. *Crit Rev Biotechnol* 37, 262–274. doi:10.1080/07388551.2016.1271767.

Ade J, DeYoung BJ, Golstein C, Innes RW (2007). Indirect activation of a plant nucleotide binding site-leucine-rich repeat protein by a bacterial protease. *PNAS* 104, 2531–2536. doi:10.1073/pnas.0608779104.

Agudelo-Romero P, Erban A, Rego C, Carbonell-Bejerano P, Nascimento T, Sousa L, Martínez-Zapater JM, Kopka J, Fortes AM (2015). Transcriptome and metabolome reprogramming in *Vitis vinifera* cv. Trincadeira berries upon infection with *Botrytis cinerea*. *J Exp Bot* 66, 1769–1785. doi:10.1093/jxb/eru517.

Alvarez ME (2000). Salicylic acid in the machinery of hypersensitive cell death and disease resistance. *Plant Mol Biol* 44, 429–442.

Ambawat S, Sharma P, Yadav NR, Yadav RC (2013). MYB transcription factor genes as regulators for plant responses: An overview. *Physiol Mol Biol Plants* 19, 307–321. doi:10.1007/s12298-013-0179-1.

Amselem J, Cuomo CA, Van Kan JAL, Viaud M, Benito EP, Couloux A, Coutinho PM, De Vries RP, Dyer PS, Fillinger S, Gout L, Hahn M, Kohn L, Lapalu N, Plummer KM, Sharon A, Simon A, Ten Have A, Que E, et al. (2011). Genomic analysis of the necrotrophic fungal pathogens *Sclerotinia sclerotiorum* and *Botrytis cinerea*. *PLoS Genet* 7, e1002230. doi:10.1371/journal.pgen.1002230.

Annis SL, Goodwin PH (1997). Recent advances in the molecular genetics of plant cell wall-degrading enzymes produced by plant pathogenic fungi. *Eur J Plant Pathol* 103, 1–14.

Asai S, Ohta K, Yoshioka H (2008). MAPK signaling regulates nitric oxide and NADPH oxidase-dependent oxidative bursts in Nicotiana benthamiana. *Plant Cell* 20, 1390–1406. doi:10.1105/tpc.107.055855.

Asai S, Shirasu K (2015). Plant cells under siege: Plant immune system versus pathogen effectors. *Curr Opin Plant Biol* 28, 1–8. doi:10.1016/j.pbi.2015.08.008.

Asselbergh B, Curvers K, França SC, Audenaert K, Vuylsteke M, Van Breusegem F, Höfte M (2007). Resistance to *Botrytis cinerea* in *sitiens*, an abscisic acid-deficient tomato mutant, involves timely production of hydrogen peroxide and cell wall modifications in the epidermis. *Plant Physiol* 144, 1863–1877. doi:10.1104/pp.107.099226.

Aziz A, Poinssot B, Daire X, Adrian M, Bézier A, Lambert B, Joubert J-M, Pugin A (2003). Laminarin elicits defense responses in grapevine and induces protection against *Botrytis cinerea* and *Plasmopara viticola*. *Mol Plant-Microbe Interact* 16, 1118–1128. doi:10.1094/MPMI.2003.16.12.1118.

Aziz A, Trotel-Aziz P, Dhuicq L, Jeandet P, Couderchet M, Vernet G (2006). Chitosan oligomers and copper sulfate induce grapevine defense reactions and resistance to gray mold and downy mildew. *Phytopathogens* 96, 1188–1194. doi:10.1094/PHYTO-96-1188.

Bailey B (1995). Purification of a protein from culture filtrates of *Fusarium oxysporum* that induces ethylene and necrosis in leaves of *Erythroxylum coca*. *Phytopathology* 85, 1250. doi:10.1094/Phyto-85-1250.

Bari R, Jones JDG (2009). Role of plant hormones in plant defence responses. *Plant Mol Biol* 69, 473–488. doi:10.1007/s11103-008-9435-0.

Benedetti M, Pontiggia D, Raggi S, Cheng Z, Scaloni F, Ferrari S, Ausubel FM, Cervone F, De Lorenzo G (2015). Plant immunity triggered by engineered in vivo release of oligogalacturonides, damage-associated molecular patterns. *PNAS* 112, 5533–5538. doi:10.1073/pnas.1504154112.

Bent AF, Mackey D (2007). Elicitors, effectors, and *R* genes: the new paradigm and a lifetime supply of questions. *Annu Rev Phytopathol* 45, 399–436. doi:10.1146/annurev.phyto.45.062806.094427.

Berger S, Sinha AK, Roitsch T (2007). Plant physiology meets phytopathology: plant primary metabolism and plant pathogen interactions. *J Exp Bot* 58, 4019–4026. doi:10.1093/jxb/erm298.

Bernsdorff F, Doering A-C, Gruner K, Schuck S, Bräutigam A, Zeier J (2016). Pipecolic acid orchestrates plant systemic acquired resistance and defense priming via salicylic acid-dependent and independent pathways. *Plant Cell* 28, 102–129. doi:10.1105/tpc.15.00496.

Bilgin DD, Zavala JA, Zhu J, Clough SJ, Ort DR, DeLucia EH (2010). Biotic stress globally downregulates photosynthesis genes. *Plant, Cell Environ* 33, 1597–1613. doi:10.1111/j.1365-3040.2010.02167.x.

Bindschedler L V, Dewdney J, Blee KA, Stone JM, Asai T, Plotnikov J, Denoux C, Hayes T, Gerrish C, Davies DR, Ausubel FM, Bolwell GP (2006). Peroxidase-dependent apoplastic oxidative burst in Arabidopsis required for pathogen resistance. *Plant J* 47, 851–863. doi:10.1111/j.1365-313X.2006.02837.x.

Birkenbihl RP, Diezel C, Somssich IE (2012). Arabidopsis WRKY33 is a key transcriptional regulator of hormonal and metabolic responses toward *Botrytis cinerea* infection. *Plant Physiol* 159, 266–285. doi:10.1104/pp.111.192641.

Blanco-Ulate B, Allen G, Powell ALT, Cantu D (2013a). Draft genome sequence of *Botrytis cinerea* BcDW1, inoculum for noble rot of grape berries. *Genome Announc* 1, e00252-13. doi:10.1128/genomeA.00252-13.Copyright.

Blanco-Ulate B, Amrine KCH, Collins TS, Rivero RM, Vicente AR, Morales-Cruz A, Doyle CL, Ye Z, Allen G, Heymann H, Ebeler SE, Cantu D (2015). Developmental and metabolic plasticity of white-skinned grape berries in response to *Botrytis cinerea* during noble rot. *Plant Physiol* 169, 2422–2443. doi:10.1104/pp.15.00852.

Blanco-Ulate B, Morales-Cruz A, Amrine KCH, Labavitch JM, Powell ALT, Cantu D (2014). Genome-wide transcriptional profiling of *Botrytis cinerea* genes targeting plant cell walls during infections of different hosts. *Front Plant Sci* 5, 435. doi:10.3389/fpls.2014.00435.

Blanco-Ulate B, Vincenti E, Powell ALT, Cantu D (2013b). Tomato transcriptome and mutant analyses suggest a role for plant stress hormones in the interaction between fruit and *Botrytis cinerea*. *Front Plant Sci* 4, 142. doi:10.3389/fpls.2013.00142.

Bleecker AB, Estelle MA, Somerville C, Kende H (1988). Insensitivity to ethylene conferred by a dominant mutation in *Arabidopsis thaliana*. *Science* 241, 1086–1089.

Bodenhausen N, Reymond P (2007). Signaling pathways controlling induced resistance to insect herbivores in *Arabidopsis*. *Mol Plant-Microbe Interact* 20, 1406–1420. doi:10.1094.

Boller T, Felix G (2009). A renaissance of elicitors: Perception of microbe-associated molecular patterns and danger signals by pattern-recognition receptors. *Annu Rev Plant Biol* 60, 379–406. doi:10.1146/annurev.arplant.57.032905.105346.

Bolton MD (2009). Primary metabolism and plant defense--fuel for the fire. *Mol Plant-Microbe Interact* 22, 487–497. doi:10.1094/MPMI-22-5-0487.

Boter M, Ruíz-Rivero O, Abdeen A, Prat S (2004). Conserved MYC transcription factors play a key role in jasmonate signaling both in tomato and *Arabidopsis*. *Genes Dev* 18, 1577–1591. doi:10.1101/gad.297704.

Broekgaarden C, Caarls L, Vos IA, Pieterse CMJ, Van Wees SCM (2015). Ethylene: traffic controller on hormonal crossroads to defense. *Plant Physiol* 169, 2371–2379. doi:10.1104/pp.15.01020.

Brutus A, Sicilia F, Macone A, Cervone F, De Lorenzo G (2010). A domain swap approach reveals a role of the plant wall-associated kinase 1 (WAK1) as a receptor of oligogalacturonides. *PNAS* 107, 9452–9457. doi:10.1073/pnas.1000675107.

Bulgarelli D, Biselli C, Collins NC, Consonni G, Stanca AM, Schulze-Lefert P, Valè G (2010). The CC-NB-LRR-Type RDG2a resistance gene confers immunity to the seed-borne barley leaf stripe pathogen in the absence of hypersensitive cell death. *PLoS ONE* 5, e12599. doi:10.1371/journal.pone.0012599.

Camañes G, Scalschi L, Vicedo B, González-Bosch C, García-Agustín P (2015). An untargeted global metabolomic analysis reveals the biochemical changes underlying basal resistance and priming in *Solanum lycopersicum*, and identifies 1-methyltryptophan as a metabolite involved in plant responses to *Botrytis cinerea* and . *Plant J* 84, 125–139. doi:10.1111/tpj.12964.

Cantu D, Blanco-Ulate B, Yang L, Labavitch JM, Bennett AB, Powell ALT (2009). Ripening-regulated susceptibility of tomato fruit to *Botrytis cinerea* requires *NOR* but not *RIN* or ethylene. *Plant Physiol* 150, 1434–1449. doi:10.1104/pp.109.138701.

Carstens M, Vivier MA, Pretorius IS (2003). The *Saccharomyces cerevisiae* chitinase, encoded by the *CTS1-2* gene, confers antifungal activity against *Botrytis cinerea* to transgenic tobacco. *Transgenic Res* 12, 497–508. doi:10.1023/A:1024220023057.

Cerrudo I, Keller MM, Cargnel MD, Demkura P V, De Wit M, Patitucci MS, Pierik R, Pieterse CMJ, Ballaré CL (2012). Low red/far-red ratios reduce Arabidopsis resistance to *Botrytis cinerea* and jasmonate responses via a COI1-JAZ10-dependent, salicylic acid-independent mechanism. *Plant Physiol* 158, 2042–2052. doi:10.1104/pp.112.193359.

Césari S, Kanzaki H, Fujiwara T, Bernoux M, Chalvon V, Kawano Y, Shimamoto K, Dodds P, Terauchi R, Kroj T (2014). The NB-LRR proteins RGA4 and RGA5 interact functionally and physically to confer disease resistance. *EMBO J* 33, 1941–1959. doi:10.15252/embj.201487923.

Cessna SG, Sears VE, Dickman MB, Low PS (2000). Oxalic acid, a pathogenicity factor for *Sclerotinia sclerotiorum*, suppresses the oxidative burst of the host plant. *Plant Cell* 12, 2191–2200. doi:10.1105/tpc.12.11.2191.

Chini A, Fonseca S, Fernández G, Adie B, Chico JM, Lorenzo O, García-Casado G, López-Vidriero I, Lozano FM, Ponce MR, Micol JL, Solano R (2007). The JAZ family of repressors is the missing link in jasmonate signalling. *Nature* 448, 666–671. doi:10.1038/nature06006.

Chisholm ST, Coaker G, Day B, Staskawicz BJ (2006). Host-microbe interactions: shaping the evolution of the plant immune response. *Cell* 124, 803–814. doi:10.1016/j.cell.2006.02.008.

Choi HW, Klessig DF (2016). DAMPs, MAMPs, and NAMPs in plant innate immunity. *BMC Plant Biol* 16, 232. doi:10.1186/s12870-016-0921-2.

Choi J, Tanaka K, Cao Y, Qi Y, Qiu J, Liang Y, Lee SY, Stacey G (2014). Identification of a plant receptor for extracellular ATP. *Science* 343, 290–294. doi:10.1126/science.343.6168.290.

Chong J, Piron MC, Meyer S, Merdinoglu D, Bertsch C, Mestre P (2014). The SWEET family of sugar transporters in grapevine: VvSWEET4 is involved in the interaction with *Botrytis cinerea*. *J Exp Bot* 65, 6589–6601. doi:10.1093/jxb/eru375.

Conrath U (2009). Priming of induced plant defense responses. *Adv Bot Res* 51, 361–395. doi:10.1016/S0065-2296(09)51009-9.

Coolen S, Proietti S, Hickman R, Davila Olivas NH, Huang PP, Van Verk MC, Van Pelt JA, Wittenberg AHJ, De Vos M, Prins M, Van Loon JJA, Aarts MGM, Dicke M, Pieterse CMJ, Van Wees SCM (2016). Transcriptome dynamics of Arabidopsis during sequential biotic and abiotic stresses. *Plant J* 86, 249–267. doi:10.1111/tpj.13167.

Cui H, Tsuda K, Parker JE (2015). Effector-triggered immunity: from pathogen perception to robust defense. *Annu Rev Plant Biol* 66, 487–511. doi:10.1146/annurev-arplant-050213-040012.

Dadakova K, Havelkova M, Kurkova B, Tlolkova I, Kasparovsky T, Zdrahal Z, Lochman J (2015). Proteome and transcript analysis of *Vitis vinifera* cell cultures subjected to *Botrytis cinerea* infection. *J Proteomics* 119, 143–153. doi:10.1016/j.jprot.2015.02.001.

De Cremer K, Mathys J, Vos C, Froenicke L, Michelmore RW, Cammue BPA, De Coninck B (2013). RNAseq-based transcriptome analysis of *Lactuca sativa* infected by the fungal necrotroph *Botrytis cinerea*. *Plant, Cell Environ* 36, 1992–2007. doi:10.1111/pce.12106.

De Lorenzo G, Brutus A, Savatin DV, Sicilia F, Cervone F (2011). Engineering plant resistance by constructing chimeric receptors that recognize damage-associated molecular patterns (DAMPs). *FEBS Lett* 585, 1521–1528. doi:10.1016/j.febslet.2011.04.043.

De Waard MA, Georgopoulos SG, Hollomon DW, Ishii H, Leroux P, Ragsdale NN, Schwinn FJ (1993). Chemical control of plant diseases: problems and prospects. *Annu Rev Phytopathol* 31, 403–421. doi:10.1146/annurev.py.31.090193.002155.

Dean R, Van Kan JAL, Pretorius ZA, Hammond-Kosack KE, Di Pietro A, Spanu PD, Rudd JJ, Dickman M, Kahmann R, Ellis J, Foster GD (2012). The Top 10 fungal pathogens in molecular plant pathology. *Mol Plant Pathol* 13, 414–430. doi:10.1111/j.1364-3703.2011.00783.x.

Deytieux-Belleau C, Geny L, Roudet J, Mayet V, Donèche B, Fermaud M (2009). Grape berry skin features related to ontogenic resistance to *Botrytis cinerea*. *Eur J Plant Pathol* 125, 551–563. doi:10.1007/s10658-009-9503-6.

Diaz J, Ten Have A, Van Kan JAL (2002). The role of ethylene and wound signalling in resistance of tomato to *Botrytis cinerea*. *Plant Physiol* 129, 1341–1351. doi:10.1104/pp.001453.1.

Dixon RA (2001). Natural products and plant disease resistance. *Nature* 411, 843–847. doi:10.1038/35081178.

Dobón A, Canet JV, García-Andrade J, Angulo C, Neumetzler L, Persson S, Vera P (2015). Novel disease susceptibility factors for fungal necrotrophic pathogens in Arabidopsis. *PLoS Pathog* 11, e1004800. doi:10.1371/journal.ppat.1004800.

Dodds PN, Rathjen JP (2010). Plant immunity: towards an integrated view of plant–pathogen interactions. *Nat Rev* 11, 539–548. doi:10.1038/nrg2812.

Doehlemann G, Ökmen B, Zhu W, Sharon A (2017). Plant pathogenic fungi. *Microbiol Spectr* 5, 75–90. doi:10.1128/microbiolspec.FUNK-0023-2016.

Dong J, Chen C, Chen Z (2003). Expression profiles of the *Arabidopsis* WRKY gene superfamily during plant defense response. *Plant Mol Biol* 51, 21–37. doi:10.1023/A:1020780022549.

D'Ovidio R, Mattei B, Roberti S, Bellincampi D (2004). Polygalacturonases, polygalacturonase-inhibiting proteins and pectic oligomers in plant-pathogen interactions. *Biochim Biophys Acta* 1696, 237–244. doi:10.1016/j.bbapap.2003.08.012.

Durrant WE, Dong X (2004). Systemic acquired resistance. *Annu Rev Phytopathol* 42, 185–209. doi:10.1146/annurev.phyto.42.040803.140421.

Eckardt NA (2002). Plant disease susceptibility genes? *Plant Cell* 14, 1983–1986. doi:10.1105/tpc.140910.

Eizner E, Ronen M, Gur Y, Gavish A, Zhu W, Sharon A (2017). Characterization of *Botrytis*-plant interactions using PathTrack© - an automated system for dynamic analysis of disease development. *Mol Plant Pathol* 18, 503–512. doi:10.1111/mpp.12410.

El Oirdi M, El Rahman TA, Rigano L, El Hadrami A, Rodriguez MC, Daayf F, Vojnov A, Bouarab K (2011). *Botrytis cinerea* manipulates the antagonistic effects between immune pathways to promote disease development in tomato. *Plant Cell* 23, 2405–2421. doi:10.1105/tpc.111.083394.

Fammartino A, Cardinale F, Göbel C, Mène-Saffrané L, Fournier J, Feussner I, Esquerré-Tugayé M-T (2007). Characterization of a divinyl ether biosynthetic pathway specifically associated with pathogenesis in tobacco. *Plant Physiol* 143, 378–388. doi:10.1104/pp.106.087304.

Faulkner C, Petutschnig E, Benitez-Alfonso Y, Beck M, Robatzek S, Lipka V, Maule AJ (2013). LYM2-dependent chitin perception limits molecular flux via plasmodesmata. *PNAS* 110, 9166–9170. doi:10.1073/pnas.1203458110.

Fernández-Calvo P, Chini A, Fernández-Barbero G, Chico J-M, Gimenez-Ibanez S, Geerinck J, Eeckhout D, Schweizer F, Godoy M, Franco-Zorrilla JM, Pauwels L, Witters E, Puga MI, Paz-Ares J, Goossens A, Reymond P, De Jaeger G, Solano R (2011). The *Arabidopsis* bHLH transcription factors MYC3 and MYC4 are targets of JAZ repressors and act additively with MYC2 in the activation of jasmonate responses. *Plant Cell* 23, 701–715. doi:10.1105/tpc.110.080788.

Ferrari S, Galletti R, Denoux C, De Lorenzo G, Ausubel FM, Dewdney J (2007). Resistance to *Botrytis cinerea* induced in *Arabidopsis* by elicitors is independent of salicylic acid, ethylene, or jasmonate signaling but requires *PHYTOALEXIN DEFICIENT3*. *Plant Physiol* 144, 367–379. doi:10.1104/pp.107.095596.

Ferrari S, Galletti R, Pontiggia D, Manfredini C, Lionetti V, Bellincampi D, Cervone F, De Lorenzo G (2008). Transgenic expression of a fungal endo-polygalacturonase increases plant resistance to pathogens and reduces auxin sensitivity. *Plant Physiol* 146, 669–681. doi:10.1104/pp.107.109686.

Ferreira RB, Monteiro SS, Freitas R, Santos CN, Chen Z, Batista LM, Duarte J, Borges AF, Teixeira AR (2007). The role of plant defence proteins in fungal pathogenesis. *Mol Plant Pathol* 8, 677–700. doi:10.1111/J.1364-3703.2007.00419.X.

Fillinger S, Elad Y (2016). Botrytis – *the Fungus, the Pathogen and its Management in Agricultural Systems*. Switzerland: Springer International Publishing doi:10.1007/978-3-319-23371-0.

Finiti I, De La O Leyva M, Vicedo B, Gómez-Pastor R, López-Cruz J, García-Agustín P, Real MD, González-Bosch C (2014). Hexanoic acid protects tomato plants against *Botrytis cinerea* by priming defence responses and reducing oxidative stress. *Mol Plant Pathol* 15, 550–562. doi:10.1111/mpp.12112.

Fonseca S, Chini A, Hamberg M, Adie B, Porzel A, Kramell R, Miersch O, Wasternack C, Solano R (2009). (+)-7-iso-Jasmonoyl-L-isoleucine is the endogenous bioactive jasmonate. *Nat Chem Biol* 5, 344–350. doi:10.1038/nchembio.161.

Fotopoulos V, Sanmartin M, Kanellis AK (2006). Effect of ascorbate oxidase over-expression on ascorbate recycling gene expression in response to agents imposing oxidative stress. *J Exp Bot* 57, 3933–3943. doi:10.1093/jxb/erl147.

Fournier E, Gladieux P, Giraud T (2013). The "Dr Jekyll and Mr Hyde fungus": Noble rot versus gray mold symptoms of *Botrytis cinerea* on grapes. *Evol Appl* 6, 960–969. doi:10.1111/eva.12079.

Frías M, González C, Brito N (2011). BcSpl1, a cerato-platanin family protein, contributes to *Botrytis cinerea* virulence and elicits the hypersensitive response in the host. *New Phytol* 192, 483–495. doi:10.1111/j.1469-8137.2011.03802.x.

Frías M, González M, González C, Brito N (2016). BcIEB1, a *Botrytis cinerea* secreted protein, elicits a defense response in plants. *Plant Sci* 250, 115–124. doi:10.1016/j.plantsci.2016.06.009.

Galletti R, Denoux C, Gambetta S, Dewdney J, Ausubel FM, De Lorenzo G, Ferrari S (2008). The AtrbohD-mediated oxidative burst elicited by oligogalacturonides in Arabidopsis is dispensable for the activation of defense responses effective against *Botrytis cinerea*. *Plant Physiol* 148, 1695–1706. doi:10.1104/pp.108.127845.

Gao Y, Jia S, Wang C, Wang F, Wang F, Zhao K (2016). BjMYB1, a transcription factor implicated in plant defence through activating *BjCHI1* chitinase expression by binding to a W-box-like element. *J Exp Bot* 67, 4647–4658. doi:10.1093/jxb/erw240.

Gijzen M, Nürnberger T (2006). Nep1-like proteins from plant pathogens: Recruitment and diversification of the NPP1 domain across taxa. *Phytochemistry* 67, 1800–1807. doi:10.1016/j.phytochem.2005.12.008.

Glazebrook J (2005). Contrasting mechanisms of defense against biotrophic and necrotrophic pathogens. *Annu Rev Phytopathol* 43, 205–227. doi:10.1146/annurev.phyto.43.040204.135923.

Gómez-Gómez L, Boller T (2002). Flagellin perception: a paradigm for innate immunity. *Trends Plant Sci* 7, 251–256.

Gong S, Hao Z, Meng J, Liu D, Wei M, Tao J (2015). Digital gene expression analysis to screen disease resistance-relevant genes from leaves of herbaceous peony (*Paeonia lactiflora* Pall.) infected by *Botrytis cinerea*. *PLoS ONE* 10, e0133305. doi:10.1371/journal.pone.0133305.

Govrin EM, Levine A (2000). The hypersensitive response facilitates plant infection by the necrotrophic pathogen *Botrytis cinerea*. *Curr Biol* 10, 751–757. doi:10.1016/S0960-9822(00)00560-1.

Granado J, Felix G, Boller T (1995). Perception of fungal sterols in plants. *Plant Physiol* 107, 485–490.

Gruau C, Trotel-Aziz P, Villaume S, Rabenoelina F, Clément C, Baillieul F, Aziz A (2015). *Pseudomonas fluorescens* PTA-CT2 triggers local and systemic immune response against *Botrytis cinerea* in grapevine. *Mol Plant-Microbe Interact* 28, 1117–1129. doi:10.1094/MPMI-04-15-0092-R.

Hain R, Reif H-J, Krause E, Langebartels R, Kindl H, Vornam B, Wiese W, Schmelzer E, Schreier PH, Stöcker RH, Stenzel K (1993). Disease resistance results from foreign phytoalexin expression in a novel plant. *Nature* 361, 153–156. doi:10.1038/361153a0.

Hatmi S, Trotel-Aziz P, Villaume S, Couderchet M, Clément C, Aziz A (2014). Osmotic stress-induced polyamine oxidation mediates defence responses and reduces stress-enhanced grapevine susceptibility to *Botrytis cinerea*. *J Exp Bot* 65, 75–88. doi:10.1093/jxb/ert351.

Heil M, Baldwin IT (2002). Fitness costs of induced resistance: Emerging experimental support for a slippery concept. *Trends Plant Sci* 7, 61–67. doi:10.1016/S1360-1385(01)02186-0.

Heil M, Hilpert A, Kaiser W, Linsenmair KE (2000). Reduced growth and seed set following chemical induction of pathogen defence: Does systemic acquired resistance (SAR) incur allocation costs? *J Ecol* 88, 645–654. doi:10.1046/j.1365-2745.2000.00479.x.

Hilker M, Schwachtje J, Baier M, Balazadeh S, Bäurle I, Geiselhardt S, Hincha DK, Kunze R, Mueller-Roeber B, Rillig MC, Rolff J, Romeis T, Schmülling T, Steppuhn A, Van Dongen J, Whitcomb SJ, Wurst S, Zuther E, Kopka J (2016). Priming and memory of stress responses in organisms lacking a nervous system. *Biol Rev* 91, 1118–1133. doi:10.1111/brv.12215.

Horbach R, Navarro-Quesada AR, Knogge W, Deising HB (2011). When and how to kill a plant cell: Infection strategies of plant pathogenic fungi. *J Plant Physiol* 168, 51–62. doi:10.1016/j.jplph.2010.06.014.

Imada K, Tanaka S, Masuda Y, Maekawa T, Ito S-I (2015). Induction of disease resistance against *Botrytis cinerea* in tomato (*Solanum lycopersicum* L.) by using electrostatic atomized water particles. *Physiol Mol Plant Pathol* 89, 1–7. doi:10.1016/j.pmpp.2014.11.001.

Ingle RA, Stoker C, Stone W, Adams N, Smith R, Grant M, Carré I, Roden LC, Denby KJ (2015). Jasmonate signalling drives time-of-day differences in susceptibility of Arabidopsis to the fungal pathogen *Botrytis cinerea*. *Plant J* 84, 937–948. doi:10.1111/tpj.13050.

Jin W, Wu F, Xiao L, Liang G, Zhen Y, Guo Z, Guo A (2012). Microarray-based analysis of tomato miRNA regulated by *Botrytis cinerea*. *J Plant Growth Regul* 31, 38–46. doi:10.1007/s00344-011-9217-9.

Jones JDG, Dangl JL (2006). The plant immune system. *Nature* 444, 323–329. doi:10.1038/nature05286.

Juge N (2006). Plant protein inhibitors of cell wall degrading enzymes. *Trends Plant Sci* 11, 359–367. doi:10.1016/j.tplants.2006.05.006.

Kalunke RM, Tundo S, Benedetti M, Cervone F, De Lorenzo G, D'Ovidio R (2015). An update on polygalacturonase-inhibiting protein (PGIP), a leucine-rich repeat protein that protects crop plants against pathogens. *Front Plant Sci* 6, 146. doi:10.3389/fpls.2015.00146.

Katagiri F (2004). A global view of defense gene expression regulation--a highly interconnected signaling network. *Curr Opin Plant Biol* 7, 506–511. doi:10.1016/j.pbi.2004.07.013.

Kelloniemi J, Trouvelot S, Héloir M-C, Simon A, Dalmais B, Frettinger P, Cimerman A, Fermaud M, Roudet J, Baulande S, Bruel C, Choquer M, Couvelard L, Duthiew M, Ferrarini A, Flors V, Le Pêcheur P, Loisel E, Morgant G, et al. (2015). Analysis of the molecular dialogue between gray mould (*Botrytis cinerea*) and grapevine (*Vitis vinifera*) reveals a clear shift in defense mechanisms during berry ripening. *Mol Plant-Microbe Interact* 28, 1167–1180. doi:10.1094/MPMI-02-15-0039-R.

Kende H (1993). Ethylene biosynthesis. *Annu Rev Plant Physiol Plant Mol Biol* 44, 283–307. doi:10.1146/annurev.arplant.44.1.283.

Kim MG, Da Cunha L, McFall AJ, Belkhadir Y, DebRoy S, Dangl JL, Mackey D (2005). Two *Pseudomonas syringae* type III effectors inhibit RIN4-regulated basal defense in *Arabidopsis*. *Cell* 121, 749–759. doi:10.1016/j.cell.2005.03.025.

Knogge W (1996). Fungal infection of plants. *Plant Cell* 8, 1711–1722. doi:10.1105/tpc.8.10.1711.

Kong W, Chen N, Liu T, Zhu J, Wang J, He X, Jin Y (2015). Large-scale transcriptome analysis of cucumber and *Botrytis cinerea* during infection. *PLoS ONE* 10, e0142221. doi:10.1371/journal.pone.0142221.

Kravchuk Z, Vicedo B, Flors V, Camañes G, González-Bosch C, García-Agustín P (2011). Priming for JA-dependent defenses using hexanoic acid is an effective mechanism to protect *Arabidopsis* against *B. cinerea*. *J Plant Physiol* 168, 359–366. doi:10.1016/j.jplph.2010.07.028.

Krol E, Mentzel T, Chinchilla D, Boller T, Felix G, Kemmerling B, Postel S, Arents M, Jeworutzki E, Al-Rasheid KAS, Becker D, Hedrich R (2010). Perception of the *Arabidopsis* danger signal peptide 1 involves the pattern recognition receptor *At*PEPR1 and its close homologue *At*PEPR2. *J Biol Chem* 285, 13471–13479. doi:10.1074/jbc.M109.097394.

Kusch S, Panstruga R (2017). *mlo*-based resistance: An apparently universal "weapon" to defeat powdery mildew disease. *Mol Plant-Microbe Interact* 30, 179–189. doi:10.1094/MPMI-12-16-0255-CR.

Lagaert S, Beliën T, Volckaert G (2009). Plant cell walls: Protecting the barrier from degradation by microbial enzymes. *Semin Cell Dev Biol* 20, 1064–1073. doi:10.1016/j.semcdb.2009.05.008.

Lamb CJ, Dixon RA (1997). The oxidative burst in disease resistance. *Annu Rev Plant Physiol Plant Mol Biol* 48, 251–275. doi:10.1146/annurev.arplant.48.1.251.

Liu S, Kracher B, Ziegler J, Birkenbihl RP, Somssich IE (2015a). Negative regulation of ABA signaling by WRKY33 is critical for *Arabidopsis* immunity towards *Botrytis cinerea* 2100. *eLife* 4, e07295. doi:10.7554/eLife.07295.

Liu X, Rockett KS, Kørner CJ, Pajerowska-Mukhtar KM (2015b). Salicylic acid signalling: new insights and prospects at a quarter-century milestone. *Essays Biochem* 58, 101–113. doi:10.1042/bse0580101.

Liu Z, Luan Y, Li J, Yin Y (2016). Expression of a tomato MYB gene in transgenic tobacco increases resistance to *Fusarium oxysporum* and *Botrytis cinerea*. *Eur J Plant Pathol* 144, 607–617. doi:10.1007/s10658-015-0799-0.

Lorenzo O, Chico JM, Sánchez-Serrano JJ, Solano R (2004). *JASMONATE-INSENSITIVE1* encodes a MYC transcription factor essential to discriminate between different jasmonate-regulated defense responses in Arabidopsis. *Plant Cell* 16, 1938–1950. doi:10.1105/tpc.022319.with.

Lori M, Van Verk MC, Hander T, Schatowitz H, Klauser D, Flury P, Gehring CA, Boller T, Bartels S (2015). Evolutionary divergence of the plant elicitor peptides (Peps) and their receptors: Interfamily incompatibility of perception but compatibility of downstream signalling. *J Exp Bot* 66, 5315–5325. doi:10.1093/jxb/erv236.

Lou B, Wang A, Lin C, Xu T, Zheng X (2011). Enhancement of defense responses by oligandrin against *Botrytis cinerea* in tomatoes. *African J Biotechnol* 10, 11442–11449. doi:10.5897/AJB11.618.

Lu D, Wu S, Gao X, Zhang Y, Shan L, He P (2010). A receptor-like cytoplasmic kinase, BIK1, associates with a flagellin receptor complex to initiate plant innate immunity. *PNAS* 107, 496–501. doi:10.1073/pnas.0909705107.

Macho AP, Zipfel C (2015). Targeting of plant pattern recognition receptor-triggered immunity by bacterial type-III secretion system effectors. *Curr Opin Microbiol* 23, 14–22. doi:10.1016/j.mib.2014.10.009.

Małolepsza U (2005). Spatial and temporal variation of reactive oxygen species and antioxidant enzymes in *o*-hydroxyethylorutin-treated tomato leaves inoculated with *Botrytis cinerea*. *Plant Pathol* 54, 317–324. doi:10.1111/j.1365-3059.2005.01167.x.

Małolepsza U, Urbanek H (2000). The oxidants and antioxidant enzymes in tomato leaves treated with *o*-hydroxyethylorutin and infected with *Botrytis cinerea*. *Eur J Plant Pathol* 106, 657–665. doi:10.1023/A:1008719820600.

Marois E, Van Den Ackerveken G, Bonas U (2002). The *Xanthomonas* type III effector protein AvrBs3 modulates plant gene expression and induces cell hypertrophy in the susceptible host. *Mol Plant-Microbe Interact* 15, 637–646. doi:10.1094/MPMI.2002.15.7.637.

Martínez-Hidalgo P, García JM, Pozo MJ (2015). Induced systemic resistance against *Botrytis cinerea* by *Micromonospora* strains isolated from root nodules. *Front Microbiol* 6, 922. doi:10.3389/fmicb.2015.00922.

Martinez-Medina A, Flors V, Heil M, Mauch-Mani B, Pieterse CMJ, Pozo MJ, Ton J, Van Dam NM, Conrath U (2016). Recognizing plant defense priming. *Trends Plant Sci* 21, 818–822. doi:10.1016/j.tplants.2016.07.009.

Mathys J, De Cremer K, Timmermans P, Van Kerckhove S, Lievens B, Vanhaecke M, Cammue BPA, De Coninck B (2012). Genome-wide characterization of ISR induced in *Arabidopsis thaliana* by *Trichoderma hamatum* T382 against *Botrytis cinerea* infection. *Front Plant Sci* 3, 108. doi:10.3389/fpls.2012.00108.

Mauch-Mani B, Baccelli I, Luna E, Flors V (2017). Defense priming: An adaptive part of induced resistance. *Annu Rev Plant Biol* 68, 485–512. doi:10.1146/annurev-arplant-042916-041132.

Mbengue M, Navaud O, Peyraud R, Barascud M, Badet T, Vincent R, Barbacci A, Raffaele S (2016). Emerging trends in molecular interactions between plants and the broad host range fungal pathogens *Botrytis cinerea* and *Sclerotinia sclerotiorum*. *Front Plant Sci* 7, 422. doi:10.3389/fpls.2016.00422.

Mehari ZH, Elad Y, Rav-David D, Graber ER, Meller Harel Y (2015). Induced systemic resistance in tomato (*Solanum lycopersicum*) against *Botrytis cinerea* by biochar amendment involves jasmonic acid signaling. *Plant Soil* 395, 31–44. doi:10.1007/s11104-015-2445-1.

Méndez-Bravo A, Calderón-Vázquez C, Ibarra-Laclette E, Raya-González J, Ramírez-Chávez E, Molina-Torres J, Guevara-García AA, López-Bucio J, Herrera-Estrella L (2011). Alkamides activate jasmonic acid biosynthesis and signaling pathways and confer resistance to *Botrytis cinerea* in *Arabidopsis thaliana*. *PLoS ONE* 6, e27251. doi:10.1371/journal.pone.0027251.

Mendgen K, Hahn M (2002). Plant infection and the establishment of fungal biotrophy. *Trends Plant Sci* 7, 352–356. doi:10.1016/S1360-1385(02)02297-5.

Meng X, Xu J, He Y, Yang K-Y, Mordorski B, Liu Y, Zhang S (2013). Phosphorylation of an ERF transcription factor by *Arabidopsis* MPK3/MPK6 regulates plant defense gene induction and fungal resistance. *Plant Cell* 25, 1126–1142. doi:10.1105/tpc.112.109074.

Mithöfer A, Boland W (2008). Recognition of herbivory-associated molecular patterns. *Plant Physiol* 146, 825–831. doi:10.1104/pp.107.113118.

Miya A, Albert P, Shinya T, Desaki Y, Ichimura K, Shirasu K, Narusaka Y, Kawakami N, Kaku H, Shibuya N (2007). CERK1, a LysM receptor kinase, is essential for chitin elicitor signaling in *Arabidopsis*. *PNAS* 104, 19613–19618. doi:10.1073/pnas.0705147104.

Mohamed N, Lherminier J, Farmer M-J, Fromentin J, Béno N, Houot V, Milat M-L, Blein J-P (2007). Defense responses in grapevine leaves against *Botrytis cinerea* induced by application of a *Pythium oligandrum* strain or its elicitin, oligandrin, to roots. *Phytopathology* 97, 611–620. doi:10.1094/PHYTO-97-5-0611.

Mulema JMK, Denby KJ (2012). Spatial and temporal transcriptomic analysis of the *Arabidopsis thaliana-Botrytis cinerea* interaction. *Mol Biol Rep* 39, 4039–4049. doi:10.1007/s11033-011-1185-4.

Nakajima M, Akutsu K (2013). Virulence factors of *Botrytis cinerea*. *J Gen Plant Pathol* 80, 15–23. doi:10.1007/s10327-013-0492-0.

Nambeesan S, AbuQamar S, Laluk K, Mattoo AK, Mickelbart M V, Ferruzzi MG, Mengiste T, Handa AK (2012). Polyamines attenuate ethylene-mediated defense responses to abrogate resistance to <i>Botrytis cinerea<i> in tomato. *Plant Physiol* 158, 1034–1045. doi:10.1104/pp.111.188698.

Narusaka Y, Shinya T, Narusaka M, Motoyama N, Shimada H, Murakami K, Shibuya N (2013). Presence of LYM2 dependent but CERK1 independent disease resistance in Arabidopsis. *Plant Signal Behav* 8, 13–15. doi:10.4161/psb.25345.

O'Brien JA, Daudi A, Butt VS, Bolwell GP (2012). Reactive oxygen species and their role in plant defence and cell wall metabolism. *Planta* 236, 765–779. doi:10.1007/s00425-012-1696-9.

Östlund G, Sonnhammer ELL (2012). Quality criteria for finding genes with high mRNA-protein expression correlation and coexpression correlation. *Gene* 497, 228–236. doi:10.1016/j.gene.2012.01.029.

Pane C, Parisi M, Zaccardelli M, Graziani G, Fogliano V (2011). Putative role of antioxidant activity of high pigment tomato cultivars in resistance against *Botrytis cinerea* post-harvest infection. *Acta Hortic* 914, 429–432.

Pastor V, Luna E, Ton J, Cerezo M, García-Agustín P, Flors V (2013). Fine tuning of reactive oxygen species homeostasis regulates primed immune responses in *Arabidopsis*. *Mol Plant-Microbe Interact* 26, 1334–1344. doi:10.1094/MPMI-04-13-0117-R.

Ravensdale M, Bernoux M, Ve T, Kobe B, Thrall PH, Ellis JG, Dodds PN (2012). Intramolecular interaction influences binding of the flax L5 and L6 resistance proteins to their AvrL567 ligands. *PLoS Pathog* 8, e1003004. doi:10.1371/journal.ppat.1003004.

Ren D, Liu Y, Yang K-Y, Han L, Mao G, Glazebrook J, Zhang S (2008). A fungal-responsive MAPK cascade regulates phytoalexin biosynthesis in *Arabidopsis*. *PNAS* 105, 5638–5643. doi:10.1073/pnas.0711301105.

Reymond P, Farmer EE (1998). Jasmonate and salicylate as global signals for defense gene expression. *Curr Opin Plant Biol* 1, 404–411.

Römer P, Hahn S, Jordan T, Strauss T, Bonas U, Lahaye T (2007). Plant pathogen recognition mediated by promoter activation of the pepper *Bs3* resistance gene. *Science* 318, 645–648. doi:10.1126/science.1144958.

Ross AF (1961). Systemic acquired resistance induced by localized virus infections in plants. *Virology* 14, 340–358. doi:10.1016/0042-6822(61)90319-1.

Rossi FR, Gárriz A, Marina M, Romero FM, Gonzalez ME, Collado IG, Pieckenstain FL (2011). The sesquiterpene botrydial produced by *Botrytis cinerea* induces the hypersensitive response on plant tissues and its action is modulated by salicylic acid and jasmonic acid signaling. *Mol Plant-Microbe Interact* 24, 888–896. doi:10.1094/MPMI-10-10-0248.

Ryals JA, Neuenschwander UH, Willits MG, Molina A, Steiner H-Y, Hunt MD (1996). Systemic acquired resistance. *Plant Cell* 8, 1809–1819. doi:10.2307/3870231.

Ryan CA, Pearce G (1998). SYSTEMIN: A polypeptide signal for plant defensive genes. *Annu Rev Cell Dev Biol* 14, 1–17. doi:10.1146/annurev.cellbio.14.1.1.

Sacristán S, García-Arenal F (2008). The evolution of virulence and pathogenicity in plant pathogen populations. *Mol Plant Pathol* 9, 369–384. doi:10.1111/j.1364-3703.2007.00460.x.

Sarosh BR, Danielsson J, Meijer J (2009). Transcript profiling of oilseed rape (*Brassica napus*) primed for biocontrol differentiate genes involved in microbial interactions with beneficial *Bacillus amyloliquefaciens* from pathogenic *Botrytis cinerea*. *Plant Mol Biol* 70, 31–45. doi:10.1007/s11103-009-9455-4.

Schenk ST, Hernandez-Reyes C, Samans B, Stein E, Neumann C, Schikora M, Reichelt M, Mithöfer A, Becker A, Kogel K-H, Schikora A (2014). N-acyl-homoserine lactone primes plants for cell wall reinforcement and induces resistance to bacterial pathogens via the salicylic acid/oxylipin pathway. *Plant Cell* 26, 2708–2723. doi:10.1105/tpc.114.126763.

Schornack S, Moscou MJ, Ward ER, Horvath DM (2013). Engineering plant disease resistance based on TAL effectors. *Annu Rev Phytopathol* 51, 383–406. doi:10.1146/annurev-phyto-082712-102255.

Schouten A, Van Baarlen P, Van Kan JAL (2008). Phytotoxic Nep1-like proteins from the necrotrophic fungus *Botrytis cinerea* associate with membranes and the nucleus of plant cells. *New Phytol* 177, 493–505. doi:10.1111/j.1469-8137.2007.02274.x.

Schweizer P, Felix G, Buchala A, Müller C, Métraux JP (1996). Perception of free cutin monomers by plant cells. *Plant J* 10, 331–341. doi:10.1046/j.1365-313X.1996.10020331.x.

Segarra G, Elena G, Trillas I (2013). Systemic resistance against *Botrytis cinerea* in Arabidopsis triggered by an olive marc compost substrate requires functional SA signalling. *Physiol Mol Plant Pathol* 82, 46–50. doi:10.1016/j.pmpp.2013.02.002.

Segmüller N, Kokkelink L, Giesbert S, Odinius D, Van Kan JAL, Tudzynski P (2008). NADPH oxidases are involved in differentiation and pathogenicity in *Botrytis cinerea*. *Mol Plant-Microbe Interact* 21, 808–819. doi:10.1094/MPMI-21-6-0808.

Sela D, Buxdorf K, Shi JX, Feldmesser E, Schreiber L, Aharoni A, Levy M (2013). Overexpression of *AtSHN1/WIN1* provokes unique defense responses. *PLoS ONE* 8, e70146. doi:10.1371/journal.pone.0070146.

Seo E, Choi D (2015). Functional studies of transcription factors involved in plant defenses in the genomics era. *Brief Funct Genomics* 14, 260–267. doi:10.1093/bfgp/elv011.

Shah J (2003). The salicylic acid loop in plant defense. *Curr Opin Plant Biol* 6, 365–371. doi:10.1016/S1369-5266(03)00058-X.

Shah P, Powell ALT, Orlando R, Bergmann C, Gutierrez-Sanchez G (2012). Proteomic analysis of ripening tomato fruit infected by *Botrytis cinerea*. *J Proteome Res* 11, 2178–2192. doi:10.1021/pr200965c.

Sham A, Al-Azzawi A, Al-Ameri S, Al-Mahmoud B, Awwad F, Al-Rawashdeh A, Iratni R, AbuQamar S (2014). Transcriptome analysis reveals genes commonly induced by *Botrytis cinerea* infection, cold, drought and oxidative stresses in *Arabidopsis*. *PLoS ONE* 9, e113718. doi:10.1371/journal.pone.0113718.

Shaul O, Galili S, Volpin H, Ginzberg I, Elad Y, Chet I, Kapulnik Y (1999). Mycorrhiza-induced changes in disease severity and PR protein expression in tobacco leaves. *Mol Plant-Microbe Interact* 12, 1000–1007. doi:10.1094/MPMI.1999.12.11.1000.

Shigenaga AM, Argueso CT (2016). No hormone to rule them all: Interactions of plant hormones during the responses of plants to pathogens. *Semin Cell Dev Biol* 56, 174–189. doi:10.1016/j.semcdb.2016.06.005.

Shin J, Heidrich K, Sanchez-Villarreal A, Parker JE, Davis SJ (2012). TIME FOR COFFEE represses accumulation of the MYC2 transcription factor to provide time-of-day regulation of jasmonate signaling in Arabidopsis. *Plant Cell* 24, 2470–2482. doi:10.1105/tpc.111.095430.

Shinya T, Motoyama N, Ikeda A, Wada M, Kamiya K, Hayafune M, Kaku H, Shibuya N (2012). Functional characterization of CEBiP and CERK1 homologs in arabidopsis and rice reveals the presence of different chitin receptor systems in plants. *Plant Cell Physiol* 53, 1696–1706. doi:10.1093/pcp/pcs113.

Shlezinger N, Doron A, Sharon A (2011a). Apoptosis-like programmed cell death in the grey mould fungus *Botrytis cinerea*: genes and their role in pathogenicity. *Biochem Soc Trans* 39, 1493–1498.

Shlezinger N, Minz A, Gur Y, Hatam I, Dagdas YF, Talbot NJ, Sharon A (2011b). Anti-apoptotic machinery protects the necrotrophic fungus *Botrytis cinerea* from host-induced apoptotic-like cell death during plant infection. *PLoS Pathog* 7, e1002185. doi:10.1371/journal.ppat.1002185.

Shulaev V, Silverman P, Raskin I (1997). Airborne signalling by methyl salicylate in plant pathogen resistance. *Nature* 385, 718–721. doi:10.1038/385718a0.

Smith JE, Mengesha B, Tang H, Mengiste T, Bluhm BH (2014). Resistance to *Botrytis cinerea* in *Solanum lycopersicoides* involves widespread transcriptional reprogramming. *BMC Genomics* 15, 334. doi:10.1186/1471-2164-15-334.

Staats M, Van Kan JAL (2012). Genome update of *Botrytis cinerea* strains B05.10 and T4. *Eukaryot Cell* 11, 1413–1414. doi:10.1128/EC.00164-12.

Stahl EA, Bishop JG (2000). Plant – pathogen arms races at the molecular level. *Curr Opin Plant Biol* 3, 299–304. doi:10.1016/S1369-5266(00)00083-2.

Staswick PE, Su W, Howell SH (1992). Methyl jasmonate inhibition of root growth and induction of a leaf protein are decreased in an *Arabidopsis thaliana* mutant. *PNAS* 89, 6837–6840. doi:10.1073/pnas.89.15.6837.

Staswick PE, Tiryaki I (2004). The oxylipin signal jasmonic acid is activated by an enzyme that conjugates it to isoleucine in Arabidopsis. *Plant Cell* 16, 2117–2127. doi:10.1105/tpc.104.023549.

Stefanato FL, Abou-Mansour E, Buchala A, Kretschmer M, Mosbach A, Hahn M, Bochet CG, Métraux JP, Schoonbeek HJ (2009). The ABC transporter BcatrB from *Botrytis cinerea* exports camalexin and is a virulence factor on *Arabidopsis thaliana*. *Plant J* 58, 499–510. doi:10.1111/j.1365-313X.2009.03794.x.

Strange RN, Scott PR (2005). Plant disease: a threat to global food security. *Annu Rev Phytopathol* 43, 83–116. doi:10.1146/annurev.phyto.43.113004.133839.

Tada Y, Spoel SH, Pajerowska-Mukhtar K, Mou Z, Song J, Wang C, Zuo J, Dong X (2008). Plant immunity requires conformational charges of NPR1 via S-nitrosylation and thioredoxins. *Science* 321, 952–956. doi:10.1126/science.1156970.

Takken FLW, Goverse A (2012). How to build a pathogen detector: Structural basis of NB-LRR function. *Curr Opin Plant Biol* 15, 375–384. doi:10.1016/j.pbi.2012.05.001.

Tanaka K, Choi J, Cao Y, Stacey G (2014). Extracellular ATP acts as a damage-associated molecular pattern (DAMP) signal in plants. *Front Plant Sci* 5, 446. doi:10.3389/fpls.2014.00446.

Thomma BPHJ, Eggermont K, Penninckx IAMA, Mauch-Mani B, Vogelsang R, Cammue BPA, Broekaert WF (1998). Separate jasmonate-dependent and salicylate-dependent defense-response pathways in *Arabidopsis* are essential for resistance to distinct microbial pathogens. *PNAS* 95, 15107–15111. doi:10.1073/pnas.95.25.15107.

Thomma BPHJ, Nürnberger T, Joosten MHAJ (2011). Of PAMPs and effectors: the blurred PTI-ETI dichotomy. *Plant Cell* 23, 4–15. doi:10.1105/tpc.110.082602.

Trdá L, Boutrot F, Claverie J, Brulé D, Dorey S, Poinssot B (2015). Perception of pathogenic or beneficial bacteria and their evasion of host immunity: pattern recognition receptors in the frontline. *Front Plant Sci* 6, 219. doi:10.3389/fpls.2015.00219.

Tsuda K, Katagiri F (2010). Comparing signaling mechanisms engaged in pattern-triggered and effector-triggered immunity. *Curr Opin Plant Biol* 13, 459–465. doi:10.1016/j.pbi.2010.04.006.

Van Kan JAL (2006). Licensed to kill: the lifestyle of a necrotrophic plant pathogen. *Trends Plant Sci* 11, 247–253. doi:10.1016/j.tplants.2006.03.005.

Van Kan JAL, Stassen JHM, Mosbach A, Van Der Lee TAJ, Faino L, Farmer AD, Papasotiriou D, Zhou S, Seidl MF, Cottam E, Edel D, Hahn M, Schwartz DC, Dietrich RA, Widdison S, Scalliet G (2017). A gapless genome sequence of the fungus *Botrytis cinerea*. *Mol Plant Pathol* 8, 75–89. doi:10.1111/mpp.12384.

Van Wees SCM, Van Der Ent S, Pieterse CMJ (2008). Plant immune responses triggered by beneficial microbes. *Curr Opin Plant Biol* 11, 443–448. doi:10.1016/j.pbi.2008.05.005.

Vandenabeele S, Van Der Kelen K, Dat J, Gadjev I, Boonefaes T, Morsa S, Rottiers P, Slooten L, Van Montagu M, Zabeau M, Inzé D, Van Breusegem F (2003). A comprehensive analysis of hydrogen peroxide-induced gene expression in tobacco. *PNAS* 100, 16113–16118. doi:10.1073/pnas.2136610100.

VanEtten HD, Mansfield JW, Bailey JA, Farmer EE (1994). Two classes of plant antibiotics: Phytoalexins versus “phytoanticipins”. *Plant Cell* 6, 1191–1192. doi:10.1105/tpc.6.9.1191.

Vega A, Canessa P, Hoppe G, Retamal I, Moyano TC, Canales J, Gutiérrez RA, Rubilar J (2015). Transcriptome analysis reveals regulatory networks underlying differential susceptibility to *Botrytis cinerea* in response to nitrogen availability in *Solanum lycopersicum*. *Front Plant Sci* 6, 911. doi:10.3389/fpls.2015.00911.

Vicedo B, Flors V, De La O Leyva M, Finiti I, Kravchuk Z, Real MD, García-Agustín P, González-Bosch C (2009). Hexanoic acid-induced resistance against *Botrytis cinerea* in tomato plants. *Mol Plant-Microbe Interact* 22, 1455–1465. doi:10.1094/MPMI-22-11-1455.

Villegas-Fernández ÁM, Krajinski F, Schlereth A, Madrid E, Rubiales D (2014). Characterization of transcription factors following expression profiling of *Medicago truncatula–Botrytis* spp. interactions. *Plant Mol Biol Report* 32, 1030–1040. doi:10.1007/s11105-014-0710-8.

Wang C, Ding Y, Yao J, Zhang Y, Sun Y, Colee J, Mou Z (2015b). Arabidopsis elongator subunit 2 positively contributes to resistance to the necrotrophic fungal pathogens *Botrytis cinerea* and *Alternaria brassicicola*. *Plant J* 83, 1019–1033. doi:10.1111/tpj.12946.

Wang D, Amornsiripanitch N, Dong X (2006). A genomic approach to identify regulatory nodes in the transcriptional network of systemic acquired resistance in plants. *PLoS Pathog* 2, e123. doi:10.1371/journal.ppat.0020123.

Wang F, Feng G, Chen K (2009). Defense responses of harvested tomato fruit to burdock fructooligosaccharide, a novel potential elicitor. *Postharvest Biol Technol* 52, 110–116. doi:10.1016/j.postharvbio.2008.09.002.

Wang K, Liao Y, Kan J, Han L, Zheng Y (2015c). Response of direct or priming defense against *Botrytis cinerea* to methyl jasmonate treatment at different concentrations in grape berries. *Int J Food Microbiol* 194, 32–39. doi:10.1016/j.ijfoodmicro.2014.11.006.

Wang L, Albert M, Einig E, Fürst U, Krust D, Felix G (2016). The pattern-recognition receptor CORE of Solanaceae detects bacterial cold-shock protein. *Nat Plants* 2, 16185. doi:10.1038/nplants.2016.185.

Wang M, Weiberg A, Dellota E, Yamane D, Jin H (2017). Botrytis small RNA *Bc*-siR37 suppresses plant defense genes by cross-kingdom RNAi. *RNA Biol* 14, 421–428. doi:10.1080/15476286.2017.1291112.

Wang M, Weiberg A, Jin H (2015a). Pathogen small RNAs: A new class of effectors for pathogen attacks. *Mol Plant Pathol* 16, 219–223. doi:10.1111/mpp.12233.

Wang X, Jiang N, Liu J, Liu W, Wang G-L (2014). The role of effectors and host immunity in plant–necrotrophic fungal interactions. *Virulence* 5, 722–732. doi:10.4161/viru.29798.

Wasternack C (2007). Jasmonates: an update on biosynthesis, signal transduction and action in plant stress response, growth and development. *Ann Bot* 100, 681–697. doi:10.1093/aob/mcm079.

Wasternack C, Hause B (2013). Jasmonates: biosynthesis, perception, signal transduction and action in plant stress response, growth and development. An update to the 2007 review in Annals of Botany. *Ann Bot* 111, 1021–1058. doi:10.1093/aob/mct067.

Wasternack C, Parthier B (1997). Jasmonate-signalled plant gene expression. *Trends Plant Sci* 2, 302–307.

Weber H, Chételat A, Caldelari D, Farmer EE (1999). Divinyl ether fatty acid synthesis in late blight-diseased potato leaves. *Plant Cell* 11, 485–494.

Weiberg A, Wang M, Lin F-M, Zhao H, Zhang Z, Kaloshian I, Huang H-D, Jin H (2013). Fungal small RNAs suppress plant immunity by hijacking host RNA interference pathways. *Science* 342, 118–123. doi:10.1126/science.1239705.

Weng J-K, Chapple C (2010). The origin and evolution of lignin biosynthesis. *New Phytol* 187, 273–285.

Williamson B, Tudzynski B, Tudzynski P, Van Kan JAL (2007). *Botrytis cinerea*: the cause of grey mould disease. *Mol Plant Pathol* 8, 561–580. doi:10.1111/J.1364-3703.2007.00417.X.

Windram O, Madhou P, McHattie S, Hill C, Hickman R, Cooke E, Jenkins DJ, Penfold CA, Baxter L, Breeze E, Kiddle SJ, Rhodes J, Atwell S, Kliebenstein DJ, Kim Y, Stegle O, Borgwardt K, Zhang C, Tabrett A, et al. (2012). *Arabidopsis* defense against *Botrytis cinerea*: chronology and regulation deciphered by high-resolution temporal transcriptomic analysis. *Plant Cell* 24, 3530–3557. doi:10.1105/tpc.112.102046.

Wojtaszek P (1997). Oxidative burst: an early plant response to pathogen infection. *Biochem J* 322, 681–692. doi:10.1042/bj3220681.

Wu Y, Zhang D, Chu JY, Boyle P, Wang Y, Brindle ID, De Luca V, Després C (2012). The Arabidopsis NPR1 protein is a receptor for the plant defense hormone salicylic acid. *Cell Rep* 1, 639–647. doi:10.1016/j.celrep.2012.05.008.

Xie D-X, Feys BF, James S, Nieto-Rostro M, Turner JG (1998). *COI1*: An *Arabidopsis* gene required for jasmonate-regulated defense and fertility. *Science* 280, 1091–1094. doi:10.1126/science.280.5366.1091.

Xu J, Li Y, Wang Y, Liu H, Lei L, Yang H, Liu G, Ren D (2008). Activation of MAPK kinase 9 induces ethylene and camalexin biosynthesis and enhances sensitivity to salt stress in Arabidopsis. *J Biol Chem* 283, 26996–27006. doi:10.1074/jbc.M801392200.

Yamaguchi Y, Pearce G, Ryan CA (2006). The cell surface leucine-rich repeat receptor for *At*Pep1, an endogenous peptide elicitor in *Arabidopsis*, is functional in transgenic tobacco cells. *PNAS* 103, 10104–10109. doi:10.1073/pnas.0603729103.

Zhang J, Li W, Xiang T, Liu Z, Laluk K, Ding X, Zou Y, Gao M, Zhang X, Chen S, Mengiste T, Zhang Y, Zhou J-M (2010). Receptor-like cytoplasmic kinases integrate signaling from multiple plant immune receptors and are targeted by a *Pseudomonas syringae* effector. *Cell Host Microbe* 7, 290–301. doi:10.1016/j.chom.2010.03.007.

Zhang L, Kars I, Essenstam B, Liebrand TWH, Wagemakers L, Elberse J, Tagkalaki P, Tjoitang D, Van Den Ackerveken G, Van Kan JAL (2014). Fungal endopolygalacturonases are recognized as microbe-associated molecular

patterns by the Arabidopsis receptor-like protein RESPONSIVENESS TO BOTRYTIS POLYGALACTURONASES1. *Plant Physiol* 164, 352–364. doi:10.1104/pp.113.230698.

Zhang S, Klessig DF (2001). MAPK cascades in plant defense signaling. *Trends Plant Sci* 6, 520–527. doi:10.1016/S1360-1385(01)02103-3.

Zhang Y, Zhang Y, Qiu D, Zeng H, Guo L, Yang X (2015). BcGs1, a glycoprotein from *Botrytis cinerea*, elicits defence response and improves disease resistance in host plants. *Biochem Biophys Res Commun* 457, 627–634. doi:10.1016/j.bbrc.2015.01.038.

Zhang Z, Wu Y, Gao M, Zhang J, Kong Q, Liu Y, Ba H, Zhou J, Zhang Y (2012). Disruption of PAMP-induced MAP kinase cascade by a *Pseudomonas syringae* effector activates plant immunity mediated by the NB-LRR protein SUMM2. *Cell Host Microbe* 11, 253–263. doi:10.1016/j.chom.2012.01.015.

Zhao D, Gong S, Hao Z, Tao J (2015). Identification of miRNAs responsive to *Botrytis cinerea* in herbaceous peony (*Paeonia lactiflora* Pall.) by high-throughput sequencing. *Genes* 6, 918–934. doi:10.3390/genes6030918.

Zheng Y, Sheng J, Zhao R, Zhang J, Lv S, Liu L, Shen L (2011). Preharvest l-arginine treatment induced postharvest disease resistance to *Botrytis cinerea* in tomato fruits. *J Agric Food Chem* 59, 6543–6549. doi:10.1021/jf2000053.

Zimmerli L, Métraux JP, Mauch-Mani B (2001). β-Aminobutyric acid-induced protection of Arabidopsis against the necrotrophic fungus *Botrytis cinerea*. *Plant Physiol* 126, 517–523. doi:10.1104/pp.126.2.517.

Zipfel C (2014). Plant pattern-recognition receptors. *Trends Immunol* 35, 345–351. doi:10.1016/j.it.2014.05.004.

Zipfel C, Robatzek S (2010). Pathogen-associated molecular pattern-triggered immunity: Veni, Vidi...? *Plant Physiol* 154, 551–554. doi:10.1104/pp.110.161547.

Zvereva AS, Pooggin MM (2012). Silencing and innate immunity in plant defense against viral and non-viral pathogens. *Viruses* 4, 2578–2597. doi:10.3390/v4112578.

Chapter 3

Obtaining a baseline of the early transcriptional responses of tobacco when infected by *Botrytis cinerea*

Obtaining a baseline of the early transcriptional responses of tobacco when infected by *Botrytis cinerea*

3.1 Introduction

The plant immune system is composed of a multi-layered network, including recognition, response and regulatory elements (Jones and Dangl, 2006; Łaźniewska et al., 2010). This system perceives the potential outcomes of symbiotic relationships with many organisms. Although mutualistic and neutral interactions may trigger the immune system, the life-or-death nature of parasitic pathogenic interactions has led to an evolutionary arms-race (Stahl and Bishop, 2000); the outcome of the interaction could be susceptibility (where the plant host cannot arrest pathogen growth) or resistance/tolerance (where pathogen growth is wholly or partly restrained). The lifestyle of the pathogen (e.g. biotrophic or necrotrophic), its host range (species-specific, narrow or broad) and genetic background dictate disease progression, virulence factors and vulnerabilities, whereas plant species have evolved diverse mechanisms to respond to pathogens (Poland et al., 2009; Roux et al., 2014). However, the specific outcome is strongly influenced by the plant species, the population genetics of a species as well as the environmental context of the specific individuals being attacked (Dodds and Rathjen, 2010; Walters and Fountaine, 2009). Understanding the features of specific plant-pathogen interactions, which may be unique to the plant host and/or pathogen, or wide-spread across different species, is the key to developing workable crop protection strategies.

Model species, of both plants and pathogens, are useful to generate this type of fundamental knowledge, and this has been exemplified by the use of the archetypal model plant *Arabidopsis thaliana*. Using a single species as host for numerous pathogens (e.g. *Fusarium oxysporum*: Berrocal-Lobo and Molina, 2007; *Pseudomonas syringae*: Katagiri et al., 2002; fungal necrotrophs: Łaźniewska et al., 2010; powdery mildews: Micali et al., 2008) has provided the ability to profile/compare responses between different types of pathogens, for example contrasting necrotroph- and biotroph-induced defence (Glazebrook, 2005). Although the use of *A. thaliana* as model host plant has been highly effective in understanding plant defence mechanisms, other plant models are equally important to establish whether findings are conserved across plant species.

Tobacco (*Nicotiana tabacum*) has long been a model plant to study fundamental questions in plant-pathogen interactions (Fournier et al., 1993; Piedras et al., 1998; Ross, 1961; Sasabe et al., 2000; Van Loon, 1985) and has the distinction of being the first plant to be genetically modified (Hoekema et al., 1983). The virulence of pathogens, gene functions and disease resistance mechanisms have been studied in the tobacco system, amongst others (Baillieul et al., 1995; Cessna et al., 2000; Marchive et al., 2007; Oliver et al., 2014; Taguchi et al., 2010). In addition, its relative ease of

transformation has made it a popular host for heterologous expression of candidate defence genes for functional characterisation studies (Carstens et al., 2003; Jach et al., 1995; Joubert et al., 2006; Maher et al., 1994). Despite the long history as a model host plant, genetic characterisation of tobacco has been delayed, since its allotetraploid genome complicated genome sequence assembly (Sierro et al., 2014). Recently, however, more genetic resources for tobacco have become available, including the genome sequences of three commercially important cultivars, two ancestral species (Bombarely et al., 2012; Edwards et al., 2017; Sierro et al., 2013, 2014) as well as two mutant libraries (Liu et al., 2014; Wang et al., 2017) deposited in the Sol Genomic Database (Mueller et al., 2005).

Improvements in the molecular resources for tobacco also created increased scope for transcript profiling of tobacco-pathogen systems. Untargeted transcriptomic analyses of tobacco have already been reported for infections with *Xanthomonas campestris* pv. *vesicatoria* (Zurbriggen et al., 2009), *X. axonopodis* pv. *citri* (Daurelio et al., 2011), *Pseudomonas syringae* pv. *syringae hrcC*- (Bozsó et al., 2016; Szatmári et al., 2014) and tobacco mosaic virus (TMV, Jada et al., 2014). Similar data for tobacco-fungal infections has not been reported yet; here we will report a transcriptomic analysis of the tobacco-*Botrytis cinerea* pathosystem during the early stages of infection.

In terms of fungal pathogens, *Botrytis cinerea* is considered a model for broad host range necrotrophs (Mbengue et al., 2016). It is an obligate necrotrophic filamentous fungus that causes grey mould on over 500 plant genera, including many of the most widely used crops (Elad et al., 2016). Its commercial and scientific importance (Dean et al., 2012) has spurred research into its epidemiology, virulence factors and infection strategy. As a necrotrophic pathogen, it depends on dead cells for nutrients and therefore has an arsenal of necrotising agents that trigger host programmed cell death (PCD), including proteins and secondary metabolites (Frías et al., 2011, 2016; Govrin et al., 2006; Kars et al., 2005; Noda et al., 2010; Zhang et al., 2015), while also possessing critical anti-apoptosis systems that prevent its own death during infections amidst the active PCD processes (Shlezinger et al., 2011).

The progression of *B. cinerea* infection on leaf tissue has been extensively studied in *Arabidopsis* (AbuQamar et al., 2006; Windram et al., 2012) and appears to follow a similar pattern on vegetative tissues of other species (Caires et al., 2015; Eizner et al., 2017; Elad, 1988; McKeen, 1974). The visible sign of disease progression follows a four-stage development and expansion of necrotic lesions, that are formed by the combined action of plant defence mechanisms and fungal necrotising activity (Eizner et al., 2017). In the first ~12 h after inoculation, the conidia attach to the leaf surface, form germ tubes and develop appressoria (Van Kan, 2006). These appressoria release cell wall degrading enzymes (CWDE) that assist in penetration of the epidermal cells. Primary lesion formation occurs from 12 to 20 hours after inoculation, followed by a lag phase, before the active lesion expansion starts from ~36 hours after inoculation. The lag phase was shown to be the stage

when the *B. cinerea* anti-apoptotic system prevents death of a limited number of fungal cells within the primary lesion where PCD was activated (Shlezinger et al., 2011). These cells, now protected from direct plant defence, initiate the secondary lesion formation/expansion. From the plant's perspective, it is in this early phase of the infection, when *B. cinerea* is most vulnerable to host defence mechanisms, that an effective defence response must be activated. Resistance is mostly correlated with faster, earlier, or stronger plant defence responses (Asselbergh et al., 2007). As is classically seen against necrotrophs, plant defence responses to *B. cinerea* are coordinated through signalling by jasmonates (JA) and ethylene (ET) and include pathogenesis-related (PR) proteins, cell wall strengthening, detoxification and control of redox homeostasis (Asselbergh et al., 2007; Ingle et al., 2015; Małolepsza and Urbanek, 2000).

The *Arabidopsis-B. cinerea* interaction has been well characterised on several levels: using mutants (AbuQamar et al., 2006; Liu et al., 2015); resistance inducers (Ferrari et al., 2007; Kravchuk et al., 2011; Zimmerli et al., 2001); and evaluating natural variation among ecotypes (Rowe and Kliebenstein, 2008). Availability of transcriptome analysis platforms has prompted gene expression profiling of *A. thaliana* infected with at least three strains of *B. cinerea* (AbuQamar et al., 2006; Birkenbihl et al., 2012; Coolen et al., 2016; Ingle et al., 2015; Liu et al., 2015; Mathys et al., 2012; Mulema and Denby, 2012; Segarra et al., 2013; Sela et al., 2013; Sham et al., 2014; Wang et al., 2015; Windram et al., 2012). Similar profiling studies have been reported for cucumber (Kong et al., 2015), grapevine (Agudelo-Romero et al., 2015; Blanco-Ulate et al., 2015; Kelloniemi et al., 2015), peony (Gong et al., 2015), lettuce (De Cremer et al., 2013) and tomato (Asselbergh et al., 2007; Blanco-Ulate et al., 2013; Cantu et al., 2009; Finiti et al., 2014; Vega et al., 2015) against this pathogen. Studies that used a tobacco-*B. cinerea* pathosystem reported gene expression analyses that have mainly been confined to marker genes for defence (Keller et al., 1999; Lee et al., 2014; Shaul et al., 1999; Sohn et al., 2007; Zhang et al., 2015), or specific pathways, such as phenylpropanoid synthesis (Vera et al., 2012), oxylipin synthesis (Cawoy et al., 2014) or antioxidant mechanisms (Fotopoulos et al., 2006).

In the present study, we examined, using microarrays, the transcriptional changes in tobacco tissue at the site of infection, and in tissues from leaves distal to the infection. The primary objective of this study was to provide a baseline for subsequent studies using the *B. cinerea*-tobacco pathosystem. By including five sampling points within the first two days after infection, we were able to examine temporal patterns in tobacco gene expression during the critical initial stages of lesion development. Profiling temporal changes in gene expression in leaves distal to the infection has, to our knowledge, not been reported in any other *B. cinerea* pathosystem, nor has it been routinely done in other model plants for plant-pathogen studies. The transcriptomic analysis was validated with real-time PCR and volatile secondary metabolite profiling was used to support some of the main findings.

3.2 Materials and methods

3.2.1 Fungal material

The inoculum was prepared from a strain of *B. cinerea* isolated from a South African vineyard which was described as a hyper-virulent strain (first reported in Joubert et al., 2006). The strain was cultured at 23°C on sterile apricot halves (Naturlite, Tiger Food Brands Limited, South Africa), in a dark growth chamber. Following sporulation, sterile water was used to harvest spores. The viability and germination potential of the spore suspension was determined by plating the suspension on 1% (w/v) water agar. Prior to infection, freshly harvested spores were hydrated overnight in sterile water at 4°C. Spore concentration was determined using light microscopy of a haemocytometer. The fungal inoculum was prepared in 50% sterile red grape juice (Liquifruit, Pioneer Foods, Paarl, South Africa) to a concentration of 1000 spores per microliter.

3.2.2 Plant material and whole plant infection assay

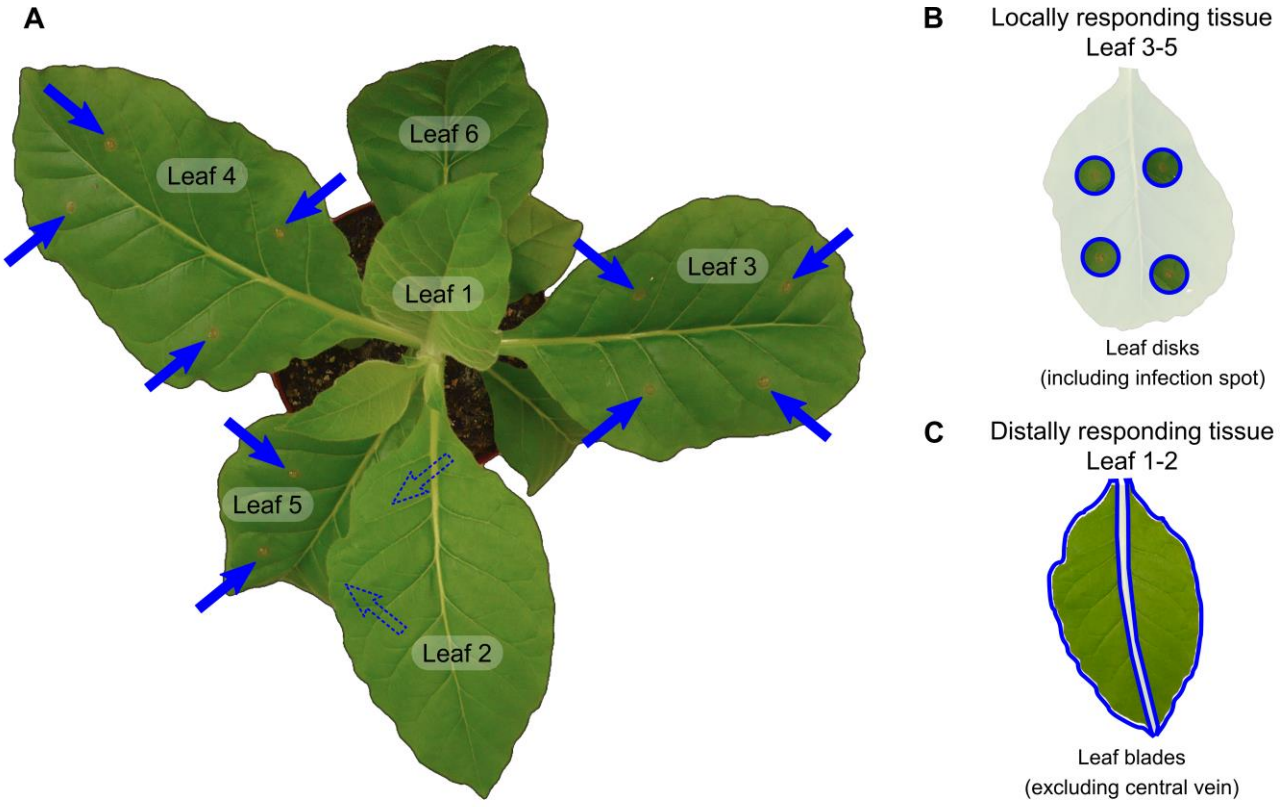

Figure 3.1 Tobacco material used for the whole plant infection assay. A. Leaf positions of representative tobacco plant (eight-leaf stage). Arrows indicate the positions of the infection spots on leaves 3,4 and 5 (the dashed arrows indicate the positions of two lesions obscured by an uninoculated leaf). B. For the profiling of lesion responses, leaf disks from leaf 3-5, centred around the inoculation sites were harvested. C. Tissue used for the leaves distal to the infection, from leaf 1 and 2, consisted of the leaf blades with the central vein removed. Harvested tissue is delineated by blue borders, whereas unused tissue is faded in B and C.

N. tabacum (cv Petit Havana SR1) seeds were sterilised using chlorine vapour (Clough and Bent, 1998) and germinated on Murashige and Skoog (MS) media without sucrose supplementation (Murashige and Skoog, 1962). Seedlings were hardened off in peat moss (Jiffy Products International AS, Norway) prior to transfer to a mixture of DoubleGrow “All Purpose” potting soil

(DoubleGrow, Durbanville, South Africa), peat moss and DoubleGrow vermiculite, in a 1:2:3 ratio. Plants were maintained under artificial lighting (Fluorescent Cool White bulbs, Osram, Munich, Germany), with a 16 h photoperiod at 23°C. Liquid organic fertilizer (Nitrosol®, Fleuron (Pty) Ltd, South Africa) was supplied every two weeks. The infection assay took place at the eight-leaf stage, when 6 fully expanded leaves were available. Prior to the whole plant infection assay, plants were acclimatised to 100% humidity for 24 hours in Perspex humidity chambers.

The infections were performed as previously described (Alexandersson et al., 2011; Joubert et al., 2006). Leaf position was determined by counting from the apex (Figure 3.1A), and leaf positions 3, 4 and 5 were inoculated, while the other leaf positions were not inoculated. The infected leaves were inoculated, 9 hours after dawn, on the adaxial side with four droplets of spore suspension, equivalent to 5000 spores each, two on either side of the central vein (Figure 3.1A). Samples were collected every 12 h over a 48 h period, beginning with t0, immediately after inoculation. Samples from four biological repeats (individually infected plants) were pooled at each sampling point, keeping the leaf positions separate. This enabled the evaluation of potential ontogenic effects, while also providing sufficient material for downstream analyses. Samples of the tissue at and surrounding the inoculation site were considered to represent the localised response, and consisted of 16 leaf disks (15 mm diameter) per leaf position (Figure 3.1B). Samples of leaf tissue from leaves distal to the infection were collected by excising the central vein and retaining the remaining tissue of those leaves and keeping leaf positions separate (Figure 3.1C). When harvested, all samples were flash frozen in liquid nitrogen and were subsequently hand-ground to a fine powder in liquid nitrogen in a mortar and pestle and stored at -80°C until further use.

3.2.3 RNA isolation and microarray analysis

Leaves 3 to 5 were infected and sampling was done at/around the infection spot, thus representing the localised defence response to *B. cinerea* at the infection spots (local expression profile: LEP), whereas leaves 1 and 2 were uninfected, thus representing the transcriptomes of leaves distal to the infection (distal expression profile: DEP). Gene expression profiling, using microarray analysis, was performed on tissue from leaf position two (as a representative leaf distal to the infection) and leaf three (as a representative leaf reacting with a localised response at and around the infection spot). Tissue from leaf positions 1 (distal), 4 and 5 (local lesions) were used for quantitative reverse-transcriptase PCR (qRT-PCR) analysis for selected transcripts (subsequent to and based on the microarray analysis) to test for possible leaf-age (ontogenic) effects. The whole plant infection assay was performed in parallel for wild-type tobacco (presented in this Chapter) and transgenic tobacco expressing *Vitis vinifera polygalacturonase-inhibiting protein 1* (*Vvipgip1*) (data presented in Chapter 4 of this dissertation). The MIAME documentation relating to sample preparation and microarray analysis for this study is attached as Appendix A to Chapter 3.

The RNA extraction protocol was adapted from Coutos-Thévenot et al. (2001). RNA extractions were done by extracting 50 mg ground tissue in 3.2 M phenol, 100 mM Tris pH 8.0, 1.5% (w/v) SDS, 300 mM LiCl, 10 mM Na_2EDTA, 1% (w/v) sodium deoxycholate, 1% (w/v) IGEPAL CA-630, 5 mM thiourea and 1% (w/v) sodium metabisulphite. Two chloroform extractions removed residual phenol prior to isopropanol precipitation. RNA was precipitated in 2.5 M LiCl and suspended in 30 µL nuclease free water. RNA extracts were DNase treated with RNase-free DNase (Roche Diagnostics GmbH, Mannheim, Germany). Quality was evaluated on a formaldehyde agarose gel, while concentration was estimated with a Nanodrop™ (Thermo Scientific, Waltham, USA) and standardised.

Both gene expression analyses of the local and distal expression profiles were performed using the Agilent Tobacco Gene Expression Microarray (G2519F-021113, Agilent Technologies, Santa Clara, CA, USA), an expressed sequence tag (EST)-based oligonucleotide array with two channels per slide. Three independent RNA extracts from each sampling point were used for microarray analysis, representing three technical replicates of a pooled biological sample. RNA extracts were sent as ethanol precipitates and quality was assessed using Agilent Bioanalyzer before cDNA synthesis, hybridisation to the arrays and data capture. Three arrays were used for each sampling point. Leaf 3 (local expression profile) transcripts were analysed by MOgene, LC (St. Louis, MO, USA) and leaf 2 (distal expression profile) by Oxford Gene Technology (OGT, Begbroke, Oxfordshire, UK) since the infected and systemic samples were processed at different times. One channel per array was used for wild-type tobacco samples, while the VviPGIP1-expressing tobacco samples (reported in Chapter 4 of this dissertation) were analysed on the second channel (Table 3.1). The microarray data will be deposited in the Gene Expression Omnibus.

An annotation of the microarray probes was obtained from the manufacturer website (www.genomics.agilent.com), but was not conducive to biological interpretation, since many probes were described as uncharacterised EST sequences. Re-annotation of the microarray probes was performed using Ortho-MCL as described previously, using the EST sequences that the probes were designed from (Bengtsson et al., 2014). This increased the number of probes with GO annotations and putative protein functions from 500 (<2% of array) to 14964 (34% of array). Analysis of expression data

Data preparation and preliminary analysis

Log ratio-mean average plots (MA-plots, Dudoit et al., 2002) were used to evaluate the quality of the microarray data (Appendix B to Chapter 3). The fluorescence intensities were processed in R, using linear models with the limma package (Smyth, 2005) for background correction and surrogate variable analysis (SVA) using the sva package (Leek et al., 2016) for normalisation. Normalised expression data consisted of three replicates for each sample. In Excel, these data were used to

calculate the average and standard error, and fold change between sampling points (always using the earlier sampling point as baseline). These data were imported into SIMCA 14 (Sartorius Stedim Data Analytics AB, Umeå, Sweden). Unsupervised principal component analysis (PCA) was performed and revealed two distinct groups corresponding to the local and distal expression profiles.

Table 3.1 Experimental design for microarray analysis, showing which samples were analysed on each channel of the Agilent Tobacco Gene Expression Microarray.

Response profiled	Leaf position	Dye: Cy3	Dye: Cy5	Company performing analysis
Distal	2	VviPGIP1 0 h A*	Wild-type 0 h A	OGT
Distal	2	VviPGIP1 0 h B*	Wild-type 0 h B	OGT
Distal	2	VviPGIP1 0 h C*	Wild-type 0 h C	OGT
Distal	2	VviPGIP1 12 h A*	Wild-type 12 h A	OGT
Distal	2	VviPGIP1 12 h B*	Wild-type 12 h B	OGT
Distal	2	VviPGIP1 12 h C*	Wild-type 12 h C	OGT
Distal	2	VviPGIP1 24 h A*	Wild-type 24 h A	OGT
Distal	2	VviPGIP1 24 h B*	Wild-type 24 h B	OGT
Distal	2	VviPGIP1 24 h C*	Wild-type 24 h C	OGT
Distal	2	VviPGIP1 36 h A*	Wild-type 36 h A	OGT
Distal	2	VviPGIP1 36 h B*	Wild-type 36 h B	OGT
Distal	2	VviPGIP1 36 h C*	Wild-type 36 h C	OGT
Distal	2	VviPGIP1 48 h A*	Wild-type 48 h A	OGT
Distal	2	VviPGIP1 48 h B*	Wild-type 48 h B	OGT
Distal	2	VviPGIP1 48 h C*	Wild-type 48 h C	OGT
Local	3	Wild-type 0 h A	VviPGIP1 0 h A*	MOgene
Local	3	Wild-type 0 h B	VviPGIP1 0 h B*	MOgene
Local	3	VviPGIP1 0 h C*	Wild-type 0 h C	MOgene
Local	3	Wild-type 12 h A	VviPGIP1 12 h A*	MOgene
Local	3	Wild-type 12 h B	VviPGIP1 12 h B*	MOgene
Local	3	VviPGIP1 12 h C*	Wild-type 12 h C	MOgene
Local	3	Wild-type 24 h A	VviPGIP1 24 h A*	MOgene
Local	3	Wild-type 24 h B	VviPGIP1 24 h B*	MOgene
Local	3	VviPGIP1 24 h C*	Wild-type 24 h C	MOgene
Local	3	Wild-type 36 h A	VviPGIP1 36 h A*	MOgene
Local	3	Wild-type 36 h B	VviPGIP1 36 h B*	MOgene
Local	3	VviPGIP1 36 h C*	Wild-type 36 h C	MOgene
Local	3	Wild-type 48 h A	VviPGIP1 48 h A*	MOgene
Local	3	Wild-type 48 h B	VviPGIP1 48 h B*	MOgene
Local	3	VviPGIP1 48 h C*	Wild-type 48 h C	MOgene

*data presented in Chapter 4. Colours are those used in figures throughout Chapter 3 and Chapter 4.

To identify probes that did not contribute to transcriptional differences between sampling points, Orthogonal Partial Least Squares Discriminate Analyses (OPLS-DA) was performed, using Pareto scaling, a scaling method that retains the original unit of the data (Van Den Berg et al., 2006). Unsupervised principal component analysis (PCA) and OPLS-DA was used to identify global patterns and microarray probes with altered expression during the time course. The threshold for

exclusion from subsequent analyses was a Variable Importance to the Projection (VIP) score of less than one. In addition, OPLS-DA revealed that probes with low normalised fluorescence intensity measured across all samples generated identical VIP scores, unlike probes with a wider range of measured fluorescence. For this reason, a minimum of 100 normalised fluorescence measurement was selected to minimise the artefacts caused by these probes. The remaining probes were curated further as described below.

Curation of expression data

Probes with a standard error (between technical replicates) greater than 20% of average were removed. The probe sequences of the remaining probes were analysed using the basic local alignment search tool for highly similar sequences (BLAST, Altschul et al., 1990) against *N. tabacum*. Where no verified annotation was available, the predicted annotation was used. Probes with annotations described as "uncharacterised" were analysed using megablast against all *Nicotiana* species. Probes with no BLAST hit retained the GenBank IDs listed in the Agilent array description. Finally, GenBank IDs assigned to multiple probes were identified and the replicate, average (with standard error) and fold changes were recalculated for each unique gene model. It should be noted that the re-annotation did not attempt to identify how many unique genes were represented by the gene models, unlike the more robust method used by Coetzer et al. (2011). Gene models where the standard error of any of the sampling points was greater than 50% of maximum average signal observed were removed. A lookup function was used to identify GO terms assigned to each group of probes, however, no more than one of the probes in each group had been annotated with GO terms. This probe was therefore used in subsequent analyses of GO term enrichment. Where no *Nicotiana* BLAST hit was found, the most informative annotation from either the Ortho-MCL re-annotation or the original Agilent array description were used.

Analysis of curated expression data

The Ortho-MCL generated GO annotation was used to functionally categorise the probes identified by calculating GO enrichment using the online GOEAST platform (Zheng and Wang, 2008). The “customized result analysis” tool of GOEAST was used with the Ortho-MCL-generated GO annotation file, using the default parameters, namely a hypergeometric statistical test with Yekutieli multi-test adjustment and a maximum of 0.1 significance level.

Targeted analysis of specific gene families and metabolic pathways was performed using the publicly available Mapman (Thimm et al., 2004) annotation and manual searches of the protein top hits. Hierarchical clustering was performed using Gene Cluster 3.0 (De Hoon et al., 2004). Data were log scaled where appropriate, mean-centred and normalised (arrays and genes) before clustering with complete linkage using uncentred Pearson correlation of array and Spearman rank correlation for genes. Java Treeview (Saldanha, 2004) was used to generate the heatmaps.

Data represented in figures and tables were either represented as fold changes (represented by the prefix "Δt") calculated relative to the earlier sampling point, or as normalised fluorescence intensities at a specific sampling point (represented by the prefix "t") that were expressed relative to the relevant uninfected control (i.e. the t0 samples always have a value of 1).

Meta-analysis using transcriptome data in public databases

The Agilent Tobacco Gene Expression Microarray derived data deposited in ArrayExpress (Kolesnikov et al. 2015) and Gene Expression Omnibus (Edgar et al. 2002) was retrieved and normalised expression data for the curated gene models from this study were extracted from GSM2433207-GSM2433213 (Zurbriggen et al. 2009) and E-MEXP-3934 (Jada et al. 2014). For cross-comparison between datasets, data were expressed relative to appropriate controls within each dataset.

In order to cross-compare tobacco expression patterns with those in *Arabidopsis*, expression patterns of differentially expressed genes reported in Mathys et al. (2012) were compared to expression patterns of their homologous gene models in tobacco. To obtain homologs for tobacco gene models, protein sequences corresponding to the microarray probe targets were sourced from NCBI. These sequences were aligned using BLAST to the entire Uniprot database to identify *Arabidopsis* homologs.

3.2.4 qRT-PCR analysis

The plant material used for qRT-PCR analysis was the same that was used for microarray analysis, however leaf positions (1, 4 and 5) that were not used for microarray analysis, but were harvested during the same experiment, were included. With the exception of leaf 3, where the RNA-extraction method of Coutos-Thévenot et al. (2001) was used, RNA extracts for qRT-PCR analysis were obtained using the Sigma Spectrum Total Plant RNA kit (Merck, Darmstadt, Germany). RNA extracts were DNase treated with RNase-free DNase (Roche) and purified using the Qiagen RNeasy mini kit (Qiagen, Hilden, Germany). Leaf 3 RNA was reverse transcribed using oligo-dT primers and the ImProm-II Reverse Transcriptase System (Promega, Madison, WI, USA). RNA extracts from other leaves were reverse transcribed using the SensiFast cDNA Synthesis Kit (Bioline, London, UK). Quantitative PCR was performed using an Applied Biosystems 7500 Instrument (Life Technologies, Carlsbad, CA, USA) using the KAPA SYBR® FAST qPCR kit (Roche).

Commonly used reference genes for tobacco were initially sourced from literature, but since no reference genes have been reported to remain stable during infection, instead absolute quantification using an external optical calibration standard and linear regression of expression (LRE) analysis was used (Rutledge, 2011; Rutledge and Stewart, 2008).

Primers (Table 3.2) were designed using the online PrimerQuest tool (Integrated DNA Technologies, Leuven, Belgium) with similar melting temperatures to those of the primers used for the external calibration. Targets were selected from the metabolic pathways that were identified during data analysis. For targets represented by a microarray probes, primers designed were to amplify products that partially overlapped with the microarray probes wherever possible.

Table 3.2 Primers used for reverse-transcriptase quantitative PCR analysis

Sequence ID	Microarray probe	Gene name	Primers	Amplicon
AF070976	A_95_P190077	9-divinyl ether synthase	5'-GGCAGGCTAATGTTGGTGGAGTTT-3' 5'-GCGCACACACACTTGATGACTTGA-3'	162 bp
X84040	A_95_P095528	linoleate 9S-lipoxygenase 5	5'-GGAATTCCTAACAGTGTGTCAAT-3' 5'-CCTTTAGCTGTAGCTGGAACTT-3'	150 bp
D85912	A_95_P017821	L-ascorbate peroxidase 2, cytosolic-like	5'-AGGCTCTCCTTTCTGATCCTGCTTTC-3' 5'-CAGCCCTCCCAACACAAGCTTAAA-3'	147 bp
XM_009773747.1	A_95_P297428	GIGANTEA-like	5'-GAGGATGGAGAAAGGGCAGAAGCATA-3' 5'-TACAACCAGAGAAGGACTATCTAGCGTACA-3'	126 bp
U07627.1	n/a	Catalase	5'-CTCGCGTTTAACCCTGGCCATATT-3' 5'-TGGCACCATCGCGGTGATTATT-3'	178 bp
AB091430.1	n/a	HRS203J	5'-GGTTAGCTTTACCCGTAGGGAGCAATAAG-3' 5'-GTCCTTCATCAGATCTTTCTCCGCTACAC-3'	134 bp
M20618	n/a	beta-1,3-glucanase	5'-GTGAGATGTGAGCTGATGAGACACTTGA-3' 5'-GTCACTGGATAACAATCCACGAGGACTTAC-3'	154 bp
EB439640	n/a	superoxide dismutase [Cu-Zn]	5'-CATGGTGCTCCTGAAGATGA-3' 5'-ACAACCACAGCTCTTCCAATGA-3'	146 bp

3.2.5 Analysis of volatile organic compounds

Plant material

Analysis of the volatile organic compounds (VOC) that remained trapped in the harvested tissue (residual VOC), was performed on a subset of samples (leaf 2 - leaf distal to the infection; leaves 4 and 5 (infected samples) and sampling points (t0, t24 [not leaf 4] and t48). These samples, as generated in section 3.2.2 were used for microarray and qRT-PCR analysis in addition to VOC analysis. A second round of analysis was performed on samples from an independent whole plant infection assay from tissue harvested at t0 and t48 from leaf positions 4 to 6 which were infected.

Chemicals and extractions

The volatile authentic standards, namely 1-octen-3-ol, pseudo-ionone, r-(+)-limonene, linalool, β-caryophyllene, trans-2-hexenal, trans-2-hexenol, 6-methyl-6-heptan-2-one, geraniol, nerol, (+)-α-terpineol, R-(+)-β-citronellol, 2,6 dimethyl-6-hepten-2-ol, trans-2-octenal, (1R)-(+)-fenchone, octanal, methyl jasmonate, α-ionone, β-ionone, damascenone, hexanal, decanal, trans-2-cis-6-nonadienal, trans-2-heptenal, 1-hexanol, trans-2-nonenal, the internal standard (IS), anisol-d_8, as well as the other chemicals such as tartaric acid, ascorbic acid, sodium chloride (NaCl), sodium azide (NaN_3) and methanol were all purchased from Sigma.

Head space (HS) solid phase microextraction (SPME), using a grey divinylbenzene/carboxen/poly-dimethylsiloxane (DVB/CAR/PDMS, 50/30 µm) fibre (Supelco, Bellefonte, PA, USA) was used for the extraction of volatile organic compounds, essentially according to Joubert et al. (2016), with a

few modifications. Approximately 100 mg of ground, frozen leaf tissue (exact weight recorded) was weighed into a 20 mL SPME vial and 1 mL of tartaric acid buffer (2 g/L tartrate, 2.1 g/L ascorbic acid and 0.8 mg/L sodium azide; pH 3.2) was added to each vial. Twenty µL of IS (100 ppm) and 0.5 g of NaCl were added before the vial was sealed for SPME.

Volatile analysis on gas chromatography mass spectrometry

The gas chromatography (GC) separation and analysis major volatile organic compounds in leaf tissues was carried out on a Thermo Scientific Trace 1300 GC system (Palo Alto, CA, Switzerland) coupled to a Triple Plus RSH auto-sampler and a Thermo Scientific TSQ 8000 Triple quadrupole mass spectrometer (MS) detector through a transfer line. Analysis was done using a Zebron FFAP capillary column (30 m × 250 µm ID, 0.25 µm). Desorption of analytes from the SPME fibre was performed in the injection port at 250°C by pulsed splitless mode for 1 min. The purge flow was 50 mL/min (for 2 min). The column operating head pressure was raised from 111 kPa to obtain a pulse pressure of 300 kPa for 1 min. Helium was used as carrier gas with a constant flow rate of 1 mL/min. The oven parameters were as follows: initial temperature of 40°C (2 min), a linear increase to a final temperature of 240°C (at a rate of 0.8°C/min), and the temperature was held at 240°C for a final 2 min. The total run time was 28 min. The MS detector was operated in scan mode (electron ionisation) and both the transfer line and ion source temperatures were maintained at 250°C. The scan masses ranged from 35 to 350 amu and the scan time was 0.2 second. The system was controlled with Xcalibur software version 1.4 (Thermo Scientific).

Data analysis

Volatiles in samples were identified according to their elution times and masses compared to those of the respective authentic standards and quantified using the calibration parameters. Compounds without available authentic standard were identified by matching their mass spectrum with the NIST/EPA/NIH Mass Spectra Library (Nist MS search, FairCom Corporation, 2011). For relative quantification, single ion count (SIC) was performed to integrate peak areas for specific compounds (Table 3.3). The peak area integration of total ion count (TIC) was used for untargeted analysis. SIC and TIC peak areas were normalised to the SIC peak area of the IS and sample fresh weight. The selected ions used for the integration of peak areas of the respective compounds of interest, their retention time on the Zebron column, and quantifier molecules are summarized in Table 3.3. Normalised SIC and TIC peak areas were analysed in SIMCA 14, using unsupervised PCA of univariate scaled data. Statistical significance was calculated in Excel using Student's T-tests.

Table 3.3 Quantifier and qualifier ions and retention times used for GC-MS integration

Compounds	Retention time (min)	Ion	Quantifier
N-Hexanal	4.76	82	Trans-2-Hexanal
β-Myrcene	4.94	93	Limonene
α-Pinene	5.78	93	Limonene
α-terpinene	5.96	93	Limonene
Limonene	6.26	93	Limonene
Sabinene	6.41	93	Limonene
Cineol	6.49	93	Limonene
2-Hexanal	6.56	83	Trans-2-Hexanal
Trans-2-Hexanal	6.86	83	Trans-2-Hexanal
Gama-Terpinene	7.03	93	Limonene
α-Terpinolene	7.62	93	Limonene
Octanal	7.86	55	2-Octenal
1-Octen-3-one	8.05	55	MHO
2-Heptanal	8.41	55	2-Heptanal
6-Methyl-6-heptan-2-one	8.58	108	MHO
IS(Anisol)	8.67	116	-
1-Hexanol	8.77	55	1-Hexanol
3-Hexanol	9.20	55	1-Hexanol
Nonenal	9.34	55	2-Octenal
Fenchone	9.32	81	Fenchone
2,4-Hexadienal	9.51	81	Trans-2-Hexanal
2-Octenal	9.86	55	2-Octenal
Cis-Linolool oxide	9.97	111	Cis-Linolool oxide
Trans-Linalool oxide	10.35	111	Trans-Linalool oxide
Cis-2,4-Heptadienal	10.38	81	2-Heptanal
Trans-2,4-Heptadienal	10.77	81	2-Heptanal
2-Nonenal	11.23	93	2-Octenal
Linalool	11.29	93	Linalool
Junipene	11.57	93	Linalool
Trans-b-caryophyllene	11.73	93	Linalool
Trans-b-caryophyllene	11.92	93	Linalool
4-Terpineol	12.03	71	4-Terpineol
Hotrienol	12.09	71	1-Hexanol
b-Cyclocitral	12.29	123	Linalool
2-Decanal	12.50	93	2-Octenal
α-Humulene	12.81	93	Linalool
α-Humulene	12.87	93	Linalool
a-Terpineol	13.14	93	a-Terpineol
Trans-trans-nona-2,4-dienal	13.31	81	2-Octenal
α-Farnesene	13.54	93	a-Terpineol
EE-α-Farnesene	13.77	93	a-Terpineol
Delta-Cadinene	13.87	161	Linalool
2,4-Nonadienal	13.99	81	2-Octenal
Citronellol	13.83	69	Citronellol
Nerol	14.31	69	Nerol
2,4-Nonadienal	14.51	81	2-Octenal
β-damascone	14.53	177	β-damascone
β-Damascenone	14.58	69	β-Damascenone
Geraniol	14.81	69	Geraniol
Geranylacetone	14.91	69	Geranylacetone
α-ionone	14.91	177	α-ionone
Propanoic acid	15.22	69	2-Octenal
Cis-Farnesol	15.69	69	1-Hexanol
β-ionone	15.83	177	β-ionone
Trans-β-ionone-5,6-epoxide	16.40	123	β-ionone
Trans-β-ionone-5,6-epoxide	16.54	123	β-ionone
Pseudo-ionone	16.87	124	Pseudo-ionone
Pseudo-ionone	17.76	124	Pseudo-ionone
Nonanoic acid	18.01	124	2-Octenal

3.3 Results

Curation of expression data was performed in parallel for the lesion and distal expression profiles, using the same parameters for both datasets (Appendix C to Chapter 3). Sixty-four percent of probes (27822) were removed due to low signal or excessive variation between replicates. After filtering for 2-fold expression change between any two sampling points and VIP score, 9970 probes were removed. 1011 of the remaining probes targeted the same gene models (some gene models were represented by more than two probes). Data from probes targeting the same gene models were averaged, leaving 3521 gene models (represented by a GO annotated probe) with a 2-fold change in expression between any two of the sampling points. Finally, only gene models with a 2-fold transcriptional response between consecutive sampling points (in other words, within a 12 h period), were selected for subsequent analyses, giving a total of 2529 gene models. Preliminary analysis had revealed that this approach (using only the 12 h period) encompassed all biological processes responding to infection. Genes were selected for RT-qPCR analysis to confirm the microarray-derived expression patterns (Figure 3.2). Good correlations were observed between RT-qPCR and microarray-derived expression patterns for highly induced transcripts *ascorbate peroxidase* (*APX*), *9-divinyl ether synthase* (*DES)* and *9-lipoxygenase (LOX*). *GIGANTEA* on leaf 2 displayed the same diurnal pattern using microarray and RT-qPCR, while a single sampling point (t12) differed between the two methods for leaf 3.

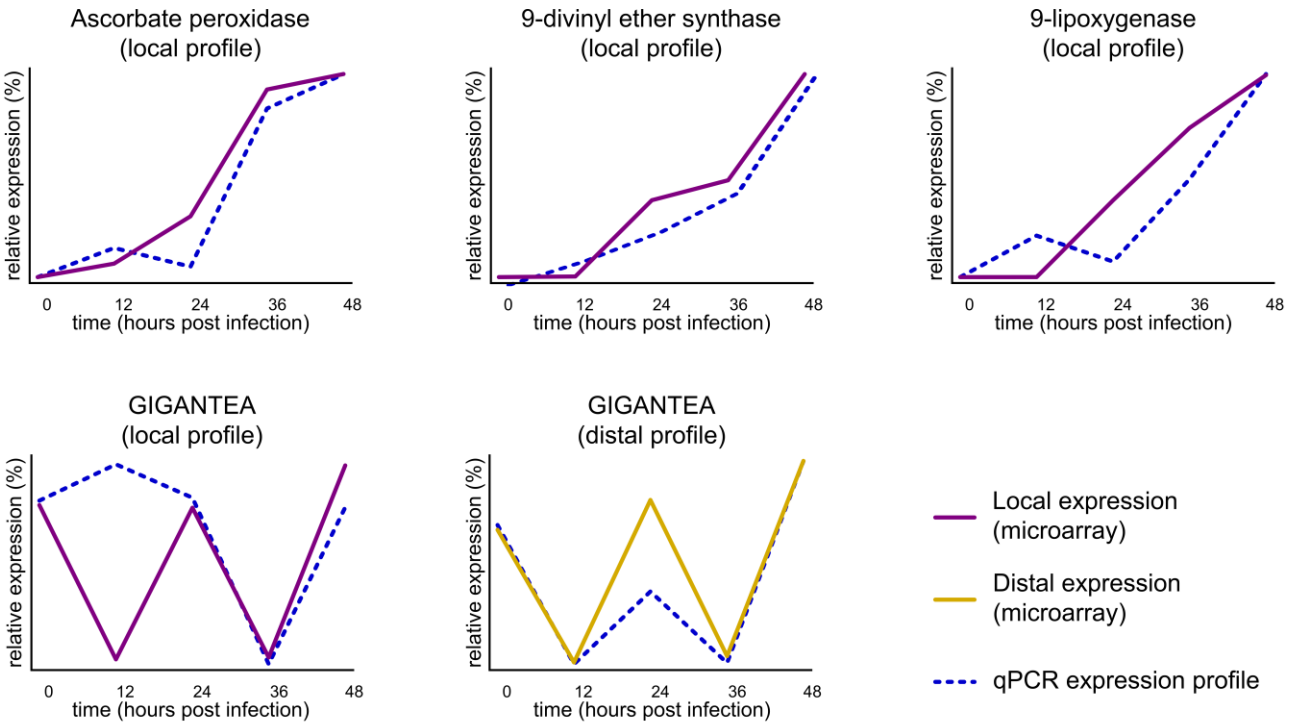

Figure 3.2 Validation of microarray expression patterns using quantitative reverse-transcriptase PCR. Four genes were targeted in leaf 3 (lesion expression profile), and one gene was targeted in leaf 2 (distal expression profile). Expression data were scaled so that maximum and minimum levels were at 100% and 0% respectively.

3.3.1 Symptom development and markers of defence response

Mature plants were challenged with a hypervirulent *B. cinerea* strain. The first clear macroscopic indication of lesion formation was observed at t36 (Figure 3.3A). Common markers for a local defence response, namely induction of chitinase (CHIT, Figure 3.3B), phenylalanine ammonia lyase (PAL, Figure 3.3C) and hypersensitive response-related (HSR203J, Figure 3.3D) were induced after t12 in tissue that included the infection spot, but not in the leaf distal to the infection. PAL expression levels continued to increase, while CHIT and HSR203J expression levels remained stable. Enhanced disease susceptibility 1 (EDS1, Figure 3.3E) and phytoalexin-deficient 4 (PAD4, Figure 3.3F), components of salicylic acid (SA)-mediated signalling were activated after t12 during lesion development, but were not induced in the leaf distal to the infection.

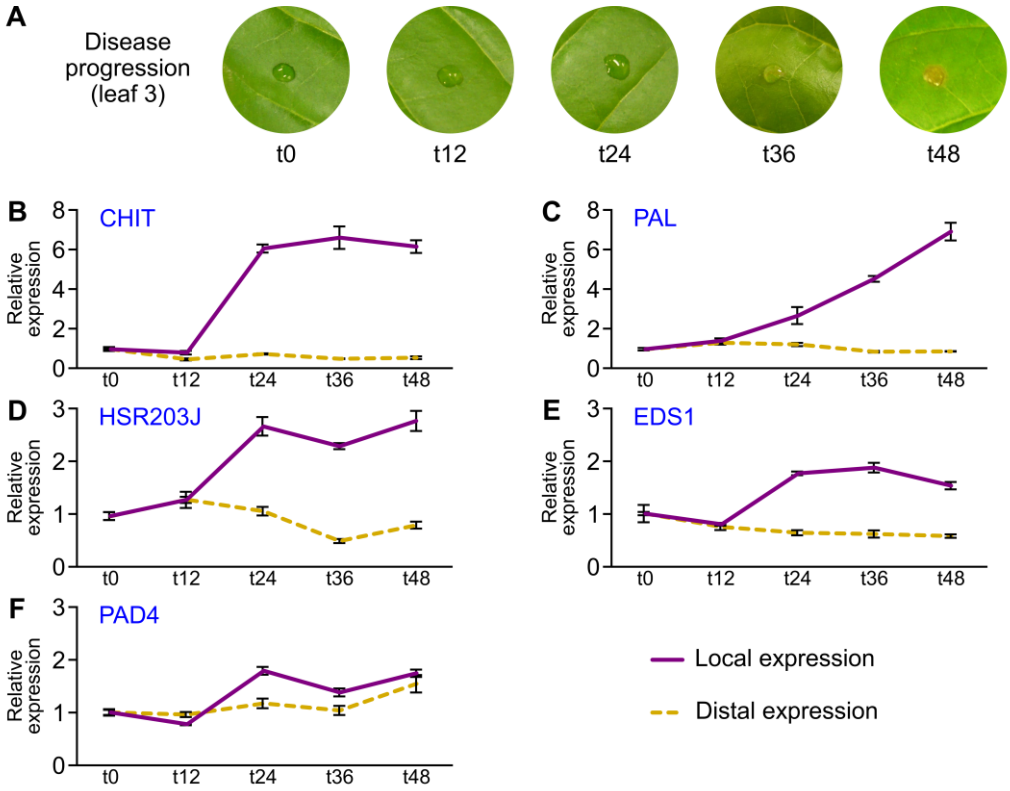

Figure 3.3 Disease progression and microarray expression profiles of marker genes. A: Photographs of representative inoculation sites of leaf 3 at each sampling point. Expression profiles of basal resistance chitinase (CHIT, B), phenylalanine ammonia lyase (PAL, C), hypersensitive response-related (HSR203J, D), enhanced disease susceptibility 1 (EDS1, E), phytoalexin-deficient 4 (PAD4, F). Expression profiles were normalised to their respective t0 and error bars represent standard error (n=3).

3.3.2 General features of transcriptional regulation

In the curated list of the transcriptionally regulated genes, 1018 were regulated both in leaf 2 (leaf distal to the infection) and leaf 3 (tissue including infection spot), while 1065 were regulated only during lesion development and 446 only in the leaf distal to the infection. PCA showed that the three replicates from each sampling point formed distinct groupings in both local (Figure 3.4A) and distal tissue (Figure 3.4B) and that two components explained 81% and 76% of the variance in the data respectively.

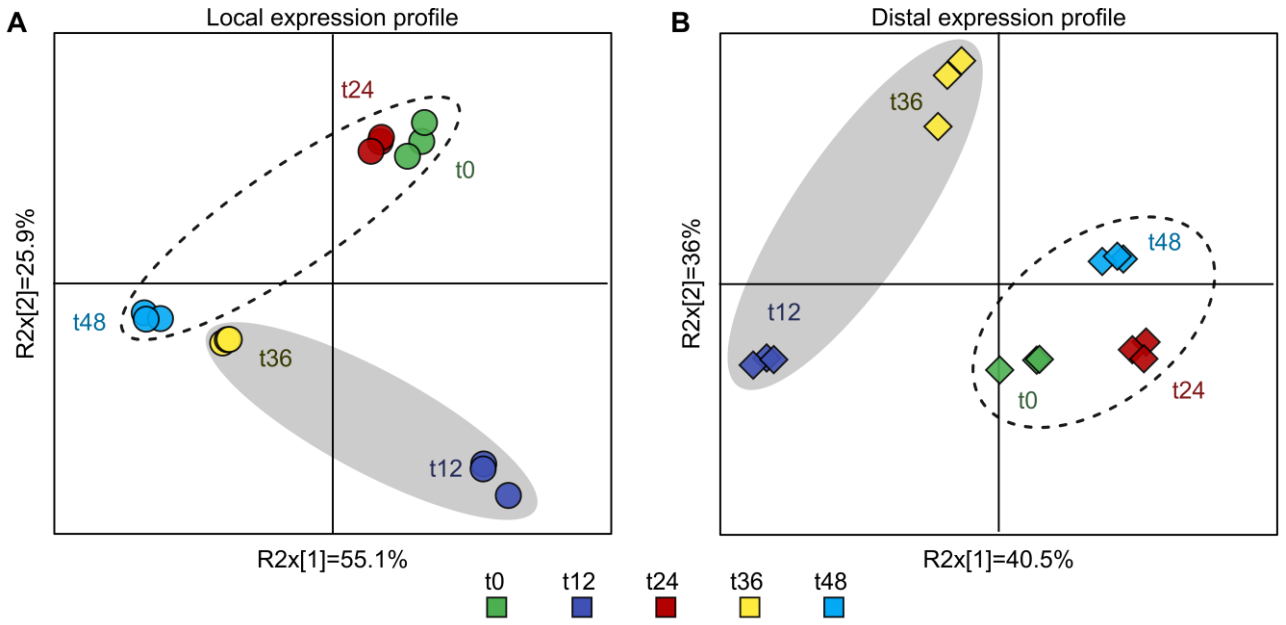

Figure 3.4 Principal component analysis score plots of curated expression data. A. Local expression profile. B. Distal expression profile. The samples inside the dotted line were harvested in the light phase of the photoperiod, whereas samples inside the shaded area were harvested in the dark phase. Axes are annotated with the percentage variance (R2x) explained by each principal component.

The distinction between samples harvested during the light and dark phases of the photoperiod was evident in the leaf distal to the infection, as well as in the samples t0-t24 at the infection sites, but thereafter (t36-t48) the influence of the diurnal pattern was less pronounced. Multivariate analysis therefore suggests that the driving force of gene expression in the leaf distal to the infection (Figure 3.5B) was the photoperiod, while lesion development and photoperiod exerted strong influences on gene expression in tissue surrounding the inoculation site (Figure 3.5A).

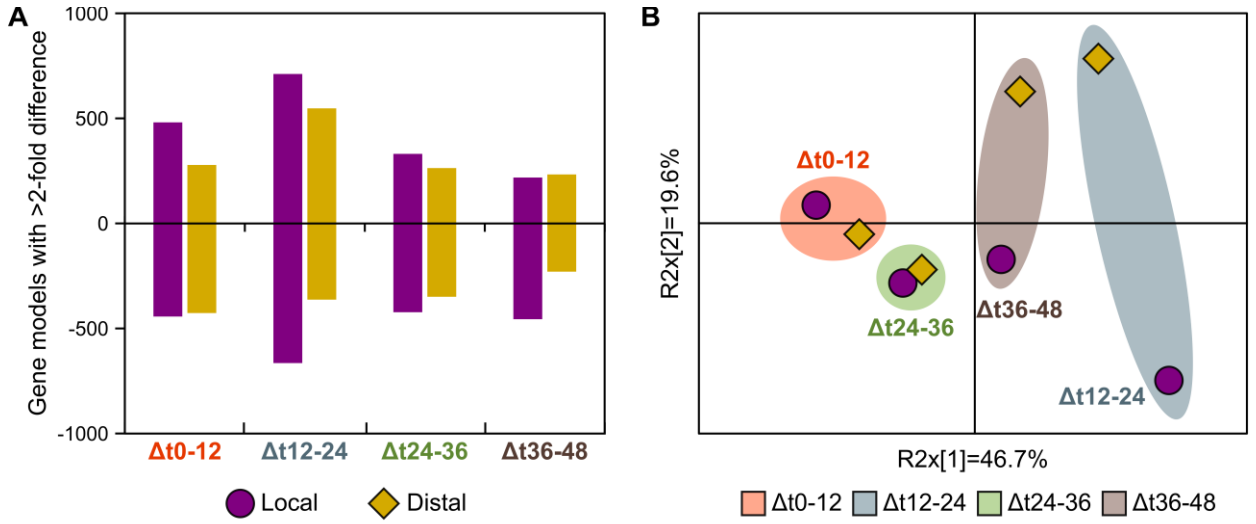

Figure 3.5 The transcriptional response between consecutive sampling points in leaf 3 (local expression profile, purple) and leaf 2 (distal expression profile, yellow). A. Number of gene models that passed initial curation steps and showed a two-fold or more change in expression between consecutive sampling points. B. Principal component analysis score plot of fold changes (Δt, relative to earlier sampling point). Axes are annotated with the percentage variance (R2x) explained by each principal component.

The number of regulated transcripts (Figure 3.5A) peaked between t12 and t24. In addition to the smaller number of transcripts regulated between sampling points in the leaf distal to the infection,

PCA revealed that the regulated transcripts were different, or responded differently, especially during the transition from the dark phase (t12/t36) to the light phase (t24/t48) of the photoperiod (Figure 3.5B).

A

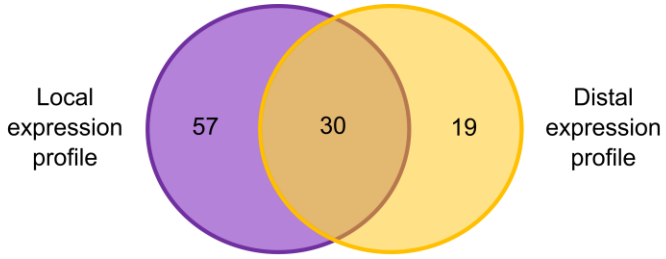

B

Local expression profile only	Local and distal expression profiles	Distal expression profile only
DEFENCE-RELATED	DEFENCE-RELATED	DEFENCE-RELATED
chitin catabolism	defence response	toxin catabolism
defence response to bacterium	defence response to fungus	
	defence response to other organism	METABOLIC PROCESSES
RESPONSES TO STIMULI	response to fungus	chromatin assembly
response to acid chemical	response to external biotic stimulus	cofactor biosynthesis
response to cadmium ion	response to other organism	nucleosome assembly
response to endoplasmic reticulum stress		secondary metabolite catabolism
response to heat	RESPONSES TO STIMULI	protein-DNA complex assembly
response to hormone	response to abiotic stimulus	
response to metal ion	response to biotic stimulus	PHOTOSYNTHESIS/LIGHT-RELATED
response to organic cyclic compound	response to chemical	chlorophyll biosynthesis
response to osmotic stress	response to cold	pigment biosynthesis
response to oxidative stress	response to endogenous stimulus	tetrapyrrole biosynthesis
response to water deprivation	response to inorganic substance	response to blue light
	response to organic substance	response to far red light
METABOLIC PROCESSES	response to stress	
aminoglycan catabolism	response to temperature stimulus	
carbohydrate derivative catabolism	response to wounding	
cell wall macromolecule catabolism		
coumarin biosynthesis	PHOTOSYNTHESIS/LIGHT-RELATED	
phenylpropanoid biosynthesis	photosynthesis	
transition metal ion homeostasis	photosynthesis, light harvesting	
	photosynthesis, light reaction	
PHOTOSYNTHESIS/LIGHT-RELATED	response to radiation	
circadian rhythm	response to light stimulus	

Figure 3.6 Enriched biological processes of the local and distal expression profiles. A. Venn diagram overlaying the enriched biological processes differentially expressed in 12-hour intervals. B. Summary of the processes that are unique to or shared between the lesion and distal expression profiles.

GO enrichment analysis served as a guideline for more specific mining of expression data, since the statistical test is sensitive to changes in GO annotation. For each 12 h interval between sampling points, GO enrichment analysis was performed separately for induced and repressed transcripts (Appendix D to Chapter 3). All significantly ($p<0.001$) enriched terms across the four periods were analysed using a Venn diagram (Figure 3.6A) to identify common and unique processes regulated during lesion development and/or in the leaf distal to the infection. The analysis revealed that transcriptional regulation of photosynthesis and defence responses was detected in both infected and distal tissues, along with responses to many stimuli, including biotic and abiotic factors, stress and light (Figure 3.6B). Transcriptional regulation uniquely enriched in the infection spot included chitin catabolism, defence response to bacterium, phenylpropanoid biosynthesis and responses to endoplasmic reticulum stress, water and oxidative stress and hormones. The leaf distal to the

infection, on the other hand, uniquely regulated chlorophyll biosynthesis, protein-DNA complex assembly and toxin catabolism on the transcriptional level.

Since GO enrichment analysis highlighted circadian rhythm and photosynthesis as being differentially regulated during the time-course, we used the Mapman annotation to quantify the cumulative expression of light signalling and photosynthesis (Figure 3.7A), as well as identifying circadian clock genes (Figure 3.7B). In the leaf distal to the infection, light signalling, photosynthesis light reaction, photorespiration and the Calvin cycle (Figure 3.7A) and the circadian clock genes (Figure 3.7B) continued to oscillate throughout the time-course. During local lesion development however, the expression levels of the gene models related to the light reaction were significantly ($P<0.01$) lower in the later sampling points (t36 and t48 compared to t12 and t24). During local lesion development, a disruption of the oscillation after t24 was observed in all four Mapman categories. The clock genes *GIGANTEA* and *pseudo response regulator 5* (Figure 3.7B) were no longer induced at t48, irrespective of the diurnal cycle.

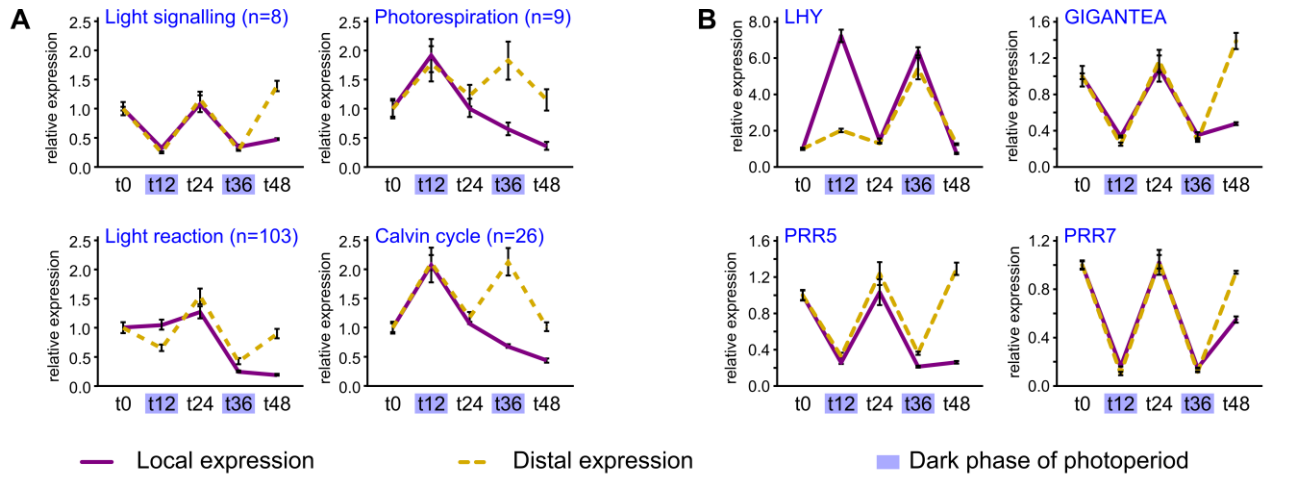

Figure 3.7 Photosynthesis-, light signalling and circadian clock regulation. A. The cumulative expression levels the Mapman bins signalling-light, PS-light reaction, PS-Calvin cycle and PS-photorespiration. n = gene models with the associated Mapman annotation. B. Circadian clock genes. Expression profiles were normalised to their respective t0 and error bars represent standard error (n=3). LHY: Late-elongating hypocotyl; PRR: Pseudo-response regulator.

Temporal regulation at and around the infection spot

Closer inspection of the GO terms enriched in each 12 h-period revealed that the local defence response ontologies were primarily activated after t12 and repressed after t36 (Table 3.4). The interval Δt12-24 was characterised by activation of diverse response-type GO terms, including responses to osmotic and oxidative stress and defence responses to bacteria and fungi. Light response and photosynthesis were repressed from t12 onwards, while the circadian rhythm ontology was repressed after t36. Coumarin biosynthesis (an indicator of monolignol biosynthesis) had a biphasic induction pattern (after t12 and again after t36), while cell wall macromolecule catabolism was activated after t12.

Table 3.4 Enriched (p<0.001) GO terms differentially expressed during the local defence response.

	Δt0-12*	Δt12-24	Δt24-36	Δt36-48
DEFENCE-RELATED				
chitin catabolic process		5.5E-06		
defence response		5.3E-06		
defence response to bacterium				2.1E-04
defence response to fungus		5.3E-04		
response to other organism		5.5E-10		5.1E-04
response to fungus	6.1E-05	6.7E-07		
RESPONSES TO STIMULI				
response to cold	5.1E-06	3.3E-06		1.5E-04
response to endoplasmic reticulum stress		6.4E-04		
response to hormone		7.1E-04		
response to osmotic stress		7.6E-04		
response to oxidative stress		1.6E-07		
response to metal ion		2.9E-10	4.3E-06	
response to temperature stimulus	1.9E-04			9.4E-04
response to water deprivation		4.1E-07		
response to wounding	5.3E-04	3.0E-06		
METABOLIC PROCESSES				
carbohydrate metabolic process	1.3E-05	1.9E-04	7.6E-05	
cell wall macromolecule catabolic process		5.5E-04		
cofactor metabolic process			3.9E-04	
coumarin biosynthetic process		5.3E-04		3.3E-05
nitrogen compound metabolic process		3.7E-04		
LIGHT- AND PHOTOSYNTHESIS-RELATED				
circadian rhythm				5.1E-04
photosynthesis	2.7E-04	2.5E-08	4.9E-21	1.7E-09
response to light stimulus		7.8E-09	3.5E-05	6.0E-08

Blocks with red/green highlight represent induced and repressed processes respectively. Yellow blocks indicate both induction and repression. * Δt: Underlying fold-change data were expressed relative to the earlier time point.

Highly induced/repressed transcripts during lesion development

During local lesion development (Table 3.5), three of the most highly induced transcripts (over 60-fold induction from t0 to t48) are predicted to encode for premnaspirodiene oxygenase, a key cytochrome P450 in the synthesis of the antifungal phytoalexin solavetivone (Takahashi et al., 2007). A sesquiterpene synthase was induced 15-fold at t12, while two genes involved in phenylpropanoid biosynthesis were also highly induced. Proteinase inhibitors and PR proteins also numbered among the most highly induced. Of the 27 PR protein transcripts that responded during lesion development, only one, described as chitinase-like protein 1, was repressed at t48, whereas only three transcripts did not increase at least two-fold. Several PR proteins were among the most highly induced on the microarray, including a basic chitinase, osmotin-like protein and acidic beta-1,3-glucanase. Chlorophyll-binding protein and circadian rhythm-related transcripts (*late-elongated hypocotyl*, *GIGANTEA*), were highly differentially expressed in a diurnal pattern.

Table 3.5 Gene models with >10-fold change between sampling points during the local defence response.

Probe ID	Mapman	Putative protein function	Δt0-12*	Δt12-24	Δt24-36	Δt36-48
HOUSEKEEPING						
A_95_P000401	Co-factor & vitamin metabolism	thiazole biosynthetic gene	-1.94	1.88	-4.32	1.36
A_95_P105552	development	dormancy-associated protein	-3.32	3.40	-2.74	0.70
A_95_P110457		dormancy-associated protein	-3.47	4.34	-3.32	0.40
A_95_P005551		senescence-associated protein-related	3.37	-1.79	1.94	-0.56
A_95_P025081		GIGANTEA-like	-3.06	3.67	-3.84	3.07
A_95_P186307		thiosulfate sulfurtransferase 16	-3.47	2.15	-0.47	-1.03
A_95_P154807	abscisic acid metabolism	nine-cis-epoxycarotenoid dioxygenase	-2.47	2.92	-4.06	0.44
A_95_P131032	metal handling	ferric reduction oxidase 6-like	3.52	-3.06	0.49	-1.51
A_95_P112417	RNA-regulation of transcription	Cys2-His2 type zinc finger	-2.06	3.40	-1.25	0.34
A_95_P127602		late-elongated hypocotyl (LHY)	2.85	-2.32	2.24	-3.47
A_95_P016256		LHY-like	3.28	-2.00	2.01	-3.32
A_95_P176787	transport	tonoplast intrinsic protein	3.39	-2.64	1.44	-1.69
METABOLIC PROCESSES						
A_95_P006901	amino acid synthesis	asparagine synthetase	-3.47	3.77	-0.45	-1.36
A_95_P026906		S-adenosylmethionine synthase 2-like	-0.09	3.60	0.64	1.12
A_95_P177242		S-adenosylmethionine synthetase	-0.10	3.42	0.71	1.2
A_95_P002686	cell wall-cell wall proteins	arabinogalactan protein	3.40	-3.84	1.06	-1.84
A_95_P188387		classical arabinogalactan protein 9-like	3.19	-3.32	2.03	-2.00
A_95_P212112		cellulose synthase-like protein H1	4.00	-1.89	4.50	-3.06
A_95_P223662		expansin-related B1	-1.64	3.66	-1.18	0.96
A_95_P199267		invertase/pectin methylesterase inhibitor	-2.4	3.39	-0.76	0.36
A_95_P187637		invertase/pectin methylesterase inhibitor	-3.84	4.29	-2.94	1.88
A_95_P206483	misc	mannose-binding lectin	-1.94	3.87	-1.12	0.96
A_95_P203282		short-chain dehydrogenase/reductase	-0.32	4.31	-0.94	1.66
A_95_P141577	N-degradation	Rho GDP dissociation inhibitor	-3.32	2.90	1.54	0.32
A_95_P301143	Not assigned	carboxymethylenebutenolidase	-3.06	2.35	-3.32	1.65
A_95_P023016		CCG-binding protein	-3.32	2.86	-2.06	0.55
A_95_P262981		epoxide hydrolase, putative	-1.51	4.40	1.34	0.83
A_95_P249062		extracellular Ca2+ sensing receptor	3.18	-3.64	1.12	-2.56
A_95_P033314		mitochondrial phosphate transporter	-0.38	3.39	0.16	0.92
A_95_P193007		pterin-4-alpha-carbinolamine dehydratase	3.46	-3.64	1.61	-2.25
A_95_P223057	protein-degradation	BTB AND TAZ DOMAIN PROTEIN 2	-4.06	3.87	-3.18	0.88
A_95_P134087	S-assimilation-APR	5'-adenylylsulfate reductase 1	4.38	-2.64	1.63	-0.54
A_95_P186367	secondary metabolism-carotenoids	phytoene synthase 2	3.61	-3.32	1.58	-2.06
A_95_P306888		phytoene synthase 2	3.55	-3.47	2.29	-1.84
A_95_P180402	secondary metabolism-terpenoids	hydroxymethylglutaryl-CoA reductase	-0.23	3.37	1.79	0.72
A_95_P004346		acetyl-CoA acetyltransferase	-0.69	4.15	-0.36	1.18
A_95_P210797		farnesyl diphosphate synthase	-0.22	3.45	0.20	0.88
A_95_P133452		geranylgeranyl diphosphate reductase	2.39	-3.32	1.02	-3.18
A_95_P250577		geranylgeranyl diphosphate reductase	2.34	-3.32	1.17	-3.47
A_95_P152722		sesquiterpene synthase	-0.62	3.97	-1.84	2.18
A_95_P240179	secondary metabolism-phenylpropanoids	acyltransferase-like protein	0.04	5.84	1.30	0.16
A_95_P007991		caffeoyl-CoA O-methyltransferase 3	-1.29	3.55	-0.54	1.47
A_95_P194292	misc-cytochrome P450	premnaspirodiene oxygenase-like	0.00	5.66	1.66	0.30
A_95_P193607		premnaspirodiene oxygenase-like	-0.51	5.33	1.18	0.61
A_95_P115107		premnaspirodiene oxygenase-like	-0.36	5.36	1.16	0.44
ENERGY GENERATION AND PHOTOSYNTHESIS						
A_95_P249012	gluconeogenese/ glyoxylate cycle	isocitrate lyase	-4.64	1.95	-1.47	0.12
A_95_P202867		malate synthase	-4.32	3.01	-1.22	-0.27
A_95_P026051	oxidative pentose phosphate	6-phosphogluconate dehydrogenase	-0.51	3.43	0.32	2.04
A_95_P133687	PS-Calvin cycle	Rubisco activase 1	5.77	-5.64	2.87	-3.32
A_95_P002906	PS-light reaction	chlorophyll a/b-binding protein	-3.18	0.70	-3.32	0.16
A_95_P003266		chlorophyll a-b binding protein 21	-3.84	2.38	-3.64	0.06
A_95_P026346		chlorophyll a-b binding protein 4	-0.64	-0.54	-3.32	0.14
A_95_P106952		chlorophyll a-b binding protein 6A- P	-1.74	2.99	-6.64	1.18
A_95_P105332		chlorophyll a-b binding protein 1	-3.84	2.23	-3.32	0.38
A_95_P006596		chlorophyll a-b binding protein 2	-3.18	3.95	-5.64	-0.20
A_95_P107847		chlorophyll binding protein	-2.25	1.34	-3.32	0.32
A_95_P195147		chloroplast-targeted protein	-1.84	1.82	-3.47	1.62
A_95_P012501		photosystem I light harvesting complex	-1.84	1.36	-3.84	1.56
A_95_P005626		photosystem I reaction centre subunit VI-2	-2.32	1.12	-4.06	1.55
A_95_P221817	tetrapyrrole synthesis	chlorophyllase-1-like	-0.54	5.00	-0.06	1.45
A_95_P249767		Mg protoporphyrin IX chelatase	2.34	-3.18	1.50	-3.84
A_95_P154167	tri-carboxylic acid cycle	carbonic anhydrase	2.82	-3.47	0.42	-2.47
A_95_P178237		carbonic anhydrase	4.10	-5.64	1.14	-1.84

Table 3.5 continues on next page

Table 3.5 continued

Probe ID	Mapman	Putative protein function	Δt0-12	Δt12-24	Δt24-36	Δt36-48
STRESS-RELATED						
A_95_P190077	jasmonate metabolism	9-divinyl ether synthase	0.18	**4.09**	-0.04	**1.05**
A_95_P177857	misc	glutathione S-transferase	**-3.84**	**3.80**	-0.29	0.59
A_95_P013836		ascorbate oxidase	**3.46**	**-3.18**	**1.96**	**-2.25**
A_95_P184047	stress-abiotic	17.3 kDa class II heat shock protein	0.19	**3.60**	**-3.06**	**3.15**
A_95_P149797		auxin-binding protein ABP19a-like	**3.70**	**-3.64**	0.39	**-1.64**
A_95_P029586		chaperone protein dnaJ 8, chloroplastic	**-3.84**	**2.63**	**-1.18**	0.26
A_95_P003006		dehydration stress-induced protein	**-2.94**	**4.05**	-0.18	-0.43
A_95_P242477		heat shock transcription factor B3	-0.29	**3.39**	**1.46**	**1.61**
A_95_P187597		osmotin-like	-0.07	0.15	**3.63**	0.96
A_95_P007686	stress-biotic	acidic beta-1,3 glucanase	-0.20	**1.43**	**4.57**	0.32
A_95_P103767		acidic beta-1,3 glucanase	-0.17	**1.56**	**4.15**	0.16
A_95_P108772		pathogenesis-related 1b	**-1.94**	**3.63**	**1.11**	0.78
A_95_P004306		systemic acquired resistance (SAR) 8.2a	**-2.40**	**3.53**	-0.56	0.43
A_95_P004321		SAR8.2b	**-2.40**	**3.52**	-0.40	0.41
A_95_P028711		SAR-related chitinase, basic	**-3.32**	**3.12**	0.81	0.66
A_95_P180617		SAR-related chitinase, basic	-0.12	**1.67**	**4.43**	0.31
A_95_P000771	misc-protease inhibitor...	microbial serine proteinase inhibitor	**-4.64**	**4.94**	**-1.43**	-0.32
A_95_P000776		microbial serine proteinase inhibitor	**-3.64**	**4.17**	-0.71	-0.34
A_95_P185737		proteinase inhibitor type-2	**-1.89**	**4.34**	**2.82**	0.70
A_95_P019016		proteinase inhibitor type-2	**-1.74**	**4.61**	**2.03**	0.32
A_95_P122247		trypsin inhibitor 1	-0.29	0.57	**3.71**	**1.91**
A_95_P185277		trypsin and protease inhibitor family	**2.83**	**-1.64**	**4.00**	0.16

* ΔtFold-change data were expressed relative to the earlier time point and log-scaled. Significant (fold change>2) induction and repression are highlighted in bold red/green respectively. Fold changes >10 are shaded for emphasis.

Detailed analysis of processes that were temporally regulated during localised defence

Cell wall modification

According to GO term enrichment, cell wall macromolecule degradation was differentially regulated during lesion development (Figure 3.6). Cell wall modification is represented on the microarray by three families of proteins, the xyloglucan endotransglycosylase/hydrolase (XTHs), extensins, and expansins. Hierarchical clustering of these genes (Figure 3.8) show that they group into four general expression patterns (A-D in Figure 3.8). During lesion development, most alpha-expansins and XTHs transiently increased at t12 (patterns C and D), whereas a small group of expansins and XTHs were induced after t24 (pattern A). Pattern B represented expansins and XTHs that responded to infection after t12.

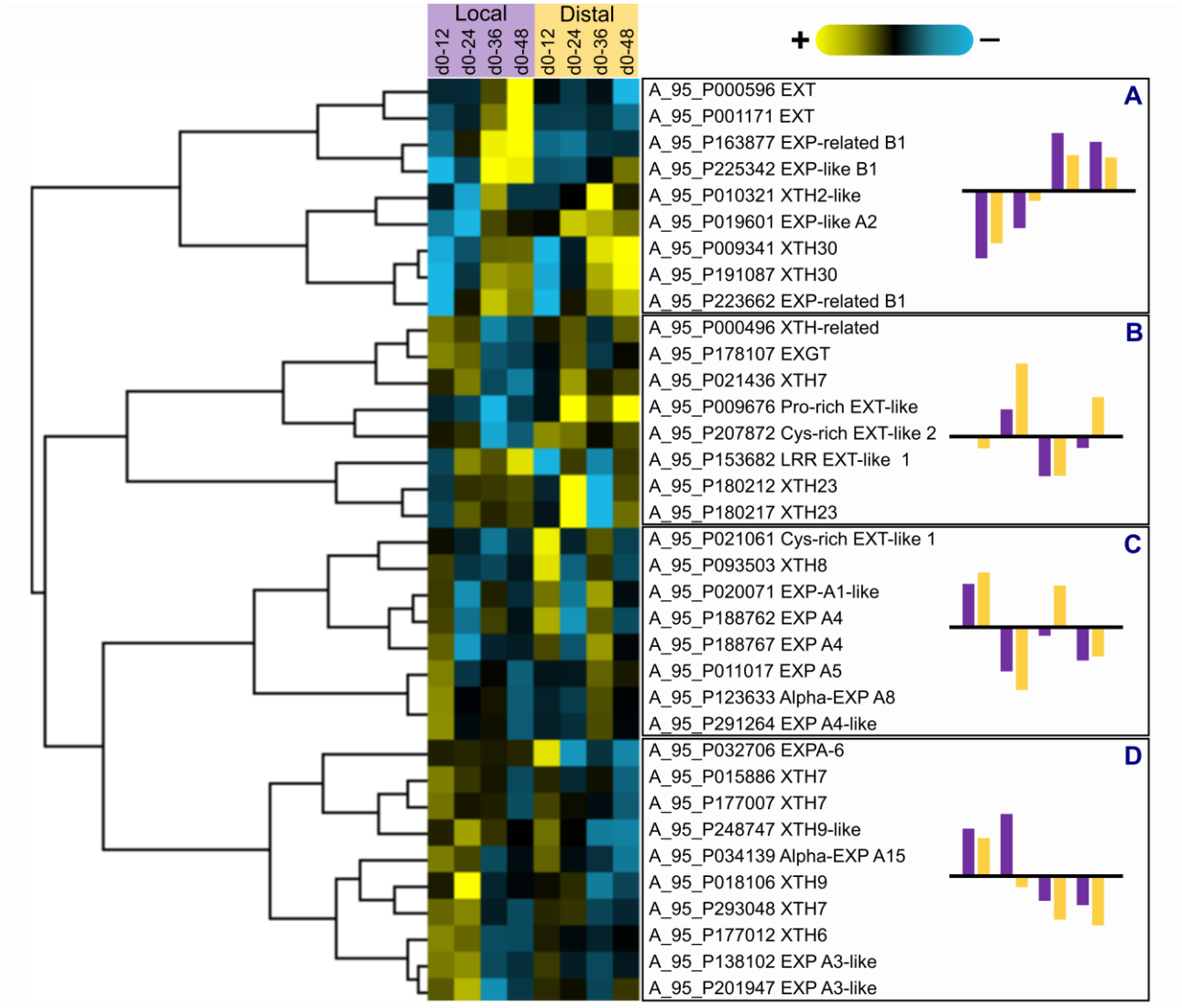

Figure 3.8 Cell wall modification-related transcripts. Hierarchical clustering of lesion and distal expression profile based on Spearman rank correlation. The subgroups (A-D) are outlined and the average expression profile is given as a bar graph. Expression levels are shown relative to t0. EXP: expansin; EXT: extensin; XTH: xyloglucan endotransglycosylase/hydrolase; XTR: XTH-related, EXGT: *N. tabacum* XTH.

Response to oxidative stress

In tissue surrounding the developing lesion, response to oxidative stress was induced after t12 (Table 3.4). Thirty transcriptionally regulated gene models were involved in redox metabolism, either generating or detoxifying ROS (summarised in Figure 3.9). Transcript levels of enzymes known to generate ROS included a single NADPH oxidase (NtNOX1) and two predicted polyamine oxidase isoforms (POA2 and POA4). NtNOX1 (Figure 3.9A) and POA4 (Figure 3.9B) displayed diurnal expression patterns with higher transcript levels in the light phase of the photoperiod. However, after t12 transcript levels doubled relative to basal levels. POA2 (Figure 3.9C) was induced 3-fold by t48 during lesion development.

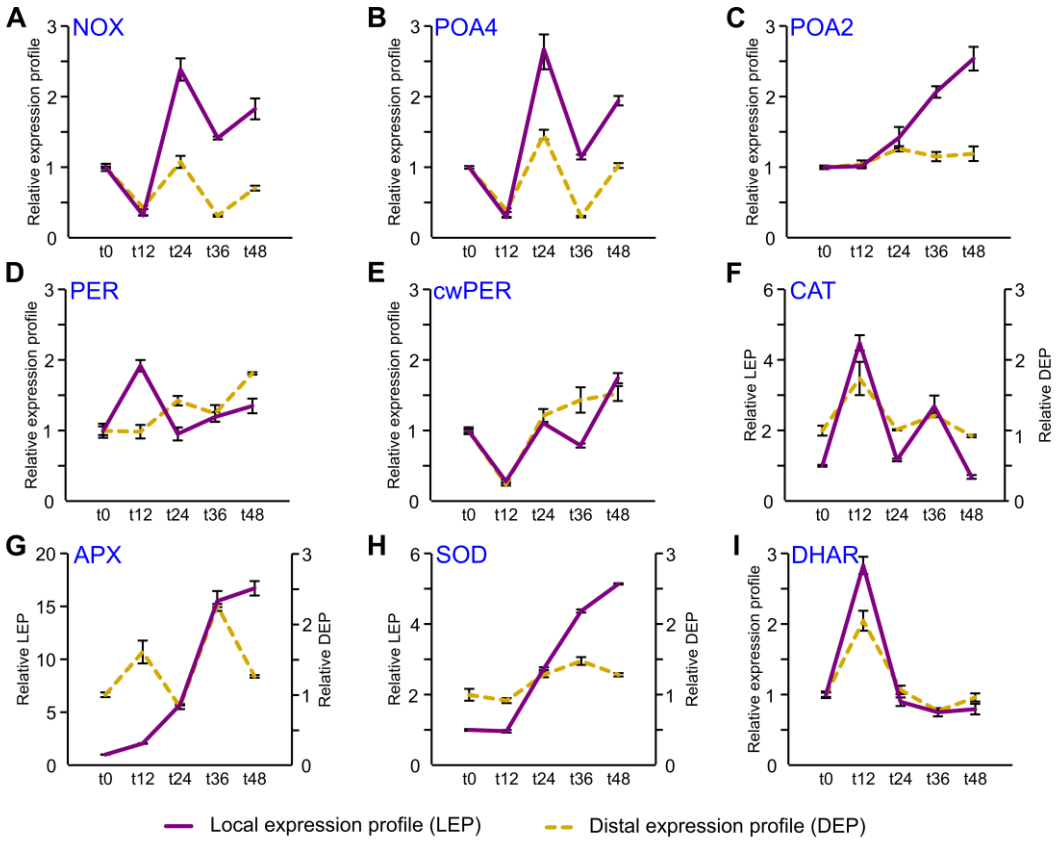

Figure 3.9 Redox related transcripts. NADPH oxidase (NOX, A). Polyamine oxidase 4 (POA4, B). Polyamine oxidase 2 (POA2, C). Peroxidase (PER, D). Cell wall peroxidase (cwPER, E). Catalase (CAT, F). Cytosolic ascorbate peroxidase (APX, G). Cytosolic superoxide dismutase (SOD, H). Dehydroascorbate reductase glutathione S-transferase (DHAR, I). Expression profiles were normalised to their respective t0 and error bars represent standard error (n=3).

Peroxidases (PER) are a large family that have a key role during plant development, and can consume or release ROS (Passardi et al., 2004). Transcripts of four PER transcripts, including a highly-expressed secretory PER (Figure 3.9D) were transiently induced at t12. The second most abundant transcript, a cell wall-bound PER (Figure 3.9E) decreased 5-fold at t12 but recovered to 1.5 times basal levels at t48. Transcripts of ROS detoxification enzymes catalase (CAT, Figure 3.9F), ascorbate peroxidase (APX, Figure 3.9G) and superoxide dismutase (SOD, Figure 3.9H), along with

ascorbate recycling enzyme dehydroascorbate reductase glutathione S-transferase (DHAR, Figure 3.9I) were also among the genes transcriptionally regulated. Cytosolic isoforms of these enzymes were highly induced during lesion development.

Phenylpropanoid metabolism

Since GO enrichment analysis (Table 3.4) and highly regulated transcripts (Table 3.5) highlighted phenylpropanoid metabolism, we investigated the phenylpropanoid pathways leading to monolignol synthesis (Figure 3.10) or other phenolic compounds (Figure 3.11).

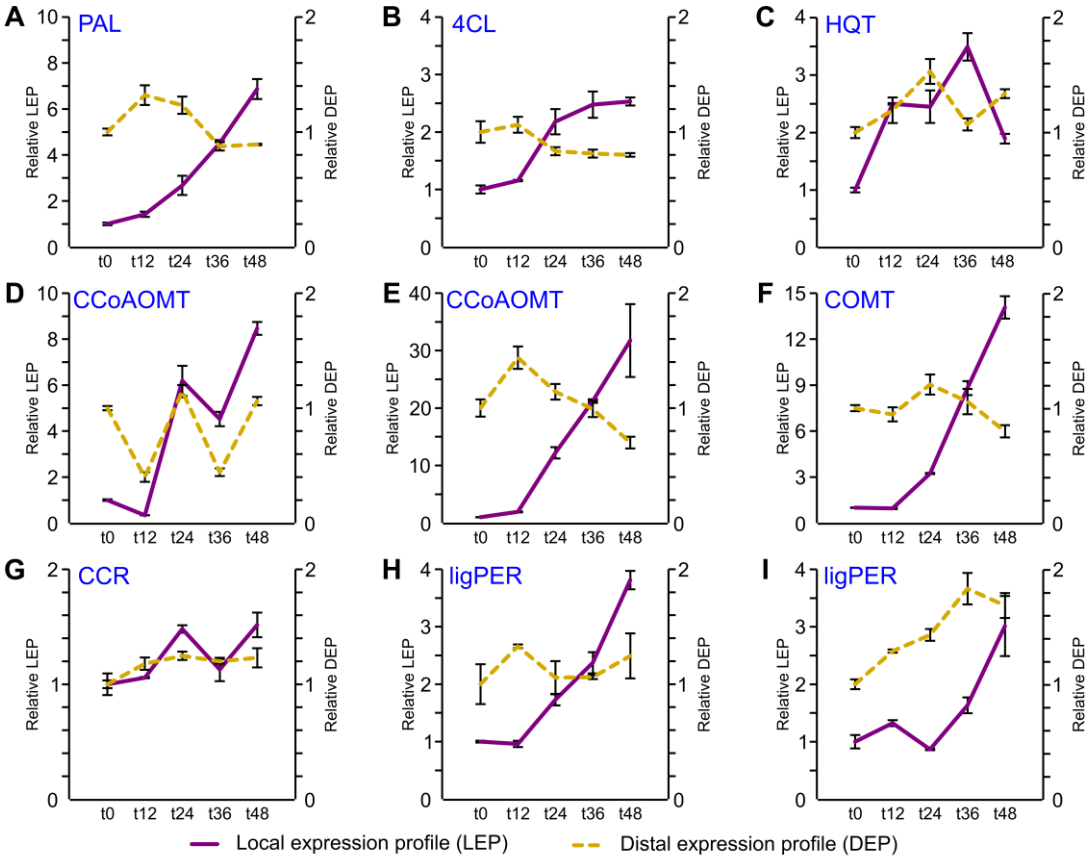

Figure 3.10 Phenylpropanoid metabolism leading to lignin synthesis. The general phenylpropanoid pathway is represented by phenylalanine ammonia-lyase (PAL, A) and 4-coumarate-CoA ligase (4CL, B). Monolignol synthesis is represented by hydroxycinnamoyl CoA quinate transferase (HQT, panel C), caffeoyl-CoA O-methyltransferase (CCoAOMT, D and E), caffeic acid 3-O-methyltransferase (COMT, F) and cinnamoyl-CoA reductase (CCR, G). In the cell wall, lignin-forming peroxidases (ligPER, H and I) incorporate monolignols into lignin. Expression profiles were normalised to their respective t0 and error bars represent standard error (n=3).

There was an significant induction of the phenylpropanoid pathway, with maximal expression of PAL (Figure 3.10A), caffeoyl-CoA O-methyltransferase (CCoAOMT; Figure 3.10D, E), caffeic acid 3-O-methyltransferase (COMT; Figure 3.10F) and lignin-forming anionic peroxidase (ligPER; Figure 3.10H, I) at t48 during the localised defence response. Other genes assigned to the Mapman bin for phenylpropanoid biosynthesis were significantly induced at the infection spot and surrounding tissue. Acyltransferase (Figure 3.11A), uncharacterised acetyltransferases (Figure 3.11B), agmatine coumaroyl-transferase (Figure 3.11C), aldehyde dehydrogenase (Figure 3.11D) and NADPH-

cytochrome P450 reductases (Figure 3.11E) were significantly induced after t12 during the local defence response.

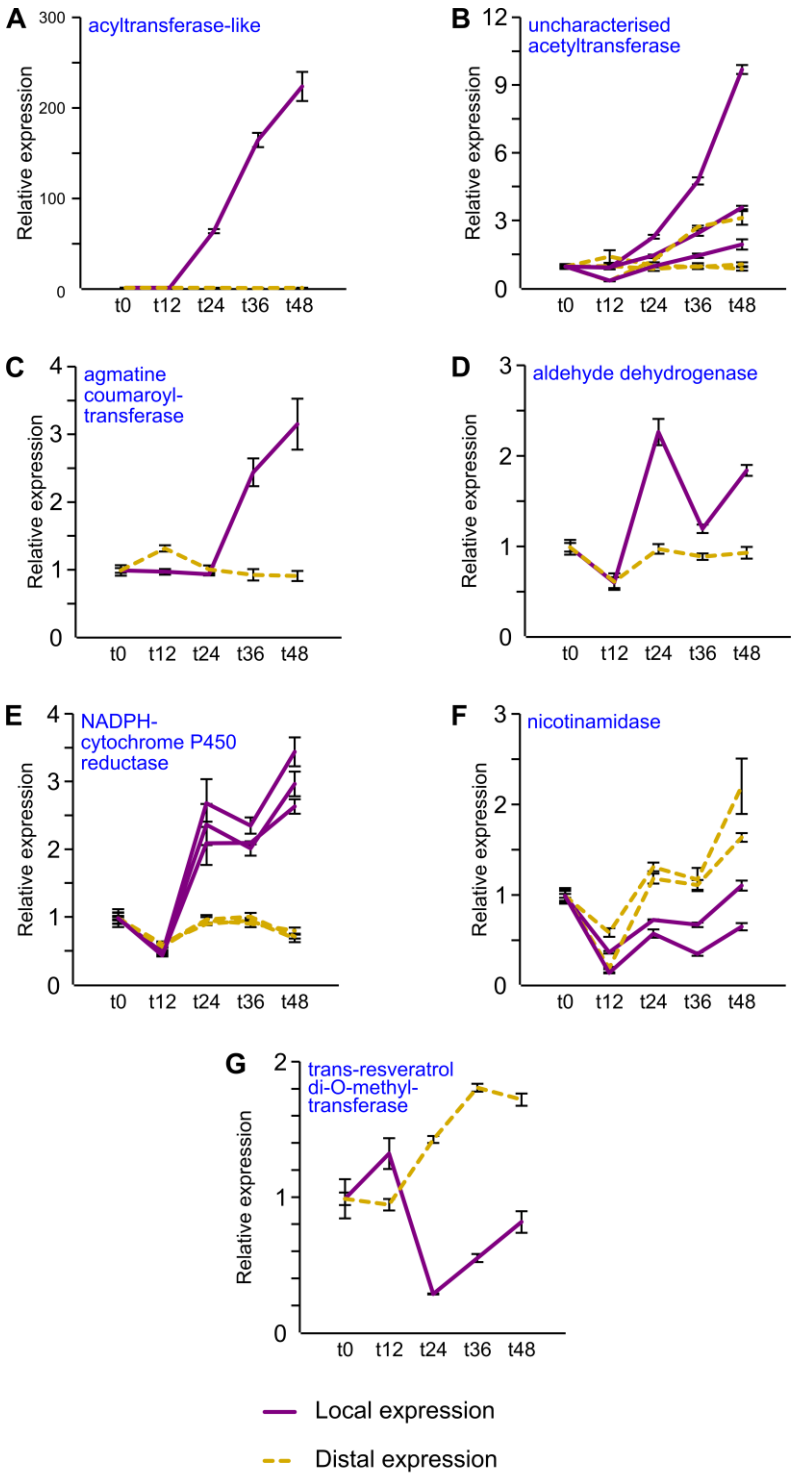

Figure 3.11 Phenylpropanoid-related transcripts, based on Mapman annotation. A. acyltransferase-like. B. three uncharacterised acetyltransferases. C. agmatine coumaroyltransferase. D. aldehyde dehydrogenase. E. three NADPH-cytochrome P450 reductases. F. two nicotinamidases. G. resveratrol di-O-methyltransferase. Expression profiles were normalised to their respective t0 and error bars represent standard error (n=3).

Defence hormone synthesis

Response to hormone, and JA and ET biosynthesis were enriched GO terms in the locally infected tissue (Figure 3.12). Since ET and polyamine biosynthesis depend on the same precursor (S-adenosylmethionine; SAM), and flux through the polyamine pathway can negatively affect ET biosynthesis (Nambeesan et al., 2012), transcripts related to polyamine biosynthesis were inspected alongside ethylene and JA biosynthetic pathways (Figure 3.12). SAM synthase (SAMS)-encoding transcripts for three isoforms increased after t12 (Figure 3.12A). Aminocyclopropane-1-carboxylic acid oxidase (ACO) was characterised by three expression patterns, representing inductions at t12, t24 or t36. The most induced isoform displayed a 15-fold increase in expression at t36. Arginine decarboxylase (ADC) was induced after t12, while spermidine synthase (SPDS) displayed a diurnal pattern that was slightly enhanced during local lesion development.

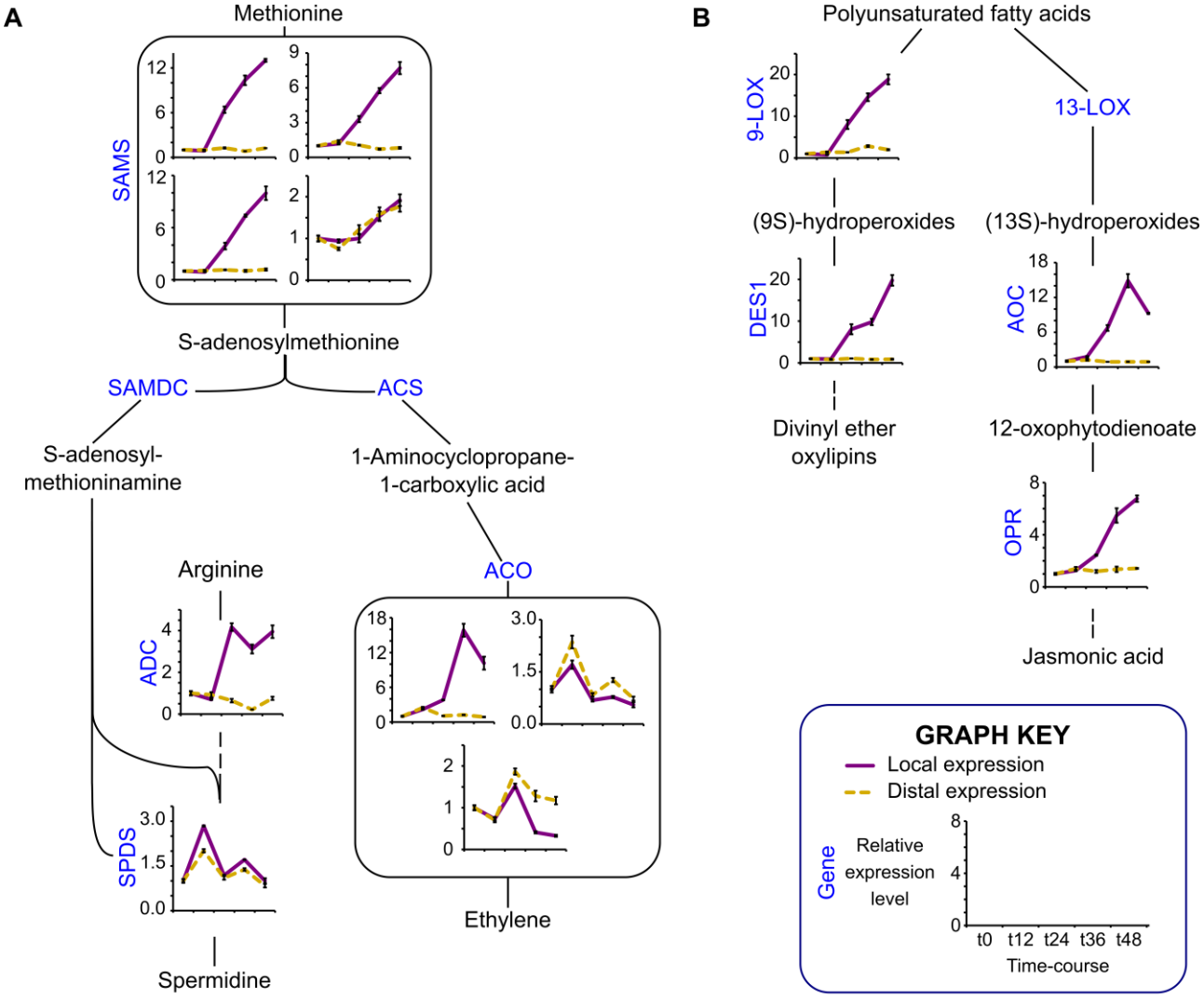

Figure 3.12 Defence-related hormone synthesis pathways. A. Polyamine and ethylene biosynthetic pathways originate from methionine. B. The 9S and 13S branches of the lipoxygenase pathway, leading to divinyl ether and jasmonate oxylipin biosynthesis. Data are expressed relative to the associated t0. Error bars represent standard error (n=3). ACC: 1-aminocyclopropane-1-carboxylic acid, ACO: ACC oxidase, ACS: ACC synthase, ADC: arginine decarboxylase, AOC: allene oxide cyclase, DES1: divinyl ether synthase 1, LOX: lipoxygenase with 9S or 13S positional specificity, OPR: 12-oxophytodienoate reductase, SAM: S-adenosylmethionine, SAMDC: SAM decarboxylase, SAMS: SAM synthase, SPDS: spermidine synthase.

The lipoxygenase (LOX) pathway (Figure 3.12B) forms a range of metabolites including JA and divinyl ethers (DVEs; Feussner and Wasternack, 2002). Two branches of the pathway are formed by LOXs with different positional specificities; 13-LOX initiates the synthesis of JA by the successive action of allene oxide cyclase (AOC), 12-oxyphytodienoic acid reductase (OPR) and beta-oxidation, while DVEs are formed by 9-LOX and divinyl ether synthase (DES). One LOX has been characterised in tobacco, producing predominantly (9S)-hydroperoxides (Fournier et al., 1993). Both branches of the LOX pathway were strongly induced during lesion development, particularly after t12, with *9-DES* being induced more than 17 times (Table 3.5).

Terpenoid biosynthesis and VOC content

Among the transcripts that were highly induced, terpenoid biosynthesis was activated after t12 (Table 3.5). These were representatives of the cytosolic mevalonate (MEV) pathway, and plastidial 2-C-methyl-D-erythritol 4-phosphate (MEP) pathway that produce sesquiterpenes and monoterpenes respectively. The MEV pathway (Table 3.6) was significantly induced after t12, as were two transcripts relating to sesquiterpene synthesis. In contrast, the MEP pathway was not significantly affected by lesion development.

Table 3.6 Terpenoid biosynthesis-related gene models during the local defence response.

Probe ID	Putative protein identity	Δt0-12$	Δt12-24	Δt24-36	Δt36-48
Plastidial 2-C-methyl-D-erythritol 4-phosphate (MEP) pathway					
A_95_P033161	1-deoxy-D-xylulose 5-phosphate synthase	0.36	-0.58	**-1.00**	-0.49
A_95_P184777	1-deoxy-D-xylulose 5-phosphate reductoisomerase	0.28	-0.51	0.03	0.07
A_95_P001031	2-C-methyl-D-erythritol 2,4-cyclodiphosphate synthase	**1.07**	**-1.29**	0.31	-0.20
A_95_P016076	4-hydroxy-3-methylbut-2-enyl diphosphate reductase	0.04	-0.69	**1.18**	0.19
Cytosolic mevalonate (MEV) pathway					
A_95_P004346	acetyl-CoA acetyltransferase*	-0.69	**4.15**	-0.36	**1.18**
A_95_P160452	hydroxymethylglutaryl-CoA synthase	0.04	**2.27**	-0.86	0.55
A_95_P180402	3-hydroxy-3-methylglutaryl-CoA reductase*	-0.23	**3.37**	**1.79**	0.72
A_95_P075045	mevalonate kinase	0.12	**3.23**	**-1.74**	**1.64**
A_95_P154872	diphosphomevalonate decarboxylase	0.19	**1.49**	-0.23	0.9
A_95_P142272	isopentenyl-diphosphate δ-isomerase I	0.16	**1.27**	**1.50**	0.78
A_95_P106557	phosphomevalonate kinase-like	-0.29	**1.69**	0.57	0.72
A_95_P190047	farnesyl diphosphate synthase	0.45	**2.98**	-0.62	**1.68**
A_95_P210797	farnesyl diphosphate synthase*	-0.22	**3.45**	0.20	0.88
Additional terpenoid-synthesis-related					
A_95_P018576	8-hydroxygeraniol dehydrogenase-like	**1.15**	**-1.32**	-0.60	**-1.00**
A_95_P255989	(+)-neomenthol dehydrogenase-like	**-1.94**	**1.82**	**1.24**	**-1.22**
A_95_P001231	5-epiaristolochene synthase	-0.84	**2.99**	**-1.69**	**1.22**
A_95_P152722	sesquiterpene synthase*	-0.62	**3.97**	**-1.84**	**2.18**

* also reported in Table 3.5. $Fold-change data were expressed relative to the earlier time point and log-scaled. Significant (fold change>2) induction and repression are highlighted in bold red/green respectively.

To further investigate secondary metabolites formed during infection, we analysed compounds in the tissue that volatilised during extraction and heating. VOCs were quantified relative to the IS (Anisol-D_8), using both a targeted approach based on the available standards (Appendix E to Chapter 3), and an untargeted approach where the chromatograms were aligned and total peak area was calculated (Appendix F to Chapter 3). PCA was used to provide a global overview of the data (Figure 3.13). Multivariate analysis of SIC data, representing C_{18}-norisoprenoids, C_6, C_8- and C_9-

compounds from the LOX pathway, monoterpenes and aldehydes (targeted analysis; Figure 3.13A), and TIC data (untargeted analysis; Figure 3.13B) showed a clear distinction between the leaf distal to the infection and tissue surrounding the inoculum, but TIC data did not clearly discriminate between t0 and t24, although t48 was distinct in both datasets.

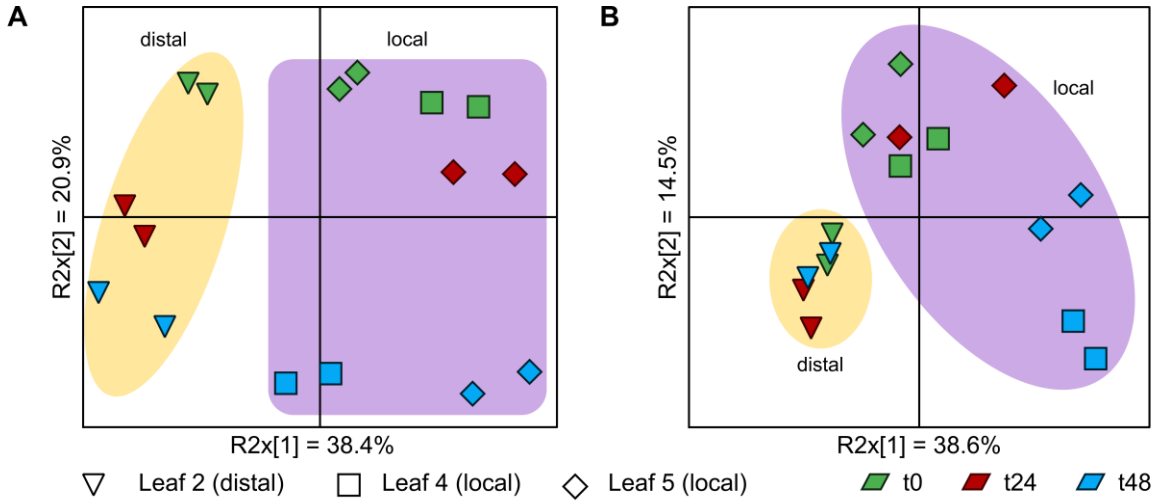

Figure 3.13 Principal component analysis of volatile organic compounds. A. Score plot of the leaf distal to the infection and tissue at/around the inoculum using single ion count (SIC) data. B. Score plot of the leaf distal to the infection and tissue at/around the inoculum using total ion count (TIC) data.

To identify compounds associated with each sampling point during lesion development, scores and loadings were calculated and plotted for SIC data of leaf 5, where data for all three of the analysed sampling points were available (Figure 3.14).

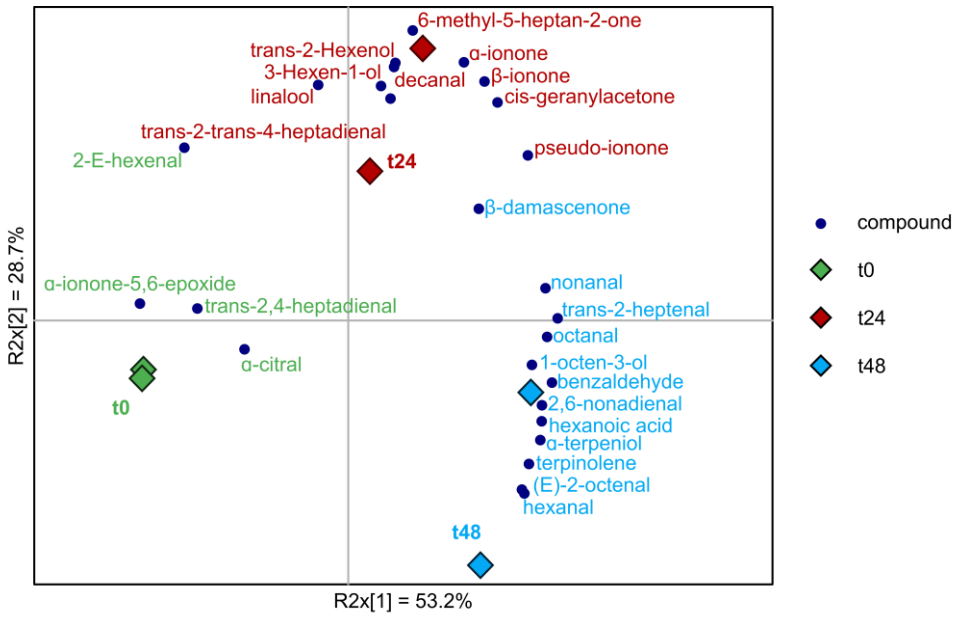

Figure 3.14 Biplot of score (samples) and loadings (compounds) of volatile organic compounds extracted from leaf 5 (local infection) using targeted quantification. Compound names are coloured according to the sampling point where their concentration is highest.

Of the 26 compounds identified, only four (2-E-hexenal, α-ionone-5,6-epoxide, α-citral, trans-2,4-heptadienal) were more abundant in uninfected tissue (t0). Several C_{18}-norisoprenoids (pseudo-, α-

and β-ionone, 6-methyl-heptan-2-one), LOX-derived green leaf volatiles (GLVs, 3-hexen-1-ol, trans-2-hexenol) and terpenoids (linalool, cis-geranylacetone) were enhanced at t24, while other LOX-derived compounds (hexanal, (E)-2-octenal, 1-octen-3-ol, octanal, 2,6-nonadienal, nonanal) and monoterpenoids (terpinolene, α-terpineol) were enhanced at t48. The individual compounds quantified during SIC were combined per type of compound to observe general changes during the time course (Figure 3.15). In tissues surrounding the developing lesion C_8-compounds ($p<0.05$) and C_9-compounds ($p<0.005$) as well as aldehydes ($p<0.1$) were accumulated. Since the analysis was performed on a single pooled biological sample, the same compounds were analysed in tissue from a second infection assay to investigate biological variability. Though infected and uninfected tissues could still be distinguished using PCA, the two experiments formed discrete groups along the first principal component (Figure 3.16).

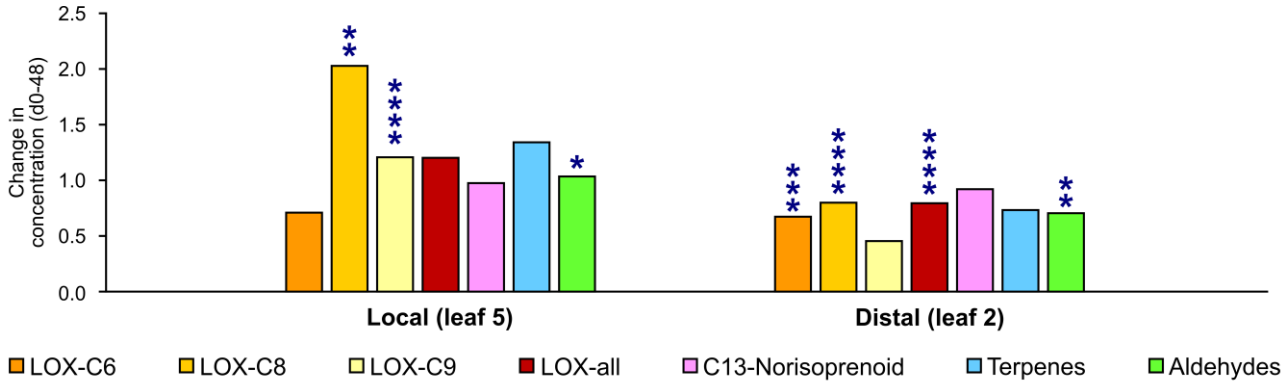

Figure 3.15 Change in concentration of six classes of volatile organic compounds (VOC) quantified during time-course. Data were quantified using single ion count peak areas and normalised to the internal standard and fresh weight. Asterisks represent significant difference between t0 and t48 per leaf position, based on Student's T-test. * p<0.1; ** p<0.05; *** p<0.01; **** p<0.005. LOX: Lipoxygenase pathway.

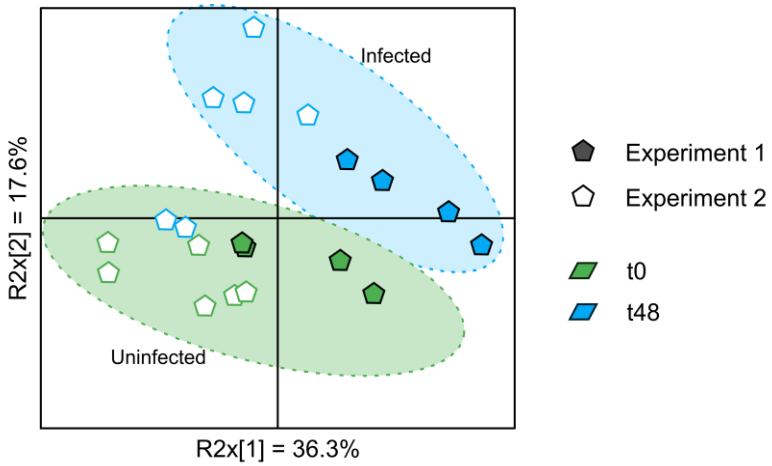

Figure 3.16 Multivariate analysis of volatile organic compounds in tissue from two independent experiments. Experiment 1 was used for VOC and gene expression analyses, while experiment 2 was an independent whole plant infection performed using the same *B. cinerea* strain and tobacco cultivar.

Temporal regulation during infection in a leaf distal to the infection

In contrast to tissue surrounding the infection spot, in the leaf distal to the infection, most GO terms displayed a diurnal pattern in the first 48 hours following infection (Table 3.7). Defence-related responses and photosynthesis-related responses followed a similar diurnal pattern, beginning with repression after t0. The diurnal pattern was confirmed when viewing the cumulative expression of photosynthesis-related transcripts based on Mapman ontology (Figure 3.7). Response to wounding was repressed at t12, before being induced. Hormone response was activated after t12 and t36. In the leaf distal to the infection, the majority of highly responsive transcripts (Table 3.8) were related to photosynthesis and followed a distinct diurnal pattern. Osmotin (PR-5), SAR8.2b and two microbial serine proteinase inhibitors were also highly induced after t12.

Table 3.7 Enriched (p<0.001) GO terms differentially expression in the leaf distal to the infection.

	Δt0-12*	Δt12-24	Δt24-36	Δt36-48
DEFENCE-RELATED				
defence response	4.6E-04		3.2E-03	7.2E-04
defence response to fungus	1.0E-03	1.7E-06		
response to biotic stimulus	5.3E-03	7.5E-07	5.8E-03	2.0E-03
response to fungus	1.5E-03	1.6E-07		
response to other organism	9.3E-03	1.1E-06		1.3E-03
response to stress			3.6E-07	8.8E-09
RESPONSES TO STIMULI				
response to cadmium ion			2.6E-03	4.2E-03
response to cold	6.1E-07	5.4E-04		
response to hormone		4.5E-03		9.6E-03
response to light stimulus				
response to metal ion	3.7E-03		2.6E-03	1.1E-03
response to osmotic stress				2.4E-03
response to temperature stimulus	1.7E-06	3.8E-04		7.1E-03
response to wounding	4.6E-04	1.2E-06		
LIGHT- AND PHOTOSYNTHESIS-RELATED				
chlorophyll biosynthetic process			8.2E-06	
chloroplast organization	4.2E-03			
photosynthesis	3.9E-07	3.2E-10	1.6E-26	2.2E-17
photosynthesis, light harvesting	1.7E-11	1.6E-09	2.5E-15	4.2E-16
photosynthesis, light reaction	9.2E-11	8.2E-11	5.7E-20	1.4E-18
tetrapyrrole biosynthetic process			4.4E-07	

* Δt: underlying fold-change data were expressed relative to the earlier time point. Blocks with red/green highlight represent induced and repressed processes respectively. Yellow blocks indicate both induction and repression.

Distal expression profiles of processes active in localised defence

In contrast to locally infected tissue, only 11 PR protein transcripts were induced more than two-fold and then only at the latest sampling point (t48). Included were the basic forms of PR1 and osmotins; the latter were in fact more strongly induced in the leaf distal to the infection compared to their expression at the site of infection. Phenylpropanoid biosynthesis-related nicotinamidase (Figure 3.11F) and trans-resveratrol di-O-methyltransferase (Figure 3.11G) were significantly induced in the leaf distal to the infection.

Table 3.8 Gene models with >10-fold change between sampling points a leaf distal to the infection.

Probe ID	Mapman	Putative protein function	Δt0-12*	Δt12-24	Δt24-36	Δt36-48
PHOTOSYNTHESIS-RELATED						
A_95_P010526	tetrapyrrole synthesis	NADPH-protochlorophyllide oxidoreductase	-1.32	2.10	-3.84	2.30
A_95_P133687	PS-Calvin cycle	Rubisco activase 1	4.45	-3.84	2.66	-3.32
A_95_P002906	PS-light reaction	chlorophyll a/b-binding protein	-5.64	6.43	-6.64	6.05
A_95_P179537		chlorophyll a-b binding protein 13	-3.32	4.34	-5.64	3.99
A_95_P003266		chlorophyll a-b binding protein 21	-5.64	6.51	-6.64	5.31
A_95_P003321		chlorophyll a-b binding protein 36	-2.74	3.62	-6.64	5.09
A_95_P177727		chlorophyll a-b binding protein 37	-2.84	3.87	-5.64	4.88
A_95_P026346		chlorophyll a-b binding protein 4	-2.84	3.13	-4.64	4.19
A_95_P106952		chlorophyll a-b binding protein 6A- P	-3.18	3.60	-5.64	4.27
A_95_P247017		chlorophyll a-b binding protein CP24 10A	-2.47	2.71	-4.32	3.36
A_95_P003231		chlorophyll a-b binding protein 1	-5.06	5.57	-5.64	4.79
A_95_P006596		chlorophyll a-b binding protein 2	-5.64	6.23	-6.64	4.91
A_95_P008206		chlorophyll binding protein 3	-3.64	3.94	-4.64	3.75
A_95_P009366		chlorophyll binding protein 6	-2.40	2.57	-4.32	3.51
A_95_P107827		chlorophyll binding protein Lhcb2.4	-5.64	5.16	-5.64	5.12
A_95_P078000		chlorophyll binding protein PSII type I	-4.32	4.81	-4.32	2.81
A_95_P111232		chlorophyll binding protein	-3.64	4.70	-4.64	3.99
A_95_P005701		photosystem I subunit O-like	-1.64	2.83	-3.47	2.83
A_95_P012501		PS I light harvesting complex	-3.06	3.28	-4.64	4.14
A_95_P188122		PS I light harvesting complex gene 4	-2.32	2.61	-3.47	2.74
A_95_P005626		PS I reaction centre subunit VI-2	-2.47	3.45	-4.64	3.29
A_95_P002626		rubisco large subunit-binding subunit alpha	-1.74	1.90	-3.32	2.57
HOUSEKEEPING						
A_95_P105552	development	dormancy-associated protein	-3.84	2.93	-0.92	1.62
A_95_P106782		dormancy-associated protein 1	-3.06	3.55	-0.69	0.92
A_95_P020166	regulation of transcription	pseudo-response regulator 7	-3.32	3.40	-3.47	3.54
A_95_P154807	abscisic acid metabolism	nine-cis-epoxycarotenoid dioxygenase 4	-3.47	2.88	-2.56	3.39
A_95_P110457	auxin metabolism	dormancy-associated protein	-4.06	4.94	-1.00	0.96
A_95_P187637	misc	invertase/pectin methylesterase inhibitor	-3.47	2.70	-0.94	2.15
A_95_P301143	Not assigned	carboxymethylenebutenolidase	-2.64	2.64	-3.47	3.82
A_95_P005551	Not assigned	senescence-associated protein-related	3.06	-3.32	2.90	-1.60
A_95_P223057	protein-degradation	BTB AND TAZ DOMAIN PROTEIN 2	-3.32	3.20	-2.56	2.63
STRESS-RELATED						
A_95_P015286	jasmonate metabolism	LOX homology domain	-3.64	3.44	-0.10	0.55
A_95_P003006	stress-abiotic	dehydration stress-induced protein	-3.32	2.97	-0.23	0.82
A_95_P176202		osmotin	-2.74	3.52	-0.12	0.58
A_95_P115287		osmotin-like	-3.32	2.85	1.24	1.16
A_95_P004306	stress-biotic	Systemic acquired resistance (SAR) 8.2a	-3.64	2.55	0.99	0.38
A_95_P004321		SAR8.2b	-3.64	2.58	1.14	0.23
A_95_P000771	misc-protease inhibitor...	microbial serine proteinase inhibitor	-5.06	3.97	1.82	0.26
A_95_P000776		microbial serine proteinase inhibitor	-4.06	3.13	1.10	0.31
A_95_P238389		P-rich protein EIG-I30	-4.32	1.78	-0.38	2.27
A_95_P000541		proline-rich protein DC2.15-like	-3.64	3.14	-2.84	3.35
A_95_P163972	transport-misc	DETOXIFICATION 27-like	0.29	-0.09	3.37	-2.84

*Δt: Fold-change data were expressed relative to the earlier time point and log-scaled. Significant (fold change>2) induction and repression are highlighted in red/green respectively. Fold changes >10 are shaded for emphasis.

Diurnal patterns in the leaf distal to the infection were observed for several processes that were activated during localised defence, including expansins and XTHs (Figure 3.8, pattern A), ROS generating enzymes NOX (Figure 3.9A), POA4 (Figure 3.9B), ROS detoxifying enzymes catalase (Figure 3.9F) and APX (Figure 3.9G), monolignol biosynthesis (CCoAOMT, Figure 3.10D) and ethylene and polyamine biosynthesis (ACO and SPDS, Figure 3.12).

Transcriptionally regulated processes/genes in a leaf distal to the infection

As could be seen from the smaller number of regulated genes in the leaf distal to the infection (Figure 3.5), local transcriptional changes in response to lesion development were generally more pronounced than those in the distal leaf. Comparison of the strength of transcriptional responses in local and distal tissues showed, as expected, that more transcripts changed prominently during lesion development, with only 5% of the 1924 gene models that responded at t48 in local tissues also responding in distal tissues. The maximum fold change in locally responding tissues at t48 was 50 times more than in distal tissues. However, some processes were activated more in the leaf distal to the infection (Figure 3.17).

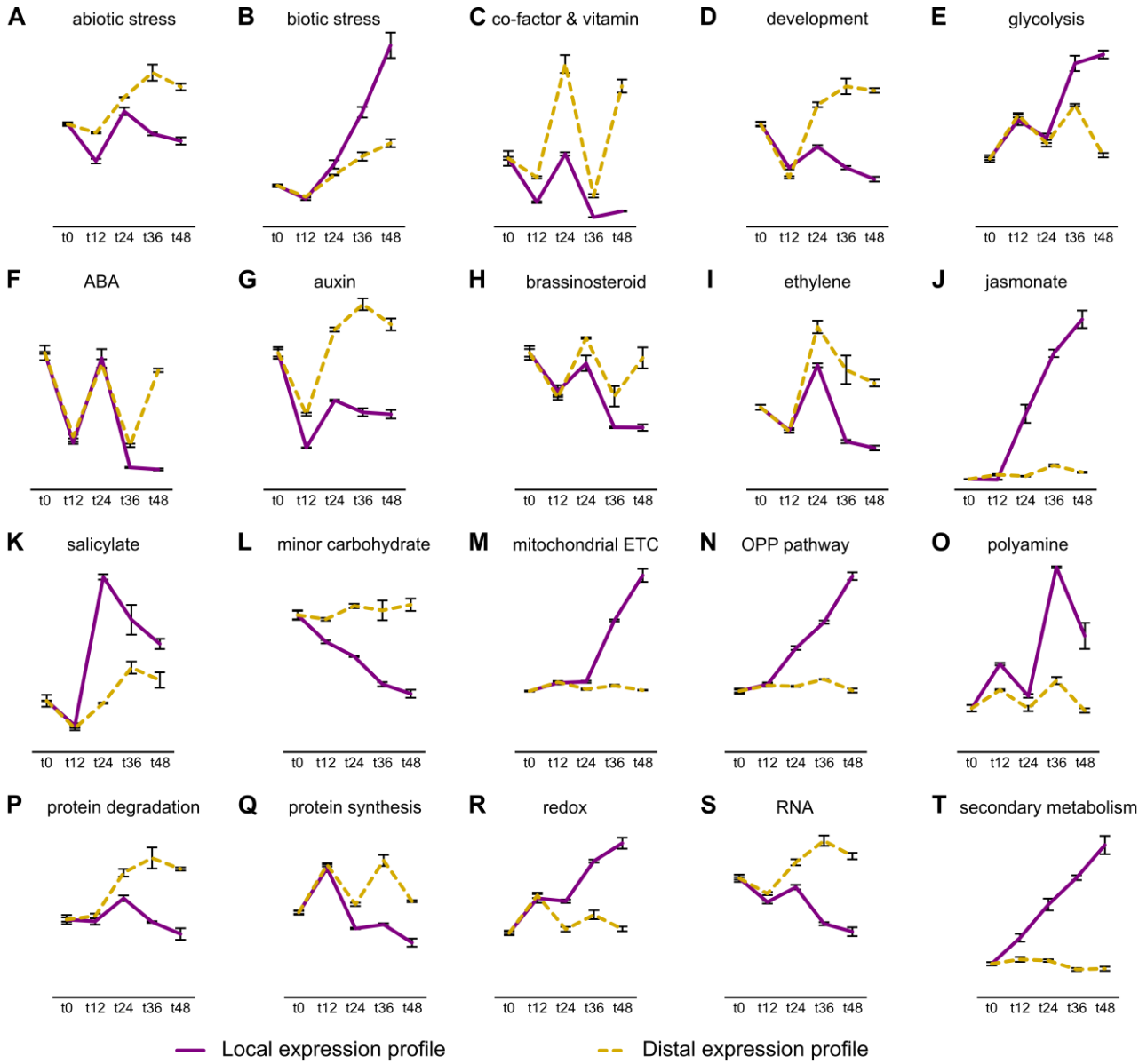

Figure 3.17 Cumulative expression of selected Mapman bins for the local and distal expression profiles. Data are expressed relative to the associated t0. Error bars represent standard error.

By calculating the cumulative transcript levels across high-level Mapman categories (Figure 3.17), diurnal patterns were observed for co-factor and vitamin metabolism (Figure 3.17C), jasmonate

(Figure 3.17J), brassinosteroid (Figure 3.17H) and ABA synthesis/degradation (Figure 3.17F), mitochondrial ATP synthesis (Figure 3.17M), glycolysis (Figure 3.17E) and oxidative pentose phosphate (Figure 3.17N), polyamine synthesis (Figure 3.17O), protein synthesis (Figure 3.17Q) and redox metabolism (Figure 3.17R). Development (Figure 3.17D), abiotic stress (Figure 3.17A), auxin synthesis/degradation/response (Figure 3.17G), RNA (Figure 3.17S) and ethylene synthesis/ degradation/response (Figure 3.17I) were induced in the leaf distal to the infection while being repressed in tissue with active local defence responses. Although biotic stress transcripts were also induced after t24, it occurred to a lesser extent than in locally infected tissue.

To identify transcripts with a stronger response in the leaf distal to the infection, the transcript levels were calculated relative to their associated t0 levels and those transcripts with a stronger induction at t48 were identified. In distal tissue, 27 transcripts were induced to a greater extent, of which five were of unknown function. The remaining transcripts (Table 3.9) included transcripts for SAR8.2n and osmotins.

Table 3.9 Top ten transcripts displaying higher induction in the leaf distal to the infection (orange dotted line) than during lesion development (purple solid line). The $\log_2$ of fluorescence intensity (±standard error) are given, along with the expression pattern.

	Pattern*		t0$		t12		t24		t36		t48	
glutathione S-transferase	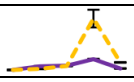	Local	9.4	±0.07	10.5	±0.06	10.7	±0.02	11.5	±0.03	10.0	±0.05
		Distal	8.6	±0.05	9.0	±0.05	9.7	±0.04	12.6	±0.13	10.3	±0.03
glutathione S-transferase	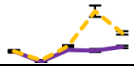	Local	11.1	±0.05	7.2	±0.04	11.2	±0.01	11.2	±0.12	11.5	±0.06
		Distal	8.4	±0.10	6.1	±0.04	9.0	±0.05	10.6	±0.10	9.8	±0.05
Invertase/PMEI	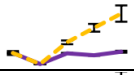	Local	11.1	±0.02	8.7	±0.04	11.1	±0.02	10.9	±0.02	11.3	±0.05
		Distal	9.9	±0.13	7.5	±0.10	10.7	±0.06	11.4	±0.09	11.8	±0.13
protease inhibitor/seed storage/LTP		Local	7.3	±0.04	6.4	±0.04	6.8	±0.01	7.1	±0.05	7.4	±0.03
		Distal	7.5	±0.12	6.0	±0.09	8.8	±0.09	6.0	±0.09	8.8	±0.16
cold, circadian rhythm, and RNA binding 2		Local	13.4	±0.07	12.7	±0.04	14.0	±0.12	12.7	±0.04	13.4	±0.07
		Distal	12.6	±0.08	12.3	±0.03	13.2	±0.03	12.9	±0.09	13.9	±0.13
uncharacterized acetyltransferase		Local	8.9	±0.07	7.5	±0.04	8.9	±0.04	9.5	±0.05	9.9	±0.10
		Distal	8.3	±0.05	6.9	±0.05	8.7	±0.06	9.8	±0.02	10.0	±0.08
osmotin-like	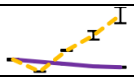	Local	11.3	±0.05	9.6	±0.12	10.9	±0.03	11.9	±0.04	12.1	±0.08
		Distal	9.7	±0.05	6.6	±0.10	10.5	±0.02	11.2	±0.10	11.8	±0.12
osmotin-like		Local	12.2	±0.04	10.5	±0.05	12.0	±0.02	13.2	±0.05	13.3	±0.07
		Distal	10.3	±0.02	6.9	±0.04	10.8	±0.01	11.7	±0.05	12.3	±0.07
antifungal protein CBP20	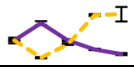	Local	12.4	±0.06	11.1	±0.09	14.3	±0.19	14.7	±0.07	15.0	±0.06
		Distal	11.3	±0.10	9.3	±0.10	11.1	±0.03	12.4	±0.02	12.4	±0.13
SAR8.2n	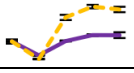	Local	13.6	±0.08	12.2	±0.03	13.6	±0.02	14.0	±0.02	13.9	±0.09
		Distal	12.2	±0.02	10.0	±0.05	13.2	±0.05	13.5	±0.03	13.5	±0.04

*Values depicted as expression patterns were normalised to t0 per tissue type
$ Normalised fluorescence values were log scaled (not expressed relative to t0)

SAR8.2n (Figure 3.18A) forms part of a multi-gene family that is induced by TMV and SA-treatment of tobacco (Alexander et al., 1992). Inspection of the other SAR8.2 family members revealed that they too were more strongly induced in distal tissue, but to a lesser extent than SAR8.2n (Figure 3.18B). Due to sequence similarity, it is likely that cross-hybridisation occurred between SAR 8.2c

and SAR 8.2n (Figure 3.18A) and between SAR8.2a and SAR8.2b (Figure 3.18B). Consequently their expression patterns were nearly identical. A single isoform, SAR8.2d (Figure 3.18C), was induced during local lesion development, but not in the leaf distal to the infection.

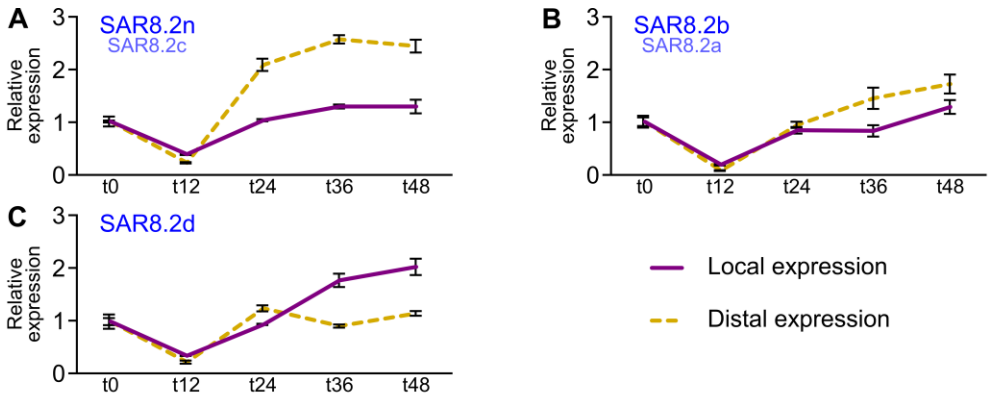

Figure 3.18 Systemic acquired resistance (SAR)-related family 8.2 members. Expression profiles were normalised to their respective t0 and error bars represent standard error (n=3). Potential targets for cross-hybridising microarray probes are shown below the gene with 100% sequence identity to the probe.

Secondary metabolism and VOC analysis of a leaf distal to the infection

In contrast to tissue around the developing lesion, the leaf distal to the infection did not induce either MEV or MEP pathways for terpenoid biosynthesis (Table 3.10). In addition, the content of the six classes of VOC (C_6-, C_8- and C_9-compounds from LOX pathway, C_{13}-norisoprenoids, terpenes and aldehydes) were slightly lower at t48 than at t0 (Figure 3.15), being highly significant ($p<0.001$) for C_6- and C_8-compounds from the LOX pathway and also significant ($p<0.05$) for aldehydes. α-ionone was the only compound that increased significantly ($p<0.05$) during infection, while octanal, decanal and trans-2,4-heptadienal decreased significantly (Figure 3.19).

Table 3.10 Secondary metabolite biosynthesis-related gene models of a leaf distal to the infection

Probe ID	Putative protein function	Δt0-12*	Δt12-24	Δt24-36	Δt36-48
A_95_P029636	LOX	0.83	0.14	**1.36**	**-1.60**
A_95_P178227	LOX-like	0.48	0.12	0.55	-0.79
A_95_P234754	LOX-like	**-1.29**	**1.82**	-0.25	-0.14
A_95_P052251	LOX-like	-0.71	**1.28**	-0.12	-0.38
A_95_P150027	alcohol dehydrogenase-like 4	**-1.15**	0.06	-0.54	**1.19**
A_95_P014261	1-deoxy-D-xylulose 5-phosphate synthase	-0.69	**1.67**	**-1.09**	0.14
A_95_P184777	1-deoxy-D-xylulose 5-phosphate reductoisomerase	0.33	**-1.06**	-0.14	0.32
A_95_P255989	(+)-neomenthol dehydrogenase-like	-0.92	**1.06**	**1.37**	**1.37**

* Δt: Fold change data were expressed relative to the earlier time point and log-scaled. Significant (fold change>2) induction and repression are highlighted in bold red/green respectively.

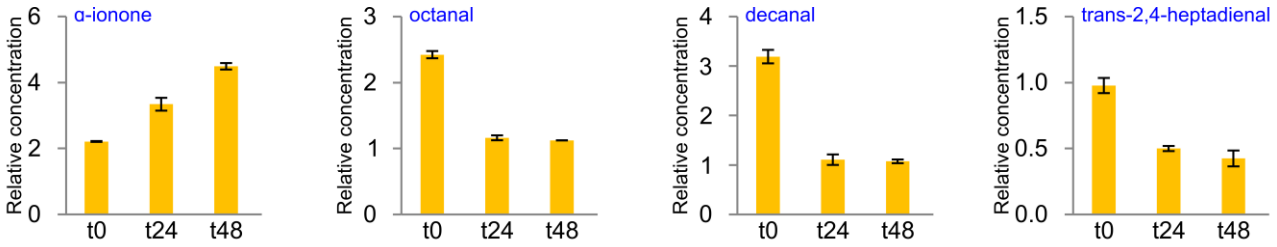

Figure 3.19 Volatile organic compounds extracted from leaf 2, a leaf distal to the infection. Only compounds with significant difference ($p<0.05$) between t0 and t48 are shown. The full dataset is included as Appendix E to Chapter 3. Error bars represent standard error (n=2).

3.3.3 Ontogenic differences in metabolite and gene expression profiles

VOC profiles of uninfected leaves were compared to clarify possible ontogenic effects before and during *B. cinerea* infection (Figure 3.20). The multivariate analysis revealed a clear ontogenic pattern with respect to leaf age. Several compounds were significantly ($p<0.05$) different between leaf two and leaves four and/or five, while only hexanoic (L4>L5) acid and β-damascenone (L4<L5) were significantly different between leaf four and leaf five. In infected tissue, only trans-2-trans-4-heptadienal was significantly different between leaves four and five, being higher in the older leaf.

Targeted transcript analysis of genes, though not of those encoding enzymes involved in VOC metabolism (Figure 3.21), revealed ontogenic effects in locally infected tissue and in uninfected leaves, suggesting that ontogenic effects may extend to other biological processes, such as PR proteins and ROS detoxification.

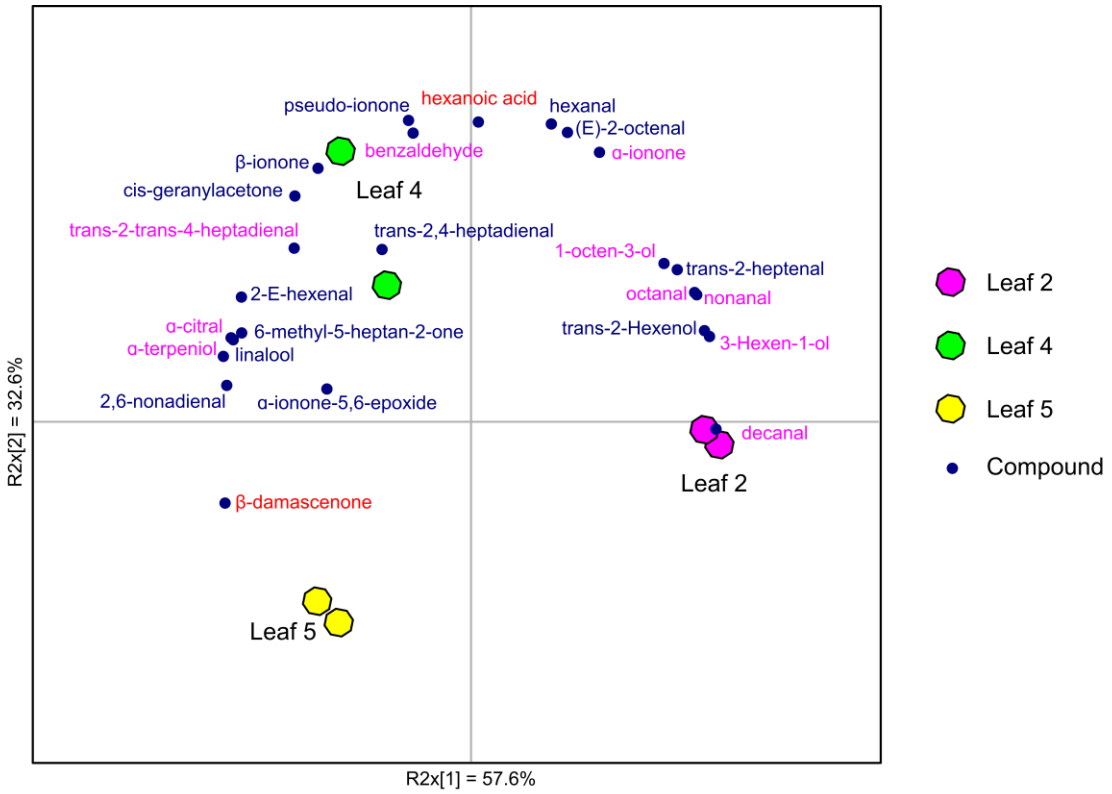

Figure 3.20 Biplots of principal component scores (samples) and loadings (compounds) of volatile organic compounds extracted from uninfected tissue from three leaf positions. Compound names in pink were significantly ($p<0.05$) different in leaf 2 compared to leaf 4 or 5. Compound names in red were significantly ($p<0.05$) different between leaf 4 and leaf 5.

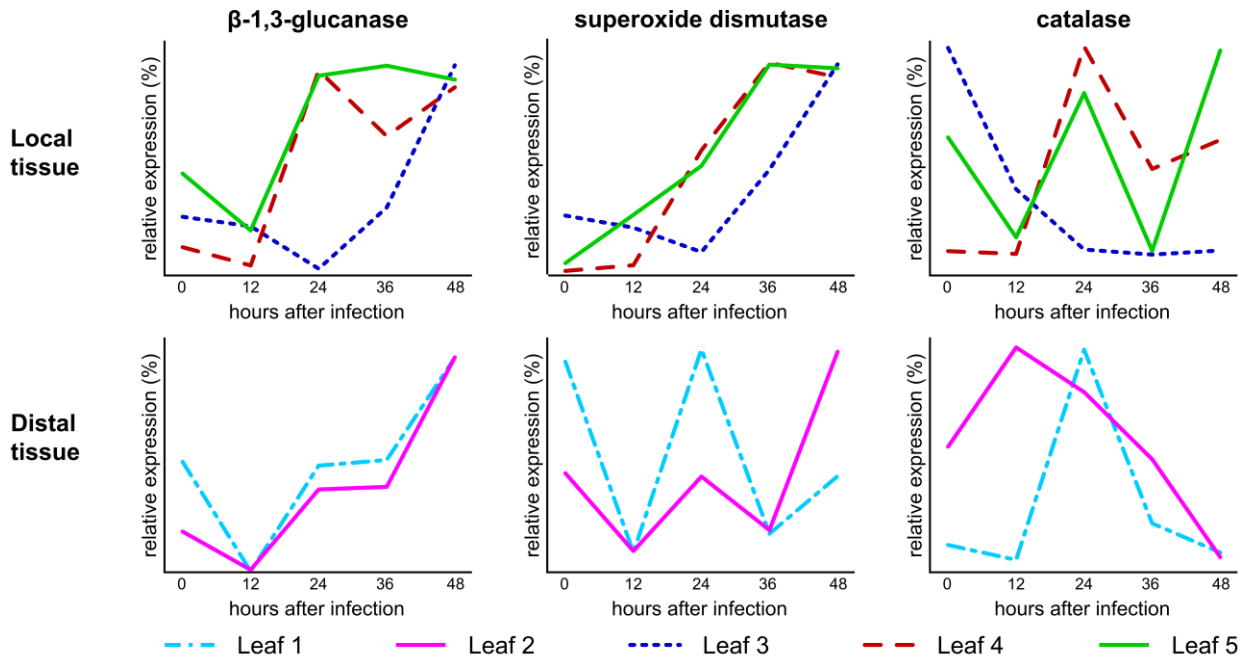

Figure 3.21 Expression profiles across leaf positions, showing an ontogenic effect. Expression levels were determined using quantitative PCR and the linear regression of expression (LRE) method. Expression data were scaled so that maximum and minimum levels were at 100% and 0% respectively.

3.3.4 Comparison of tobacco transcriptional responses to those in an *Arabidopsis-B. cinerea* pathosystem

Expression patterns observed in this study were compared to those obtained using *Arabidopsis* as host plant by identifying homologous genes in *Arabidopsis* (Mathys et al., 2012; Appendix G to Chapter 3). Four groups of gene models and homologous *Arabidopsis* genes were identified: those that were induced in both species; those that were repressed in both species; those that were induced in tobacco, but repressed in *Arabidopsis*; and those that were repressed in tobacco, but induced in *Arabidopsis*. Most gene models belonged to the first two categories, i.e. their responses in the two species were comparable (Figure 3.22). A smaller group of gene models showed different responses in tobacco than in *Arabidopsis*. For example, in tobacco, S-adenosylmethionine decarboxylase (involved in polyamine synthesis) and UDP-glucose:salicylic acid glucosyltransferase (involved in salicylic acid metabolism) were induced while being repressed in *Arabidopsis*.

3.3.5 Tobacco transcriptional response to *B. cinerea* compared to responses to a bacterial and viral pathogen

To further explore the transcriptional response of tobacco to *B. cinerea*, additional data were sourced from Gene Expression Omnibus (Edgar et al., 2002) and ArrayExpress (Kolesnikov et al., 2015). Studies using the same Agilent Tobacco Gene Expression microarray utilised in the study were identified and represented the tobacco cultivar Havana Petit infected with *Xanthomonas campestris* pv. *vesicatoria* (Xcv; GSM2433207-GSM2433213; Zurbriggen et al. 2009) and the tobacco cultivar Xanthi infected with tobacco mosaic virus (TMV) or expressing the full-length TMV genome (E-MEXP-3934; Jada et al., 2014).

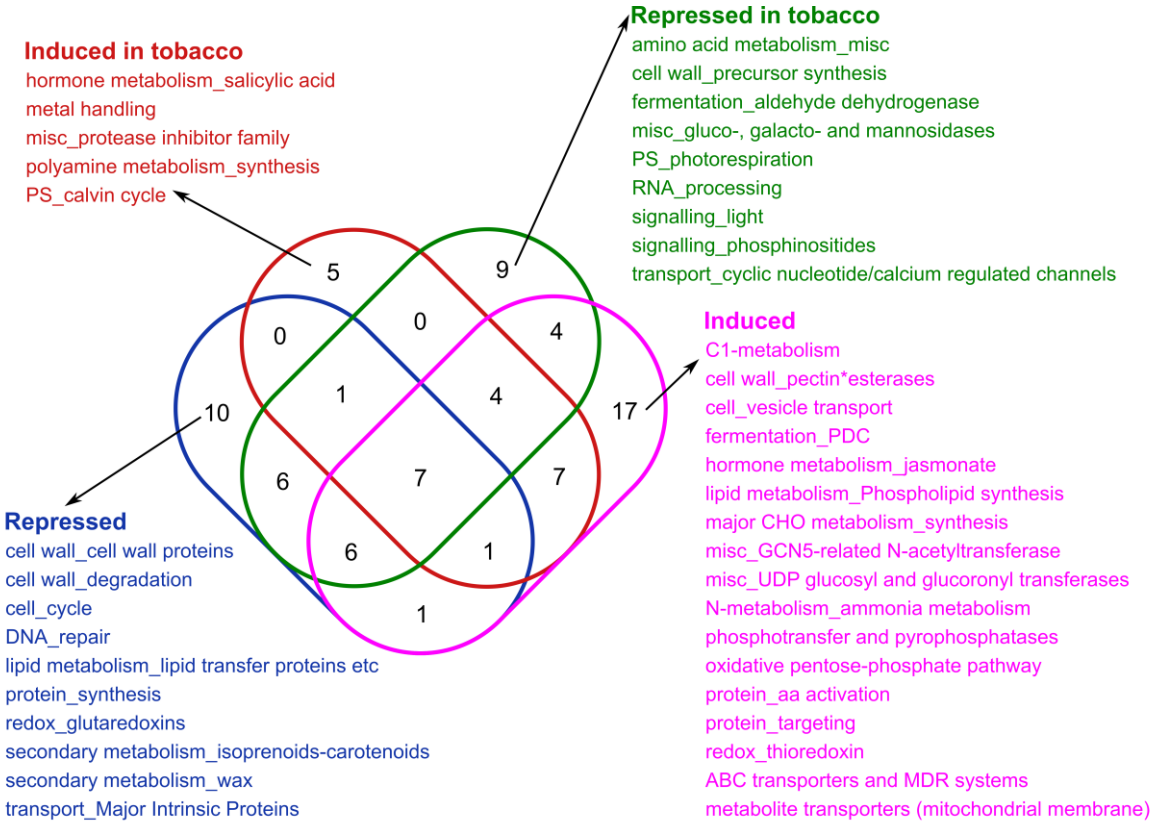

Figure 3.22 Similar and contrasting expression patterns in tobacco- and *Arabidopsis-B. cinerea* pathosystems. Venn diagram shows distribution of Mapman annotations. Annotations represent tobacco gene models that responded to *B. cinerea* infection and their *Arabidopsis* homologs (from Mathys et al., 2012) with similar or contrasting expression patterns.

In addition, Xcv infection had been performed on transgenic plants expressing a chloroplast-targeted cyanobacterial flavodoxin that reduced chloroplastic ROS accumulation during infection (Zurbriggen et al. 2009). Firstly, the significantly differentially expressed (2-fold change) gene models of wild-type tobacco challenged with Xcv or TMV were compared, along with the gene models that were differentially expressed between leaf position three of 8-week-old and 6-week-old plants (Figure 3.23). Venn diagram analysis showed that 49% of gene models that display a two-fold induction or repression between t0 and t48 in response to *B. cinerea* displayed the same expression pattern (induction/repression) in response to Xcv infection (19 h after inoculation vs mock inoculation). A correlation between ontogenic effect and *B. cinerea* infection was observed for 22% of gene models. Only 2% of gene models displayed the same expression pattern in response to TMV infection. Gene models within the lipoxygenase and mevalonate pathways were significantly induced by both Xcv and *B. cinerea* (Table 3.11), while TMV-infection and aging repressed these gene models. Expression patterns of models for cell wall modification genes, i.e. *XTH*, *extensin* and *expansin* (Figure 3.24) revealed ontogenic expression patterns were mirrored in defence responses to *B. cinerea*, Xcv and constitutive expression of the TMV genome.

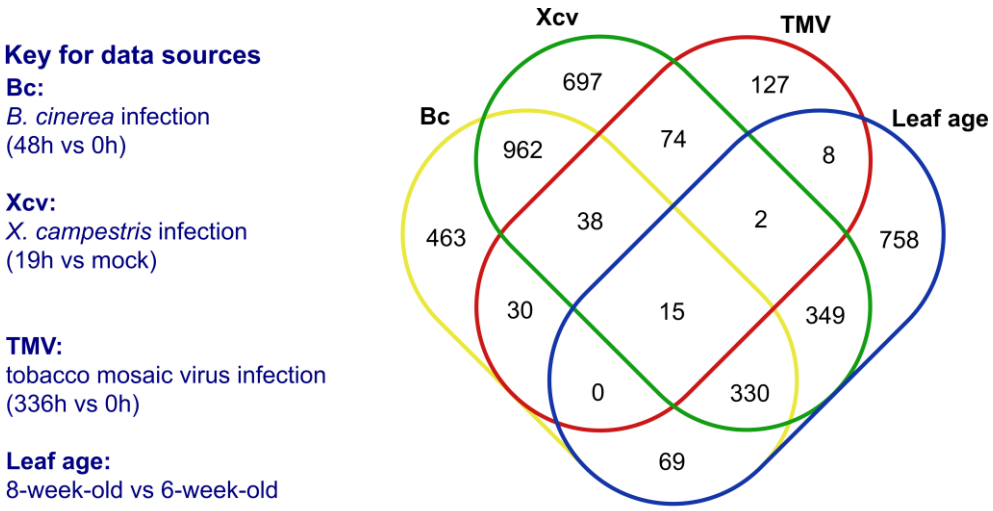

Figure 3.23 Venn diagram overlaying the differentially expressed gene models in three tobacco pathosystems. Gene models that were differentially expressed (2-fold change) during *B. cinerea* infection compared to those differentially expressed in tobacco pathosystems with *Xanthomonas campestris* pv. *vesicatoria* (Xcv) or tobacco mosaic virus (TMV) or between the third leaf from the apex collected two weeks apart (Jada et al., 2014; Zurbriggen et al., 2009). For Xcv, differential expression was relative to a mock inoculation, while *B. cinerea* and TMV expression levels were calculated relative to uninfected plants.

Table 3.11 Cross-experiment comparison of gene models related to the lipoxygenase and mevalonate pathways.

	Probe ID	Putative protein function	Bc 48hpi*	Xcv[1] 19hpi	TMV[2] 336hpi	Aging[2]
lipoxygenase pathway	A_95_P029636	lipoxygenase (LOX)	**5.11**	**5.90**	**1.03**	**2.19**
	A_95_P033299	9S-LOX	**1.69**	**1.78**	**-1.07**	**-1.49**
	A_95_P095528	9S-LOX	**1.64**	**2.12**	**2.26**	**1.81**
	A_95_P015286	LOX homology domain	**1.66**	**4.34**	**-1.26**	**-2.13**
	A_95_P015286	LOX homology domain	**1.66**	**4.34**	**-2.12**	**-2.46**
	A_95_P091193	12-oxo-phytodienoate reductase 2	**2.76**	**1.56**	**-1.36**	**-1.20**
	A_95_P250517	allene oxide cyclase	**3.21**	**1.97**	**1.19**	**1.12**
	A_95_P014126	allene oxide cyclase	**3.23**	**1.81**	**-2.23**	**-2.00**
	A_95_P190077	9-divinyl ether synthase	**5.29**	**8.88**	**-1.29**	**-1.33**
mevalonate pathway	A_95_P004346	acetyl-CoA acetyltransferase	**4.66**	**2.54**	**1.82**	**1.46**
	A_95_P160452	hydroxymethylglutaryl-CoA synthase	**2.12**	**1.89**	**-1.23**	**-1.27**
	A_95_P125232	3-hydroxy-3-methylglutaryl-CoA reductase	**1.57**	**1.48**	**-1.02**	**-2.12**
	A_95_P180402	3-hydroxy-3-methylglutaryl-CoA reductase	**5.92**	**5.14**	**-1.04**	**-1.02**
	A_95_P075045	mevalonate kinase	**2.64**	**1.58**	**2.22**	**1.91**
	A_95_P154872	diphosphomevalonate decarboxylase	**2.24**	**1.10**	**-1.02**	**-1.67**
	A_95_P142272	isopentenyl-diphosphate δ-isomerase I	**3.99**	0.98	**-1.28**	**3.72**
	A_95_P106557	phosphomevalonate kinase-like	**2.66**	**1.82**	**1.83**	-0.45
	A_95_P190047	farnesyl diphosphate synthase	**4.41**	**1.25**	**1.85**	-0.42
	A_95_P210797	farnesyl diphosphate synthase	**4.26**	**2.84**	**1.77**	-0.26

*Data are expressed relative to uninfected control (Bc and TMV), mock inoculation (Xcv) and younger leaf (Aging) and log-scaled. Significant (fold change>2) induction and repression are highlighted in bold red/green respectively. Data sourced from [1]Zurbriggen et al. (2009) and [2]Jada et al. (2014)

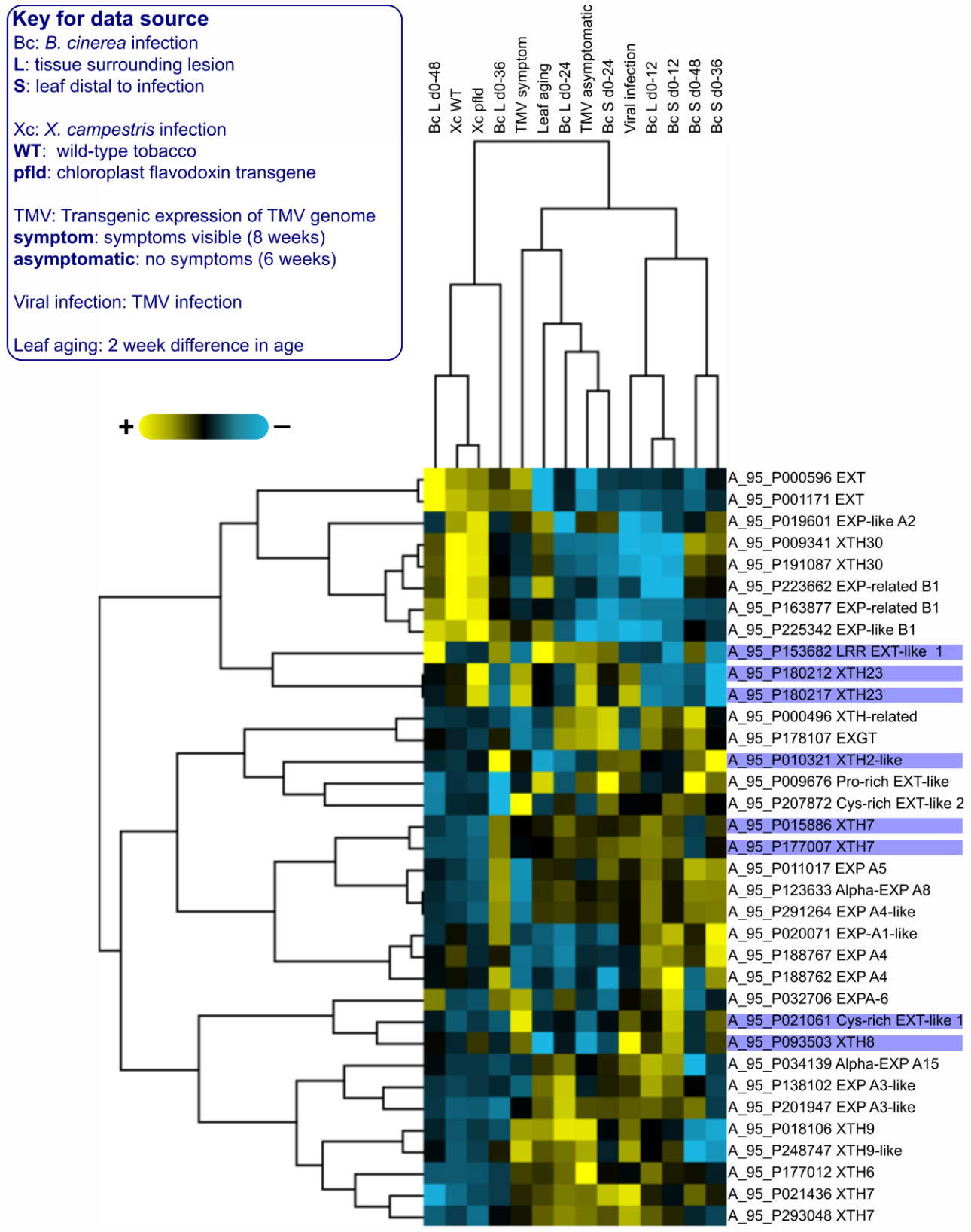

Figure 3.24 Cross-experiment clustering of cell wall modification gene models. Fold changes were calculated between infected and control samples (Bc, Xcv, Viral), or uninfected transgenic and wild-type (TMV), or between leaves from older and younger plants (Leaf aging). Data were log transformed and clustered according to gene model (Spearman rank correlation) and experiment (Pearson correlation). Shaded gene models were clustered differently in this analysis and the one represented in Figure 3.8.

In addition, the majority of cell wall modification-related gene models retained the groupings that had been observed when only *B. cinerea* infected samples were considered (Figure 3.8), with only eight gene models shifting to different clusters when additional experiments were considered (Figure 3.24). Furthermore, the majority of gene models that responded differently to *B. cinerea* infection in *Arabidopsis* (Figure 3.22), displayed the same expression patterns in *B. cinerea*- and Xcv-infected tobacco (Figure 3.25). Xcv, like *B. cinerea*, is known to induce hypersensitive response and programmed cell death in tobacco (Zurbriggen et al. 2009), therefore the cohesion in transcriptional responses against these different pathogens provides valuable support for the validity of the findings reported here.

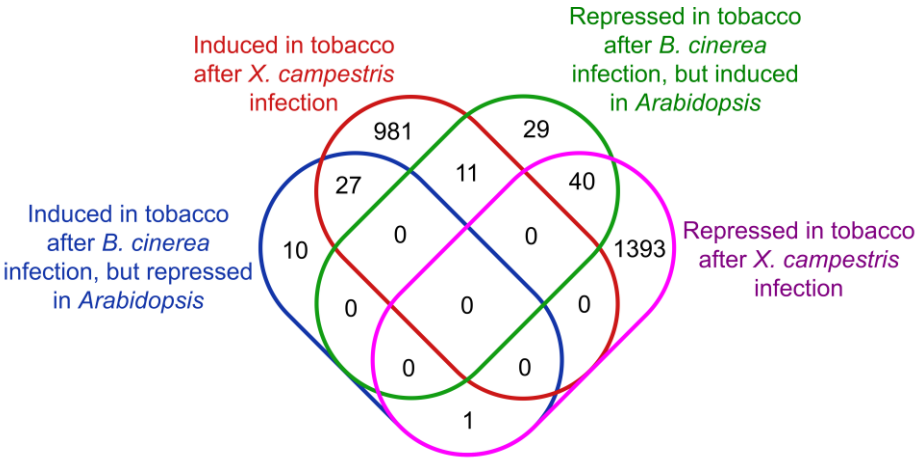

Figure 3.25 Venn overlay of gene models that responded differently to *B. cinerea* infection in tobacco and *Arabidopsis*, and the gene models that were induced or repressed in response to a *Xanthomonas campestris* pv *vesicatoria* infection. Tobacco/*Arabidopsis* controls were uninfected (t0) plants, *X. campestris* control was a mock-inoculated plant.

3.4 Discussion

The tobacco-*Botrytis* pathosystem we used in this study provided the opportunity to study both the transcriptional response at the site of lesion development, as well as in a leaf distal to the infection. In this pathosystem, infection is known to lead to complete maceration of inoculated leaves within two weeks (Joubert et al., 2006). The transcriptional analyses were limited to the first 48 hours after infection, providing an important description of the initial reaction of tobacco to *Botrytis* attack. Based on reports in other plant species (Eizner et al., 2017; Stefanato et al., 2009; Windram et al., 2012) and visual inspection of the inoculation sites, the sampled time-course (0-48 h post infection) spanned primary lesion formation, the lag phase and the intermediate phase of lesion expansion. The microarray analysis of the tissues at and surrounding the infection spot confirmed that the plant mounted a defence response; expression of several transcripts associated with localised defence to pathogens, including acidic and basic isoforms of chitinase (Kasprzewska, 2003), β-1,3-glucanases (Renault et al., 2000), HSR203J (Pontier et al., 1994, 1998), PAD4 and EDS1 (Feys et al., 2001) and PAL (Szatmári et al., 2014) were induced. These markers for defence responses were furthermore clearly linked to the defence response at the infection site, since their expression were not upregulated in the leaf distal to the infection. Moreover, meta-analysis of *Arabidopsis* response

to *B. cinerea* (Figure 3.22 and Appendix G to Chapter 3) and tobacco response to *X. campestris* pv *vesicatoria* (Figure 3.23 and Figure 3.24), an HR-inducing bacterial pathogen, confirmed that a defence response had been observed on the transcriptional level.

Overall the results showed that the plant mounted defence responses both at the spot of infection, as well as in the distal organs, but the timing of events was different, and the responses were inherently distinct, as could be expected. By contrasting the responses, it was possible to identify shared responses, even though time-frames might be different, as well as responses that were unique to either the infections spot, or the distal response. Furthermore, since the infections spanned two day-night cycles, the diurnal patterns could also be explored and were confirmed to play an important role, but that the infection progression/defence response diminished their impact over time. The main findings are contextualised below.

Tobacco presents a typical, though ultimately ineffective defence response

Key features of localised responses to *B. cinerea* infections tend to be conserved across different species (Agudelo-Romero et al., 2015; Blanco-Ulate et al., 2013; Finiti et al., 2014; Kong et al., 2015; Mathys et al., 2012; Smith et al., 2014; Vega et al., 2015; Windram et al., 2012). In all species analysed to date, *B. cinerea* infection leads to massive transcriptional reprogramming. In this study, an increasing difference between the number of induced and repressed transcripts emphasised the disruption of diurnal patterns, which were most evident for photosynthesis (Figure 3.5A; Table 3.4). In the leaf distal to the infection, the oscillation of both photosynthesis, light signalling, and the circadian clock was not significantly affected, suggesting that the changes were specific to the local defence responses at the infection spot. In addition to the repression of photosynthesis, it appeared that the infection lead to the dampening of the oscillation of some clock genes (Figure 3.7B), as has been reported in *Arabidopsis* (Windram et al., 2012). Susceptibility to *B. cinerea* has been shown to follow a diurnal pattern that is governed by the regulation of defence hormone signalling by the circadian clock (Ingle et al., 2015; Zhou et al., 2015). The initial preservation of the diurnal pattern during lesion development (Figure 3.7) has been observed in *B. cinerea*-infected lettuce, where their sampling strategy also allowed observation of diurnal gene expression (De Cremer et al., 2013).

B. cinerea infection has been reported to increase expression of jasmonate biosynthetic genes in *Arabidopsis* (Windram et al., 2012), tomato (Blanco-Ulate et al., 2013) and grapevine (Agudelo-Romero et al., 2015). We observed an induction of both the 9S- and 13S-LOX branches of the lipoxygenase pathway, though only 9S-LOX was significantly induced during infection (Figure 3.12B). In Solanaceous species the activation of the lipoxygenase pathway, primarily the 9S-branch, has primarily been investigated from the perspective of its response to oxidative stress, induced by high light or hydrogen peroxide treatments (Fammartino et al., 2007; Montillet et al., 2005; Thoma et al., 2003). Since the oxidative burst and associated HR is a key feature of *B. cinerea* infection (Govrin

and Levine, 2000; Shlezinger et al., 2011), these studies provided an analogue for *B. cinerea* infection.

As expected, ROS generating enzymes were induced during local lesion development, particularly after t12 (Figure 3.9A, B). This timing likely coincides with initial stage of *B. cinerea* infection, where toxic metabolites and necrosis-inducing proteins are released to activate PCD (Shlezinger et al., 2011). The continual induction of APX (Figure 3.9G) and SOD (Figure 3.9H) suggest the activation and enhancement of ROS detoxification processes in the subsequent lesion expansion phase, when *B. cinerea* is launching its second wave of necrosis-inducing compounds.

Given the importance of CWDE in the *B. cinerea* infection strategy, one would expect that cell wall modifying enzymes would, during infection, be regulated so as to improve the resistance of the cell wall to degradation (Bhuiyan et al., 2009a, 2009b; Bradley et al., 1992; Cantu et al., 2008; Juge, 2006). We observed diverse expression patterns for three classes of wall-modifying enzymes, which were mirrored in Xcv-infected tobacco (Figure 3.24). One of the most abundant classes of cell wall modifying enzymes is that of XTHs, a large group of enzymes that cleave the xyloglucan backbone of hemicellulose, either cutting the xyloglucan backbone or transferring sections of xyloglucan to different strands (Rose et al., 2002). Since minimal information is available about XTH functions *in vivo*, a preliminary *in silico* study of the tobacco XTH family (presented in Chapter 5 of this dissertation), was conducted, but could not provide putative functions for XTH transcripts with diverging expression patterns observed here.

Secondary metabolism pathways activated during localised defence response

Accumulation of phytoalexins is often seen in response to *B. cinerea* (Charles et al., 2008; Jeandet et al., 1995). We observed the induction of phenylpropanoid (Figure 3.10) and sesquiterpenoid (Table 3.6) pathways and of transcripts encoding enzymes responsible for phenolamide and sesquiterpenoid phytoalexin synthesis (Bird and Smith, 1982; Muroi et al., 2009; Ward et al., 1974; Whitehead et al., 1989). We profiled the volatile secondary metabolites that remained in the sampled tissue and observed a temporal shift in VOC profile during infection (Figure 3.14, Figure 3.15). Our analysis revealed that C_8- and C_9-LOX-derived compounds were generated during infection, suggesting that the LOX pathway may be responsible for additional compounds, beyond the oxylipins that are normally studied in relation to defence. Since several LOX-derived volatiles have confirmed anti-fungal activity against *B. cinerea* (Archbold et al., 1997), sufficient activation of this pathway may play an important role in defence.

Despite the induction of the MEV pathway (Table 3.6), our targeted analysis could not identify sesquiterpene volatiles responsive to infection. In contrast, the MEP pathway was suppressed by infection, but we detected several monoterpenoid volatiles. Since our method only detected compounds that volatilised during analysis, non-volatile sesquiterpenes could not be detected, but

may have been present. The role of volatile emissions in defence against herbivorous pathogens has been extensively studied (Pare and Tumlinson, 1999), but they can also function in defence against fungi (Nandi and Fries, 1976). In some cases, emission of VOCs can be used to diagnose *Botrytis* infection before symptoms are evident (Jansen et al., 2009). VOCs can act as signalling molecules that induce defence gene expression (Kishimoto et al., 2005) or directly inhibit growth of *B. cinerea* (Archbold et al., 1997). Since metabolite profiling was, in this study, an exploratory analysis, future studies into this aspect of response to infection would include a more comprehensive profile of volatile and non-volatile products of these pathways, since many of these compounds can directly affect the invading pathogen without volatilisation.

Leaves distal to the infection maintain diurnal patterns, but activate some defence pathways

Systemic induced resistance has commonly been studied in tobacco and other species by application of a known inducer, such as SA (Murphy et al., 2000) or microbe-associated molecular patterns (Cordelier et al., 2003; Frías et al., 2013; Kulye et al., 2012), but only rarely by mimicking the natural process where pathogen infection on one plant organ induces a systemic response. Transcriptomic analysis of fully developed systemic acquired resistance (SAR) has been reported in *Arabidopsis* challenged with compatible strains of *Pseudomonas syringae* (Bernsdorff et al., 2016; Gruner et al., 2013) and an incompatible interaction with the fungal pathogen *Alternaria brassicola* (Schenk et al., 2003) at a single sampling point where SAR was fully established, namely two days for *P. syringae* and three days for *A. brassicola*. Responses to *B. cinerea* have been extensively studied in cells and plant organs that are in close proximity to the pathogen, however, necrotizing pathogens are also known to induce systemic responses such as SAR in plant organs distal to the infection (Ryals et al., 1996). Though *B. cinerea* is a necrotising pathogen, it did not induce SAR within two days, but induced a subset of defence genes systemically according to Govrin and Levine (2002). In tobacco, however, SAR was induced by *B. cinerea* strain B05.10 in distal leaves by 8 days post infection and shown to be effective against *P. syringae* and itself (Frías et al., 2013). Because the authors, following the results reported in *Arabidopsis* (Govrin and Levine, 2002), did not expect SAR-induction by *B. cinerea*, SA accumulation was only tested at three and eight days post infection (dpi). Since SA accumulation had not occurred by 3 dpi, but was comparable to *P. syringae*-induced SA accumulation at 8 dpi, *B. cinerea* could have induced SAR at any point after 3 days (Frías et al., 2013). In contrast, *P. syringae* accumulates SA and activates SAR within three days in the leaves distal to the infection. Our transcriptional profile then falls well within the pre-SAR distal response, and was therefore substantially different from fully realised SAR in *Arabidopsis*. This study therefore provides a novel perspective into the transcriptional changes in the distal tissue of tobacco when an infection starts in a distal organ of the plant.

In *Arabidopsis*, infection by *B. cinerea* activated the induction of PR5 and Glutathione S-transferase 1 (GST1), but without induction of SAR markers, PR1 and plant defensin 1.2 (PDF1.2), in distal leaves (Govrin and Levine, 2002). Despite the early time-frame, we observed a cumulative increase in biotic stress-related transcripts (Figure 3.17B). The strongest inductions were observed for chitinases B (class I) and endochitinase, also reported in systemic *Arabidopsis* leaves following *Alternaria brassicola* infection (Schenk et al., 2003), osmotins, described in *Arabidopsis* distally challenged with *P. syringae* (Gruner et al., 2013) and the basic form of PR protein 1. The biotic stress category also included homologs for *Arabidopsis* PAD4 and EDS1, both considered essential for SAR (Bernsdorff et al., 2016; Feys et al., 2001). In tobacco, PAD4 was slightly induced (1.5-fold) in the last sampling point (Figure 3.2F), while EDS1 (Figure 3.2E) was slightly repressed (1.5-1.7-fold), further illustrating that the tobacco has not yet fully developed SAR in the analysis window.

Both studies in *Arabidopsis* (Bernsdorff et al., 2016; Gruner et al., 2013) concluded that the SAR state is characterised by a shift from vegetative growth and development to defence metabolism, akin to the shift seen in locally infected tissue (Bilgin et al., 2010). One of the key features described a significant drop in photosynthetic rate, coupled to a massive repression of photosynthesis-associated genes. In contrast, we did not see a disruption of the diurnal pattern of photosynthetic genes (Figure 3.7A), nor a shift in energy metabolism (Figure 3.17E, M, N). Given the interrelationship between photosynthesis and the circadian clock (Haydon et al., 2013), this explains why circadian clock genes (Figure 3.7B) continued to oscillate throughout the time-course in the leaf distal to the infection.

Although the transcriptional changes in distal tissue were more limited in scope than in tissue with active local defence, some transcripts were more responsive in distal tissues. The most pronounced differences were observed for numerous metabolic categories, which spanned abiotic stress (Figure 3.17A), protein degradation (Figure 3.17P), development (Figure 3.17D) and ethylene synthesis and response (Figure 3.17I). One of the markers for SAR, a gene family originally identified following TMV infection (Alexander et al., 1992), is *SAR8.2*, which was consistently more induced in the leaf distal to the infection (Figure 3.18). SAR8.2 proteins are induced by SA, ET and, in resistant tobacco cultivars, by TMV (Guo et al., 2000) and are toxic to a range of pathogens, including *B. cinerea* (Lee and Hwang, 2006). In addition, neomenthol dehydrogenase (Table 3.10) and trans-resveratrol di-O-methyltransferase (Figure 3.11G) transcripts were highly induced. Neomenthol dehydrogenase synthesizes menthone, a monoterpene with fungitoxic activity against *B. cinerea* (Tsao and Zhou, 2000), while trans-resveratrol di-O-methyltransferase produces pterostilbene, a phytoalexin associated with resistance to *B. cinerea* in grapevine (Pezet et al., 1991). We also observed an induction of α-ionone, an apocarotenoid. Though α-ionone has not been reported in defence signalling, other compounds of this type have been found to participate in defence signalling (Ramel et al., 2012; Vallabhaneni et al., 2010). Therefore, even at this every early phase of infection, tobacco

seemed to have increased its capacity to deter subsequent pathogens in the leaf distal to the infection.

Leaf age effects in tobacco – considerations for profiling approaches

Since the majority of profiling studies focus on tissues from a specific leaf position, it is important to consider potential differences in response of older and younger tissues to the same stimulus. Age-related resistance (ARR) has been extensively studied in *Arabidopsis*, where ARR to *P. syringae* is dependent on SA accumulation (Kus et al., 2002). Both local and systemic defence responses are influenced by leaf age in *Arabidopsis* and younger leaves displayed accelerated induction of PAL and GST, while accumulating more SA and camalexin (Zeier, 2005). In tobacco, leaf age influences sensitivity to ethylene (Bailey et al., 1995) and susceptibility to pathogens (Reuveni et al., 1986; Stavely and Slana, 1971). We observed differences in baseline (t0) VOC profiles (Figure 3.20) between leaves of different ages, while targeted transcript analysis revealed differences in expression patterns of β-1,3-glucanase (PR-2), SOD and catalase during the infection assay. The leaf-age effect on VOC profiles in uninfected (t0) tissue (Figure 3.20) has been observed in tomato (Zhang and Chen, 2009), though the effect was less pronounced between adjacent leaf positions, with only two compounds differing significantly. Since we also observed marked differences in VOC profiles between independent experiments (Figure 3.16), robust biological replication would be essential in discerning such subtle ontogenic effects.

3.5 Conclusion

The objective of this study was to profile transcriptional changes of tobacco over 48 hours, in tissue that included and surrounded a developing lesion and in tissue of a leaf distal to the infection. Our sampling strategy, harvesting tissue every 12 hours, meant that two diurnal cycles were represented in the samples, making it possible to also interpret the results against the influence of the photoperiod. In both types of tissue, the diurnal cycle was clear and continued to dominate gene expression patterns up to t24 in tissue responding to lesion development, and throughout the time-course in the leaf distal to the infection.

Despite the early time-frame, the leaf distal to the infection began to activate, to a limited extent, defence-related genes, including PR-proteins and SAR-related proteins, and genes involved in secondary metabolite synthesis. In tissue surrounding the developing lesion, a clear activation of defence was observed, along with a shift in energy metabolism from photosynthesis to glycolytic and mitochondrial ATP synthesis. Typical markers for defence against *B. cinerea* were observed, namely enhancement of ROS generation followed by activation of ROS scavenging, activation of the phenylpropanoid and sesquiterpenoid pathways, chitinase expression and JA/ET biosynthesis. Profiling volatile secondary metabolites further highlighted the activation of the LOX pathway during the localised response to infection. Despite apparently inducing a fully-fledged defence response in

tissue surrounding the infection spot, the outcome of this interaction favours *B. cinerea*, since complete maceration of infected leaves occurs after two weeks (Joubert et al., 2006). It appears that, once *B. cinerea* has survived the first wave of the defence response, typified by the oxidative burst and PCD, the activation of secondary metabolism and defence gene expression, occurring in living tissue adjacent to the necrotic lesion, was not sufficient to prevent further ingress by the pathogen. Comparison of the tobacco response to *B. cinerea* to its response to other pathogens highlighted that pathogens that induce PCD, such as *B. cinerea* and *X. campestris* pv *vesicatoria*, elicit similar types of responses, despite having different lifestyles. The response of tobacco to *B. cinerea* was, in the main, consistent with the response of *Arabidopsis*, although it appears that salicylic acid and polyamine metabolism differed slightly. This profile of transcriptional changes in tobacco infected with *B. cinerea*, has provided a novel resource for subsequent studies using this pathosystem, however, ontogenic effects on gene expression and secondary metabolites emphasise the need to expand this profile to other tissues.

3.6 Literature cited

AbuQamar S, Chen X, Dhawan R, Bluhm B, Salmeron J, Lam S, Dietrich RA, Mengiste T (2006). Expression profiling and mutant analysis reveals complex regulatory networks involved in Arabidopsis response to *Botrytis* infection. *Plant J* 48, 28–44. doi:10.1111/j.1365-313X.2006.02849.x.

Agudelo-Romero P, Erban A, Rego C, Carbonell-Bejerano P, Nascimento T, Sousa L, Martínez-Zapater JM, Kopka J, Fortes AM (2015). Transcriptome and metabolome reprogramming in *Vitis vinifera* cv. Trincadeira berries upon infection with *Botrytis cinerea*. *J Exp Bot* 66, 1769–1785. doi:10.1093/jxb/eru517.

Alexander D, Stinson J, Pear J, Glascock C, Ward E, Goodman RM, Ryals JA (1992). A new multigene family inducible by tobacco mosaic virus or salicylic acid in tobacco. *Mol Plant-Microbe Interact* 5, 513–515.

Alexandersson E, Becker JVW, Jacobson D, Nguema-Ona E, Steyn C, Denby KJ, Vivier MA (2011). Constitutive expression of a grapevine polygalacturonase-inhibiting protein affects gene expression and cell wall properties in uninfected tobacco. *BMC Res Notes* 4, 493. doi:10.1186/1756-0500-4-493.

Altschul SF, Gish W, Miller W, Myers EW, Lipman DJ (1990). Basic local alignment search tool. *J Mol Biol* 215, 403–410. doi:10.1016/S0022-2836(05)80360-2.

Archbold DD, Hamilton-Kemp TR, Barth MM, Langlois BE (1997). Identifying natural volatile compounds that control gray mold (*Botrytis cinerea*) during postharvest storage of strawberry, blackberry, and grape. *J Agric Food Chem* 45, 4032–4037. doi:10.1021/jf970332w.

Asselbergh B, Curvers K, França SC, Audenaert K, Vuylsteke M, Van Breusegem F, Höfte M (2007). Resistance to *Botrytis cinerea* in *sitiens*, an abscisic acid-deficient tomato mutant, involves timely production of hydrogen peroxide and cell wall modifications in the epidermis. *Plant Physiol* 144, 1863–1877. doi:10.1104/pp.107.099226.

Bailey BA, Avni A, Anderson JD (1995). The influence of ethylene and tissue age on the sensitivity of Xanthi tobacco leaves to a *Trichoderma viride* xylanase. *Plant Cell Physiol* 36, 1669–1676. doi:10.1093/oxfordjournals.pcp.a078934.

Baillieul F, Genetet I, Kopp M, Saindrenan P, Fritig B, Kauffmann S (1995). A new elicitor of the hypersensitive response in tobacco: a fungal glycoprotein elicits cell death, expression of defence genes, production of salicylic acid, and induction of systemic acquired resistance. *Plant J* 8, 551–560. doi:10.1046/j.1365-313X.1995.8040551.x.

Bengtsson T, Weighill D, Proux-Wéra E, Levander F, Resjö S, Burra DD, Moushib LI, Hedley PE, Liljeroth E, Jacobson D, Alexandersson E, Andreasson E (2014). Proteomics and transcriptomics of the BABA-induced resistance response in potato using a novel functional annotation approach. *BMC Genomics* 15, 315. doi:10.1186/1471-2164-15-315.

Bernsdorff F, Doering A-C, Gruner K, Schuck S, Bräutigam A, Zeier J (2016). Pipecolic acid orchestrates plant systemic acquired resistance and defense priming via salicylic acid-dependent and independent pathways. *Plant Cell* 28, 102–129. doi:10.1105/tpc.15.00496.

Berrocal-Lobo M, Molina A (2007). *Arabidopsis* defense response against *Fusarium oxysporum*. *Trends Plant Sci* 13, 145–150. doi:10.1016/j.tplants.2007.12.004.

Bhuiyan NH, Selvaraj G, Wei Y, King J (2009a). Gene expression profiling and silencing reveal that monolignol biosynthesis plays a critical role in penetration defence in wheat against powdery mildew invasion. *J Exp Bot* 60, 509–521. doi:10.1093/jxb/ern290.

Bhuiyan NH, Selvaraj G, Wei Y, King J (2009b). Role of lignification in plant defense. *Plant Signal Behav* 4, 158–159. doi: 10.1093/jxb/ern290.8.

Bilgin DD, Zavala JA, Zhu J, Clough SJ, Ort DR, DeLucia EH (2010). Biotic stress globally downregulates photosynthesis genes. *Plant, Cell Environ* 33, 1597–1613. doi:10.1111/j.1365-3040.2010.02167.x.

Bird CR, Smith TA (1982). Agmatine coumaroyltransferase, an enzyme involved in the formation of the antifungal hordatines in barley (*Hordeum vulgare*) seedlings. *Biochem Soc Trans* 10, 400–401. doi:10.1042/bst0100400.

Birkenbihl RP, Diezel C, Somssich IE (2012). Arabidopsis WRKY33 is a key transcriptional regulator of hormonal and metabolic responses toward *Botrytis cinerea* infection. *Plant Physiol* 159, 266–285. doi:10.1104/ pp.111.192641.

Blanco-Ulate B, Amrine KCH, Collins TS, Rivero RM, Vicente AR, Morales-Cruz A, Doyle CL, Ye Z, Allen G, Heymann H, Ebeler SE, Cantu D (2015). Developmental and metabolic plasticity of white-skinned grape berries in response to *Botrytis cinerea* during noble rot. *Plant Physiol* 169, 2422–2443. doi:10.1104/pp.15.00852.

Blanco-Ulate B, Vincenti E, Powell ALT, Cantu D (2013). Tomato transcriptome and mutant analyses suggest a role for plant stress hormones in the interaction between fruit and *Botrytis cinerea*. *Front Plant Sci* 4, 142. doi:10.3389/ fpls.2013.00142.

Bombarely A, Edwards KD, Sanchez-Tamburrino J, Mueller LA (2012). Deciphering the complex leaf transcriptome of the allotetraploid species *Nicotiana tabacum*: a phylogenomic perspective. *BMC Genomics* 13, 406. doi:10.1186/ 1471-2164-13-406.

Bozsó Z, Ott PG, Kámán-Tóth E, Bognár GF, Pogány M, Szatmári Á (2016). Overlapping yet response-specific transcriptome alterations characterize the nature of tobacco-*Pseudomonas syringae* interactions. *Front Plant Sci* 7, 251. doi:10.3389/fpls.2016.00251.

Bradley DJ, Kjellbom P, Lamb CJ (1992). Elicitor- and wound-induced oxidative cross-linking of a proline-rich plant cell wall protein: a novel, rapid defense response. *Cell* 70, 21–30.

Caires NP, Rodrigues FA, Furtado GQ (2015). Infection process of *Botrytis cinerea* on eucalypt leaves. *J Phytopathol* 163, 604–611. doi:10.1111/jph.12360.

Cantu D, Blanco-Ulate B, Yang L, Labavitch JM, Bennett AB, Powell ALT (2009). Ripening-regulated susceptibility of tomato fruit to *Botrytis cinerea* requires *NOR* but not *RIN* or ethylene. *Plant Physiol* 150, 1434–1449. doi: 10.1104/pp.109.138701.

Cantu D, Vicente AR, Greve LC, Dewey FM, Bennett AB, Labavitch JM, Powell ALT (2008). The intersection between cell wall disassembly, ripening, and fruit susceptibility to *Botrytis cinerea*. *PNAS* 105, 859–864. doi:10.1073/ pnas.0709813105.

Carstens M, Vivier MA, Pretorius IS (2003). The *Saccharomyces cerevisiae* chitinase, encoded by the *CTS1-2* gene, confers antifungal activity against *Botrytis cinerea* to transgenic tobacco. *Transgenic Res* 12, 497–508. doi: 10.1023/A:1024220023057.

Cawoy H, Mariutto M, Henry G, Fisher C, Vasilyeva N, Thonart P, Dommes J, Ongena M (2014). Plant defense stimulation by natural isolates of *Bacillus* depends on efficient surfactin production. *Mol Plant-Microbe Interact* 27, 87–100. doi:10.1094/MPMI-09-13-0262-R.

Cessna SG, Sears VE, Dickman MB, Low PS (2000). Oxalic acid, a pathogenicity factor for *Sclerotinia sclerotiorum*, suppresses the oxidative burst of the host plant. *Plant Cell* 12, 2191–2200. doi:10.1105/tpc.12.11.2191.

Charles MT, Mercier J, Makhlouf J, Arul J (2008). Physiological basis of UV-C-induced resistance to *Botrytis cinerea* in tomato fruit. I. Role of pre- and post-challenge accumulation of the phytoalexin-rishitin. *Postharvest Biol Technol* 47, 10–20. doi:10.1016/j.postharvbio.2007.05.013.

Clough SJ, Bent AF (1998). Floral dip: A simplified method for *Agrobacterium*-mediated transformation of *Arabidopsis thaliana*. *Plant J* 16, 735–743. doi:10.1046/j.1365-313X.1998.00343.x.

Coolen S, Proietti S, Hickman R, Davila Olivas NH, Huang PP, Van Verk MC, Van Pelt JA, Wittenberg AHJ, De Vos M, Prins M, Van Loon JJA, Aarts MGM, Dicke M, Pieterse CMJ, Van Wees SCM (2016). Transcriptome dynamics of Arabidopsis during sequential biotic and abiotic stresses. *Plant J* 86, 249–267. doi:10.1111/tpj.13167.

Cordelier S, De Ruffray P, Fritig B, Kauffmann S (2003). Biological and molecular comparison between localized and systemic acquired resistance induced in tobacco by a *Phytophthora megasperma* glycoprotein elicitin. *Plant Mol Biol* 51, 109–118. doi:10.1023/A:1020722102871.

Coutos-Thévenot P, Poinssot B, Bonomelli A, Yean H, Breda C, Buffard D, Esnault R, Hain R, Boulay M (2001). *In vitro* tolerance to *Botrytis cinerea* of grapevine 41B rootstock in transgenic plants expressing the stilbene synthase *Vst1* gene under the control of a pathogen-inducible PR10 promoter. *J Exp Bot* 52, 901–910. doi:10.1093/ jexbot/52.358.901.

Daurelio LD, Petrocelli S, Blanco F, Holuigue L, Ottado J, Orellano EG (2011). Transcriptome analysis reveals novel genes involved in nonhost response to bacterial infection in tobacco. *J Plant Physiol* 168, 382–391. doi:10.1016/j.jplph.2010.07.014.

De Cremer K, Mathys J, Vos C, Froenicke L, Michelmore RW, Cammue BPA, De Coninck B (2013). RNAseq-based transcriptome analysis of *Lactuca sativa* infected by the fungal necrotroph *Botrytis cinerea*. *Plant, Cell Environ* 36, 1992–2007. doi:10.1111/pce.12106.

De Hoon MJL, Imoto S, Nolan J, Miyano S (2004). Open source clustering software. *Bioinformatics* 20, 1453–1454. doi:10.1093/bioinformatics/bth078.

Dean R, Van Kan JAL, Pretorius ZA, Hammond-Kosack KE, Di Pietro A, Spanu PD, Rudd JJ, Dickman M, Kahmann R, Ellis J, Foster GD (2012). The Top 10 fungal pathogens in molecular plant pathology. *Mol Plant Pathol* 13, 414–430. doi:10.1111/j.1364-3703.2011.00783.x.

Dodds PN, Rathjen JP (2010). Plant immunity: towards an integrated view of plant–pathogen interactions. *Nat Rev* 11, 539–548. doi:10.1038/nrg2812.

Dudoit S, Yang YH, Callow MJ, Speed TP (2002). Statistical methods for identifying differentially expressed genes in replicated cDNA microarray experiments. *Stat Sin* 12, 111–139. doi:10.1.1.117.9702.

Edwards KD, Fernandez-Pozo N, Drake-Stowe K, Humphry M, Evans AD, Bombarely A, Allen F, Hurst R, White B, Kernodle SP, Bromley JR, Sanchez-Tamburrino JP, Lewis RS, Mueller LA (2017). A reference genome for *Nicotiana tabacum* enables map-based cloning of homeologous loci implicated in nitrogen utilization efficiency. *BMC Genomics* 18, 448. doi:10.1186/s12864-017-3791-6.

Eizner E, Ronen M, Gur Y, Gavish A, Zhu W, Sharon A (2017). Characterization of *Botrytis*-plant interactions using PathTrack© - an automated system for dynamic analysis of disease development. *Mol Plant Pathol* 18, 503–512. doi:10.1111/mpp.12410.

Elad Y (1988). Scanning electron microscopy of parasitism of *Botrytis cinerea* on flowers and fruits of cucumber. *Trans Br Mycol Soc* 91, 185–190. doi:10.1016/S0007-1536(88)80025-1.

Elad Y, Pertot I, Cotes Prado AM, Stewart A (2016). Plant hosts of Botrytis spp. In *Botrytis - the Fungus, the Pathogen and its Management in Agricultural Systems*, eds S Fillinger and Y Elad (Switzerland: Springer International Publishing), 413–486. doi:10.1007/978-3-319-23371-0_20.

Fammartino A, Cardinale F, Göbel C, Mène-Saffrané L, Fournier J, Feussner I, Esquerré-Tugayé M-T (2007). Characterization of a divinyl ether biosynthetic pathway specifically associated with pathogenesis in tobacco. *Plant Physiol* 143, 378–388. doi:10.1104/pp.106.087304.

Ferrari S, Galletti R, Denoux C, De Lorenzo G, Ausubel FM, Dewdney J (2007). Resistance to *Botrytis cinerea* induced in *Arabidopsis* by elicitors is independent of salicylic acid, ethylene, or jasmonate signaling but requires *PHYTOALEXIN DEFICIENT3*. *Plant Physiol* 144, 367–379. doi:10.1104/pp.107.095596.

Feussner I, Wasternack C (2002). The lipoxygenase pathway. *Annu Rev Plant Biol* 53, 275–297. doi:10.1146/annurev.arplant.53.100301.135248.

Feys BJ, Moisan LJ, Newman MA, Parker JE (2001). Direct interaction between the *Arabidopsis* disease resistance signaling proteins, EDS1 and PAD4. *EMBO J* 20, 5400–5411. doi:10.1093/emboj/20.19.5400.

Finiti I, De La O Leyva M, Vicedo B, Gómez-Pastor R, López-Cruz J, García-Agustín P, Real MD, González-Bosch C (2014). Hexanoic acid protects tomato plants against *Botrytis cinerea* by priming defence responses and reducing oxidative stress. *Mol Plant Pathol* 15, 550–562. doi:10.1111/mpp.12112.

Fotopoulos V, Sanmartin M, Kanellis AK (2006). Effect of ascorbate oxidase over-expression on ascorbate recycling gene expression in response to agents imposing oxidative stress. *J Exp Bot* 57, 3933–3943. doi:10.1093/jxb/erl147.

Fournier J, Pouéhat M-L, Rickauer M, Rabinovich-Chable H, Rigaud M, Esquerré-Tugayé M-T (1993). Purification and characterization of elicitor-induced lipoxygenase in tobacco cells. *Plant J* 3, 63–70.

Frías M, Brito N, González C (2013). The *Botrytis cinerea* cerato-platanin BcSpl1 is a potent inducer of systemic acquired resistance (SAR) in tobacco and generates a wave of salicylic acid expanding from the site of application. *Mol Plant Pathol* 14, 191–196. doi:10.1111/j.1364-3703.2012.00842.x.

Frías M, González C, Brito N (2011). BcSpl1, a cerato-platanin family protein, contributes to *Botrytis cinerea* virulence and elicits the hypersensitive response in the host. *New Phytol* 192, 483–495. doi:10.1111/j.1469-8137.2011.03802.x.

Frías M, González M, González C, Brito N (2016). BcIEB1, a *Botrytis cinerea* secreted protein, elicits a defense response in plants. *Plant Sci* 250, 115–124. doi:10.1016/j.plantsci.2016.06.009.

Glazebrook J (2005). Contrasting mechanisms of defense against biotrophic and necrotrophic pathogens. *Annu Rev Phytopathol* 43, 205–227. doi:10.1146/annurev.phyto.43.040204.135923.

Gong S, Hao Z, Meng J, Liu D, Wei M, Tao J (2015). Digital gene expression analysis to screen disease resistance-relevant genes from leaves of herbaceous peony (*Paeonia lactiflora* Pall.) infected by *Botrytis cinerea*. *PLoS ONE* 10, e0133305. doi:10.1371/journal.pone.0133305.

Govrin EM, Levine A (2000). The hypersensitive response facilitates plant infection by the necrotrophic pathogen *Botrytis cinerea*. *Curr Biol* 10, 751–757. doi:10.1016/S0960-9822(00)00560-1.

Govrin EM, Levine A (2002). Infection of *Arabidopsis* with a necrotrophic pathogen, *Botrytis cinerea*, elicits various defense responses but does not induce systemic acquired resistance (SAR). *Plant Mol Biol* 48, 267–276. doi:10.1023/A:1013323222095.

Govrin EM, Rachmilevitch S, Tiwari BS, Solomon M, Levine A (2006). An elicitor from *Botrytis cinerea* induces the hypersensitive response in *Arabidopsis thaliana* and other plants and promotes the gray mold disease. *Phytopathology* 96, 299–307. doi:10.1094/PHYTO-96-0299.

Gruner K, Griebel T, Návarová H, Attaran E, Zeier J (2013). Reprogramming of plants during systemic acquired resistance. *Front Plant Sci* 4, 252. doi:10.3389/fpls.2013.00252.

Guo A, Salih G, Klessig DF (2000). Activation of a diverse set of genes during the tobacco resistance response to TMV is independent of salicylic acid; induction of a subset is also ethylene independent. *Plant J* 21, 409–418. doi:10.1046/j.1365-313X.2000.00692.x.

Haydon MJ, Mielczarek O, Robertson FC, Hubbard KE, Webb AAR (2013). Photosynthetic entrainment of the *Arabidopsis thaliana* circadian clock. *Nature* 502, 689–692. doi:10.1038/nature12603.

Hoekema A, Hirsch PR, Hooykaas PJJ, Schilperoort RA (1983). A binary plant vector strategy based on separation of *vir*- and T-region of the *Agrobacterium tumefaciens* Ti-plasmid. *Nature* 303, 179–180. doi:10.1038/303179a0.

Ingle RA, Stoker C, Stone W, Adams N, Smith R, Grant M, Carré I, Roden LC, Denby KJ (2015). Jasmonate signalling drives time-of-day differences in susceptibility of Arabidopsis to the fungal pathogen *Botrytis cinerea*. *Plant J* 84, 937–948. doi:10.1111/tpj.13050.

Jach G, Gornhardt B, Mundy J, Logemann J, Pinsdorf E, Leah R, Schell J, Maas C (1995). Enhanced quantitative resistance against fungal disease by combinatorial expression of different barley antifungal proteins in transgenic tobacco. *Plant J* 8, 97–109. doi:10.1046/j.1365-313X.1995.08010097.x.

Jada B, Soitamo AJ, Siddiqui SA, Murukesan G, Aro E-M, Salakoski T, Lehto K (2014). Multiple different defense mechanisms are activated in the young transgenic tobacco plants which express the full length genome of the tobacco mosaic virus, and are resistant against this virus. *PLoS ONE* 9, e107778. doi:10.1371/journal.pone.0107778.

Jansen RMC, Miebach M, Kleist E, Van Henten EJ, Wildt J (2009). Release of lipoxygenase products and monoterpenes by tomato plants as an indicator of *Botrytis cinerea*-induced stress. *Plant Biol* 11, 859–868. doi:10.1111/j.1438-8677.2008.00183.x.

Jeandet P, Bessis R, Sbaghi M, Meunier P (1995). Production of the phytoalexin resveratrol by grapes as a response to *Botrytis* attack under natural conditions. *J Phytopathol* 143, 135–139. doi:10.1111/1439-0434.ep14258424.

Jones JDG, Dangl JL (2006). The plant immune system. *Nature* 444, 323–329. doi:10.1038/nature05286.

Joubert C, Young PR, Eyéghé-Bickong HA, Vivier MA (2016). Field-grown grapevine berries use carotenoids and the associated xanthophyll cycles to acclimate to UV exposure differentially in high and low light (shade) conditions. *Front Plant Sci* 7, 786. doi:10.3389/FPLS.2016.00786.

Joubert DA, Slaughter AR, Kemp G, Becker JVW, Krooshof GH, Bergmann CW, Benen JAE, Pretorius IS, Vivier MA (2006). The grapevine polygalacturonase-inhibiting protein (VvPGIP1) reduces *Botrytis cinerea* susceptibility in transgenic tobacco and differentially inhibits fungal polygalacturonases. *Transgenic Res* 15, 687–702. doi:10.1007/s11248-006-9019-1.

Juge N (2006). Plant protein inhibitors of cell wall degrading enzymes. *Trends Plant Sci* 11, 359–367. doi:10.1016/j.tplants.2006.05.006.

Kars I, Krooshof GH, Wagemakers L, Joosten R, Benen JAE, Van Kan JAL (2005). Necrotizing activity of five *Botrytis cinerea* endopolygalacturonases produced in *Pichia pastoris*. *Plant J* 43, 213–225. doi:10.1111/j.1365-313X.2005.02436.x.

Kasprzewska A (2003). Plant chitinases - regulation and function. *Cell Mol Biol Lett* 8, 809–824.

Katagiri F, Thilmony R, He SY (2002). The *Arabidopsis thaliana-Pseudomonas syringae* interaction. *Arabidopsis Book* 1, e0039. doi:10.1199/tab.0039.

Keller H, Pamboukdjian N, Ponchet M, Poupet A, Delon R, Verrier J, Roby D, Ricci P (1999). Pathogen-induced elicitin production in transgenic tobacco generates a hypersensitive response and nonspecific disease resistance. *Plant Cell* 11, 223–235. doi:10.2307/3870852.

Kelloniemi J, Trouvelot S, Héloir M-C, Simon A, Dalmais B, Frettinger P, Cimerman A, Fermaud M, Roudet J, Baulande S, Bruel C, Choquer M, Couvelard L, Duthiew M, Ferrarini A, Flors V, Le Pêcheur P, Loisel E, Morgant G, et al. (2015). Analysis of the molecular dialogue between gray mould (*Botrytis cinerea*) and grapevine (*Vitis vinifera*) reveals a clear shift in defense mechanisms during berry ripening. *Mol Plant-Microbe Interact* 28, 1167–1180. doi:10.1094/MPMI-02-15-0039-R.

Kishimoto K, Matsui K, Ozawa R, Takabayashi J (2005). Volatile C6-aldehydes and allo-ocimene activate defense genes and induce resistance against *Botrytis cinerea* in *Arabidopsis thaliana*. *Plant Cell Physiol* 46, 1093–1102. doi: 10.1093/pcp/pci122.

Kong W, Chen N, Liu T, Zhu J, Wang J, He X, Jin Y (2015). Large-scale transcriptome analysis of cucumber and *Botrytis cinerea* during infection. *PLoS ONE* 10, e0142221. doi:10.1371/journal.pone.0142221.

Kravchuk Z, Vicedo B, Flors V, Camañes G, González-Bosch C, García-Agustín P (2011). Priming for JA-dependent defenses using hexanoic acid is an effective mechanism to protect *Arabidopsis* against *B. cinerea*. *J Plant Physiol* 168, 359–366. doi:10.1016/j.jplph.2010.07.028.

Kulye M, Liu H, Zhang Y, Zeng H, Yang X, Qiu D (2012). Hrip1, a novel protein elicitor from necrotrophic fungus, *Alternaria tenuissima*, elicits cell death, expression of defence-related genes and systemic acquired resistance in tobacco. *Plant, Cell Environ* 35, 2104–2120. doi:10.1111/j.1365-3040.2012.02539.x.

Kus J V, Zaton K, Sarkar R, Cameron RK (2002). Age-related resistance in Arabidopsis is a developmentally regulated defense response to *Pseudomonas syringae*. *Plant Cell* 14, 479–490. doi:10.1105/tpc.010481.tions.

Łaźniewska J, Macioszek VK, Lawrence CB, Kononowicz AK (2010). Fight to the death: *Arabidopsis thaliana* defense response to fungal necrotrophic pathogens. *Acta Physiol Plant* 32, 1–10. doi:10.1007/s11738-009-0372-6.

Lee SW, Lee SH, Balaraju K, Park KS, Nam KW, Park JW, Park K (2014). Growth promotion and induced disease suppression of four vegetable crops by a selected plant growth-promoting rhizobacteria (PGPR) strain *Bacillus subtilis* 21-1 under two different soil conditions. *Acta Physiol Plant* 36, 1353–1362. doi:10.1007/s11738-014-1514-z.

Lee SC, Hwang BK (2006). CASAR82A, a pathogen-induced pepper SAR8.2, exhibits an antifungal activity and its overexpression enhances disease resistance and stress tolerance. *Plant Mol Biol* 61, 95–109. doi:10.1007/ s11103-005-6102-6.

Leek JT, Johnson WE, Parker HS, Fertig EJ, Jaffe AE, Storey JD (2016). sva: Surrogate Variable Analysis. R package version 3.22.0.

Liu F, Gong D, Zhang Q, Wang D, Cui M, Zhang Z, Liu G, Wu J, Wang Y (2014). High-throughput generation of an activation-tagged mutant library for functional genomic analyses in tobacco. *Planta* 241, 629–640. doi: 10.1007/s00425-014-2186-z.

Liu S, Kracher B, Ziegler J, Birkenbihl RP, Somssich IE (2015). Negative regulation of ABA signaling by WRKY33 is critical for *Arabidopsis* immunity towards *Botrytis cinerea* 2100. *eLife* 4, e07295. doi:10.7554/eLife.07295.

Maher EA, Bate NJ, Ni W, Elkind Y, Dixon RA, Lamb CJ (1994). Increased disease susceptibility of transgenic tobacco plants with suppressed levels of preformed phenylpropanoid products. *PNAS* 91, 7802–7806.

Małolepsza U, Urbanek H (2000). The oxidants and antioxidant enzymes in tomato leaves treated with *o*-hydroxyethylorutin and infected with *Botrytis cinerea*. *Eur J Plant Pathol* 106, 657–665. doi:10.1023/A:1008719820600.

Marchive C, Mzid R, Deluc LG, Barrieu F, Pirrello J, Gauthier A, Corio-Costet M-F, Regad F, Cailleteau B, Hamdi S, Lauvergeat V (2007). Isolation and characterization of a *Vitis vinifera* transcription factor, VvWRKY1, and its effect on responses to fungal pathogens in transgenic tobacco plants. *J Exp Bot* 58, 1999–2010. doi:10.1093/ jxb/erm062.

Mathys J, De Cremer K, Timmermans P, Van Kerckhove S, Lievens B, Vanhaecke M, Cammue BPA, De Coninck B (2012). Genome-wide characterization of ISR induced in *Arabidopsis thaliana* by *Trichoderma hamatum* T382 against *Botrytis cinerea* infection. *Front Plant Sci* 3, 108. doi:10.3389/fpls.2012.00108.

Mbengue M, Navaud O, Peyraud R, Barascud M, Badet T, Vincent R, Barbacci A, Raffaele S (2016). Emerging trends in molecular interactions between plants and the broad host range fungal pathogens *Botrytis cinerea* and *Sclerotinia sclerotiorum*. *Front Plant Sci* 7, 422. doi:10.3389/fpls.2016.00422.

McKeen WE (1974). Mode of penetration of epidermal cell walls of *Vicia faba* by *Botrytis cinerea*. *Phytopathology* 64, 461. doi:10.1094/Phyto-64-461.

Micali C, Göllner K, Humphry M, Consonni C, Panstruga R (2008). The powdery mildew disease of Arabidopsis: A paradigm for the interaction between plants and biotrophic fungi. *Arabidopsis Book* 6, e0115. doi:10.1199/ tab.0115.

Montillet J, Chamnongpol S, Rustérucci C, Dat J, Van De Cotte B, Agnel J, Battesti C, Inzé D, Van Breusegem F, Triantaphylidès C (2005). Fatty acid hydroperoxides and H_2O_2 in the execution of hypersensitive cell death in tobacco leaves. *Plant Physiol* 138, 1516–1526. doi:10.1104/pp.105.059907.The.

Mueller LA, Solow TH, Taylor N, Skwarecki B, Buels R, Binns J, Lin C, Wright MH, Ahrens R, Wang Y, Herbst E V, Keyder ER, Menda N, Zamir D, Tanksley SD (2005). The SOL Genomics Network: a comparative resource for Solanaceae biology and beyond. *Plant Physiol* 138, 1310–1317. doi:10.1104/pp.105.060707.

Mulema JMK, Denby KJ (2012). Spatial and temporal transcriptomic analysis of the *Arabidopsis thaliana-Botrytis cinerea* interaction. *Mol Biol Rep* 39, 4039–4049. doi:10.1007/s11033-011-1185-4.

Murashige T, Skoog F (1962). A revised medium for rapid growth and bio assays with tobaoco tissue cultures. *Physiol Plant* 15, 473–497. doi:10.1111/j.1399-3054.1962.tb08052.x.

Muroi A, Ishihara A, Tanaka C, Ishizuka A, Takabayashi J, Miyoshi H, Nishioka T (2009). Accumulation of hydroxycinnamic acid amides induced by pathogen infection and identification of agmatine coumaroyltransferase in *Arabidopsis thaliana*. *Planta* 230, 517–527. doi:10.1007/s00425-009-0960-0.

Murphy AM, Holcombe LJ, Carr JP (2000). Characteristics of salicylic acid-induced delay in disease caused by a necrotrophic fungal pathogen in tobacco. *Physiol Mol Plant Pathol* 57, 47–54. doi:10.1006/pmpp.2000.0280.

Nambeesan S, AbuQamar S, Laluk K, Mattoo AK, Mickelbart M V, Ferruzzi MG, Mengiste T, Handa AK (2012). Polyamines attenuate ethylene-mediated defense responses to abrogate resistance to <i>Botrytis cinerea<i> in tomato. *Plant Physiol* 158, 1034–1045. doi:10.1104/pp.111.188698.

Nandi B, Fries N (1976). Volatile aldehydes, ketones, esters and terpenoids as preservatives against storage fungi in wheat. *J Plant Dis Prot* 83, 284–294.

Noda J, Brito N, González C (2010). The *Botrytis cinerea* xylanase Xyn11A contributes to virulence with its necrotizing activity, not with its catalytic activity. *BMC Plant Biol* 10, 38. doi:10.1186/1471-2229-10-38.

Oliver JE, Sefick SA, Parker JK, Arnold T, Cobine PA, De La Fuente L (2014). Ionome changes in *Xylella fastidiosa*-infected *Nicotiana tabacum* correlate with virulence and discriminate between subspecies of bacterial isolates. *Mol Plant-Microbe Interact* 27, 1048–1058. doi:10.1094/MPMI-05-14-0151-R.

Pare PW, Tumlinson JH (1999). Plant volatiles as a defense against insect herbivores. *Plant Physiol* 121, 325–331. doi: 10.1104/pp.121.2.325.

Passardi F, Penel C, Dunand C (2004). Performing the paradoxical: How plant peroxidases modify the cell wall. *Trends Plant Sci* 9, 534–540. doi:10.1016/j.tplants.2004.09.002.

Pezet R, Pontt V, Hoang-Van K (1991). Evidence for oxidative detoxication of pterostilbene and resveratrol by a laccase-like stilbene oxidase produced by *Botrytis cinerea*. *Physiol Mol Plant Pathol* 39, 441–450. doi:10.1016/0885-5765(91)90010-F.

Piedras P, Hammond-Kosack KE, Harrison K, Jones JDG (1998). Rapid, *Cf*-9- and Avr9-dependent production of active oxygen species in tobacco suspension cultures. *Mol Plant-Microbe Interact* 11, 1155–1166. doi:10.1094/MPMI.1998.11.12.1155.

Poland JA, Balint-Kurti PJ, Wisser RJ, Pratt RC, Nelson RJ (2009). Shades of gray: the world of quantitative disease resistance. *Trends Plant Sci* 14, 21–29. doi:10.1016/j.tplants.2008.10.006.

Pontier D, Godiard L, Marco Y, Roby D (1994). *hsr*203J, a tobacco gene whose activation is rapid, highly localized and specific for incompatible plant/pathogen interactions. *Plant J* 5, 507–521. doi:10.1046/j.1365-313X.1994.05040507.x.

Pontier D, Tronchet M, Rogowsky P, Lam E, Roby D (1998). Activation of *hsr*203, a plant gene expressed during incompatible plant-pathogen interactions, is correlated with programmed cell death. *Mol Plant-Microbe Interact* 11, 544–554. doi:10.1094/MPMI.1998.11.6.544.

Ramel F, Birtic S, Ginies C, Soubigou-Taconnat L, Triantaphylidès C, Havaux M (2012). Carotenoid oxidation products are stress signals that mediate gene responses to singlet oxygen in plants. *PNAS* 109, 5535–5540. doi:10.1073/pnas.1115982109.

Renault AS, Deloire A, Letinois I, Kraeva E, Tesniere C, Ageorges A, Redon C, Bierne J (2000). β-1,3-glucanase gene expression in grapevine leaves as a response to infection with *Botrytis cinerea*. *Am J Enol Vitic* 51, 81–87.

Reuveni M, Tuzun S, Cole JS, Siegel MR, Kuć J (1986). The effects of plant age and leaf position on the susceptibility of tobacco to blue mold caused by *Peronospora tabacina*. *Phytopathology* 76, 455–458. doi:10.1094/Phyto-76-455.

Rose JKC, Braam J, Fry SC, Nishitani K (2002). The XTH family of enzymes involved in xyloglucan endotransglycosylation and endohydrolysis: Current perspectives and a new unifying nomenclature. *Plant Cell Physiol* 43, 1421–1435. doi:10.1093/pcp/pcf171.

Ross AF (1961). Systemic acquired resistance induced by localized virus infections in plants. *Virology* 14, 340–358. doi: 10.1016/0042-6822(61)90319-1.

Roux F, Voisin D, Badet T, Balagué C, Barlet X, Huard-Chauveau C, Roby D, Raffaele S (2014). Resistance to phytopathogens *e tutti quanti*: Placing plant quantitative disease resistance on the map. *Mol Plant Pathol* 15, 427–432. doi:10.1111/mpp.12138.

Rowe HC, Kliebenstein DJ (2008). Complex genetics control natural variation in *Arabidopsis thaliana* resistance to *Botrytis cinerea*. *Genetics* 180, 2237–2250. doi:10.1534/genetics.108.091439.

Rutledge RG (2011). A java program for LRE-based real-time qPCR that enables large-scale absolute quantification. *PLoS ONE* 6, e17636. doi:10.1371/journal.pone.0017636.

Rutledge RG, Stewart D (2008). A kinetic-based sigmoidal model for the polymerase chain reaction and its application to high-capacity absolute quantitative real-time PCR. *BMC Biotechnol* 8, 47. doi:10.1186/1472-6750-8-47.

Ryals JA, Neuenschwander UH, Willits MG, Molina A, Steiner H-Y, Hunt MD (1996). Systemic acquired resistance. *Plant Cell* 8, 1809–1819. doi:10.2307/3870231.

Saldanha AJ (2004). Java Treeview - Extensible visualization of microarray data. *Bioinformatics* 20, 3246–3248. doi: 10.1093/bioinformatics/bth349.

Sasabe M, Takeuchi K, Kamoun S, Ichinose Y, Govers F, Toyoda K, Shiraishi T, Yamada T (2000). Independent pathways leading to apoptotic cell death, oxidative burst and defense gene expression in response to elicitin in tobacco cell suspension culture. *Eur J Biochem* 267, 5005–5013. doi:10.1046/j.1432-1327.2000.01553.x.

Schenk PM, Kazan K, Manners JM, Anderson JP, Simpson RS, Wilson IW, Somerville SC, Maclean DJ (2003). Systemic gene expression in Arabidopsis during an incompatible interaction with *Alternaria brassicicola*. *Plant Physiol* 132, 999–1010. doi:10.1104/pp.103.021683.

Segarra G, Elena G, Trillas I (2013). Systemic resistance against *Botrytis cinerea* in Arabidopsis triggered by an olive marc compost substrate requires functional SA signalling. *Physiol Mol Plant Pathol* 82, 46–50. doi:10.1016/ j.pmpp.2013.02.002.

Sela D, Buxdorf K, Shi JX, Feldmesser E, Schreiber L, Aharoni A, Levy M (2013). Overexpression of *AtSHN1/WIN1* provokes unique defense responses. *PLoS ONE* 8, e70146. doi:10.1371/journal.pone.0070146.

Sham A, Al-Azzawi A, Al-Ameri S, Al-Mahmoud B, Awwad F, Al-Rawashdeh A, Iratni R, AbuQamar S (2014). Transcriptome analysis reveals genes commonly induced by *Botrytis cinerea* infection, cold, drought and oxidative stresses in *Arabidopsis*. *PLoS ONE* 9, e113718. doi:10.1371/journal.pone.0113718.

Shaul O, Galili S, Volpin H, Ginzberg I, Elad Y, Chet I, Kapulnik Y (1999). Mycorrhiza-induced changes in disease severity and PR protein expression in tobacco leaves. *Mol Plant-Microbe Interact* 12, 1000–1007. doi:10.1094/ MPMI.1999.12.11.1000.

Shlezinger N, Minz A, Gur Y, Hatam I, Dagdas YF, Talbot NJ, Sharon A (2011). Anti-apoptotic machinery protects the necrotrophic fungus *Botrytis cinerea* from host-induced apoptotic-like cell death during plant infection. *PLoS Pathog* 7, e1002185. doi:10.1371/journal.ppat.1002185.

Sierro N, Battey JND, Ouadi S, Bakaher N, Bovet L, Willig A, Goepfert S, Peitsch MC, Ivanov N V (2014). The tobacco genome sequence and its comparison with those of tomato and potato. *Nat Commun* 5, 3833. doi:10.1038/ ncomms4833.

Sierro N, Battey JN, Ouadi S, Bovet L, Goepfert S, Bakaher N, Peitsch MC, Ivanov N V (2013). Reference genomes and transcriptomes of *Nicotiana sylvestris* and *Nicotiana tomentosiformis*. *Genome Biol* 14, R60. doi:10.1186/gb-2013-14-6-r60.

Smith JE, Mengesha B, Tang H, Mengiste T, Bluhm BH (2014). Resistance to *Botrytis cinerea* in *Solanum lycopersicoides* involves widespread transcriptional reprogramming. *BMC Genomics* 15, 334. doi:10.1186/1471-2164-15-334.

Smyth GK (2005). Limma: Linear models for microarray data. *Bioinforma Comput Biol Solut using R Bioconductor*, 397–420. doi:10.1007/0-387-29362-0_23.

Sohn SI, Kim YH, Kim BR, Lee SY, Lim CK, Hur JH, Lee JY (2007). Transgenic tobacco expressing the *hrpN*$_{EP}$ gene from *Erwinia pyrifoliae* triggers defense responses against *Botrytis cinerea*. *Mol Cells* 24, 232–239. doi:1124 [pii].

Stahl EA, Bishop JG (2000). Plant – pathogen arms races at the molecular level. *Curr Opin Plant Biol* 3, 299–304. doi: 10.1016/S1369-5266(00)00083-2.

Stavely JR, Slana LJ (1971). Relation of leaf age to the reaction of tobacco to *Alternaria alternata*. *Phytopathology* 61, 73–78. doi:10.1094/Phyto-61-73.

Stefanato FL, Abou-Mansour E, Buchala A, Kretschmer M, Mosbach A, Hahn M, Bochet CG, Métraux JP, Schoonbeek HJ (2009). The ABC transporter BcatrB from *Botrytis cinerea* exports camalexin and is a virulence factor on *Arabidopsis thaliana*. *Plant J* 58, 499–510. doi:10.1111/j.1365-313X.2009.03794.x.

Szatmári Á, Zvara Á, Móricz ÁM, Besenyei E, Szabó E, Ott PG, Puskás LG, Bozsó Z (2014). Pattern triggered immunity (PTI) in tobacco: Isolation of activated genes suggests role of the phenylpropanoid pathway in inhibition of bacterial pathogens. *PLoS ONE* 9, e102869. doi:10.1371/journal.pone.0102869.

Taguchi F, Suzuki T, Inagaki Y, Toyoda K, Shiraishi T, Ichinose Y (2010). The siderophore pyoverdine of *Pseudomonas syringae* pv. tabaci 6605 is an intrinsic virulence factor in host tobacco infection. *J Bacteriol* 192, 117–126. doi:10.1128/JB.00689-09.

Takahashi S, Yeo YS, Zhao Y, O'Maille PE, Greenhagen BT, Noel JP, Coates RM, Chappell J (2007). Functional characterization of premnaspirodiene oxygenase, a cytochrome P450 catalyzing regio- and stereo-specific hydroxylations of diverse sesquiterpene substrates. *J Biol Chem* 282, 31744–31754. doi:10.1074/ jbc.M703378200.

Thimm O, Bläsing OE, Gibon Y, Nagel A, Meyer S, Krüger P, Selbig J, Müller LA, Rhee SY, Stitt M (2004). Mapman: a user-driven tool to display genomics data sets onto diagrams of metabolic pathways and other biological processes. *Plant J* 37, 914–939. doi:10.1111/j.1365-313X.2004.02016.x.

Thoma I, Loeffler C, Sinha AK, Gupta M, Krischke M, Steffan B, Roitsch T, Mueller MJ (2003). Cyclopentenone isoprostanes induced by reactive oxygen species trigger defense gene activation and phytoalexin accumulation in plants. *Plant J* 34, 363–375. doi:10.1046/j.1365-313X.2003.01730.x.

Tsao R, Zhou T (2000). Antifungal activity of monoterpenoids against postharvest pathogens *Botrytis cinerea* and *Monilinia fructicola*. *J Essent Oil Res* 12, 113–121. doi:10.1080/10412905.2000.9712057.

Vallabhaneni R, Bradbury LMT, Wurtzel ET (2010). The carotenoid dioxygenase gene family in maize, sorghum, and rice. *Arch Biochem Biophys* 504, 104–111. doi:10.1016/j.abb.2010.07.019.

Van Den Berg RA, Hoefsloot HCJ, Westerhuis JA, Smilde AK, Van Der Werf MJ (2006). Centering, scaling, and transformations: improving the biological information content of metabolomics data. *BMC Genomics* 7, 142. doi:10.1186/1471-2164-7-142.

Van Kan JAL (2006). Licensed to kill: the lifestyle of a necrotrophic plant pathogen. *Trends Plant Sci* 11, 247–253. doi: 10.1016/j.tplants.2006.03.005.

Van Loon LC (1985). Pathogenesis-related proteins. *Plant Mol Biol* 116, 111–116.

Vega A, Canessa P, Hoppe G, Retamal I, Moyano TC, Canales J, Gutiérrez RA, Rubilar J (2015). Transcriptome analysis reveals regulatory networks underlying differential susceptibility to *Botrytis cinerea* in response to nitrogen availability in *Solanum lycopersicum*. *Front Plant Sci* 6, 911. doi:10.3389/fpls.2015.00911.

Vera J, Castro J, Contreras RA, González A, Moenne A (2012). Oligo-carrageenans induce a long-term and broad-range protection against pathogens in tobacco plants (var. Xanthi). *Physiol Mol Plant Pathol* 79, 31–39. doi:10.1016/ j.pmpp.2012.03.005.

Walters DR, Fountaine JM (2009). Practical application of induced resistance to plant diseases: an appraisal of effectiveness under field conditions. *J Agric Sci* 147, 523–535. doi:10.1017/S0021859609008806.

Wang D, Wang S, Chao J, Wu X, Sun Y, Li F, Lv J, Gao X, Liu G, Wang Y (2017). Morphological phenotyping and genetic analyses of a new chemical-mutagenized population of tobacco (*Nicotiana tabacum* L.). *Planta* 246, 149–163. doi:10.1007/s00425-017-2690-z.

Wang K, Liao Y, Kan J, Han L, Zheng Y (2015). Response of direct or priming defense against *Botrytis cinerea* to methyl jasmonate treatment at different concentrations in grape berries. *Int J Food Microbiol* 194, 32–39. doi:10.1016/ j.ijfoodmicro.2014.11.006.

Ward EWB, Unwin CH, Stoessl A (1974). Postinfectional inhibitors from plants. XIII. Fungitoxicity of the phytoalexin, capsidiol, and related sesquiterpenes. *Can J Bot* 52, 2481–2488. doi:10.1139/b75-115.

Whitehead IM, Threlfall DR, Ewing DF (1989). 5-epi-aristolochene is a common precursor of the sesquiterpenoid phytoalexins capsidiol and debneyol. *Phytochemistry* 28, 775–779. doi:10.1016/0031-9422(89)80114-1.

Windram O, Madhou P, McHattie S, Hill C, Hickman R, Cooke E, Jenkins DJ, Penfold CA, Baxter L, Breeze E, Kiddle SJ, Rhodes J, Atwell S, Kliebenstein DJ, Kim Y, Stegle O, Borgwardt K, Zhang C, Tabrett A, et al. (2012). *Arabidopsis* defense against *Botrytis cinerea*: chronology and regulation deciphered by high-resolution temporal transcriptomic analysis. *Plant Cell* 24, 3530–3557. doi:10.1105/tpc.112.102046.

Yu M, Shen L, Fan B, Zhao D, Zheng Y, Sheng J (2009). The effect of MeJA on ethylene biosynthesis and induced disease resistance to *Botrytis cinerea* in tomato. *Postharvest Biol Technol* 54, 153–158. doi:10.1016/ j.postharvbio.2009.07.001.

Zeier J (2005). Age-dependent variations of local and systemic defence responses in *Arabidopsis* leaves towards an avirulent strain of *Pseudomonas syringae*. *Physiol Mol Plant Pathol* 66, 30–39. doi:10.1016/ j.pmpp.2005.03.007.

Zhang P, Chen K (2009). Age-dependent variations of volatile emissions and inhibitory activity toward *Botrytis cinerea* and *Fusarium oxysporum* in tomato leaves treated with chitosan oligosaccharide. *J Plant Biol* 52, 332–339. doi: 10.1007/s12374-009-9043-9.

Zhang Y, Zhang Y, Qiu D, Zeng H, Guo L, Yang X (2015). BcGs1, a glycoprotein from *Botrytis cinerea*, elicits defence response and improves disease resistance in host plants. *Biochem Biophys Res Commun* 457, 627–634. doi: 10.1016/j.bbrc.2015.01.038.

Zheng Q, Wang X-J (2008). GOEAST: a web-based software toolkit for Gene Ontology enrichment analysis. *Nucleic Acids Res* 36, W358–W363. doi:10.1093/nar/gkn276.

Zhou M, Wang W, Karapetyan S, Mwimba M, Marqués J, Buchler NE, Dong X (2015). Redox rhythm reinforces the circadian clock to gate immune response. *Nature* 523, 472–476. doi:10.1038/nature14449.

Zimmerli L, Métraux JP, Mauch-Mani B (2001). β-Aminobutyric acid-induced protection of Arabidopsis against the necrotrophic fungus *Botrytis cinerea*. *Plant Physiol* 126, 517–523. doi:10.1104/pp.126.2.517.

Zurbriggen MD, Carrillo N, Tognetti VB, Melzer M, Peisker M, Hause B, Hajirezaei M-R (2009). Chloroplast-generated reactive oxygen species play a major role in localized cell death during the non-host interaction between tobacco and *Xanthomonas campestris* pv. *vesicatoria*. *Plant J* 60, 962–973. doi:10.1111/j.1365-313X.2009.04010.x.

Appendix A to Chapter 3

MIAME documentation

(based on the MIAME/PLANT protocol:
https://www.arabidopsis.org/portals/expression/microarray/MIAME-plant_Dec2005.pdf)

Experiment design:

To identify differentially expressed genes in *Nicotiana tabacum* cv. Havana Petit SR1 in response to *Botrytis cinerea* lesion development and distal infection and to identify transcriptional changes induced by constitutive *Vitis vinifera polygalacturonase-inhibiting protein 1* (*Vvipgip1*) expression.

I. Array Design Description

Agilent Tobacco Gene Expression Microarray is a 44k format dual-colour array. The array contains 43803 60-mer oligonucleotide probes sourced from UniGene (Build 11, July 2008), TIGR (Release 3, September 2006) and IGR Plant Transcript Assemblies (Release 5, June 2007). It is manufactured by Agilent Technologies (Palo Alto, CA 94304 USA). Catalogue number for the 4 x 44K array is 021113. Three GEO accessions represent this array, namely GPL21158, GPL21056 and GPL10098.

II. Experiment Description

1. Plant experimental design

1) Pooling of samples

Tobacco leaf position had previously been established to affect response to *B. cinerea*, therefore it was decided to keep leaf positions separate, but combine samples from four biological repeats. For example, the sample for leaf 3 consisted of tissue (from the youngest third leaf) from four individual plants. This provided sufficient material for analysis of gene expression and metabolite levels. During sample collection, tissue from each individual plant was flash-frozen separately (per leaf and per time point). During preparation for sample extraction, the tissue from the four biological replicates was combined (in liquid nitrogen) prior to grinding, and ground and homogenised by hand for at least two minutes using a liquid nitrogen-cooled pestle and mortar.

2) Experimental design

Experimental design for microarray analysis, showing which samples were analysed on each channel.

Response profiled	Leaf position	Dye: Cy3	Dye: Cy5	Company performing analysis
Distal	2	VviPGIP1 0 h A	Wild-type 0 h A	OGT
Distal	2	VviPGIP1 0 h B	Wild-type 0 h B	OGT
Distal	2	VviPGIP1 0 h C	Wild-type 0 h C	OGT
Distal	2	VviPGIP1 12 h A	Wild-type 12 h A	OGT
Distal	2	VviPGIP1 12 h B	Wild-type 12 h B	OGT
Distal	2	VviPGIP1 12 h C	Wild-type 12 h C	OGT
Distal	2	VviPGIP1 24 h A	Wild-type 24 h A	OGT
Distal	2	VviPGIP1 24 h B	Wild-type 24 h B	OGT
Distal	2	VviPGIP1 24 h C	Wild-type 24 h C	OGT
Distal	2	VviPGIP1 36 h A	Wild-type 36 h A	OGT
Distal	2	VviPGIP1 36 h B	Wild-type 36 h B	OGT
Distal	2	VviPGIP1 36 h C	Wild-type 36 h C	OGT
Distal	2	VviPGIP1 48 h A	Wild-type 48 h A	OGT
Distal	2	VviPGIP1 48 h B	Wild-type 48 h B	OGT
Distal	2	VviPGIP1 48 h C	Wild-type 48 h C	OGT
Local	3	Wild-type 0 h A	VviPGIP1 0 h A*	MOgene
Local	3	Wild-type 0 h B	VviPGIP1 0 h B*	MOgene
Local	3	VviPGIP1 0 h C	Wild-type 0 h C	MOgene
Local	3	Wild-type 12 h A	VviPGIP1 12 h A*	MOgene
Local	3	Wild-type 12 h B	VviPGIP1 12 h B*	MOgene
Local	3	VviPGIP1 12 h C	Wild-type 12 h C	MOgene
Local	3	Wild-type 24 h A	VviPGIP1 24 h A*	MOgene
Local	3	Wild-type 24 h B	VviPGIP1 24 h B*	MOgene
Local	3	VviPGIP1 24 h C	Wild-type 24 h C	MOgene
Local	3	Wild-type 36 h A	VviPGIP1 36 h A*	MOgene
Local	3	Wild-type 36 h B	VviPGIP1 36 h B*	MOgene
Local	3	VviPGIP1 36 h C	Wild-type 36 h C	MOgene
Local	3	Wild-type 48 h A	VviPGIP1 48 h A*	MOgene
Local	3	Wild-type 48 h B	VviPGIP1 48 h B*	MOgene
Local	3	VviPGIP1 48 h C	Wild-type 48 h C	MOgene

Plants were grown in the same growth chamber. Twenty plants (from each line) with 6 fully expanded leaves were moved to clear Perspex humidity chambers one day before inoculation and acclimatised to 100% relative humidity. Each humidity chamber contained the plants harvested at one sampling point. Humidity chambers were identically positioned under lights. All six leaves were harvested from each plant at each sampling point.

2. Plant Samples used, RNA extraction and labelling

1) Biosource properties

Plant/Strain of line/Genotype

Nicotiana tabacum cv Havana Petit SR1 was used as wild-type. Transgenic tobacco was generated as described by Joubert et al. 2006.

Starting material

Seeds were sterilised using chlorine gas and germinated on MS medium (Murashige and Skoog, 1962) without supplemental sucrose. Transgenic seeds were germinated under Kanamycin

selection. Seedlings at the 4-leaf stage were transferred to peat moss plugs (Jiffy Products International AS, Norway) and hardened off before the plug was transferred to pots containing a 1:2:3 mix of DoubleGrow “All Purpose” potting soil (DoubleGrow, Durbanville, South Africa), peat moss and DoubleGrow vermiculite. Liquid organic fertilizer was supplied every two weeks, plants were water twice a week.

Developmental stage

Plant were mature, but not flowering.

Organism part

Fully expanded leaves at the third to fifth position from the apex of the plant were used for inoculation. Tissue surrounding the inoculation site was collected on leave 3-5. The central vein of non-inoculated leaves was excised, and the remaining leaf blade was collected.

2) Biomaterial manipulations

Growth substrates

Peat moss (Jiffy Products International AS, Norway). Commercial potting soil and vermiculite (DoubleGrow, Durbanville, South Africa) in 12 cm pots.

Growth environment

Growth room in greenhouse (prior to infection). Infection lab with identical lighting. Both with temperature control. Paper sheets were used to increase humidity in sealed Perspex chambers. Tinytag data loggers (Gemini Data Loggers, Chinchester, West Sussex, UK) confirmed that 100% humidity is reached 1h after sealing the chamber.

Environmental conditions

Duration: 16 hours day / 9 hours night. Light intensity 120 µmol m^2s^{-1}. Light source: Lumilux Cool White (Osram GmbH, Munich, Germany). Temperature: 24°C. Relative humidity: 55% prior to infection, 100% from 24 h prior to infection.

3) Treatment type

Biotic factors

Fungus: *Botrytis cinerea*. Pathogenic culture of *B. cinerea* was isolated from a South African vineyard and maintained on sterile apricot halves (Naturlite, Tiger Food Brands Limited, South Africa). Spores were collected by washing the apricot with sterile water and filtering the spore suspension through glass wool to remove mycelial debris. After hydrating for 16 hours, spore concentration was determined using a haemocytometer and adjusted to 1000 spore per microliter in 50% grape juice. Inoculations were performed simultaneously for all 20 plants. Inoculations were performed by

pipetting 5 µL of spore suspension onto the leaf. Inoculations were performed on three leaves per plant and each inoculated leaf received four inoculation spots.

4) Extraction method

The RNA extraction protocol was adapted from Coutos-Thévenot et al. (2001). Three RNA extractions were done from each sample by extracting 50 mg ground tissue in 3.2 M phenol, 100 mM Tris pH 8.0, 1.5% SDS, 300 mM LiCl, 10 mM Na_2EDTA, 1% (w/v) sodium deoxycholate, 1% (w/v) IGEPAL CA-630, 5 mM thiourea and 1% sodium metabisulphite. Two chloroform extractions removed residual phenol prior to isopropanol precipitation. RNA was precipitated in 2.5 M LiCl and suspended in 30 µL nuclease free water. Quality was evaluated on a formaldehyde agarose gel, while concentration was estimated with a Nanodrop™ (Thermo Scientific, Waltham, USA).

RNA extraction of leaf 3 was performed in 2011. RNA concentration was standardised to 160 ng/µL before shipping. Column purification using the RNeasy mini kit (Qiagen, Hilden, Germany) was performed by MOgene, LC (St. Louis, MO, USA).

RNA extraction of leaf 2 was performed in 2015 and was followed by DNase I (Roche Diagnositcs GmbH, Mannheim, Germany) treatment and column purification using the RNeasy midi kit (Qiagen). RNA concentration was standardised to 20 ng/µL prior to shipping.

Array hybridizations, data processing and data quality assessment

RNA quality was determined using Agilent Bioanalyzer before cDNA synthesis. The array hybridizations and data capture procedures were completed at MOgene, LC (St. Louis, MO, USA) for leaf 3 and Oxford Gene Technology (Begbroke, Oxfordshire, UK) for leaf 2. Procedures followed the standard protocol recommended by Agilent.

Data processing and normalisation: The raw intensity data was processed in R, using linear models with the limma package for background correction and surrogate variable analysis (SVA) using the sva package for normalisation.

Cited references

Coutos-Thévenot P, Poinssot B, Bonomelli A, Yean H, Breda C, Buffard D, Esnault R, Hain R, Boulay M (2001). *In vitro* tolerance to *Botrytis cinerea* of grapevine 41B rootstock in transgenic plants expressing the stilbene synthase *Vst1* gene under the control of a pathogen-inducible PR10 promoter. *J Exp Bot* 52, 901–910. doi:10.1093/jexbot/52.358.901.

Joubert DA, Slaughter AR, Kemp G, Becker JVW, Krooshof GH, Bergmann CW, Benen JAE, Pretorius IS, Vivier MA (2006). The grapevine polygalacturonase-inhibiting protein (VvPGIP1) reduces *Botrytis cinerea* susceptibility in transgenic tobacco and differentially inhibits fungal polygalacturonases. *Transgenic Res* 15, 687–702. doi:10.1007/s11248-006-9019-1.

Appendix B to Chapter 3

Microarray quality control

Gene expression analysis of leaf 3 (control and transgenic)

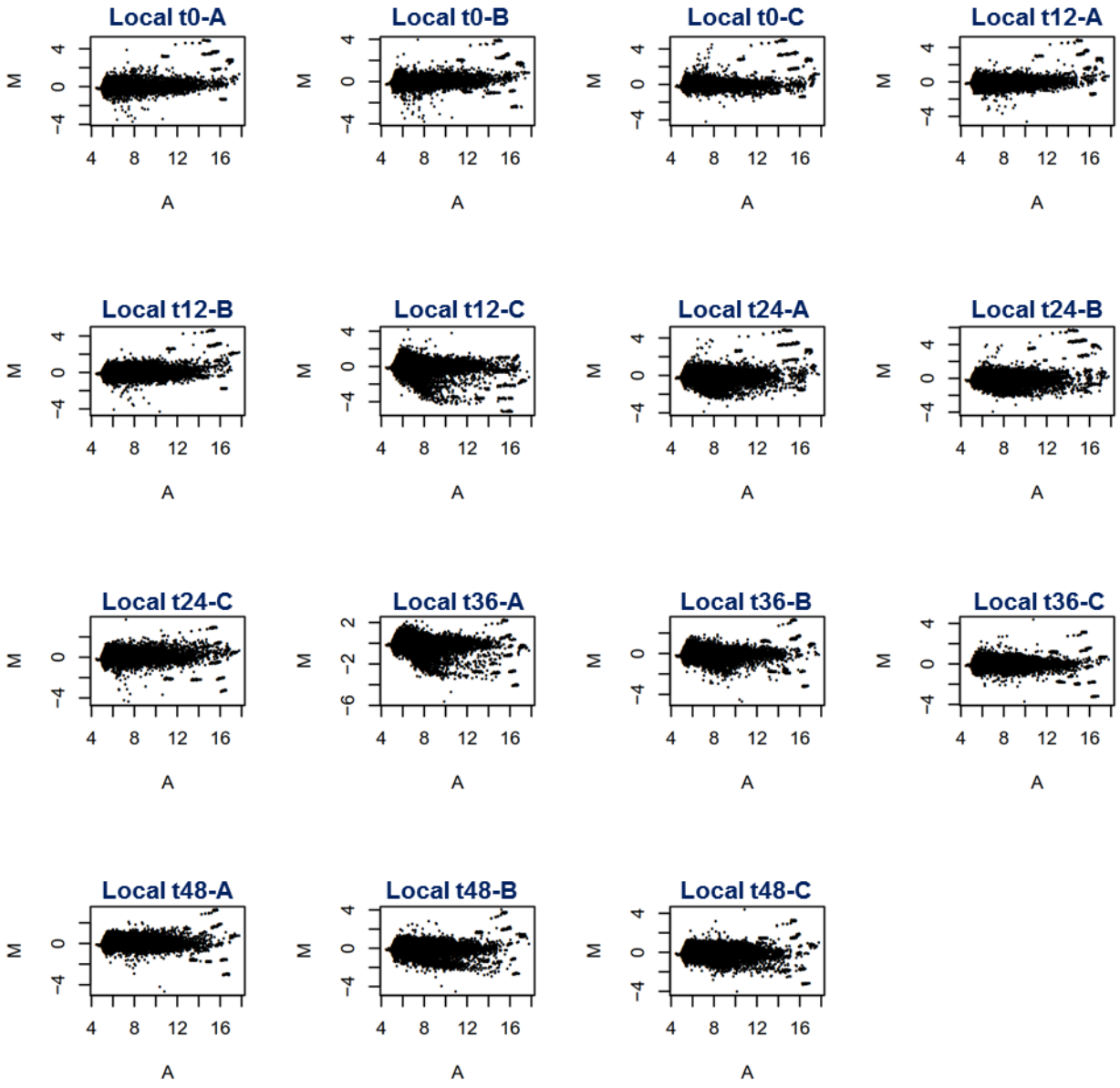

Gene expression analysis of leaf 2 (control and transgenic). Note the t12-C plot (boxed in red), where the transgenic sample was analysed on a bad channel and was omitted from subsequent analyses.

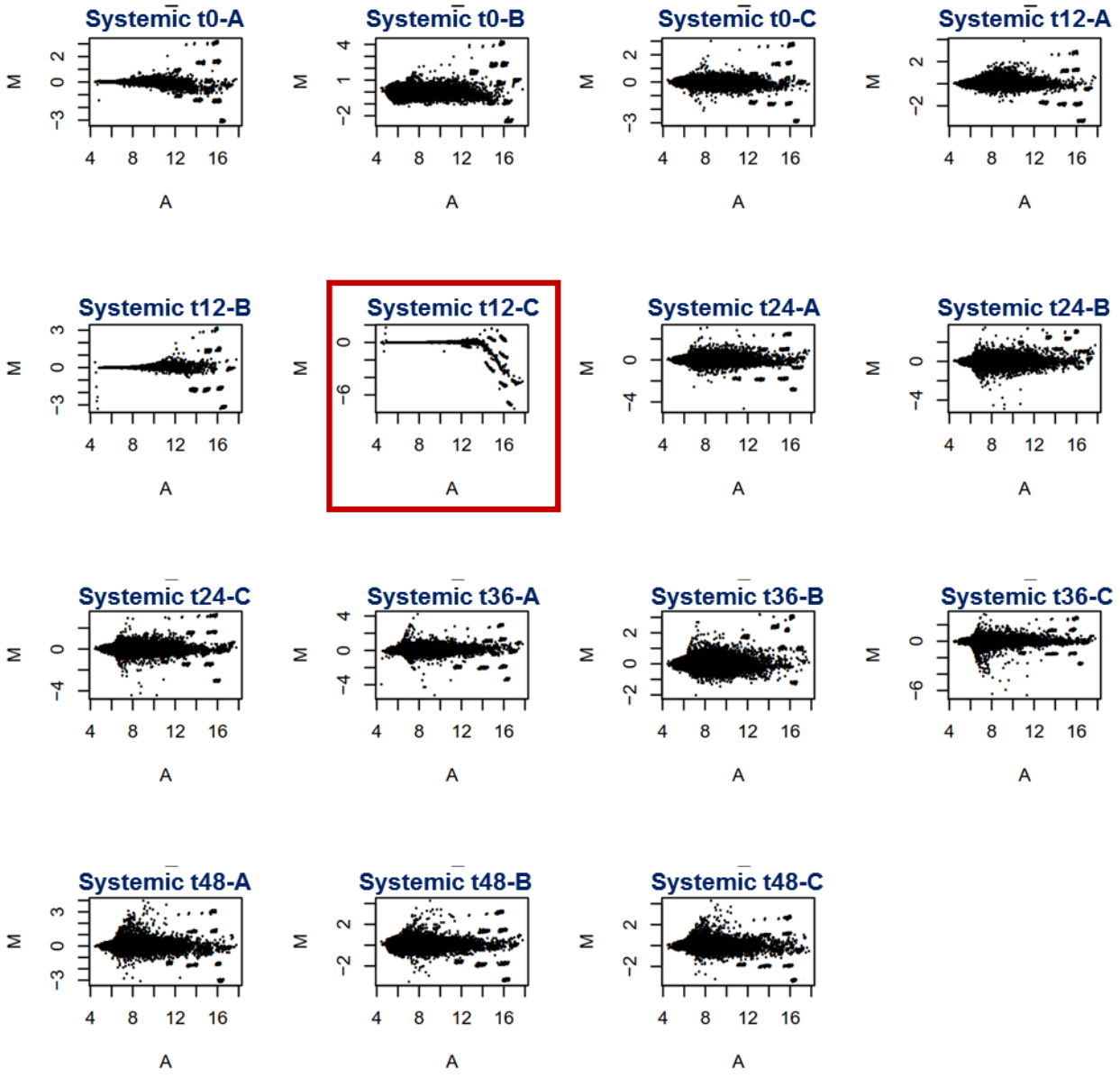

Appendix C to Chapter 3

Microarray data curation steps

Blue block: Core dataset subjected to further curation steps (presented in Chapters 3 and 4)

Green blocks: data used for each curation step.

Red blocks: curation steps and record of data points (probes/gene models) removed at each step

Yellow block: curation step and record of gene models added

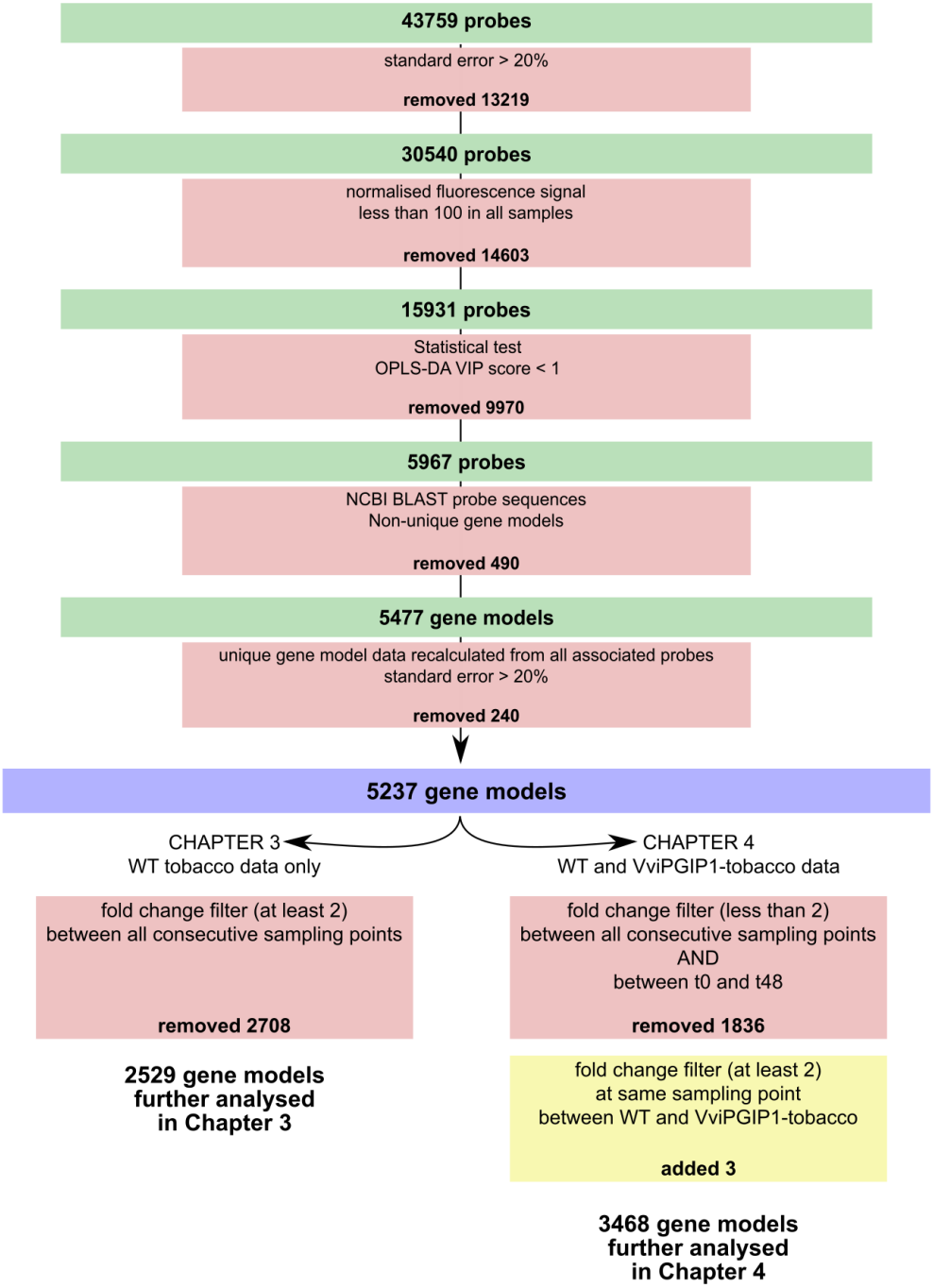

Appendix D to Chapter 3

GO enrichment analysis of gene models with a 2-fold change between consecutive time points

Δt: Fold-change data calculated relative to earlier sampling point

GOID	Term	Local expression profile								Distal expression profile							
		Induced				Repressed				Induced				Repressed			
		Δt0-12	Δt12-24	Δt24-36	Δt36-48	Δt0-12	Δt12-24	Δt24-36	Δt36-48	Δt0-12	Δt12-24	Δt24-36	Δt36-48	Δt0-12	Δt12-24	Δt24-36	Δt36-48
GO:0007568	aging					8.E-02											
GO:0006915	apoptotic process				1.E-01			1.E-01					4.E-02				
GO:0046034	ATP metabolic process			6.E-02													
GO:0009058	biosynthetic process	3.E-02		6.E-02			1.E-05		8.E-02								
GO:0016051	carbohydrate biosynthetic process			4.E-02						2.E-02							
GO:0005975	carbohydrate metabolic process	1.E-05		8.E-05			2.E-04		1.E-01	6.E-02					3.E-02		
GO:0015976	carbon utilization			7.E-03						6.E-03							
GO:0019752	carboxylic acid metabolic process	1.E-01	4.E-02	1.E-01													
GO:0016998	cell wall macromolecule catabolic process		6.E-04	1.E-02							1.E-01						
GO:0009063	cellular amino acid catabolic process	5.E-02															7.E-02
GO:0006725	cellular aromatic compound metabolic process				1.E-01												
GO:0044262	cellular carbohydrate metabolic process	2.E-03					4.E-04		1.E-01	5.E-02						2.E-02	
GO:0006073	cellular glucan metabolic process	3.E-03					1.E-02			7.E-02					8.E-02	3.E-02	
GO:0044237	cellular metabolic process	2.E-05	2.E-02	3.E-02	8.E-02		1.E-11	3.E-05	3.E-04	2.E-02	1.E-01		4.E-05		3.E-02	3.E-04	
GO:0009987	cellular process	2.E-07	2.E-03	4.E-03	2.E-02		5.E-12	4.E-09	2.E-06	4.E-04	4.E-02		2.E-06		2.E-05	4.E-06	5.E-02
GO:0042631	cellular response to water deprivation					1.E-01								8.E-02			
GO:0030244	cellulose biosynthetic process									1.E-01					7.E-02		
GO:0006032	chitin catabolic process		5.E-06	2.E-03							1.E-02			7.E-02			
GO:0015995	chlorophyll biosynthetic process	2.E-03					8.E-03	9.E-02	2.E-03							8.E-06	

GOID	Term	Local expression profile								Distal expression profile							
		Induced				Repressed				Induced				Repressed			
		Δt0-12	Δt12-24	Δt24-36	Δt36-48	Δt0-12	Δt12-24	Δt24-36	Δt36-48	Δt0-12	Δt12-24	Δt24-36	Δt36-48	Δt0-12	Δt12-24	Δt24-36	Δt36-48
GO:0015994	chlorophyll metabolic process	8.E-03					4.E-02	4.E-02	1.E-02							8.E-05	
GO:0009658	chloroplast organization	4.E-03					3.E-03		5.E-02	4.E-03							
GO:0009902	chloroplast relocation						1.E-01			3.E-02					7.E-02		
GO:0006333	chromatin assembly or disassembly															7.E-03	
GO:0006325	chromatin organization															1.E-01	
GO:0007623	circadian rhythm	3.E-02					3.E-03		5.E-04			1.E-02	2.E-02				
GO:0051186	cofactor metabolic process	1.E-03		4.E-04					5.E-02		8.E-02					3.E-02	
GO:0055070	copper ion homeostasis	3.E-03					6.E-03		3.E-03	5.E-02							
GO:0009805	coumarin biosynthetic process		5.E-04		3.E-05												
GO:0019344	cysteine biosynthetic process	6.E-02															
GO:0006534	cysteine metabolic process	1.E-01															
GO:0006952	defence response		5.E-06	7.E-05	1.E-02	4.E-02	3.E-02	5.E-06	1.E-01	1.E-01	1.E-06		7.E-04	5.E-04	2.E-03	3.E-03	
GO:0042742	defence response to bacterium		1.E-01	4.E-03			2.E-03	6.E-02	2.E-04	2.E-02	9.E-02						
GO:0050832	defence response to fungus		5.E-04			5.E-03		1.E-01			2.E-06			1.E-03			
GO:0006323	DNA packaging															1.E-03	
GO:0022900	electron transport chain								2.E-03								
GO:0009693	ethylene biosynthetic process		1.E-01								5.E-02						
GO:0009250	glucan biosynthetic process						1.E-01								5.E-02		
GO:0006114	glycerol biosynthetic process									7.E-02							
GO:0006662	glycerol ether metabolic process						4.E-02										
GO:0006546	glycine catabolic process	6.E-02					1.E-01										
GO:0019464	glycine decarboxylation via glycine cleavage system	1.E-02					3.E-02			1.E-01							
GO:0006096	glycolytic process	1.E-02		1.E-02						1.E-01					1.E-01		
GO:0015969	guanosine tetraphosphate metabolic process												1.E-01				
GO:0006783	heme biosynthetic process												2.E-02			4.E-02	
GO:0006971	hypotonic response																7.E-02
GO:0045087	innate immune response		2.E-02														
GO:0055072	iron ion homeostasis	1.E-01															
GO:0019288	isopentenyl diphosphate biosynthetic process, methylerythritol 4-phosphate pathway															1.E-01	

GOID	Term	Local expression profile								Distal expression profile							
		Induced				Repressed				Induced				Repressed			
		Δt0-12	Δt12-24	Δt24-36	Δt36-48	Δt0-12	Δt12-24	Δt24-36	Δt36-48	Δt0-12	Δt12-24	Δt24-36	Δt36-48	Δt0-12	Δt12-24	Δt24-36	Δt36-48
GO:0009695	jasmonic acid biosynthetic process		3.E-02	3.E-02													
GO:0009694	jasmonic acid metabolic process		5.E-02	4.E-02													
GO:0008610	lipid biosynthetic process						4.E-02										
GO:0006629	lipid metabolic process		2.E-02				1.E-01										
GO:0048571	long-day photoperiodism	1.E-01		5.E-02						6.E-02							7.E-02
GO:0008152	metabolic process	6.E-07	9.E-04	1.E-04			2.E-17	4.E-05	3.E-07	2.E-02			2.E-04		1.E-02	2.E-03	6.E-02
GO:0006555	methionine metabolic process				1.E-01												
GO:0006346	methylation-dependent chromatin silencing				8.E-02												
GO:0009435	NAD biosynthetic process			5.E-03													
GO:0006807	nitrogen compound metabolic process	3.E-02					4.E-04										
GO:0009116	nucleoside metabolic process			4.E-02					1.E-01								
GO:0006334	nucleosome assembly															1.E-03	
GO:0009117	nucleotide metabolic process			2.E-03													1.E-01
GO:0006730	one-carbon metabolic process		2.E-02		5.E-04												
GO:0055114	oxidation-reduction process	6.E-04	5.E-03	6.E-05			2.E-05	1.E-02	2.E-06	4.E-02						6.E-02	
GO:0016559	peroxisome fission	6.E-02		3.E-02			1.E-01		1.E-01			9.E-02			7.E-02		
GO:0015979	photosynthesis	3.E-04					2.E-08	5.E-21	2.E-09		3.E-10		2.E-17	4.E-07		2.E-26	
GO:0019685	photosynthesis, dark reaction															1.E-01	
GO:0009765	photosynthesis, light harvesting					3.E-02	2.E-03	8.E-10	2.E-03		2.E-09		4.E-16	2.E-11		3.E-15	
GO:0019684	photosynthesis, light reaction						3.E-03	3.E-15	2.E-05		8.E-11		1.E-18	9.E-11		6.E-20	
GO:0009773	photosynthetic electron transport in photosystem I							1.E-01	1.E-01							4.E-02	
GO:0000271	polysaccharide biosynthetic process														9.E-02		
GO:0006779	porphyrin-containing compound biosynthetic process	2.E-02					1.E-01	2.E-02	4.E-02		5.E-02		6.E-02			2.E-07	
GO:0006813	potassium ion transport			5.E-02													
GO:0012501	programmed cell death												1.E-01				
GO:0006562	proline catabolic process																7.E-02
GO:0006461	protein complex assembly															7.E-02	
GO:0006457	protein folding		2.E-02					3.E-03									

GOID	Term	Local expression profile								Distal expression profile							
		Induced				Repressed				Induced				Repressed			
		Δt0-12	Δt12-24	Δt24-36	Δt36-48	Δt0-12	Δt12-24	Δt24-36	Δt36-48	Δt0-12	Δt12-24	Δt24-36	Δt36-48	Δt0-12	Δt12-24	Δt24-36	Δt36-48
GO:0010731	protein glutathionylation	1.E-01								6.E-02							
GO:0019538	protein metabolic process						2.E-02										
GO:0018298	protein-chromophore linkage										1.E-01		1.E-02	9.E-02		2.E-02	
GO:0009150	purine ribonucleotide metabolic process			6.E-02													
GO:0019363	pyridine nucleotide biosynthetic process			2.E-02													
GO:0009218	pyrimidine ribonucleotide metabolic process											8.E-02					5.E-02
GO:0035304	regulation of protein dephosphorylation							7.E-02			1.E-01						
GO:0051246	regulation of protein metabolic process								8.E-02								
GO:0009737	response to abscisic acid		5.E-03	4.E-02									4.E-03				
GO:0010044	response to aluminium ion										1.E-01						
GO:0009617	response to bacterium		3.E-03	3.E-03			8.E-03	4.E-03	1.E-03	6.E-02	1.E-02				1.E-01		
GO:0009607	response to biotic stimulus		5.E-10	3.E-06		1.E-03	9.E-03	7.E-05	9.E-04		7.E-07		2.E-03	5.E-03	3.E-02	6.E-03	
GO:0009637	response to blue light					5.E-02		1.E-02			6.E-03		5.E-05	2.E-03		3.E-04	
GO:0046686	response to cadmium ion	4.E-02	1.E-10	4.E-06	2.E-03					2.E-02		3.E-03			1.E-01		4.E-03
GO:0010037	response to carbon dioxide			6.E-03						4.E-03							
GO:0042221	response to chemical	4.E-02	8.E-19	9.E-06	8.E-04	3.E-02				2.E-03	3.E-05	2.E-04	8.E-03		1.E-01	9.E-03	1.E-06
GO:0010200	response to chitin		8.E-02														
GO:0009409	response to cold	5.E-06	8.E-03	1.E-02			3.E-06		1.E-04	6.E-07			1.E-02		5.E-04		
GO:0046688	response to copper ion	8.E-02							1.E-01								
GO:0010583	response to cyclopentenone		5.E-03	9.E-02								3.E-02					7.E-02
GO:0009269	response to desiccation		2.E-02														
GO:0034976	response to endoplasmic reticulum stress		6.E-04														
GO:0010218	response to far red light					3.E-02		5.E-02			4.E-03		2.E-04	1.E-02		1.E-03	
GO:0009620	response to fungus		7.E-07	1.E-01		6.E-05		3.E-02			2.E-07		2.E-02	2.E-03			
GO:0009739	response to gibberellin			9.E-02													
GO:0009629	response to gravity						8.E-02										
GO:0009408	response to heat		6.E-04		1.E-02			1.E-01					1.E-01				
GO:0009644	response to high light intensity		1.E-01				1.E-02										
GO:0009725	response to hormone		7.E-04								5.E-03		1.E-02			7.E-02	
GO:0042542	response to hydrogen peroxide		9.E-02		9.E-02												
GO:0001666	response to hypoxia		3.E-02														
GO:0009642	response to light intensity						4.E-03	4.E-02	9.E-02								

GOID	Term	Local expression profile								Distal expression profile							
		Induced				Repressed				Induced				Repressed			
		Δt0-12	Δt12-24	Δt24-36	Δt36-48	Δt0-12	Δt12-24	Δt24-36	Δt36-48	Δt0-12	Δt12-24	Δt24-36	Δt36-48	Δt0-12	Δt12-24	Δt24-36	Δt36-48
GO:0009416	response to light stimulus	3.E-03		7.E-02			8.E-09	3.E-05	6.E-08		4.E-03	2.E-03	1.E-03		3.E-03	3.E-05	8.E-03
GO:0010038	response to metal ion	1.E-03	3.E-10	4.E-06	6.E-03		7.E-02			4.E-03		3.E-03			1.E-01		1.E-03
GO:0010243	response to organonitrogen compound		2.E-02														
GO:0006970	response to osmotic stress		8.E-04	4.E-03						1.E-01	6.E-02	4.E-03	2.E-03			2.E-03	7.E-02
GO:0051707	response to other organism		5.E-10	4.E-06		2.E-03	5.E-03	1.E-04	5.E-04		1.E-06		1.E-03	9.E-03	2.E-02	1.E-02	
GO:0006979	response to oxidative stress		2.E-07	6.E-02	5.E-02						6.E-02		6.E-02				
GO:0010114	response to red light										7.E-02		2.E-03	5.E-02		7.E-03	
GO:0009639	response to red or far red light					1.E-01			1.E-01		1.E-02		1.E-03	7.E-02		1.E-03	
GO:0009651	response to salt stress		4.E-03	2.E-03							3.E-02	8.E-03	1.E-03			1.E-03	
GO:0006950	response to stress	6.E-05	3.E-15	3.E-06	7.E-06	1.E-07	2.E-05	4.E-07	1.E-03	4.E-06	2.E-12		9.E-09	4.E-07	6.E-05	4.E-07	
GO:0009610	response to symbiotic fungus												1.E-01				
GO:0009266	response to temperature stimulus	2.E-04	3.E-04	2.E-02	3.E-02		1.E-04		9.E-04	2.E-06		9.E-02	7.E-03		4.E-04		
GO:0010353	response to trehalose												2.E-02				
GO:0009615	response to virus		4.E-02														
GO:0009414	response to water deprivation		4.E-07								9.E-02		3.E-02				
GO:0009611	response to wounding		3.E-06		4.E-02	5.E-04		5.E-02			1.E-06			5.E-04		1.E-02	
GO:0005985	sucrose metabolic process	5.E-02															
GO:0006949	syncytium formation	4.E-03					1.E-02			6.E-02					1.E-01		7.E-02
GO:0033014	tetrapyrrole biosynthetic process	4.E-02						3.E-02	6.E-02		2.E-02		9.E-02			4.E-07	
GO:0009228	thiamine biosynthetic process							4.E-02					1.E-01				
GO:0009407	toxin catabolic process		2.E-02	9.E-03								9.E-05					1.E-02
GO:0006412	translation						3.E-03										
GO:0055085	transmembrane transport			3.E-02					1.E-01								
GO:0006099	tricarboxylic acid cycle			1.E-01													
GO:0006636	unsaturated fatty acid biosynthetic process						2.E-02										
GO:0006833	water transport															1.E-01	

Appendix E to Chapter 3

VOC data generated using targeted integration

Peak areas from single-ion counts were normalised to internal standard (Anisol D8) and fresh weight. Each sample was extracted in duplicate (A/B).

		Tissue from experiment used for transcriptome study															
		Leaf 2 (leaf distal to the infection)						Leaf 4 (includes infection spot)				Leaf 5 (includes infection spot)					
	Compound type	t0		t24		t48		t0		t48		t0		t24		t48	
		A	B	A	B	A	B	A	B	A	B	A	B	A	B	A	B
Benzaldehyde	Aldehyde	0.34	0.36	0.28	0.26	0.28	0.24	0.44	0.46	0.38	0.39	0.31	0.32	0.46	0.44	0.52	0.55
Decanal	Aldehyde	0.21	0.19	0.06	0.08	0.07	0.07	0.07	0.06	0.05	0.07	0.06	0.06	0.06	0.10	0.07	0.06
Trans-2,4-Heptadienal	Aldehyde	3.27	2.91	1.64	1.52	1.53	1.15	3.52	4.54	1.28	1.58	3.12	3.20	2.48	2.38	2.18	2.06
Trans-2-Trans-4-Heptadienal	Aldehyde	5.25	5.44	3.63	3.74	4.75	3.67	18.44	24.98	7.00	7.47	11.24	12.30	14.07	13.14	11.74	11.96
2-E-Hexenal	LOX-derived C6	4.90	5.25	6.31	5.07	4.30	4.10	9.93	7.93	3.79	3.96	8.08	7.57	6.88	7.11	5.75	4.04
3-Hexen-1-ol	LOX-derived C6	1.38	1.43	1.12	1.15	0.36	0.28	1.06	1.08	0.82	0.75	0.89	0.91	1.99	1.68	0.88	0.96
Trans-2-Hexenol	LOX-derived C6	0.57	0.62	0.47	0.49	0.15	0.12	0.46	0.46	0.35	0.33	0.38	0.38	0.84	0.73	0.37	0.41
Hexanal	LOX-derived C6	0.19	0.19	0.18	0.16	0.24	0.20	0.22	0.20	0.20	0.20	0.14	0.13	0.17	0.18	0.31	0.35
Octanal	LOX-derived C8	0.23	0.22	0.11	0.10	0.10	0.10	0.15	0.16	0.11	0.13	0.10	0.08	0.16	0.20	0.21	0.21
(E)-2-Octenal	LOX-derived C8	0.81	0.79	0.68	0.67	0.70	0.54	0.88	0.79	1.02	1.20	0.63	0.65	0.74	0.78	1.48	1.37
1-Octen-3-ol	LOX-derived C8	1.13	1.09	1.13	1.26	1.07	0.89	1.04	0.76	0.82	0.92	0.70	0.67	0.87	0.93	1.44	1.01
Nonanal	LOX-derived C9	1.07	1.08	0.50	0.54	0.47	0.49	0.74	0.65	0.46	0.60	0.43	0.35	0.48	0.63	0.68	0.58
2,6-Nonadienal	LOX-derived C9	0.20	0.21	0.14	0.14	0.26	0.22	0.34	0.29	0.36	0.39	0.34	0.30	0.38	0.42	0.59	0.50
Hexanoic acid	Monocarboxylic acid	0.24	0.27	0.24	0.25	0.38	0.27	0.31	0.32	0.36	0.29	0.19	0.22	0.33	0.31	0.39	0.46
6-Methyl-5-heptan-2-one	Norisoprenoid	0.42	0.41	0.40	0.42	0.37	0.34	0.57	0.49	0.33	0.35	0.53	0.50	0.62	0.74	0.59	0.46
alpha-Citral	Norisoprenoid	0.08	0.07	0.06	0.07	0.06	0.04	0.14	0.12	0.06	0.06	0.12	0.12	0.10	0.12	0.11	0.11
beta-Damascenone	Norisoprenoid	0.30	0.33	0.31	0.43	0.58	0.50	1.69	1.67	1.60	1.93	2.36	2.32	2.33	2.85	2.92	2.36
Alpha-Ionone	Norisoprenoid	0.62	0.63	0.89	1.00	1.30	1.25	0.71	0.55	0.62	0.86	0.29	0.28	0.80	1.01	0.66	0.46
Beta-Ionone	Norisoprenoid	7.59	7.65	5.38	6.32	8.36	7.71	17.75	13.43	11.36	15.44	9.58	9.21	13.92	17.19	13.74	9.55
a-ionon-5,6-epoxide	Norisoprenoid	2.10	2.12	1.28	1.07	1.52	1.33	2.72	1.98	0.86	0.96	2.62	2.25	1.67	2.16	1.98	1.75
Pseudoionone	Norisoprenoid	0.19	0.20	0.25	0.34	0.28	0.23	0.28	0.22	0.37	0.39	0.18	0.17	0.33	0.41	0.37	0.28
Terpinolene	Terpene	0.00	0.00	0.00	0.00	0.00	0.00	0.02	0.02	0.04	0.06	0.03	0.03	0.03	0.05	0.08	0.08
Linalool	Terpene	0.59	0.71	0.52	0.57	0.75	0.65	0.97	0.90	0.62	0.81	0.89	0.88	0.88	0.94	0.91	0.74
alpha-Terpeniol	Terpene	0.10	0.10	0.14	0.20	0.15	0.11	0.35	0.33	0.43	0.36	0.30	0.31	0.38	0.36	0.44	0.47
cis-Geranylacetone	Terpene	0.57	0.59	0.56	0.74	0.64	0.56	1.18	0.92	0.76	0.84	0.79	0.70	1.15	1.42	1.12	0.95

Tissue from independent infection assay												
Samples	Compound type	Leaf 2 (includes infection spot)				Leaf 3 (includes infection spot)				Leaf 4 (includes infection spot)			
		t0		t48		t0		t48		t0		t48	
		A	B	A	B	A	B	A	B	A	B	A	B
Benzaldehyde	Aldehyde	0.25	0.27	0.24	0.27	0.31	0.33	0.34	0.31	0.19	0.20	0.28	0.26
Decanal	Aldehyde	0.06	0.06	0.09	0.10	0.09	0.08	0.13	0.15	0.14	0.13	0.08	0.06
Trans-2,4-Heptadienal	Aldehyde	4.30	5.11	5.34	5.71	3.49	3.48	2.70	1.86	5.90	5.10	2.09	2.01
Trans-2-Trans-4-Heptadienal	Aldehyde	11.29	13.18	7.20	8.71	12.39	13.28	16.15	11.57	6.47	6.31	12.53	12.23
2-E-Hexenal	LOX-derived C6	5.83	5.21	2.35	2.72	10.60	11.82	8.73	5.74	5.66	4.94	6.15	4.99
3-Hexen-1-ol	LOX-derived C6	0.87	1.02	0.21	0.21	1.00	1.04	0.21	0.14	0.58	0.53	0.11	0.10
Trans-2-Hexenol	LOX-derived C6	0.37	0.43	0.09	0.09	0.43	0.45	0.09	0.06	0.24	0.22	0.05	0.05
Hexanal	LOX-derived C6	0.16	0.20	0.22	0.15	0.20	0.20	0.17	0.13	0.20	0.18	0.11	0.11
Octanal	LOX-derived C8	0.10	0.10	0.09	0.09	0.10	0.11	0.23	0.22	0.08	0.07	0.18	0.15
(E)-2-Octenal	LOX-derived C8	0.80	0.96	0.75	0.80	0.94	0.91	0.82	0.55	0.84	0.73	0.63	0.54
1-Octen-3-ol	LOX-derived C8	0.65	0.79	0.64	0.67	0.79	0.76	0.82	0.60	0.61	0.56	0.71	0.57
Nonanal	LOX-derived C9	0.51	0.47	0.46	0.54	0.57	0.56	0.91	1.10	0.44	0.47	0.66	0.53
2,6-Nonadienal	LOX-derived C9	0.20	0.24	0.19	0.26	0.39	0.38	0.49	0.37	0.20	0.16	0.35	0.30
Hexanoic acid	Monocarboxylic acid	0.23	0.24	0.24	0.30	0.22	0.25	0.33	0.33	0.23	0.21	0.29	0.24
6-Methyl-5-heptan-2-one	Norisoprenoid	0.88	1.30	0.40	0.43	1.38	1.22	0.74	0.55	1.05	1.05	0.84	0.77
alpha-Citral	Norisoprenoid	0.19	0.24	0.12	0.15	0.27	0.25	0.15	0.12	0.31	0.29	0.15	0.14
beta-Damascenone	Norisoprenoid	2.45	2.33	1.40	1.91	4.00	3.98	3.66	3.02	5.54	5.99	3.29	3.43
Alpha-Ionone	Norisoprenoid	0.42	0.50	0.20	0.26	0.59	0.53	0.45	0.39	0.35	0.34	0.40	0.37
Beta-Ionone	Norisoprenoid	7.83	7.56	8.83	11.28	10.55	10.77	13.84	12.21	9.53	8.91	9.24	8.80
a-ionon-5,6-epoxide	Norisoprenoid	1.78	2.37	2.93	3.79	2.81	2.41	1.08	0.72	4.24	3.17	0.74	0.68
Pseudoionone	Norisoprenoid	0.32	0.34	0.25	0.28	0.39	0.34	0.56	0.55	0.40	0.38	0.45	0.43
Terpinolene	Terpene	0.01	0.01	0.00	0.00	0.02	0.03	0.03	0.03	0.00	0.00	0.04	0.04
Linalool	Terpene	0.72	0.65	0.69	0.79	0.77	0.75	0.69	0.50	0.64	0.68	0.56	0.52
alpha-Terpeniol	Terpene	0.19	0.14	0.13	0.15	0.17	0.14	0.24	0.23	0.15	0.19	0.28	0.28
cis-Geranylacetone	Terpene	0.95	1.30	0.63	0.80	1.53	1.31	1.29	1.15	1.32	1.14	1.26	1.14

Appendix F to Chapter 3

VOC data generated using chromatogram alignment and automated integration

Peak areas from total-ion counts were normalised to internal standard (Anisol D8) and fresh weight.

	Tissue from experiment used for transcriptome study															
	Leaf 2 (leaf distal to the infection)						Leaf 4 (includes infection spot)					Leaf 5 (includes infection spot)				
	t0	t0	t24	t24	t48	t48	t0	t0	t48	t48	t0	t0	t24	t24	t48	t48
	A	B	A	B	A	B	A	B	A	B	A	B	A	B	A	B
4-Penten-2-one, 4 methyl	7.56	8.88	10.35	12.95	5.22	7.73	8.33	5.89	11.01	9.62	3.18	4.98	2.68	4.37	8.06	8.57
Pentanol, 2-methyl	0.00	0.57	0.00	0.00	0.99	0.00	1.91	0.00	0.00	0.86	1.95	2.29	0.00	0.93	0.00	0.00
Comp_1	0.00	0.00	1.44	2.19	0.44	0.00	0.74	0.00	0.00	0.00	0.40	0.41	0.00	0.00	0.00	0.00
Comp_2	0.00	0.00	0.00	0.00	0.00	0.00	0.00	0.00	0.00	0.00	0.74	1.02	0.00	0.48	0.00	0.00
Hexanal	0.96	1.26	1.44	1.60	0.55	0.00	0.97	0.62	0.20	0.00	0.61	0.88	0.00	0.65	0.35	0.32
Comp_3	0.70	0.91	3.21	0.00	0.00	0.00	0.23	0.11	0.00	0.00	0.00	0.00	0.17	0.12	0.00	0.18
Comp_4	0.00	0.00	0.00	0.00	0.00	0.00	0.00	0.00	0.00	0.00	0.00	0.00	0.00	0.00	0.00	1.36
Cyclopentasiloxane, decamethyl	5.96	8.53	4.73	4.25	2.09	7.18	1.83	2.76	3.39	3.33	1.30	3.44	3.70	0.93	2.92	2.16
Comp_5	0.00	0.00	0.00	0.00	0.29	0.00	0.48	0.47	0.55	0.70	0.36	0.74	0.75	0.32	0.81	0.88
Comp_6	0.00	0.95	0.92	0.00	0.50	0.88	0.36	0.28	0.45	0.48	0.32	0.44	0.63	0.32	0.54	0.50
(E) 2-Hexanal	0.00	0.00	0.00	0.00	0.00	0.00	0.30	0.20	0.00	0.17	0.42	0.54	0.31	0.21	0.00	0.00
(E) 2-Hexanal	12.25	12.63	14.56	10.64	6.52	9.92	13.28	9.12	7.55	7.26	12.44	16.28	12.89	7.08	9.70	8.20
Comp_7	0.00	0.00	0.93	2.95	0.00	0.00	0.00	0.00	0.00	0.00	0.00	0.00	0.00	0.00	0.00	0.00
Comp_8	0.38	0.00	0.00	0.00	0.29	0.00	1.13	1.08	1.26	1.57	0.81	1.38	1.39	0.51	1.82	1.84
Comp_9	0.00	0.00	0.00	0.00	0.00	0.00	0.00	0.00	0.00	0.00	0.00	0.00	0.00	0.00	0.00	0.00
Comp_10	0.51	0.52	0.00	0.00	0.00	0.00	0.00	0.18	0.32	0.80	0.00	0.00	0.15	0.26	0.54	0.43
Comp_11	0.00	0.00	0.00	0.00	0.00	0.00	0.00	0.00	0.00	0.00	0.00	0.00	0.00	0.00	0.64	0.00
Cyclohexanol, 2 methyl-5-(1-methylenyl)	0.93	0.85	0.00	1.33	0.55	0.00	0.53	0.36	1.06	1.43	0.53	0.50	0.60	0.66	1.09	2.00
Comp_12	0.58	0.57	1.15	1.74	0.39	0.00	0.34	0.30	0.21	0.29	0.00	0.00	0.33	0.22	0.40	0.31
Comp_13	0.00	0.00	0.00	0.00	0.35	0.00	0.16	0.23	0.00	0.25	0.00	0.00	0.00	0.11	0.00	0.00
1-Octyltrifluotoacetate	2.18	2.10	1.89	2.33	1.20	1.57	0.99	1.10	0.93	1.53	0.60	0.85	1.16	0.74	1.89	1.91
Comp_14	9.62	10.19	10.03	6.68	0.00	8.62	0.00	0.00	5.96	8.13	0.00	6.16	4.77	0.00	7.95	4.50
Comp_15	0.00	0.00	0.00	0.00	0.00	0.00	0.00	0.00	0.00	0.00	0.00	0.00	0.00	0.00	0.00	0.00
Comp_16	0.00	0.00	0.00	0.00	0.00	0.00	0.00	0.00	0.00	0.00	0.00	0.00	0.00	0.00	0.00	0.00
(E) 3-Hexen-1-ol	1.20	1.26	0.97	0.00	0.00	0.00	0.64	0.52	0.74	0.54	0.52	0.75	1.71	0.73	0.69	0.90
Cyclodecanol	2.65	2.82	1.61	1.93	0.94	1.34	1.75	1.25	1.50	1.54	1.07	1.54	1.73	1.04	1.92	1.90
Comp_17	0.00	0.00	0.00	0.00	0.42	0.00	0.00	0.00	0.00	0.00	0.00	0.00	0.00	0.00	0.00	0.00

	Tissue from experiment used for transcriptome study															
	Leaf 2 (leaf distal to the infection)						Leaf 4 (includes infection spot)					Leaf 5 (includes infection spot)				
	t0	t0	t24	t24	t48	t48	t0	t0	t48	t48	t0	t0	t24	t24	t48	t48
	A	B	A	B	A	B	A	B	A	B	A	B	A	B	A	B
2-Octenal	1.47	1.44	1.09	1.20	0.78	0.96	1.20	0.84	2.15	2.18	0.83	1.08	1.35	0.67	2.21	3.00
1-Octen-3-ol	0.62	0.59	0.00	0.00	0.34	0.00	0.45	0.24	0.56	0.48	0.21	0.00	0.46	0.25	0.60	0.75
Comp_18	0.00	0.00	0.00	0.00	0.00	0.00	0.20	0.14	0.32	0.27	0.00	0.00	0.22	0.14	0.00	0.39
(E,E)-2,4-Heptadienal	2.50	1.99	1.15	1.30	0.74	0.94	2.05	1.94	1.31	1.22	1.56	2.20	1.81	1.09	1.35	1.86
Comp_19	0.00	0.00	0.00	0.00	0.00	0.00	0.45	0.26	0.29	0.33	0.25	0.31	0.28	0.29	0.28	0.35
Comp_20	0.40	0.00	0.00	0.00	0.33	0.00	0.39	0.18	0.29	0.37	0.00	0.00	0.19	0.24	0.00	0.00
Oxonin, 4,5,6,7 tetrahydro	0.43	0.00	0.00	0.00	0.00	0.00	0.40	0.34	0.32	0.42	0.41	0.59	0.26	0.26	0.00	0.33
(E,E)-2,4-Heptadienal	2.84	2.44	1.88	2.09	1.57	1.92	7.63	8.46	4.02	3.93	4.07	6.64	7.47	3.69	5.45	6.73
Comp_21	4.09	6.20	3.67	2.08	1.20	4.54	0.00	0.00	0.00	0.00	0.00	0.00	0.00	0.00	0.00	0.00
Comp_22	0.00	0.00	0.00	0.00	0.00	0.00	1.45	0.95	2.76	3.88	0.84	2.90	2.72	0.88	3.13	1.81
Comp_23	0.00	0.00	0.00	0.00	0.00	0.00	0.36	0.20	0.24	0.26	0.21	0.36	0.33	0.14	0.33	0.24
Comp_24	0.53	0.00	0.00	0.00	0.30	0.00	0.48	0.32	0.52	0.59	0.25	0.40	0.56	0.30	0.50	0.67
Linalool	1.72	1.67	1.31	1.48	1.05	1.58	2.02	1.44	1.73	2.13	1.77	2.40	2.33	1.34	2.15	2.28
1-Octyn-3-ol, 4-methyl	0.47	0.00	0.00	0.00	0.00	0.00	0.25	0.14	0.28	0.30	0.21	0.00	0.00	0.00	0.00	0.24
Comp_24	0.00	0.00	0.00	0.00	0.00	0.00	0.29	0.11	0.00	0.00	0.00	0.00	0.59	0.26	0.00	0.28
2-Decenal	1.13	0.93	0.96	0.00	0.35	0.00	1.20	0.75	0.90	0.77	1.21	1.87	1.38	0.65	0.66	0.90
Comp_25	0.00	0.00	0.00	0.00	0.00	0.00	0.34	0.26	0.33	0.20	0.00	0.27	0.46	0.17	0.26	0.32
2,6-Nonadienal	0.00	0.00	0.00	0.00	0.00	0.00	0.18	0.14	0.43	0.38	0.23	0.00	0.37	0.20	0.58	0.62
Comp_26	0.00	0.00	0.00	0.00	0.00	0.00	0.00	0.00	0.00	0.00	0.00	0.24	0.17	0.10	0.00	0.26
Cyclohexanol, 2,6-dimethyl	0.97	0.90	0.70	0.00	0.62	0.00	1.23	0.79	0.96	0.77	0.74	1.00	1.47	0.66	0.91	0.98
Comp_27	0.00	0.00	0.00	0.00	0.00	0.00	0.00	0.00	0.00	0.00	0.00	0.00	0.00	0.00	0.00	0.00
Comp_28	0.00	0.00	0.00	0.00	0.00	0.00	0.20	0.14	0.00	0.20	0.00	0.26	0.36	0.21	0.40	0.52
Comp_29	0.00	0.00	0.00	0.00	0.00	0.00	0.00	0.00	0.00	0.00	0.00	0.00	0.00	0.00	0.00	0.00
1-cyclohexene-1-carboxaldehyde, 2,6,6-trimethyl	3.82	3.99	3.20	3.14	2.90	3.74	6.08	3.83	5.70	5.84	3.95	5.81	7.97	4.32	6.51	6.32
Comp_30	0.00	0.00	0.00	0.00	0.33	0.00	0.49	0.28	0.48	0.43	0.32	0.59	0.77	0.55	0.53	0.47
Comp_31	0.73	0.62	0.72	1.34	0.44	0.00	0.52	0.42	0.72	1.09	0.50	0.67	1.03	0.86	0.96	1.26
Comp_32	0.00	0.00	0.00	0.00	0.00	0.00	0.15	0.13	0.00	0.00	0.00	0.87	0.17	0.23	0.21	0.19
Comp_33	0.00	1.28	0.99	0.00	0.00	1.11	0.00	0.19	0.48	0.71	0.00	0.77	0.46	0.21	0.31	0.00
Comp_34	0.00	0.00	0.00	0.00	0.00	0.00	0.00	0.00	0.00	0.00	0.00	0.00	0.00	0.11	0.00	0.00
alpha-Terpineol	0.00	0.00	0.00	0.00	0.00	0.00	0.19	0.00	0.00	0.21	0.00	0.00	0.30	0.22	0.53	0.51
Comp_34	0.00	0.00	0.00	0.00	0.00	0.00	0.55	0.50	0.58	0.59	0.49	0.00	0.73	0.44	0.83	1.04
Comp_35	0.00	0.00	0.00	0.00	0.00	0.00	0.00	0.00	0.00	0.00	0.00	0.00	2.45	1.41	1.80	2.01
Comp_36	2.01	2.08	1.71	2.06	1.35	1.75	1.77	1.36	0.74	0.88	1.50	2.18	0.00	0.00	0.39	0.40
Comp_37	0.00	0.00	0.00	0.00	0.00	0.00	0.19	0.15	0.00	0.30	0.26	0.25	0.00	0.16	0.35	0.34
6-epi-shyobunol	0.00	0.00	0.00	0.00	0.00	0.00	0.31	0.27	0.00	0.00	0.00	0.34	0.00	0.00	0.00	0.00

	Tissue from experiment used for transcriptome study															
	Leaf 2 (leaf distal to the infection)						Leaf 4 (includes infection spot)					Leaf 5 (includes infection spot)				
	t0	t0	t24	t24	t48	t48	t0	t0	t48	t48	t0	t0	t24	t24	t48	t48
	A	B	A	B	A	B	A	B	A	B	A	B	A	B	A	B
Comp_38	0.00	0.00	0.00	0.00	0.58	0.00	0.59	0.37	13.18	11.49	0.29	0.46	3.83	3.00	14.68	14.98
Comp_39	0.00	0.00	0.00	0.00	0.33	0.00	0.14	0.12	0.00	0.00	0.00	0.00	0.00	0.00	0.00	0.00
Comp_40	0.74	0.66	0.00	0.00	0.61	0.00	1.79	1.25	2.04	0.83	1.31	1.90	2.89	1.97	3.67	4.26
Comp_41	0.00	0.00	0.00	0.00	0.00	0.00	0.24	0.11	1.35	0.00	0.00	0.00	0.20	0.00	1.33	1.48
Comp_42	0.00	0.00	0.00	0.00	0.00	0.00	0.67	0.37	0.89	0.00	0.51	0.75	0.60	0.54	1.35	1.49
Cyclohexanol, 3,5-dimethyl	0.41	0.50	0.00	0.00	0.65	0.00	1.37	0.74	3.12	2.36	0.68	0.98	1.81	0.95	3.49	3.71
Comp_43	0.00	0.00	0.00	0.00	0.00	0.00	0.73	0.27	0.35	0.59	0.00	0.00	0.20	0.00	0.00	0.00
2-Buten-1-one,	0.00	0.73	0.00	0.00	0.45	0.00	1.41	1.38	1.76	2.54	1.78	2.63	2.48	1.37	2.97	2.09
Comp_44	0.00	0.00	0.00	0.00	0.00	0.00	0.43	0.00	0.63	0.00	0.00	0.00	0.73	0.29	0.00	0.00
Comp_45	0.00	0.46	0.00	0.00	0.36	0.00	0.30	0.27	0.53	0.33	0.00	0.00	0.37	0.00	0.29	0.00
3-Buten-1-one, 4(5,5-dimethyl-1-oxaspiro[2,5]oct-5-yl)	0.00	0.00	0.00	0.00	0.00	0.00	0.68	0.41	0.63	0.63	0.29	0.36	0.86	0.10	0.37	0.21
Comp_46	0.00	0.00	0.00	0.00	0.00	0.00	0.41	0.28	0.44	0.42	0.00	0.00	0.62	0.00	0.33	0.20
(Z) 5,9 Undecadien-2-one, 6,10-dimethyl	1.73	1.75	2.41	2.41	2.23	3.35	1.82	1.16	1.79	2.24	0.72	0.83	2.49	1.38	1.45	0.27
Propanoic acid, 2-methyl	3.44	5.12	5.60	8.36	4.58	5.17	5.09	3.43	8.77	8.00	2.75	4.29	8.05	3.09	6.95	6.71
2,2,4-Trimethyl-1,3-pentanediol diisobutyrate	1.95	2.50	3.44	4.42	2.62	2.95	2.49	2.01	5.54	5.05	1.38	2.31	4.56	1.54	4.03	3.61
Comp_47	0.00	0.00	1.08	0.00	0.56	0.00	0.42	0.41	1.11	0.84	0.00	0.00	0.59	0.00	0.00	0.24
Comp_48	0.00	0.50	0.00	0.00	0.00	0.00	0.52	0.65	0.78	0.98	0.24	0.37	0.90	0.50	0.72	0.83
Comp_49	0.00	0.00	0.00	0.00	0.00	0.00	0.34	0.22	0.37	0.30	0.00	0.00	0.40	0.24	0.32	0.28
Comp_50	0.00	0.00	0.00	0.00	0.32	0.00	0.33	0.28	0.84	0.61	0.00	0.29	0.39	0.25	0.39	0.44
beta-Ionone	6.23	6.20	4.56	5.87	4.31	6.14	11.40	7.37	11.97	13.09	5.75	8.01	13.41	8.28	11.28	10.02
Comp_51	0.00	0.00	0.00	0.00	0.00	0.00	0.00	0.00	0.00	0.00	0.00	0.00	0.00	0.13	0.00	0.00
Comp_52	0.92	0.77	0.74	0.00	0.00	0.00	0.45	0.29	0.00	0.00	0.42	0.78	0.44	0.17	0.00	0.00
Comp_53	0.00	0.00	0.00	0.00	0.00	0.00	0.00	0.00	0.00	0.00	0.00	0.00	0.00	0.00	0.00	0.00
Comp_54	0.00	0.00	0.00	0.00	0.00	0.00	0.24	0.16	1.29	1.07	0.00	0.00	0.33	0.10	1.46	1.09
Comp_55	0.00	0.00	0.00	0.00	0.00	0.00	0.00	0.11	0.00	0.00	0.00	0.00	0.25	0.00	0.00	0.00
3-Buten-1-one, 4(2,2,6-dimethyl-7-oxaspiro[2,5]oct-5-yl)	0.88	0.88	0.00	0.00	0.33	0.86	0.49	0.70	0.00	0.00	0.95	1.24	1.06	0.62	0.96	1.07
2-Butyloxycarbonyloxy-1,1,10-trimethyl	0.62	1.77	2.07	3.03	1.45	2.08	3.46	3.50	19.26	8.17	4.61	3.07	10.82	3.37	7.62	5.23
Comp_56	0.00	0.00	0.00	0.00	0.00	0.00	0.00	0.00	0.00	1.75	0.00	2.63	0.00	0.00	1.42	5.10
Comp_57	0.00	0.00	0.00	0.00	0.00	0.00	0.00	0.00	0.00	10.10	0.00	0.00	0.00	2.55	9.91	10.77
Melezitose	0.00	0.46	0.00	0.00	0.34	0.00	0.48	0.37	0.97	0.87	0.31	0.39	0.68	0.33	0.74	0.93
Comp_58	0.00	0.00	0.00	0.00	0.00	0.00	0.28	0.22	0.52	0.76	0.24	0.34	0.40	0.20	0.44	0.68
Comp_59	0.00	0.00	0.00	0.00	0.00	0.00	0.26	0.15	0.70	0.66	0.00	0.00	0.35	0.14	0.34	0.34
Comp_60	0.00	0.00	0.00	0.00	0.00	0.00	0.00	0.00	1.24	1.41	0.00	0.00	0.18	0.10	0.69	0.95

	Tissue from experiment used for transcriptome study															
	Leaf 2 (leaf distal to the infection)						Leaf 4 (includes infection spot)					Leaf 5 (includes infection spot)				
	t0	t0	t24	t24	t48	t48	t0	t0	t48	t48	t0	t0	t24	t24	t48	t48
	A	B	A	B	A	B	A	B	A	B	A	B	A	B	A	B
Comp_61	0.00	0.00	0.00	0.00	0.00	0.00	0.00	0.00	0.00	0.00	0.00	0.00	0.00	0.00	0.00	0.00
Comp_62	0.00	0.00	0.00	0.00	0.00	0.00	0.00	0.00	0.00	0.00	0.00	0.00	0.18	0.08	0.00	0.00
Cyclopentasiloxane, 2-hydroxy	0.72	1.15	0.95	1.28	0.82	0.81	0.94	0.70	1.57	1.45	0.00	0.00	0.86	0.09	0.90	0.91
Comp_63	0.00	0.00	0.00	0.00	0.00	0.00	0.00	0.00	0.24	1.03	0.45	0.67	0.00	0.61	0.37	0.54
Comp_64	0.00	0.00	0.00	0.00	0.00	0.00	0.00	0.00	0.88	1.87	0.00	0.00	0.00	0.00	0.88	1.08
Aristol-1(10)-en-9yl isovalerate	0.00	0.00	0.00	0.00	0.00	0.00	0.00	0.00	3.13	2.94	0.00	0.00	0.00	0.00	2.39	2.38
Comp_65	0.00	0.00	0.00	0.00	0.00	0.00	0.00	0.00	1.91	1.84	0.00	0.00	0.00	0.00	1.14	1.27
Comp_66	0.00	0.00	0.00	0.00	0.00	0.00	0.00	0.00	0.00	0.42	0.00	0.00	0.00	0.00	0.00	0.00
1-Heptadriacatanol	0.00	0.00	0.00	0.00	0.00	0.00	0.14	0.33	2.93	4.53	0.24	0.36	0.27	0.25	2.03	2.56
Comp_67	0.00	0.00	0.00	0.00	0.00	0.00	0.00	0.12	0.00	0.37	0.00	0.00	0.00	0.00	0.00	0.00
Comp_68	0.00	0.00	0.00	0.00	0.00	0.00	0.00	0.16	1.31	2.15	0.00	0.00	0.20	0.00	1.03	1.12
Comp_69	0.00	0.00	0.00	0.00	0.00	0.00	0.00	0.00	0.00	0.00	0.00	0.00	0.14	0.00	0.00	0.00
2,4 Di-tert-butylphenol	1.43	2.80	4.05	7.34	2.31	2.29	4.25	1.80	5.83	5.37	1.04	3.41	3.92	1.63	3.42	2.67
Comp_70	0.00	0.00	0.00	0.00	0.00	0.00	0.14	0.00	0.50	0.42	0.00	0.00	0.00	0.00	0.22	0.30
Comp_71	0.00	0.00	0.00	0.00	0.00	0.00	0.00	0.00	0.88	0.86	0.00	0.00	0.18	0.10	0.58	0.71
Comp_72	0.00	0.00	0.00	0.00	0.00	0.00	0.00	0.00	1.72	1.90	0.00	0.00	1.53	1.18	1.45	1.45
2-(4H)-Benzofuranone	1.13	0.99	0.81	0.00	0.48	0.00	1.51	0.87	0.93	0.62	1.07	1.10	0.14	0.10	1.27	1.19
Comp_73	0.00	0.00	0.00	0.00	0.00	0.00	0.00	0.00	0.45	0.41	0.00	0.00	0.00	0.00	0.37	0.41
Comp_74	0.00	0.00	0.00	0.00	0.00	0.00	0.00	0.10	0.27	0.22	0.00	0.00	0.00	0.00	0.00	0.00
Comp_75	0.00	0.00	0.00	0.00	0.00	0.00	0.00	0.00	0.00	0.00	0.00	0.00	0.00	0.00	0.00	0.00
Comp_76	0.00	0.00	0.00	0.00	0.00	0.00	0.00	0.00	0.28	0.90	0.00	0.00	0.00	0.00	0.00	0.00
Comp_77	0.00	0.00	0.00	0.00	0.00	0.00	0.00	0.00	1.02	16.65	0.00	0.00	0.29	0.11	0.61	0.98
Comp_78	0.00	0.00	0.00	0.00	0.00	0.00	0.00	0.00	20.14	0.25	0.00	0.00	0.00	0.16	20.96	17.93
Comp_79	0.00	0.00	0.00	0.00	0.00	0.00	0.17	0.11	0.55	0.35	0.00	0.00	0.33	0.00	0.40	0.25
Comp_80	0.00	0.00	0.00	0.00	0.00	0.00	0.00	0.00	0.00	0.00	0.00	0.00	0.00	0.00	0.00	0.00
Comp_81	0.00	0.00	0.00	0.00	0.00	0.00	0.00	0.00	0.27	0.24	0.00	0.00	0.00	0.00	0.23	0.36
Comp_82	0.00	0.00	0.00	0.00	0.00	0.00	0.29	0.19	0.23	0.22	0.00	0.27	0.47	0.11	0.00	0.37
Comp_83	0.00	0.00	0.00	0.00	0.00	0.00	0.00	0.00	0.00	0.00	0.00	0.00	0.00	0.00	0.00	0.00
Comp_84	0.00	0.00	0.00	0.00	0.00	0.00	0.00	0.00	0.00	0.00	0.00	0.00	0.00	0.00	0.00	0.00
Comp_85	0.00	0.00	0.00	0.00	0.00	0.00	0.00	0.00	0.00	0.00	0.00	0.00	0.00	0.00	0.00	0.00
Comp_86	0.00	0.00	0.00	0.00	0.00	0.00	0.21	0.15	0.35	0.17	0.00	0.00	0.26	0.14	0.00	0.18
Comp_87	0.00	0.00	0.00	0.00	0.00	0.00	0.00	0.00	2.63	0.43	0.00	0.00	0.00	0.00	1.40	1.98
Comp_88	0.00	0.00	0.00	0.00	0.00	0.00	0.00	0.00	2.09	3.20	0.00	0.00	0.00	0.00	1.32	1.69
Comp_89	0.00	0.00	0.00	0.00	0.00	0.00	0.20	0.11	0.58	2.38	0.00	0.00	0.00	0.00	0.00	0.00
Comp_90	0.00	0.00	0.00	0.00	0.00	0.00	0.38	0.15	0.27	0.76	0.00	0.25	0.14	0.00	0.49	0.41

	Tissue from experiment used for transcriptome study															
	Leaf 2 (leaf distal to the infection)						Leaf 4 (includes infection spot)					Leaf 5 (includes infection spot)				
	t0	t0	t24	t24	t48	t48	t0	t0	t48	t48	t0	t0	t24	t24	t48	t48
	A	B	A	B	A	B	A	B	A	B	A	B	A	B	A	B
Comp_91	0.00	0.00	0.00	0.00	0.00	0.00	0.00	0.30	0.41	0.37	0.00	0.00	0.50	0.00	0.22	0.45
Comp_92	0.00	0.00	0.00	0.00	0.00	0.00	0.00	0.00	0.20	0.41	0.31	0.48	0.76	0.48	0.47	0.52
Comp_93	0.00	0.00	0.00	0.00	0.00	0.00	0.00	0.00	0.00	0.00	0.00	0.00	0.00	0.00	0.00	0.00
Comp_94	0.00	0.00	0.00	0.00	0.00	0.00	0.00	0.00	0.00	0.21	0.00	0.00	0.00	0.00	0.00	0.00
Comp_95	0.00	0.00	0.00	0.00	0.00	0.00	0.00	0.16	0.00	0.00	0.00	0.00	0.00	0.00	0.00	0.00
Comp_96	0.00	0.00	0.00	0.00	0.00	0.00	0.00	0.00	0.24	0.00	0.00	0.00	0.00	0.00	0.00	0.00
Comp_97	0.00	0.00	0.00	0.00	0.00	0.00	0.00	0.00	0.00	0.00	0.00	0.00	0.00	0.00	0.00	0.00
Comp_98	0.00	0.00	0.00	0.00	0.00	0.00	0.00	0.00	0.00	0.00	0.00	0.00	0.00	0.00	0.00	0.00
Comp_99	0.00	0.00	0.00	0.00	0.00	0.00	0.45	0.25	0.67	0.62	0.00	0.00	0.23	0.28	0.47	0.44

	Tissue from independent infection assay											
	Leaf 2 (includes infection spot)				Leaf 3 (includes infection spot)				Leaf 4 (includes infection spot)			
	t0	t0	t48	t48	t0	t0	t48	t48	t0	t0	t48	t48
	A	B	A	B	A	B	A	B	A	B	A	B
4-Penten-2-one, 4 methyl	9.92	1.06	1.11	7.05	7.10	5.90	10.37	8.49	1.73	4.13	5.96	5.78
Pentanol, 2-methyl	0.00	0.00	0.00	0.00	0.00	1.43	0.00	0.00	0.00	0.00	0.00	0.00
Comp_1	0.00	0.00	0.00	0.00	2.00	1.20	2.25	0.52	0.32	3.68	0.34	0.71
Comp_2	0.99	0.28	0.84	1.05	0.00	0.00	0.00	0.00	2.28	0.00	0.00	0.00
Hexanal	0.88	0.68	1.32	1.17	0.88	0.84	0.55	0.41	1.59	0.00	0.00	0.00
Comp_3	0.00	0.00	0.09	0.00	0.00	0.00	0.89	0.00	0.00	0.00	0.00	0.00
Comp_4	0.00	0.67	0.00	0.89	0.00	0.75	0.00	0.00	0.00	0.00	0.00	0.00
Cyclopentasiloxane, decamethyl	6.30	0.78	2.67	1.05	2.83	1.39	3.84	4.16	1.79	4.09	0.93	1.52
Comp_5	1.12	0.44	1.80	2.04	0.35	0.65	0.43	0.45	0.84	1.00	0.50	0.51
Comp_6	0.71	0.00	0.00	0.00	0.63	0.52	0.65	0.36	0.00	0.00	0.45	0.00
(E) 2-Hexanal	0.47	0.35	0.18	0.00	0.19	0.70	0.15	0.15	0.42	0.38	0.26	0.21
(E) 2-Hexanal	12.65	6.68	3.60	4.94	15.83	18.32	14.17	10.54	8.50	6.69	7.67	5.91
Comp_7	0.00	0.00	0.00	0.00	2.99	0.00	0.90	2.11	0.00	0.00	0.00	0.00
Comp_8	1.46	0.92	0.79	0.86	0.94	0.88	1.18	0.76	0.45	0.33	0.71	0.52
Comp_9	0.00	0.00	0.00	0.00	0.30	0.00	0.21	0.24	0.00	0.00	0.00	0.16
Comp_10	0.00	0.00	0.00	0.00	0.00	0.00	0.21	0.28	0.00	0.00	0.14	0.11
Comp_11	0.00	0.00	0.00	0.00	0.00	0.00	0.00	0.00	0.00	0.00	0.00	0.00
Cyclohexanol, 2 methyl-5-(1-methylenyl)	0.70	0.62	0.52	0.64	0.92	0.85	0.71	0.92	0.52	0.42	0.46	0.56
Comp_12	0.63	0.31	0.58	0.00	0.44	0.46	1.31	0.26	0.16	0.53	0.20	0.33
Comp_13	0.41	0.30	0.00	0.00	0.39	0.37	0.00	0.00	0.00	0.00	0.00	0.16
1-Octyltrifluotoacetate	1.60	1.27	1.14	0.86	1.64	1.51	1.73	0.88	0.95	0.79	0.67	0.78
Comp_14	10.38	0.00	0.00	0.00	4.39	3.36	4.69	0.00	0.00	0.00	0.00	0.00
Comp_15	0.00	0.00	0.00	0.00	0.16	0.00	0.20	9.35	0.00	0.00	0.00	0.00
Comp_16	0.00	0.00	0.00	0.00	0.00	0.00	0.14	0.21	0.12	0.00	0.00	0.00
(E) 3-Hexen-1-ol	0.67	0.54	0.13	0.00	0.67	0.65	0.00	0.00	0.37	0.00	0.00	0.00
Cyclodecanol	1.93	1.18	1.03	1.31	2.13	1.74	2.39	2.85	1.55	0.61	1.37	1.10
Comp_17	0.32	0.00	0.00	0.00	0.21	0.21	0.00	0.00	0.00	0.00	0.00	0.00
2-Octenal	1.32	0.98	0.75	1.06	1.42	1.20	1.35	0.88	0.95	0.74	0.73	0.56
1-Octen-3-ol	0.00	0.38	0.17	0.00	0.40	0.46	0.47	0.35	0.36	0.00	0.43	0.34
Comp_18	0.00	0.00	0.00	0.00	0.17	0.00	0.22	0.00	0.00	0.00	0.00	0.00
(E,E)-2,4-Heptadienal	2.56	1.87	2.14	2.60	2.11	1.66	2.03	1.50	2.34	1.77	1.15	1.06
Comp_19	0.00	0.00	0.28	0.00	0.38	0.25	0.55	0.39	0.20	0.00	0.25	0.25
Comp_20	0.00	0.00	0.28	0.00	0.26	0.00	0.37	0.28	0.19	0.00	0.15	0.18
Oxonin, 4,5,6,7 tetrahydro	0.42	0.42	0.50	0.62	0.67	0.42	0.71	0.30	0.53	0.33	0.26	0.23
(E,E)-2,4-Heptadienal	5.46	3.88	2.32	3.20	5.40	5.21	7.32	5.83	2.10	1.75	4.43	4.09

Tissue from independent infection assay

	Leaf 2 (includes infection spot)				Leaf 3 (includes infection spot)				Leaf 4 (includes infection spot)			
	t0	t0	t48	t48	t0	t0	t48	t48	t0	t0	t48	t48
	A	B	A	B	A	B	A	B	A	B	A	B
Comp_21	0.00	0.00	0.00	0.00	0.00	0.00	0.00	0.00	0.00	0.00	0.10	0.11
Comp_22	3.49	0.58	1.26	1.48	1.60	1.31	2.00	3.20	0.96	1.12	1.07	1.14
Comp_23	0.00	0.00	0.18	0.00	0.34	0.19	0.17	0.00	0.11	0.00	0.11	0.11
Comp_24	0.00	0.00	0.15	0.00	0.00	0.32	0.48	0.00	0.19	0.00	0.21	0.22
Linalool	1.72	0.92	0.98	1.27	1.65	1.34	1.57	1.12	1.15	1.06	0.89	0.83
1-Octyn-3-ol, 4-methyl	0.00	0.00	0.00	0.00	0.00	0.00	0.24	0.24	0.00	0.00	0.26	0.00
Comp_24	0.00	0.00	0.00	0.00	0.00	0.00	0.37	0.00	0.00	0.00	0.00	0.00
2-Decenal	1.04	0.59	0.41	0.54	2.23	1.87	2.33	1.34	0.86	0.73	0.84	0.51
Comp_25	0.00	0.00	0.00	0.00	0.21	0.20	0.46	0.39	0.00	0.00	0.21	0.14
2,6-Nonadienal	0.00	0.00	0.12	0.00	0.27	0.21	0.33	0.30	0.12	0.00	0.18	0.12
Comp_26	0.00	0.00	0.31	0.00	0.20	0.19	0.00	0.00	0.96	0.00	0.00	0.00
Cyclohexanol, 2,6-dimethyl	0.90	0.57	0.63	0.78	0.70	0.63	1.04	0.82	0.51	1.16	0.56	0.22
Comp_27	0.00	0.00	0.00	0.00	0.20	0.00	0.00	0.28	0.16	0.00	0.00	0.00
Comp_28	0.35	0.00	0.23	0.00	0.34	0.00	0.26	0.23	0.23	0.00	0.21	0.10
Comp_29	0.00	0.00	0.00	0.00	0.00	0.00	0.23	0.00	0.00	0.00	0.00	0.00
1-cyclohexene-1-carboxaldehyde, 2,6,6-trimethyl	4.01	2.35	2.58	3.62	4.49	4.28	5.75	5.24	2.53	2.23	3.19	2.81
Comp_30	0.44	0.25	0.24	0.00	0.54	0.44	0.57	0.47	0.20	0.00	0.28	0.24
Comp_31	0.54	0.35	0.37	0.00	0.61	0.54	1.13	1.06	0.42	0.31	0.82	0.57
Comp_32	0.00	0.00	0.10	0.00	0.00	0.00	0.00	0.00	0.00	0.00	0.09	0.12
Comp_33	0.99	0.00	0.38	0.00	0.29	0.00	0.18	0.80	0.11	0.00	0.16	0.11
Comp_34	0.00	0.00	0.13	0.00	0.00	0.00	0.00	0.00	0.00	0.00	0.00	0.00
alpha-Terpineol	0.00	0.00	0.42	0.55	0.00	0.00	0.22	0.35	0.63	0.27	0.33	0.11
Comp_34	0.00	0.00	0.00	0.00	0.00	0.00	0.43	0.45	0.00	0.00	0.00	0.35
Comp_35	0.00	0.00	0.00	0.00	0.00	0.00	0.00	0.00	0.00	0.00	0.00	0.00
Comp_36	1.41	0.91	1.13	1.47	1.35	1.24	2.13	1.91	0.79	0.63	1.26	1.16
Comp_37	0.42	0.23	0.09	0.00	0.23	0.22	0.27	0.34	0.11	0.00	0.17	0.16
6-epi-shyobunol	0.00	0.00	0.22	0.00	0.51	0.37	0.52	0.43	0.42	0.32	0.35	0.28
Comp_38	0.57	0.28	0.41	0.57	0.61	0.48	0.71	0.61	0.37	0.41	0.45	0.20
Comp_39	0.00	0.00	0.00	0.00	0.00	0.00	0.00	0.00	0.00	0.00	0.00	0.00
Comp_40	0.88	0.84	0.78	1.04	1.88	1.75	1.94	1.62	1.14	0.99	1.20	0.95
Comp_41	0.00	0.00	0.00	0.00	0.23	0.00	0.14	0.29	0.14	0.00	0.09	0.00
Comp_42	0.47	0.35	0.34	0.00	0.80	0.72	0.83	0.83	0.48	0.38	0.44	0.33
Cyclohexanol, 3,5-dimethyl	0.56	0.38	0.53	0.67	0.65	0.61	1.03	0.88	0.48	0.34	0.37	0.56
Comp_43	0.00	0.00	0.00	0.00	0.00	0.00	1.10	1.32	0.55	0.28	0.24	0.21
2-Buten-1-one,	2.14	1.20	1.12	1.83	3.77	3.27	3.33	3.79	3.72	3.52	2.53	2.46

	Tissue from independent infection assay											
	Leaf 2 (includes infection spot)				Leaf 3 (includes infection spot)				Leaf 4 (includes infection spot)			
	t0	t0	t48	t48	t0	t0	t48	t48	t0	t0	t48	t48
	A	B	A	B	A	B	A	B	A	B	A	B
Comp_44	0.00	0.00	0.00	0.00	0.00	0.00	0.00	0.00	0.00	0.00	0.00	0.00
Comp_45	0.00	0.00	0.25	0.00	0.19	0.00	0.14	0.43	0.28	0.38	0.17	0.14
3-Buten-1-one, 4(5,5-dimethyl-1-oxaspiro[2,5]oct-5-yl)	0.00	0.00	0.25	0.00	0.33	0.21	0.27	0.80	0.43	0.00	0.23	0.20
Comp_46	0.00	0.00	0.00	0.00	0.00	0.00	0.19	0.57	0.12	0.00	0.15	0.16
(Z) 5,9 Undecadien-2-one, 6,10-dimethyl	0.00	0.96	0.00	0.00	1.57	1.25	0.00	0.00	0.00	0.00	0.72	0.00
Propanoic acid, 2-methyl	8.31	2.32	4.08	5.35	3.64	3.09	6.80	10.66	5.69	4.40	3.58	3.82
2,2,4-Trimethyl-1,3-pentanediol diisobutyrate	3.60	1.23	2.11	2.80	1.83	1.64	3.19	5.64	2.53	2.13	1.90	1.78
Comp_47	1.04	0.23	0.61	0.80	0.00	0.00	0.51	1.04	0.00	0.00	0.22	0.21
Comp_48	0.37	0.00	0.22	0.00	0.24	0.22	0.51	0.57	0.59	0.87	0.18	0.18
Comp_49	0.00	0.00	0.13	0.00	0.25	0.19	0.39	0.36	0.18	0.00	0.21	0.18
Comp_50	0.00	0.00	0.24	0.00	0.00	0.28	0.50	0.59	0.29	0.28	0.37	0.32
beta-Ionone	6.15	3.45	4.70	6.85	7.67	6.89	11.60	12.01	5.05	4.21	6.28	5.67
Comp_51	0.00	0.00	0.00	0.00	0.00	0.00	0.00	0.00	0.00	0.00	0.00	0.11
Comp_52	0.65	0.37	0.88	0.91	0.74	0.52	0.66	0.50	1.94	1.44	0.24	0.09
Comp_53	0.00	0.00	0.00	0.00	0.00	0.00	0.00	0.15	0.12	0.00	0.00	0.00
Comp_54	0.00	0.00	0.00	0.00	0.00	0.00	0.28	0.29	0.11	0.00	0.12	0.14
Comp_55	0.00	0.00	0.00	0.00	0.00	0.00	0.00	0.00	0.12	0.00	0.00	0.10
3-Buten-1-one, 4(2,2,6-dimethyl-7-oxaspiro[2,5]oct-5-yl)	0.87	0.56	0.89	1.30	1.20	0.91	0.53	0.00	1.36	0.83	0.00	0.00
2-Butyloxycarbonyloxy-1,1,10-trimethyl	2.66	0.74	0.90	1.23	2.29	2.60	7.96	10.39	2.80	2.08	4.09	3.56
Comp_56	0.00	0.00	0.00	0.00	0.00	0.00	0.00	0.00	0.00	0.00	5.12	4.47
Comp_57	0.00	0.00	0.00	0.00	0.00	0.00	0.00	0.00	0.00	0.00	0.00	0.00
Melezitose	0.37	0.23	0.29	0.00	0.34	0.32	0.65	0.98	0.33	0.30	0.48	0.42
Comp_58	0.35	0.26	0.24	0.00	0.48	0.34	0.44	0.30	0.35	0.00	0.30	0.25
Comp_59	0.00	0.00	0.16	0.00	0.00	0.00	0.34	0.42	0.11	0.00	0.17	0.16
Comp_60	0.00	0.00	0.00	0.00	0.00	0.00	0.00	0.16	0.44	0.00	0.20	0.24
Comp_61	0.00	0.00	0.00	0.00	0.00	0.00	0.16	0.00	0.00	0.00	0.00	0.00
Comp_62	0.00	0.00	0.08	0.00	0.00	0.00	0.21	0.23	0.10	0.00	0.10	0.08
Cyclopentasiloxane, 2-hydroxy	0.00	0.00	0.61	0.95	0.81	0.66	1.57	2.17	0.70	0.64	1.06	0.79
Comp_63	1.02	0.45	0.00	0.00	0.00	0.00	0.00	0.00	0.00	0.00	0.00	0.00
Comp_64	0.00	0.00	0.00	0.00	0.00	0.00	0.00	0.00	0.00	0.00	0.00	0.00
Aristol-1(10)-en-9yl isovalerate	0.00	0.00	0.00	0.00	0.00	0.00	0.00	0.00	0.00	0.00	0.00	0.00
Comp_65	0.00	0.00	0.00	0.00	0.00	0.00	0.00	0.00	0.00	0.00	0.00	0.00
Comp_66	0.00	0.00	0.00	0.00	0.00	0.00	0.00	0.00	0.00	0.00	0.00	0.00
1-Heptadriacatanol	0.46	0.24	0.67	0.00	0.66	0.58	0.28	0.25	0.93	1.08	0.57	0.36
Comp_67	0.00	0.00	0.00	0.00	0.00	0.00	0.00	0.00	0.00	0.00	0.15	0.00

Tissue from independent infection assay

	Leaf 2 (includes infection spot)				Leaf 3 (includes infection spot)				Leaf 4 (includes infection spot)			
	t0	t0	t48	t48	t0	t0	t48	t48	t0	t0	t48	t48
	A	B	A	B	A	B	A	B	A	B	A	B
Comp_68	0.00	0.00	0.00	0.00	0.00	0.20	0.00	0.32	0.19	0.00	0.24	0.13
Comp_69	0.00	0.00	0.00	0.00	0.00	0.00	0.00	0.00	0.00	0.00	0.00	0.00
2,4 Di-tert-butylphenol	5.50	0.96	3.48	5.09	1.76	1.46	4.61	4.83	3.52	4.59	2.38	1.90
Comp_70	0.00	0.00	0.00	0.00	0.00	0.00	0.18	0.00	0.12	0.00	0.10	0.00
Comp_71	0.00	0.00	0.17	0.00	0.00	0.00	0.19	0.00	0.35	0.00	0.00	0.00
Comp_72	0.00	0.00	0.00	0.00	0.00	0.00	0.00	0.00	0.00	0.00	0.11	0.00
2-(4H)-Benzofuranone	0.74	0.97	0.85	1.16	1.65	1.12	1.24	0.98	1.50	1.00	0.73	0.58
Comp_73	0.00	0.00	0.00	0.00	0.00	0.00	0.00	0.00	0.00	0.00	0.00	0.00
Comp_74	0.00	0.00	0.00	0.00	0.73	0.25	0.17	0.14	0.49	0.27	0.10	0.00
Comp_75	0.00	0.00	0.00	0.00	0.40	0.19	0.00	0.00	0.24	0.00	0.00	0.00
Comp_76	0.00	0.00	0.00	0.00	0.00	0.00	0.00	0.00	0.00	0.00	0.00	0.00
Comp_77	0.00	0.00	0.00	0.00	0.00	0.00	0.00	0.00	0.00	0.00	0.41	0.00
Comp_78	0.00	0.00	0.18	0.00	0.00	0.00	0.26	0.32	0.20	0.00	0.11	0.00
Comp_79	0.00	0.00	0.00	0.00	0.00	0.00	0.00	0.00	0.00	0.00	0.00	0.00
Comp_80	0.00	0.00	0.00	0.00	0.18	0.00	0.00	0.00	0.14	0.00	0.10	0.00
Comp_81	0.00	0.00	0.00	0.00	0.00	0.00	0.17	0.00	0.11	0.00	0.00	0.44
Comp_82	0.00	0.00	0.13	0.00	0.25	0.00	0.28	0.37	0.46	0.27	1.97	0.11
Comp_83	0.00	0.00	0.00	0.00	0.00	0.00	0.00	0.00	0.00	0.00	0.18	0.00
Comp_84	0.00	0.00	0.09	0.00	0.20	0.00	0.22	0.20	0.19	0.00	0.17	0.12
Comp_85	0.00	0.00	0.00	0.00	0.00	0.00	0.00	0.00	0.00	0.00	0.08	0.08
Comp_86	0.00	0.00	0.00	0.00	0.19	0.00	0.00	0.00	0.16	0.00	0.00	0.00
Comp_87	0.00	0.00	0.00	0.00	0.21	0.00	0.00	0.00	0.21	0.00	0.00	0.00
Comp_88	0.00	0.00	0.00	0.00	0.00	0.00	0.00	0.00	0.00	0.00	0.00	0.00
Comp_89	0.00	0.00	0.00	0.00	0.00	0.00	0.00	0.00	0.00	0.00	0.00	0.00
Comp_90	0.00	0.00	0.14	0.00	0.67	0.45	0.16	0.15	0.56	0.28	0.16	0.11
Comp_91	0.33	0.00	0.18	0.00	0.00	0.00	0.21	0.52	0.26	0.00	0.13	0.11
Comp_92	0.39	0.26	0.09	0.00	0.59	0.45	0.66	0.56	0.44	0.28	0.58	0.43
Comp_93	0.00	0.00	0.00	0.00	0.21	0.00	0.00	0.00	0.00	0.00	0.00	0.00
Comp_94	0.00	0.00	0.00	0.00	0.19	0.00	0.00	0.00	0.00	0.00	0.00	0.00
Comp_95	0.00	0.00	0.00	0.00	0.67	0.30	0.00	0.13	0.24	0.00	0.09	0.14
Comp_96	0.00	0.00	0.00	0.00	0.17	0.00	0.00	0.00	0.00	0.00	0.00	0.00
Comp_97	0.00	0.00	0.00	0.00	0.00	0.23	0.17	0.00	0.00	0.00	0.00	0.09
Comp_98	0.00	0.00	0.00	0.00	0.27	0.00	0.00	0.00	0.24	0.00	0.00	0.00
Comp_99	0.54	0.00	0.36	0.00	0.39	0.35	0.52	0.57	0.31	0.44	0.23	0.25

Appendix G to Chapter 3

Meta-analysis of tobacco- and *Arabidopsis* response to *B. cinerea*

Arabidopsis data were sourced from Mathys et al. (2012).

Δt: *B. cinerea* infected tobacco, fold-change data calculated relative to earlier sampling point

ISR-prime 2dpTi: *Trichoderma hamatum* treatment after 2 days, compared to untreated control

ISR-boost: *T. hamatum* treated and *B. cinerea* infected *Arabidopsis* at the indicated days after infection (dpi)

BDIR: *B. cinerea* infected *Arabidopsis* at the indicated days after infection (dpi)

Arabidopsis and tobacco identifiers				WT tobacco		VviPGIP1-tobacco		Primed *Arabidopsis*	Primed and infected *Arabidopsis*		*B. cinerea* infected *Arabidopsis*	
Locus Identifier Arabidopsis	Agilent microarray probe	Tobacco GenBank Accession	Tobacco UNIPROT ID	Δt0-24	Δt0-48	Δt0-24	Δt0-48	ISR-prime 2dpTi	ISR-boost 1dpi	ISR-boost 2dpi	BIDR 1dpi	BIDR 2dpi
AT4G14090	A_95_P025216	AB000623.1	Q0WW21	-0.67	-1.60	0.60	-1.25	1.85		1.49		
AT4G15550	A_95_P025216	AB000623.1	O23406	-0.67	-1.60	0.60	-1.25	1.85		1.49		
AT2G43820	A_95_P025216	AB000623.1	O22822	-0.67	-1.60	0.60	-1.25	1.85		1.49		
AT1G05680	A_95_P025216	AB000623.1	Q9SYK9	-0.67	-1.60	0.60	-1.25	1.85		1.49		
AT2G31750	A_95_P025216	AB000623.1	Q9SKC5	-0.67	-1.60	0.60	-1.25	1.85		1.49		
AT4G08950	A_95_P008351	AB018441.1	Q9ZPE7	-0.54	0.31	-0.60	-0.67				1.43	
AT1G35140	A_95_P008351	AB018441.1	Q9C6E4	-0.54	0.31	-0.60	-0.67				1.43	
AT5G64260	A_95_P008351	AB018441.1	Q9FE06	-0.54	0.31	-0.60	-0.67				1.43	
AT5G51550	A_95_P008351	AB018441.1	Q9FHM9	-0.54	0.31	-0.60	-0.67				1.43	
AT2G17230	A_95_P008351	AB018441.1	Q9SII5	-0.54	0.31	-0.60	-0.67				1.43	
AT4G31550	A_95_P237924	AB020023.1	Q9SV15	0.46	-0.69	-0.30	-0.60					0.91
AT2G23320	A_95_P237924	AB020023.1	O22176	0.46	-0.69	-0.30	-0.60					0.91
AT5G28650	A_95_P237924	AB020023.1	Q93WU6	0.46	-0.69	-0.30	-0.60					0.91
AT3G04670	A_95_P237924	AB020023.1	Q9SR07	0.46	-0.69	-0.30	-0.60					0.91
AT4G01250	A_95_P237924	AB020023.1	O04609	0.46	-0.69	-0.30	-0.60					0.91
AT3G58710	A_95_P237924	AB020023.1	Q93WV5	0.46	-0.69	-0.30	-0.60					0.91
AT1G10200	A_95_P238629	AB023479.1	Q94JX5	-0.47	-1.03	-0.64	-1.32				-0.88	
AT2G39900	A_95_P238629	AB023479.1	O04193	-0.47	-1.03	-0.64	-1.32				-0.88	
AT2G45800	A_95_P238629	AB023479.1	O80839	-0.47	-1.03	-0.64	-1.32				-0.88	
AT4G12490	A_95_P034613	AB035125.1	Q9SU34	1.74	4.33	0.84	4.64	2.20	2.33			
AT4G00165	A_95_P034613	AB035125.1	Q8RW93	1.74	4.33	0.84	4.64	2.20	2.33			
AT4G11600	A_95_P250097	AB041518.1	O48646	0.39	1.23	0.39	1.36				-1.88	
AT1G63460	A_95_P250097	AB041518.1	Q8LBU2	0.39	1.23	0.39	1.36				-1.88	
AT2G25080	A_95_P250097	AB041518.1	P52032	0.39	1.23	0.39	1.36				-1.88	
AT1G30040	A_95_P032526	AB125232.1	Q9XFR9	0.59	-0.84	-0.76	-2.32	0.93		-1.14		1.79
AT1G02400	A_95_P032526	AB125232.1	Q9FZ21	0.59	-0.84	-0.76	-2.32	0.93		-1.14		1.79
AT5G24530	A_95_P032526	AB125232.1	Q9FLV0	0.59	-0.84	-0.76	-2.32	0.93		-1.14		1.79

Arabidopsis and tobacco identifiers				WT tobacco		VviPGIP1-tobacco		Primed *Arabidopsis*	Primed and infected *Arabidopsis*		*B. cinerea* infected *Arabidopsis*	
Locus Identifier Arabidopsis	Agilent microarray probe	Tobacco GenBank Accession	Tobacco UNIPROT ID	Δt0-24	Δt0-48	Δt0-24	Δt0-48	ISR-prime 2dpTi	ISR-boost 1dpi	ISR-boost 2dpi	BIDR 1dpi	BIDR 2dpi
AT3G13610	A_95_P032526	AB125232.1	Q9LHN8	0.59	-0.84	-0.76	-2.32	0.93		-1.14		1.79
AT1G15550	A_95_P032526	AB125232.1	Q39103	0.59	-0.84	-0.76	-2.32	0.93		-1.14		1.79
AT5G08640	A_95_P032526	AB125232.1	Q96330	0.59	-0.84	-0.76	-2.32	0.93		-1.14		1.79
AT5G51810	A_95_P032526	AB125232.1	Q39111	0.59	-0.84	-0.76	-2.32	0.93		-1.14		1.79
AT4G10500	A_95_P032526	AB125232.1	Q9ZSA8	0.59	-0.84	-0.76	-2.32	0.93		-1.14		1.79
AT1G22400	A_95_P239709	AB176524.1	Q9SK82	-1.00	-0.40	-0.06	-0.12	0.95				1.94
AT1G22360	A_95_P239709	AB176524.1	Q9ZWJ3	-1.00	-0.40	-0.06	-0.12	0.95				1.94
AT1G22370	A_95_P239709	AB176524.1	Q9LMF0	-1.00	-0.40	-0.06	-0.12	0.95				1.94
AT1G78270	A_95_P239709	AB176524.1	Q9M9E7	-1.00	-0.40	-0.06	-0.12	0.95				1.94
AT3G46660	A_95_P239709	AB176524.1	Q94AB5	-1.00	-0.40	-0.06	-0.12	0.95				1.94
AT3G29670	A_95_P293088	AB176525.1	Q9LRQ8	1.29	2.37	2.01	2.77	-2.00		1.23		
AT1G03940	A_95_P293088	AB176525.1	Q9ZWB4	1.29	2.37	2.01	2.77	-2.00		1.23		
AT3G29590	A_95_P293088	AB176525.1	Q9LJB4	1.29	2.37	2.01	2.77	-2.00		1.23		
AT5G39050	A_95_P293088	AB176525.1	Q940Z5	1.29	2.37	2.01	2.77	-2.00		1.23		
AT3G29680	A_95_P293088	AB176525.1	Q9LRQ7	1.29	2.37	2.01	2.77	-2.00		1.23		
AT5G61160	A_95_P293088	AB176525.1	Q9FNP9	1.29	2.37	2.01	2.77	-2.00		1.23		
AT5G23940	A_95_P293088	AB176525.1	Q9FF86	1.29	2.37	2.01	2.77	-2.00		1.23		
AT3G50280	A_95_P293088	AB176525.1	Q9SND9	1.29	2.37	2.01	2.77	-2.00		1.23		
AT3G10010	A_95_P222627	AB281587.1	Q9SR66	0.58	-1.00	-0.22	-0.84	0.87				
AT4G34060	A_95_P222627	AB281587.1	O49498	0.58	-1.00	-0.22	-0.84	0.87				
AT1G11670	A_95_P259986	AB286961.1	Q9SAB0	0.75	3.24	0.69	2.97			-1.03		0.94
AT1G61890	A_95_P259986	AB286961.1	O80695	0.75	3.24	0.69	2.97			-1.03		0.94
AT1G33110	A_95_P259986	AB286961.1	Q8W488	0.75	3.24	0.69	2.97			-1.03		0.94
AT5G65380	A_95_P259986	AB286961.1	Q9FKQ1	0.75	3.24	0.69	2.97			-1.03		0.94
AT4G35920	A_95_P219252	AB622811.1	Q8L7E9	-0.30	-1.43	-0.62	-1.69	-1.25				-0.92
AT1G49030	A_95_P219252	AB622811.1	Q9M9A5	-0.30	-1.43	-0.62	-1.69	-1.25				-0.92
AT1G14870	A_95_P219252	AB622811.1	Q9LQU4	-0.30	-1.43	-0.62	-1.69	-1.25				-0.92
AT1G52200	A_95_P219252	AB622811.1	Q9M815	-0.30	-1.43	-0.62	-1.69	-1.25				-0.92
AT1G69530	A_95_P188762	AF049353.1	Q9C554	-0.32	-0.06	0.86	0.69					-1.05
AT2G03090	A_95_P188762	AF049353.1	O80622	-0.32	-0.06	0.86	0.69					-1.05
AT1G26770	A_95_P188762	AF049353.1	Q9LDR9	-0.32	-0.06	0.86	0.69					-1.05
AT5G56320	A_95_P188762	AF049353.1	Q9FMA0	-0.32	-0.06	0.86	0.69					-1.05
AT2G40610	A_95_P188762	AF049353.1	O22874	-0.32	-0.06	0.86	0.69					-1.05
AT3G29030	A_95_P188762	AF049353.1	Q38864	-0.32	-0.06	0.86	0.69					-1.05
AT2G37640	A_95_P188762	AF049353.1	O80932	-0.32	-0.06	0.86	0.69					-1.05
AT5G63450	A_95_P191682	AF092915.1	Q9FMV7	1.02	1.23	0.86	1.34			-1.74		4.47
AT3G48520	A_95_P191682	AF092915.1	Q9SMP5	1.02	1.23	0.86	1.34			-1.74		4.47
AT2G27690	A_95_P191682	AF092915.1	Q9ZUX1	1.02	1.23	0.86	1.34			-1.74		4.47
AT2G45970	A_95_P191682	AF092915.1	O80823	1.02	1.23	0.86	1.34			-1.74		4.47
AT1G63710	A_95_P191682	AF092915.1	Q9CAD6	1.02	1.23	0.86	1.34			-1.74		4.47
AT1G57750	A_95_P191682	AF092915.1	Q9FVS9	1.02	1.23	0.86	1.34			-1.74		4.47
AT4G21960	A_95_P249287	AF149251.1	Q9SB81	0.66	-1.00	0.50	-1.25					0.92
AT2G37130	A_95_P249287	AF149251.1	Q42580	0.66	-1.00	0.50	-1.25					0.92

Arabidopsis and tobacco identifiers				WT tobacco		VviPGIP1-tobacco		Primed *Arabidopsis*	Primed and infected *Arabidopsis*		*B. cinerea* infected *Arabidopsis*	
Locus Identifier Arabidopsis	Agilent microarray probe	Tobacco GenBank Accession	Tobacco UNIPROT ID	Δt0-24	Δt0-48	Δt0-24	Δt0-48	ISR-prime 2dpTi	ISR-boost 1dpi	ISR-boost 2dpi	BIDR 1dpi	BIDR 2dpi
AT5G40150	A_95_P249287	AF149251.1	Q9FL16	0.66	-1.00	0.50	-1.25					0.92
AT4G36430	A_95_P249287	AF149251.1	O23237	0.66	-1.00	0.50	-1.25					0.92
AT2G31790	A_95_P254344	AF190634.1	Q9SKC1	1.77	1.08	1.98	1.93					-0.99
AT1G24100	A_95_P254344	AF190634.1	O48676	1.77	1.08	1.98	1.93					-0.99
AT4G15480	A_95_P254344	AF190634.1	Q5XF20	1.77	1.08	1.98	1.93					-0.99
AT3G56400	A_95_P252864	AF193770.1	Q9LY00	0.70	0.51	0.93	0.82	0.99		-1.00		
AT2G40750	A_95_P252864	AF193770.1	Q93WU8	0.70	0.51	0.93	0.82	0.99		-1.00		
AT1G66550	A_95_P252864	AF193770.1	Q93WV7	0.70	0.51	0.93	0.82	0.99		-1.00		
AT5G22570	A_95_P252864	AF193770.1	Q8GWF1	0.70	0.51	0.93	0.82	0.99		-1.00		
AT1G66600	A_95_P252864	AF193770.1	Q9C6H5	0.70	0.51	0.93	0.82	0.99		-1.00		
AT5G24110	A_95_P252864	AF193770.1	Q9FL62	0.70	0.51	0.93	0.82	0.99		-1.00		
AT2G46400	A_95_P252864	AF193770.1	Q9SKD9	0.70	0.51	0.93	0.82	0.99		-1.00		
AT5G01900	A_95_P252864	AF193770.1	Q9LZV6	0.70	0.51	0.93	0.82	0.99		-1.00		
AT1G80590	A_95_P252864	AF193770.1	Q9M8M6	0.70	0.51	0.93	0.82	0.99		-1.00		
AT2G40740	A_95_P252864	AF193770.1	Q9SHB5	0.70	0.51	0.93	0.82	0.99		-1.00		
AT4G23810	A_95_P252864	AF193770.1	Q9SUP6	0.70	0.51	0.93	0.82	0.99		-1.00		
AT4G11070	A_95_P252864	AF193770.1	Q8H0Y8	0.70	0.51	0.93	0.82	0.99		-1.00		
AT4G18170	A_95_P252864	AF193770.1	Q8VWJ2	0.70	0.51	0.93	0.82	0.99		-1.00		
AT3G57550	A_95_P029471	AF205130.1	Q9M682	1.23	1.46	0.99	1.55					1.45
AT2G41880	A_95_P029471	AF205130.1	P93757	1.23	1.46	0.99	1.55					1.45
AT1G76650	A_95_P023776	AF329729.1	Q9SRE6	-0.84	-1.89	-0.60	-1.47		-1.89	-1.87		3.61
AT5G42380	A_95_P023776	AF329729.1	Q9FIH9	-0.84	-1.89	-0.60	-1.47		-1.89	-1.87		3.61
AT1G76640	A_95_P023776	AF329729.1	Q9SRE7	-0.84	-1.89	-0.60	-1.47		-1.89	-1.87		3.61
AT3G50770	A_95_P023776	AF329729.1	Q8L3R2	-0.84	-1.89	-0.60	-1.47		-1.89	-1.87		3.61
AT3G01830	A_95_P023776	AF329729.1	Q9SGI8	-0.84	-1.89	-0.60	-1.47		-1.89	-1.87		3.61
AT1G18210	A_95_P023776	AF329729.1	Q9LE22	-0.84	-1.89	-0.60	-1.47		-1.89	-1.87		3.61
AT3G62410	A_95_P000630	AF359459.2	Q9LZP9	-0.79	-2.00	-0.97	-2.64				-1.01	
AT1G76560	A_95_P000630	AF359459.2	Q9C9K2	-0.79	-2.00	-0.97	-2.64				-1.01	
AT1G64390	A_95_P217357	AF362949.1	Q42059	0.19	-0.34	0.25	-0.20					-1.92
AT2G32990	A_95_P217357	AF362949.1	O48766	0.19	-0.34	0.25	-0.20					-1.92
AT4G35100	A_95_P243347	AF440272.1	P93004	0.74	-1.06	-0.05	-1.36	-1.49				-1.43
AT2G16850	A_95_P243347	AF440272.1	Q9ZVX8	0.74	-1.06	-0.05	-1.36	-1.49				-1.43
AT3G53420	A_95_P243347	AF440272.1	P43286	0.74	-1.06	-0.05	-1.36	-1.49				-1.43
AT3G15020	A_95_P239759	AJ006974.1	Q9LKA3	0.28	1.50	0.24	1.66				-0.89	-0.99
AT1G53240	A_95_P239759	AJ006974.1	Q9ZP06	0.28	1.50	0.24	1.66				-0.89	-0.99
AT5G40780	A_95_P019116	AJ299255.1	Q9FKS8	1.10	1.50	0.91	1.45	1.53				2.69
AT1G25530	A_95_P019116	AJ299255.1	Q9C6M2	1.10	1.50	0.91	1.45	1.53				2.69
AT3G25780	A_95_P014126	AJ308487.1	Q9LS01	2.76	3.23	2.12	3.80	1.24		-1.35		5.55
AT1G13280	A_95_P014126	AJ308487.1	Q93ZC5	2.76	3.23	2.12	3.80	1.24		-1.35		5.55
AT3G25770	A_95_P014126	AJ308487.1	Q9LS02	2.76	3.23	2.12	3.80	1.24		-1.35		5.55
AT3G25760	A_95_P014126	AJ308487.1	Q9LS03	2.76	3.23	2.12	3.80	1.24		-1.35		5.55
AT3G54420	A_95_P183832	AJ880384.1	Q9M2U5	2.59	2.61	1.76	3.01	1.44		-1.05		2.18
AT2G43590	A_95_P183832	AJ880384.1	O24658	2.59	2.61	1.76	3.01	1.44		-1.05		2.18

Arabidopsis and tobacco identifiers				WT tobacco		VviPGIP1-tobacco		Primed *Arabidopsis*	Primed and infected *Arabidopsis*		*B. cinerea* infected *Arabidopsis*	
Locus Identifier Arabidopsis	Agilent microarray probe	Tobacco GenBank Accession	Tobacco UNIPROT ID	Δt0-24	Δt0-48	Δt0-24	Δt0-48	ISR-prime 2dpTi	ISR-boost 1dpi	ISR-boost 2dpi	BIDR 1dpi	BIDR 2dpi
AT2G43580	A_95_P183832	AJ880384.1	O24598	2.59	2.61	1.76	3.01	1.44		-1.05		2.18
AT4G02520	A_95_P178192	AJ937852.1	P46422	0.72	0.90	0.30	1.53	1.43				2.79
AT2G02930	A_95_P178192	AJ937852.1	Q9SLM6	0.72	0.90	0.30	1.53	1.43				2.79
AT1G02930	A_95_P178192	AJ937852.1	P42760	0.72	0.90	0.30	1.53	1.43				2.79
AT1G02920	A_95_P178192	AJ937852.1	Q9SRY5	0.72	0.90	0.30	1.53	1.43				2.79
AT1G09940	A_95_P245277	AM746200.1	P49294	-0.12	-1.32	-1.40	-2.06	-0.90	-1.05			1.81
AT3G47340	A_95_P006901	AY061820.1	P49078	-0.76	-2.74	-0.34	-2.18	-1.15			1.80	3.17
AT5G65010	A_95_P006901	AY061820.1	Q9LV77	-0.76	-2.74	-0.34	-2.18	-1.15			1.80	3.17
AT5G67340	A_95_P239164	AY219234.1	Q5XEZ8	1.61	1.29	0.19	1.92	2.99		-0.90		2.86
AT3G46510	A_95_P239164	AY219234.1	Q9SNC6	1.61	1.29	0.19	1.92	2.99		-0.90		2.86
AT1G23030	A_95_P239164	AY219234.1	Q8GUG9	1.61	1.29	0.19	1.92	2.99		-0.90		2.86
AT3G54850	A_95_P239164	AY219234.1	Q8VZ40	1.61	1.29	0.19	1.92	2.99		-0.90		2.86
AT2G29110	A_95_P034678	AY220478.1	Q9C5V5	0.65	-1.06	0.24	-0.60	2.30				2.06
AT2G29120	A_95_P034678	AY220478.1	Q8LGN0	0.65	-1.06	0.24	-0.60	2.30				2.06
AT2G29100	A_95_P034678	AY220478.1	O81078	0.65	-1.06	0.24	-0.60	2.30				2.06
AT5G11210	A_95_P034678	AY220478.1	Q9LFN5	0.65	-1.06	0.24	-0.60	2.30				2.06
AT3G07520	A_95_P034678	AY220478.1	Q8LGN1	0.65	-1.06	0.24	-0.60	2.30				2.06
AT5G48400	A_95_P034678	AY220478.1	Q9LV72	0.65	-1.06	0.24	-0.60	2.30				2.06
AT3G51480	A_95_P034678	AY220478.1	Q84W41	0.65	-1.06	0.24	-0.60	2.30				2.06
AT5G48410	A_95_P034678	AY220478.1	Q9FH75	0.65	-1.06	0.24	-0.60	2.30				2.06
AT2G37630	A_95_P034753	AY559043.1	O80931	-0.01	-1.56	-0.23	-1.69				1.22	-1.65
AT1G66370	A_95_P034753	AY559043.1	Q9FNV9	-0.01	-1.56	-0.23	-1.69				1.22	-1.65
AT5G59780	A_95_P034753	AY559043.1	Q4JL84	-0.01	-1.56	-0.23	-1.69				1.22	-1.65
AT5G52600	A_95_P034753	AY559043.1	Q9LTF7	-0.01	-1.56	-0.23	-1.69				1.22	-1.65
AT5G44210	A_95_P034768	AY627865.1	Q9FE67	-0.36	-0.94	-0.32	-0.84		-1.89			2.99
AT3G15210	A_95_P034768	AY627865.1	O80340	-0.36	-0.94	-0.32	-0.84		-1.89			2.99
AT1G50640	A_95_P034768	AY627865.1	O80339	-0.36	-0.94	-0.32	-0.84		-1.89			2.99
AT1G28370	A_95_P034768	AY627865.1	Q9C5I3	-0.36	-0.94	-0.32	-0.84		-1.89			2.99
AT1G03800	A_95_P034768	AY627865.1	Q9ZWA2	-0.36	-0.94	-0.32	-0.84		-1.89			2.99
AT2G33710	A_95_P034768	AY627865.1	P93007	-0.36	-0.94	-0.32	-0.84		-1.89			2.99
AT5G13330	A_95_P034768	AY627865.1	Q9LYU3	-0.36	-0.94	-0.32	-0.84		-1.89			2.99
AT5G51190	A_95_P034768	AY627865.1	Q8VY90	-0.36	-0.94	-0.32	-0.84		-1.89			2.99
AT1G34300	A_95_P199987	AY775028.1	Q9XID3	1.07	0.03	-0.12	-0.10					1.09
AT2G19130	A_95_P199987	AY775028.1	O64477	1.07	0.03	-0.12	-0.10					1.09
AT5G66210	A_95_P195052	AY971376.1	Q9FKW4	0.65	-0.14	0.44	0.52			-1.03	1.33	2.19
AT3G50530	A_95_P195052	AY971376.1	Q9SCS2	0.65	-0.14	0.44	0.52			-1.03	1.33	2.19
AT1G49580	A_95_P195052	AY971376.1	Q9FX86	0.65	-0.14	0.44	0.52			-1.03	1.33	2.19
AT3G20410	A_95_P195052	AY971376.1	Q38868	0.65	-0.14	0.44	0.52			-1.03	1.33	2.19
AT5G06730	A_95_P135667	D11396.1	Q9FG34	-0.07	0.43	1.05	0.25					1.87
AT5G19880	A_95_P135667	D11396.1	P59120	-0.07	0.43	1.05	0.25					1.87
AT3G32980	A_95_P135667	D11396.1	Q9LHB9	-0.07	0.43	1.05	0.25					1.87
AT3G49120	A_95_P135667	D11396.1	Q9SMU8	-0.07	0.43	1.05	0.25					1.87
AT2G06850	A_95_P000496	D86730.1	Q39099	0.31	-1.51	-0.20	-1.69	-0.88				

Arabidopsis and tobacco identifiers				WT tobacco		VviPGIP1-tobacco		Primed *Arabidopsis*	Primed and infected *Arabidopsis*		*B. cinerea* infected *Arabidopsis*	
Locus Identifier Arabidopsis	Agilent microarray probe	Tobacco GenBank Accession	Tobacco UNIPROT ID	Δt0-24	Δt0-48	Δt0-24	Δt0-48	ISR-prime 2dpTi	ISR-boost 1dpi	ISR-boost 2dpi	BIDR 1dpi	BIDR 2dpi
AT5G65730	A_95_P000496	D86730.1	Q8LF99	0.31	-1.51	-0.20	-1.69	-0.88				
AT4G37800	A_95_P000496	D86730.1	Q8LER3	0.31	-1.51	-0.20	-1.69	-0.88				
AT4G35770	A_95_P115072	DQ116561.1	Q38853	-0.81	-1.43	-1.06	-1.43	-2.49			1.31	3.22
AT5G66170	A_95_P115072	DQ116561.1	Q9FKW8	-0.81	-1.43	-1.06	-1.43	-2.49			1.31	3.22
AT4G27700	A_95_P115072	DQ116561.1	Q94A65	-0.81	-1.43	-1.06	-1.43	-2.49			1.31	3.22
AT1G55850	A_95_P013646	DQ127171.1	Q8VZK9	-0.64	-2.56	-0.10	-2.32				0.97	1.48
AT4G24000	A_95_P013646	DQ127171.1	Q8VYR4	-0.64	-2.56	-0.10	-2.32				0.97	1.48
AT4G23990	A_95_P013646	DQ127171.1	Q0WVN5	-0.64	-2.56	-0.10	-2.32				0.97	1.48
AT5G09870	A_95_P013646	DQ127171.1	Q8L778	-0.64	-2.56	-0.10	-2.32				0.97	1.48
AT2G32530	A_95_P013646	DQ127171.1	Q8RX83	-0.64	-2.56	-0.10	-2.32				0.97	1.48
AT2G32540	A_95_P013646	DQ127171.1	O80891	-0.64	-2.56	-0.10	-2.32				0.97	1.48
AT3G28740	A_95_P217592	DQ350320.1	Q9LHA1	0.44	-0.51	0.33	-0.27					4.08
AT4G37410	A_95_P217592	DQ350320.1	Q9SZU1	0.44	-0.51	0.33	-0.27					4.08
AT5G57220	A_95_P217592	DQ350320.1	Q9LVD6	0.44	-0.51	0.33	-0.27					4.08
AT5G07990	A_95_P217592	DQ350320.1	Q9SD85	0.44	-0.51	0.33	-0.27					4.08
AT3G14690	A_95_P216157	DQ350355.1	Q9LUC5	-0.04	-1.25	-0.49	-1.51					-0.95
AT3G14650	A_95_P216157	DQ350355.1	Q9LUC9	-0.04	-1.25	-0.49	-1.51					-0.95
AT1G17060	A_95_P216157	DQ350355.1	Q9SHG5	-0.04	-1.25	-0.49	-1.51					-0.95
AT2G26710	A_95_P216157	DQ350355.1	O48786	-0.04	-1.25	-0.49	-1.51					-0.95
AT4G27710	A_95_P216157	DQ350355.1	Q9T093	-0.04	-1.25	-0.49	-1.51					-0.95
AT1G79750	A_95_P252079	DQ923119.2	Q9CA83	-0.14	-1.12	-0.51	-1.09			0.88		
AT2G19900	A_95_P252079	DQ923119.2	O82191	-0.14	-1.12	-0.51	-1.09			0.88		
AT5G11670	A_95_P252079	DQ923119.2	Q9LYG3	-0.14	-1.12	-0.51	-1.09			0.88		
AT2G05920	A_95_P143337	EU364874.1	Q9ZUF6	0.49	-0.89	0.51	-1.29					-1.19
AT5G67360	A_95_P143337	EU364874.1	O65351	0.49	-0.89	0.51	-1.29					-1.19
AT5G51750	A_95_P143337	EU364874.1	Q9FLI4	0.49	-0.89	0.51	-1.29					-1.19
AT1G04110	A_95_P143337	EU364874.1	O64495	0.49	-0.89	0.51	-1.29					-1.19
AT2G45290	A_95_P076215	EU647214.1	F4IW47	-0.17	-0.18	-0.03	-0.25					2.13
AT3G60750	A_95_P076215	EU647214.1	Q8RWV0	-0.17	-0.18	-0.03	-0.25					2.13
AT4G26850	A_95_P286393	EU700061.1	Q8RWE8	0.72	0.26	0.79	0.76				1.16	-1.67
AT5G55120	A_95_P286393	EU700061.1	Q9FLP9	0.72	0.26	0.79	0.76				1.16	-1.67
AT3G02380	A_95_P223997	JN022535.1	Q96502	0.11	-0.18	-0.06	-0.07				1.34	-3.24
AT5G15850	A_95_P223997	JN022535.1	O50055	0.11	-0.18	-0.06	-0.07				1.34	-3.24
AT2G21320	A_95_P223997	JN022535.1	Q9SJU5	0.11	-0.18	-0.06	-0.07				1.34	-3.24
AT2G47890	A_95_P223997	JN022535.1	O82256	0.11	-0.18	-0.06	-0.07				1.34	-3.24
AT4G38960	A_95_P223997	JN022535.1	C0SVM5	0.11	-0.18	-0.06	-0.07				1.34	-3.24
AT1G28050	A_95_P223997	JN022535.1	Q9C7E8	0.11	-0.18	-0.06	-0.07				1.34	-3.24
AT1G65790	A_95_P206483	JQ031357.1	Q39086	0.59	0.43	1.01	0.86	1.47				2.33
AT1G11330	A_95_P206483	JQ031357.1	Q9SXB8	0.59	0.43	1.01	0.86	1.47				2.33
AT4G21380	A_95_P206483	JQ031357.1	O81905	0.59	0.43	1.01	0.86	1.47				2.33
AT5G59845	A_95_P019246	JQ031364.1	Q8LFM2	0.14	0.10	0.31	-0.15					-1.24
AT2G14900	A_95_P019246	JQ031364.1	O82328	0.14	0.10	0.31	-0.15					-1.24
AT1G74670	A_95_P019246	JQ031364.1	Q6NMQ7	0.14	0.10	0.31	-0.15					-1.24

Arabidopsis and tobacco identifiers				WT tobacco		VviPGIP1-tobacco		Primed *Arabidopsis*	Primed and infected *Arabidopsis*		*B. cinerea* infected *Arabidopsis*	
Locus Identifier Arabidopsis	Agilent microarray probe	Tobacco GenBank Accession	Tobacco UNIPROT ID	Δt0-24	Δt0-48	Δt0-24	Δt0-48	ISR-prime 2dpTi	ISR-boost 1dpi	ISR-boost 2dpi	BIDR 1dpi	BIDR 2dpi
AT5G15230	A_95_P019246	JQ031364.1	P46690	0.14	0.10	0.31	-0.15					-1.24
AT5G14920	A_95_P019246	JQ031364.1	Q9LFR3	0.14	0.10	0.31	-0.15					-1.24
AT2G30540	A_95_P018826	JQ654633.1	O04341	-1.32	-2.06	-0.40	-2.56					-0.91
AT3G62950	A_95_P018826	JQ654633.1	Q9LYC6	-1.32	-2.06	-0.40	-2.56					-0.91
AT5G18600	A_95_P018826	JQ654633.1	Q8L8Z8	-1.32	-2.06	-0.40	-2.56					-0.91
AT4G15680	A_95_P018826	JQ654633.1	O23419	-1.32	-2.06	-0.40	-2.56					-0.91
AT4G15660	A_95_P018826	JQ654633.1	O23417	-1.32	-2.06	-0.40	-2.56					-0.91
AT4G15700	A_95_P018826	JQ654633.1	O23421	-1.32	-2.06	-0.40	-2.56					-0.91
AT2G02100	A_95_P206692	JQ654635.1	Q39182	0.83	1.43	-0.30	1.48		-0.98		-2.90	
AT1G61070	A_95_P206692	JQ654635.1	Q9C947	0.83	1.43	-0.30	1.48		-0.98		-2.90	
AT3G19390	A_95_P222812	KF113573.1	Q9LT78	0.31	0.29	-0.06	-0.06					2.15
AT4G11310	A_95_P222812	KF113573.1	Q9SUT0	0.31	0.29	-0.06	-0.06					2.15
AT5G06860	A_95_P126117	KF317204.1	Q9M5J9	-0.20	0.07	0.01	-0.06					2.57
AT5G06870	A_95_P126117	KF317204.1	Q9M5J8	-0.20	0.07	0.01	-0.06					2.57
AT3G12610	A_95_P126117	KF317204.1	Q00874	-0.20	0.07	0.01	-0.06					2.57
AT2G26330	A_95_P126117	KF317204.1	Q42371	-0.20	0.07	0.01	-0.06					2.57
AT5G46330	A_95_P126117	KF317204.1	Q9FL28	-0.20	0.07	0.01	-0.06					2.57
AT5G01890	A_95_P126117	KF317204.1	Q9LZV7	-0.20	0.07	0.01	-0.06					2.57
AT1G35710	A_95_P126117	KF317204.1	Q9LP24	-0.20	0.07	0.01	-0.06					2.57
AT1G04220	A_95_P117952	KJ423103.1	Q5XEP9	0.10	-0.15	0.03	-0.07					-4.04
AT2G26640	A_95_P117952	KJ423103.1	O48780	0.10	-0.15	0.03	-0.07					-4.04
AT4G34250	A_95_P117952	KJ423103.1	Q9SYZ0	0.10	-0.15	0.03	-0.07					-4.04
AT2G15090	A_95_P117952	KJ423103.1	Q4V3C9	0.10	-0.15	0.03	-0.07					-4.04
AT3G10280	A_95_P117952	KJ423103.1	Q9SS39	0.10	-0.15	0.03	-0.07					-4.04
AT1G11545	A_95_P293048	KJ730270.1	Q8L9A9	0.49	-1.69	-0.40	-2.12	-1.04				
AT5G57560	A_95_P293048	KJ730270.1	Q38857	0.49	-1.69	-0.40	-2.12	-1.04				
AT5G57550	A_95_P293048	KJ730270.1	Q38907	0.49	-1.69	-0.40	-2.12	-1.04				
AT5G14740	A_95_P149917	KJ874399.1	P42737	-0.51	-1.51	-0.97	-1.74					-1.02
AT3G01500	A_95_P149917	KJ874399.1	P27140	-0.51	-1.51	-0.97	-1.74					-1.02
AT1G58180	A_95_P149917	KJ874399.1	Q9C6F5	-0.51	-1.51	-0.97	-1.74					-1.02
AT2G18790	A_95_P237279	L10114.1	P14713	-0.17	-0.89	-0.36	-1.03					1.06
AT4G16250	A_95_P237279	L10114.1	P42497	-0.17	-0.89	-0.36	-1.03					1.06
AT3G12160	A_95_P176182	L29268.1	Q9LH50	-0.74	-1.43	-0.43	-1.43					-1.19
AT5G47960	A_95_P176182	L29268.1	Q9FE79	-0.74	-1.43	-0.43	-1.43					-1.19
AT1G42990	A_95_P163012	NM_001324734.1	Q9C7S0	-0.23	-0.43	0.04	-0.51	1.06		-0.97	0.87	1.44
AT2G40950	A_95_P163012	NM_001324734.1	O22208	-0.23	-0.43	0.04	-0.51	1.06		-0.97	0.87	1.44
AT5G15730	A_95_P019536	NM_001325136.1	Q9LFV3	0.70	1.33	0.32	1.65			-0.98		2.00
AT5G61350	A_95_P019536	NM_001325136.1	Q9FLJ8	0.70	1.33	0.32	1.65			-0.98		2.00
AT1G49730	A_95_P019536	NM_001325136.1	Q9FX99	0.70	1.33	0.32	1.65			-0.98		2.00
AT1G16130	A_95_P019536	NM_001325136.1	Q7X8C5	0.70	1.33	0.32	1.65			-0.98		2.00
AT5G38710	A_95_P283429	NM_001325364.1	Q6NKX1	-1.32	-0.22	-0.17	-0.12			-1.06		4.81
AT3G30775	A_95_P283429	NM_001325364.1	P92983	-1.32	-0.22	-0.17	-0.12			-1.06		4.81
AT4G24570	A_95_P250542	NM_001325368.1	Q9SB52	-0.07	1.90	0.19	2.12	-1.26	-2.13	-1.83	1.57	

Arabidopsis and tobacco identifiers				WT tobacco		VviPGIP1-tobacco		Primed *Arabidopsis*	Primed and infected *Arabidopsis*		*B. cinerea* infected *Arabidopsis*	
Locus Identifier Arabidopsis	Agilent microarray probe	Tobacco GenBank Accession	Tobacco UNIPROT ID	Δt0-24	Δt0-48	Δt0-24	Δt0-48	ISR-prime 2dpTi	ISR-boost 1dpi	ISR-boost 2dpi	BIDR 1dpi	BIDR 2dpi
AT2G22500	A_95_P250542	NM_001325368.1	Q9SJY5	-0.07	1.90	0.19	2.12	-1.26	-2.13	-1.83	1.57	
AT5G09470	A_95_P250542	NM_001325368.1	Q9FY68	-0.07	1.90	0.19	2.12	-1.26	-2.13	-1.83	1.57	
AT3G54110	A_95_P250542	NM_001325368.1	O81845	-0.07	1.90	0.19	2.12	-1.26	-2.13	-1.83	1.57	
AT2G39030	A_95_P000336	NM_001325476.1	Q9ZV05	1.66	3.57	1.36	3.82	2.19	1.06	-1.28		5.97
AT1G72310	A_95_P211877	NM_001325503.1	Q9XF63	2.41	2.16	2.06	2.29	-1.10				-1.10
AT3G16720	A_95_P211877	NM_001325503.1	Q8L9T5	2.41	2.16	2.06	2.29	-1.10				-1.10
AT1G04360	A_95_P211877	NM_001325503.1	P93823	2.41	2.16	2.06	2.29	-1.10				-1.10
AT4G15975	A_95_P211877	NM_001325503.1	Q8LF65	2.41	2.16	2.06	2.29	-1.10				-1.10
AT2G47560	A_95_P211877	NM_001325503.1	O22255	2.41	2.16	2.06	2.29	-1.10				-1.10
AT5G17600	A_95_P211877	NM_001325503.1	Q9LF64	2.41	2.16	2.06	2.29	-1.10				-1.10
AT2G42360	A_95_P211877	NM_001325503.1	Q9SLC3	2.41	2.16	2.06	2.29	-1.10				-1.10
AT5G22300	A_95_P007556	NM_001325754.1	P46011	-0.30	-1.12	-0.36	-1.15	1.78				2.16
AT3G44300	A_95_P007556	NM_001325754.1	P32962	-0.30	-1.12	-0.36	-1.15	1.78				2.16
AT3G44320	A_95_P007556	NM_001325754.1	P46010	-0.30	-1.12	-0.36	-1.15	1.78				2.16
AT5G37490	A_95_P239404	NM_001325854.1	Q5PNY6	1.50	1.18	1.13	1.86			-3.50		3.83
AT1G66160	A_95_P239404	NM_001325854.1	Q9C8D1	1.50	1.18	1.13	1.86			-3.50		3.83
AT2G35930	A_95_P239404	NM_001325854.1	Q84TG3	1.50	1.18	1.13	1.86			-3.50		3.83
AT3G52450	A_95_P239404	NM_001325854.1	Q9SVC6	1.50	1.18	1.13	1.86			-3.50		3.83
AT1G49780	A_95_P239404	NM_001325854.1	Q9FXA4	1.50	1.18	1.13	1.86			-3.50		3.83
AT3G19380	A_95_P239404	NM_001325854.1	Q9LT79	1.50	1.18	1.13	1.86			-3.50		3.83
AT3G11840	A_95_P239404	NM_001325854.1	Q9SF15	1.50	1.18	1.13	1.86			-3.50		3.83
AT5G65920	A_95_P239404	NM_001325854.1	Q9FHN9	1.50	1.18	1.13	1.86			-3.50		3.83
AT5G09800	A_95_P239404	NM_001325854.1	Q9LXE3	1.50	1.18	1.13	1.86			-3.50		3.83
AT3G18710	A_95_P239404	NM_001325854.1	Q9LSA6	1.50	1.18	1.13	1.86			-3.50		3.83
AT4G00430	A_95_P245117	NM_001325992.1	Q39196	0.16	0.15	0.61	0.14					-1.38
AT2G45960	A_95_P245117	NM_001325992.1	Q06611	0.16	0.15	0.61	0.14					-1.38
AT1G01620	A_95_P245117	NM_001325992.1	Q08733	0.16	0.15	0.61	0.14					-1.38
AT4G23400	A_95_P245117	NM_001325992.1	Q8LAA6	0.16	0.15	0.61	0.14					-1.38
AT3G61430	A_95_P245117	NM_001325992.1	P61837	0.16	0.15	0.61	0.14					-1.38
AT2G45560	A_95_P234719	NM_001326128.1	O64636	1.70	2.27	1.55	2.61				-1.73	-1.24
AT2G45570	A_95_P234719	NM_001326128.1	O64637	1.70	2.27	1.55	2.61				-1.73	-1.24
AT4G05390	A_95_P010631	NM_001326155.1	Q9M0V6	-0.12	1.61	0.31	1.66	1.30				
AT1G20020	A_95_P010631	NM_001326155.1	Q8W493	-0.12	1.61	0.31	1.66	1.30				
AT5G66190	A_95_P010631	NM_001326155.1	Q9FKW6	-0.12	1.61	0.31	1.66	1.30				
AT4G34135	A_95_P001761	NM_001326177.1	Q94C57	1.69	1.25	1.84	1.68	2.36		1.58		1.71
AT4G18800	A_95_P223807	NM_001326230.1	Q9SN35	-0.29	-0.64	-0.06	-0.76	1.03				1.44
AT5G45750	A_95_P223807	NM_001326230.1	Q9FK68	-0.29	-0.64	-0.06	-0.76	1.03				1.44
AT2G45050	A_95_P238279	NM_001326262.1	O49741	-0.62	-1.32	-0.45	-1.36			0.93		
AT4G36240	A_95_P238279	NM_001326262.1	O65515	-0.62	-1.32	-0.45	-1.36			0.93		
AT3G60530	A_95_P238279	NM_001326262.1	O49743	-0.62	-1.32	-0.45	-1.36			0.93		
AT5G66320	A_95_P238279	NM_001326262.1	Q9FH57	-0.62	-1.32	-0.45	-1.36			0.93		
AT3G51080	A_95_P238279	NM_001326262.1	Q9SD38	-0.62	-1.32	-0.45	-1.36			0.93		
AT2G17800	A_95_P007861	U64924.1	Q38902	-0.18	-1.00	-0.49	-1.12	-1.21				

Arabidopsis and tobacco identifiers				WT tobacco		VviPGIP1-tobacco		Primed *Arabidopsis*	Primed and infected *Arabidopsis*		*B. cinerea* infected *Arabidopsis*	
Locus Identifier Arabidopsis	Agilent microarray probe	Tobacco GenBank Accession	Tobacco UNIPROT ID	Δt0-24	Δt0-48	Δt0-24	Δt0-48	ISR-prime 2dpTi	ISR-boost 1dpi	ISR-boost 2dpi	BIDR 1dpi	BIDR 2dpi
AT4G35950	A_95_P007861	U64924.1	Q9SBJ6	-0.18	-1.00	-0.49	-1.12	-1.21				
AT4G01010	A_95_P237494	U65390.2	Q9LD40	0.12	0.39	0.30	0.41	1.34				2.05
AT4G30560	A_95_P237494	U65390.2	Q9M0A4	0.12	0.39	0.30	0.41	1.34				2.05
AT2G46430	A_95_P237494	U65390.2	Q9SKD7	0.12	0.39	0.30	0.41	1.34				2.05
AT2G46440	A_95_P237494	U65390.2	Q9SKD6	0.12	0.39	0.30	0.41	1.34				2.05
AT1G20330	A_95_P010161	U71108.1	Q39227	-0.42	-1.64	-0.17	-1.84					-0.87
AT1G76090	A_95_P010161	U71108.1	Q94JS4	-0.42	-1.64	-0.17	-1.84					-0.87
AT3G57240	A_95_P007726	X54456.1	F4J270	1.01	4.88	1.35	4.56	2.91				3.94
AT3G57260	A_95_P007726	X54456.1	P33157	1.01	4.88	1.35	4.56	2.91				3.94
AT3G57270	A_95_P007726	X54456.1	Q9M2M0	1.01	4.88	1.35	4.56	2.91				3.94
AT1G60690	A_95_P007701	X56267.1	O22707	-0.64	-0.34	0.31	-0.14					-0.88
AT1G60730	A_95_P007701	X56267.1	Q9ASZ9	-0.64	-0.34	0.31	-0.14					-0.88
AT5G42020	A_95_P195212	X60060.1	Q39043	0.64	2.01	2.57	2.34	1.83		-0.95		1.07
AT5G28540	A_95_P195212	X60060.1	Q9LKR3	0.64	2.01	2.57	2.34	1.83		-0.95		1.07
AT1G09080	A_95_P195212	X60060.1	Q8H1B3	0.64	2.01	2.57	2.34	1.83		-0.95		1.07
AT3G12580	A_95_P239889	X63106.1	Q9LHA8	2.58	1.54	1.89	2.30	0.85	1.07			
AT5G02490	A_95_P239889	X63106.1	P22954	2.58	1.54	1.89	2.30	0.85	1.07			
AT1G68620	A_95_P007651	X77136.1	Q9SX25	1.42	1.48	1.15	1.96	3.55				3.10
AT5G06570	A_95_P007651	X77136.1	Q9FG13	1.42	1.48	1.15	1.96	3.55				3.10
AT2G45610	A_95_P007651	X77136.1	O64641	1.42	1.48	1.15	1.96	3.55				3.10
AT1G47480	A_95_P007651	X77136.1	Q9SX78	1.42	1.48	1.15	1.96	3.55				3.10
AT5G62180	A_95_P007651	X77136.1	Q9LVB8	1.42	1.48	1.15	1.96	3.55				3.10
AT3G10230	A_95_P205022	X81787.1	Q38933	-0.64	-1.25	-0.42	-1.56					-1.03
AT5G57030	A_95_P205022	X81787.1	Q38932	-0.64	-1.25	-0.42	-1.56					-1.03
AT1G69880	A_95_P254304	XM_016577579.1	Q9CAS1	0.58	0.32	1.01	1.08					1.98
AT5G42980	A_95_P254304	XM_016577579.1	Q42403	0.58	0.32	1.01	1.08					1.98
AT1G65430	A_95_P004151	XM_016577676.1	Q8W468	0.10	0.14	0.21	0.58					1.03
AT1G05890	A_95_P004151	XM_016577676.1	Q8L829	0.10	0.14	0.21	0.58					1.03
AT1G17180	A_95_P018851	XM_016578159.1	Q9SHH7	1.51	4.30	1.93	3.73	2.32				4.94
AT1G17170	A_95_P018851	XM_016578159.1	Q9SHH6	1.51	4.30	1.93	3.73	2.32				4.94
AT1G53680	A_95_P018851	XM_016578159.1	Q9C8M3	1.51	4.30	1.93	3.73	2.32				4.94
AT3G43800	A_95_P018851	XM_016578159.1	Q9LZG7	1.51	4.30	1.93	3.73	2.32				4.94
AT5G56760	A_95_P093408	XM_016578294.1	Q42538	0.49	-0.15	0.44	-0.14					0.91
AT4G35640	A_95_P093408	XM_016578294.1	Q8W2B8	0.49	-0.15	0.44	-0.14					0.91
AT1G63850	A_95_P213332	XM_016578667.1	Q9CAJ9	-0.45	-1.43	-0.58	-1.47					-1.48
AT5G60050	A_95_P213332	XM_016578667.1	Q9LVG9	-0.45	-1.43	-0.58	-1.47					-1.48
AT2G13690	A_95_P213332	XM_016578667.1	Q9SKH2	-0.45	-1.43	-0.58	-1.47					-1.48
AT1G56280	A_95_P191692	XM_016579066.1	Q39083	-0.32	-0.34	-0.07	0.25					0.89
AT4G02200	A_95_P191692	XM_016579066.1	O04259	-0.32	-0.34	-0.07	0.25					0.89
AT5G45090	A_95_P269781	XM_016579227.1	Q9FHE5	0.20	-0.74	-0.14	-1.09	2.44				2.54
AT5G45080	A_95_P269781	XM_016579227.1	Q9FHE8	0.20	-0.74	-0.14	-1.09	2.44				2.54
AT2G29170	A_95_P192817	XM_016579409.1	Q9ZW04	2.34	3.31	2.27	3.14					1.25
AT2G29150	A_95_P192817	XM_016579409.1	Q9ZW03	2.34	3.31	2.27	3.14					1.25

Arabidopsis and tobacco identifiers				WT tobacco		VviPGIP1-tobacco		Primed *Arabidopsis*	Primed and infected *Arabidopsis*		*B. cinerea* infected *Arabidopsis*	
Locus Identifier Arabidopsis	Agilent microarray probe	Tobacco GenBank Accession	Tobacco UNIPROT ID	Δt0-24	Δt0-48	Δt0-24	Δt0-48	ISR-prime 2dpTi	ISR-boost 1dpi	ISR-boost 2dpi	BIDR 1dpi	BIDR 2dpi
AT2G29290	A_95_P192817	XM_016579409.1	Q9ZW13	2.34	3.31	2.27	3.14					1.25
AT2G29300	A_95_P192817	XM_016579409.1	Q42182	2.34	3.31	2.27	3.14					1.25
AT2G29350	A_95_P192817	XM_016579409.1	Q9ZW18	2.34	3.31	2.27	3.14					1.25
AT4G22200	A_95_P131432	XM_016580254.1	Q38898	0.50	-0.67	0.33	-1.12					-1.09
AT2G26650	A_95_P131432	XM_016580254.1	Q38998	0.50	-0.67	0.33	-1.12					-1.09
AT4G33050	A_95_P138437	XM_016581049.1	O82645	-0.30	-0.69	0.11	-0.43	2.00		-0.94		3.82
AT2G26190	A_95_P138437	XM_016581049.1	O64851	-0.30	-0.69	0.11	-0.43	2.00		-0.94		3.82
AT5G57010	A_95_P138437	XM_016581049.1	Q058N0	-0.30	-0.69	0.11	-0.43	2.00		-0.94		3.82
AT3G13600	A_95_P138437	XM_016581049.1	Q9LHN9	-0.30	-0.69	0.11	-0.43	2.00		-0.94		3.82
AT3G52870	A_95_P138437	XM_016581049.1	Q9LFA4	-0.30	-0.69	0.11	-0.43	2.00		-0.94		3.82
AT5G13490	A_95_P012211	XM_016581441.1	P40941	0.07	1.29	0.42	1.69	1.90		-1.03		2.45
AT4G28390	A_95_P012211	XM_016581441.1	O49447	0.07	1.29	0.42	1.69	1.90		-1.03		2.45
AT2G34500	A_95_P216932	XM_016581479.1	O64697	1.36	1.61	1.19	1.84	2.72		-1.32		4.34
AT2G34490	A_95_P216932	XM_016581479.1	O64698	1.36	1.61	1.19	1.84	2.72		-1.32		4.34
AT1G66400	A_95_P225782	XM_016581521.1	Q9C8Y1	-0.30	-1.12	-0.92	-1.09	-1.28				
AT2G15680	A_95_P225782	XM_016581521.1	Q9ZQE6	-0.30	-1.12	-0.92	-1.09	-1.28				
AT1G32170	A_95_P009341	XM_016581891.1	Q38908	-0.23	1.03	0.06	1.14					1.15
AT4G18990	A_95_P009341	XM_016581891.1	Q8L7H3	-0.23	1.03	0.06	1.14					1.15
AT1G10550	A_95_P009341	XM_016581891.1	Q8LC45	-0.23	1.03	0.06	1.14					1.15
AT3G44990	A_95_P009341	XM_016581891.1	P93046	-0.23	1.03	0.06	1.14					1.15
AT2G36870	A_95_P009341	XM_016581891.1	Q9SJL9	-0.23	1.03	0.06	1.14					1.15
AT5G16370	A_95_P021681	XM_016582131.1	Q9FFE6	0.00	-0.51	-0.40	-1.15					1.37
AT1G75960	A_95_P021681	XM_016582131.1	Q9LQS1	0.00	-0.51	-0.40	-1.15					1.37
AT1G65890	A_95_P021681	XM_016582131.1	Q9SS00	0.00	-0.51	-0.40	-1.15					1.37
AT2G25450	A_95_P001501	XM_016582216.1	Q9SKK4	-0.56	-0.86	-0.58	-1.22			-1.00		
AT5G43450	A_95_P001501	XM_016582216.1	Q9LSW6	-0.56	-0.86	-0.58	-1.22			-1.00		
AT4G03510	A_95_P294183	XM_016582883.1	O64425	1.31	0.69	0.68	0.67			0.89		
AT4G28270	A_95_P294183	XM_016582883.1	P93030	1.31	0.69	0.68	0.67			0.89		
AT5G17860	A_95_P155007	XM_016583176.1	Q9FKP1	-0.32	0.24	0.28	0.03	0.97	1.00			2.39
AT5G17850	A_95_P155007	XM_016583176.1	Q9FKP2	-0.32	0.24	0.28	0.03	0.97	1.00			2.39
AT5G18240	A_95_P012316	XM_016583235.1	Q9FK47	-0.43	-1.56	-0.49	-1.51			-0.94		
AT3G04450	A_95_P012316	XM_016583235.1	F4J3P7	-0.43	-1.56	-0.49	-1.51			-0.94		
AT5G54280	A_95_P285483	XM_016583682.1	F4K0A6	-0.47	-1.56	-0.18	-1.56					0.85
AT1G50360	A_95_P285483	XM_016583682.1	F4I507	-0.47	-1.56	-0.18	-1.56					0.85
AT2G20290	A_95_P285483	XM_016583682.1	F4IUG9	-0.47	-1.56	-0.18	-1.56					0.85
AT1G09930	A_95_P159532	XM_016584005.1	O04514	0.16	-0.23	1.48	-0.13	1.43				-0.86
AT4G10770	A_95_P159532	XM_016584005.1	O82485	0.16	-0.23	1.48	-0.13	1.43				-0.86
AT5G55930	A_95_P159532	XM_016584005.1	Q9FG72	0.16	-0.23	1.48	-0.13	1.43				-0.86
AT3G21620	A_95_P164717	XM_016584372.1	Q9LVE4	-0.47	-1.79	-0.45	-1.74					-1.60
AT1G11960	A_95_P164717	XM_016584372.1	B5TYT3	-0.47	-1.79	-0.45	-1.74					-1.60
AT4G15430	A_95_P164717	XM_016584372.1	Q8VZM5	-0.47	-1.79	-0.45	-1.74					-1.60
AT1G69450	A_95_P164717	XM_016584372.1	F4I248	-0.47	-1.79	-0.45	-1.74					-1.60
AT1G58520	A_95_P164717	XM_016584372.1	F4IBD7	-0.47	-1.79	-0.45	-1.74					-1.60

Arabidopsis and tobacco identifiers				WT tobacco		VviPGIP1-tobacco		Primed *Arabidopsis*	Primed and infected *Arabidopsis*		*B. cinerea* infected *Arabidopsis*	
Locus Identifier Arabidopsis	Agilent microarray probe	Tobacco GenBank Accession	Tobacco UNIPROT ID	Δt0-24	Δt0-48	Δt0-24	Δt0-48	ISR-prime 2dpTi	ISR-boost 1dpi	ISR-boost 2dpi	BIDR 1dpi	BIDR 2dpi
AT1G10090	A_95_P164717	XM_016584372.1	Q94A87	-0.47	-1.79	-0.45	-1.74					-1.60
AT4G27410	A_95_P020736	XM_016584562.1	Q93VY3	0.24	1.24	0.08	1.30					1.44
AT1G52890	A_95_P020736	XM_016584562.1	Q9C932	0.24	1.24	0.08	1.30					1.44
AT3G15500	A_95_P020736	XM_016584562.1	Q9LDY8	0.24	1.24	0.08	1.30					1.44
AT5G08790	A_95_P020736	XM_016584562.1	Q9C598	0.24	1.24	0.08	1.30					1.44
AT1G61110	A_95_P020736	XM_016584562.1	Q8GY42	0.24	1.24	0.08	1.30					1.44
AT5G63790	A_95_P020736	XM_016584562.1	Q8H115	0.24	1.24	0.08	1.30					1.44
AT1G69490	A_95_P020736	XM_016584562.1	O49255	0.24	1.24	0.08	1.30					1.44
AT3G44260	A_95_P015901	XM_016586275.1	Q9LXM2	-0.71	-1.06	-0.76	-1.09	-1.03				1.06
AT5G22250	A_95_P015901	XM_016586275.1	Q9FMS6	-0.71	-1.06	-0.76	-1.09	-1.03				1.06
AT2G40900	A_95_P117397	XM_016586447.1	F4IJ08	0.54	-0.79	-0.04	-0.47					-1.21
AT4G08300	A_95_P117397	XM_016586447.1	Q501F8	0.54	-0.79	-0.04	-0.47					-1.21
AT4G08290	A_95_P117397	XM_016586447.1	Q9SUF1	0.54	-0.79	-0.04	-0.47					-1.21
AT4G39620	A_95_P280488	XM_016586483.1	Q9SV96	-0.74	0.69	-0.60	0.85	-0.89				
AT5G48730	A_95_P280488	XM_016586483.1	Q9FKC3	-0.74	0.69	-0.60	0.85	-0.89				
AT1G74750	A_95_P280488	XM_016586483.1	Q9SSF9	-0.74	0.69	-0.60	0.85	-0.89				
AT2G35130	A_95_P280488	XM_016586483.1	O82178	-0.74	0.69	-0.60	0.85	-0.89				
AT4G34610	A_95_P120297	XM_016587250.1	O65685	-0.06	-0.40	0.19	0.03					-1.29
AT1G19700	A_95_P120297	XM_016587250.1	Q9FXG8	-0.06	-0.40	0.19	0.03					-1.29
AT2G23760	A_95_P120297	XM_016587250.1	Q94KL5	-0.06	-0.40	0.19	0.03					-1.29
AT2G27990	A_95_P120297	XM_016587250.1	Q9SJJ3	-0.06	-0.40	0.19	0.03					-1.29
AT4G32980	A_95_P120297	XM_016587250.1	P48731	-0.06	-0.40	0.19	0.03					-1.29
AT2G35760	A_95_P224147	XM_016587825.1	Q8L924	0.31	-0.34	-0.22	-0.34					-1.31
AT4G16442	A_95_P224147	XM_016587825.1	Q8L9B5	0.31	-0.34	-0.22	-0.34					-1.31
AT3G61220	A_95_P255989	XM_016588434.1	Q9M2E2	-1.00	0.01	0.39	0.42					-1.21
AT2G24190	A_95_P255989	XM_016588434.1	Q9ZUH5	-1.00	0.01	0.39	0.42					-1.21
AT1G74360	A_95_P119352	XM_016588630.1	C0LGJ1	1.32	1.01	1.21	1.77	1.65		-1.58		3.46
AT3G13380	A_95_P119352	XM_016588630.1	Q9LJF3	1.32	1.01	1.21	1.77	1.65		-1.58		3.46
AT1G64150	A_95_P280608	XM_016588671.1	Q94AX5	-0.09	-0.76	-0.09	-0.81					-1.13
AT5G36290	A_95_P280608	XM_016588671.1	Q93Y38	-0.09	-0.76	-0.09	-0.81					-1.13
AT1G12360	A_95_P211412	XM_016588739.1	Q9C5X3	0.49	0.82	0.68	1.08					1.47
AT4G12120	A_95_P211412	XM_016588739.1	Q9SZ77	0.49	0.82	0.68	1.08					1.47
AT2G44790	A_95_P106582	XM_016589545.1	O80517	1.50	0.99	0.29	1.03					2.91
AT2G25060	A_95_P106582	XM_016589545.1	Q9SK27	1.50	0.99	0.29	1.03					2.91
AT5G20230	A_95_P106582	XM_016589545.1	Q07488	1.50	0.99	0.29	1.03					2.91
AT4G27520	A_95_P106582	XM_016589545.1	Q9T076	1.50	0.99	0.29	1.03					2.91
AT5G15350	A_95_P106582	XM_016589545.1	Q39131	1.50	0.99	0.29	1.03					2.91
AT1G29395	A_95_P184147	XM_016589585.1	Q94AL8	-0.34	-0.18	-0.15	-0.49				-1.90	1.87
AT2G15970	A_95_P184147	XM_016589585.1	Q9XIM7	-0.34	-0.18	-0.15	-0.49				-1.90	1.87
AT3G48890	A_95_P027011	XM_016589783.1	Q9M2Z4	0.77	2.36	0.70	2.32					1.97
AT5G52240	A_95_P027011	XM_016589783.1	Q9XFM6	0.77	2.36	0.70	2.32					1.97
AT1G13960	A_95_P195282	XM_016589826.1	Q9XI90	0.30	1.54	0.36	1.70					0.92
AT2G38470	A_95_P195282	XM_016589826.1	Q8S8P5	0.30	1.54	0.36	1.70					0.92

Arabidopsis and tobacco identifiers				WT tobacco		VviPGIP1-tobacco		Primed *Arabidopsis*	Primed and infected *Arabidopsis*		*B. cinerea* infected *Arabidopsis*	
Locus Identifier Arabidopsis	Agilent microarray probe	Tobacco GenBank Accession	Tobacco UNIPROT ID	Δt0-24	Δt0-48	Δt0-24	Δt0-48	ISR-prime 2dpTi	ISR-boost 1dpi	ISR-boost 2dpi	BIDR 1dpi	BIDR 2dpi
AT2G30250	A_95_P195282	XM_016589826.1	O22921	0.30	1.54	0.36	1.70					0.92
AT4G12020	A_95_P195282	XM_016589826.1	Q9SZ67	0.30	1.54	0.36	1.70					0.92
AT3G01080	A_95_P195282	XM_016589826.1	Q93WU7	0.30	1.54	0.36	1.70					0.92
AT1G05260	A_95_P034843	XM_016589949.1	O23044	0.26	0.32	0.06	0.43					-1.09
AT4G08770	A_95_P034843	XM_016589949.1	Q9LDN9	0.26	0.32	0.06	0.43					-1.09
AT5G35735	A_95_P004401	XM_016590826.1	Q9FKH6	0.70	-0.42	0.61	0.31			-1.26		3.29
AT3G25290	A_95_P004401	XM_016590826.1	Q9LSE7	0.70	-0.42	0.61	0.31			-1.26		3.29
AT4G12980	A_95_P004401	XM_016590826.1	Q9SV71	0.70	-0.42	0.61	0.31			-1.26		3.29
AT2G04850	A_95_P004401	XM_016590826.1	Q9SJ74	0.70	-0.42	0.61	0.31			-1.26		3.29
AT3G61750	A_95_P004401	XM_016590826.1	Q9M363	0.70	-0.42	0.61	0.31			-1.26		3.29
AT4G18260	A_95_P004401	XM_016590826.1	Q0WPS2	0.70	-0.42	0.61	0.31			-1.26		3.29
AT2G30890	A_95_P004401	XM_016590826.1	O80854	0.70	-0.42	0.61	0.31			-1.26		3.29
AT1G74590	A_95_P203612	XM_016590881.1	Q9CA57	1.05	0.52	0.93	0.96	2.71				3.53
AT5G62480	A_95_P203612	XM_016590881.1	Q9FUT0	1.05	0.52	0.93	0.96	2.71				3.53
AT2G29420	A_95_P203612	XM_016590881.1	Q9ZW24	1.05	0.52	0.93	0.96	2.71				3.53
AT3G09270	A_95_P203612	XM_016590881.1	Q9SR36	1.05	0.52	0.93	0.96	2.71				3.53
AT2G29480	A_95_P203612	XM_016590881.1	Q9ZW29	1.05	0.52	0.93	0.96	2.71				3.53
AT2G29490	A_95_P203612	XM_016590881.1	Q9ZW30	1.05	0.52	0.93	0.96	2.71				3.53
AT2G29450	A_95_P203612	XM_016590881.1	P46421	1.05	0.52	0.93	0.96	2.71				3.53
AT1G10370	A_95_P203612	XM_016590881.1	Q9FUS8	1.05	0.52	0.93	0.96	2.71				3.53
AT3G48460	A_95_P315968	XM_016591009.1	Q9STM6	-0.25	-0.22	-0.18	-0.32					-2.42
AT1G28670	A_95_P315968	XM_016591009.1	Q38894	-0.25	-0.22	-0.18	-0.32					-2.42
AT1G31550	A_95_P315968	XM_016591009.1	Q9C857	-0.25	-0.22	-0.18	-0.32					-2.42
AT2G27360	A_95_P315968	XM_016591009.1	Q9ZQI3	-0.25	-0.22	-0.18	-0.32					-2.42
AT1G28610	A_95_P315968	XM_016591009.1	Q9SHP6	-0.25	-0.22	-0.18	-0.32					-2.42
AT4G37760	A_95_P191387	XM_016591191.1	Q8VYH2	-0.43	-0.84	-0.49	-0.97					-1.45
AT5G24150	A_95_P191387	XM_016591191.1	O65404	-0.43	-0.84	-0.49	-0.97					-1.45
AT2G33270	A_95_P131737	XM_016591520.1	O22779	0.24	0.01	-0.22	0.30					1.10
AT5G61440	A_95_P131737	XM_016591520.1	Q9XFI1	0.24	0.01	-0.22	0.30					1.10
AT2G29970	A_95_P115712	XM_016591521.1	O80875	-0.42	-1.00	0.00	-0.94					-0.86
AT2G40130	A_95_P115712	XM_016591521.1	F4IGZ2	-0.42	-1.00	0.00	-0.94					-0.86
AT4G30350	A_95_P115712	XM_016591521.1	Q9M0C5	-0.42	-1.00	0.00	-0.94					-0.86
AT4G29920	A_95_P115712	XM_016591521.1	Q9SZR3	-0.42	-1.00	0.00	-0.94					-0.86
AT2G46680	A_95_P195092	XM_016591580.1	P46897	0.15	0.20	0.03	1.12	1.43				
AT2G22430	A_95_P195092	XM_016591580.1	P46668	0.15	0.20	0.03	1.12	1.43				
AT1G69780	A_95_P195092	XM_016591580.1	Q8LC03	0.15	0.20	0.03	1.12	1.43				
AT2G47520	A_95_P184897	XM_016591614.1	O22259	-0.12	-1.12	0.60	-1.56					3.70
AT1G72360	A_95_P184897	XM_016591614.1	Q8H0T5	-0.12	-1.12	0.60	-1.56					3.70
AT5G61890	A_95_P184897	XM_016591614.1	Q9FH54	-0.12	-1.12	0.60	-1.56					3.70
AT5G47230	A_95_P184897	XM_016591614.1	O80341	-0.12	-1.12	0.60	-1.56					3.70
AT4G17500	A_95_P184897	XM_016591614.1	O80337	-0.12	-1.12	0.60	-1.56					3.70
AT1G01360	A_95_P205442	XM_016591683.1	Q84MC7	-0.23	-1.12	-0.69	-1.40				1.00	
AT5G05440	A_95_P205442	XM_016591683.1	Q9FLB1	-0.23	-1.12	-0.69	-1.40				1.00	

Arabidopsis and tobacco identifiers				WT tobacco		VviPGIP1-tobacco		Primed *Arabidopsis*	Primed and infected *Arabidopsis*		*B. cinerea* infected *Arabidopsis*	
Locus Identifier Arabidopsis	Agilent microarray probe	Tobacco GenBank Accession	Tobacco UNIPROT ID	Δt0-24	Δt0-48	Δt0-24	Δt0-48	ISR-prime 2dpTi	ISR-boost 1dpi	ISR-boost 2dpi	BIDR 1dpi	BIDR 2dpi
AT2G38310	A_95_P205442	XM_016591683.1	O80920	-0.23	-1.12	-0.69	-1.40				1.00	
AT2G40330	A_95_P205442	XM_016591683.1	Q8S8E3	-0.23	-1.12	-0.69	-1.40				1.00	
AT5G46790	A_95_P205442	XM_016591683.1	Q8VZS8	-0.23	-1.12	-0.69	-1.40				1.00	
AT3G06020	A_95_P119727	XM_016591826.1	Q9SFG6	-0.14	-0.58	-0.25	-0.71					-0.98
AT4G02810	A_95_P119727	XM_016591826.1	Q9SY06	-0.14	-0.58	-0.25	-0.71					-0.98
AT1G03170	A_95_P119727	XM_016591826.1	Q8GXU9	-0.14	-0.58	-0.25	-0.71					-0.98
AT4G39330	A_95_P015641	XM_016592682.1	P42734	0.36	1.53	0.56	1.16					-1.98
AT4G37990	A_95_P015641	XM_016592682.1	Q02972	0.36	1.53	0.56	1.16					-1.98
AT2G21730	A_95_P015641	XM_016592682.1	Q9SJ25	0.36	1.53	0.56	1.16					-1.98
AT3G22890	A_95_P033279	XM_016592790.1	Q9LIK9	1.30	2.71	1.62	2.85					0.94
AT4G14680	A_95_P033279	XM_016592790.1	O23324	1.30	2.71	1.62	2.85					0.94
AT5G43780	A_95_P033279	XM_016592790.1	Q9S7D8	1.30	2.71	1.62	2.85					0.94
AT2G38750	A_95_P002741	XM_016592813.1	Q9ZVJ6	-0.20	-0.64	-1.15	-0.49		1.32			
AT1G35720	A_95_P002741	XM_016592813.1	Q9SYT0	-0.20	-0.64	-1.15	-0.49		1.32			
AT2G38760	A_95_P002741	XM_016592813.1	Q9SE45	-0.20	-0.64	-1.15	-0.49		1.32			
AT1G07820	A_95_P193178	XM_016592917.1	P59259	-0.09	-0.97	-0.29	-1.06					1.16
AT3G45930	A_95_P193178	XM_016592917.1	P59259	-0.09	-0.97	-0.29	-1.06					1.16
AT3G46320	A_95_P193178	XM_016592917.1	P59259	-0.09	-0.97	-0.29	-1.06					1.16
AT5G61790	A_95_P185712	XM_016593002.1	P29402	0.77	1.89	1.23	2.17	1.69				
AT5G07340	A_95_P185712	XM_016593002.1	Q38798	0.77	1.89	1.23	2.17	1.69				
AT1G01520	A_95_P196562	XM_016593008.1	Q6R0H0	0.21	0.06	0.00	-0.06					-3.44
AT5G52660	A_95_P196562	XM_016593008.1	Q8H0W3	0.21	0.06	0.00	-0.06					-3.44
AT4G30340	A_95_P211722	XM_016593227.1	F4JQ95	1.72	1.44	1.33	1.98					1.65
AT2G20900	A_95_P211722	XM_016593227.1	Q9C5E5	1.72	1.44	1.33	1.98					1.65
AT4G28130	A_95_P211722	XM_016593227.1	F4JKI3	1.72	1.44	1.33	1.98					1.65
AT2G17700	A_95_P115872	XM_016593269.1	O22558	0.71	1.31	0.63	1.56					0.97
AT4G38470	A_95_P115872	XM_016593269.1	F4JTP5	0.71	1.31	0.63	1.56					0.97
AT3G47570	A_95_P221787	XM_016593270.1	C0LGP4	0.14	-0.54	-0.12	-0.36					2.42
AT5G20480	A_95_P221787	XM_016593270.1	C0LGT6	0.14	-0.54	-0.12	-0.36					2.42
AT3G47110	A_95_P221787	XM_016593270.1	Q9SD62	0.14	-0.54	-0.12	-0.36					2.42
AT3G17420	A_95_P221787	XM_016593270.1	Q9LRP3	0.14	-0.54	-0.12	-0.36					2.42
AT3G53380	A_95_P221787	XM_016593270.1	Q9LFH9	0.14	-0.54	-0.12	-0.36					2.42
AT4G28490	A_95_P221787	XM_016593270.1	P47735	0.14	-0.54	-0.12	-0.36					2.42
AT3G14310	A_95_P136407	XM_016593961.1	O49006	0.30	0.40	-0.20	0.14					2.06
AT1G53830	A_95_P136407	XM_016593961.1	Q42534	0.30	0.40	-0.20	0.14					2.06
AT3G05620	A_95_P136407	XM_016593961.1	Q9M9W7	0.30	0.40	-0.20	0.14					2.06
AT5G53370	A_95_P136407	XM_016593961.1	Q9FK05	0.30	0.40	-0.20	0.14					2.06
AT3G49220	A_95_P136407	XM_016593961.1	Q9M3B0	0.30	0.40	-0.20	0.14					2.06
AT5G62920	A_95_P133212	XM_016594217.1	Q9ZWS6	-0.49	-0.29	0.55	0.07	-2.11				-1.32
AT1G74890	A_95_P133212	XM_016594217.1	Q7G8V2	-0.49	-0.29	0.55	0.07	-2.11				-1.32
AT3G48100	A_95_P133212	XM_016594217.1	Q9SB04	-0.49	-0.29	0.55	0.07	-2.11				-1.32
AT1G19050	A_95_P133212	XM_016594217.1	Q9ZWS7	-0.49	-0.29	0.55	0.07	-2.11				-1.32
AT2G40670	A_95_P133212	XM_016594217.1	Q9SHC2	-0.49	-0.29	0.55	0.07	-2.11				-1.32

Arabidopsis and tobacco identifiers				WT tobacco		VviPGIP1-tobacco		Primed *Arabidopsis*	Primed and infected *Arabidopsis*		*B. cinerea* infected *Arabidopsis*	
Locus Identifier Arabidopsis	Agilent microarray probe	Tobacco GenBank Accession	Tobacco UNIPROT ID	Δt0-24	Δt0-48	Δt0-24	Δt0-48	ISR-prime 2dpTi	ISR-boost 1dpi	ISR-boost 2dpi	BIDR 1dpi	BIDR 2dpi
AT2G41310	A_95_P133212	XM_016594217.1	O80365	-0.49	-0.29	0.55	0.07	-2.11				-1.32
AT3G57040	A_95_P133212	XM_016594217.1	O80366	-0.49	-0.29	0.55	0.07	-2.11				-1.32
AT2G39470	A_95_P003716	XM_016594399.1	O80634	-0.30	-1.32	-0.67	-1.60					-0.91
AT3G05410	A_95_P003716	XM_016594399.1	F4J7A7	-0.30	-1.32	-0.67	-1.60					-0.91
AT4G15510	A_95_P003716	XM_016594399.1	O23403	-0.30	-1.32	-0.67	-1.60					-0.91
AT5G62670	A_95_P212737	XM_016594734.1	Q9LV11	0.08	-1.03	0.18	-1.09					-1.48
AT3G47950	A_95_P212737	XM_016594734.1	Q9SU58	0.08	-1.03	0.18	-1.09					-1.48
AT4G30190	A_95_P212737	XM_016594734.1	P19456	0.08	-1.03	0.18	-1.09					-1.48
AT2G46830	A_95_P016256	XM_016594932.1	P92973	0.34	-0.32	0.72	-0.64				3.09	-2.23
AT5G37260	A_95_P016256	XM_016594932.1	F4K5X6	0.34	-0.32	0.72	-0.64				3.09	-2.23
AT1G18330	A_95_P016256	XM_016594932.1	B3H5A8	0.34	-0.32	0.72	-0.64				3.09	-2.23
AT5G17300	A_95_P016256	XM_016594932.1	F4KGY6	0.34	-0.32	0.72	-0.64				3.09	-2.23
AT3G05640	A_95_P245742	XM_016594991.1	Q9M9W9	1.88	2.25	1.21	2.32	-1.52			-3.44	
AT1G03590	A_95_P245742	XM_016594991.1	Q9LR65	1.88	2.25	1.21	2.32	-1.52			-3.44	
AT2G36830	A_95_P125462	XM_016594997.1	P25818	-0.22	-0.84	-0.49	-1.69	-1.39				-1.56
AT3G26520	A_95_P125462	XM_016594997.1	Q41963	-0.22	-0.84	-0.49	-1.69	-1.39				-1.56
AT3G16240	A_95_P125462	XM_016594997.1	Q41951	-0.22	-0.84	-0.49	-1.69	-1.39				-1.56
AT3G46620	A_95_P202457	XM_016595056.1	Q9SNB6	-0.22	-0.71	-1.12	-0.79			-0.86		1.29
AT5G59550	A_95_P202457	XM_016595056.1	Q940T5	-0.22	-0.71	-1.12	-0.79			-0.86		1.29
AT5G03630	A_95_P014911	XM_016595431.1	Q93WJ8	0.54	1.57	0.48	1.87	0.98		-0.93		2.73
AT3G09940	A_95_P014911	XM_016595431.1	Q9SR59	0.54	1.57	0.48	1.87	0.98		-0.93		2.73
AT1G10760	A_95_P207287	XM_016595549.1	Q9SAC6	-0.18	-1.22	-0.06	-0.94				-1.06	
AT5G26570	A_95_P207287	XM_016595549.1	Q6ZY51	-0.18	-1.22	-0.06	-0.94				-1.06	
AT2G01290	A_95_P007261	XM_016595785.1	Q9ZU38	-0.19	-0.44	-0.42	-0.82					-1.28
AT1G71100	A_95_P007261	XM_016595785.1	Q9C998	-0.19	-0.44	-0.42	-0.82					-1.28
AT2G13610	A_95_P041366	XM_016595823.1	Q9SIT6	0.31	-0.29	-0.12	-0.36	-1.03				
AT5G52860	A_95_P041366	XM_016595823.1	Q9FLX5	0.31	-0.29	-0.12	-0.36	-1.03				
AT3G55090	A_95_P041366	XM_016595823.1	Q9M2V7	0.31	-0.29	-0.12	-0.36	-1.03				
AT3G55100	A_95_P041366	XM_016595823.1	Q9M2V6	0.31	-0.29	-0.12	-0.36	-1.03				
AT2G39350	A_95_P041366	XM_016595823.1	O80946	0.31	-0.29	-0.12	-0.36	-1.03				
AT5G13580	A_95_P041366	XM_016595823.1	Q9FNB5	0.31	-0.29	-0.12	-0.36	-1.03				
AT1G45249	A_95_P131617	XM_016595914.1	Q9M7Q4	-0.15	-0.03	0.00	0.74	1.03				-0.87
AT1G49720	A_95_P131617	XM_016595914.1	Q9M7Q5	-0.15	-0.03	0.00	0.74	1.03				-0.87
AT4G34000	A_95_P131617	XM_016595914.1	Q9M7Q3	-0.15	-0.03	0.00	0.74	1.03				-0.87
AT3G56850	A_95_P131617	XM_016595914.1	Q9LES3	-0.15	-0.03	0.00	0.74	1.03				-0.87
AT2G41070	A_95_P131617	XM_016595914.1	Q9C5Q2	-0.15	-0.03	0.00	0.74	1.03				-0.87
AT2G36270	A_95_P131617	XM_016595914.1	Q9SJN0	-0.15	-0.03	0.00	0.74	1.03				-0.87
AT1G75250	A_95_P132842	XM_016595921.1	Q1A173	-0.92	-2.00	0.53	-2.47	-1.29				
AT2G21650	A_95_P132842	XM_016595921.1	Q9SIJ5	-0.92	-2.00	0.53	-2.47	-1.29				
AT1G61560	A_95_P220687	XM_016596069.1	Q94KB7	0.40	-1.18	0.11	-0.89			-1.15		3.70
AT1G11310	A_95_P220687	XM_016596069.1	Q9SXB6	0.40	-1.18	0.11	-0.89			-1.15		3.70
AT2G39200	A_95_P220687	XM_016596069.1	O80961	0.40	-1.18	0.11	-0.89			-1.15		3.70
AT3G45290	A_95_P220687	XM_016596069.1	Q94KB9	0.40	-1.18	0.11	-0.89			-1.15		3.70

Arabidopsis and tobacco identifiers				WT tobacco		VviPGIP1-tobacco		Primed *Arabidopsis*	Primed and infected *Arabidopsis*		*B. cinerea* infected *Arabidopsis*	
Locus Identifier Arabidopsis	Agilent microarray probe	Tobacco GenBank Accession	Tobacco UNIPROT ID	Δt0-24	Δt0-48	Δt0-24	Δt0-48	ISR-prime 2dpTi	ISR-boost 1dpi	ISR-boost 2dpi	BIDR 1dpi	BIDR 2dpi
AT5G53970	A_95_P155177	XM_016596694.1	Q9FN30	-1.89	-1.36	-0.47	-0.76					-1.01
AT4G28420	A_95_P155177	XM_016596694.1	Q67Y55	-1.89	-1.36	-0.47	-0.76					-1.01
AT2G24850	A_95_P155177	XM_016596694.1	Q9SK47	-1.89	-1.36	-0.47	-0.76					-1.01
AT4G23600	A_95_P155177	XM_016596694.1	Q9SUR6	-1.89	-1.36	-0.47	-0.76					-1.01
AT1G08450	A_95_P006216	XM_016596877.1	O04153	0.77	1.42	1.14	1.87	2.02				1.40
AT1G09210	A_95_P006216	XM_016596877.1	Q38858	0.77	1.42	1.14	1.87	2.02				1.40
AT1G56340	A_95_P006216	XM_016596877.1	O04151	0.77	1.42	1.14	1.87	2.02				1.40
AT5G21326	A_95_P002066	XM_016596880.1	Q84VQ3	0.18	-0.71	-0.94	-1.32					-0.88
AT1G30270	A_95_P002066	XM_016596880.1	Q93VD3	0.18	-0.71	-0.94	-1.32					-0.88
AT4G24400	A_95_P002066	XM_016596880.1	Q9STV4	0.18	-0.71	-0.94	-1.32					-0.88
AT2G22300	A_95_P139452	XM_016597284.1	Q8GSA7	0.72	-0.04	0.70	0.39			-0.86		
AT1G67310	A_95_P139452	XM_016597284.1	Q9FYG2	0.72	-0.04	0.70	0.39			-0.86		
AT1G33840	A_95_P201952	XM_016597352.1	Q9LQ36	-0.07	-0.49	-0.47	-0.06	1.93				2.60
AT2G14560	A_95_P201952	XM_016597352.1	Q9ZQR8	-0.07	-0.49	-0.47	-0.06	1.93				2.60
AT1G80120	A_95_P201952	XM_016597352.1	Q9SSC7	-0.07	-0.49	-0.47	-0.06	1.93				2.60
AT5G20640	A_95_P201952	XM_016597352.1	A0MFH4	-0.07	-0.49	-0.47	-0.06	1.93				2.60
AT2G29460	A_95_P180922	XM_016597679.1	Q9ZW27	0.25	0.38	0.30	0.25	3.06				7.08
AT2G29470	A_95_P180922	XM_016597679.1	Q9ZW28	0.25	0.38	0.30	0.25	3.06				7.08
AT1G54130	A_95_P120177	XM_016597761.1	Q9SYH1	1.70	1.79	1.63	2.13					1.12
AT3G14050	A_95_P120177	XM_016597761.1	Q9LVJ3	1.70	1.79	1.63	2.13					1.12
AT5G45840	A_95_P214112	XM_016597765.1	C0LGU7	0.70	0.61	0.55	1.33					0.85
AT5G48380	A_95_P214112	XM_016597765.1	Q9ASS4	0.70	0.61	0.55	1.33					0.85
AT1G60800	A_95_P214112	XM_016597765.1	Q93ZS4	0.70	0.61	0.55	1.33					0.85
AT1G64770	A_95_P233899	XM_016597909.1	Q94AQ8	-0.54	-1.60	-0.74	-1.94					-1.38
AT1G55370	A_95_P233899	XM_016597909.1	Q9C503	-0.54	-1.60	-0.74	-1.94					-1.38
AT2G46620	A_95_P199517	XM_016598081.1	F4IJ77	2.40	2.92	2.08	3.27	1.11				3.62
AT5G17760	A_95_P199517	XM_016598081.1	Q9FN75	2.40	2.92	2.08	3.27	1.11				3.62
AT3G28580	A_95_P199517	XM_016598081.1	Q9LJJ7	2.40	2.92	2.08	3.27	1.11				3.62
AT5G40010	A_95_P199517	XM_016598081.1	Q9FLD5	2.40	2.92	2.08	3.27	1.11				3.62
AT3G50930	A_95_P199517	XM_016598081.1	Q8VZG2	2.40	2.92	2.08	3.27	1.11				3.62
AT2G18193	A_95_P199517	XM_016598081.1	Q8GW96	2.40	2.92	2.08	3.27	1.11				3.62
AT3G28540	A_95_P199517	XM_016598081.1	Q9LH82	2.40	2.92	2.08	3.27	1.11				3.62
AT5G57480	A_95_P199517	XM_016598081.1	Q9FKM3	2.40	2.92	2.08	3.27	1.11				3.62
AT3G28610	A_95_P199517	XM_016598081.1	Q9LJJ5	2.40	2.92	2.08	3.27	1.11				3.62
AT3G28510	A_95_P199517	XM_016598081.1	Q9LH84	2.40	2.92	2.08	3.27	1.11				3.62
AT3G28600	A_95_P199517	XM_016598081.1	F4J0C0	2.40	2.92	2.08	3.27	1.11				3.62
AT5G41060	A_95_P129577	XM_016598156.1	Q9FLM3	0.04	-1.22	-0.10	-1.09					-0.90
AT3G48760	A_95_P129577	XM_016598156.1	Q9M306	0.04	-1.22	-0.10	-1.09					-0.90
AT4G26140	A_95_P262326	XM_016598404.1	Q9SCV0	-1.09	-2.18	-0.47	-2.12		-1.13			
AT3G13750	A_95_P262326	XM_016598404.1	Q9SCW1	-1.09	-2.18	-0.47	-2.12		-1.13			
AT5G56870	A_95_P262326	XM_016598404.1	Q9SCV8	-1.09	-2.18	-0.47	-2.12		-1.13			
AT4G36360	A_95_P262326	XM_016598404.1	Q9SCV9	-1.09	-2.18	-0.47	-2.12		-1.13			
AT4G25810	A_95_P010321	XM_016598442.1	Q38910	-1.03	-0.84	-0.45	-1.40					2.00

Arabidopsis and tobacco identifiers				WT tobacco		VviPGIP1-tobacco		Primed *Arabidopsis*	Primed and infected *Arabidopsis*		*B. cinerea* infected *Arabidopsis*	
Locus Identifier Arabidopsis	Agilent microarray probe	Tobacco GenBank Accession	Tobacco UNIPROT ID	Δt0-24	Δt0-48	Δt0-24	Δt0-48	ISR-prime 2dpTi	ISR-boost 1dpi	ISR-boost 2dpi	BIDR 1dpi	BIDR 2dpi
AT4G30270	A_95_P010321	XM_016598442.1	P24806	-1.03	-0.84	-0.45	-1.40					2.00
AT4G30280	A_95_P010321	XM_016598442.1	Q9M0D2	-1.03	-0.84	-0.45	-1.40					2.00
AT3G10500	A_95_P133377	XM_016598522.1	Q949N0	0.54	1.22	0.56	1.66	1.51				2.07
AT1G34180	A_95_P133377	XM_016598522.1	A4FVP6	0.54	1.22	0.56	1.66	1.51				2.07
AT1G32870	A_95_P133377	XM_016598522.1	F4IED2	0.54	1.22	0.56	1.66	1.51				2.07
AT3G49530	A_95_P133377	XM_016598522.1	Q9SCK6	0.54	1.22	0.56	1.66	1.51				2.07
AT5G24590	A_95_P133377	XM_016598522.1	Q9LKG8	0.54	1.22	0.56	1.66	1.51				2.07
AT4G35580	A_95_P133377	XM_016598522.1	F4JN35	0.54	1.22	0.56	1.66	1.51				2.07
AT5G20150	A_95_P198044	XM_016598643.1	Q8LBH4	0.43	0.66	1.14	0.53		1.33			
AT2G26660	A_95_P198044	XM_016598643.1	O48781	0.43	0.66	1.14	0.53		1.33			
AT2G45130	A_95_P198044	XM_016598643.1	Q5PP62	0.43	0.66	1.14	0.53		1.33			
AT1G27950	A_95_P115372	XM_016598976.1	Q9C7F7	0.26	-1.40	-0.10	-1.51					-1.11
AT2G44290	A_95_P115372	XM_016598976.1	O64864	0.26	-1.40	-0.10	-1.51					-1.11
AT5G10770	A_95_P029251	XM_016599114.1	Q8S9J6	0.25	-0.17	-0.17	-0.38	2.67				
AT5G10760	A_95_P029251	XM_016599114.1	Q9LEW3	0.25	-0.17	-0.17	-0.38	2.67				
AT1G09750	A_95_P029251	XM_016599114.1	O04496	0.25	-0.17	-0.17	-0.38	2.67				
AT1G65240	A_95_P029251	XM_016599114.1	Q9S9K4	0.25	-0.17	-0.17	-0.38	2.67				
AT2G43570	A_95_P183827	XM_016599207.1	O24603	1.58	2.56	1.29	3.05	4.40				3.00
AT2G43620	A_95_P183827	XM_016599207.1	O22841	1.58	2.56	1.29	3.05	4.40				3.00
AT2G41430	A_95_P000576	XM_016599397.1	Q39096	0.62	-0.06	0.65	0.43					1.68
AT4G14270	A_95_P000576	XM_016599397.1	Q94AR4	0.62	-0.06	0.65	0.43					1.68
AT4G25500	A_95_P289258	XM_016599807.1	P92965	0.29	-0.62	0.18	-0.38					1.18
AT3G61860	A_95_P289258	XM_016599807.1	P92964	0.29	-0.62	0.18	-0.38					1.18
AT5G26220	A_95_P189832	XM_016599844.1	Q8GY54	-0.67	-1.51	-1.09	-1.43			-1.02		
AT4G31290	A_95_P189832	XM_016599844.1	Q84MC1	-0.67	-1.51	-1.09	-1.43			-1.02		
AT1G44790	A_95_P189832	XM_016599844.1	Q84QC1	-0.67	-1.51	-1.09	-1.43			-1.02		
AT3G08640	A_95_P230404	XM_016599999.1	Q9C9Z2	0.18	1.30	0.70	1.66					0.93
AT5G12470	A_95_P230404	XM_016599999.1	Q94CJ5	0.18	1.30	0.70	1.66					0.93
AT2G37860	A_95_P230404	XM_016599999.1	B9DFK5	0.18	1.30	0.70	1.66					0.93
AT2G40400	A_95_P230404	XM_016599999.1	Q9SIY5	0.18	1.30	0.70	1.66					0.93
AT5G04930	A_95_P122077	XM_016600010.1	P98204	0.38	0.30	0.39	1.04	0.95				1.37
AT3G25610	A_95_P122077	XM_016600010.1	Q9LI83	0.38	0.30	0.39	1.04	0.95				1.37
AT1G68710	A_95_P122077	XM_016600010.1	Q9SX33	0.38	0.30	0.39	1.04	0.95				1.37
AT2G29440	A_95_P248322	XM_016600181.1	Q9ZW26	0.91	0.19	0.69	0.04			-1.41		2.99
AT1G78340	A_95_P248322	XM_016600181.1	Q8GYM1	0.91	0.19	0.69	0.04			-1.41		2.99
AT5G67190	A_95_P204502	XM_016600225.1	Q9FH94	-0.62	-0.01	-0.64	0.03			0.92		
AT3G50260	A_95_P204502	XM_016600225.1	Q9SNE1	-0.62	-0.01	-0.64	0.03			0.92		
AT4G36900	A_95_P204502	XM_016600225.1	Q9SW63	-0.62	-0.01	-0.64	0.03			0.92		
AT1G46768	A_95_P204502	XM_016600225.1	Q8LC30	-0.62	-0.01	-0.64	0.03			0.92		
AT4G06746	A_95_P204502	XM_016600225.1	Q8W3M3	-0.62	-0.01	-0.64	0.03			0.92		
AT4G28140	A_95_P204502	XM_016600225.1	Q9M0J3	-0.62	-0.01	-0.64	0.03			0.92		
AT1G21910	A_95_P204502	XM_016600225.1	Q9SFE4	-0.62	-0.01	-0.64	0.03			0.92		
AT1G74930	A_95_P204502	XM_016600225.1	Q9S7L5	-0.62	-0.01	-0.64	0.03			0.92		

Arabidopsis and tobacco identifiers				WT tobacco		VviPGIP1-tobacco		Primed *Arabidopsis*	Primed and infected *Arabidopsis*		*B. cinerea* infected *Arabidopsis*	
Locus Identifier Arabidopsis	Agilent microarray probe	Tobacco GenBank Accession	Tobacco UNIPROT ID	Δt0-24	Δt0-48	Δt0-24	Δt0-48	ISR-prime 2dpTi	ISR-boost 1dpi	ISR-boost 2dpi	BIDR 1dpi	BIDR 2dpi
AT1G19210	A_95_P204502	XM_016600225.1	Q84QC2	-0.62	-0.01	-0.64	0.03			0.92		
AT5G11590	A_95_P204502	XM_016600225.1	Q9LYD3	-0.62	-0.01	-0.64	0.03			0.92		
AT2G20880	A_95_P204502	XM_016600225.1	Q9SKT1	-0.62	-0.01	-0.64	0.03			0.92		
AT5G21960	A_95_P204502	XM_016600225.1	Q9C591	-0.62	-0.01	-0.64	0.03			0.92		
AT3G21670	A_95_P229534	XM_016600247.1	Q9LVE0	-0.62	-0.04	-0.27	-0.14					-1.06
AT1G12110	A_95_P229534	XM_016600247.1	Q05085	-0.62	-0.04	-0.27	-0.14					-1.06
AT1G62200	A_95_P229534	XM_016600247.1	Q93Z20	-0.62	-0.04	-0.27	-0.14					-1.06
AT1G59740	A_95_P229534	XM_016600247.1	Q93VV5	-0.62	-0.04	-0.27	-0.14					-1.06
AT1G68570	A_95_P229534	XM_016600247.1	Q9SX20	-0.62	-0.04	-0.27	-0.14					-1.06
AT5G46050	A_95_P229534	XM_016600247.1	Q9FNL7	-0.62	-0.04	-0.27	-0.14					-1.06
AT1G32450	A_95_P229534	XM_016600247.1	Q9LQL2	-0.62	-0.04	-0.27	-0.14					-1.06
AT5G13400	A_95_P229534	XM_016600247.1	Q9LYR6	-0.62	-0.04	-0.27	-0.14					-1.06
AT5G18670	A_95_P024336	XM_016600901.1	Q8VYW2	1.45	1.34	1.10	1.54				1.75	-2.08
AT4G17090	A_95_P024336	XM_016600901.1	O23553	1.45	1.34	1.10	1.54				1.75	-2.08
AT4G00490	A_95_P024336	XM_016600901.1	O65258	1.45	1.34	1.10	1.54				1.75	-2.08
AT4G15210	A_95_P024336	XM_016600901.1	P25853	1.45	1.34	1.10	1.54				1.75	-2.08
AT1G02280	A_95_P200122	XM_016601032.1	O23680	-0.18	0.01	-0.01	0.07				-1.25	
AT4G02510	A_95_P200122	XM_016601032.1	O81283	-0.18	0.01	-0.01	0.07				-1.25	
AT3G46010	A_95_P017976	XM_016601092.1	Q39250	0.41	1.04	0.54	1.40				-0.89	
AT5G52360	A_95_P017976	XM_016601092.1	Q8LFH6	0.41	1.04	0.54	1.40				-0.89	
AT2G24540	A_95_P204207	XM_016601374.1	Q8LAW2	-0.22	-1.22	-0.43	-1.64					-2.95
AT1G55270	A_95_P204207	XM_016601374.1	Q93W93	-0.22	-1.22	-0.43	-1.64					-2.95
AT1G67480	A_95_P204207	XM_016601374.1	Q9CAG8	-0.22	-1.22	-0.43	-1.64					-2.95
AT3G63220	A_95_P204207	XM_016601374.1	Q9M1W7	-0.22	-1.22	-0.43	-1.64					-2.95
AT3G57280	A_95_P291038	XM_016601530.1	Q93V66	0.94	1.90	0.93	2.06					1.32
AT3G20510	A_95_P291038	XM_016601530.1	Q9LJU6	0.94	1.90	0.93	2.06					1.32
AT1G50740	A_95_P291038	XM_016601530.1	Q9C6T7	0.94	1.90	0.93	2.06					1.32
AT2G38550	A_95_P291038	XM_016601530.1	Q9ZVH7	0.94	1.90	0.93	2.06					1.32
AT5G49450	A_95_P026351	XM_016601705.1	Q9FGX2	0.43	1.65	0.81	1.76	-1.36				
AT5G24800	A_95_P026351	XM_016601705.1	Q9FUD3	0.43	1.65	0.81	1.76	-1.36				
AT2G17130	A_95_P187457	XM_016601918.1	P93032	-0.03	0.00	0.15	0.15					1.23
AT5G03290	A_95_P187457	XM_016601918.1	Q945K7	-0.03	0.00	0.15	0.15					1.23
AT5G15600	A_95_P185818	XM_016602331.1	Q9LF22	-0.12	-0.94	-0.76	-1.09					-2.92
AT4G23496	A_95_P185818	XM_016602331.1	Q8LGD1	-0.12	-0.94	-0.76	-1.09					-2.92
AT5G20250	A_95_P272416	XM_016602363.1	Q8RX87	-1.03	-1.18	-0.29	-1.32	-1.99			1.08	2.32
AT3G57520	A_95_P272416	XM_016602363.1	Q94A08	-1.03	-1.18	-0.29	-1.32	-1.99			1.08	2.32
AT5G40390	A_95_P272416	XM_016602363.1	Q9FND9	-1.03	-1.18	-0.29	-1.32	-1.99			1.08	2.32
AT3G22420	A_95_P076650	XM_016602523.1	Q8S8Y9	0.03	-0.94	-0.07	-1.03					-1.03
AT3G18750	A_95_P076650	XM_016602523.1	Q8S8Y8	0.03	-0.94	-0.07	-1.03					-1.03
AT5G58350	A_95_P076650	XM_016602523.1	Q9LVL5	0.03	-0.94	-0.07	-1.03					-1.03
AT4G23920	A_95_P194092	XM_016602710.1	Q9T0A7	-1.36	-1.94	-0.42	-2.18					0.94
AT4G10960	A_95_P194092	XM_016602710.1	Q9SN58	-1.36	-1.94	-0.42	-2.18					0.94
AT4G05020	A_95_P097858	XM_016602755.1	Q94BV7	2.59	2.68	2.38	3.38	1.81		-1.32	0.91	2.11

Arabidopsis and tobacco identifiers				WT tobacco		VviPGIP1-tobacco		Primed *Arabidopsis*	Primed and infected *Arabidopsis*		*B. cinerea* infected *Arabidopsis*	
Locus Identifier Arabidopsis	Agilent microarray probe	Tobacco GenBank Accession	Tobacco UNIPROT ID	Δt0-24	Δt0-48	Δt0-24	Δt0-48	ISR-prime 2dpTi	ISR-boost 1dpi	ISR-boost 2dpi	BIDR 1dpi	BIDR 2dpi
AT1G07180	A_95_P097858	XM_016602755.1	Q8GWA1	2.59	2.68	2.38	3.38	1.81		-1.32	0.91	2.11
AT2G29990	A_95_P097858	XM_016602755.1	O80874	2.59	2.68	2.38	3.38	1.81		-1.32	0.91	2.11
AT1G79600	A_95_P151192	XM_016602908.1	Q9MA15	0.36	-0.67	-0.25	-0.81					-0.91
AT1G71810	A_95_P151192	XM_016602908.1	Q94BU1	0.36	-0.67	-0.25	-0.81					-0.91
AT4G31390	A_95_P151192	XM_016602908.1	Q8RWG1	0.36	-0.67	-0.25	-0.81					-0.91
AT3G53790	A_95_P225292	XM_016603733.1	Q9M347	-0.01	-0.32	-0.10	-0.15					1.72
AT5G59430	A_95_P225292	XM_016603733.1	Q8L7L8	-0.01	-0.32	-0.10	-0.15					1.72
AT4G31970	A_95_P154587	XM_016603885.1	O49394	2.64	3.35	2.54	3.55			-2.63		3.14
AT3G25180	A_95_P154587	XM_016603885.1	Q9LSF8	2.64	3.35	2.54	3.55			-2.63		3.14
AT2G26080	A_95_P247197	XM_016603969.1	O80988	0.12	0.06	-0.69	-0.36				1.78	-1.89
AT4G33010	A_95_P247197	XM_016603969.1	Q94B78	0.12	0.06	-0.69	-0.36				1.78	-1.89
AT2G37790	A_95_P211337	XM_016604034.1	Q84TF0	-0.42	-0.89	-0.40	-0.86					-0.92
AT2G37770	A_95_P211337	XM_016604034.1	Q0PGJ6	-0.42	-0.89	-0.40	-0.86					-0.92
AT4G13710	A_95_P117527	XM_016604443.1	Q944R1	0.28	-0.49	0.32	-0.23					-0.98
AT4G13210	A_95_P117527	XM_016604443.1	Q9SVQ6	0.28	-0.49	0.32	-0.23					-0.98
AT1G67750	A_95_P117527	XM_016604443.1	Q9FXD8	0.28	-0.49	0.32	-0.23					-0.98
AT4G24780	A_95_P117527	XM_016604443.1	Q9C5M8	0.28	-0.49	0.32	-0.23					-0.98
AT3G53190	A_95_P117527	XM_016604443.1	Q9SCP2	0.28	-0.49	0.32	-0.23					-0.98
AT3G54920	A_95_P117527	XM_016604443.1	Q93Z04	0.28	-0.49	0.32	-0.23					-0.98
AT2G34460	A_95_P008316	XM_016604720.1	Q8H124	-0.25	-1.56	-0.71	-1.84					-0.98
AT3G18890	A_95_P008316	XM_016604720.1	Q8H0U5	-0.25	-1.56	-0.71	-1.84					-0.98
AT3G53700	A_95_P264866	XM_016604851.1	Q9LFF1	-0.20	-0.89	-0.03	-0.97					-1.01
AT1G62670	A_95_P264866	XM_016604851.1	Q9SXD1	-0.20	-0.89	-0.03	-0.97					-1.01
AT2G28260	A_95_P253709	XM_016605087.1	Q9SL29	-0.18	-1.12	-0.03	-1.28				1.06	
AT1G01340	A_95_P253709	XM_016605087.1	Q9LNJ0	-0.18	-1.12	-0.03	-1.28				1.06	
AT1G03870	A_95_P196257	XM_016605093.1	Q9ZWA8	-0.47	-1.09	-0.36	-1.60	-0.96				
AT5G03170	A_95_P196257	XM_016605093.1	Q8LEJ6	-0.47	-1.09	-0.36	-1.60	-0.96				
AT2G04780	A_95_P196257	XM_016605093.1	Q9SJ81	-0.47	-1.09	-0.36	-1.60	-0.96				
AT3G46550	A_95_P196257	XM_016605093.1	Q9SNC3	-0.47	-1.09	-0.36	-1.60	-0.96				
AT2G45470	A_95_P196257	XM_016605093.1	O22126	-0.47	-1.09	-0.36	-1.60	-0.96				
AT4G12730	A_95_P196257	XM_016605093.1	Q9SU13	-0.47	-1.09	-0.36	-1.60	-0.96				
AT2G41410	A_95_P135457	XM_016605181.1	P30188	-0.27	1.03	0.01	0.65	1.19			0.85	
AT3G59440	A_95_P135457	XM_016605181.1	Q9LX27	-0.27	1.03	0.01	0.65	1.19			0.85	
AT1G73630	A_95_P135457	XM_016605181.1	Q9C9U8	-0.27	1.03	0.01	0.65	1.19			0.85	
AT1G06620	A_95_P134592	XM_016605403.1	Q84MB3	0.79	2.61	0.98	2.76					4.67
AT1G03410	A_95_P134592	XM_016605403.1	Q43383	0.79	2.61	0.98	2.76					4.67
AT5G59530	A_95_P134592	XM_016605403.1	Q9LTH8	0.79	2.61	0.98	2.76					4.67
AT5G59540	A_95_P134592	XM_016605403.1	Q9LTH7	0.79	2.61	0.98	2.76					4.67
AT1G06640	A_95_P134592	XM_016605403.1	Q9C5K7	0.79	2.61	0.98	2.76					4.67
AT1G04350	A_95_P134592	XM_016605403.1	P93824	0.79	2.61	0.98	2.76					4.67
AT1G04750	A_95_P292098	XM_016605505.1	Q9ZTW3	-0.17	-0.84	-0.22	-1.09				-1.05	1.19
AT2G32670	A_95_P292098	XM_016605505.1	O48850	-0.17	-0.84	-0.22	-1.09				-1.05	1.19
AT2G33110	A_95_P292098	XM_016605505.1	Q8VY69	-0.17	-0.84	-0.22	-1.09				-1.05	1.19

Arabidopsis and tobacco identifiers				WT tobacco		VviPGIP1-tobacco		Primed *Arabidopsis*	Primed and infected *Arabidopsis*		*B. cinerea* infected *Arabidopsis*	
Locus Identifier Arabidopsis	Agilent microarray probe	Tobacco GenBank Accession	Tobacco UNIPROT ID	Δt0-24	Δt0-48	Δt0-24	Δt0-48	ISR-prime 2dpTi	ISR-boost 1dpi	ISR-boost 2dpi	BIDR 1dpi	BIDR 2dpi
AT5G11150	A_95_P292098	XM_016605505.1	Q9LFP1	-0.17	-0.84	-0.22	-1.09				-1.05	1.19
AT1G42550	A_95_P121192	XM_016605685.1	Q9C8E6	-0.42	-0.76	-0.12	-0.76					-1.01
AT5G20610	A_95_P121192	XM_016605685.1	F4K5K6	-0.42	-0.76	-0.12	-0.76					-1.01
AT5G54490	A_95_P121297	XM_016605960.1	Q9LSQ6	0.29	-0.40	-0.42	-0.64	1.24				
AT2G46600	A_95_P121297	XM_016605960.1	Q9ZPX9	0.29	-0.40	-0.42	-0.64	1.24				
AT2G21660	A_95_P106807	XM_016606050.1	Q03250	0.39	-0.14	0.40	0.37				-5.11	
AT4G13850	A_95_P106807	XM_016606050.1	Q9SVM8	0.39	-0.14	0.40	0.37				-5.11	
AT5G64080	A_95_P144422	XM_016606364.1	Q8VYI9	-0.54	-0.18	0.73	-0.18					-1.34
AT2G13820	A_95_P144422	XM_016606364.1	Q9ZQI8	-0.54	-0.18	0.73	-0.18					-1.34
AT2G27130	A_95_P144422	XM_016606364.1	Q9ZVC7	-0.54	-0.18	0.73	-0.18					-1.34
AT3G09650	A_95_P279608	XM_016606458.1	Q9SF38	-0.17	-1.22	-0.09	-1.43					-1.04
AT1G03100	A_95_P279608	XM_016606458.1	Q9SA60	-0.17	-1.22	-0.09	-1.43					-1.04
AT1G02205	A_95_P202072	XM_016606668.1	F4HVY0	0.26	-1.32	0.10	-1.47	-1.80			-2.98	-3.58
AT1G02190	A_95_P202072	XM_016606668.1	F4HVX7	0.26	-1.32	0.10	-1.47	-1.80			-2.98	-3.58
AT3G21240	A_95_P000646	XM_016606706.1	Q9S725	2.81	4.24	2.78	4.59					0.86
AT1G65060	A_95_P000646	XM_016606706.1	Q9S777	2.81	4.24	2.78	4.59					0.86
AT1G58200	A_95_P138462	XM_016606930.1	Q8L7W1	-0.07	-0.38	0.19	-0.18					1.32
AT4G00290	A_95_P138462	XM_016606930.1	Q8VZL4	-0.07	-0.38	0.19	-0.18					1.32
AT1G80110	A_95_P026141	XM_016606946.1	Q949S5	-0.06	2.11	0.65	3.90					1.10
AT1G56240	A_95_P026141	XM_016606946.1	Q9C7J9	-0.06	2.11	0.65	3.90					1.10
AT1G56250	A_95_P026141	XM_016606946.1	Q9C7K0	-0.06	2.11	0.65	3.90					1.10
AT2G02340	A_95_P026141	XM_016606946.1	Q9ZVQ8	-0.06	2.11	0.65	3.90					1.10
AT1G65390	A_95_P026141	XM_016606946.1	Q9C5Q9	-0.06	2.11	0.65	3.90					1.10
AT2G02310	A_95_P026141	XM_016606946.1	Q9ZVR0	-0.06	2.11	0.65	3.90					1.10
AT3G60190	A_95_P210997	XM_016607079.1	Q9FNX5	0.19	0.56	0.49	1.01				-1.56	1.63
AT2G44590	A_95_P210997	XM_016607079.1	Q8S3C9	0.19	0.56	0.49	1.01				-1.56	1.63
AT3G61760	A_95_P210997	XM_016607079.1	Q84XF3	0.19	0.56	0.49	1.01				-1.56	1.63
AT4G29840	A_95_P088588	XM_016607324.1	Q9S7B5	0.12	0.60	0.06	0.65				-1.32	
AT1G72810	A_95_P088588	XM_016607324.1	Q9SSP5	0.12	0.60	0.06	0.65				-1.32	
AT2G30520	A_95_P194728	XM_016607706.1	Q682S0	-0.02	-0.91	-0.17	-1.20					-1.13
AT5G67385	A_95_P194728	XM_016607706.1	Q66GP0	-0.02	-0.91	-0.17	-1.20					-1.13
AT3G50840	A_95_P194728	XM_016607706.1	Q8LPQ3	-0.02	-0.91	-0.17	-1.20					-1.13
AT2G15480	A_95_P134427	XM_016608279.1	Q9ZQG4	0.66	-0.14	0.07	-0.36	1.27				3.13
AT2G15490	A_95_P134427	XM_016608279.1	Q7Y232	0.66	-0.14	0.07	-0.36	1.27				3.13
AT2G36780	A_95_P134427	XM_016608279.1	Q9ZQ96	0.66	-0.14	0.07	-0.36	1.27				3.13
AT3G53160	A_95_P134427	XM_016608279.1	Q9SCP5	0.66	-0.14	0.07	-0.36	1.27				3.13
AT2G36770	A_95_P134427	XM_016608279.1	Q9ZQ97	0.66	-0.14	0.07	-0.36	1.27				3.13
AT4G34131	A_95_P134427	XM_016608279.1	Q8W491	0.66	-0.14	0.07	-0.36	1.27				3.13
AT4G34138	A_95_P134427	XM_016608279.1	Q8VZE9	0.66	-0.14	0.07	-0.36	1.27				3.13
AT5G61480	A_95_P131992	XM_016608771.1	Q9FII5	0.61	-0.58	0.19	-0.67					-0.94
AT5G02800	A_95_P131992	XM_016608771.1	Q0WRY5	0.61	-0.58	0.19	-0.67					-0.94
AT1G64710	A_95_P150027	XM_016608977.1	Q8VZ49	0.93	0.51	0.26	0.79	1.14				1.56
AT1G32780	A_95_P150027	XM_016608977.1	A1L4Y2	0.93	0.51	0.26	0.79	1.14				1.56

Arabidopsis and tobacco identifiers				WT tobacco		VviPGIP1-tobacco		Primed *Arabidopsis*	Primed and infected *Arabidopsis*		*B. cinerea* infected *Arabidopsis*	
Locus Identifier Arabidopsis	Agilent microarray probe	Tobacco GenBank Accession	Tobacco UNIPROT ID	Δt0-24	Δt0-48	Δt0-24	Δt0-48	ISR-prime 2dpTi	ISR-boost 1dpi	ISR-boost 2dpi	BIDR 1dpi	BIDR 2dpi
AT1G26420	A_95_P101448	XM_016609045.1	Q9FZC8	1.21	3.00	1.61	3.03	1.86				4.44
AT1G26380	A_95_P101448	XM_016609045.1	Q9FZC4	1.21	3.00	1.61	3.03	1.86				4.44
AT1G26390	A_95_P101448	XM_016609045.1	Q9FZC5	1.21	3.00	1.61	3.03	1.86				4.44
AT1G26410	A_95_P101448	XM_016609045.1	Q9FZC7	1.21	3.00	1.61	3.03	1.86				4.44
AT4G20830	A_95_P101448	XM_016609045.1	Q9SVG4	1.21	3.00	1.61	3.03	1.86				4.44
AT2G34720	A_95_P214337	XM_016609156.1	Q8VY64	0.11	-1.00	-0.49	-1.40				1.25	
AT5G12840	A_95_P214337	XM_016609156.1	Q9LXV5	0.11	-1.00	-0.49	-1.40				1.25	
AT1G17590	A_95_P214337	XM_016609156.1	Q9LNP6	0.11	-1.00	-0.49	-1.40				1.25	
AT4G34200	A_95_P189662	XM_016609482.1	O49485	0.34	0.16	0.59	1.15					2.05
AT3G19480	A_95_P189662	XM_016609482.1	Q9LT69	0.34	0.16	0.59	1.15					2.05
AT1G17745	A_95_P189662	XM_016609482.1	O04130	0.34	0.16	0.59	1.15					2.05
AT1G13250	A_95_P069760	XM_016610267.1	Q0V7R1	-0.30	-0.56	-0.47	-0.79				0.88	-0.99
AT3G28340	A_95_P069760	XM_016610267.1	Q9LHD2	-0.30	-0.56	-0.47	-0.79				0.88	-0.99
AT1G19300	A_95_P069760	XM_016610267.1	Q9LN68	-0.30	-0.56	-0.47	-0.79				0.88	-0.99
AT3G50760	A_95_P069760	XM_016610267.1	Q9S7G2	-0.30	-0.56	-0.47	-0.79				0.88	-0.99
AT3G01040	A_95_P069760	XM_016610267.1	Q0WV13	-0.30	-0.56	-0.47	-0.79				0.88	-0.99
AT5G04660	A_95_P131967	XM_016610653.1	Q9LZ31	-0.15	0.01	-0.20	-0.17					-2.22
AT3G03470	A_95_P131967	XM_016610653.1	Q9SRQ1	-0.15	0.01	-0.20	-0.17					-2.22
AT3G48280	A_95_P131967	XM_016610653.1	Q9STK8	-0.15	0.01	-0.20	-0.17					-2.22
AT4G27030	A_95_P206522	XM_016610722.1	Q9SZ42	-0.04	0.36	0.07	0.24					-1.93
AT2G22890	A_95_P206522	XM_016610722.1	O81006	-0.04	0.36	0.07	0.24					-1.93
AT2G37430	A_95_P305928	XM_016610816.1	Q9SLD4	1.56	0.51	1.10	0.92			-2.55		3.52
AT3G46080	A_95_P305928	XM_016610816.1	Q9LX85	1.56	0.51	1.10	0.92			-2.55		3.52
AT5G59820	A_95_P305928	XM_016610816.1	Q42410	1.56	0.51	1.10	0.92			-2.55		3.52
AT3G46090	A_95_P305928	XM_016610816.1	Q42453	1.56	0.51	1.10	0.92			-2.55		3.52
AT2G28200	A_95_P305928	XM_016610816.1	Q681X4	1.56	0.51	1.10	0.92			-2.55		3.52
AT5G43170	A_95_P305928	XM_016610816.1	Q9SSW0	1.56	0.51	1.10	0.92			-2.55		3.52
AT3G19580	A_95_P305928	XM_016610816.1	Q9SSW2	1.56	0.51	1.10	0.92			-2.55		3.52
AT5G67450	A_95_P305928	XM_016610816.1	Q9SSW1	1.56	0.51	1.10	0.92			-2.55		3.52
AT1G27730	A_95_P305928	XM_016610816.1	Q96289	1.56	0.51	1.10	0.92			-2.55		3.52
AT5G04340	A_95_P305928	XM_016610816.1	O22533	1.56	0.51	1.10	0.92			-2.55		3.52
AT3G50700	A_95_P103922	XM_016611036.1	Q9SCQ6	-0.27	-1.25	-0.20	-1.36				-2.97	2.03
AT1G03840	A_95_P103922	XM_016611036.1	Q9ZWA6	-0.27	-1.25	-0.20	-1.36				-2.97	2.03
AT4G02670	A_95_P103922	XM_016611036.1	O22759	-0.27	-1.25	-0.20	-1.36				-2.97	2.03
AT1G55110	A_95_P103922	XM_016611036.1	Q8H1F5	-0.27	-1.25	-0.20	-1.36				-2.97	2.03
AT4G34220	A_95_P267611	XM_016611269.1	Q94C77	0.58	0.06	-0.09	0.03					-1.03
AT1G48480	A_95_P267611	XM_016611269.1	Q9LP77	0.58	0.06	-0.09	0.03					-1.03
AT2G26730	A_95_P267611	XM_016611269.1	O48788	0.58	0.06	-0.09	0.03					-1.03
AT2G36570	A_95_P267611	XM_016611269.1	Q9SJQ1	0.58	0.06	-0.09	0.03					-1.03
AT5G67200	A_95_P267611	XM_016611269.1	Q93Y06	0.58	0.06	-0.09	0.03					-1.03
AT1G68400	A_95_P267611	XM_016611269.1	Q9M9C5	0.58	0.06	-0.09	0.03					-1.03
AT3G08680	A_95_P267611	XM_016611269.1	Q9C9Y8	0.58	0.06	-0.09	0.03					-1.03
AT4G35180	A_95_P199632	XM_016612076.1	Q84WE9	1.06	2.49	0.86	2.15	3.83		-0.96		3.70

Arabidopsis and tobacco identifiers				WT tobacco		VviPGIP1-tobacco		Primed *Arabidopsis*	Primed and infected *Arabidopsis*		*B. cinerea* infected *Arabidopsis*	
Locus Identifier Arabidopsis	Agilent microarray probe	Tobacco GenBank Accession	Tobacco UNIPROT ID	Δt0-24	Δt0-48	Δt0-24	Δt0-48	ISR-prime 2dpTi	ISR-boost 1dpi	ISR-boost 2dpi	BIDR 1dpi	BIDR 2dpi
AT5G41800	A_95_P199632	XM_016612076.1	Q8L4X4	1.06	2.49	0.86	2.15	3.83		-0.96		3.70
AT1G20510	A_95_P021221	XM_016612245.1	Q84P21	0.93	1.79	0.92	2.12			-1.00		3.01
AT1G20490	A_95_P021221	XM_016612245.1	Q3E6Y4	0.93	1.79	0.92	2.12			-1.00		3.01
AT5G38120	A_95_P021221	XM_016612245.1	Q84P26	0.93	1.79	0.92	2.12			-1.00		3.01
AT4G38400	A_95_P225342	XM_016612308.1	Q9SVE5	0.37	2.18	0.80	2.23	-1.00				-1.01
AT3G45960	A_95_P225342	XM_016612308.1	Q9LZT5	0.37	2.18	0.80	2.23	-1.00				-1.01
AT3G45970	A_95_P225342	XM_016612308.1	Q9LZT4	0.37	2.18	0.80	2.23	-1.00				-1.01
AT4G28250	A_95_P225342	XM_016612308.1	Q9M0I2	0.37	2.18	0.80	2.23	-1.00				-1.01
AT1G11130	A_95_P118872	XM_016612659.1	Q8RWZ1	0.04	-0.38	-0.12	-0.60					-1.32
AT2G20850	A_95_P118872	XM_016612659.1	Q06BH3	0.04	-0.38	-0.12	-0.60					-1.32
AT3G59350	A_95_P118872	XM_016612659.1	B9DFG5	0.04	-0.38	-0.12	-0.60					-1.32
AT1G75040	A_95_P193372	XM_016612759.1	P28493	-0.40	-0.22	-0.23	-0.22	2.74				1.06
AT1G18250	A_95_P193372	XM_016612759.1	P50699	-0.40	-0.22	-0.23	-0.22	2.74				1.06
AT5G23660	A_95_P226219	XM_016612876.1	O82587	-0.29	-1.64	-0.09	-1.74					2.40
AT5G50800	A_95_P226219	XM_016612876.1	Q9FGQ2	-0.29	-1.64	-0.09	-1.74					2.40
AT2G26900	A_95_P132367	XM_016613140.1	Q1EBV7	-0.03	-0.64	-0.17	-0.74				-1.13	
AT3G25410	A_95_P132367	XM_016613140.1	Q8RXE8	-0.03	-0.64	-0.17	-0.74				-1.13	
AT4G12030	A_95_P132367	XM_016613140.1	F4JPW1	-0.03	-0.64	-0.17	-0.74				-1.13	
AT4G22840	A_95_P132367	XM_016613140.1	Q8VYY4	-0.03	-0.64	-0.17	-0.74				-1.13	
AT5G24270	A_95_P139762	XM_016613930.1	O81223	-0.17	-0.22	1.00	-0.42					2.26
AT4G17615	A_95_P139762	XM_016613930.1	O81445	-0.17	-0.22	1.00	-0.42					2.26
AT4G19230	A_95_P151467	XM_016614025.1	Q949P1	0.10	-1.09	0.08	-1.00					1.17
AT5G45340	A_95_P151467	XM_016614025.1	Q9FH76	0.10	-1.09	0.08	-1.00					1.17
AT3G01550	A_95_P218802	XM_016614094.1	Q8H0T6	0.18	1.56	0.52	1.71					-1.97
AT5G17630	A_95_P218802	XM_016614094.1	Q9LF61	0.18	1.56	0.52	1.71					-1.97
AT1G61800	A_95_P218802	XM_016614094.1	Q94B38	0.18	1.56	0.52	1.71					-1.97
AT5G66880	A_95_P125357	XM_016614247.1	Q39193	-0.49	-1.06	-0.30	-1.06					1.37
AT3G50500	A_95_P125357	XM_016614247.1	Q39192	-0.49	-1.06	-0.30	-1.06					1.37
AT5G63650	A_95_P125357	XM_016614247.1	Q9FFP9	-0.49	-1.06	-0.30	-1.06					1.37
AT5G22740	A_95_P187022	XM_016614587.1	Q9FNI7	0.28	-0.47	0.04	-0.45				1.11	
AT5G03760	A_95_P187022	XM_016614587.1	Q9LZR3	0.28	-0.47	0.04	-0.45				1.11	
AT1G23480	A_95_P187022	XM_016614587.1	Q9LQC9	0.28	-0.47	0.04	-0.45				1.11	
AT1G24070	A_95_P187022	XM_016614587.1	Q9LR87	0.28	-0.47	0.04	-0.45				1.11	
AT2G26510	A_95_P153792	XM_016615036.1	Q8GZD4	-0.29	-1.06	-0.14	-1.12					1.03
AT2G27810	A_95_P153792	XM_016615036.1	Q3E7D0	-0.29	-1.06	-0.14	-1.12					1.03
AT5G49740	A_95_P131032	XM_016615157.1	Q3KTM0	0.49	-0.74	-0.06	-1.12					-1.95
AT1G01580	A_95_P131032	XM_016615157.1	P92949	0.49	-0.74	-0.06	-1.12					-1.95
AT1G01590	A_95_P131032	XM_016615157.1	Q9LMM2	0.49	-0.74	-0.06	-1.12					-1.95
AT5G23980	A_95_P131032	XM_016615157.1	Q8W110	0.49	-0.74	-0.06	-1.12					-1.95
AT1G23020	A_95_P131032	XM_016615157.1	F4I4K7	0.49	-0.74	-0.06	-1.12					-1.95
AT1G64060	A_95_P131032	XM_016615157.1	O48538	0.49	-0.74	-0.06	-1.12					-1.95
AT1G30410	A_95_P198112	XM_016615378.1	Q9C8H0	0.69	1.39	1.01	1.93	1.00				
AT1G30420	A_95_P198112	XM_016615378.1	Q9C8H1	0.69	1.39	1.01	1.93	1.00				

Arabidopsis and tobacco identifiers				WT tobacco		VviPGIP1-tobacco		Primed *Arabidopsis*	Primed and infected *Arabidopsis*		*B. cinerea* infected *Arabidopsis*	
Locus Identifier Arabidopsis	Agilent microarray probe	Tobacco GenBank Accession	Tobacco UNIPROT ID	Δt0-24	Δt0-48	Δt0-24	Δt0-48	ISR-prime 2dpTi	ISR-boost 1dpi	ISR-boost 2dpi	BIDR 1dpi	BIDR 2dpi
AT2G22660	A_95_P254204	XM_016615653.1	Q9ZQ47	-0.97	-0.60	0.61	-0.76	1.60				1.32
AT4G37900	A_95_P254204	XM_016615653.1	Q9SZJ2	-0.97	-0.60	0.61	-0.76	1.60				1.32
AT2G20180	A_95_P029376	XM_016615830.1	Q8GZM7	-0.76	-1.69	-0.38	-1.64	-1.37				-1.26
AT2G46970	A_95_P029376	XM_016615830.1	Q8L5W8	-0.76	-1.69	-0.38	-1.64	-1.37				-1.26
AT5G67110	A_95_P029376	XM_016615830.1	Q9FHA2	-0.76	-1.69	-0.38	-1.64	-1.37				-1.26
AT4G00050	A_95_P029376	XM_016615830.1	Q8GZ38	-0.76	-1.69	-0.38	-1.64	-1.37				-1.26
AT4G30980	A_95_P029376	XM_016615830.1	Q8S3D5	-0.76	-1.69	-0.38	-1.64	-1.37				-1.26
AT3G56710	A_95_P133392	XM_016616102.1	Q9LDH1	-0.12	-0.97	-0.20	-0.94	0.92				2.08
AT2G41180	A_95_P133392	XM_016616102.1	O80669	-0.12	-0.97	-0.20	-0.94	0.92				2.08
AT1G73655	A_95_P267641	XM_016616417.1	Q8LB65	-0.43	-2.18	-0.89	-2.56	-0.86			-1.16	
AT4G25340	A_95_P267641	XM_016616417.1	Q93ZG9	-0.43	-2.18	-0.89	-2.56	-0.86			-1.16	
AT4G19830	A_95_P267641	XM_016616417.1	O81864	-0.43	-2.18	-0.89	-2.56	-0.86			-1.16	
AT2G26400	A_95_P116182	XM_016616463.1	O48707	-0.34	1.29	0.07	1.36	5.95				
AT5G43850	A_95_P116182	XM_016616463.1	Q8H185	-0.34	1.29	0.07	1.36	5.95				
AT1G70460	A_95_P204747	XM_016616594.1	Q9CAL8	-0.58	-1.51	-0.20	-1.40					0.86
AT3G24550	A_95_P204747	XM_016616594.1	Q9LV48	-0.58	-1.51	-0.20	-1.40					0.86
AT1G52290	A_95_P204747	XM_016616594.1	Q9C821	-0.58	-1.51	-0.20	-1.40					0.86
AT5G03270	A_95_P222277	XM_016616854.1	Q9LYV8	-0.06	-1.12	-0.09	-1.03					1.93
AT4G35190	A_95_P222277	XM_016616854.1	Q8LBB7	-0.06	-1.12	-0.09	-1.03					1.93
AT3G05200	A_95_P034903	XM_016617009.1	Q8RXX9	2.28	1.72	1.81	1.75					2.03
AT5G27420	A_95_P034903	XM_016617009.1	Q8LGA5	2.28	1.72	1.81	1.75					2.03
AT1G72200	A_95_P034903	XM_016617009.1	Q84W40	2.28	1.72	1.81	1.75					2.03
AT2G35000	A_95_P034903	XM_016617009.1	O64763	2.28	1.72	1.81	1.75					2.03
AT4G40070	A_95_P034903	XM_016617009.1	Q8W571	2.28	1.72	1.81	1.75					2.03
AT1G66250	A_95_P203102	XM_016617177.1	Q9C7U5	-0.51	-0.84	-0.60	-1.12					-1.42
AT1G11820	A_95_P203102	XM_016617177.1	O65399	-0.51	-0.84	-0.60	-1.12					-1.42
AT5G56590	A_95_P203102	XM_016617177.1	Q9FJU9	-0.51	-0.84	-0.60	-1.12					-1.42
AT2G27500	A_95_P203102	XM_016617177.1	Q9ZQG9	-0.51	-0.84	-0.60	-1.12					-1.42
AT5G42100	A_95_P203102	XM_016617177.1	Q9FHX5	-0.51	-0.84	-0.60	-1.12					-1.42
AT3G16860	A_95_P017016	XM_016617691.1	Q9LIB6	-0.22	-2.12	-0.47	-1.94					1.60
AT3G02210	A_95_P017016	XM_016617691.1	Q9SRT7	-0.22	-2.12	-0.47	-1.94					1.60
AT3G06590	A_95_P153262	XM_016618192.1	Q9C8Z9	-0.06	-1.25	-0.07	-1.09					-0.87
AT1G09250	A_95_P153262	XM_016618192.1	O80482	-0.06	-1.25	-0.07	-1.09					-0.87
AT3G05800	A_95_P153262	XM_016618192.1	Q9M9L6	-0.06	-1.25	-0.07	-1.09					-0.87
AT3G02040	A_95_P264196	XM_016618281.1	Q9SGA2	-0.49	-0.54	-0.42	-0.30	1.40	1.65		0.92	1.44
AT5G41080	A_95_P264196	XM_016618281.1	Q9FLM1	-0.49	-0.54	-0.42	-0.30	1.40	1.65		0.92	1.44
AT1G18650	A_95_P254615	XM_016618352.1	Q9FZ86	0.04	-0.42	-0.29	-0.60	-1.32				-1.36
AT5G61130	A_95_P254615	XM_016618352.1	Q9FNQ2	0.04	-0.42	-0.29	-0.60	-1.32				-1.36
AT3G16857	A_95_P089068	XM_016618413.1	Q940D0	-0.47	-1.32	-0.47	-1.47			0.98	1.04	
AT3G46640	A_95_P089068	XM_016618413.1	Q9SNB4	-0.47	-1.32	-0.47	-1.47			0.98	1.04	
AT5G29000	A_95_P089068	XM_016618413.1	Q8GUN5	-0.47	-1.32	-0.47	-1.47			0.98	1.04	
AT1G12060	A_95_P270711	XM_016619247.1	O65373	2.42	1.34	2.01	1.78					-1.10
AT2G46240	A_95_P270711	XM_016619247.1	O82345	2.42	1.34	2.01	1.78					-1.10

Arabidopsis and tobacco identifiers				WT tobacco		VviPGIP1-tobacco		Primed *Arabidopsis*	Primed and infected *Arabidopsis*		*B. cinerea* infected *Arabidopsis*	
Locus Identifier Arabidopsis	Agilent microarray probe	Tobacco GenBank Accession	Tobacco UNIPROT ID	Δt0-24	Δt0-48	Δt0-24	Δt0-48	ISR-prime 2dpTi	ISR-boost 1dpi	ISR-boost 2dpi	BIDR 1dpi	BIDR 2dpi
AT3G17840	A_95_P261566	XM_016619764.1	Q9LVI6	-0.09	-0.62	0.08	-0.38					-2.23
AT5G16590	A_95_P261566	XM_016619764.1	Q9FMD7	-0.09	-0.62	0.08	-0.38					-2.23
AT3G05880	A_95_P020291	XM_016620287.1	Q9ZNQ7	0.06	0.93	-0.40	0.58				-3.50	
AT4G30650	A_95_P020291	XM_016620287.1	Q9M095	0.06	0.93	-0.40	0.58				-3.50	
AT5G50460	A_95_P021406	XM_016620416.1	P0DI75	0.68	1.22	0.72	1.55					0.98
AT4G24920	A_95_P021406	XM_016620416.1	P0DI74	0.68	1.22	0.72	1.55					0.98
AT3G48570	A_95_P021406	XM_016620416.1	Q9SMP2	0.68	1.22	0.72	1.55					0.98
AT2G40890	A_95_P185547	XM_016620591.1	O22203	2.34	4.51	2.05	4.71				0.87	
AT5G25140	A_95_P185547	XM_016620591.1	P58050	2.34	4.51	2.05	4.71				0.87	
AT3G26310	A_95_P185547	XM_016620591.1	Q9LIP5	2.34	4.51	2.05	4.71				0.87	
AT2G42380	A_95_P124302	XM_016620773.1	F4IN23	0.38	1.00	0.23	0.90	-0.97				
AT3G58120	A_95_P124302	XM_016620773.1	Q9M2K4	0.38	1.00	0.23	0.90	-0.97				
AT5G47070	A_95_P091328	XM_016621055.1	Q9LTC0	0.99	1.06	0.57	2.00	0.91				1.93
AT1G14370	A_95_P091328	XM_016621055.1	O49839	0.99	1.06	0.57	2.00	0.91				1.93
AT1G07570	A_95_P091328	XM_016621055.1	Q06548	0.99	1.06	0.57	2.00	0.91				1.93
AT5G02290	A_95_P091328	XM_016621055.1	P43293	0.99	1.06	0.57	2.00	0.91				1.93
AT2G28930	A_95_P091328	XM_016621055.1	P46573	0.99	1.06	0.57	2.00	0.91				1.93
AT3G55450	A_95_P091328	XM_016621055.1	Q8H186	0.99	1.06	0.57	2.00	0.91				1.93
AT2G39660	A_95_P091328	XM_016621055.1	O48814	0.99	1.06	0.57	2.00	0.91				1.93
AT3G62150	A_95_P197082	XM_016621805.1	Q9M1Q9	0.46	2.06	0.59	2.26				1.90	3.08
AT2G47000	A_95_P197082	XM_016621805.1	O80725	0.46	2.06	0.59	2.26				1.90	3.08
AT4G01820	A_95_P197082	XM_016621805.1	Q9SYI2	0.46	2.06	0.59	2.26				1.90	3.08
AT1G76040	A_95_P192947	XM_016621913.1	Q8RWL2	0.80	0.80	0.44	1.14	2.94		-1.32		2.61
AT4G04740	A_95_P192947	XM_016621913.1	Q9M101	0.80	0.80	0.44	1.14	2.94		-1.32		2.61
AT4G04695	A_95_P192947	XM_016621913.1	Q9S9V0	0.80	0.80	0.44	1.14	2.94		-1.32		2.61
AT1G68190	A_95_P158767	XM_016622471.1	Q9C9F4	-0.84	-1.22	-0.43	-0.94	-1.79				
AT2G31380	A_95_P158767	XM_016622471.1	Q9SID1	-0.84	-1.22	-0.43	-0.94	-1.79				
AT4G18360	A_95_P007766	XM_016622629.1	O49506	-0.14	-2.32	-0.86	-2.64					3.85
AT3G14130	A_95_P007766	XM_016622629.1	Q9LJH5	-0.14	-2.32	-0.86	-2.64					3.85
AT1G53440	A_95_P276193	XM_016622915.1	C0LGG9	0.41	0.30	0.50	0.39			-1.37		2.65
AT1G53430	A_95_P276193	XM_016622915.1	C0LGG8	0.41	0.30	0.50	0.39			-1.37		2.65
AT1G07650	A_95_P276193	XM_016622915.1	C0LGE0	0.41	0.30	0.50	0.39			-1.37		2.65
AT3G14840	A_95_P276193	XM_016622915.1	C0LGN2	0.41	0.30	0.50	0.39			-1.37		2.65
AT1G56130	A_95_P276193	XM_016622915.1	C0LGH2	0.41	0.30	0.50	0.39			-1.37		2.65
AT1G56140	A_95_P276193	XM_016622915.1	C0LGH3	0.41	0.30	0.50	0.39			-1.37		2.65
AT4G00970	A_95_P276193	XM_016622915.1	O23081	0.41	0.30	0.50	0.39			-1.37		2.65
AT4G23190	A_95_P276193	XM_016622915.1	Q9ZP16	0.41	0.30	0.50	0.39			-1.37		2.65
AT1G70530	A_95_P276193	XM_016622915.1	Q9CAL2	0.41	0.30	0.50	0.39			-1.37		2.65
AT4G21390	A_95_P276193	XM_016622915.1	O81906	0.41	0.30	0.50	0.39			-1.37		2.65
AT5G63160	A_95_P059081	XM_016623015.1	Q9FMK7	-0.71	-1.60	-0.01	-1.36		-1.25			1.24
AT3G48360	A_95_P059081	XM_016623015.1	Q94BN0	-0.71	-1.60	-0.01	-1.36		-1.25			1.24
AT5G67480	A_95_P059081	XM_016623015.1	Q9FJX5	-0.71	-1.60	-0.01	-1.36		-1.25			1.24
AT4G37610	A_95_P059081	XM_016623015.1	Q6EJ98	-0.71	-1.60	-0.01	-1.36		-1.25			1.24

Arabidopsis and tobacco identifiers				WT tobacco		VviPGIP1-tobacco		Primed *Arabidopsis*	Primed and infected *Arabidopsis*		*B. cinerea* infected *Arabidopsis*	
Locus Identifier Arabidopsis	Agilent microarray probe	Tobacco GenBank Accession	Tobacco UNIPROT ID	Δt0-24	Δt0-48	Δt0-24	Δt0-48	ISR-prime 2dpTi	ISR-boost 1dpi	ISR-boost 2dpi	BIDR 1dpi	BIDR 2dpi
AT1G66140	A_95_P133517	XM_016623148.1	Q39263	-0.22	-1.03	-0.30	-1.51					-1.47
AT5G57520	A_95_P133517	XM_016623148.1	Q39261	-0.22	-1.03	-0.30	-1.51					-1.47
AT3G58070	A_95_P133517	XM_016623148.1	Q84WI0	-0.22	-1.03	-0.30	-1.51					-1.47
AT1G72330	A_95_P161142	XM_016623249.1	Q9LDV4	1.00	1.94	1.04	2.12					3.82
AT1G17290	A_95_P161142	XM_016623249.1	F4I7I0	1.00	1.94	1.04	2.12					3.82
AT1G70580	A_95_P161142	XM_016623249.1	Q9S7E9	1.00	1.94	1.04	2.12					3.82
AT2G45600	A_95_P144692	XM_016623315.1	O64640	-0.34	-0.97	-0.36	-1.36			1.15		
AT3G63010	A_95_P144692	XM_016623315.1	Q9LYC1	-0.34	-0.97	-0.36	-1.36			1.15		
AT4G19120	A_95_P108037	XM_016623584.1	Q94II3	-0.47	-1.09	-0.14	-0.97				-1.46	
AT1G33170	A_95_P108037	XM_016623584.1	Q9C884	-0.47	-1.09	-0.14	-0.97				-1.46	
AT1G18390	A_95_P124162	XM_016624077.1	P0C5E2	1.89	1.70	1.61	2.08	1.31				3.34
AT1G25390	A_95_P124162	XM_016624077.1	Q9C6K9	1.89	1.70	1.61	2.08	1.31				3.34
AT1G66880	A_95_P124162	XM_016624077.1	F4HQ17	1.89	1.70	1.61	2.08	1.31				3.34
AT5G38210	A_95_P124162	XM_016624077.1	Q8VYG0	1.89	1.70	1.61	2.08	1.31				3.34
AT2G23450	A_95_P124162	XM_016624077.1	Q8RY67	1.89	1.70	1.61	2.08	1.31				3.34
AT5G66790	A_95_P124162	XM_016624077.1	Q8GYF5	1.89	1.70	1.61	2.08	1.31				3.34
AT1G69730	A_95_P124162	XM_016624077.1	Q9C9L5	1.89	1.70	1.61	2.08	1.31				3.34
AT3G25490	A_95_P124162	XM_016624077.1	Q9LSV3	1.89	1.70	1.61	2.08	1.31				3.34
AT1G21240	A_95_P124162	XM_016624077.1	Q9LMN8	1.89	1.70	1.61	2.08	1.31				3.34
AT4G21990	A_95_P134087	XM_016624519.1	P92980	2.80	3.21	1.86	2.96				1.49	
AT4G04610	A_95_P134087	XM_016624519.1	P92979	2.80	3.21	1.86	2.96				1.49	
AT1G62180	A_95_P134087	XM_016624519.1	P92981	2.80	3.21	1.86	2.96				1.49	
AT4G14540	A_95_P149952	XM_016624768.1	O23310	-0.58	-2.64	-1.06	-2.40			0.98		-1.23
AT5G47640	A_95_P149952	XM_016624768.1	Q9FGJ3	-0.58	-2.64	-1.06	-2.40			0.98		-1.23
AT1G69870	A_95_P010556	XM_016625640.1	Q8RX77	-0.32	-0.94	-0.30	-0.97	0.92			-1.05	2.16
AT3G16180	A_95_P010556	XM_016625640.1	Q8LPL2	-0.32	-0.94	-0.30	-0.97	0.92			-1.05	2.16
AT1G18880	A_95_P010556	XM_016625640.1	Q9M9V7	-0.32	-0.94	-0.30	-0.97	0.92			-1.05	2.16
AT4G12420	A_95_P013836	XM_016625815.1	Q9SU40	0.37	-0.25	0.29	0.00	-0.91				
AT2G38080	A_95_P013836	XM_016625815.1	O80434	0.37	-0.25	0.29	0.00	-0.91				
AT5G03260	A_95_P013836	XM_016625815.1	Q8VZA1	0.37	-0.25	0.29	0.00	-0.91				
AT5G51640	A_95_P021576	XM_016625904.1	Q9FHM0	0.39	1.00	0.46	1.20					0.97
AT4G01080	A_95_P021576	XM_016625904.1	O04621	0.39	1.00	0.46	1.20					0.97
AT5G15900	A_95_P021576	XM_016625904.1	Q9LFT0	0.39	1.00	0.46	1.20					0.97
AT1G12420	A_95_P014551	XM_016626050.1	Q9LNA5	0.00	-1.94	-0.30	-1.94	1.02				1.39
AT4G22780	A_95_P014551	XM_016626050.1	Q8LJW1	0.00	-1.94	-0.30	-1.94	1.02				1.39
AT3G06700	A_95_P025201	XM_016626499.1	Q9M7X7	-0.29	0.62	0.31	0.53	-1.05				
AT3G06680	A_95_P025201	XM_016626499.1	Q84WM0	-0.29	0.62	0.31	0.53	-1.05				
AT1G18900	A_95_P293988	XM_016626876.1	Q8GYP6	0.24	-0.43	0.23	-0.25			-1.03		0.95
AT2G18940	A_95_P293988	XM_016626876.1	O64624	0.24	-0.43	0.23	-0.25			-1.03		0.95
AT4G39460	A_95_P209857	XM_016627029.1	Q94AG6	-0.86	-1.64	-0.58	-1.64				-1.21	
AT5G42130	A_95_P209857	XM_016627029.1	Q9FHX2	-0.86	-1.64	-0.58	-1.64				-1.21	
AT1G19360	A_95_P229539	XM_016627158.1	Q9LN62	0.38	0.99	0.38	1.10					1.02
AT4G01750	A_95_P229539	XM_016627158.1	Q9ZSJ0	0.38	0.99	0.38	1.10					1.02

Arabidopsis and tobacco identifiers				WT tobacco		VviPGIP1-tobacco		Primed *Arabidopsis*	Primed and infected *Arabidopsis*		*B. cinerea* infected *Arabidopsis*	
Locus Identifier Arabidopsis	Agilent microarray probe	Tobacco GenBank Accession	Tobacco UNIPROT ID	Δt0-24	Δt0-48	Δt0-24	Δt0-48	ISR-prime 2dpTi	ISR-boost 1dpi	ISR-boost 2dpi	BIDR 1dpi	BIDR 2dpi
AT4G35470	A_95_P020406	XM_016627238.1	Q9SVW8	1.16	0.33	1.02	0.71	-1.43				
AT3G11330	A_95_P020406	XM_016627238.1	Q8VYG9	1.16	0.33	1.02	0.71	-1.43				
AT3G26500	A_95_P020406	XM_016627238.1	Q9LRV8	1.16	0.33	1.02	0.71	-1.43				
AT5G05850	A_95_P020406	XM_016627238.1	Q9FFJ3	1.16	0.33	1.02	0.71	-1.43				
AT4G08850	A_95_P137142	XM_016627263.1	Q8VZG8	0.22	-0.63	-0.08	-0.75	1.07			1.10	1.40
AT3G56370	A_95_P137142	XM_016627263.1	Q9LY03	0.22	-0.63	-0.08	-0.75	1.07			1.10	1.40
AT1G71400	A_95_P137142	XM_016627263.1	Q9C9H7	0.22	-0.63	-0.08	-0.75	1.07			1.10	1.40
AT5G01620	A_95_P216172	XM_016627505.1	Q8RXQ1	0.08	-0.97	-0.36	-1.03					-0.87
AT2G38320	A_95_P216172	XM_016627505.1	O80919	0.08	-0.97	-0.36	-1.03					-0.87
AT2G40150	A_95_P216172	XM_016627505.1	Q94K00	0.08	-0.97	-0.36	-1.03					-0.87
AT3G55990	A_95_P216172	XM_016627505.1	Q9LY46	0.08	-0.97	-0.36	-1.03					-0.87
AT5G01360	A_95_P216172	XM_016627505.1	Q8LED3	0.08	-0.97	-0.36	-1.03					-0.87
AT5G58600	A_95_P216172	XM_016627505.1	Q9LUZ6	0.08	-0.97	-0.36	-1.03					-0.87
AT3G62390	A_95_P216172	XM_016627505.1	Q9LZQ1	0.08	-0.97	-0.36	-1.03					-0.87
AT1G30620	A_95_P089863	XM_016627785.1	Q9SA77	0.62	0.80	0.15	1.04			-1.05		2.99
AT5G44480	A_95_P089863	XM_016627785.1	Q9FI17	0.62	0.80	0.15	1.04			-1.05		2.99
AT3G52720	A_95_P251022	XM_016627861.1	O04846	-0.71	-1.03	-0.58	-1.18				1.44	-3.13
AT5G04180	A_95_P251022	XM_016627861.1	Q9FYE3	-0.71	-1.03	-0.58	-1.18				1.44	-3.13
AT2G28210	A_95_P251022	XM_016627861.1	F4IHR4	-0.71	-1.03	-0.58	-1.18				1.44	-3.13
AT1G44000	A_95_P216297	XM_016628092.1	Q94AQ9	0.07	-1.64	-1.06	-2.12					-1.72
AT4G11910	A_95_P216297	XM_016628092.1	Q66WT5	0.07	-1.64	-1.06	-2.12					-1.72
AT1G02900	A_95_P189862	XM_016628355.1	Q9SRY3	-0.49	-0.89	-0.76	-1.22					0.87
AT3G05490	A_95_P189862	XM_016628355.1	Q9MA62	-0.49	-0.89	-0.76	-1.22					0.87
AT3G23805	A_95_P189862	XM_016628355.1	Q9LK37	-0.49	-0.89	-0.76	-1.22					0.87
AT3G47420	A_95_P204352	XM_016628638.1	Q9C5L3	1.54	1.75	1.81	2.13				1.19	
AT4G17550	A_95_P204352	XM_016628638.1	O23596	1.54	1.75	1.81	2.13				1.19	
AT3G23230	A_95_P162742	XM_016628786.1	Q9LTC5	2.88	3.51	2.28	3.77					4.64
AT5G43410	A_95_P162742	XM_016628786.1	Q9LSX0	2.88	3.51	2.28	3.77					4.64
AT1G04370	A_95_P162742	XM_016628786.1	P93822	2.88	3.51	2.28	3.77					4.64
AT3G23240	A_95_P162742	XM_016628786.1	Q8LDC8	2.88	3.51	2.28	3.77					4.64
AT2G44840	A_95_P162742	XM_016628786.1	Q8L9K1	2.88	3.51	2.28	3.77					4.64
AT5G47220	A_95_P162742	XM_016628786.1	O80338	2.88	3.51	2.28	3.77					4.64
AT3G23220	A_95_P162742	XM_016628786.1	Q9LTC6	2.88	3.51	2.28	3.77					4.64
AT2G31230	A_95_P162742	XM_016628786.1	Q8VYM0	2.88	3.51	2.28	3.77					4.64
AT3G18830	A_95_P208867	XM_016629655.1	Q8VZ80	0.97	0.97	0.38	1.29	0.96				2.17
AT4G36670	A_95_P208867	XM_016629655.1	Q8GXR2	0.97	0.97	0.38	1.29	0.96				2.17
AT2G20780	A_95_P208867	XM_016629655.1	Q0WUU6	0.97	0.97	0.38	1.29	0.96				2.17
AT2G02220	A_95_P161807	XM_016630515.1	Q9ZVR7	0.54	0.69	0.63	1.21					0.98
AT4G33430	A_95_P161807	XM_016630515.1	Q94F62	0.54	0.69	0.63	1.21					0.98
AT4G39770	A_95_P205707	XM_016630959.1	Q8GWG2	-0.29	-1.40	-0.56	-1.56					-1.24
AT1G78090	A_95_P205707	XM_016630959.1	Q9C9S4	-0.29	-1.40	-0.56	-1.56					-1.24
AT5G51460	A_95_P205707	XM_016630959.1	O64896	-0.29	-1.40	-0.56	-1.56					-1.24
AT5G01410	A_95_P008541	XM_016631667.1	Q8L940	-0.40	-0.36	0.29	-0.79				1.47	-0.95

Arabidopsis and tobacco identifiers				WT tobacco		VviPGIP1-tobacco		Primed *Arabidopsis*	Primed and infected *Arabidopsis*		*B. cinerea* infected *Arabidopsis*	
Locus Identifier Arabidopsis	Agilent microarray probe	Tobacco GenBank Accession	Tobacco UNIPROT ID	Δt0-24	Δt0-48	Δt0-24	Δt0-48	ISR-prime 2dpTi	ISR-boost 1dpi	ISR-boost 2dpi	BIDR 1dpi	BIDR 2dpi
AT2G38230	A_95_P008541	XM_016631667.1	O80448	-0.40	-0.36	0.29	-0.79				1.47	-0.95
AT1G11350	A_95_P134092	XM_016632026.1	Q9LPZ9	-0.18	-0.79	-0.15	-1.06					1.36
AT1G61610	A_95_P134092	XM_016632026.1	Q9SY89	-0.18	-0.79	-0.15	-1.06					1.36
AT1G61370	A_95_P134092	XM_016632026.1	O64783	-0.18	-0.79	-0.15	-1.06					1.36
AT1G61550	A_95_P134092	XM_016632026.1	Q9SY95	-0.18	-0.79	-0.15	-1.06					1.36
AT1G61380	A_95_P134092	XM_016632026.1	O64782	-0.18	-0.79	-0.15	-1.06					1.36
AT1G61390	A_95_P134092	XM_016632026.1	O64781	-0.18	-0.79	-0.15	-1.06					1.36
AT1G61420	A_95_P134092	XM_016632026.1	O64778	-0.18	-0.79	-0.15	-1.06					1.36
AT3G16560	A_95_P121167	XM_016632045.1	Q9LUS8	-0.04	-1.29	-0.58	-1.15					-1.00
AT2G28890	A_95_P121167	XM_016632045.1	Q9ZV25	-0.04	-1.29	-0.58	-1.15					-1.00
AT1G07630	A_95_P121167	XM_016632045.1	Q9LQN6	-0.04	-1.29	-0.58	-1.15					-1.00
AT2G35350	A_95_P121167	XM_016632045.1	O82302	-0.04	-1.29	-0.58	-1.15					-1.00
AT2G16600	A_95_P026081	XM_016632052.1	Q38900	2.02	2.63	1.50	2.81	1.12				0.94
AT2G21130	A_95_P026081	XM_016632052.1	Q9SKQ0	2.02	2.63	1.50	2.81	1.12				0.94
AT2G24010	A_95_P124992	XM_016632515.1	O82229	0.03	-0.23	-0.25	-0.29					-1.31
AT4G30610	A_95_P124992	XM_016632515.1	Q9M099	0.03	-0.23	-0.25	-0.29					-1.31
AT3G02110	A_95_P124992	XM_016632515.1	Q8L9Y0	0.03	-0.23	-0.25	-0.29					-1.31
AT3G63470	A_95_P124992	XM_016632515.1	Q0WRX3	0.03	-0.23	-0.25	-0.29					-1.31
AT1G50280	A_95_P159137	XM_016632699.1	Q8RXR6	0.78	-0.20	0.16	-0.18					-1.44
AT3G22104	A_95_P159137	XM_016632699.1	Q9C5J4	0.78	-0.20	0.16	-0.18					-1.44
AT1G80820	A_95_P186892	XM_016632773.1	Q9SAH9	0.57	0.60	-0.84	0.30			-1.34		4.80
AT4G35420	A_95_P186892	XM_016632773.1	Q500U8	0.57	0.60	-0.84	0.30			-1.34		4.80
AT5G42800	A_95_P186892	XM_016632773.1	P51102	0.57	0.60	-0.84	0.30			-1.34		4.80
AT1G47830	A_95_P207472	XM_016633294.1	Q84WL9	0.90	1.63	0.66	1.90					1.03
AT2G17380	A_95_P207472	XM_016633294.1	Q8LEZ8	0.90	1.63	0.66	1.90					1.03
AT3G15850	A_95_P270791	XM_016636099.1	Q949X0	0.31	-0.69	-0.34	-1.06					-1.08
AT2G31360	A_95_P270791	XM_016636099.1	Q9SID2	0.31	-0.69	-0.34	-1.06					-1.08
AT1G06360	A_95_P270791	XM_016636099.1	Q9LMI3	0.31	-0.69	-0.34	-1.06					-1.08
AT2G31110	A_95_P223482	XM_016636214.1	Q67XC4	0.50	0.70	0.39	1.07				1.47	
AT2G30010	A_95_P223482	XM_016636214.1	O80872	0.50	0.70	0.39	1.07				1.47	
AT3G48090	A_95_P025936	XM_016636310.1	Q9SU72	1.05	0.98	1.22	1.61	2.05		-1.01		0.95
AT3G48080	A_95_P025936	XM_016636310.1	Q9SU71	1.05	0.98	1.22	1.61	2.05		-1.01		0.95
AT3G52430	A_95_P025936	XM_016636310.1	Q9S745	1.05	0.98	1.22	1.61	2.05		-1.01		0.95
AT5G14930	A_95_P025936	XM_016636310.1	Q4F883	1.05	0.98	1.22	1.61	2.05		-1.01		0.95
AT5G21222	A_95_P023441	XM_016636577.1	Q8S9D1	-0.23	-1.06	-0.38	-1.25					-1.60
AT5G25630	A_95_P023441	XM_016636577.1	Q8GZ63	-0.23	-1.06	-0.38	-1.25					-1.60
AT4G11690	A_95_P023441	XM_016636577.1	Q9T0D6	-0.23	-1.06	-0.38	-1.25					-1.60
AT4G33070	A_95_P015376	XM_016636659.1	O82647	1.82	1.81	2.07	2.28					2.02
AT5G54960	A_95_P015376	XM_016636659.1	Q9FFT4	1.82	1.81	2.07	2.28					2.02
AT2G40140	A_95_P160597	XM_016636694.1	Q9XEE6	0.79	-0.42	-0.22	-0.38		-1.28	-1.23	1.32	1.86
AT5G58620	A_95_P160597	XM_016636694.1	Q9LUZ4	0.79	-0.42	-0.22	-0.38		-1.28	-1.23	1.32	1.86
AT3G55980	A_95_P160597	XM_016636694.1	Q93ZS9	0.79	-0.42	-0.22	-0.38		-1.28	-1.23	1.32	1.86
AT2G25900	A_95_P160597	XM_016636694.1	O82307	0.79	-0.42	-0.22	-0.38		-1.28	-1.23	1.32	1.86

Arabidopsis and tobacco identifiers				WT tobacco		VviPGIP1-tobacco		Primed *Arabidopsis*	Primed and infected *Arabidopsis*		*B. cinerea* infected *Arabidopsis*	
Locus Identifier Arabidopsis	Agilent microarray probe	Tobacco GenBank Accession	Tobacco UNIPROT ID	Δt0-24	Δt0-48	Δt0-24	Δt0-48	ISR-prime 2dpTi	ISR-boost 1dpi	ISR-boost 2dpi	BIDR 1dpi	BIDR 2dpi
AT2G19810	A_95_P160597	XM_016636694.1	O82199	0.79	-0.42	-0.22	-0.38		-1.28	-1.23	1.32	1.86
AT4G28730	A_95_P068440	XM_016637118.1	Q8GWS0	-0.51	-1.47	-0.51	-1.69					-1.10
AT2G20270	A_95_P068440	XM_016637118.1	Q8LBS4	-0.51	-1.47	-0.51	-1.69					-1.10
AT2G48150	A_95_P030236	XM_016637769.1	Q8L910	0.69	-0.01	0.36	-0.15					1.62
AT3G63080	A_95_P030236	XM_016637769.1	Q9LYB4	0.69	-0.01	0.36	-0.15					1.62
AT5G35220	A_95_P130752	XM_016639376.1	Q949Y5	-0.17	-1.12	-0.30	-1.22					-1.18
AT1G17870	A_95_P130752	XM_016639376.1	Q9LMU1	-0.17	-1.12	-0.30	-1.22					-1.18
AT2G30060	A_95_P125267	XM_016640238.1	Q8RWG8	-0.10	0.84	-0.18	1.09					1.17
AT1G07140	A_95_P125267	XM_016640238.1	Q9LMK7	-0.10	0.84	-0.18	1.09					1.17
AT5G10250	A_95_P033679	XM_016640965.1	Q9LFU0	-0.17	-1.69	-0.69	-1.69					-1.23
AT5G67440	A_95_P033679	XM_016640965.1	Q9FN09	-0.17	-1.69	-0.69	-1.69					-1.23
AT1G19350	A_95_P134757	XM_016640980.1	Q9LN63	-0.07	-0.97	0.11	-0.30					-1.38
AT4G18890	A_95_P134757	XM_016640980.1	O49404	-0.07	-0.97	0.11	-0.30					-1.38
AT2G40410	A_95_P273371	XM_016641579.1	F4IH31	-0.49	-0.64	-0.56	-0.60					0.87
AT3G56170	A_95_P273371	XM_016641579.1	F4IZC5	-0.49	-0.64	-0.56	-0.60					0.87
AT3G11230	A_95_P003601	XM_016641838.1	Q9C777	-0.15	-0.92	-0.54	-1.03					1.58
AT3G55890	A_95_P003601	XM_016641838.1	Q9LY56	-0.15	-0.92	-0.54	-1.03					1.58
AT4G27860	A_95_P206552	XM_016642113.1	Q8W4P8	0.41	2.12	0.41	1.93	1.45	0.92			3.17
AT5G24290	A_95_P206552	XM_016642113.1	F4KFS7	0.41	2.12	0.41	1.93	1.45	0.92			3.17
AT3G21870	A_95_P023061	XM_016642426.1	Q9LJ45	-0.62	-2.00	-1.29	-2.56				1.14	-2.27
AT2G44740	A_95_P023061	XM_016642426.1	O80513	-0.62	-2.00	-1.29	-2.56				1.14	-2.27
AT2G45080	A_95_P023061	XM_016642426.1	Q9SHD3	-0.62	-2.00	-1.29	-2.56				1.14	-2.27
AT5G09730	A_95_P211882	XM_016642489.1	Q9LXD6	-0.30	-1.60	-0.18	-2.06					-1.91
AT5G49360	A_95_P211882	XM_016642489.1	Q9FGY1	-0.30	-1.60	-0.18	-2.06					-1.91
AT1G02640	A_95_P211882	XM_016642489.1	Q94KD8	-0.30	-1.60	-0.18	-2.06					-1.91
AT5G22630	A_95_P202537	XM_016642832.1	Q9FNJ8	2.32	3.64	2.07	4.20					1.82
AT3G44720	A_95_P202537	XM_016642832.1	O22241	2.32	3.64	2.07	4.20					1.82
AT1G11790	A_95_P202537	XM_016642832.1	Q9SA96	2.32	3.64	2.07	4.20					1.82
AT4G16390	A_95_P200517	XM_016643441.1	Q8GWE0	-0.17	-0.60	0.10	-1.00				-1.18	-1.01
AT1G62590	A_95_P200517	XM_016643441.1	Q9SXD8	-0.17	-0.60	0.10	-1.00				-1.18	-1.01
AT1G05170	A_95_P151567	XM_016643491.1	A8MRC7	0.32	0.62	0.49	1.01					-1.14
AT1G77810	A_95_P151567	XM_016643491.1	Q6NQB7	0.32	0.62	0.49	1.01					-1.14
AT2G32430	A_95_P151567	XM_016643491.1	Q9ZV71	0.32	0.62	0.49	1.01					-1.14
AT3G28210	A_95_P192482	XM_016643685.1	Q67YE6	1.85	2.59	1.14	2.95	2.70				3.51
AT2G41835	A_95_P192482	XM_016643685.1	Q8VZ42	1.85	2.59	1.14	2.95	2.70				3.51
AT3G57480	A_95_P192482	XM_016643685.1	Q9SCM4	1.85	2.59	1.14	2.95	2.70				3.51
AT5G26030	A_95_P145647	XM_016643806.1	P42043	1.76	1.93	1.10	2.02			-1.10	1.11	1.54
AT2G30390	A_95_P145647	XM_016643806.1	O04921	1.76	1.93	1.10	2.02			-1.10	1.11	1.54
AT3G13080	A_95_P006321	XM_016644669.1	Q9LK64	0.31	0.24	0.53	0.31	2.15		-1.36		1.22
AT3G13100	A_95_P006321	XM_016644669.1	Q9LK62	0.31	0.24	0.53	0.31	2.15		-1.36		1.22
AT3G13090	A_95_P006321	XM_016644669.1	Q8VZZ4	0.31	0.24	0.53	0.31	2.15		-1.36		1.22
AT3G59140	A_95_P006321	XM_016644669.1	Q9LYS2	0.31	0.24	0.53	0.31	2.15		-1.36		1.22
AT1G49430	A_95_P133442	XM_016645750.1	Q9XIA9	-0.14	-1.89	-0.43	-1.94	-1.01				-1.83

Arabidopsis and tobacco identifiers				WT tobacco		VviPGIP1-tobacco		Primed *Arabidopsis*	Primed and infected *Arabidopsis*		*B. cinerea* infected *Arabidopsis*	
Locus Identifier Arabidopsis	Agilent microarray probe	Tobacco GenBank Accession	Tobacco UNIPROT ID	Δt0-24	Δt0-48	Δt0-24	Δt0-48	ISR-prime 2dpTi	ISR-boost 1dpi	ISR-boost 2dpi	BIDR 1dpi	BIDR 2dpi
AT1G64400	A_95_P133442	XM_016645750.1	Q9C7W4	-0.14	-1.89	-0.43	-1.94	-1.01				-1.83
AT4G23850	A_95_P133442	XM_016645750.1	Q9T0A0	-0.14	-1.89	-0.43	-1.94	-1.01				-1.83
AT5G27600	A_95_P133442	XM_016645750.1	Q8LKS5	-0.14	-1.89	-0.43	-1.94	-1.01				-1.83
AT3G05970	A_95_P133442	XM_016645750.1	Q8LPS1	-0.14	-1.89	-0.43	-1.94	-1.01				-1.83
AT1G09580	A_95_P200952	XM_016646008.1	Q6IDL4	0.49	1.38	0.67	1.64	-1.05				
AT1G26690	A_95_P200952	XM_016646008.1	Q9LQY3	0.49	1.38	0.67	1.64	-1.05				
AT1G14010	A_95_P200952	XM_016646008.1	Q8GYG1	0.49	1.38	0.67	1.64	-1.05				
AT2G03770	A_95_P200482	XM_016646158.1	Q9ZPQ5	-0.09	-0.60	-0.30	-1.00					1.10
AT1G74100	A_95_P200482	XM_016646158.1	Q9C9D0	-0.09	-0.60	-0.30	-1.00					1.10
AT1G13420	A_95_P200482	XM_016646158.1	Q9FX56	-0.09	-0.60	-0.30	-1.00					1.10
AT2G03760	A_95_P200482	XM_016646158.1	P52839	-0.09	-0.60	-0.30	-1.00					1.10
AT5G07000	A_95_P200482	XM_016646158.1	Q8GZ53	-0.09	-0.60	-0.30	-1.00					1.10
AT5G07010	A_95_P200482	XM_016646158.1	Q8L5A7	-0.09	-0.60	-0.30	-1.00					1.10
AT1G02170	A_95_P011256	XM_016646741.1	Q7XJE6	-0.25	-0.36	-0.10	-0.62					1.02
AT5G64240	A_95_P011256	XM_016646741.1	Q9FMG1	-0.25	-0.36	-0.10	-0.62					1.02
AT4G25110	A_95_P011256	XM_016646741.1	Q7XJE5	-0.25	-0.36	-0.10	-0.62					1.02
AT3G05580	A_95_P202212	XM_016647599.1	Q9M9W3	0.33	0.63	0.03	0.90					0.88
AT2G29400	A_95_P202212	XM_016647599.1	P30366	0.33	0.63	0.03	0.90					0.88
AT2G37940	A_95_P162172	XM_016648619.1	Q9SH93	1.64	1.90	1.63	2.42			-0.90		2.03
AT3G54020	A_95_P162172	XM_016648619.1	Q9M325	1.64	1.90	1.63	2.42			-0.90		2.03
AT5G62100	A_95_P181387	XM_016648905.1	Q0WPX7	0.23	-1.84	-0.69	-2.40					-1.77
AT5G52060	A_95_P181387	XM_016648905.1	Q0WUQ1	0.23	-1.84	-0.69	-2.40					-1.77
AT1G52340	A_95_P017151	XM_016648914.1	Q9C826	-0.34	-1.89	-0.71	-2.25					-1.18
AT2G47140	A_95_P017151	XM_016648914.1	Q94K41	-0.34	-1.89	-0.71	-2.25					-1.18
AT2G47130	A_95_P017151	XM_016648914.1	O80713	-0.34	-1.89	-0.71	-2.25					-1.18
AT3G29250	A_95_P017151	XM_016648914.1	F4J2Z7	-0.34	-1.89	-0.71	-2.25					-1.18
AT4G22880	A_95_P269481	XM_016649365.1	Q96323	-0.69	-1.47	-0.10	-1.51	2.47	1.79	1.37		
AT1G17020	A_95_P269481	XM_016649365.1	Q39224	-0.69	-1.47	-0.10	-1.51	2.47	1.79	1.37		
AT1G19670	A_95_P221817	XM_016649385.1	O22527	4.34	5.25	4.26	5.65		0.93	-1.39		2.03
AT5G43860	A_95_P221817	XM_016649385.1	Q9M7I7	4.34	5.25	4.26	5.65		0.93	-1.39		2.03
AT1G45145	A_95_P219682	XM_016649996.1	Q39241	1.06	1.67	0.59	1.80	1.92	1.18	-1.25	-0.96	3.63
AT2G46140	A_95_P136547	XM_016650323.1	O82355	0.30	-0.84	-0.23	-0.79					1.76
AT1G01470	A_95_P136547	XM_016650323.1	O03983	0.30	-0.84	-0.23	-0.79					1.76
AT2G40000	A_95_P204522	XM_016650560.1	O04203	0.03	-1.15	-0.56	-0.86		-2.17			1.41
AT3G55840	A_95_P204522	XM_016650560.1	Q9LY61	0.03	-1.15	-0.56	-0.86		-2.17			1.41
AT2G30360	A_95_P128872	XM_016651439.1	O22932	-0.06	-0.23	-0.22	-0.27	0.99				1.89
AT5G01820	A_95_P128872	XM_016651439.1	Q9LZW4	-0.06	-0.23	-0.22	-0.27	0.99				1.89
AT5G45810	A_95_P128872	XM_016651439.1	Q9FJ55	-0.06	-0.23	-0.22	-0.27	0.99				1.89
AT4G30960	A_95_P128872	XM_016651439.1	O65554	-0.06	-0.23	-0.22	-0.27	0.99				1.89
AT5G65050	A_95_P225577	XM_016651527.1	Q9FPN7	-0.03	-0.29	-0.07	-0.32					1.21
AT5G65080	A_95_P225577	XM_016651527.1	Q683D7	-0.03	-0.29	-0.07	-0.32					1.21
AT2G33150	A_95_P009401	XM_016651715.1	Q56WD9	0.18	1.02	0.19	1.29				-0.98	1.32
AT5G48880	A_95_P009401	XM_016651715.1	Q570C8	0.18	1.02	0.19	1.29				-0.98	1.32

Arabidopsis and tobacco identifiers				WT tobacco		VviPGIP1-tobacco		Primed *Arabidopsis*	Primed and infected *Arabidopsis*		*B. cinerea* infected *Arabidopsis*	
Locus Identifier Arabidopsis	Agilent microarray probe	Tobacco GenBank Accession	Tobacco UNIPROT ID	Δt0-24	Δt0-48	Δt0-24	Δt0-48	ISR-prime 2dpTi	ISR-boost 1dpi	ISR-boost 2dpi	BIDR 1dpi	BIDR 2dpi
AT1G53310	A_95_P090053	XM_016652322.1	Q9MAH0	-0.23	-0.43	0.43	-0.10	0.88				
AT2G42600	A_95_P090053	XM_016652322.1	Q5GM68	-0.23	-0.43	0.43	-0.10	0.88				
AT5G48910	A_95_P283088	XM_016652752.1	Q9FI80	0.50	-1.12	-0.86	-1.64					-1.30
AT5G66520	A_95_P283088	XM_016652752.1	Q9FJY7	0.50	-1.12	-0.86	-1.64					-1.30
AT1G59720	A_95_P283088	XM_016652752.1	Q0WQW5	0.50	-1.12	-0.86	-1.64					-1.30
AT4G23740	A_95_P192282	XM_016652762.1	Q9SUQ3	0.78	1.70	0.93	1.72					-1.50
AT5G41680	A_95_P192282	XM_016652762.1	Q3E8J4	0.78	1.70	0.93	1.72					-1.50
AT1G49050	A_95_P065285	XM_016653041.1	Q9M9A8	-0.09	0.90	-0.29	0.65					1.11
AT5G10080	A_95_P065285	XM_016653041.1	Q9LX20	-0.09	0.90	-0.29	0.65					1.11
AT4G34860	A_95_P133527	XM_016653436.1	Q9SW48	-0.20	-0.81	-0.43	-1.03					1.47
AT1G72000	A_95_P133527	XM_016653436.1	Q9C560	-0.20	-0.81	-0.43	-1.03					1.47
AT3G06500	A_95_P133527	XM_016653436.1	B9DFA8	-0.20	-0.81	-0.43	-1.03					1.47
AT5G45680	A_95_P027821	XM_016653616.1	Q9SCY2	-0.62	-1.64	-0.74	-2.00					-0.90
AT4G39710	A_95_P027821	XM_016653616.1	Q9SCY3	-0.62	-1.64	-0.74	-2.00					-0.90
AT5G63320	A_95_P142732	XM_016653874.1	Q9FGW9	0.28	0.16	0.57	1.11			-1.34		1.07
AT5G14270	A_95_P142732	XM_016653874.1	Q93YS6	0.28	0.16	0.57	1.11			-1.34		1.07
AT3G01770	A_95_P142732	XM_016653874.1	Q93ZB7	0.28	0.16	0.57	1.11			-1.34		1.07
AT3G54960	A_95_P196252	XM_016654102.1	Q8VX13	0.62	2.15	1.03	2.30	1.97				1.16
AT5G60640	A_95_P196252	XM_016654102.1	Q9FF55	0.62	2.15	1.03	2.30	1.97				1.16
AT5G61250	A_95_P125492	XM_016654658.1	Q8L608	-0.56	-0.89	-0.43	-1.03	1.15				1.25
AT5G07830	A_95_P125492	XM_016654658.1	Q9FF10	-0.56	-0.89	-0.43	-1.03	1.15				1.25
AT5G34940	A_95_P125492	XM_016654658.1	Q9FZP1	-0.56	-0.89	-0.43	-1.03	1.15				1.25
AT5G25250	A_95_P297548	XM_016654805.1	Q501E6	1.24	1.63	1.84	2.12	1.89				3.43
AT5G64870	A_95_P297548	XM_016654805.1	Q9LV90	1.24	1.63	1.84	2.12	1.89				3.43
AT5G56860	A_95_P146607	XM_016655136.1	Q5HZ36	-0.25	-1.64	-0.22	-1.43					-1.52
AT4G26150	A_95_P146607	XM_016655136.1	Q9SZI6	-0.25	-1.64	-0.22	-1.43					-1.52
AT2G18380	A_95_P146607	XM_016655136.1	Q9ZPX0	-0.25	-1.64	-0.22	-1.43					-1.52
AT3G50870	A_95_P146607	XM_016655136.1	Q8LC79	-0.25	-1.64	-0.22	-1.43					-1.52
AT4G32890	A_95_P146607	XM_016655136.1	O82632	-0.25	-1.64	-0.22	-1.43					-1.52
AT3G22790	A_95_P200747	XM_016655520.1	Q9LUI2	0.08	-0.32	-0.01	-0.27			-0.85		
AT1G03080	A_95_P200747	XM_016655520.1	F4HZB5	0.08	-0.32	-0.01	-0.27			-0.85		
AT4G14760	A_95_P200747	XM_016655520.1	F4JIF4	0.08	-0.32	-0.01	-0.27			-0.85		
AT2G22560	A_95_P200747	XM_016655520.1	F4IJK1	0.08	-0.32	-0.01	-0.27			-0.85		
AT4G27595	A_95_P017131	XM_016656493.1	F4JJP1	0.30	-0.36	0.04	-0.58					-1.32
AT2G37080	A_95_P017131	XM_016656493.1	Q9ZQC5	0.30	-0.36	0.04	-0.58					-1.32
AT5G09510	A_95_P178632	XM_016656498.1	Q9FY64	-0.42	-0.17	0.20	-0.30				-0.95	
AT5G43640	A_95_P178632	XM_016656498.1	Q9FIX6	-0.42	-0.17	0.20	-0.30				-0.95	
AT2G21520	A_95_P241810	XM_016657327.1	F4IHJ0	0.83	1.64	0.75	1.84					1.30
AT2G21540	A_95_P241810	XM_016657327.1	Q93ZE9	0.83	1.64	0.75	1.84					1.30
AT1G01390	A_95_P014501	XM_016657469.1	Q8W4C2	0.38	1.02	0.24	1.20					-1.25
AT2G18570	A_95_P014501	XM_016657469.1	Q9ZU72	0.38	1.02	0.24	1.20					-1.25
AT5G66690	A_95_P014501	XM_016657469.1	Q9LVR1	0.38	1.02	0.24	1.20					-1.25
AT3G50740	A_95_P014501	XM_016657469.1	Q94A84	0.38	1.02	0.24	1.20					-1.25

Arabidopsis and tobacco identifiers				WT tobacco		VviPGIP1-tobacco		Primed *Arabidopsis*	Primed and infected *Arabidopsis*		*B. cinerea* infected *Arabidopsis*	
Locus Identifier Arabidopsis	Agilent microarray probe	Tobacco GenBank Accession	Tobacco UNIPROT ID	Δt0-24	Δt0-48	Δt0-24	Δt0-48	ISR-prime 2dpTi	ISR-boost 1dpi	ISR-boost 2dpi	BIDR 1dpi	BIDR 2dpi
AT4G36770	A_95_P014501	XM_016657469.1	O23205	0.38	1.02	0.24	1.20					-1.25
AT3G16520	A_95_P014501	XM_016657469.1	Q9LK73	0.38	1.02	0.24	1.20					-1.25
AT1G55490	A_95_P031841	XM_016657857.1	P21240	0.03	-0.47	0.25	-0.64					-0.99
AT3G13470	A_95_P031841	XM_016657857.1	Q9LJE4	0.03	-0.47	0.25	-0.64					-0.99
AT1G26230	A_95_P031841	XM_016657857.1	Q9C667	0.03	-0.47	0.25	-0.64					-0.99
AT4G14550	A_95_P126232	XM_016658276.1	Q38832	0.32	-0.71	-0.58	-1.25	-1.42				-1.30
AT1G04250	A_95_P126232	XM_016658276.1	P93830	0.32	-0.71	-0.58	-1.25	-1.42				-1.30
AT1G61820	A_95_P100268	XM_016658362.1	O80690	-0.36	0.70	-0.86	0.40			-1.74		3.82
AT4G21760	A_95_P100268	XM_016658362.1	Q9SVS1	-0.36	0.70	-0.86	0.40			-1.74		3.82
AT1G61810	A_95_P100268	XM_016658362.1	O80689	-0.36	0.70	-0.86	0.40			-1.74		3.82
AT1G26560	A_95_P100268	XM_016658362.1	Q9FZE0	-0.36	0.70	-0.86	0.40			-1.74		3.82
AT2G44480	A_95_P100268	XM_016658362.1	O64882	-0.36	0.70	-0.86	0.40			-1.74		3.82
AT2G02990	A_95_P296278	XM_016659615.1	P42813	-0.74	-1.12	-0.45	-1.22	1.38	2.10	0.91		1.72
AT1G26820	A_95_P296278	XM_016659615.1	P42815	-0.74	-1.12	-0.45	-1.22	1.38	2.10	0.91		1.72
AT2G03890	A_95_P149567	XM_016659643.1	Q9SI52	-0.62	-1.89	-0.20	-1.94				1.09	
AT1G13640	A_95_P149567	XM_016659643.1	Q8W4R8	-0.62	-1.89	-0.20	-1.94				1.09	
AT1G64460	A_95_P149567	XM_016659643.1	Q9SGW8	-0.62	-1.89	-0.20	-1.94				1.09	
AT1G58170	A_95_P119907	XM_016659706.1	Q9C523	0.95	1.29	1.21	1.95					-1.53
AT1G55210	A_95_P119907	XM_016659706.1	Q9C891	0.95	1.29	1.21	1.95					-1.53
AT4G38700	A_95_P119907	XM_016659706.1	F4JUF8	0.95	1.29	1.21	1.95					-1.53
AT1G14700	A_95_P213647	XM_016659920.1	Q8H129	0.45	0.39	0.33	0.64	-0.90				-1.41
AT2G01890	A_95_P213647	XM_016659920.1	Q8VYZ2	0.45	0.39	0.33	0.64	-0.90				-1.41
AT1G25230	A_95_P213647	XM_016659920.1	Q8VYU7	0.45	0.39	0.33	0.64	-0.90				-1.41
AT3G17790	A_95_P213647	XM_016659920.1	Q9SCX8	0.45	0.39	0.33	0.64	-0.90				-1.41
AT2G17500	A_95_P145757	XM_016660388.1	Q9SHL8	-0.04	-0.76	-0.29	-0.67	1.84				2.02
AT1G76520	A_95_P145757	XM_016660388.1	Q9C9K5	-0.04	-0.76	-0.29	-0.67	1.84				2.02
AT1G76530	A_95_P145757	XM_016660388.1	Q9C9K4	-0.04	-0.76	-0.29	-0.67	1.84				2.02
AT2G35980	A_95_P022806	Y07563.1	Q9SJ52	0.44	1.97	1.45	2.93	4.61				4.30
AT5G06320	A_95_P022806	Y07563.1	Q9FNH6	0.44	1.97	1.45	2.93	4.61				4.30
AT1G32270	A_95_P022806	Y07563.1	Q9C615	0.44	1.97	1.45	2.93	4.61				4.30
AT2G35960	A_95_P022806	Y07563.1	Q9SJ54	0.44	1.97	1.45	2.93	4.61				4.30
AT5G25370	A_95_P016051	Z84822.1	P58766	0.36	0.38	0.34	0.55			-2.12		
AT2G42010	A_95_P016051	Z84822.1	P93733	0.36	0.38	0.34	0.55			-2.12		
AT3G03190	A_95_P178207	XM_016617344.1	Q96324	0.75	1.14	0.37	1.74		1.33			
AT5G67300	A_95_P003546	AB032540.1	Q9FDW1	0.49	1.27	0.36	1.78					1.62
AT3G13790	A_95_P238509	AB055500.1	Q43866	1.55	3.11	1.37	3.30	1.36				2.44
AT5G05340	A_95_P178312	AB178953.2	Q9FLC0	2.53	5.33	2.51	4.99	2.27				3.76
AT5G42650	A_95_P190077	AF070976.1	Q96242	3.94	5.29	4.17	5.17			-0.91		1.14
AT4G26970	A_95_P217392	AF194945.1	Q94A28	0.62	1.75	0.58	1.74					1.01
AT1G07890	A_95_P258396	D85912.1	Q05431	2.54	3.98	1.95	3.68			-0.97	1.03	
AT3G23210	A_95_P228174	EU880279.1	Q9LTC7	-0.14	-1.64	-0.45	-2.00					-1.13
AT1G05010	A_95_P130452	HQ418209.1	Q06588	0.80	-1.60	0.62	-1.94					2.06
AT1G69720	A_95_P120422	HQ676595.1	Q9C9L4	-0.42	-1.56	-0.62	-1.69	1.50				1.52

Arabidopsis and tobacco identifiers				WT tobacco		VviPGIP1-tobacco		Primed *Arabidopsis*	Primed and infected *Arabidopsis*		*B. cinerea* infected *Arabidopsis*	
Locus Identifier Arabidopsis	Agilent microarray probe	Tobacco GenBank Accession	Tobacco UNIPROT ID	Δt0-24	Δt0-48	Δt0-24	Δt0-48	ISR-prime 2dpTi	ISR-boost 1dpi	ISR-boost 2dpi	BIDR 1dpi	BIDR 2dpi
AT5G40760	A_95_P020731	NM_001326264.1	Q9FJI5	1.38	2.18	1.53	2.55					1.33
AT2G14610	A_95_P021401	X05959.1	P33154	0.01	2.27	0.45	2.24	4.18				1.95
AT3G12500	A_95_P179847	X64519.1	P19171	0.25	1.67	0.52	1.20	1.14				4.61
AT1G21310	A_95_P000596	X71602.1	Q9FS16	0.23	2.41	0.30	1.33	3.81				3.32
AT1G15690	A_95_P250777	X77915.1	P31414	-0.79	-1.29	-0.12	-1.06					-1.21
AT3G51470	A_95_P191042	XM_016578395.1	Q9SD02	-0.42	-1.51	-0.54	-1.51					-1.05
AT3G21890	A_95_P217352	XM_016582192.1	Q9LRM4	0.19	-1.22	-0.32	-1.51					-2.28
AT5G02780	A_95_P249712	XM_016582263.1	Q6NLB0	-2.25	-2.47	-1.32	-2.18	2.86				4.88
AT4G08170	A_95_P234939	XM_016582584.1	Q9SUG3	-0.45	-2.18	-0.54	-1.89			-1.07		1.58
AT5G20910	A_95_P139122	XM_016585323.1	Q8RXD3	0.15	-1.60	-0.20	-1.29					1.29
AT1G14540	A_95_P277528	XM_016585973.1	Q9LE15	0.79	1.93	1.15	1.75			-1.57		3.99
AT2G27510	A_95_P194602	XM_016586162.1	Q9ZQG8	0.60	2.16	0.30	1.88					1.28
AT3G12930	A_95_P304098	XM_016587097.1	Q9LDY9	-0.42	-1.47	-0.67	-1.79				-1.17	-1.00
AT4G35570	A_95_P179952	XM_016587101.1	O49597	-0.20	-1.56	0.00	-1.56	0.89				1.34
AT1G28330	A_95_P108367	XM_016587715.1	B9DGG8	-0.51	-2.32	-0.09	-2.32	-1.82			-1.93	3.14
AT5G06770	A_95_P149167	XM_016589241.1	Q9FG30	-0.56	-1.22	-0.23	-1.12					-1.03
AT3G20250	A_95_P031071	XM_016591183.1	Q9LJX4	-0.12	-1.00	-0.22	-1.00	1.78				1.71
AT2G37240	A_95_P025261	XM_016591728.1	Q9ZUU2	0.03	-1.89	-0.45	-1.89					-1.62
AT1G19150	A_95_P135527	XM_016594612.1	Q8LCQ4	-0.09	-2.84	-1.12	-3.32					-1.52
AT4G31820	A_95_P210827	XM_016594749.1	Q8H1D3	-0.42	-1.47	-0.18	-1.29					1.01
AT4G21470	A_95_P269811	XM_016595555.1	Q84MD8	-0.40	-1.94	-1.09	-2.25					2.31
AT4G20260	A_95_P136002	XM_016595857.1	Q96262	-0.45	-1.40	-0.18	-1.47				-1.10	1.19
AT2G32250	A_95_P197307	XM_016596399.1	Q3EBQ3	-0.64	-1.29	-0.07	-1.06					1.43
AT5G03730	A_95_P095323	XM_016596426.1	Q05609	-0.58	-1.54	-0.68	-1.60					1.20
AT4G30210	A_95_P016661	XM_016599456.1	Q9SUM3	1.08	1.41	1.00	2.08				0.89	1.46
AT3G02360	A_95_P026051	XM_016599550.1	Q9FWA3	3.52	4.85	3.16	5.53					1.07
AT5G45650	A_95_P117802	XM_016601893.1	Q9FK76	-0.06	-1.84	-0.36	-2.25					-1.64
AT5G42560	A_95_P216627	XM_016602442.1	Q8LE10	-0.22	-1.25	-0.38	-1.40					1.46
AT5G35450	A_95_P216987	XM_016604707.1	Q9FJB5	1.43	1.25	1.35	1.83					1.08
AT1G64750	A_95_P211667	XM_016606964.1	Q9XIR8	0.48	1.06	0.30	0.92					2.86
AT2G45220	A_95_P234829	XM_016610700.1	O22149	0.79	1.35	1.57	1.45	4.50				3.10
AT4G21870	A_95_P233289	XM_016610874.1	O49710	-1.16	-1.81	-0.77	-2.19	-1.15			2.21	
AT1G62440	A_95_P242622	XM_016612257.1	O48809	-0.34	-1.15	0.32	-1.12					1.31
AT3G60100	A_95_P098838	XM_016613891.1	Q9M1D3	1.03	1.86	1.01	2.05					1.31
AT1G74070	A_95_P272466	XM_016615537.1	F4HTT6	0.37	-1.84	-0.84	-2.06					-1.58
AT5G41220	A_95_P229239	XM_016616188.1	Q9FHE1	-0.67	-1.43	-1.09	-1.74					1.32
AT5G49770	A_95_P160117	XM_016617971.1	Q9LT96	0.25	-1.06	0.34	-0.94					1.34
AT3G52800	A_95_P028551	XM_016619283.1	Q94B40	-0.60	-1.60	-0.60	-1.47					1.10
AT1G54100	A_95_P227619	XM_016619796.1	Q9SYG7	-0.86	-1.89	-0.40	-2.00					1.65
AT4G28660	A_95_P021806	XM_016619865.1	Q8W0Y8	0.01	-1.32	-0.92	-1.79					-1.32
AT2G47650	A_95_P011416	XM_016620378.1	Q8S8T4	-0.54	-1.47	-0.64	-1.64					1.88
AT5G40000	A_95_P153502	XM_016620859.1	F4KFX5	0.76	1.17	0.54	1.42			-3.60		2.19
AT5G02200	A_95_P019861	XM_016621821.1	A8MR65	-0.40	-1.29	-0.54	-1.64					2.87

Arabidopsis and tobacco identifiers				WT tobacco		VviPGIP1-tobacco		Primed *Arabidopsis*	Primed and infected *Arabidopsis*		*B. cinerea* infected *Arabidopsis*	
Locus Identifier Arabidopsis	Agilent microarray probe	Tobacco GenBank Accession	Tobacco UNIPROT ID	Δt0-24	Δt0-48	Δt0-24	Δt0-48	ISR-prime 2dpTi	ISR-boost 1dpi	ISR-boost 2dpi	BIDR 1dpi	BIDR 2dpi
AT5G12900	A_95_P149777	XM_016622928.1	Q9LXU9	-1.64	-1.03	1.96	0.44					-1.17
AT1G70980	A_95_P221757	XM_016623028.1	Q9SSK1	1.01	1.13	1.10	1.53					1.02
AT3G22060	A_95_P152142	XM_016623302.1	Q9LRJ9	1.72	3.29	1.97	3.46				1.85	1.08
AT4G26910	A_95_P014386	XM_016623967.1	Q8H107	0.59	1.39	0.79	1.68	1.21				2.00
AT1G69370	A_95_P044461	XM_016624201.1	Q9C544	0.86	2.46	0.84	2.66					1.03
AT5G50100	A_95_P301758	XM_016624223.1	Q8W485	-0.30	-1.06	-0.74	-1.22					-1.54
AT1G15980	A_95_P198287	XM_016624266.1	Q9S9N6	0.00	-1.40	-0.62	-1.94					-1.03
AT4G09350	A_95_P004041	XM_016629465.1	Q9SMS0	-0.79	-2.56	-1.12	-3.06					-1.66
AT5G37600	A_95_P179627	XM_016631329.1	Q56WN1	0.87	1.69	1.03	1.76	1.46			-2.23	3.26
AT4G26760	A_95_P222107	XM_016633514.1	Q8LEG3	0.12	-1.18	0.00	-1.40					-1.07
AT1G03055	A_95_P146007	XM_016634432.1	Q7XA78	-0.49	-1.22	-0.49	-1.29					-2.04
AT5G58260	A_95_P270266	XM_016635843.1	Q9LVM2	-0.47	-1.94	-1.00	-2.32					-1.01
AT2G02390	A_95_P024886	XM_016636544.1	Q9ZVQ3	-0.12	1.21	0.21	1.43	0.99				1.71
AT4G17340	A_95_P117862	XM_016640248.1	Q41975	-0.97	-1.29	-0.43	-1.64					-1.27
AT1G52710	A_95_P179807	XM_016642137.1	Q9SSS5	-0.12	1.21	0.25	1.37					1.24
AT2G40100	A_95_P106952	XM_016644161.1	Q9S7W1	1.25	-4.21	-1.15	-4.66				1.01	-1.33
AT3G42790	A_95_P019366	XM_016644480.1	Q9M2B4	-0.62	-1.43	-0.69	-1.60					1.33
AT5G12110	A_95_P004086	XM_016645592.1	Q84WM9	-0.51	-1.00	0.42	-0.76					-2.02
AT2G23680	A_95_P190187	XM_016645749.1	O64834	-0.53	-1.30	-0.76	-1.26	1.76				2.63
AT2G19570	A_95_P002021	XM_016648049.1	O65896	-0.03	1.04	-0.03	0.93					1.08
AT5G62520	A_95_P029451	XM_016649922.1	Q9FJJ3	0.83	1.14	0.70	1.61			-1.58		2.49
AT5G17380	A_95_P021756	XM_016652331.1	Q9LF46	1.70	2.33	1.60	2.95	1.38				2.23
AT5G14780	A_95_P028351	XM_016654388.1	Q9S7E4	2.19	1.68	2.82	1.95					1.30
AT5G42300	A_95_P000586	XM_016654765.1	Q9FGZ9	-0.22	1.00	0.00	1.05					1.05
AT4G12970	A_95_P150532	XM_016654878.1	Q9SV72	-0.64	-1.15	-0.76	-1.43	-1.61		0.99		-1.97
AT5G10860	A_95_P242972	XM_016655454.1	Q9LEV3	-0.19	-1.03	-0.63	-1.21				-1.30	1.26
AT1G56170	A_95_P014846	XM_016655575.1	Q8LCG7	-0.22	-1.09	-0.62	-1.56					-1.44
AT4G28950	A_95_P033599	XM_016655733.1	O82480	-0.64	-1.56	-0.79	-1.84					-1.48
AT2G01530	A_95_P247147	XM_016656857.1	Q9ZVF2	-0.18	-1.06	-0.23	-1.25					1.44
AT3G24520	A_95_P155197	XM_016657160.1	Q9LV52	-0.47	-1.06	-0.54	-0.74	-1.18				-1.30
AT2G25930	A_95_P288873	XM_016658320.1	O82804	-0.62	-1.03	-0.09	-0.76					1.98
AT4G39800	A_95_P176887	AB009881.1	P42801	0.21	-0.79	-0.18	-0.64					-1.46
AT4G36990	A_95_P238019	AB014483.1	Q96320	1.53	2.30	1.30	3.16	1.93				
AT4G03210	A_95_P178107	AB017025.1	Q8LDW9	0.70	-0.86	-0.20	-1.22	-1.50		1.07		
AT5G59870	A_95_P016011	AB032543.1	Q9FJE8	-0.36	-1.25	-0.76	-1.40				-1.24	
AT1G28260	A_95_P011806	AB041352.1	Q9FZ99	-0.34	-0.79	-0.42	-0.45					1.18
AT2G41110	A_95_P021516	AB050839.1	P0DH97	0.16	-0.43	0.12	-0.29					1.20
AT5G17310	A_95_P250107	AB055502.1	P57751	0.24	-0.03	0.20	-0.43					-1.15
AT4G27440	A_95_P010526	AB074570.1	P21218	0.46	-2.94	-0.92	-3.47				-2.97	
AT3G55270	A_95_P025971	AB117525.1	Q9C5S1	0.81	0.38	1.06	1.00	1.00				
AT4G24040	A_95_P143422	AB501123.1	Q9SU50	-0.12	0.56	0.28	0.37					1.69
AT4G24190	A_95_P226409	AB689675.1	Q9STX5	0.36	0.81	1.40	1.12	1.89		-0.96		3.89
AT5G13630	A_95_P249767	AF014052.1	Q9FNB0	1.29	-2.47	-1.51	-3.84					-0.86

Arabidopsis and tobacco identifiers				WT tobacco		VviPGIP1-tobacco		Primed *Arabidopsis*	Primed and infected *Arabidopsis*		*B. cinerea* infected *Arabidopsis*	
Locus Identifier Arabidopsis	Agilent microarray probe	Tobacco GenBank Accession	Tobacco UNIPROT ID	Δt0-24	Δt0-48	Δt0-24	Δt0-48	ISR-prime 2dpTi	ISR-boost 1dpi	ISR-boost 2dpi	BIDR 1dpi	BIDR 2dpi
AT4G18480	A_95_P184912	AF014053.1	P16127	0.12	-0.70	-0.30	-1.42					-1.08
AT1G49760	A_95_P008431	AF190657.1	Q9FXA2	0.12	0.72	1.21	1.56				-0.99	
AT3G63060	A_95_P026596	AF368237.1	Q93ZT5	0.16	-0.94	-0.20	-0.45	0.92		-1.01		
AT5G15950	A_95_P004020	AH013088.2	Q9S7T9	0.63	1.61	1.10	1.90			-0.86	2.60	-2.41
AT5G26751	A_95_P196872	AJ002315.1	P43288	0.61	0.44	0.20	0.76					1.18
AT5G03240	A_95_P005841	AJ309010.1	Q1EC66	1.30	0.25	1.34	0.32				-0.88	
AT5G48930	A_95_P249212	AJ582651.1	Q9FI78	1.29	0.92	1.63	1.17					-1.11
AT5G12860	A_95_P236429	AY123847.1	Q9LXV3	0.33	0.82	0.37	0.64					-0.95
AT3G23810	A_95_P034773	AY639866.1	Q9LK36	-0.15	1.55	0.14	1.63					-1.41
AT4G26070	A_95_P237524	D31964.1	Q94A06	0.25	0.97	0.16	1.04					1.43
AT2G29630	A_95_P289068	EF588039.1	O82392	-0.16	-1.01	-0.22	-1.21				-0.94	
AT5G08380	A_95_P145667	HQ877671.1	Q9FT97	-0.40	-0.60	-0.30	-0.69	0.93				
AT1G75750	A_95_P000261	JQ031366.1	P46689	-0.32	1.23	0.23	0.87				2.53	
AT4G36810	A_95_P149112	KF316933.1	P34802	0.20	1.37	0.10	1.51					-0.94
AT1G23760	A_95_P008201	KF701474.1	P92982	0.14	-0.76	0.15	-0.92					0.93
AT2G47490	A_95_P133072	KF856280.1	O22261	0.56	0.70	0.08	1.00				1.54	-1.04
AT5G05580	A_95_P237544	KJ551512.1	P48622	0.24	-0.22	-0.54	-0.10					-1.73
AT4G11650	A_95_P176202	M29279.1	P50700	-0.42	0.73	0.99	0.21					3.90
AT4G20360	A_95_P133117	M94204.1	P17745	0.16	-1.15	-0.36	-1.43					-0.86
AT3G51160	A_95_P298558	NM_001325224.1	P93031	0.85	1.01	0.79	1.07					0.88
AT3G16000	A_95_P032811	NM_001325545.1	Q9LW85	-0.12	-0.84	-0.29	-1.29			-1.18		
AT5G51890	A_95_P238334	NM_001325829.1	Q9LT91	0.70	-0.12	-0.03	-0.07					-0.91
AT5G59590	A_95_P259746	NM_001325837.1	Q9LTH2	-0.47	-0.49	-0.27	0.07					2.32
AT4G10120	A_95_P235469	NM_001326164.1	F4JLK2	-0.09	-0.92	-0.22	-1.25					-1.75
AT1G06160	A_95_P034798	NM_001326275.1	Q9LND1	-0.22	0.16	0.03	-0.07					3.97
AT5G50250	A_95_P239919	X53932.1	Q9FGS0	-0.56	-0.43	-0.32	-0.20				-1.24	
AT3G04720	A_95_P018316	X58546.1	P43082	0.33	0.89	0.18	1.46	1.05				2.62
AT5G52640	A_95_P014536	X63195.1	P27323	3.51	2.78	3.31	3.81	1.52		-0.86		
AT3G22400	A_95_P029636	X84040.1	Q9LUW0	3.78	5.11	3.52	5.32	0.93				
AT3G53150	A_95_P016151	XM_016576986.1	Q9SCP6	-0.27	-0.97	0.37	-0.58	4.22				1.66
AT5G39860	A_95_P219782	XM_016577282.1	Q9FLE9	0.37	-0.71	-0.18	-0.92	-1.15				-1.07
AT4G35290	A_95_P146837	XM_016577533.1	Q93YT1	0.40	-0.51	0.89	0.04					-1.77
AT3G54250	A_95_P154872	XM_016577721.1	F4JCU3	1.26	2.24	1.55	2.21					-0.89
AT4G12040	A_95_P183177	XM_016578123.1	Q9SZ69	-0.12	-0.42	-0.15	-0.07					1.02
AT5G43420	A_95_P271411	XM_016578588.1	Q9LSW9	-0.10	-0.23	-0.07	-0.01	1.35		-1.34		3.38
AT5G27520	A_95_P022571	XM_016579360.1	Q8VZS0	0.92	0.69	0.61	1.14					3.58
AT1G13270	A_95_P230039	XM_016580504.1	Q9FV52	-0.34	-1.60	-0.56	-1.94				-2.07	
AT4G20070	A_95_P124602	XM_016580862.1	O49434	-0.88	-1.62	-0.26	-1.15				1.16	
AT2G43350	A_95_P253794	XM_016582394.1	O22850	0.10	-0.71	-0.74	-1.00	1.20				
AT3G12320	A_95_P199442	XM_016582529.1	Q9LHH5	0.32	-0.17	-0.34	-0.60				1.27	-1.53
AT1G06690	A_95_P290578	XM_016582546.1	Q94A68	-0.36	-1.29	-0.12	-1.32					-0.96
AT1G03370	A_95_P196152	XM_016582635.1	Q9ZVT9	-0.06	-0.94	-0.09	-1.12					2.12
AT5G46290	A_95_P268111	XM_016582863.1	P52410	-0.29	-1.51	-0.43	-1.36				-1.20	

Arabidopsis and tobacco identifiers				WT tobacco		VviPGIP1-tobacco		Primed *Arabidopsis*	Primed and infected *Arabidopsis*		*B. cinerea* infected *Arabidopsis*	
Locus Identifier Arabidopsis	Agilent microarray probe	Tobacco GenBank Accession	Tobacco UNIPROT ID	Δt0-24	Δt0-48	Δt0-24	Δt0-48	ISR-prime 2dpTi	ISR-boost 1dpi	ISR-boost 2dpi	BIDR 1dpi	BIDR 2dpi
AT3G47370	A_95_P198512	XM_016583959.1	Q9STY6	-0.25	0.12	0.10	-0.12				-1.26	
AT3G13450	A_95_P193182	XM_016584020.1	Q9LDY2	-0.51	-0.62	-0.40	-0.74					1.15
AT4G24230	A_95_P002156	XM_016584254.1	Q9STX1	-0.69	-0.62	-0.54	-0.38	-1.29			1.14	0.94
AT5G37300	A_95_P202612	XM_016585921.1	Q93ZR6	0.88	1.37	0.88	1.90					-3.78
AT3G09600	A_95_P146592	XM_016586289.1	Q8RWU3	-0.20	-0.92	-0.34	-1.06					-1.81
AT1G14030	A_95_P290163	XM_016586550.1	Q9XI84	0.01	0.11	-0.17	-0.09					-0.87
AT2G28190	A_95_P001976	XM_016586559.1	O78310	0.21	-1.09	-0.71	-1.89	-2.06				
AT4G26520	A_95_P002881	XM_016586812.1	P22197	1.37	3.17	1.36	3.00	-1.03				-1.26
AT5G45040	A_95_P061765	XM_016588305.1	Q93VA3	-0.38	-1.06	-0.54	-1.22	-1.65				
AT3G56480	A_95_P137212	XM_016588742.1	Q8GX05	-0.03	0.18	-0.12	0.20				0.94	
AT3G53460	A_95_P200817	XM_016588919.1	Q43349	-0.22	-1.12	-0.14	-1.36			1.07	-1.93	
AT4G21980	A_95_P188217	XM_016589225.1	Q8LEM4	-0.60	-0.43	-0.20	-0.81	1.52				
AT1G23740	A_95_P247907	XM_016589682.1	Q9ZUC1	-0.03	-1.59	-0.14	-1.56					-0.91
AT5G20630	A_95_P119912	XM_016589792.1	P94072	0.06	-0.01	0.04	-0.03				-2.50	-2.15
AT3G60245	A_95_P020706	XM_016589858.1	Q8RXU5	0.08	0.98	0.43	1.16				-0.87	
AT1G36240	A_95_P018341	XM_016590092.1	Q9C8F7	-0.10	0.52	0.69	1.10				-2.32	1.45
AT2G26310	A_95_P229729	XM_016591646.1	Q84RK2	0.04	-0.76	-0.40	-1.18	1.00				2.45
AT3G27210	A_95_P195442	XM_016591939.1	Q9LK32	0.01	0.58	-0.06	0.63					2.48
AT1G62750	A_95_P243737	XM_016592179.1	Q9SI75	-0.18	-0.25	-0.06	-0.47					-0.90
AT5G07470	A_95_P271396	XM_016592204.1	Q9LY14	-0.34	-0.92	-0.34	-1.18					0.88
AT2G28840	A_95_P203932	XM_016592906.1	Q94B55	-0.17	-0.64	-0.32	-0.64				-1.53	1.92
AT1G19570	A_95_P224547	XM_016593011.1	Q9FWR4	-0.15	-0.32	-0.07	-0.40					1.29
AT1G14150	A_95_P219217	XM_016593061.1	Q9XI73	-0.51	-0.94	-1.03	-1.79					-1.22
AT1G65520	A_95_P208727	XM_016593180.1	O04469	0.18	0.96	0.48	1.12					1.38
AT2G18600	A_95_P000806	XM_016593705.1	Q9ZU75	-0.01	0.06	0.11	0.07					0.85
AT5G51070	A_95_P025561	XM_016593934.1	P42762	1.14	0.89	0.83	1.53					2.04
AT1G68050	A_95_P253064	XM_016594093.1	Q9C9W9	-0.20	-1.29	-0.25	-1.22				-1.86	
AT2G32060	A_95_P107207	XM_016594197.1	Q9SKZ3	-0.67	-1.09	-0.01	-1.00				-1.41	
AT2G32720	A_95_P270277	XM_016594312.1	O48845	0.33	1.11	0.50	1.43					-0.88
AT1G72740	A_95_P214822	XM_016594728.1	F4IEY4	0.00	-0.92	-0.09	-0.94					0.92
AT3G52180	A_95_P207642	XM_016595441.1	Q9FEB5	-0.43	-0.97	-0.09	-1.29				-1.53	
AT4G15530	A_95_P210027	XM_016596105.1	O23404	0.10	0.93	0.31	0.79	1.62			2.29	
AT1G48100	A_95_P200497	XM_016596164.1	Q949Z1	-0.25	-0.97	-0.32	-1.56					-2.86
AT1G67360	A_95_P184877	XM_016596172.1	Q9FYF7	-0.25	-0.10	-0.12	0.14	1.49				
AT3G63130	A_95_P002446	XM_016596268.1	Q9LE82	-0.40	-0.89	-0.32	-1.00					2.85
AT2G45170	A_95_P123532	XM_016596561.1	Q8S926	-1.03	-0.79	-0.67	-1.09				0.88	
AT2G20740	A_95_P203367	XM_016596597.1	Q940P5	-0.67	-0.84	-0.45	-1.25			0.86		
AT4G28080	A_95_P268341	XM_016596794.1	F4JKH6	0.10	-0.09	0.11	-0.10					-1.23
AT2G32560	A_95_P164202	XM_016596858.1	Q8RY82	1.10	1.96	0.68	1.99					-0.87
AT5G49520	A_95_P260116	XM_016598355.1	Q9FGZ4	2.31	0.15	0.68	0.30					2.62
AT3G01180	A_95_P211267	XM_016598590.1	Q9MAC8	0.24	0.26	0.11	0.23					-1.07
AT3G62030	A_95_P193967	XM_016599418.1	P34791	-0.32	-0.74	-0.23	-0.79					-0.99
AT3G55800	A_95_P132377	XM_016599639.1	P46283	-0.14	-1.79	-1.03	-2.32					-0.97

Arabidopsis and tobacco identifiers				WT tobacco		VviPGIP1-tobacco		Primed *Arabidopsis*	Primed and infected *Arabidopsis*		*B. cinerea* infected *Arabidopsis*	
Locus Identifier Arabidopsis	Agilent microarray probe	Tobacco GenBank Accession	Tobacco UNIPROT ID	Δt0-24	Δt0-48	Δt0-24	Δt0-48	ISR-prime 2dpTi	ISR-boost 1dpi	ISR-boost 2dpi	BIDR 1dpi	BIDR 2dpi
AT3G26710	A_95_P105892	XM_016599863.1	Q9LSE4	0.24	-0.12	-0.50	-0.41					-1.01
AT5G60800	A_95_P160277	XM_016599993.1	Q9FJH5	-1.03	-2.18	-1.09	-1.79	1.91				
AT3G08720	A_95_P129857	XM_016600009.1	Q39030	0.73	0.99	0.61	1.50	1.27		-1.18		3.08
AT4G28100	A_95_P008051	XM_016600486.1	Q9SUC9	-0.07	0.43	0.00	0.36					-1.17
AT1G53870	A_95_P152152	XM_016600649.1	Q8LG32	-0.43	-2.32	-0.84	-2.56	-0.93			-1.08	0.98
AT5G53120	A_95_P194162	XM_016600766.1	Q94BN2	0.25	0.00	0.07	0.00	0.99				
AT3G02990	A_95_P290463	XM_016600975.1	Q9SCW5	-0.12	-0.67	-0.27	-0.38					0.95
AT5G54980	A_95_P141692	XM_016601316.1	Q9FFT2	-0.43	0.19	-0.25	0.10	-1.00				-1.02
AT4G35090	A_95_P132372	XM_016601638.1	P25819	-0.76	-0.71	-0.74	-0.92				1.02	
AT5G16970	A_95_P016006	XM_016601701.1	Q39172	0.08	-1.03	-0.51	-1.47				-1.10	
AT1G01820	A_95_P011321	XM_016602682.1	Q9LQ73	-0.74	-1.12	-0.71	-1.60					0.95
AT4G34730	A_95_P017881	XM_016602997.1	O65693	-0.01	-1.56	-0.56	-1.69					-0.90
AT4G04955	A_95_P013386	XM_016603413.1	Q94AP0	-0.09	-0.54	-0.47	-0.64	-1.43			1.85	
AT3G08710	A_95_P021026	XM_016603418.1	Q9C9Y6	0.54	0.40	-0.04	1.10					1.36
AT1G10700	A_95_P144742	XM_016603793.1	Q93Z66	-0.76	-0.79	-0.14	-1.18					1.20
AT3G25920	A_95_P226929	XM_016603870.1	P25873	-0.11	-1.14	-0.19	-1.19				-0.90	
AT4G03320	A_95_P018616	XM_016604052.1	Q9ZQZ9	-0.47	-0.74	-0.38	-0.94	1.49				2.67
AT2G14620	A_95_P093503	XM_016604292.1	Q9ZVK1	-0.12	-0.32	0.26	-0.01	4.37				
AT3G19130	A_95_P210567	XM_016604763.1	Q0WW84	0.04	-0.58	-0.25	-0.30					1.13
AT5G22440	A_95_P003941	XM_016605080.1	P59231	-0.22	-0.89	-0.81	-1.06				-1.14	
AT2G27040	A_95_P267016	XM_016605278.1	Q9ZVD5	-0.09	-0.36	-0.32	-0.49					-1.06
AT5G13010	A_95_P264551	XM_016605877.1	F4K2E9	0.18	-1.18	0.24	-1.03					0.97
AT3G07770	A_95_P142462	XM_016605998.1	F4JFN3	0.06	0.19	0.61	0.37					-1.09
AT1G08630	A_95_P213327	XM_016606047.1	Q8RXU4	-0.79	-0.54	-0.62	-0.60					5.64
AT1G76700	A_95_P120362	XM_016606921.1	Q8GYX8	0.04	-0.84	-0.14	-0.79					1.73
AT3G47430	A_95_P186702	XM_016607004.1	Q9STY0	-0.15	-0.15	-0.38	-0.58				1.01	-1.92
AT1G21400	A_95_P193622	XM_016607438.1	Q9LPL5	-0.94	-0.29	-0.74	-0.27	1.75				1.31
AT5G59310	A_95_P003971	XM_016607791.1	Q9LLR6	-0.92	-1.89	-0.49	-2.32	3.78		2.73		
AT2G32610	A_95_P212112	XM_016608017.1	O80898	1.78	3.40	2.29	3.71					-2.18
AT3G59760	A_95_P200982	XM_016608617.1	Q43725	-0.57	-1.03	-0.29	-1.54					0.88
AT5G05140	A_95_P020621	XM_016608649.1	Q9FHK9	0.12	-0.38	0.03	-0.10					1.55
AT1G09430	A_95_P300288	XM_016609171.1	O80526	2.03	2.73	1.56	2.94					0.96
AT4G17490	A_95_P202397	XM_016610186.1	Q8VZ91	0.00	0.21	0.68	0.32					1.83
AT3G16150	A_95_P230709	XM_016610556.1	Q8GXG1	-0.32	-1.22	-0.45	-1.56				2.30	
AT5G13800	A_95_P158892	XM_016611144.1	Q9FFZ1	0.55	0.79	0.14	1.13					0.99
AT3G26570	A_95_P155452	XM_016611925.1	Q38954	0.00	-0.43	-0.07	-1.18					-1.61
AT1G08830	A_95_P004446	XM_016612374.1	P24704	1.60	2.44	1.33	2.36				0.89	
AT1G19660	A_95_P008951	XM_016612689.1	Q93VH2	-0.10	-2.18	-0.51	-2.18					0.86
AT4G35480	A_95_P003881	XM_016612805.1	Q9ZT49	-0.29	-0.89	-0.12	-0.81					2.37
AT2G13650	A_95_P213347	XM_016613180.1	Q941R4	1.10	0.45	0.84	0.91					1.22
AT1G75100	A_95_P207302	XM_016613378.1	Q9C9Q4	-0.09	-1.64	-0.45	-1.94				0.92	-1.00
AT2G29090	A_95_P233549	XM_016613468.1	O81077	-0.06	-0.18	-0.07	-0.20	1.26				
AT3G63530	A_95_P153927	XM_016613693.1	Q8L649	-0.23	-0.34	-0.15	-0.47					-1.25

Arabidopsis and tobacco identifiers				WT tobacco		VviPGIP1-tobacco		Primed *Arabidopsis*	Primed and infected *Arabidopsis*		*B. cinerea* infected *Arabidopsis*	
Locus Identifier Arabidopsis	Agilent microarray probe	Tobacco GenBank Accession	Tobacco UNIPROT ID	Δt0-24	Δt0-48	Δt0-24	Δt0-48	ISR-prime 2dpTi	ISR-boost 1dpi	ISR-boost 2dpi	BIDR 1dpi	BIDR 2dpi
AT1G55060	A_95_P186027	XM_016614723.1	Q3E7K8	1.03	0.94	0.95	1.02					1.57
AT1G22770	A_95_P297428	XM_016615027.1	Q9SQI2	0.11	-1.06	-0.32	-1.22				-2.68	
AT4G16760	A_95_P015756	XM_016615669.1	O65202	0.18	0.90	0.45	1.06					1.48
AT5G49910	A_95_P115797	XM_016616306.1	Q9LTX9	-0.17	-0.79	0.31	-0.58				-1.28	
AT5G53490	A_95_P114542	XM_016616431.1	P81760	-0.36	-0.89	-0.42	-1.12				-0.89	
AT4G29010	A_95_P029151	XM_016616680.1	Q9ZPI6	0.37	1.46	0.29	1.65					0.87
AT5G64570	A_95_P008501	XM_016617387.1	Q9FLG1	-0.14	-0.17	-0.15	-0.14				1.02	1.50
AT2G42840	A_95_P291973	XM_016617882.1	Q9S728	0.82	0.11	-0.03	0.01			0.99		-2.37
AT1G17650	A_95_P179902	XM_016618380.1	F4I907	0.39	-1.40	-0.34	-1.69				-1.17	-0.92
AT5G61380	A_95_P127877	XM_016618561.1	Q9LKL2	-0.17	0.81	-0.07	0.80					2.38
AT1G64860	A_95_P221482	XM_016618636.1	O24629	-0.01	-1.12	-0.69	-1.51					-0.97
AT1G51700	A_95_P133022	XM_016619422.1	O82155	0.58	0.00	0.18	0.18			-1.01		
AT3G62600	A_95_P176252	XM_016619916.1	Q9LZK5	0.71	1.42	1.20	1.98	1.33				
AT5G17230	A_95_P306888	XM_016619957.1	P37271	0.23	0.93	0.28	0.73					-0.94
AT5G36880	A_95_P296688	XM_016620129.1	B9DGD6	0.42	0.10	0.39	0.29					0.97
AT4G25050	A_95_P018521	XM_016621124.1	Q9SW21	0.42	1.98	0.76	1.89					-0.88
AT3G51860	A_95_P178907	XM_016621451.1	Q93Z81	-0.25	-0.36	0.34	-0.81	1.31				
AT1G07420	A_95_P134702	XM_016621855.1	Q8VWZ8	-0.12	-1.64	-0.43	-1.22				-1.65	0.95
AT1G59900	A_95_P141087	XM_016622093.1	P52901	0.73	1.89	0.94	2.00				-0.91	
AT5G55730	A_95_P144992	XM_016622323.1	Q9FM65	-0.10	0.23	0.06	0.31					-1.29
AT5G09420	A_95_P148587	XM_016622490.1	F4KCL7	-0.06	0.37	0.14	0.39	1.00				1.61
AT5G65220	A_95_P134807	XM_016622535.1	Q9FJP3	-0.04	-0.92	-0.17	-1.29				-1.96	
AT5G02120	A_95_P131142	XM_016623812.1	O81208	0.32	-0.97	-0.84	-2.00					-1.02
AT1G72540	A_95_P097073	XM_016625539.1	Q9CAH1	0.28	-0.04	0.28	0.26	2.98				2.46
AT2G28800	A_95_P022606	XM_016625742.1	Q8LBP4	-0.18	-0.86	-0.14	-1.00					-1.24
AT5G06690	A_95_P295468	XM_016626383.1	Q9FG36	-0.62	-2.25	-1.32	-2.64				-1.57	
AT5G08280	A_95_P198297	XM_016626401.1	Q43316	-0.36	-1.25	-0.81	-1.64				-1.57	
AT5G24470	A_95_P276723	XM_016626415.1	Q6LA42	-0.15	0.37	-0.10	0.85				-5.75	
AT5G07100	A_95_P101338	XM_016627164.1	Q9C5T3	1.04	-0.06	0.48	0.29					3.34
AT3G54500	A_95_P095268	XM_016627622.1	F4JCX9	0.75	-1.03	-0.03	-1.29				2.04	
AT2G01180	A_95_P123327	XM_016629129.1	Q9ZU49	1.00	-0.43	0.06	-0.06				0.94	1.58
AT1G68010	A_95_P129652	XM_016629378.1	Q9C9W5	-0.29	-0.74	-0.79	-1.43				1.02	-1.08
AT4G14220	A_95_P268221	XM_016629553.1	Q4TU14	-0.17	-0.43	0.25	-0.38					1.29
AT5G47560	A_95_P141122	XM_016630055.1	Q8LG88	-0.36	-1.29	-0.60	-1.64				1.94	-0.98
AT2G20450	A_95_P183752	XM_016630134.1	Q9SIM4	-0.01	-0.06	0.50	0.03				-0.96	
AT1G14880	A_95_P142762	XM_016630354.1	Q9LQU2	0.24	-0.15	-0.49	-0.07	3.08			-1.81	2.08
AT4G33670	A_95_P013391	XM_016630716.1	O81884	-0.56	-0.76	-0.30	-1.09				-1.03	
AT1G60890	A_95_P094558	XM_016630791.1	Q8RY89	-0.92	-1.47	-0.14	-1.29	0.85				
AT1G08290	A_95_P124327	XM_016632141.1	Q9SGD1	-0.47	-0.81	-0.36	-0.76					1.20
AT1G76990	A_95_P008976	XM_016633016.1	O49285	-0.79	-1.89	-0.86	-2.25				1.45	
AT2G22450	A_95_P230879	XM_016633744.1	Q6NLQ7	-0.12	-0.27	-0.29	-0.40				-2.84	
AT4G26670	A_95_P011006	XM_016634477.1	Q94EH2	-0.36	-0.69	-0.18	-0.89				-4.15	
AT1G78580	A_95_P124277	XM_016635437.1	Q9SYM4	0.07	-0.67	-0.10	-0.69					-1.46

Arabidopsis and tobacco identifiers				WT tobacco		VviPGIP1-tobacco		Primed *Arabidopsis*	Primed and infected *Arabidopsis*		*B. cinerea* infected *Arabidopsis*	
Locus Identifier Arabidopsis	Agilent microarray probe	Tobacco GenBank Accession	Tobacco UNIPROT ID	Δt0-24	Δt0-48	Δt0-24	Δt0-48	ISR-prime 2dpTi	ISR-boost 1dpi	ISR-boost 2dpi	BIDR 1dpi	BIDR 2dpi
AT3G03780	A_95_P177577	XM_016635962.1	Q9SRV5	1.32	2.81	1.46	3.12					-1.13
AT1G35260	A_95_P013731	XM_016636170.1	Q9C7I7	0.04	-0.51	-0.51	-1.06		1.62			
AT5G07180	A_95_P189767	XM_016637134.1	Q6XAT2	0.12	-0.49	-0.25	-0.56					-1.91
AT2G24270	A_95_P133327	XM_016637789.1	Q1WIQ6	0.36	0.14	-0.40	-0.60				0.90	-1.15
AT3G48700	A_95_P200257	XM_016638708.1	Q9SMM9	-0.15	-0.60	-0.15	-0.45					-1.64
AT5G55260	A_95_P241920	XM_016639329.1	P48528	-0.12	-0.25	-0.34	-0.30					-1.37
AT5G13450	A_95_P009611	XM_016639554.1	Q96251	0.01	1.01	0.18	0.86				-1.04	
AT1G19870	A_95_P199367	XM_016639603.1	Q9FXI5	-0.30	-1.94	-0.71	-1.84				1.22	
AT5G23210	A_95_P013526	XM_016640306.1	Q0WPR4	0.03	-1.22	-0.10	-1.00			1.33		
AT1G50250	A_95_P132852	XM_016641914.1	Q39102	0.07	-1.29	-0.06	-1.47					-0.87
AT1G78320	A_95_P187112	XM_016642056.1	Q9M9F1	3.01	2.90	2.64	3.31					-1.59
AT4G04020	A_95_P218767	XM_016642070.1	O81439	-0.43	-0.69	0.08	-1.09				1.27	-0.88
AT3G28900	A_95_P001136	XM_016642912.1	Q9LJW6	-0.27	-0.89	-0.14	-1.03				-1.02	
AT1G79940	A_95_P031501	XM_016643891.1	Q0WT48	0.42	0.81	0.44	1.21					0.86
AT1G78895	A_95_P133817	XM_016644023.1	Q8GWH5	0.78	0.86	0.51	1.22					1.14
AT1G76405	A_95_P013761	XM_016644192.1	Q9FPG2	-0.92	-1.40	-0.34	-1.36	-1.01				
AT1G11430	A_95_P267636	XM_016644371.1	Q9LPZ1	0.07	-0.86	-0.14	-1.03				-1.72	
AT5G48545	A_95_P133867	XM_016644904.1	F4K1R2	-0.15	-0.76	-0.47	-1.06	-1.18				-1.14
AT3G59290	A_95_P028296	XM_016645013.1	Q93YP4	1.00	1.61	0.99	2.09					0.94
AT2G15890	A_95_P023016	XM_016645570.1	Q9XIM0	-0.81	-1.79	-0.42	-1.89	-1.10			-2.92	
AT1G60600	A_95_P137272	XM_016645906.1	Q0WUA3	-0.06	-1.25	-0.47	-1.29	-1.51				-0.99
AT5G38510	A_95_P002986	XM_016647065.1	Q9FFX0	0.31	-2.12	-0.79	-2.64					-0.86
AT4G31950	A_95_P186802	XM_016647788.1	O49396	0.90	-0.07	0.58	0.30			-1.74		2.91
AT3G55400	A_95_P139252	XM_016647988.1	Q9M2T9	-0.12	-1.25	-0.17	-1.29				-0.90	
AT3G28200	A_95_P177717	XM_016648002.1	Q9LHA7	-0.05	-0.61	-0.53	-1.01	-1.10			-0.93	
AT4G17486	A_95_P013926	XM_016648510.1	Q93VG8	0.99	0.59	0.40	0.86					1.12
AT2G39570	A_95_P150957	XM_016649203.1	O80644	-0.62	-0.86	-0.67	-0.92				1.70	
AT4G16260	A_95_P202527	XM_016650401.1	Q8VZJ2	0.15	-0.56	0.03	-0.47	1.00		-0.98		5.73
AT3G06980	A_95_P204567	XM_016650666.1	Q8GUG7	-0.10	-0.76	-0.04	-1.00					-1.24
AT4G26540	A_95_P193632	XM_016650945.1	C0LGR3	0.07	0.86	0.14	0.70	-0.86				-1.35
AT1G65590	A_95_P269001	XM_016651789.1	Q8L7S6	-0.67	-1.32	-0.29	-1.69	-0.88		0.90		
AT2G18950	A_95_P203402	XM_016652007.1	Q8VWJ1	-0.25	-0.69	-0.38	-0.74					1.08
AT4G14450	A_95_P223337	XM_016652649.1	Q6NN02	0.49	0.34	0.01	-0.09		-3.34	-1.45		1.71
AT3G20770	A_95_P127302	XM_016653788.1	O24606	-0.10	-0.71	0.03	-0.30					0.97
AT2G33255	A_95_P263056	XM_016653964.1	Q8RYE9	-0.18	-0.20	-0.14	-0.07					-1.14
AT4G33150	A_95_P141327	XM_016654377.1	Q9SMZ4	-1.22	-0.29	-0.76	0.10					2.47
AT5G46800	A_95_P017346	XM_016654794.1	Q93XM7	0.03	-0.10	-0.62	-0.36					-1.23
AT1G07320	A_95_P103182	XM_016655906.1	O50061	0.12	-0.69	0.15	-1.06					-0.91
AT5G26742	A_95_P310398	XM_016655944.1	Q8L7S8	0.03	0.46	-0.07	-0.01				-0.94	-1.40
AT2G47060	A_95_P204127	XM_016656372.1	O80719	1.24	1.93	0.86	1.84				0.89	
AT4G36830	A_95_P128397	XM_016656572.1	Q9SYY4	-0.01	0.33	-0.17	0.04					-1.82
AT5G54660	A_95_P123157	XM_016657129.1	Q9FIT9	2.14	2.88	2.27	3.62					-1.12
AT5G61210	A_95_P030971	XM_016657869.1	Q9S7P9	1.24	0.85	0.60	1.10					1.60

Arabidopsis and tobacco identifiers				WT tobacco		VviPGIP1-tobacco		Primed *Arabidopsis*	Primed and infected *Arabidopsis*		*B. cinerea* infected *Arabidopsis*	
Locus Identifier Arabidopsis	**Agilent microarray probe**	**Tobacco GenBank Accession**	**Tobacco UNIPROT ID**	**Δt0-24**	**Δt0-48**	**Δt0-24**	**Δt0-48**	**ISR-prime 2dpTi**	**ISR-boost 1dpi**	**ISR-boost 2dpi**	**BIDR 1dpi**	**BIDR 2dpi**
AT2G32710	A_95_P136517	XM_016658417.1	Q8GYJ3	-0.51	-1.79	-0.40	-1.69				0.94	
AT4G35060	A_95_P020276	XM_016659717.1	O49613	-0.62	-2.06	-1.22	-2.47	-1.49				
AT3G11750	A_95_P266811	XM_016659755.1	Q9SF23	-0.76	-1.12	-0.62	-1.22					-0.90
AT2G06530	A_95_P248172	XM_016659774.1	Q9SKI2	0.62	0.74	0.03	0.70					0.96
AT1G51500	A_95_P205667	XM_016660158.1	Q9C8K2	-0.23	-1.36	-0.34	-1.56					-0.90
AT5G01190	A_95_P048726	XM_016660205.1	Q6ID18	-0.14	-0.94	-0.34	-1.32					-1.09
AT2G44160	A_95_P120637	XM_016660347.1	O80585	1.65	3.59	1.95	3.92					-0.88
AT2G28720	A_95_P185322	Y11208.1	Q9SI96	-0.07	-0.92	-0.29	-1.51				-1.24	
AT2G47470	A_95_P190742	Y11209.1	O22263	0.38	1.37	1.15	1.83	1.04				

Chapter 4

In a *Botrytis*-tobacco pathosystem, overexpression of a grapevine PGIP reduced oxidative stress during lesion development and enhanced secondary metabolism in infected leaves and leaves distal to the infection

In a *Botrytis*-tobacco pathosystem, overexpression of a grapevine PGIP reduced oxidative stress during lesion development and enhanced secondary metabolism in infected leaves and leaves distal to the infection

4.1 Introduction

Botrytis cinerea is an obligate necrotrophic filamentous fungus that causes grey mould on over 500 plant genera (Fillinger and Elad, 2016). As a classical example of necrotrophic phytopathogens, *B. cinerea* both requires and stimulates host plants to activate the hypersensitive response (HR, Govrin and Levine, 2000), possessing numerous HR-inducing toxins (Frías et al., 2011, 2016; Rossi et al., 2011; Zhang et al., 2015) and anti-apoptotic machinery that enables the fungus to survive the initial plant defence response (Shlezinger et al., 2011).

A critical component of its infection strategy is the degradation of the plant cell wall, firstly to penetrate the host tissue, and secondly to colonise the surrounding tissue. To aid in this, *B. cinerea* possesses an array of cell wall degrading enzymes (Kars and Van Kan, 2007), with the degradation of pectin in the anticlinal cell wall being an essential step in the penetration of the host tissue. Pectin, a polymer with a galacturonic acid backbone, is degraded by polygalacturonases (PGs), of which *B. cinerea* possesses six isoforms (BcPG1-6) with varying pH optima and expression patterns (Kars et al., 2005). Two BcPGs, BcPG1 and BcPG2, are required for full virulence on several hosts, being important for secondary infection and primary lesion formation respectively (Kars et al., 2005; Ten Have et al., 1998).

Given the importance of PGs for successful infection, the evolution of plant proteins that inhibit them comes as no surprise. Polygalacturonase-inhibiting proteins (PGIPs) are plant leucine-rich repeat (LRR) proteins with the capacity to inhibit specific PGs (Cervone et al., 1989; De Lorenzo and Ferrari, 2002; Kalunke et al., 2015). Increased resistance to *B. cinerea* has been observed following expression, among others, of bean PGIP in tobacco (Manfredini et al., 2005), pear PGIPs in grapevine (Agüero et al., 2005) and tomato (Powell et al., 2000) and overexpression of native PGIPs in *Arabidopsis* (Ferrari et al., 2003). The classical mode-of-action of PGIPs relies on their ability to enhance the oligogalacturonide (OG)-dependent activation of defences, since they delay the degradation of elicitor-active OGs (Kalunke et al., 2015). Furthermore, this mode-of-action appears to rely on salicylic acid (SA) activated defence signalling (Benedetti et al., 2015; Liu et al., 2017).

Vitis vinifera possesses one isoform of PGIP, namely VviPGIP1 (Joubert et al., 2006). Expression analysis in grapevine showed that it had organ-specific and developmentally-regulated expression

patterns (Joubert et al., 2013). Expression was detected in berries at the véraison stage and in roots, while analysis of the promoter in tobacco showed that it was induced in all plant organs by infection with *B. cinerea*. It was confirmed that VviPGIP1 effectively inhibited BcPG1, BcPG2 and BcPG6 (Joubert et al., 2006, 2007). Interestingly, *in vivo* infiltration studies in *Nicotiana benthamiana* established that although VviPGIP1 effectively inhibited BcPG2, the protein pair was found not to interact directly, using plasmon resonance analysis (Joubert et al., 2007).

To study the defence roles of VviPGIP1, the gene was constitutively expressed in *Nicotiana tabacum* (Joubert et al., 2006). Following inoculation, *B. cinerea* was able to form primary lesions and initiate lesion expansion, but, in contrast to the unhindered maceration of wild-type tobacco, lesion expansion on transgenic plants was delayed and restricted and no fungal reproductive structures were formed. Though many PGIP genes have been similarly expressed in heterologous plant systems and subjected to pathogen infections to determine defense phenotypes, few studies have analysed the biological processes that were affected by overexpression, whether before or during infection. Prior studies have already profiled VviPGIP1-expressing tobacco lines prior to infection, identifying transcriptional and metabolic changes indicative of a pre-infection primed defence state (Alexandersson et al., 2011; Nguema-Ona et al., 2013). In this study, the aim was therefore to evaluate the transcriptional response of the VviPGIP1-expressing tobacco lines when challenged with *Botrytis*. The transcriptional response of tobacco to *Botrytis* (presented in Chapter 3) will be used as baseline to compare the susceptible (WT) and the resistant (PGIP) phenotypes at the infection spots as well as in a leaf distal to the infection over the first 48 hours post challenge.

4.2 Materials and methods

4.2.1 Plant and fungal material

Wild-type *Nicotiana tabacum* SR1 cv Petit Havana (WT tobacco) and a fully characterised transgenic tobacco line constitutively expressing the VviPGIP1 gene (VviPGIP1-tobacco line 37 as reported in Alexandersson et al., 2011; Joubert et al., 2006; Nguema-Ona et al., 2013) was grown and maintained as described in Alexandersson et al. (2011). Transgenic seeds were germinated under kanamycin selection. Growth conditions, pre-infection acclimation, whole plant infection assay and sampling were performed as described in Chapter 3 of this thesis. The hypervirulent grape isolate of *B. cinerea* (Joubert et al., 2006; Rowe et al., 2010) was cultured, harvested and prepared as described in Chapter 3.

4.2.2 Gene expression analysis and data analysis

RNA extraction, quantitative reverse-transcriptase PCR (qRT-PCR) and microarray analyses were performed as described in Chapter 3. Transgene expression was confirmed using qRT-PCR with gene specific primers 5'- AGCACCACACAAGCACCGATT-3' and 5'- ACGTCGTTGGACCTTTCG-CATAAC-3'. Samples from VviPGIP1-tobacco were analysed on the second channel of the dual-

colour array used as described in Chapter 3. Channel allocations (see Table 3.1 and MIAME documentation; Appendix A to Chapter 3) for leaf 3 (local response) included a dye swap for one of the three technical repeats, but a misunderstanding with Oxford Gene Technologies regarding experimental design meant that no dye swaps were included for leaf 2 (distal response). Data normalisation, curation (Appendix C to Chapter 3) and analysis was performed in parallel for data presented here and in Chapter 3. Log ratio-mean average plots (MA-plots, Dudoit et al., 2002) were used to evaluate the quality of the microarray data (refer to Appendix B to Chapter 3). A single replicate (Systemic t12-c) of VviPGIP1-tobacco had been analysed on a faulty channel and was therefore omitted from data processing. Data from leaf two, representative of a younger leaf undergoing a distal response on an infected plant, and leaf three, representing a leaf reacting with a localised response at and around the infection spot (refer to Figure 3.1 of Chapter 3), were analysed as separate experiments, using identical workflows. The annotation of the probe targets was performed as described in Chapter 3, using the Basic Local Alignment Search Tool (BLAST) in NCBI (Johnson et al., 2008), an in-house Ortho-MCL workflow (Bengtsson et al., 2014) or the original Agilent microarray annotation (www.genomics.agilent.com). The Ortho-MCL approach generated a custom gene ontology (GO) annotation that was used for GO enrichment analyses in GOEAST (Zheng and Wang, 2008). To calculate significant differences between transcript levels of wild-type and VviPGIP1-expressing tobacco, fold change was calculated between the VviPGIP1-tobacco line and WT at each sampling point. Only probes with a fold change of two or more were considered, to avoid artefacts due to dye bias.

Data represented in figures and tables were either represented as 1) fold changes between sampling points (represented by the prefix “Δt”) calculated relative to the earlier sampling point, or 2) as a fold changes between the WT and VviPGIP1-tobacco genotypes at one sampling point (relative to WT expression and represented by the prefix “Δg”) or 3) as normalised fluorescence intensities (represented by the prefix “t”) that were expressed relative to the relevant uninfected control (i.e. the t0 samples always have a value of 1).

4.2.3 Analysis of residual volatile organic compounds

Volatile organic compound (VOC) analysis and quantification proceeded as presented in Chapter 3.

4.2.4 Analysis of redox-related compounds in *B. cinerea* infected tissue

Antioxidant capacity

Ground leaf disks from leaf 4 were used to perform an oxygen radical absorbance capacity (ORAC) assay (Ou et al., 2001). Extracts were prepared as described according to Marnewick et al. (2003) and using 50 µM Trolox (6-hydroxy-2,5,7,8-tetramethylchroman-2-carboxylic acid) as standard. The ORAC values were normalised to fresh weight and expressed as µmol Trolox equivalents per mg fresh weight.

Leaf disk infection, histochemical staining and image analysis

A leaf disk infection assay was performed to investigate the progression of hydrogen peroxide production during infection (Asselbergh et al., 2007; Thordal-Christensen et al., 1997). Plants were maintained as described before until the eight-leaf stage. Three plants and six leaf disks per plant line were used for each sampling point. Leaf disks were excised from the third leaf position using a 1 cm diameter cork-borer and floated adaxial side up on sterile water in covered 24-well cell culture plates (Nunc, Roskilde, Denmark). As negative control for the infection, two leaf disks per leaf were used for mock inoculation and an assay control was included by floating one leaf disk from each leaf on a catalase solution (1100 U/mL). *B. cinerea* was prepared as described before and were pre-germinated for 2 hours in 50% sterile grape juice in the dark. The infection was initiated by inoculating 5000 spores in a single droplet onto each leaf disk. Leaf disks were incubated in the dark at 23°C for the duration of the infection. In order to visualise hydrogen peroxide formation, leaf disks were transferred to a 1 mg/mL 3,3-diaminobenzidine-HCl (pH 4, DAB) staining solution. Leaf disks were fixed by boiling for 10 minutes in 96% ethanol, causing the formation of a brown precipitate and were stored in 96% ethanol until further analysis. Preliminary assays with an extended time series (every three hours until 48 h post infection) showed that infected leaf disks became too fragile for staining around t48 due to the maceration activity of the infections, and that staining only became visible from t12 onwards; sampling/fixing was therefore conducted at t15, t18, t24 and t48.

Image capture of the leaf disks was done by placing the leaf disks between two sheets of clear cellulose acetate and scanning the disks in Red-Green-Blue colour at a resolution of 600 dots per inch. The resulting images were stored as JPEG. For quantitative analysis, the colour images were converted to greyscale and brightness and contrast were auto-adjusted before analysis with ImageJ software (National Institutes of Health, Bethesda, MD, USA). The threshold tool was used to delineate browned areas and the wound-induced hydrogen peroxide stain (Figure 4.1) was excluded using the wand tool. The *Botrytis*-induced hydrogen peroxide stain was quantified by counting the pixels in the browned area. The analyses distinguished between the wound-induced hydrogen peroxide, that was visible as a distinct ring on the border of the leaf disk, and the *Botrytis*-induced hydrogen peroxide, that was defined as internal browning distinct from the wound-induced hydrogen peroxide stain.

Qualitative analysis of the *Botrytis*-induced hydrogen peroxide stains was included by scoring the different stains and counting the occurrence of each of these classes for comparative purposes (expressed as % of occurrence). Two main features were observed: spots with a clear border with a uniform dark stain, or a speckled/diffuse spot, with darker and lighter areas within the bounds of the internal browned area. Examples of stained disks are shown in Figure 4.1 to contextualise the scoring and typical features of the stained leaf disks.

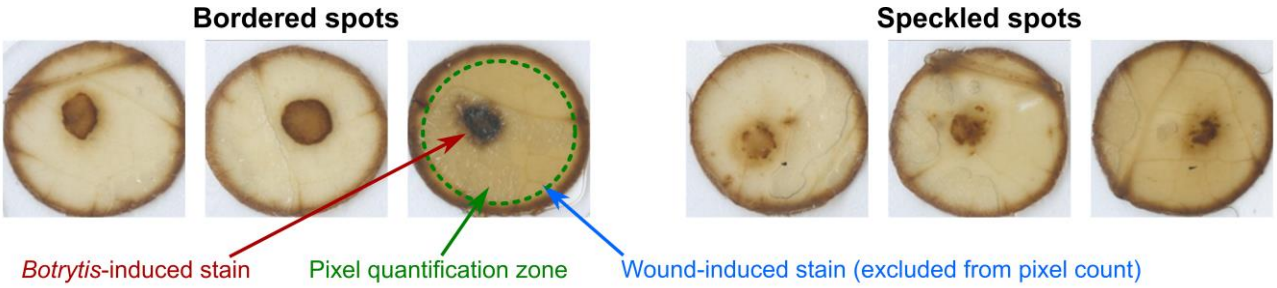

Figure 4.1 Qualitative and quantitative analysis of *in situ* hydrogen peroxide staining of infected leaf disks at 24 hours after infection by *Botrytis cinerea*. Qualitative analysis of diaminobenzidine stained leaf disks categorised infection-induced stains as bordered or speckled spots. For quantification of the stained area (red arrow), the wound-induced H_2O_2 stain (blue arrow) was excluded and the number of dark pixels of the remaining area (green dotted line) were counted.

4.3 Results

4.3.1 Lesion morphology showed characteristics of *B. cinerea* resistance

To verify expression of the transgene (*Vvipgip1*), qRT-PCR was performed on samples collected during the infection assay and confirmed expression of *Vvipgip1* in all leaves (Figure 4.2). The gene expression analysis was conducted in the first 48 hours after infection and there was no visual difference between WT and the VviPGIP1-tobacco line in primary lesion formation (t36) and the first stage of lesion expansion (t48) (Figure 4.3A). Differences in lesion morphology were clear at nine days after infection (Figure 4.3B), where the lesions on the transgenic leaves were dry and necrotic, while WT leaf lesions had a wide zone of macerated tissue. The edge of the lesions on the VviPGIP1-tobacco plants were clearly delineated, compared to the blurred boundary of the lesions on WT tobacco.

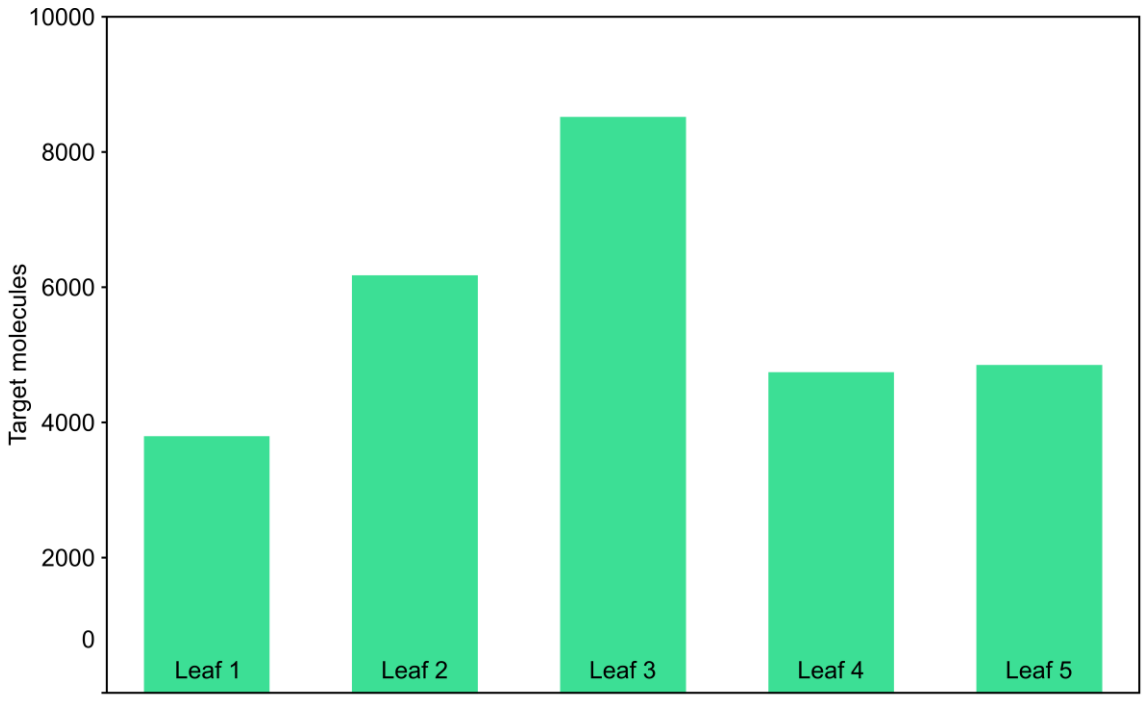

Figure 4.2 VviPGIP1 expression in leaves collected at 0 hours post infection during the whole-plant infection assay. Target molecules were quantified using linear regression of expression.

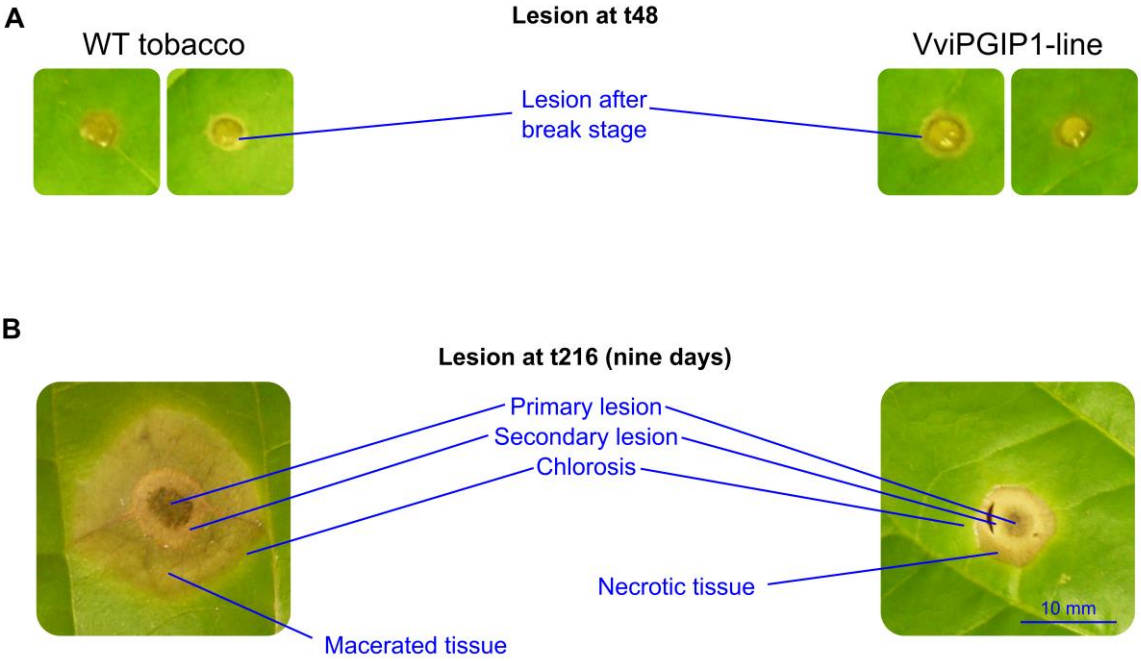

Figure 4.3 *B. cinerea* lesion appearance after infection with 5000 spores of a hypervirulent grapevine isolate on WT and VviPGIP1-tobacco. A. At t48 lesions have passed the "break stage", spreading past the boundaries of the inoculation spot. B. Nine days after infection clear differences in lesion morphology were observed between WT and the VviPGIP1-line.

4.3.2 Curation of expression data

Expression data from leaves two (distal to the infection) and three (infected, local lesion analysed) were curated to remove data from probes that showed consistently low signal or excessive variation (Appendix C to Chapter 3). This removed 64% of the probes on the array. Following filtering based on fold change, orthogonal partial least squares discriminate analysis (OPLS-DA) and identification of duplicate targets, 3521 transcripts were transcriptionally regulated in tissue including and surrounding the infection spot or in the leaf distal to the infection in WT tobacco (see Chapter 3). An additional 294 transcripts were identified as regulated in the VviPGIP1-tobacco plants, comprising a total of 3815 transcripts. Thirty-one transcripts did not pass the fold change or OPLS-DA filter, but had a minimum two-fold difference between samples from WT and VviPGIP1-expressing tobacco at the same sampling point. Finally, only transcripts that were significantly (fold change ≥ 2) regulated between two consecutive sampling points (i.e. 12 h-intervals) or between uninfected (t0) and t48 were used for further analysis. Therefore, subsequent analyses were performed on 3468 genes that were transcriptionally regulated during the time-course. 2491 transcripts were transcriptionally regulated between consecutive sampling points in tissue including and surrounding the infection spot, while 754 transcripts were only significantly regulated between t0 and t48. In the leaf distal to the infection, 2187 transcripts were regulated between consecutive sampling points and 43 were regulated between t0 and t48. Only three transcripts were significantly different between WT and VviPGIP1-expressing tobacco at one or more sampling points while not passing the 2-fold threshold for regulation between sampling points.

4.3.3 The local expression profile of the VviPGIP1-line in comparison with WT tobacco

Overview of expression levels and biological processes during lesion development

Multivariate analysis was used to identify broad patterns in the transcriptomic data. Figure 4.4 shows the principal component analysis (PCA) score plot of the curated transcripts representing the lesion expression profiles of WT tobacco and the VviPGIP1-expressing line. Two principal components were able to explain 79% of variation in the lesion expression profile. PCA score points of replicate samples were grouped according to sampling times in the time-course. Separation between WT and VviPGIP1-expressing tobacco increased gradually in the first three sampling-points (t0, t12 and t24) of the time-course, but this separation was not evident for the two latter sampling-points (t36 and t48).

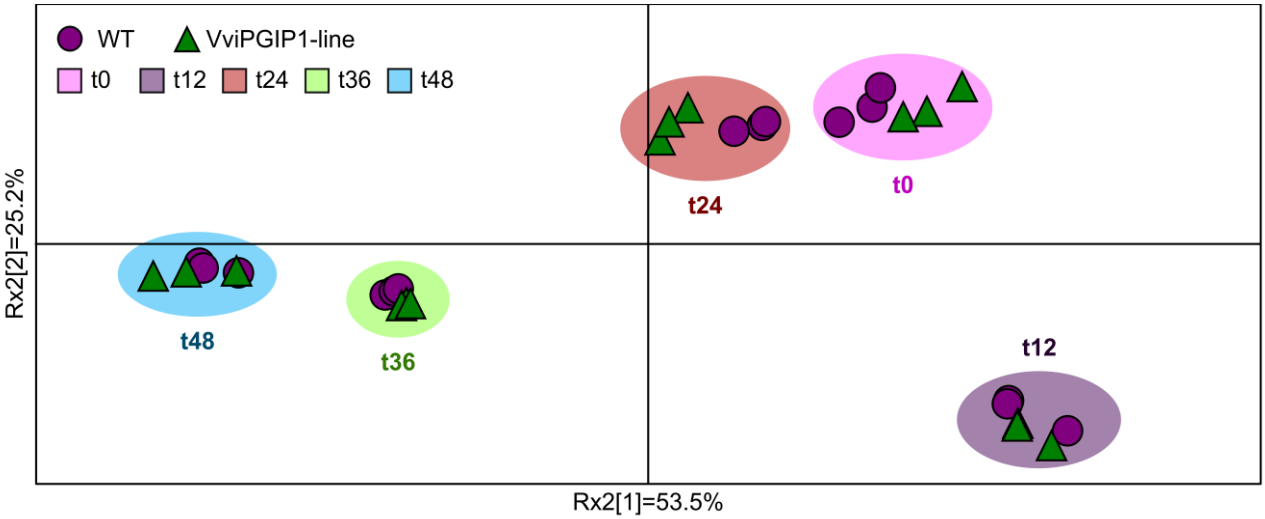

Figure 4.4 Principal component analysis score plots of curated transcriptional data for the local expression profile in WT- and VviPGIP1-tobacco. Axes are annotated with the percentage variance (R2x) explained by each principal component.

To identify biological processes that were operating differently over time in WT and VviPGIP1-expressing tobacco, GO enrichment analysis was performed on genes within each 12 h-interval that were differentially induced (fold change ≥ 2) or repressed (fold change ≤ 0.5). The significantly ($p<0.001$) enriched terms (Appendix A to Chapter 4) across the four periods were analysed using a Venn diagram (Figure 4.5A) to identify common and unique processes regulated in WT tobacco and/or the VviPGIP1-line.

Many defence/stress-related ontologies were transcriptionally regulated in both lines (Figure 4.5B), however chitin catabolism, phenylpropanoid biosynthesis and responses to endoplasmic reticulum stress, oxidative stress and osmotic stress were not enriched in the VviPGIP1-line but only in WT. Several energy generation-related ontologies were uniquely enriched in VviPGIP1-expressing tobacco, including ATP generation from ADP, glycolytic process, carbohydrate catabolism and pyruvate metabolism, as were key photosynthesis-related aspects such as chloroplast organisation,

tetrapyrrole biosynthesis and responses of blue and far-red light. Translation and peptide biosynthesis was uniquely enriched in VviPGIP1, suggesting altered protein synthesis in the resistant line.

A

B

VviPGIP1-tobacco local expression profile only	WT and VviPGIP1 tobacco local expression profiles	WT tobacco local expression profile only
DEFENCE-RELATED	DEFENCE-RELATED	DEFENCE-RELATED
response to bacterium	defence response	chitin catabolism
	defence response to bacterium	
METABOLIC PROCESSES	defence response to fungus	RESPONSES TO STIMULI
ATP generation from ADP		response to endogenous stimulus
amide biosynthesis	RESPONSES TO STIMULI	response to endoplasmic reticulum stress
carbohydrate catabolism	response to cold	response to heat
glucan metabolism	response to metal ion	response to hormone
glycolytic process	response to organic substance	response to organic cyclic compound
peptide biosynthesis	response to oxygen-containing compound	response to osmotic stress
pyruvate metabolism	response to stress	response to oxidative stress
translation	response to temperature stimulus	response to water deprivation
	response to wounding	
LIGHT/PHOTOSYNTHESIS-RELATED		METABOLIC PROCESSES
chloroplast organization	METABOLIC PROCESSES	carbohydrate derivative catabolism
plastid organization	carbohydrate metabolism	cell wall macromolecule catabolism
tetrapyrrole biosynthesis	coumarin biosynthesis	coenzyme metabolism
response to blue light	nicotinamide nucleotide metabolism	cofactor metabolism
response to far red light	nitrogen compound metabolism	monocarboxylic acid metabolism
	organonitrogen compound biosynthesis	one-carbon metabolism
	oxidoreduction coenzyme metabolism	organonitrogen compound catabolism
	pyridine nucleotide metabolism	phenylpropanoid biosynthesis
		primary metabolism
	LIGHT/PHOTOSYNTHESIS-RELATED	secondary metabolism
	photosynthesis	transition metal ion homeostasis
	response to radiation	
	response to light stimulus	LIGHT/PHOTOSYNTHESIS-RELATED
		circadian rhythm

Figure 4.5 Enriched biological processes of the local expression profiles of WT and VviPGIP1-tobacco. A. Venn diagram overlaying the enriched biological processes differentially expressed in 12-hour intervals. B. Summary of the processes that are unique to or shared between the WT and VviPGIP1-line lesion expression profiles.

Enhanced or accelerated expression in infected VviPGIP1-tobacco tissue

When transcript levels were compared at individual sampling points (Appendix C to Chapter 4), the number of transcripts with a minimum fold change of two between WT and the VviPGIP1 line (Figure 4.6A) confirmed the patterns observed using PCA. The Mapman annotations of these transcripts (Figure 4.6B,) revealed that the most represented category was the light reaction of photosynthesis (31 transcripts), while biotic and abiotic stress was the second most common category (13 and 9 transcripts respectively). The expression levels of photosynthesis-related transcripts were higher at t0 in the transgenic lines, but lower at t24. The transcripts mainly encoded chlorophyll binding proteins, with some components of the photosystem I light harvesting complex.

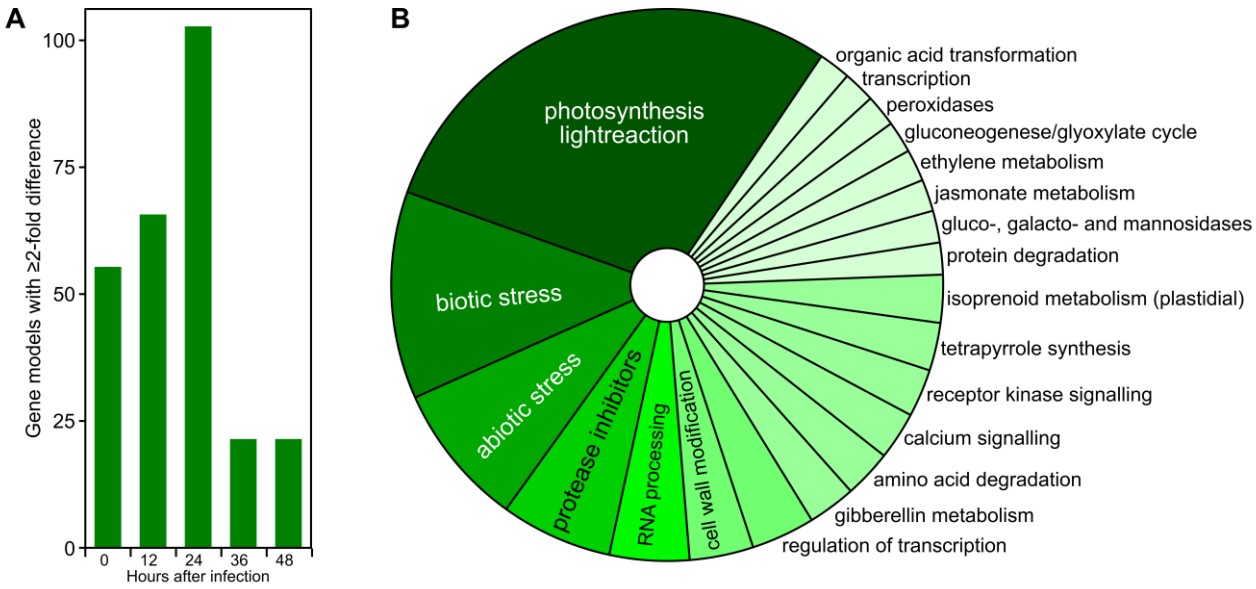

Figure 4.6 Comparison of WT- and VviPGIP1-tobacco at individual sampling points in the local expression profile. A. Number of gene models with a minimum two-fold difference between lines. B. Mapman annotations of gene models differing at one or more sampling point. Shading indicates the number of gene models with the specified annotation. Only bins representing at least two gene models are shown. The full data table is available as Appendix C to Chapter 4.

Pathogenesis-related (PR) protein transcripts for PR-1A, PR4-A, PR-1B and PR-5 (osmotin) were enhanced at t24 or t36, but other osmotin transcripts, systemic acquired resistance-related protein family 8.2 (SAR8.2), antimicrobial peptide (SN1a) and two Avr9/Cf-9 rapidly elicited proteins were repressed at t12 in the PGIP line. In contrast, heat shock protein-encoding genes were enhanced at t48. Two transcripts coding for WRKY transcription factors were enhanced at t36 and t48, while two transcripts encoding ethylene (ET) responsive transcription factors (ERFs) were repressed. Cell wall-related transcripts were also affected, with two *beta-galactosidases* enhanced at t24, whereas those for *expansin-related* genes and an *XTH* gene were repressed at t48 and t36 respectively. Two *lipoxygenase* (*LOX*) genes were enhanced at t12 and t24 respectively, representing jasmonate (JA) biosynthesis. At t24 a transcript encoding trans-resveratrol di-O-methyltransferase-like (ROMT) was induced three-fold, while a *geranylgeranyl pyrophosphate (GGPP) reductase* transcript was repressed.

To identify protein transcripts that displayed accelerated induction in VviPGIP1-tobacco, the 24 h response intervals (Δt0-24) and 48 h response intervals (Δt0-48) of gene models were used. An accelerated response was defined as one where VviPGIP1-tobacco displayed significant induction/repression in d0-24, while WT tobacco displayed significant induction/repression in Δt0-48, without significant induction/repression in Δt0-24. Gene models matching these criteria are summarised in Table 4.1. The enhanced activation of transcripts related to energy metabolism (glycolysis, tricarboxylic acid cycle and oxidative pentose phosphate pathway), combined with the accelerated repression of photosynthesis suggested a more rapid shift from source to sink metabolism in VviPGIP1-tobacco. Although *Arabidopsis* homologs of most of these gene models were not enhanced in *Trichoderma hamatum*-primed *Arabidopsis* (Mathys et al., 2012; Appendix G

to Chapter 3), several were homologous to Arabido*psis* genes that were primed prior to *B. cinerea* infection. Following infection, both primed *Arabidopsis* and VviPGIP1-tobacco repressed genes involved in gibberellin catabolism (gibberellin 2-oxidase), and ethylene synthesis (1-aminoacyclopropane 1-carboxylate synthase) and signalling (ethylene-responsive transcription factor RAP2-3-like). Allene oxide cyclase and 4-coumarate--CoA ligase were enhanced in both cases.

Table 4.1 A summary of gene models that were induced at 24 hours after infection in VviPGIP1-tobacco, while being induced at 48 hours after infection in WT tobacco.

Probe ID	Mapman annotation	Putative protein function	WT		VviPGIP1-tobacco	
			Δt0-24*	Δt0-48	Δt0-24	Δt0-48
A_95_P108772	stress-biotic	basic pathogenesis-related protein 1	0.31	**3.13**	**1.43**	**3.33**
A_95_P119907		dirigent protein 22-like	0.95	**1.29**	**1.21**	**1.95**
A_95_P305858		endochitinase	0.42	**2.34**	**1.22**	**2.18**
A_95_P022806		harpin inducing protein 1	0.44	**1.97**	**1.45**	**2.93**
A_95_P183437		lesion inducing protein-related	0.94	**3.02**	**1.30**	**3.25**
A_95_P185277		trypsin and protease inhibitor family	0.81	**5.79**	**1.23**	**5.39**
A_95_P005501		thionin-like protein	-0.64	**-1.89**	**-1.56**	**-2.12**
A_95_P177082	stress-abiotic	cytosolic heat shock protein AtHSP90.1	0.86	**1.42**	**1.01**	**1.82**
A_95_P176252		dnaJ protein ERDJ3B	0.71	**1.42**	**1.20**	**1.98**
A_95_P183997		ER-resident HSP90-like protein	0.51	**1.20**	**1.16**	**1.48**
A_95_P195212		luminal binding protein	0.64	**2.01**	**2.57**	**2.34**
A_95_P029586		chaperone protein dnaJ 8, chloroplastic-like	-0.76	**-2.84**	**-1.25**	**-2.12**
A_95_P113807		latex-like protein	0.03	**-1.33**	**-1.38**	**-2.69**
A_95_P105622		MLP-like protein 34	0.50	**-1.84**	**-1.29**	**-2.47**
A_95_P216297		STAY-GREEN LIKE, chloroplastic-like	0.07	**-1.64**	**-1.06**	**-2.12**
A_95_P209592		wound-responsive protein	-0.89	**-1.84**	**-1.32**	**-2.40**
A_95_P052251	jasmonate metabolism	LOX-like	-0.71	**-1.79**	**-1.03**	**-2.06**
A_95_P004020	polyamine metabolism	S-adenosylmethionine decarboxylase	0.63	**1.61**	**1.10**	**1.90**
A_95_P219057		polyamine oxidase 2	0.51	**1.34**	**1.57**	**1.71**
A_95_P105952	glycolysis	cytosolic GADPH (C subunit)	0.92	**1.68**	**1.21**	**1.81**
A_95_P022366		enolase LOS2	0.99	**1.74**	**1.15**	**2.13**
A_95_P247317	tricarboxylic acid cycle	aconitate hydratase	0.77	**1.30**	**1.01**	**1.69**
A_95_P160697		ATP Citrate Lyase	0.88	**1.67**	**1.12**	**2.12**
A_95_P184492	oxidative pentose phosphate pathway	6-phosphogluconate dehydrogenase	0.93	**1.69**	**1.04**	**1.94**
A_95_P106272		transaldolase-like	0.65	**2.66**	**1.06**	**2.45**
A_95_P008651	photosynthesis-Calvin cycle	fructose-bisphosphate aldolase 3	0.89	**2.97**	**1.42**	**3.12**
A_95_P176937		RuBisCo activase 1	-0.22	**-2.64**	**-1.15**	**-3.32**
A_95_P105332	photosynthesis-light reaction	chlorophyll a-b binding protein 1	0.93	**-4.06**	**-2.74**	**-5.64**
A_95_P113182		ferredoxin	-0.34	**-1.64**	**-1.29**	**-2.84**
A_95_P028586		NAD(P)H-quinone oxidoreductase subunit M	-0.04	**-1.84**	**-1.03**	**-2.47**
A_95_P248737		oxygen-evolving enhancer protein 2-1	0.32	**-2.12**	**-1.15**	**-2.56**
A_95_P002746		photosystem I subunit O	0.16	**-3.64**	**-1.12**	**-3.64**
A_95_P108687		photosystem II subunit T	0.79	**-1.84**	**-1.09**	**-2.94**
A_95_P250577	secondary metabolism	geranylgeranyl diphosphate reductase	0.96	**-2.32**	**-1.36**	**-3.84**
A_95_P003626		lignin-forming anionic peroxidase-like	-0.20	**1.59**	**1.54**	**1.44**
A_95_P223662	cell wall	expansin-related B1	0.38	**1.01**	**1.42**	**1.19**
A_95_P018106		xyloglucan endotransglycosylase/hydrolase 9	0.95	**-1.32**	**-1.29**	**-1.36**
A_95_P234829		pectin esterase/pectin esterase inhibitor U1	0.79	**1.35**	**1.57**	**1.45**

Table 4.1 continues on next page

Table 4.1 continued

Probe ID	Mapman annotation	Putative protein function	WT		VviPGIP1-tobacco	
			Δt0-24*	Δt0-48	Δt0-24	Δt0-48
A_95_P023061	cell	cyclin-U1-1	-0.62	**-2.00**	**-1.29**	**-2.56**
A_95_P189972		annexin D2	0.96	**2.05**	**1.11**	**1.87**
A_95_P115072	development	senescence-associated protein (didiA9)	-0.81	**-1.43**	**-1.06**	**-1.43**
A_95_P103112		senescence-associated protein 12	-0.69	**-1.51**	**-1.09**	**-1.40**
A_95_P192132	lipid metabolism	pyruvate kinase 1, cytosolic	0.78	**2.28**	**1.22**	**2.59**
A_95_P016686	metal handling	heavy metal-associated isoprenylated protein	-0.12	**-3.84**	**-1.29**	**-3.32**
A_95_P229239	miscellaneous	glutathione S-transferase T1-like	-0.67	**-1.43**	**-1.09**	**-1.74**
A_95_P030766		peroxidase 53 precursor	-0.06	**2.14**	**1.35**	**1.91**
A_95_P290528		proline-rich protein DC2.15-like	0.46	**-2.25**	**-1.03**	**-2.56**
A_95_P179627	N-metabolism	glutamine synthetase	0.87	**1.69**	**1.03**	**1.76**
A_95_P016036	Not assigned	adenosylhomocysteinase	0.70	**1.65**	**1.20**	**2.32**
A_95_P030936		gamma-glutamyl cyclotransferases	-0.69	**-1.47**	**-1.03**	**-1.32**
A_95_P269811		NHL repeat-containing protein 2	-0.40	**-1.94**	**-1.09**	**-2.25**
A_95_P298028		putative lipid-binding	0.08	**-2.00**	**-1.43**	**-2.40**
A_95_P258956		Uncharacterised ncRNA	-0.69	**-1.22**	**-1.32**	**-1.74**
A_95_P185032	redox	peroxiredoxin Q	0.04	**-1.43**	**-1.03**	**-1.94**
A_95_P097848		protein disulfide isomerase-like	0.24	**2.43**	**1.74**	**2.58**
A_95_P139967		thioredoxin-like protein	-0.84	**-1.32**	**-1.03**	**-1.74**
A_95_P215942	RNA	tRNA (cytidine(34)-2'-O)-methyltransferase	0.10	**-1.40**	**-1.12**	**-1.47**
A_95_P149952		nuclear transcription factor Y subunit B-3-like	-0.58	**-2.64**	**-1.06**	**-2.40**
A_95_P017036	signalling-calcium	calnexin homolog 1-like	0.73	**1.95**	**1.39**	**2.51**
A_95_P240269		calreticulin	0.46	**1.52**	**1.20**	**1.68**
A_95_P198112	transport	ABC transporters C2	0.69	**1.39**	**1.01**	**1.93**
A_95_P015251		DELTA-TIP	-0.62	**-1.15**	**-1.64**	**-2.18**
A_95_P178727		mitochondrial phosphate transporter	0.41	**1.81**	**1.12**	**2.17**

* ΔtFold-change data were expressed relative to the earlier time point and log-scaled. Significant (fold change>2) induction and repression are highlighted in bold red/green respectively.

Differentially regulated proteins/processes during lesion development in VviPGIP1-tobacco

The transcriptional response of VviPGIP1-tobacco line was, except for the initial (Δt0-12) response, muted in the subsequent periods with a 22% lowering in the number of regulated transcripts in the Δt12-24, Δt24-36 and Δt36-48 periods (Figure 4.7A). This effect was even more pronounced when only repressed transcripts were considered. Unsupervised PCA (Figure 4.7B) showed that the most pronounced differences occurred in the 12 h-periods Δt12-24 and Δt36-48, that also represented the transition from the dark phase to the light phase of the diurnal pattern.

To further explore the divergence of WT and VviPGIP1-tobacco during lesion development, the most responsive transcripts were compared (Figure 4.8). Chlorophyll binding proteins were most prominently associated with the VviPGIP1-line, while proteinase inhibitors and lipoxygenase, phenylpropanoid and terpenoid pathways were represented in both lines. WT tobacco highly induced transcripts encoding PR proteins, namely a systemic acquired resistance (SAR) related basic chitinase and acidic beta-1,3-glucanase, as well as two components of the circadian clock, GIGANTEA and late-elongated hypocotyl (LHY).

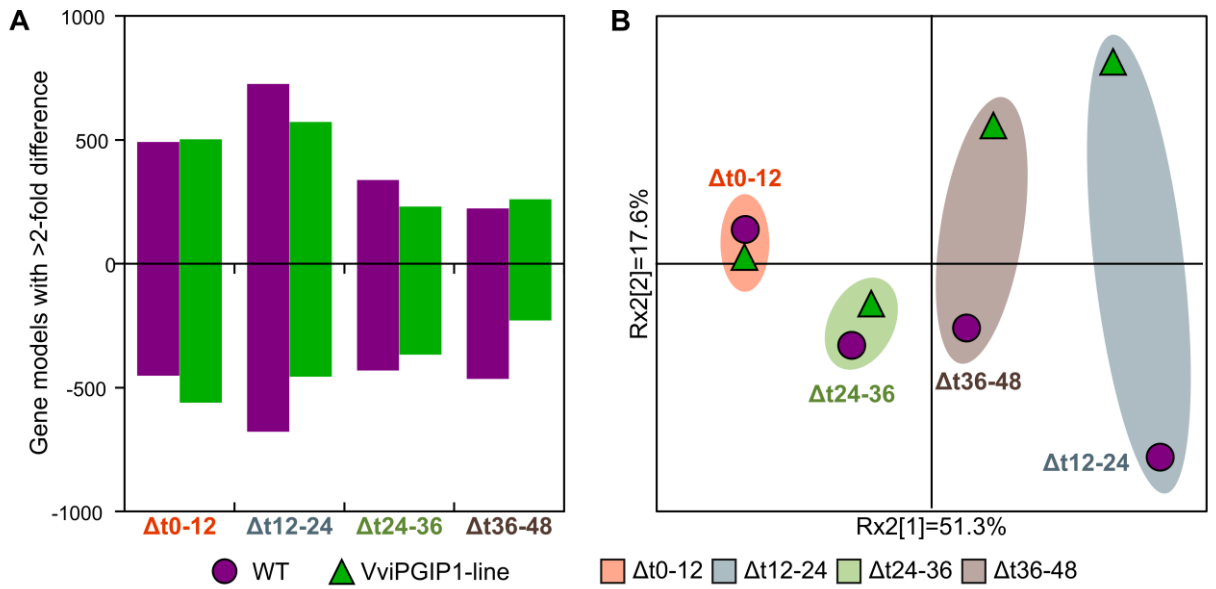

Figure 4.7 The local transcriptional response between consecutive sampling points (Δt, relative to earlier sampling point) in WT- and VviPGIP1-tobacco. A. Number of transcripts that passed initial curation steps and showed a two-fold or more change in expression between consecutive sampling points. B. Principal component analysis score plot of fold changes. Axes are annotated with the percentage variance (R2x) explained by each principal component.

To identify more subtle changes caused by *VviPGIP1* expression, genes involved in biotic stress responses, hormone signalling and synthesis, oxidative stress response and secondary metabolism were investigated. The selection of these categories was based on the analysis of the WT tobacco baseline (Chapter 3), enriched GO terms (Figure 4.5) and highly responsive transcripts (Figure 4.8). A summary of these transcripts is presented in Table 4.2.

Defence-related genes

In the VviPGIP1-tobacco lines, defence-related genes mirrored a general trend where lower expression levels were observed at t12 compared to WT-tobacco. These included transcripts encoding protease inhibitors, antimicrobial peptides and five SAR8.2 isoforms. Some of these, such as basic PR1 and three SAR8.2 isoforms, displayed higher expression at t24, along with acidic PR1, chitinases, type-2 proteinase inhibitor and antimicrobial peptide snakin 2a. At t36, *phytoalexin deficient 4* (*PAD4*) and *enhanced disease susceptibility 1* (*EDS1*), both associated with SA signalling, were induced. Two proteinase inhibitors were repressed at t48, while *harpin inducing protein 1* was induced. VviPGIP1-tobacco expression of *WRKY41* and *WRKY3* was significantly different from WT at t0 (1.85-fold) and t24 (0.62-fold) respectively. *WRKY41* expression levels were two-fold higher at t48, but this was not significantly ($p<0.05$) different.

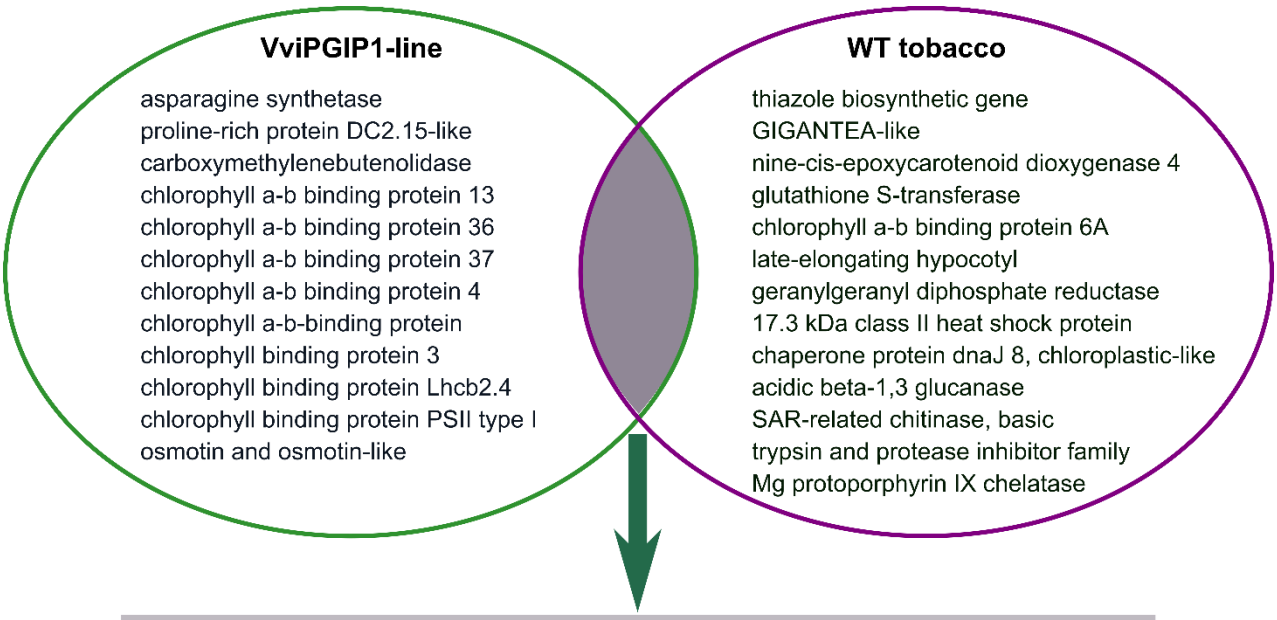

Figure 4.8 Comparison of all highly responsive transcripts in the local response of WT- and VviPGIP1-tobacco. The top 2% was selected based on absolute fold change between consecutive sampling points. Genes unique to either line are inside the Venn diagram, while gene names that were highly responsive in both lines are listed in the grey block.

Hormones and hormone signalling

The 9S- and 13S-branches of the lipoxygenase pathway were enhanced in VviPGIP1-expressing tobacco, with enhanced expression of three *LOX* genes at t12 or t24, and heightened induction of allene oxide cyclase at t48. This amounted to a shift in the timing of 9S- and 13S-LOX pathway induction in the VviPGIP1-tobacco lines, with the 9S-LOX pathway more strongly induced at an earlier sampling point, and a delayed, but eventually stronger induction of the 13S-LOX pathway. Expression of JA-regulated transcription factor *myelocytomatosis oncogene 2* (*MYC2*) was repressed at t12, compared to WT. Ethylene synthesis (represented by *1-aminocyclopropane-1-carboxylate oxidase*) was enhanced at t36, but transcripts encoding ethylene-responsive transcription factors were generally repressed, with the exception of ethylene-responsive transcription factors *RELATED TO APETALA 2-3* (*RAP2-3*) and *RAP2-12* that were induced at t24.

Expression of three *ethylene-insensitive 3 (EIN3)-binding F-box protein* transcripts, encoding proteins that are involved in degradation of EIN3 transcription factors, were induced at t24.

Table 4.2 Summary of transcripts with different expression patterns during lesion development in WT- and VviPGIP1-expressing tobacco.

	Probe ID	Putative protein function	Δg0*	Δg12	Δg24	Δg36	Δg48
Biotic stress-related	A_95_P113527	cysteine-rich protease inhibitor	*0.33*	0.52	-0.51	*0.59*	0.23
	A_95_P000776	microbial serine proteinase inhibitor	-0.47	*-0.47*	**1.42**	*-0.76*	**-1.47**
	A_95_P019016	proteinase inhibitor type-2	*-0.60*	0.19	*0.81*	-0.12	*-0.71*
	A_95_P185277	trypsin and protease inhibitor family	*-0.64*	*-0.62*	-0.25	-0.01	**-1.06**
	A_95_P004201	osmotin	*-0.60*	**-1.12**	**1.36**	-0.49	**-1.29**
	A_95_P187597	osmotin-like	-0.17	*0.53*	-0.36	*0.82*	-0.22
	A_95_P007686	acidic beta-1,3 glucanase	**-1.12**	-0.18	-0.25	*0.56*	-0.15
	A_95_P027946	Avr9/Cf-9 rapidly elicited protein 76	-0.43	**-1.22**	*-0.71*	-0.03	-0.23
	A_95_P019246	antimicrobial peptide (SN1a)	0.06	**-1.06**	0.15	-0.06	-0.27
	A_95_P000261	antimicrobial peptide (SN2a)	-0.14	0.26	*0.38*	0.07	-0.54
	A_95_P183832	basal resistance-related chitinase	0.12	-0.09	*-0.54*	-0.34	0.69
	A_95_P179847	Chitinase B (class I)	0.04	0.06	*0.31*	0.30	-0.43
	A_95_P305858	endochitinase	-0.18	-0.71	*0.60*	0.01	-0.34
	A_95_P293053	enhanced disease susceptibility 1	-0.06	*0.81*	-0.20	0.06	0.07
	A_95_P220487	enhanced disease susceptibility 1	0.08	0.49	*-0.56*	0.49	0.31
	A_95_P025936	enhanced disease susceptibility 1-like	-0.32	-0.38	*-0.15*	*0.44*	0.31
	A_95_P022806	harpin inducing protein 1	*-0.67*	-0.10	0.32	-0.27	*0.28*
	A_95_P226559	lipase-like phytoalexin-deficient 4	-0.38	-0.07	-0.09	*0.31*	0.25
	A_95_P184512	pathogenesis-related protein STH-2-like	0.06	-0.07	*-0.47*	-0.18	-0.60
	A_95_P021401	Pathogenesis-related 1a	0.01	-0.32	*0.44*	**1.80**	-0.03
	A_95_P003871	Pathogenesis-related 1b	*-0.15*	*-0.71*	**1.09**	-0.03	-0.47
	A_95_P032861	Pathogenesis-related 38	0.50	-0.06	0.34	*0.70*	-0.76
	A_95_P018316	Pathogenesis-related 4A	-0.09	0.01	*-0.29*	**1.14**	0.44
	A_95_P184987	Pathogenesis-related 4B	*-0.40*	0.00	-0.38	0.06	0.06
	A_95_P185867	Pathogenesis-related p27	-0.14	*-0.49*	0.18	-0.14	-0.23
	A_95_P002681	systemic acquired resistance-related chitinase, basic	*-0.29*	*-0.60*	-0.04	*0.21*	-0.03
	A_95_P004321	systemic acquired resistance 8.2b	-0.81	*-0.97*	*0.43*	0.07	-0.15
	A_95_P000196	systemic acquired resistance 8.2d	*-0.58*	**-1.15**	0.39	-0.06	-0.34
	A_95_P004441	systemic acquired resistance 8.2n	-0.62	**-1.00**	*0.58*	-0.14	-0.36
	A_95_P299943	virus-specific-signalling-pathway	0.29	*-0.30*	*-0.47*	0.40	-0.15
	A_95_P260116	WRKY 41	*0.89*	-0.45	-0.67	-0.18	**1.11**
	A_95_P237924	WRKY 3	0.16	-0.09	*-0.69*	-0.12	0.14
Hormone synthesis	A_95_P010991	1-aminocyclopropane-1-carboxylate oxidase	*0.36*	-0.01	-0.03	*0.57*	0.14
	A_95_P003016	1-aminocyclopropane-1-carboxylate oxidase	-0.03	-0.27	-0.07	*0.29*	-0.25
	A_95_P095528	9S-lipoxygenase	-0.36	-0.22	*0.67*	0.00	0.07
	A_95_P250517	allene oxide cyclase	-0.06	-0.14	*-0.79*	-0.58	*0.53*
	A_95_P029636	lipoxygenase	0.16	**1.24**	-0.10	0.30	0.38
	A_95_P015286	lipoxygenase homology domain	-0.40	*-0.60*	**1.28**	-0.01	*-0.64*
Hormone signalling	A_95_P034768	ethylene-responsive element binding protein 5	-0.18	*-0.94*	-0.17	**-1.00**	-0.10
	A_95_P203507	ethylene-responsive element binding protein 6	-0.29	*-0.94*	*-0.32*	-0.51	-0.23
	A_95_P006976	ethylene-responsive transcription factor 1	-0.32	-0.22	-0.23	-0.32	**-1.18**
	A_95_P162742	ethylene-responsive transcription factor 14-like	0.08	-0.07	-0.56	*-0.71*	0.30
	A_95_P092958	ethylene-responsive transcriptional coactivator	0.10	-0.07	*-0.67*	-0.92	0.16
	A_95_P201377	Ethylene insensitive (EIN)3-binding F-box protein	0.16	*0.31*	0.40	0.12	0.08
	A_95_P015091	EIN3-binding F-box protein 1-like	-0.09	*-0.62*	*0.90*	-0.12	0.06
	A_95_P202397	ethylene-responsive transcription factor RAP2-12-like	-0.18	-0.01	*0.57*	-0.01	-0.01
	A_95_P184897	ethylene-responsive transcription factor RAP2-3-like	-0.04	*-0.40*	*0.62*	0.23	-0.54
	A_95_P206662	MYC2	-0.01	*-0.62*	-0.43	0.06	0.03
Secondary meta-bolism	A_95_P250577	geranylgeranyl diphosphate reductase	0.03	0.15	0.01	-0.49	0.39
	A_95_P000646	4-coumarate--CoA ligase	0.03	*0.34*	*0.11*	0.01	*0.38*
	A_95_P180427	coumarate 3-hydroxylase	0.00	0.19	-0.06	*-0.64*	0.42
	A_95_P000346	caffeoyl-CoA O-methyltransferase	0.14	0.21	*-0.38*	0.33	-0.01
	A_95_P188507	cinnamoyl-CoA reductase family	*0.78*	0.57	*-0.62*	0.93	0.46
	A_95_P186892	cinnamoyl-CoA reductase 1	*-0.23*	*-0.74*	*0.43*	*-0.71*	-0.49
	A_95_P006386	caffeic acid 3-O-methyltransferase	-0.45	**-1.00**	**1.34**	0.70	-0.56
	A_95_P003626	lignin-forming anionic peroxidase-like	-0.10	0.23	-0.17	*-0.32*	*0.58*
	A_95_P008966	trans-resveratrol di-O-methyltransferase-like	*-0.54*	*-0.97*	**1.61**	-0.45	**-1.32**
	A_95_P252279	uncharacterised acetyltransferase	0.03	0.23	*-0.14*	*-0.30*	0.44
	A_95_P047686	laccase	0.01	0.00	-0.15	*0.73*	0.28

Table 4.2 continues on next page

Table 4.2 (continued)

	Probe ID	Putative protein function	Δg0	Δg12	Δg24	Δg36	Δg48
Secondary meta-bolism	A_95_P016661	NADPH--cytochrome P450 reductase	0.03	*0.31*	0.16	-0.04	0.34
	A_95_P096873	cytochrome P450 734A1-like	*0.43*	0.12	-0.60	0.14	-0.15
	A_95_P016076	hydroxymethylbutenyl diphosphate reductase	0.12	*0.73*	*-0.54*	0.20	0.34
	A_95_P075045	mevalonate kinase	*0.85*	0.58	**-1.40**	*0.32*	*-0.49*
	A_95_P106557	phosphomevalonate kinase-like	-0.07	-0.04	*-0.27*	*0.55*	-0.25
	A_95_P033161	1-deoxy-D-xylulose 5-phosphate synthase	0.00	0.67	-0.07	*-0.67*	0.18
	A_95_P132877	geranylgeranyl diphosphate synthase	0.03	0.15	0.01	*-0.49*	0.39
	A_95_P149112	geranylgeranyl diphosphate synthase	0.03	*0.34*	*0.11*	0.01	*0.38*
Redox	A_95_P298383	NADPH oxidase	0.06	0.16	*-0.29*	-0.23	0.58
	A_95_P219057	Polyamine oxidase 2	*-0.42*	*-0.23*	*0.62*	*-0.45*	-0.07
	A_95_P188127	Polyamine oxidase 4	*0.15*	-0.04	-0.58	*-0.42*	*0.68*
	A_95_P016471	Cell wall-bound peroxidase	0.14	-0.30	*0.33*	*0.39*	*-0.69*
	A_95_P135667	Peroxidase	-0.15	**-1.22**	**1.00**	*0.62*	-0.30
	A_95_P212837	Peroxidase 47 precursor	0.03	0.06	*-0.23*	*0.4*	-0.30
	A_95_P030766	Peroxidase 53 precursor	*-0.23*	*-0.84*	**1.14**	0.42	-0.51
	A_95_P018841	glutamate-cysteine ligase	-0.27	*-0.54*	*0.76*	*-0.40*	-0.64
	A_95_P066415	monodehydroascorbate reductase, chloroplast	-0.27	*0.75*	-0.04	*0.61*	0.11
	A_95_P183327	monodehydroascorbate reductase, cytoplasmic	-0.06	0.28	-0.10	0.10	*0.44*
	A_95_P181492	phospholipid hydroperoxide glutathione peroxidase	*-0.29*	*-0.40*	0.00	-0.29	-0.29
	A_95_P253794	phospholipid hydroperoxide glutathione peroxidase	*0.26*	0.31	*-0.62*	0.15	-0.07
	A_95_P236294	transmembrane ascorbate ferrireductase 1-like	-0.22	*-0.67*	0.24	0.29	-0.10
	A_95_P286393	Vitamin C (VTC) 2-like protein	0.07	-0.25	0.18	-0.12	*0.60*
	A_95_P259416	Catalase 1-like	*0.39*	0.57	-0.49	-0.03	0.11
	A_95_P001976	superoxide dismutase [Cu-Zn], chloroplastic	*0.70*	00	-0.20	0.16	-0.04
	A_95_P019621	iron superoxide dismutase	0.23	0.10	*0.30*	-0.22	-0.6
	A_95_P018826	glutaredoxin	0.10	*-0.86*	*0.95*	-0.07	-0.54
	A_95_P186062	2-Cys peroxiredoxin BAS1-like	0.07	0.46	*-0.12*	*0.38*	-0.20
	A_95_P109682	peroxiredoxin Q	0.34	*-0.42*	*-0.56*	0.14	0.11
	A_95_P111412	thioredoxin-dependent peroxidase 1	-0.01	*-0.56*	-0.04	-0.04	-0.23
	A_95_P013686	thioredoxin F-type,	0.54	-0.22	*-0.56*	0.08	0.04
	A_95_P254304	thioredoxin H2-like	-0.60	*-0.49*	-0.10	0.61	0.23
	A_95_P219682	thioredoxin H4-1-like	-0.09	*-0.34*	-0.43	-0.38	0.15
	A_95_P147437	thioredoxin M3	-0.27	*0.21*	-0.23	*0.44*	-0.18

* Δg Fold-change data were expressed relative to the wild-type and log-scaled. Significant (fold change>2) induction and repression are highlighted in bold red/green respectively. Italicised induction/repression were significant (p≤0.05) according to Student's t-test.

Secondary metabolism

With the exception of the 2-C-methyl-d-erythritol 4-phosphate (MEP) pathway of terpenoid biosynthesis, the cumulative expression levels of secondary metabolism pathways of VviPGIP1-tobacco were generally similar to WT (Figure 4.9). Although carotenoid biosynthesis (Figure 4.9B) was not distinctly different in VviPGIP1-tobacco, transcripts encoding GGPP reductase, responsible for, among others, chlorophyll biosynthesis, was elevated in uninfected VviPGIP1-tobacco and repressed at t24.

Although phenylpropanoid metabolism was uniquely enriched in WT-tobacco (Figure 4.5), the cumulative expression pattern (Figure 4.9C) of WT and VviPGIP1-expressing tobacco were nearly identical, with reduced levels at t36 and elevated levels at t48, though the latter was not significant (p=0.06). Expression of coumarate 3-hydroxylase (C3H)-encoding genes, a component of the general phenylpropanoid pathway, was enhanced at t12, t24 and t48. VviPGIP1-tobacco displayed enhanced accumulation of transcripts encoding for caffeic acid 3-O-methyltransferase (COMT), while *caffeoyl-CoA O-methyltransferase* (*CCoAOMT*) was reduced at t24. At t48, enhanced expression was not significant for individual probes, the combined expression levels of all *CCoAOMT*-targeting probes (A_95_P101153, A_95_P007991, A_95_P010531 and A_95_P000346) were significantly (P<0.05) different between WT and VviPGIP1-tobacco. A lignin-forming

peroxidase isoform displayed an accelerated induction in VviPGIP1, being induced after t12, rather than after t24.

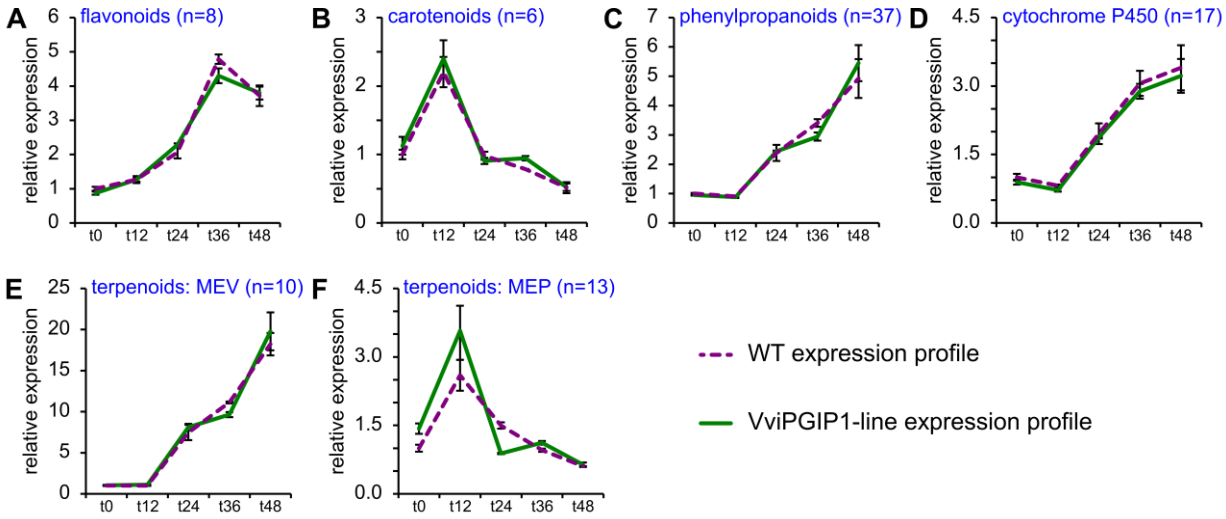

Figure 4.9 Secondary metabolism local expression patterns, calculated across Mapman bins and normalised to WT-t0. A. flavonoids B. phenylpropanoids C. carotenoids D. cytochrome P450 E. mevalonate pathway F. non-mevalonate pathway. n = number of probes included in each bin. MEV, mevalonate; MEP, 2-C-methyl-d-erythritol 4-phosphate.

A single, highly-induced laccase encoding gene displayed higher transcript levels in VviPGIP1-tobacco after t24. WT and VviPGIP1-tobacco profiles of *ROMT* transcript expression were negatively correlated, with VviPGIP1-tobacco displaying a transient induction at t24 before repressing expression levels, consequently *ROMT* transcript levels were significantly lower at t12 and t48, while being three-fold higher at t24. Transcripts encoding NADPH-cytochrome P450 reductase and cytochrome P450 734A1-like displayed a significant induction after t36 in VviPGIP1-tobacco, and were consequently significantly higher than in WT.

Terpenoid biosynthesis via the mevalonate pathway was, as in WT tobacco, highly induced, and was cumulatively induced to the same extent in both lines (Figure 4.9E), but 3-hydroxy-3-methylglutaryl-CoA reductase (HMGR), mevalonate kinase and phosphomevalonate kinase were enhanced at t48. In the MEP pathway, 1-deoxy-D-xylulose 5-phosphate synthase (DXS) transcript expression was significantly higher in uninfected (t0) VviPGIP1-tobacco. Two isoforms with distinct WT expression profiles were differentially affected in VviPGIP1-expressing tobacco. One displayed a transient but non-significant increase at t12, but was significantly lower at t36, while the other was significantly lower at t24 and higher at t36, since the transcripts were not as rapidly repressed after t24.

To further study secondary metabolites, residual VOC analysis was performed on VviPGIP1-expressing tobacco tissue, to be compared with those of WT under infection. Due to technical difficulties (column degradation leading to standard deviations exceeded 50% for nearly all compounds), the data were not usable and are not reported further here.

Oxidative stress metabolism

Unlike WT tobacco, response to oxidative stress was not enriched among transcriptionally regulated genes in VviPGIP1-expressing tobacco (Figure 4.5B). Closer inspection of redox-related transcripts revealed that more than half of the redox-annotated transcripts displayed significant differences between WT and VviPGIP1-tobacco at one or more sampling point. These included important contributors to reactive oxygen species (ROS) producers, NADPH oxidase (1.5-fold higher at t48), polyamine oxidase (PAO) 2 (1.5-fold higher at t24) and PAO4 (1.6-fold higher at t48). Several peroxidase isoforms were more highly expressed at t24 or t36. Thioredoxins were repressed at t12 or t24, with the exception of thioredoxin M3, that was enhanced during the dark phase of the photoperiod (t12 and t36). A chloroplastic isoform of monodehydroascorbate reductase (MDHAR) was more highly expressed during the dark phase of the photoperiod, while a cytosolic isoform was more highly expressed at t48. Overall, five of the seven proteins that were more highly transcribed at t24 were suppressed at t12.

Since some of the redox-related gene products can act as oxidants or reducers (e.g. peroxidases), we analysed the total antioxidant capacity of the tissue to supplement the transcriptional data (Figure 4.10). Significant ($p<0.05$) differences in total antioxidant capacity were observed after t12, with VviPGIP1-tobacco exhibiting reduced antioxidant capacity at t24 and t48, and enhanced antioxidant capacity at t36.

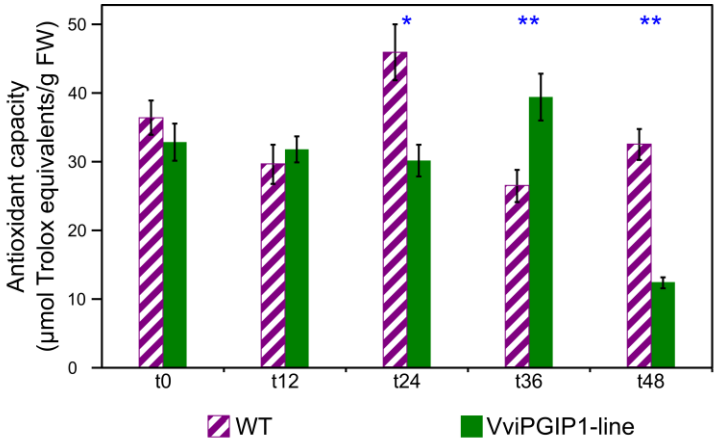

Figure 4.10 Antioxidant capacity of WT- and VviPGIP1-tobacco tissue including and surrounding the infection spot. Error bars represent standard error of three technical replicates. Asterisks indicate significance according to Student's t-test. * $p<0.05$; ** $p<0.01$.

These data prompted a further analysis of the *in situ* hydrogen peroxide evolution during infection. A histochemical staining of infected leaf disks of WT and transgenic VviPGIP1 expressing tobacco was used (Figure 4.11, Appendix C to Chapter 4). It was clear that both lines displayed a gradual increase in H_2O_2 associated with lesion formation, while the wound response from leaf disk preparation also caused a stained edge (Figure 4.11A). By t48 few of the leaf disks were still intact enough to stain; on the WT leaf disks, the *B. cinerea*-induced H_2O_2 could no longer be clearly distinguished from the wound response (i.e. most of leaf disks were stained uniformly between the

inoculation site and wound response). The leaf disks from the resistant lines (*VviPGIP1* expressing) displayed uniquely a distinct second dark ring of H_2O_2 that originated from the infection. Using the scoring system adopted (refer to Section 4.2.4b and Figure 4.1 in Materials & Methods), the qualitative assessment of the leaf disks (Figure 4.11B) showed that WT tobacco mostly produced the solid/bordered spots under the infection drop, whereas the VviPGIP1-tobacco line's leaf disks displayed more mottled hydrogen peroxide stains (speckled spots) in response to infection. The amount of hydrogen peroxide (Figure 4.11C) was significantly ($p<0.05$) lower at t24 in the VviPGIP1-line.

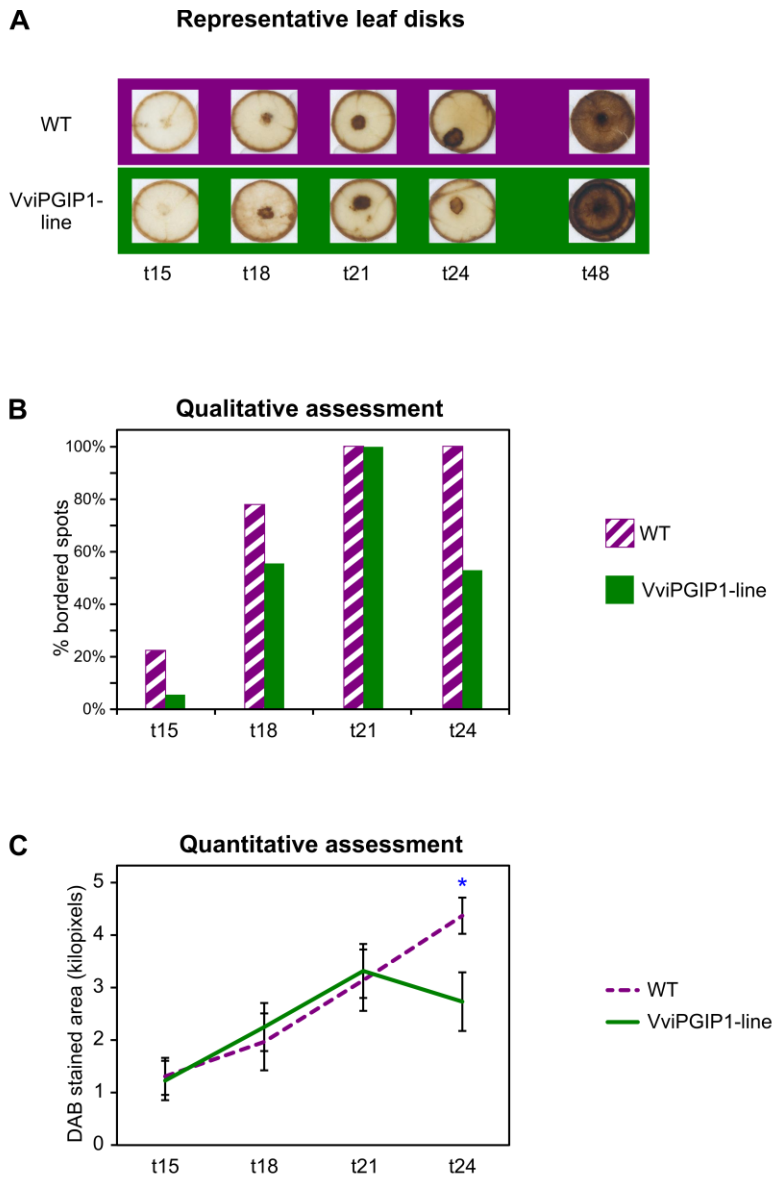

Figure 4.11 Hydrogen peroxide production during leaf disk assay. A. Representative leaf disks showing the brown precipitate formed by diaminobenzidine staining. The full complement of leaf disk images is available as Appendix C to Chapter 4. B. Qualitative analysis of the histochemical staining. The bars represent the percentage of bordered spots, representing a stained area of homogenous density. C. Quantitative analysis of the histochemical staining calculated using pixel counts in the area excluding the wound response. Error bars represent standard error (N=16-18). * $p<0.05$ (Student's t-test)

4.3.4 The distal expression profile of VviPGIP1-tobacco

Overview of expression levels and biological processes in a leaf distal to the infection

Multivariate analysis reveals diverging expression profiles in a leaf distal to the infection

The first round of PCA confirmed the MA-plot analysis (Addendum B to Chapter 3) that revealed that one technical replicate (systemic t12-C) was an outlier (data not shown) and was therefore omitted from subsequent analyses and calculations. Two principal components were able to explain 65% of variation in the distal expression profile (Figure 4.12). Since (erroneously) no dye swaps were included in this analysis, the difference between WT and VviPGIP1-expressing tobacco was more distinct than for the lesion expression profile.

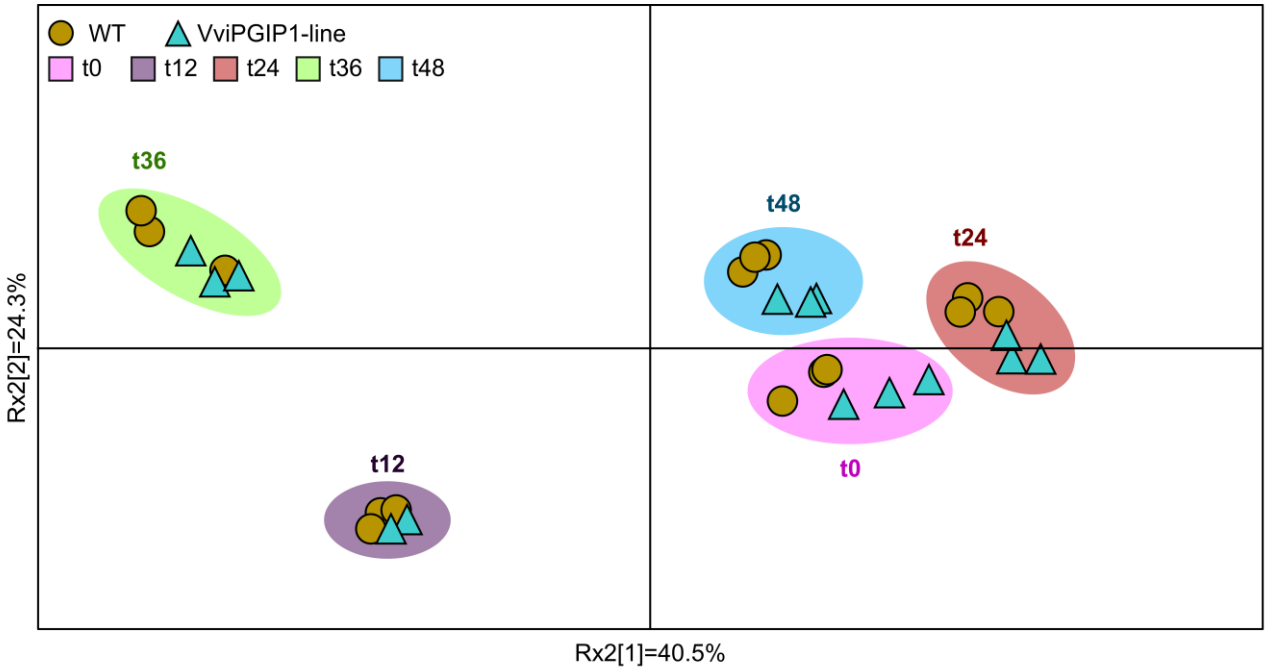

Figure 4.12 Principal component analysis score plots of curated transcriptional data for the distal expression profile. Axes are annotated with the percentage variance (R2x) explained by each principal component.

However, when viewing the transcriptional responses between sampling points in the leaf distal to the infection (Figure 4.13) the influence of dye bias could be removed, and the differences between WT- and VviPGIP1-tobacco were readily apparent after t12 in terms of magnitude of response (Figure 4.13A) and expression patterns visualised with PCA (Figure 4.13B). This was further highlighted when determining the transcripts that displayed a minimum 2-fold difference between WT and VviPGIP1-tobacco (Figure 4.14, Appendix D to Chapter 4).

Biological processes that were altered in VviPGIP1-tobacco compared to WT in the leaf distal to the infection

Differences between transcript levels of WT and the VviPGIP1-expressing tobacco increased sharply after t12 (Figure 4.14A). Inspection of the biological functions of these transcripts showed that the Mapman annotation biotic stress was the most prevalent (Figure 4.14B). The majority of

significantly different transcripts were repressed at t24-t48 in the VviPGIP1-line compared to WT and encoded, among others, beta-galactosidases, ethylene responsive element binding proteins and transcription factors, protease inhibitors, calcium-binding proteins, PR-1B, SAR8.2a-c and osmotins. On the other hand, several histones were induced, particularly at t24, and LOX-encoding transcripts were induced at t36.

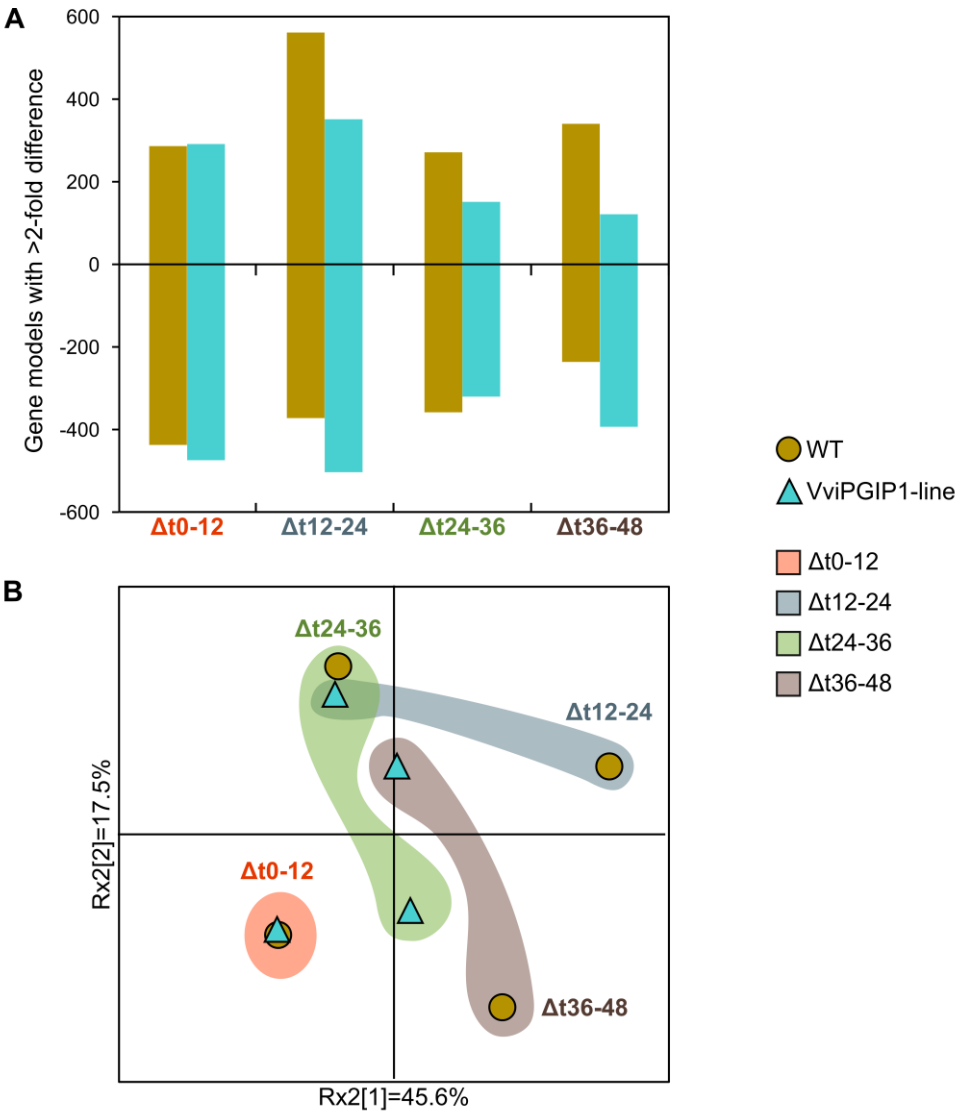

Figure 4.13 The distal transcriptional response between consecutive sampling points (Δt, relative to earlier sampling point) in WT tobacco and the VviPGIP1-tobacco line. A. Number of transcripts that passed initial curation steps and showed a two-fold or more change in expression between consecutive sampling points. B. Principal component analysis score plot of fold changes. Axes are annotated with the percentage variance (R2x) explained by each principal component.

Divergence in temporal regulation of biological processes in the leaf distal to the infection

Examination of the GO terms enriched in each 12 h-period (Table 4.3, Appendix E to Chapter 4) revealed differential regulation of defence response-related ontologies, being repressed in VviPGIP1-tobacco and induced in WT in the 12 h-intervals d12-24 and d36-48. Several stress responses were repressed in VviPGIP1-tobacco after t36, while not being significantly enriched in

WT, whereas response to wounding was repressed after t0 and t12 in VviPGIP1 tobacco, but induced after t12 in WT.

Peptide biosynthesis, ribosome biogenesis and translation were induced after t0 in VviPGIP1-tobacco. A number of metabolite biosynthetic and catabolic processes were uniquely enriched in VviPGIP1-expressing tobacco, and were repressed after t36 (Table 4.3). Photosynthesis-related terms once again distinguished VviPGIP1-tobacco from WT in the 12 h-interval d12-24, where photosynthesis, pigment biosynthesis and light responses were repressed in WT, but followed a typical diurnal oscillating pattern in WT.

As was expected after observing the PCA results, comparison of VviPGIP1-tobacco with WT with respect to transcripts with the greatest change in abundance between t0 and t12 (Table 4.4) were largely similar, with only three transcripts, *senescence-associated protein*, *thiosulfate sulfurtransferase* and a *chloroplastic chaperone protein dnaJ* being highly repressed. In the subsequent 12 h-intervals however, several biological processes were represented among transcripts that displayed tremendous transcriptional changes between sampling points.

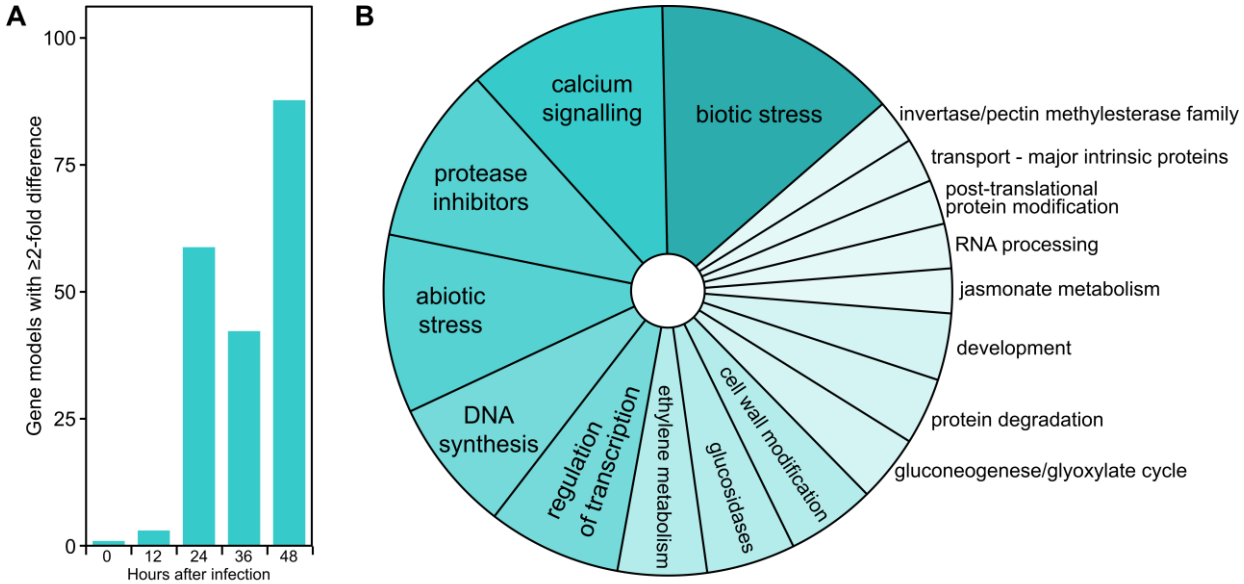

Figure 4.14 Comparison of WT- and VviPGIP1-tobacco at individual sampling points in the distal expression profile. A. Number of transcripts with a minimum two-fold difference between lines. B. Mapman annotations of transcripts differing at one or more sampling point. Shading indicates the number of transcripts with the specified annotation. Only bins representing at least two transcripts are shown. The full data table is available as Appendix D to Chapter 4.

These included repressions after t36 of transcripts encoding S-adenosylmethionine (SAM) synthesising enzymes, jasmonate-synthesising LOX, 9-divinyl ether synthase (DES) and several heat shock proteins, as well as enzymes responsible for isoprenoid synthesis via the MEV pathway, and those involved with phenylpropanoid synthesis. The MEP pathway transcripts were significantly repressed after t24 in the resistant lines. Similarly, several photosynthesis-related transcripts were repressed in these lines after t12 or t24, including *photosystem I subunit O* and transcripts encoding genes involved in tetrapyrrole synthesis.

Table 4.3 Enriched GO terms in the distal expression profile in susceptible WT tobacco (yellow shading) and the resistant transgenic VviPGIP1 line (blue shading).

	Δt0-12*		Δt12-24		Δt24-36		Δt36-48	
DEFENCE-RELATED	VviPGIP1	WT	VviPGIP1	WT	VviPGIP1	WT	VviPGIP1	WT
chitin catabolism							8.8E-07	
defence response	1.2E-04	4.6E-04	3.0E-04	1.3E-06				7.2E-04
defence response to fungus	2.8E-05	1.0E-03		1.7E-06				
response to biotic stimulus	1.1E-04		7.5E-05	7.5E-07			1.0E-06	
response to fungus	1.0E-05			1.6E-07				
RESPONSES TO STIMULI								
response to abiotic stimulus	2.1E-09	9.0E-08	7.9E-08		1.1E-07		2.5E-08	
response to cadmium ion	4.9E-04		2.1E-04				5.3E-16	
response to cold	2.7E-07	6.1E-07		5.4E-04				
response to heat							1.9E-05	
response to metal ion	1.2E-04		2.5E-04				5.3E-16	
response to osmotic stress	8.4E-04						4.9E-06	
response to oxidative stress							2.8E-04	
response to reactive oxygen species							3.8E-04	
response to salt stress	4.1E-04						6.1E-06	
response to temperature stimulus	3.9E-09	1.7E-06		3.8E-04			5.2E-05	
response to wounding	1.1E-04	4.6E-04	8.2E-04	1.2E-06				
METABOLIC PROCESSES								
alpha-amino acid biosynthesis							1.6E-04	
amide biosynthesis	2.2E-09							
carbohydrate derivative catabolism							1.1E-05	
cell wall macromolecule catabolism							4.0E-05	
coumarin biosynthesis							6.2E-07	
organic acid biosynthesis							9.5E-04	
phenylpropanoid biosynthesis							1.8E-05	
secondary metabolite biosynthesis							1.6E-04	
PROTEIN BIOSYNTHESIS								
peptide biosynthesis	2.2E-09							
protein folding			1.6E-05					
ribonucleoprotein complex biogenesis	1.8E-04							
ribosome biogenesis	1.4E-04							
translation	2.2E-09							
LIGHT & PHOTOSYNTHESIS-RELATED								
photosynthesis	2.9E-08	3.9E-07	3.3E-31	3.2E-10		1.6E-26		2.2E-17
pigment biosynthesis			3.4E-04			1.2E-06		
response to light intensity			3.7E-05					
response to light stimulus			5.0E-08		1.6E-07	2.5E-05		

* Δt: Underlying fold-change data are expressed relative to the earlier time point. Significance of enrichment is shown in red/green for induction/repression. Yellow cells indicate significant induction and repression of the term.

Table 4.4 Transcripts with the biggest transcriptional change (top 30) between sampling points in distal leaf tissue of VviPGIP1-expressing tobacco that were not in the equivalent WT list.

Mapman annotation	Probe ID	Putative protein function	Δt0-12	Δt12-24	Δt24-36	Δt36-48
HOUSEKEEPING						
development	A_95_P025081	GIGANTEA-like	**-1.94**	**-3.32**	**2.58**	0.34
	A_95_P115072	senescence-associated protein	**-3.18**	-0.25	-0.40	0.81
	A_95_P186307	thiosulfate sulfurtransferase	**-3.18**	**-1.00**	-0.74	**1.20**
	A_95_P016256	late elongated hypocotyl	0.92	**2.77**	**-3.47**	-0.34
transport-misc	A_95_P163972	DETOXIFICATION 27-like	0.70	-0.29	**3.33**	**-3.06**
METABOLIC PROCESSES						
amino acid synthesis	A_95_P026906	S-adenosylmethionine synthase 2-like	0.67	0.90	0.43	**-3.64**
cell wall-cellulose synthesis	A_95_P212112	cellulose synthase-like protein	**2.55**	**4.64**	**-3.06**	**-1.79**
	A_95_P111912	thiazole biosynthetic gene	-0.97	**-4.06**	**1.34**	0.08
misc-cytochrome P450	A_95_P194292	premnaspirodiene oxygenase-like	-0.03	**1.97**	0.45	**-5.64**
secondary metabolism-mevalonate pathway	A_95_P180402	hydroxymethylglutaryl-CoA reductase	-0.74	**1.97**	0.45	**-3.47**
	A_95_P004346	acetyl-CoA acetyltransferase	-0.22	0.29	0.68	**-3.64**
	A_95_P190047	farnesyl diphosphate synthase	0.00	-0.30	**1.20**	**-3.47**
	A_95_P250577	geranylgeranyl diphosphate reductase	0.29	-0.54	**-2.74**	-0.94
secondary metabolism-phenylpropanoids	A_95_P240179	acyltransferase-like protein	-0.01	**1.37**	0.44	**-5.64**
	A_95_P010531	caffeoyl-CoA 3-O-methyltransferase	0.52	0.84	0.84	**-4.06**
	A_95_P000346	caffeoyl-CoA 3-O-methyltransferase	0.46	0.80	0.58	**-3.64**
PHOTOSYNTHESIS AND ENERGY GENERATION						
glyoxylate cycle	A_95_P249012	isocitrate lyase	-0.49	0.39	**-1.00**	**3.71**
oxidative pentose phosphate	A_95_P026051	6-phosphogluconate dehydrogenase	-0.27	0.42	0.91	**-3.47**
PS-Calvin cycle	A_95_P010701	fructose-bisphosphate aldolase	0.66	-0.20	**-2.64**	0.44
	A_95_P176937	Rubisco activase 1	1.20	0.04	**-2.40**	0.23
PS-light reaction	A_95_P234784	chlorophyll a-b binding protein 8	**-1.84**	1.75	**-2.84**	**2.60**
	A_95_P003241	photosystem I subunit O	**-1.40**	**-4.32**	0.40	-0.45
	A_95_P103872	PS I reaction centre subunit VI	**-1.43**	**-3.84**	0.33	-0.71
	A_95_P002626	rubisco large subunit-binding protein	**-2.12**	**2.01**	**-3.18**	**2.45**
tetrapyrrole synthesis	A_95_P221817	chlorophyllase-1-like	-0.29	0.06	0.85	**-4.32**
	A_95_P249767	Mg protoporphyrin IX chelatase	-0.56	-0.62	**-3.18**	-1.29
	A_95_P105012	ZIP	-0.17	**-1.29**	**-2.47**	-0.74
hormone metabolism-jasmonate	A_95_P190077	9-divinyl ether synthase	0.06	0.31	**1.03**	**-3.84**
	A_95_P029636	lipoxygenase	**1.04**	0.90	0.42	**-3.84**
STRESS-RELATED						
misc-GDSL-motif lipase	A_95_P200862	GDSL-motif lipase	0.80	**1.86**	0.52	**-3.32**
misc-protease inhibitor...	A_95_P185737	proteinase inhibitor type-2	-0.89	**3.84**	**1.27**	**-1.15**
misc-SDR	A_95_P203282	short-chain dehydrogenase/reductase	-0.34	-0.92	**1.62**	**-4.06**
stress-abiotic	A_95_P184047	17.3 kDa class II heat shock protein	0.30	**-1.94**	**1.20**	**-4.32**
	A_95_P029586	chaperone protein dnaJ, chloroplastic	**-3.18**	**-1.74**	-0.29	0.77
	A_95_P000306	heat shock cognate 70 kDa protein	0.24	-0.89	-0.01	**-3.47**
	A_95_P014536	heat shock protein 82	0.08	-0.81	0.07	**-3.47**
	A_95_P242477	heat shock transcription factor B3	-0.17	**1.10**	0.44	**-3.84**

* Δt: Fold-change data are expressed relative to the earlier time point and log-scaled. Italicised Mapman annotations were not represented in the top 30 transcripts of WT tobacco. Significant (fold change>2) induction and repression are highlighted in bold red/green respectively. “Top 30” fold changes are shaded for emphasis.

Similar to the approach used to analyse the transcriptional profile of the localised defence response, the transcripts relating to hormone signalling and synthesis, oxidative stress response and secondary metabolism were examined (Table 4.5). The WT tobacco baseline (Chapter 3), enriched GO terms (Table 4.3) and highly responsive transcripts (Table 4.4) directed the choice of processes that were investigated.

Genes involved in ET- and JA biosynthesis were enhanced in VviPGIP1-tobacco, but, from t24, ET signalling, via *ET-responsive transcription factor 1* (*ERF1*), *ET-responsive element binding protein 5*

(*EREBP5*) and *EREBP6* were suppressed. *APX* transcripts were slightly enhanced in VviPGIP1-tobacco, whereas those encoding catalase isozyme 3-like were suppressed, along with one *glutaredoxin* transcript, while another was enhanced at t36.

Table 4.5 Summary of transcripts with altered distal expression patterns in WT- and VviPGIP1-expressing tobacco, with the expression of VviPGIP1-tobacco normalised to WT at each sampling point.

Biological process	Probe ID	Putative protein function	Δg0	Δg12	Δg24	Δg36	Δg48
ethylene synthesis or signalling	A_95_P010991	1-aminocyclopropane-1-carboxylate oxidase	0.23	0.00	0.04	*0.44*	*0.11*
	A_95_P178962	1-aminocyclopropane-1-carboxylate oxidase	0.04	0.20	*0.48*	*0.53*	0.30
	A_95_P009111	ethylene-insensitive 3 (EIN3)	0.00	-0.20	-0.01	*0.23*	-0.07
	A_95_P034768	ethylene-responsive element binding protein 5	*-0.30*	-0.79	*-0.43*	***-0.89***	***-1.09***
	A_95_P203507	ethylene-responsive element binding protein 6	*-0.09*	-0.42	*-0.60*	*-0.54*	***-1.56***
	A_95_P006976	ethylene-responsive transcription factor 1	*-0.34*	-0.10	***-0.84***	*-0.54*	***-4.06***
	A_95_P034798	ethylene-responsive transcription factor 1B	*-0.07*	0.06	***-0.84***	***-0.76***	***-1.09***
	A_95_P184897	ethylene-responsive transcription factor RAP2-3	-0.06	-0.09	***-0.64***	*-0.32*	*-0.62*
jasmonate synthesis	A_95_P014126	allene oxide cyclase	0.03	0.01	***0.69***	*0.30*	-0.03
	A_95_P029636	lipoxygenase	0.21	0.42	***0.83***	***1.05***	-0.03
	A_95_P015286	lipoxygenase homology domain	-0.34	0.04	***-1.12***	***-1.60***	-0.23
redox	A_95_P017821	ascorbate peroxidase (cytosolic)	-0.06	0.62	***0.66***	*0.37*	*0.48*
	A_95_P001321	catalase	0.30	0.24	0.32	*0.33*	*0.61*
	A_95_P132372	catalase isozyme 3-like	*-0.43*	-0.18	*-0.45*	***-0.79***	*-0.34*
	A_95_P268211	glutaredoxin	0.24	-0.25	***-0.89***	*0.53*	0.06
	A_95_P018826	glutaredoxin	*-0.29*	-0.14	***-1.12***	-0.25	***-0.89***
secondary metabolism	A_95_P190047	farnesyl diphosphate synthase	0.08	-0.09	0.44	*0.54*	*0.33*
	A_95_P010531	caffeoyl-CoA O-methyltransferase	0.54	0.28	***0.63***	*0.56*	***0.82***
	A_95_P180592	caffeoyl-CoA O-methyltransferase	*-0.06*	0.03	-0.25	0.12	-0.54
	A_95_P034873	4-coumarate-CoA ligase	0.06	0.21	*0.57*	*0.21*	0.14
	A_95_P018576	8-hydroxygeraniol dehydrogenase-like	-0.01	0.04	0.38	0.20	-0.07
	A_95_P180372	caffeic acid 3-O-methyltransferase	0.06	-0.20	0.34	-0.15	-0.10
	A_95_P008921	hydroxycinnamoyltransferase	0.06	0.06	-0.15	0.55	*-0.34*
	A_95_P017176	NADPH-cytochrome P450 oxidoreductase	-0.15	-0.06	-0.27	0.14	*0.61*
	A_95_P008966	trans-resveratrol di-O-methyltransferase-like	-0.34	-0.23	***-0.89***	***-0.86***	***-1.00***
	A_95_P124057	uncharacterised acetyltransferase	-0.32	-0.03	*-0.42*	-0.18	***-1.25***

* Δg: Fold-change data were expressed relative to the wild-type and log-scaled. Near-significant (fold change>1.5) induction and repression are highlighted in bold red/green respectively. Italicised induction/repression were significant (p≤0.05) according to Student's t-test.

Despite minimal transcriptional regulation of the phenylpropanoid pathway in the leaf distal to the infection (Figure 4.15B), enhanced transcript levels were observed for *CCoAOMT*, and *4-coumarate-CoA ligase* (*4CL*). VviPGIP1-tobacco displayed slightly enhanced activation of the MEV pathway (Figure 4.15D), and elevated levels of MEP-pathway transcripts (Figure 4.15E). As mentioned before, the VOC analysis of these samples did not render usable data due to technical problems and are not reported on further.

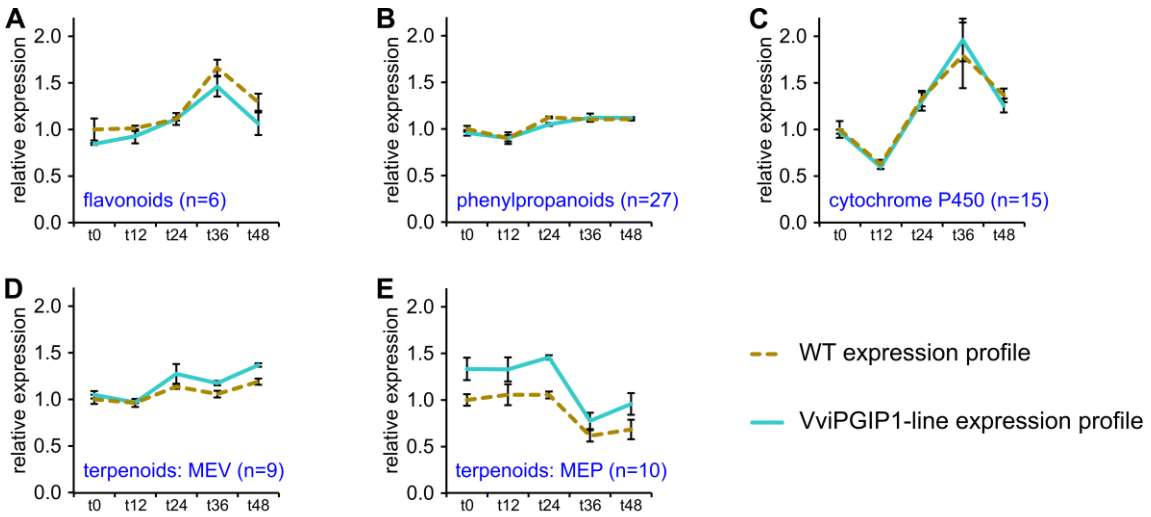

Figure 4.15 Secondary metabolism distal expression patterns, calculated across Mapman bins and normalised to WT-t0 (leaf 2). A. secondary metabolism-flavonoids B. secondary metabolism-phenylpropanoids C. misc-cytochrome P450 E. secondary metabolism-isoprenoids-mevalonate pathway F. secondary metabolism-isoprenoids-non-mevalonate pathway. n = number of probes included in each bin. MEV, mevalonate; MEP, 2-C-methyl-d-erythritol 4-phosphate.

4.3.5 Transcript analysis using RT-qPCR

Genes were selected for RT-qPCR analysis to confirm the microarray-derived expression patterns (Figure 4.16). Enhanced induction (compared to WT) of *ascorbate peroxidase* (*APX*), *9-divinyl ether synthase* (*DES), 9-lipoxygenase (LOX*) in VviPGIP1-tobacco was confirmed and good correlations were observed between the microarray- and RT-qPCR expression patterns.

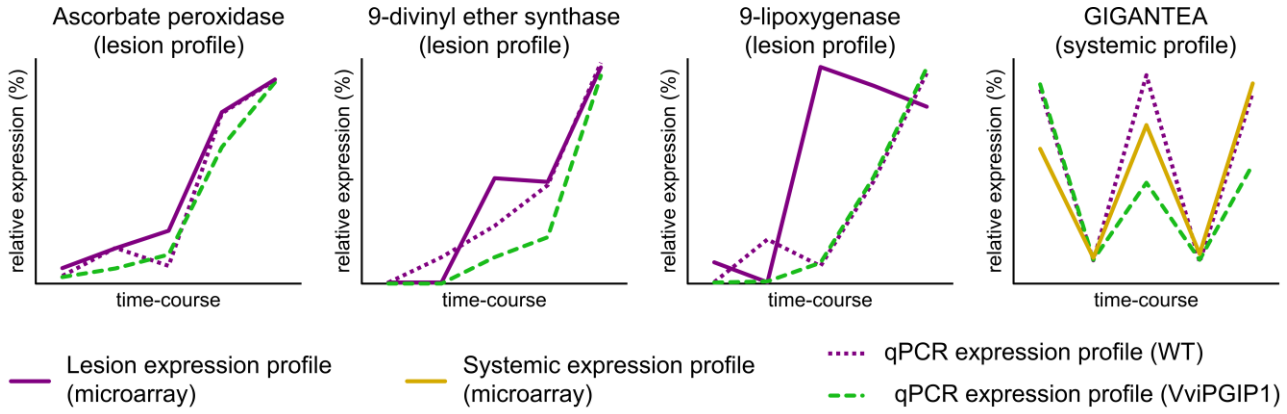

Figure 4.16 Validation of microarray expression patterns using quantitative reverse-transcriptase PCR. Three genes were targeted in leaf 3 (lesion expression profile), and one gene was targeted in leaf 2 (distal expression profile).

As in WT tobacco (Figure 3.21), there was an ontogenic effect on the expression patterns in locally infected tissue and the leaf distal to the infection (Figure 4.17). *APX*, *DES* and *LOX* were induced more in leaf four, compared to leaf three. *β-1,3-glucanase* and *superoxide dismutase* displayed different expression patterns in infected and distal tissue.

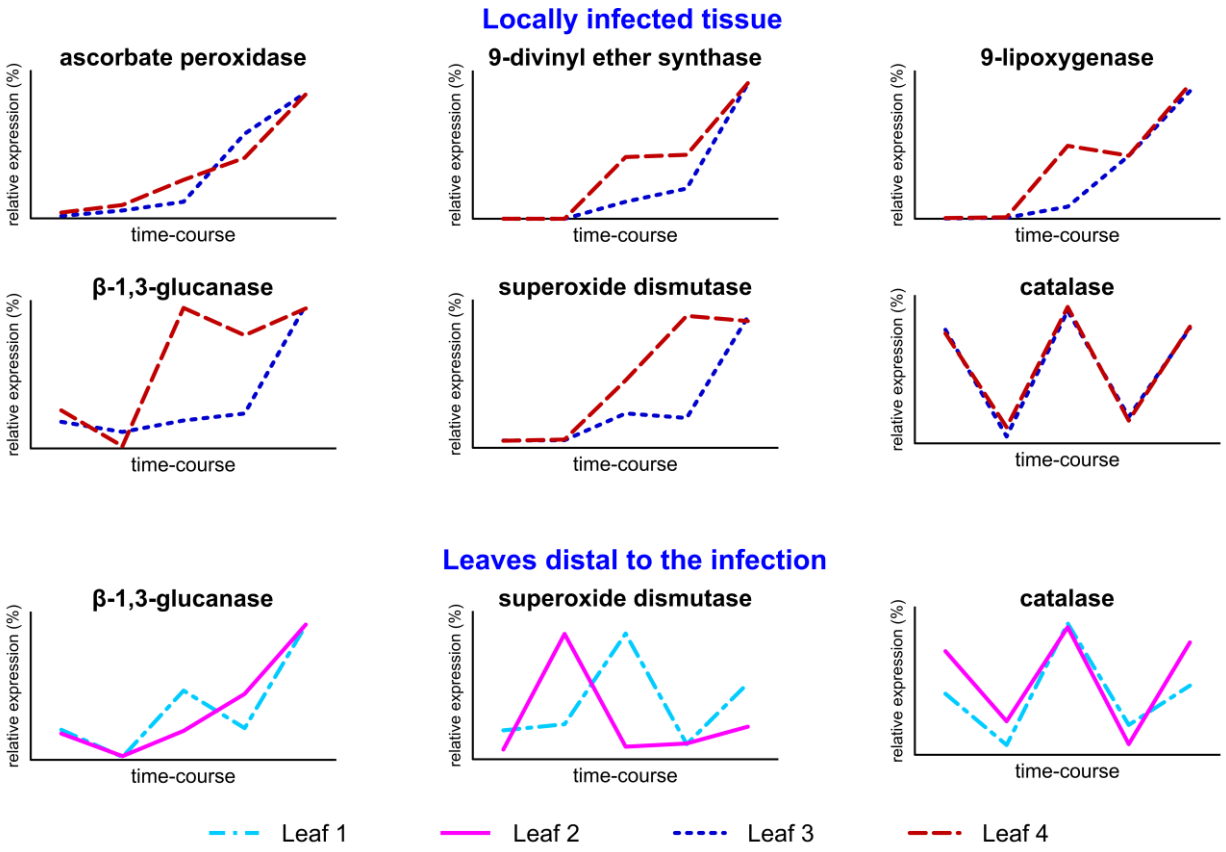

Figure 4.17 Expression profiles across leaf positions, showing an ontogenic effect. Expression levels were determined using quantitative PCR and the linear regression of expression (LRE) method.

4.4 Discussion

Since PGIPs were first identified as inhibitors of fungal PGs (Albersheim and Anderson, 1971), their status as a defensive mechanism has been reinforced by the resistance phenotypes of plants expressing *PGIP* transgenes or overexpressing native *PGIPs* (see Table 1.2 of Chapter 1). Despite this, only a few studies (Alexandersson et al., 2011; Benedetti et al., 2015; Liu et al., 2017) have investigated the basis of the PGIP-specific resistance phenotypes on the transcriptional level. To our knowledge, large-scale analysis of gene expression during infection has not been performed, making this the first report of untargeted transcriptome analysis of an infected PGIP-expressing transgenic line, with a confirmed resistance phenotype against the challenging pathogen (*B. cinerea*). Although transcriptional regulation of PGIP-specific resistance has not been reported, a wealth of information has been generated on characteristics of resistance to *B. cinerea* (reviewed in Chapter 2).

This study relied on a single pooled sample, representing the transcriptomes of four individually infected plants. Though this approach provides a “normalised view” of plant defence induction (Smith et al., 2014), it is limiting in the assessment of inherent biological variability in the identified processes, however it enabled us to assess ontogenic responses. For this reason, this report emphasised the biological processes and not so much the specific genes, that support the hypothesis that VviPGIP1-tobacco displayed a potentiated defence response.

Evidence of local and distal priming in VviPGIP1-tobacco

Martinez-Medina et al. (2016) recently proposed a guideline to analyse the presence of defence priming, where the criteria were summarised as memory (storing information about a priming stimulus), low fitness cost, more robust defence response and better performance (resistance against a pathogen). In terms of VviPGIP1-tobacco, all four of these criteria have been observed (Alexandersson et al., 2011; Joubert et al., 2006). The study specifically focussed on characterising the more robust defence response.

The involvement of PR proteins in defence priming is well documented (Finiti et al., 2014; Mahesh et al., 2017; Roylawar et al., 2015; Sun et al., 2017; Wang et al., 2015; Xue and Yi, 2018), however the modes of priming depended on the pathosystem. We observed stronger activation of several PR proteins (Figure 4.6) and faster induction of the basic form of PR1 (Table 4.1). The stronger induction of *ROMT* at t24 further underscores the primed state, as activation this enzyme was also enhanced in mycorrhiza-primed grapevine leaves (Bruisson et al., 2016). Furthermore, the enhanced transcription of histones in a leaf distal to the infection suggests that VviPGIP1 may enhance the memory of a stress signal as well.

A direct comparison (Appendix G to Chapter 3) of transcriptional changes in *Trichoderma hamatum* T382-primed *Arabidopsis* (Mathys et al., 2012) and VviPGIP1-tobacco revealed only a few induced and repressed gene models that were similarly enhanced in *Arabidopsis*, while WT/unprimed responses to *B. cinerea* were more similar (Figure 3.22), suggesting that priming signatures may be much more specific than general defence responses. Nevertheless, both species appear to have enhanced jasmonate biosynthesis while repressing ethylene synthesis and signalling.

Features of *B. cinerea* resistance in VviPGIP1-tobacco

While SA-mediated defences have been associated with *B. cinerea* resistance (Imada et al., 2015; Zimmerli et al., 2001), most resistant phenotypes require intact JA signalling or display enhanced JA synthesis (Finiti et al., 2014; Kravchuk et al., 2011; Liu et al., 2016; Martínez-Hidalgo et al., 2015; Mathys et al., 2012; Sarosh et al., 2009). Since enhanced JA accumulation during infection had previously been reported of VviPGIP1-expressing tobacco lines (Alexandersson et al., 2011), the transcriptional enhancement of both 9S- and 13S-LOX pathways (Table 4.2) supported a JA-mediated resistance phenotype. Products of the LOX pathways have diverse roles in defence, including phytoalexins and intracellular and volatile signalling (Griffiths, 2015), and so even slight changes in the timing of JA and divinyl ether oxylipin synthesis could have substantial effects on the defence response.

Ethylene sensitivity is important for resistance against *B. cinerea* (Geraats et al., 2003), but since ethylene also promotes senescence, which favours *B. cinerea*, ethylene perception, synthesis and

response must be carefully controlled to ensure an effective defence (Van Loon et al., 2006). Tomato primed with hexanoic acid more strongly induced ethylene synthesis via ACC oxidase (Finiti et al. 2014), and ethylene itself, exogenously applied, can activate resistance to *Botrytis* through the induction of defence gene expression (Diaz et al., 2002), however, reduced ethylene response was associated with *Trichoderma hamatum* T382-induced systemic resistance (ISR) in *Arabidopsis* (Mathys et al., 2012). In VviPGIP1-tobacco, ethylene synthesis was transiently enhanced, but transcripts encoding ethylene-responsive transcriptional regulators were suppressed, while transcripts encoding proteins that target them for degradation were enhanced (Table 4.2). One exception to this was *RAP2-3* and *RAP2-12*, encoding APETALA 2/Ethylene Response Factor (AP2/ERF)-domain containing transcription factors. RAP2-3 has not been functionally characterised in tobacco or *Arabidopsis*, however, other AP2/ERF transcription factors are associated with HR-like cell death phenotypes (Ogata et al., 2012) and reduced HR-lesions during viral infection (Fischer and Dröge-Laser, 2004), so it is possible that the differences in ethylene-responsive proteins and transcription factors may have contributed to the development of a necrotic, rather than hypersensitive lesion in the VviPGIP1-tobacco line.

Lignin deposition is known to inhibit penetration (Bhuiyan et al., 2009), and *B. cinerea* resistance often involves enhanced activation of the phenylpropanoid pathway (Gong et al., 2015; Gruau et al., 2015; Kelloniemi et al., 2015; Lou et al., 2011; Mathys et al., 2012). We observed enhanced induction of several phenylpropanoid and monolignol synthesis pathway transcripts in the VviPGIP1-tobacco line, however *COMT* induction was restrained (Table 4.2). Downregulation of *COMT* and *CCoAOMT* in alfalfa revealed that these enzymes determine total lignin content and lignin composition (Guo et al., 2001), which suggest that the *VviPGIP1*-expression may alter lignin composition. Infection of *Arabidopsis* mutants with differing lignin composition by *Botrytis* revealed variations in susceptibility (Lloyd et al., 2011), so it is possible that a modified lignin composition may have contributed to resistance. In addition to changes in monolignol synthesis, we observed increases in *ROMT* transcript levels at t24, suggesting that VviPGIP1-tobacco has increased capacity to synthesise pterostilbene, a phytoalexin that is toxic to *B. cinerea* (Pezet et al., 1991), at a key phase of lesion development when the fungus is most vulnerable to plant defence responses (Shlezinger et al., 2011).

B. cinerea resistance often correlates with activation of *PR* gene expression or PR protein accumulation (Gong et al., 2015; Imada et al., 2015; Smith et al., 2014; Zhang et al., 2015; Zimmerli et al., 2001). Intriguingly, VviPGIP1-tobacco repressed diverse defence-related transcripts, including those that encode PR proteins, proteinase-inhibitors, antimicrobial peptides and members of the fungitoxic SAR8.2 family at t12, but subsequently enhanced transcript levels (Table 4.2). This pattern again suggests that VviPGIP1-tobacco defence responses are preferentially activated at the point where the fungus is highly vulnerable to plant defence mechanisms. The later suppression of protease

inhibitor transcription appears to support this notion, since the restriction of lesion expansion may effectively have already occurred at t24.

Given the ubiquity of the oxidative burst in plant defence responses (Lamb and Dixon, 1997) and the ability of *B. cinerea* to not only survive the HR-induced PCD (Shlezinger et al., 2011), but to actively promote it (Govrin and Levine, 2000), it is not surprising that an altered redox state is often reported in *B. cinerea*-resistant plants (Finiti et al., 2014; Gong et al., 2015; Liu et al., 2016; Mathys et al., 2012). We observed widespread changes in redox-related transcripts (Table 4.2) that prompted investigation of the antioxidant capacity (Figure 4.10) and hydrogen peroxide generation (Figure 4.11) during infection. Hydrogen peroxide staining patterns suggested clear differences between WT and VviPGIP1-tobacco, pointing to more efficient ROS-scavenging systems, that reduce oxidative stress in the early phase of the infection. This is the phase when *B. cinerea* needs to survive the plant cells' PCD and initiate secondary lesion formation (Shlezinger et al., 2011), therefore it follows that VviPGIP1 may have prevented the runaway cell death characteristic of susceptible responses to *B. cinerea*. The striking resemblance of the VviPGIP1-tobacco plant's hydrogen peroxide staining pattern at t48 (Figure 4.11A) to the lesion morphology after nine days (Figure 4.3B) further underscores the key role that hydrogen peroxide scavenging may play in the resistance phenotype. The reduced antioxidant capacity of VviPGIP1-tobacco at t24 and t48 (Figure 4.10), combined with the enhanced transcription of NADPH oxidase and POA2 (Table 4.2) suggests that VviPGIP1-tobacco regulates oxidative stress differently than the WT. Given that photosynthesis is an important source of ROS (Foyer and Shigeoka, 2011), and that VviPGIP1-tobacco quickly repressed photosynthesis after infection (Table 4.1), it is possible that it activated alternative ROS-regulating mechanisms.

VviPGIP1 function/mode-of-action in *B. cinerea* infected tissue

Gene expression analysis of the transgenic population tobacco expressing *VviPGIP1* revealed transcriptional changes in cell wall metabolism and lignin biosynthesis (Alexandersson et al., 2011). These changes were observed in the uninfected VviPGIP1-tobacco line, thus not yet activating the PGIP-PG inhibition that is typically linked to PGIP function (D'Ovidio et al., 2004; Kalunke et al., 2015). The VviPGIP1-lines were found to have decreased xyloglucan endotransglycosylase/ hydrolase (XTH) activity in leaves and increased lignin deposits in stems and leaves (Alexandersson et al., 2011). A more detailed cell wall analysis found changes in the arabinoxyloglucan network of the leaves that suggested a more cross-linked hemicellulose network (Nguema-Ona et al., 2013), which, together with the increased lignin deposition, suggested that these uninfected VviPGIP1-tobacco lines show increased defensive reactions, suggesting a primed phenotype that would therefore display more rapid and/or stronger defence responses during infection (Balmer et al., 2015). The aim of study was to profile the transcriptional changes during infection, when the classical

PGIP function (inhibiting cell wall degradation) and the putative constitutive priming function intersect.

The enzymatic activity of PGs, acting on the plant cell wall, generates OGs that can act as damage-associated molecular patterns (D'Ovidio et al., 2004). Elicitation by OGs induces numerous defence mechanisms, including proteinase inhibitors, biosynthesis of phenylpropanoid compounds like lignin and phytoalexins, PR proteins, and the induction of the oxidative burst (Aziz et al., 2004; Ferrari et al., 2013; Galletti et al., 2008; Ridley et al., 2001). In terms of PG inhibitory activity, VviPGIP1 is able to inhibit the two main BcPGs required for virulence (Joubert et al., 2006, 2007; Kars et al., 2005; Ten Have et al., 1998). During infection therefore, plant gene expression would be influenced by the constitutive effect of VviPGIP1 expression and the OGs formed by the combined effect of BcPG degradation and inhibition of BcPGs by VviPGIP1. Though OGs generally induce a strong oxidative burst (Aziz et al., 2004; Binet et al., 1998; Galletti et al., 2008), VviPGIP1-tobacco produced less hydrogen peroxide in the first phase of infection (Figure 4.11), as has recently been reported for *Arabidopsis* expressing a PGIP from cotton (GhPGIP1) and infected with *Verticillium dahliae* or *Fusarium oxysporum* (Liu et al., 2017). *V. dahliae*-infected plants, expressing *GhPGIP1*, displayed enhanced induction of several PR proteins, SA synthesis via isochorismate synthase (ICS) and markers for SA signalling (PAD4 and EDS1). Since we observed enhanced expression of several of these genes (Table 4.2), it appears that there may be some commonality between GhPGIP1 and VviPGIP1. The degree of polymerisation (DP) of OGs plays a role in their elicitor activity (Ridley et al., 2001), therefore the capacity of these proteins to alter induced defence responses may rely on their capacity to alter the DP of OGs generated by PG activity.

It is, however, important to note that induced defence by GhPGIP1 and bean PGIP2 (PvPGIP2) was associated with SA-mediated signalling and accumulation of SA respectively (Benedetti et al., 2015; Liu et al., 2017), whereas *B. cinerea*-induced SA accumulation in VviPGIP1-tobacco did not significantly differ from WT (Alexandersson et al., 2011). Instead, in the VviPGIP1-line used in this study (VviPGIP1-37), post-infection JA levels were consistently higher than WT, while a second line (VviPGIP1-45) displayed a transient increase in JA (Alexandersson et al., 2011). The enhanced activation of JA synthesis has been reported in connection with defence primed by non-pathogenic soil microbes (Martínez-Hidalgo et al., 2015; Mehari et al., 2015; Nair et al., 2015; Van Wees et al., 1999). Therefore, considering that we observed an enhanced/accelerated activation of the LOX pathway at the site of the infection (Table 4.2), it appears that VviPGIP1 primes defence by potentiating the activation of the LOX pathway. A positive correlation between JA-induced resistance and pathogen-induced oxidative stress has been proposed (Kariola et al., 2005) which suggests that the potentiation of JA biosynthesis and inhibition of hydrogen peroxide evolution may constitute an important mechanism whereby VviPGIP1 primes tobacco for resistance against *B. cinerea*.

VviPGIP1 induced diverse transcriptional changes in a leaf distal to the infection

SAR, and other forms of defence priming, are important sources of resistance against *B. cinerea* (Frías et al., 2013; Mathys et al., 2012; Vicedo et al., 2009; Zimmerli et al., 2001). *B. cinerea* induced SAR has not been studied in detail, and the time-course considered in this study occurs prior to systemic SA accumulation, which functions as a marker for SAR (Frías et al., 2013). Since Alexandersson et al. (2011) and Nguema-Ona et al. (2013) posited the hypothesis that VviPGIP1 induced a primed state in tobacco, as evidenced by increased lignin deposition and cell wall cross-linking, profiling the transcriptional regulation of VviPGIP1-tobacco leaves that were not infected, but were on infected plants, provides an additional viewpoint to study its role in the absence of fungal PG activity, but with potential danger signals transduced from infected leaves. Intriguingly, VviPGIP1-tobacco displayed enhanced transcript accumulation of histones, which may function to "store" the primed state by altering chromatin structure (Conrath et al., 2015). The enhanced induction of secondary metabolism, including phenylpropanoid, mono- and sesquiterpene pathways are reminiscent of primed local defences (Finiti et al., 2014; Mathys et al., 2012). However, the enhanced induction of *SAR8.2* genes observed in the leaf distal to the infection in WT tobacco (Figure 3.13, Chapter 3) was negated, and the suppression of ethylene signalling observed in infected tissue was also seen in distal tissue (Table 4.5). In future, transcriptional regulation in the leaves distal to the infection may provide an interesting avenue to explore VviPGIP1 defence functions apart from those triggered by the elicitors (including OGs) that induce localised defence responses at the site of infection.

4.5 Conclusion

The first 48 hours after *B. cinerea* infection, the interval covered by our time-course, is a phase where *B. cinerea* is most vulnerable to plant defence responses, since it is not yet fully protected within a necrotic zone (Shlezinger et al., 2011). We observed the greatest differences between WT and resistant VviPGIP1-tobacco during the 24-48 h phase. This is typically the phase when only a few fungal cells are thought to survive plant PCD and then activate the further attack and spreading lesion formation in susceptible hosts. Several features of the VviPGIP1-tobacco response occurred around t24, including enhanced capacity to synthesise pterostilbene, detoxify ROS and produce fungitoxic proteins and microbial proteinase inhibitors. Since timing of defence responses is known to affect the outcome of host-*B. cinerea* interactions (Asselbergh et al., 2007; Smith et al., 2014), and VviPGIP1-tobacco appears to activate important defence mechanisms at a crucial early time, this may play an important role in the subsequent restriction of lesion expansion. In addition, our time-course infection assay allowed us to evaluate whether VviPGIP1-expressing tobacco plants displayed characteristics of priming. At the site of infection, a range of biological processes responded more rapidly, including changes indicative of an accelerated transition from source- to sink metabolism. Taken together with the enhanced defence responses, we can therefore conclude

that VviPGIP1 primed tobacco for *B. cinerea* infection at the site of infection. Although we did not observe accelerated responses in distal tissues, enhanced transcription of histones suggested that VviPGIP1 may have primed distal tissues for enhanced induced resistance.

Constitutive expression of PGIPs, including VviPGIP1 have been reported to alter host plant metabolism prior to infection (Agüero et al., 2005; Alexandersson et al., 2011; Masci et al., 2015; Matsaunyane et al., 2016; Nguema-Ona et al., 2013), but this study aimed to investigate the role that VviPGIP1 plays when its inhibitory activity against PGs leads to the production of OGs that themselves induce defence responses. Our findings contrast with those reported for transgenic *Arabidopsis* expressing PvPGIP2 and GhPGIP1, that appeared to activate defence via salicylic acid signalling (Benedetti et al., 2015; Liu et al., 2017). Since there have only been three reports, excluding this one, where plants expressing foreign PGIPs have been characterised with respect to hormone signalling/accumulation and/or defence gene activation after infection (Alexandersson et al., 2011; Benedetti et al., 2015; Liu et al., 2017), conclusive statements about a general PGIP mode-of-action would be premature. Since this is the first large-scale transcriptomic analysis of a *PGIP*-expressing transgenic during infection, it provides a useful benchmark for subsequent studies, and hints at diverse mechanisms that cause resistance, depending on the PGIP being studied.

4.6 Literature cited

Agüero CB, Uratsu SL, Greve LC, Powell ALT, Labavitch JM, Meredith CP, Dandekar AM, Ave OS (2005). Evaluation of tolerance to Pierce's disease and *Botrytis* in transgenic plants of *Vitis vinifera* L. expressing the pear PGIP gene. *Mol Plant Pathol* 6, 43–51. doi:10.1111/J.1364-3703.2004.00262.X.

Albersheim P, Anderson AJ (1971). Proteins from plant cell walls inhibit polygalacturonases secreted by plant pathogens. *PNAS* 68, 1815–1819.

Alexandersson E, Becker JVW, Jacobson D, Nguema-Ona E, Steyn C, Denby KJ, Vivier MA (2011). Constitutive expression of a grapevine polygalacturonase-inhibiting protein affects gene expression and cell wall properties in uninfected tobacco. *BMC Res Notes* 4, 493. doi:10.1186/1756-0500-4-493.

Asselbergh B, Curvers K, França SC, Audenaert K, Vuylsteke M, Van Breusegem F, Höfte M (2007). Resistance to *Botrytis cinerea* in *sitiens*, an abscisic acid-deficient tomato mutant, involves timely production of hydrogen peroxide and cell wall modifications in the epidermis. *Plant Physiol* 144, 1863–1877. doi:10.1104/pp.107.099226.

Aziz A, Heyraud A, Lambert B (2004). Oligogalacturonide signal transduction, induction of defense-related responses and protection of grapevine against *Botrytis cinerea*. *Planta* 218, 767–774. doi:10.1007/s00425-003-1153-x.

Balmer A, Pastor V, Gamir J, Flors V, Mauch-Mani B (2015). The "prime-ome": Towards a holistic approach to priming. *Trends Plant Sci* 20, 443–452. doi:10.1016/j.tplants.2015.04.002.

Benedetti M, Pontiggia D, Raggi S, Cheng Z, Scaloni F, Ferrari S, Ausubel FM, Cervone F, De Lorenzo G (2015). Plant immunity triggered by engineered in vivo release of oligogalacturonides, damage-associated molecular patterns. *PNAS* 112, 5533–5538. doi:10.1073/pnas.1504154112.

Bengtsson T, Weighill D, Proux-Wéra E, Levander F, Resjö S, Burra DD, Moushib LI, Hedley PE, Liljeroth E, Jacobson D, Alexandersson E, Andreasson E (2014). Proteomics and transcriptomics of the BABA-induced resistance response in potato using a novel functional annotation approach. *BMC Genomics* 15, 315. doi:10.1186/1471-2164-15-315.

Bhuiyan NH, Selvaraj G, Wei Y, King J (2009). Gene expression profiling and silencing reveal that monolignol biosynthesis plays a critical role in penetration defence in wheat against powdery mildew invasion. *J Exp Bot* 60, 509–521. doi:10.1093/jxb/ern290.

Binet MN, Bourque S, Lebrun-Garcia A, Chiltz A, Pugin A (1998). Comparison of the effects of cryptogein and oligogalacturonides on tobacco cells and evidence of different forms of desensitization induced by these elicitors. *Plant Sci* 137, 33–41. doi:10.1016/S0168-9452(98)00132-0.

Bruisson S, Maillot P, Schellenbaum P, Walter B, Gindro K, Deglène-Benbrahim L (2016). Arbuscular mycorrhizal symbiosis stimulates key genes of the phenylpropanoid biosynthesis and stilbenoid production in grapevine leaves in response to downy mildew and grey mould infection. *Phytochemistry* 131, 92–99. doi:10.1016/j.phytochem.2016.09.002.

Cervone F, Hahn MG, De Lorenzo G, Darvill AG, Albersheim P (1989). Host-pathogen interactions XXXIII A plant protein converts a fungal pathogenesis factor into an elicitor of plant defense responses. *Plant Physiol* 90, 542–548. doi:10.1104/pp.90.2.542.

Cheng W, Xiao Z, Cai H, Wang C, Hu Y, Xiao Y, Zheng Y, Shen L, Yang S, Liu Z, Mou S, Qiu A, Guan D, He S (2016). A novel leucine-rich repeat protein, CaLRR51, acts as a positive regulator in the response of pepper to Ralstonia solanacearum infection. *Mol Plant Pathol* 18, 1089–1100. doi:10.1111/mpp.12462.

Conrath U, Beckers GJM, Langenbach CJG, Jaskiewicz MR (2015). Priming for enhanced defense. *Annu Rev Phytopathol* 53, 97–119. doi:10.1146/annurev-phyto-080614-120132.

De Lorenzo G, Ferrari S (2002). Polygalacturonase-inhibiting proteins in defense against phytopathogenic fungi. *Curr Opin Plant Biol* 5, 1–5. doi:10.1016/S1369-5266(02)00271-6.

Diaz J, Ten Have A, Van Kan JAL (2002). The role of ethylene and wound signalling in resistance of tomato to *Botrytis cinerea*. *Plant Physiol* 129, 1341–1351. doi:10.1104/pp.001453.1.

D'Ovidio R, Mattei B, Roberti S, Bellincampi D (2004). Polygalacturonases, polygalacturonase-inhibiting proteins and pectic oligomers in plant-pathogen interactions. *Biochim Biophys Acta* 1696, 237–244. doi:10.1016/j.bbapap.2003.08.012.

Dudoit S, Yang YH, Callow MJ, Speed TP (2002). Statistical methods for identifying differentially expressed genes in replicated cDNA microarray experiments. *Stat Sin* 12, 111–139. doi:10.1.1.117.9702.

Ferrari S, Savatin D V, Sicilia F, Gramegna G, Cervone F, De Lorenzo G (2013). Oligogalacturonides: plant damage-associated molecular patterns and regulators of growth and development. *Front Plant Sci* 4, 49. doi:10.3389/fpls.2013.00049.

Ferrari S, Vairo D, Ausubel FM, Cervone F, De Lorenzo G (2003). Tandemly duplicated Arabidopsis genes that encode polygalacturonase-inhibiting proteins are regulated coordinately by different signal transduction pathways in response to fungal infection. *Plant Cell* 15, 93–106. doi:10.1105/tpc.005165.

Fillinger S, Elad Y (2016). Botrytis – *the Fungus, the Pathogen and its Management in Agricultural Systems*. Switzerland: Springer International Publishing doi:10.1007/978-3-319-23371-0.

Finiti I, De La O Leyva M, Vicedo B, Gómez-Pastor R, López-Cruz J, García-Agustín P, Real MD, González-Bosch C (2014). Hexanoic acid protects tomato plants against *Botrytis cinerea* by priming defence responses and reducing oxidative stress. *Mol Plant Pathol* 15, 550–562. doi:10.1111/mpp.12112.

Fischer R, Nölke G, Orecchia M, Schillberg S, Twyman RM (2004). Improvement of grapevine using current biotechnology. *Acta Hortic* 652, 383–390.

Foyer CH, Shigeoka S (2011). Understanding oxidative stress and antioxidant functions to enhance photosynthesis. *Plant Physiol* 155, 93–100. doi:10.1104/pp.110.166181.

Frías M, Brito N, González C (2013). The *Botrytis cinerea* cerato-platanin BcSpl1 is a potent inducer of systemic acquired resistance (SAR) in tobacco and generates a wave of salicylic acid expanding from the site of application. *Mol Plant Pathol* 14, 191–196. doi:10.1111/j.1364-3703.2012.00842.x.

Frías M, González C, Brito N (2011). BcSpl1, a cerato-platanin family protein, contributes to *Botrytis cinerea* virulence and elicits the hypersensitive response in the host. *New Phytol* 192, 483–495. doi:10.1111/j.1469-8137.2011.03802.x.

Frías M, González M, González C, Brito N (2016). BcIEB1, a *Botrytis cinerea* secreted protein, elicits a defense response in plants. *Plant Sci* 250, 115–124. doi:10.1016/j.plantsci.2016.06.009.

Galletti R, Denoux C, Gambetta S, Dewdney J, Ausubel FM, De Lorenzo G, Ferrari S (2008). The AtrbohD-mediated oxidative burst elicited by oligogalacturonides in Arabidopsis is dispensable for the activation of defense responses effective against *Botrytis cinerea*. *Plant Physiol* 148, 1695–1706. doi:10.1104/pp.108.127845.

Geraats BPJ, Bakker PAHM, Lawrence CB, Achuo EA, Höfte M, Van Loon LC (2003). Ethylene-insensitive tobacco shows differentially altered susceptibility to different pathogens. *Phytopathology* 93, 813–821. doi:10.1094/PHYTO.2003.93.7.813.

Gong S, Hao Z, Meng J, Liu D, Wei M, Tao J (2015). Digital gene expression analysis to screen disease resistance-relevant genes from leaves of herbaceous peony (*Paeonia lactiflora* Pall.) infected by *Botrytis cinerea*. *PLoS ONE* 10, e0133305. doi:10.1371/journal.pone.0133305.

Govrin EM, Levine A (2000). The hypersensitive response facilitates plant infection by the necrotrophic pathogen *Botrytis cinerea*. *Curr Biol* 10, 751–757. doi:10.1016/S0960-9822(00)00560-1.

Griffiths G (2015). Biosynthesis and analysis of plant oxylipins. *Free Radic Res* 49, 565–582. doi:10.3109/10715762.2014.1000318.

Gruau C, Trotel-Aziz P, Villaume S, Rabenoelina F, Clément C, Baillieul F, Aziz A (2015). *Pseudomonas fluorescens* PTA-CT2 triggers local and systemic immune response against *Botrytis cinerea* in grapevine. *Mol Plant-Microbe Interact* 28, 1117–1129. doi:10.1094/MPMI-04-15-0092-R.

Guo D, Chen F, Inoue K, Blount JW, Dixon RA (2001). Downregulation of caffeic acid 3-O-methyltransferase and caffeoyl CoA 3-O-methyltransferase in transgenic alfalfa: Impacts on lignin structure and implications for the biosynthesis of G and S lignin. *Plant Cell* 13, 73–88. doi:10.1105/tpc.13.1.73.

Imada K, Tanaka S, Masuda Y, Maekawa T, Ito S-I (2015). Induction of disease resistance against *Botrytis cinerea* in tomato (*Solanum lycopersicum* L.) by using electrostatic atomized water particles. *Physiol Mol Plant Pathol* 89, 1–7. doi:10.1016/j.pmpp.2014.11.001.

Johnson M, Zaretskaya I, Raytselis Y, Merezhuk Y, McGinnis S, Madden TL (2008). NCBI BLAST: a better web interface. *Nucleic Acids Res* 36, 5–9. doi:10.1093/nar/gkn201.

Joubert DA, De Lorenzo G, Vivier MA (2013). Regulation of the grapevine polygalacturonase-inhibiting protein encoding gene: expression pattern, induction profile and promoter analysis. *J Plant Res* 126, 267–281. doi:10.1007/s10265-012-0515-5.

Joubert DA, Kars I, Wagemakers L, Bergmann CW, Kemp G, Vivier MA, Van Kan JAL (2007). A polygalacturonase-inhibiting protein from grapevine reduces the symptoms of the endopolygalacturonase BcPG2 from *Botrytis cinerea* in *Nicotiana benthamiana* leaves without any evidence for in vitro interaction. *Mol Plant-Microbe Interact* 20, 392–402. doi:10.1094/MPMI-20-4-0392.

Joubert DA, Slaughter AR, Kemp G, Becker JVW, Krooshof GH, Bergmann CW, Benen JAE, Pretorius IS, Vivier MA (2006). The grapevine polygalacturonase-inhibiting protein (VvPGIP1) reduces *Botrytis cinerea* susceptibility in transgenic tobacco and differentially inhibits fungal polygalacturonases. *Transgenic Res* 15, 687–702. doi:10.1007/s11248-006-9019-1.

Kalunke RM, Tundo S, Benedetti M, Cervone F, De Lorenzo G, D'Ovidio R (2015). An update on polygalacturonase-inhibiting protein (PGIP), a leucine-rich repeat protein that protects crop plants against pathogens. *Front Plant Sci* 6, 146. doi:10.3389/fpls.2015.00146.

Kariola T, Brader G, Li J, Palva ET (2005). Chlorophyllase 1, a damage control enzyme, affects the balance between defense pathways in plants. *Plant Cell* 17, 282–294. doi:10.1105/tpc.104.025817.

Kars I, Krooshof GH, Wagemakers L, Joosten R, Benen JAE, Van Kan JAL (2005). Necrotizing activity of five *Botrytis cinerea* endopolygalacturonases produced in *Pichia pastoris*. *Plant J* 43, 213–225. doi:10.1111/j.1365-313X.2005.02436.x.

Kars I, Van Kan JAL (2007). Extracellular enzymes and metabolites involved in pathogenesis of *Botrytis*. In *Botrytis: Biology, Pathology and Control*, eds B Y Elad, B Williamson, P Tudzynski, and N Delen (Springer Netherlands), 99–118. doi:10.1007/978-1-4020-2626-3_7.

Kelloniemi J, Trouvelot S, Héloir M-C, Simon A, Dalmais B, Frettinger P, Cimerman A, Fermaud M, Roudet J, Baulande S, Bruel C, Choquer M, Couvelard L, Duthiew M, Ferrarini A, Flors V, Le Pêcheur P, Loisel E, Morgant G, et al. (2015). Analysis of the molecular dialogue between gray mould (*Botrytis cinerea*) and grapevine (*Vitis vinifera*) reveals a clear shift in defense mechanisms during berry ripening. *Mol Plant-Microbe Interact* 28, 1167–1180. doi:10.1094/MPMI-02-15-0039-R.

Kobe B, Deisenhofer J (1995). Proteins with leucine-rich repeats. *Curr Opin Struct Biol* 5, 409–416. doi:10.1016/0959-440X(95)80105-7.

Kravchuk Z, Vicedo B, Flors V, Camañes G, González-Bosch C, García-Agustín P (2011). Priming for JA-dependent defenses using hexanoic acid is an effective mechanism to protect *Arabidopsis* against *B. cinerea*. *J Plant Physiol* 168, 359–366. doi:10.1016/j.jplph.2010.07.028.

Lamb CJ, Dixon RA (1997). The oxidative burst in disease resistance. *Annu Rev Plant Physiol Plant Mol Biol* 48, 251–275. doi:10.1146/annurev.arplant.48.1.251.

Liu N, Zhang X, Sun Y, Wang P, Li X, Pei Y, Li F, Hou Y (2017). Molecular evidence for the involvement of a polygalacturonase-inhibiting protein, GhPGIP1, in enhanced resistance to Verticillium and Fusarium wilts in cotton. *Sci Rep* 7, 39840. doi:10.1038/srep39840.

Liu Z, Luan Y, Li J, Yin Y (2016). Expression of a tomato MYB gene in transgenic tobacco increases resistance to *Fusarium oxysporum* and *Botrytis cinerea*. *Eur J Plant Pathol* 144, 607–617. doi:10.1007/s10658-015-0799-0.

Lloyd AJ, Allwood JW, Winder CL, Dunn WB, Heald JK, Cristescu SM, Sivakumaran A, Harren FJM, Mulema J, Denby K, Goodacre R, Smith AR, Mur LAJ (2011). Metabolomic approaches reveal that cell wall modifications play a major role in ethylene-mediated resistance against *Botrytis cinerea*. *Plant J* 67, 852–868. doi:10.1111/j.1365-313X.2011.04639.x.

Lou B, Wang A, Lin C, Xu T, Zheng X (2011). Enhancement of defense responses by oligandrin against *Botrytis cinerea* in tomatoes. *African J Biotechnol* 10, 11442–11449. doi:10.5897/AJB11.618.

Mahesh HM, Murali M, Anup Chandra Pal M, Melvin P, Sharada MS (2017). Salicylic acid seed priming instigates defense mechanism by inducing PR-Proteins in *Solanum melongena* L. upon infection with *Verticillium dahliae* Kleb. *Plant Physiol Biochem* 117, 12–23. doi:10.1016/j.plaphy.2017.05.012.

Manfredini C, Sicilia F, Ferrari S, Pontiggia D, Salvi G, Caprari C, Lorito M, De Lorenzo G (2005). Polygalacturonase-inhibiting protein 2 of *Phaseolus vulgaris* inhibits BcPG1, a polygalacturonase of *Botrytis cinerea* important for pathogenicity, and protects transgenic plants from infection. *Physiol Mol Plant Pathol* 67, 108–115. doi:10.1016/j.pmpp.2005.10.002.

Marnewick JL, Joubert E, Swart P, Van Der Westhuizen F, Gelderblom WC (2003). Modulation of hepatic drug metabolism enzymes and oxidative status by rooibos (*Aspalathus linearis*), honeybush (*Cyclopia intermedia*) tea, as well as green and black (*Camellia sinensis*) teas in rats. *J Agric Food Chem* 51, 8113–8119.

Martínez-Hidalgo P, García JM, Pozo MJ (2015). Induced systemic resistance against *Botrytis cinerea* by *Micromonospora* strains isolated from root nodules. *Front Microbiol* 6, 922. doi:10.3389/fmicb.2015.00922.

Martinez-Medina A, Flors V, Heil M, Mauch-Mani B, Pieterse CMJ, Pozo MJ, Ton J, Van Dam NM, Conrath U (2016). Recognizing plant defense priming. *Trends Plant Sci* 21, 818–822. doi:10.1016/j.tplants.2016.07.009.

Masci S, Laino P, Janni M, Botticella E, Di Carli M, Benvenuto E, Danieli PP, Lilley KS, Lafiandra D, D'Ovidio R (2015). Analysis of quality-related parameters in mature kernels of polygalacturonase inhibiting protein (PGIP) transgenic bread wheat infected with *Fusarium graminearum*. *J Agric Food Chem* 63, 3962–3969. doi:10.1021/jf506003t.

Mathys J, De Cremer K, Timmermans P, Van Kerckhove S, Lievens B, Vanhaecke M, Cammue BPA, De Coninck B (2012). Genome-wide characterization of ISR induced in *Arabidopsis thaliana* by *Trichoderma hamatum* T382 against *Botrytis cinerea* infection. *Front Plant Sci* 3, 108. doi:10.3389/fpls.2012.00108.

Matsaunyane LBT, Oelofse D, Dubery IA (2016). Detailed molecular characterisation of the transgenic potato line, AppA6, modified with the apple (*Malus domestica*) polygalacturonase inhibiting protein 1 (pgip1) gene. *Potato Res* 59, 129–147. doi:10.1007/s11540-016-9316-x.

Mehari ZH, Elad Y, Rav-David D, Graber ER, Meller Harel Y (2015). Induced systemic resistance in tomato (*Solanum lycopersicum*) against *Botrytis cinerea* by biochar amendment involves jasmonic acid signaling. *Plant Soil* 395, 31–44. doi:10.1007/s11104-015-2445-1.

Nair A, Kolet SP, Thulasiram H V, Bhargava S (2015). Systemic jasmonic acid modulation in mycorrhizal tomato plants and its role in induced resistance against *Alternaria alternata*. *Plant Biol* 17, 625–631. doi:10.1111/plb.12277.

Nguema-Ona E, Moore JP, Fagerström AD, Fangel JU, Willats WGT, Hugo A, Vivier MA (2013). Overexpression of the grapevine PGIP1 in tobacco results in compositional changes in the leaf arabinoxyloglucan network in the absence of fungal infection. *BMC Plant Biol* 13, 46. doi:10.1186/1471-2229-13-46.

Ogata T, Kida Y, Arai T, Kishi Y, Manago Y, Murai M, Matsushita Y (2012). Overexpression of tobacco ethylene response factor *NtERF3* gene and its homologues from tobacco and rice induces hypersensitive response-like cell death in tobacco. *J Gen Plant Pathol* 78, 8–17. doi:10.1007/s10327-011-0355-5.

Ou B, Hampsch-Woodill M, Prior RL (2001). Development and validation of an improved oxygen radical absorbance capacity assay using fluorescein as the fluorescent probe development and validation of an improved oxygen radical absorbance capacity assay using fluorescein as the fluorescent probe. *J Agric Food Chem* 49, 4619–4626. doi:10.1021/jf010586o.

Pezet R, Pontt V, Hoang-Van K (1991). Evidence for oxidative detoxication of pterostilbene and resveratrol by a laccase-like stilbene oxidase produced by *Botrytis cinerea*. *Physiol Mol Plant Pathol* 39, 441–450. doi:10.1016/0885-5765(91)90010-F.

Powell ALT, Van Kan JAL, Ten Have A, Visser J, Greve LC, Bennett AB, Labavitch JM (2000). Transgenic expression of pear PGIP in tomato limits fungal colonization. *Mol Plant-Microbe Interact* 13, 942–950. doi:10.1094/MPMI.2000.13.9.942.

Ridley BL, Neill MAO, Mohnen D (2001). Pectins: structure, biosynthesis, and oligogalacturonide-related signaling. *Phytochemistry* 57, 929–967. doi:10.1016/S0031-9422(01)00113-3.

Rossi FR, Gárriz A, Marina M, Romero FM, Gonzalez ME, Collado IG, Pieckenstain FL (2011). The sesquiterpene botrydial produced by *Botrytis cinerea* induces the hypersensitive response on plant tissues and its action is modulated by salicylic acid and jasmonic acid signaling. *Mol Plant-Microbe Interact* 24, 888–896. doi:10.1094/MPMI-10-10-0248.

Rowe HC, Walley JW, Corwin J, Chan EK-F, Dehesh K, Kliebenstein DJ (2010). Deficiencies in jasmonate-mediated plant defense reveal quantitative variation in *Botrytis cinerea* pathogenesis. *PLoS Pathog* 6, e1000861. doi:10.1371/journal.ppat.1000861.

Roylawar P, Panda S, Kamble A (2015). Comparative analysis of BABA and *Piriformospora indica* mediated priming of defence-related genes in tomato against early blight. *Physiol Mol Plant Pathol* 91, 88–95. doi:10.1016/j.pmpp.2015.06.004.

Sarosh BR, Danielsson J, Meijer J (2009). Transcript profiling of oilseed rape (*Brassica napus*) primed for biocontrol differentiate genes involved in microbial interactions with beneficial *Bacillus amyloliquefaciens* from pathogenic *Botrytis cinerea*. *Plant Mol Biol* 70, 31–45. doi:10.1007/s11103-009-9455-4.

Shlezinger N, Minz A, Gur Y, Hatam I, Dagdas YF, Talbot NJ, Sharon A (2011). Anti-apoptotic machinery protects the necrotrophic fungus *Botrytis cinerea* from host-induced apoptotic-like cell death during plant infection. *PLoS Pathog* 7, e1002185. doi:10.1371/journal.ppat.1002185.

Smith JE, Mengesha B, Tang H, Mengiste T, Bluhm BH (2014). Resistance to *Botrytis cinerea* in *Solanum lycopersicoides* involves widespread transcriptional reprogramming. *BMC Genomics* 15, 334. doi:10.1186/1471-2164-15-334.

Sun G, Wang H, Shi B, Shangguan N, Wang Y, Ma Q (2017). Control efficiency and expressions of resistance genes in tomato plants treated with ε-poly-L-lysine against *Botrytis cinerea*. *Pestic Biochem Physiol*. doi:10.1016/j.pestbp.2017.07.007.

Ten Have A, Mulder W, Visser J, Van Kan JAL (1998). The endopolygalacturonase gene *Bcpg1* is required for full virulence of *Botrytis cinerea*. *Mol Plant-Microbe Interact* 11, 1009–1016. doi:10.1094/MPMI.1998.11.10.1009.

Thordal-Christensen H, Zhang Z, Wei Y, Collinge DB (1997). Subcellular localization of H_2O_2 in plants. H_2O_2 accumulation in papillae and hypersensitive response during the barley-powdery mildew interaction. *Plant J* 11, 1187–1194. doi:10.1046/j.1365-313X.1997.11061187.x.

Torres MA (2010). ROS in biotic interactions. *Physiol Plant* 138, 414–429. doi:10.1111/j.1399-3054.2009.01326.x.

Van Loon LC, Geraats BPJ, Linthorst HJM (2006). Ethylene as a modulator of disease resistance in plants. *Trends Plant Sci* 11, 184–191. doi:10.1016/j.tplants.2006.02.005.

Van Wees SCM, Luijendijk M, Smoorenburg I, Van Loon LC, Pieterse CMJ (1999). Rhizobacteria-mediated induced systemic resistance (ISR) in *Arabidopsis* is not associated with a direct effect on expression of known defense-related genes but stimulates the expression of the jasmonate-inducible gene Atvsp upon challenge. *Plant Mol Biol* 41, 537–549. doi:10.1023/A:1006319216982.

Vicedo B, Flors V, De La O Leyva M, Finiti I, Kravchuk Z, Real MD, García-Agustín P, González-Bosch C (2009). Hexanoic acid-induced resistance against *Botrytis cinerea* in tomato plants. *Mol Plant-Microbe Interact* 22, 1455–1465. doi:10.1094/MPMI-22-11-1455.

Wang L, Jin P, Wang J, Jiang L, Shan T, Zheng Y (2015). Methyl jasmonate primed defense responses against *Penicillium expansum* in sweet cherry fruit. *Plant Mol Biol Report* 33, 1464–1471. doi:10.1007/s11105-014-0844-8.

Xue M, Yi H (2018). Enhanced *Arabidopsis* disease resistance against *Botrytis cinerea* induced by sulfur dioxide. *Ecotoxicol Environ Saf* 147, 523–529. doi:10.1016/j.ecoenv.2017.09.011.

Zhang Y, Zhang Y, Qiu D, Zeng H, Guo L, Yang X (2015). BcGs1, a glycoprotein from *Botrytis cinerea*, elicits defence response and improves disease resistance in host plants. *Biochem Biophys Res Commun* 457, 627–634. doi:10.1016/j.bbrc.2015.01.038.

Zheng Q, Wang X-J (2008). GOEAST: a web-based software toolkit for Gene Ontology enrichment analysis. *Nucleic Acids Res* 36, W358–W363. doi:10.1093/nar/gkn276.

Zhou L, Cheung MY, Zhang Q, Lei CL, Zhang SH, Sun SSM, Lam HM (2009). A novel simple extracellular leucine-rich repeat (eLRR) domain protein from rice (OsLRR1) enters the endosomal pathway and interacts with the hypersensitive-induced reaction protein 1 (OsHIR1). *Plant, Cell Environ* 32, 1804–1820. doi:10.1111/j.1365-3040.2009.02039.x.

Zimmerli L, Métraux JP, Mauch-Mani B (2001). β-Aminobutyric acid-induced protection of Arabidopsis against the necrotrophic fungus *Botrytis cinerea*. *Plant Physiol* 126, 517–523. doi:10.1104/pp.126.2.517.

Appendix A to Chapter 4

GO enrichment analysis of differentially expressed transcripts in tissue including the infection spot.

Transcripts with a minimum fold change of two were analysed using GOEAST. Only biological process ontologies with p<0.01 are shown.

* Δt: Fold-change data are expressed relative to the earlier time point and log-scaled.

GOID	Term	Induced in WT				Repressed in WT				Induced in VviPGIP1-line				Repressed in VviPGIP1-line			
		Δt0-12	Δt12-24	Δt24-36	Δt36-48	Δt0-12	Δt12-24	Δt24-36	Δt36-48	Δt0-12	Δt12-24	Δt24-36	Δt36-48	Δt0-12	Δt12-24	Δt24-36	Δt36-48
GO:0046031	ADP metabolism									6.4E-04					1.4E-03		
GO:0006757	ADP phosphorylation									6.4E-04					1.4E-03		
GO:0043604	amide biosynthesis						3.0E-03								2.3E-04		
GO:0046348	amino sugar catabolism		5.5E-06														
GO:0006040	amino sugar metabolism		7.7E-06														
GO:0006026	aminoglycan catabolism		9.3E-06														
GO:0006022	aminoglycan metabolism		1.0E-05														
GO:0009058	biosynthesis						1.4E-05			8.3E-05					1.6E-04		
GO:0016052	carbohydrate catabolism									1.8E-03					6.0E-04		
GO:1901136	carbohydrate derivative catabolism		1.5E-04	8.7E-04													
GO:1901135	carbohydrate derivative metabolism			8.7E-04													
GO:0005975	carbohydrate metabolism	1.3E-05		7.6E-05			1.9E-04			4.4E-04							
GO:0009056	catabolism		8.4E-04	7.8E-06													
GO:0016998	cell wall macromolecule catabolism		5.5E-04														
GO:0043603	cellular amide metabolism						3.0E-03								4.1E-04		
GO:0044249	cellular biosynthesis						8.5E-06			2.5E-04					2.1E-05		
GO:0044262	cellular carbohydrate metabolism						4.5E-04									1.1E-05	
GO:0044248	cellular catabolism		1.5E-04														
GO:0006073	cellular glucan metabolism						1.0E-02									2.7E-06	
GO:0044237	cellular metabolism	1.5E-05					1.2E-11	2.6E-05	3.5E-04	6.6E-06					1.7E-06	1.1E-04	
GO:0044264	cellular polysaccharide metabolism															5.0E-06	
GO:0009987	cellular process	2.1E-07					5.4E-12	3.6E-09	2.3E-06	1.6E-07			1.5E-04		7.3E-11	5.5E-07	
GO:0006032	chitin catabolism		5.5E-06														
GO:0006030	chitin metabolism		5.5E-06														
GO:0009658	chloroplast organization						3.4E-03								2.2E-04		
GO:0007623	circadian rhythm						3.2E-03		5.1E-04								

GOID	Term	Induced in WT				Repressed in WT				Induced in VviPGIP1-line				Repressed in VviPGIP1-line			
		Δt0-12	Δt12-24	Δt24-36	Δt36-48	Δt0-12	Δt12-24	Δt24-36	Δt36-48	Δt0-12	Δt12-24	Δt24-36	Δt36-48	Δt0-12	Δt12-24	Δt24-36	Δt36-48
GO:0006732	coenzyme metabolism			2.0E-04						4.8E-03							
GO:0051186	cofactor metabolism			3.9E-04						1.3E-03							
GO:0009805	coumarin biosynthesis		5.3E-04		3.3E-05					6.4E-05							
GO:0009804	coumarin metabolism		5.3E-04		3.3E-05					6.4E-05							
GO:0006952	defence response		5.3E-06	6.8E-05				5.0E-06		1.0E-03	1.6E-05		1.6E-04		4.1E-05	1.0E-05	
GO:0042742	defence response to bacterium						1.7E-03		2.1E-04	1.9E-04					2.3E-04		
GO:0050832	defence response to fungus		5.3E-04			5.4E-03					2.7E-05						
GO:0098542	defence response to other organism		4.9E-04					4.0E-03	6.5E-03		6.8E-05					1.9E-03	
GO:0006091	generation of precursor metabolites and energy						2.4E-04	2.7E-11	3.5E-08	8.7E-04	1.3E-05		8.6E-09		1.9E-03	3.7E-13	
GO:0044042	glucan metabolism						1.0E-02									2.7E-06	
GO:1901072	glucosamine-containing compound catabolism		5.5E-06														
GO:1901071	glucosamine-containing compound metabolism		5.5E-06														
GO:0006096	glycolytic process									6.4E-04					1.4E-03		
GO:0008152	metabolism	6.3E-07	8.9E-04	1.3E-04			1.6E-17	4.3E-05	3.1E-07	5.8E-06					3.8E-06	1.2E-04	
GO:0032787	monocarboxylic acid metabolism			8.7E-04						2.2E-03							
GO:0051704	multi-organism process		5.0E-09	3.0E-06				2.7E-03			2.6E-05				3.2E-03	4.8E-03	
GO:0046496	nicotinamide nucleotide metabolism			7.6E-05						4.8E-05					9.1E-03		
GO:0006807	nitrogen compound metabolism						3.7E-04			6.1E-03					2.9E-04		
GO:0009132	nucleoside diphosphate metabolism									8.3E-04					2.9E-04		
GO:0006165	nucleoside diphosphate phosphorylation									6.4E-04					1.4E-03		
GO:0046939	nucleotide phosphorylation									6.4E-04					1.4E-03		
GO:0006730	one-carbon metabolism				4.6E-04												
GO:1901576	organic substance biosynthesis						7.6E-05			9.9E-04					1.2E-04		
GO:1901575	organic substance catabolism			6.0E-04													
GO:0071704	organic substance metabolism						7.4E-09			3.4E-03					1.4E-03		
GO:1901566	organonitrogen compound biosynthesis						3.9E-04								1.6E-04		
GO:1901565	organonitrogen compound catabolism		1.6E-05														
GO:1901564	organonitrogen compound metabolism						6.1E-05			6.2E-04					2.4E-05		
GO:0055114	oxidation-reduction process	6.1E-04		5.8E-05			1.8E-05		2.3E-06	1.2E-04						6.0E-04	
GO:0006733	oxidoreduction coenzyme metabolism			1.5E-04						1.1E-04							
GO:0043043	peptide biosynthesis						3.0E-03								2.3E-04		
GO:0006518	peptide metabolism						4.0E-03								3.0E-04		
GO:0009699	phenylpropanoid biosynthesis				4.6E-04					1.2E-03							
GO:0015979	photosynthesis	2.7E-04					2.5E-08	4.9E-21	1.7E-09		2.3E-07		4.4E-14		4.8E-03	5.5E-26	
GO:0015979	photosynthesis	2.7E-04					2.5E-08	4.9E-21	1.7E-09		2.3E-07		4.4E-14		4.8E-03	5.5E-26	

GOID	Term	Induced in WT				Repressed in WT				Induced in VviPGIP1-line				Repressed in VviPGIP1-line			
		Δt0-12	Δt12-24	Δt24-36	Δt36-48	Δt0-12	Δt12-24	Δt24-36	Δt36-48	Δt0-12	Δt12-24	Δt24-36	Δt36-48	Δt0-12	Δt12-24	Δt24-36	Δt36-48
GO:0009765	photosynthesis, light harvesting						2.0E-03	8.1E-10	2.1E-03		5.3E-08		2.9E-12	3.8E-04		4.5E-15	
GO:0019684	photosynthesis, light reaction						2.8E-03	2.9E-15	2.4E-05		2.9E-09		1.8E-13	1.8E-03		1.2E-19	
GO:0009657	plastid organization														4.1E-04		
GO:0005976	polysaccharide metabolism															2.3E-05	
GO:0006779	porphyrin-containing compound biosynthesis															4.6E-04	
GO:0044238	primary metabolism						3.0E-07								7.0E-03		
GO:0009135	purine nucleoside diphosphate metabolism									6.4E-04					1.4E-03		
GO:0009179	purine ribonucleoside diphosphate metabolism									6.4E-04					1.4E-03		
GO:0019362	pyridine nucleotide metabolism			1.1E-04						7.2E-05							
GO:0072524	pyridine-containing compound metabolism			1.4E-04						9.8E-05							
GO:0006090	pyruvate metabolism									1.3E-03					4.5E-04		
GO:0009628	response to abiotic stimulus	1.7E-08	1.5E-06	1.8E-04			2.3E-11	1.3E-04	6.3E-11	1.7E-10	3.0E-03	2.8E-04	1.0E-03		5.8E-09	4.4E-08	1.8E-03
GO:0001101	response to acid chemical		1.0E-09											2.9E-03			
GO:0009617	response to bacterium						7.5E-03	3.9E-03	1.1E-03	2.5E-04					5.5E-05		
GO:0009607	response to biotic stimulus		5.5E-10	3.0E-06		1.5E-03	9.5E-03	7.2E-05	9.4E-04	2.4E-03	2.3E-06		1.6E-03	4.2E-03	3.5E-03	6.3E-05	
GO:0009637	response to blue light												9.6E-05			3.6E-04	
GO:0046686	response to cadmium ion		1.2E-10	3.8E-06						7.1E-06		1.0E-03			5.7E-04		
GO:0042221	response to chemical		7.8E-19	8.9E-06	7.9E-04					7.2E-04	1.7E-03	4.1E-04	2.8E-04	2.9E-03		6.4E-04	1.6E-03
GO:0009409	response to cold	5.1E-06					3.3E-06		1.5E-04	8.5E-06					5.5E-10		
GO:0009719	response to endogenous stimulus		1.1E-04								5.8E-03		1.7E-03	3.6E-03			
GO:0034976	response to endoplasmic reticulum stress		6.4E-04														
GO:0043207	response to external biotic stimulus		5.5E-10	4.3E-06		2.1E-03	5.1E-03	1.3E-04	5.1E-04	1.4E-03	8.6E-07		3.4E-03	5.9E-03	2.1E-03	1.3E-04	
GO:0009605	response to external stimulus		3.5E-10	1.7E-05		1.4E-04	1.1E-03	2.1E-04	9.4E-04	2.3E-03	3.5E-07		5.3E-04	1.2E-03	7.5E-03	1.3E-04	
GO:0010218	response to far red light										5.8E-03		4.2E-04			1.8E-03	
GO:0009620	response to fungus		6.7E-07			6.1E-05					3.5E-07			3.8E-04			
GO:0009408	response to heat		5.5E-04														
GO:0009725	response to hormone		7.1E-04								4.5E-03						
GO:0010035	response to inorganic substance		1.3E-15	5.9E-06						3.5E-07		9.1E-04			3.3E-03		1.5E-03
GO:0009416	response to light stimulus						7.8E-09	3.5E-05	6.0E-08			8.1E-03				1.8E-06	
GO:0010038	response to metal ion		2.9E-10	4.3E-06						6.5E-08		1.0E-03			2.8E-04		
GO:0014070	response to organic cyclic compound		3.0E-04														
GO:0010033	response to organic substance		3.6E-08								5.1E-03		2.7E-05	1.0E-03		1.0E-04	
GO:0006970	response to osmotic stress		7.6E-04									5.8E-03				3.5E-03	
GO:0051707	response to other organism		5.5E-10	4.3E-06		2.1E-03	5.1E-03	1.3E-04	5.1E-04	1.4E-03	8.6E-07		3.4E-03	5.9E-03	2.1E-03	1.3E-04	
GO:0006979	response to oxidative stress		1.6E-07														

GOID	Term	Induced in WT				Repressed in WT				Induced in VviPGIP1-line				Repressed in VviPGIP1-line			
		Δt0-12	Δt12-24	Δt24-36	Δt36-48	Δt0-12	Δt12-24	Δt24-36	Δt36-48	Δt0-12	Δt12-24	Δt24-36	Δt36-48	Δt0-12	Δt12-24	Δt24-36	Δt36-48
GO:1901700	response to oxygen-containing compound		2.7E-11	9.4E-04		9.3E-03							1.2E-03	3.2E-04		7.2E-04	
GO:0009314	response to radiation						1.5E-08	4.9E-05	1.0E-07			9.5E-03				2.7E-06	
GO:0050896	response to stimulus	2.8E-06	2.0E-19	1.3E-09	5.1E-06	5.5E-07	3.4E-08	3.7E-07	2.4E-05	5.4E-12	3.6E-10	2.0E-03	7.2E-11	9.5E-07	4.6E-08	2.2E-11	
GO:0006950	response to stress	6.5E-05	2.6E-15	3.4E-06	7.2E-06	9.6E-08	2.0E-05	4.1E-07	9.7E-04	1.4E-08	1.6E-09		5.4E-08	7.5E-06	1.1E-07	5.1E-09	
GO:0009266	response to temperature stimulus	1.9E-04	2.7E-04				1.0E-04		9.4E-04	2.3E-05					1.7E-08		
GO:0009415	response to water		5.0E-07														
GO:0009414	response to water deprivation		4.1E-07														
GO:0009611	response to wounding		3.0E-06			5.3E-04					8.9E-04			1.8E-03			
GO:0048511	rhythmic process						3.4E-03		5.6E-04								
GO:0009185	ribonucleoside diphosphate metabolism									6.4E-04					1.4E-03		
GO:0019748	secondary metabolism		5.3E-04														
GO:0044723	single-organism carbohydrate metabolism						5.5E-04			8.5E-05					3.3E-03		
GO:0044763	single-organism cellular process		7.6E-06	1.7E-05	8.9E-05		1.7E-03		1.7E-03	5.4E-05					1.6E-05		
GO:0044710	single-organism metabolism	6.0E-04	1.5E-08	4.3E-06			6.4E-08	2.5E-03	2.4E-06	1.5E-06					1.9E-03	4.7E-04	
GO:0044699	single-organism process		7.5E-07	2.4E-06			8.8E-06	2.8E-04	3.2E-05	1.0E-05			4.4E-03	6.6E-03	7.3E-05	2.2E-04	
GO:0033014	tetrapyrrole biosynthesis															9.1E-04	
GO:0055076	transition metal ion homeostasis	8.1E-04					4.4E-03			8.1E-03							
GO:0006412	translation						3.0E-03								2.3E-04		

Appendix C to Chapter 4

Comparison of WT- and VviPGIP1-expressing tobacco at individual sampling points (local expression profile)

Transcripts showing at least two-fold difference between WT and VviPGIP1-tobacco at one or more sampling points, with putative protein function, Mapman annotation and VviPGIP1 expression normalised to WT expression (per sampling point)

* Δg Fold-change data were expressed relative to the wild-type and log-scaled. Significant (fold change>2) induction and repression are highlighted in bold red/green respectively.

Probe ID	Mapman annotation	Putative protein function	Δg0*	Δg12	Δg24	Δg36	Δg48
A_95_P283429	amino acid metabolism-degradation	proline dehydrogenase 2, mitochondrial-like	0.00	**-1.25**	**1.14**	-0.23	0.10
A_95_P155177	amino acid metabolism-degradation	aminotransferase TAT2	**-1.06**	-0.89	0.41	-0.15	-0.40
A_95_P239420	amino acid metabolism-degradation	proline dehydrogenase 2, mitochondrial-like	-0.17	-0.67	**1.35**	-0.20	0.08
A_95_P017016	cell wall-cellulose synthesis	COBRA-like protein 7	-0.15	**-1.22**	-0.42	0.45	0.01
A_95_P200872	cell wall-degradation	BURP domain protein USPL1-like	0.32	**-1.09**	0.03	0.44	-0.27
A_95_P223662	cell wall-modification	Expansin-related B1	-0.51	-0.97	0.65	**-1.40**	-0.22
A_95_P177012	cell wall-modification	NtXTH6	**1.01**	-0.15	-0.06	0.38	0.29
A_95_P015886	cell wall-modification	NtXTH7	**1.05**	0.14	-0.20	0.28	0.34
A_95_P018106	cell wall-modification	NtXTH9	0.64	0.92	**-1.60**	0.04	0.59
A_95_P026141	cell-organisation	F-box protein PP2-B11-like	**-1.22**	0.07	-0.56	0.89	0.52
A_95_P231234	DNA-synthesis/chromatin structure	DEAD-box ATP-dependent RNA helicase 5-like	-0.58	-0.97	**1.24**	-0.62	-0.67
A_95_P249012	gluconeogenese/ glyoxylate cycle	isocitrate lyase	-0.09	0.28	**1.26**	-0.60	0.54
A_95_P183537	gluconeogenese/ glyoxylate cycle	isocitrate lyase	-0.07	0.10	**1.34**	-0.43	0.50
A_95_P110457	hormone metabolism-auxin	dormancy-associated protein	-0.03	**-1.06**	0.11	-0.14	-0.34
A_95_P034768	hormone metabolism-ethylene	ethylene-responsive element binding protein 5	-0.18	-0.94	-0.17	**-1.00**	-0.10
A_95_P006976	hormone metabolism-ethylene	ethylene-responsive transcription factor 1	-0.32	-0.22	-0.23	-0.32	**-1.18**
A_95_P019246	hormone metabolism-gibberellin	antimicrobial peptide (SN1a)	0.06	**-1.06**	0.15	-0.06	-0.27
A_95_P207447	hormone metabolism-gibberellin	gibberellin-responsive protein	0.26	0.41	**-1.00**	0.20	-0.23
A_95_P032526	hormone metabolism-gibberellin	gibberellin 2-oxidase 1	**1.27**	0.00	-0.03	0.64	-0.15
A_95_P029636	hormone metabolism-jasmonate	LOX	0.16	**1.24**	-0.10	0.30	0.38
A_95_P015286	hormone metabolism-jasmonate	LOX homology domain	-0.40	-0.60	**1.28**	-0.01	-0.64
A_95_P070265	lipid metabolism-lipid degradation	beta-oxidation of fatty acids	-0.06	0.00	-0.29	**-1.03**	0.77
A_95_P145447	metal handling	farnesylated protein	0.06	-0.27	0.28	0.11	**-1.15**
A_95_P197557	minor CHO metabolism	inositol 2-dehydrogenase-like	-0.23	**-1.22**	**1.25**	-0.42	**-1.22**
A_95_P113847	misc-gluco-, galacto- and mannosidases	beta-galactosidase	-0.12	-0.54	**1.08**	0.03	-0.09
A_95_P205727	misc-gluco-, galacto- and mannosidases	beta-galactosidase-like	-0.10	-0.25	**1.13**	0.00	-0.29
A_95_P206483	misc-myrosinases-lectin-jacalin	mannose-binding lectin	-0.20	**-1.09**	0.21	-0.36	0.21
A_95_P135667	misc-peroxidases	Peroxidase	-0.15	**-1.22**	**1.00**	0.62	-0.30
A_95_P030766	misc-peroxidases	Peroxidase 53 precursor	-0.23	-0.84	**1.14**	0.42	-0.51
A_95_P197852	misc-plastocyanin-like	early nodulin-like protein 1	0.80	**1.14**	-0.60	0.29	0.73
A_95_P000776	misc-protease inhibitor...	microbial serine proteinase inhibitor	-0.47	-0.47	**1.42**	-0.76	**-1.47**
A_95_P197867	misc-protease inhibitor...	protease inhibitor/seed storage/LTP	-0.38	-0.81	**1.06**	-0.25	**-1.64**

Probe ID	Mapman annotation	Putative protein function	Δg0*	Δg12	Δg24	Δg36	Δg48
A_95_P034613	misc-protease inhibitor...	glycine-rich protein	-0.01	0.43	-0.92	1.42	0.30
A_95_P144422	misc-protease inhibitor...	non-specific lipid-transfer protein-like protein	-0.62	-1.06	0.59	0.01	-0.69
A_95_P113567	misc-protease inhibitor...	protease inhibitor/seed storage/LTP	-1.00	-1.00	0.83	-0.09	-0.42
A_95_P254204	misc-protease inhibitor...	glycine-rich domain-containing protein 1-like	-0.49	-0.56	1.14	-0.15	-0.60
A_95_P001181	misc-protease inhibitor...	glycine-rich protein-like	-0.25	-1.12	0.19	0.08	-0.25
A_95_P007297	N-metabolism-nitrate metabolism	nitrate reductase	0.01	0.36	0.29	1.02	-0.04
A_95_P234979	Not assigned	unknown	-1.79	-1.74	1.46	-1.12	-1.18
A_95_P219702	Not assigned	zinc finger BED domain-containing protein RICESLEEPER 2-like	-1.22	-1.25	1.21	-1.03	-1.03
A_95_P260266	Not assigned	mitotic checkpoint serine/threonine-protein kinase BUB1-like	-2.94	-1.56	2.89	-1.18	-0.49
A_95_P027896	Not assigned	unknown	-1.56	-1.00	1.22	-0.54	-0.49
A_95_P149777	Not assigned	inflorescence and root apices receptor-like kinase-interacting protein	-1.84	-2.56	1.77	-0.18	-0.34
A_95_P221952	Not assigned	pentatricopeptide repeat-containing protein	1.24	1.02	-1.32	0.58	0.53
A_95_P118642	Not assigned	UBP1-associated protein 2B-like	-1.56	-1.56	1.61	-0.43	-0.45
A_95_P006266	Not assigned	unknown	-0.23	-1.06	-1.15	-1.51	-0.17
A_95_P154777	Not assigned	unknown	-2.32	-1.84	2.05	-0.76	-0.43
A_95_P105277	Not assigned	unknown	-1.94	-1.64	1.74	-0.94	-0.30
A_95_P131437	Not assigned	gamma-secretase subunit PEN-2	1.26	0.78	-0.94	1.04	0.58
A_95_P005501	Not assigned	thionin-like protein	-0.04	1.27	-0.86	1.03	-0.22
A_95_P100653	Not assigned	unknown	-0.94	-1.56	1.13	0.04	-0.29
A_95_P093913	Not assigned	unknown	-1.22	-0.94	1.02	-0.49	-0.20
A_95_P080600	Not assigned	unknown	-1.25	-0.22	1.04	-0.15	-0.03
A_95_P029526	Not assigned	unknown	-1.15	-0.74	1.10	-0.36	-0.56
A_95_P020641	Not assigned	unknown	1.06	0.12	-1.69	0.25	-0.10
A_95_P298028	Not assigned	putative lipid-binding	0.50	0.00	-1.09	0.07	0.07
A_95_P026581	Not assigned	unknown	1.02	0.45	-0.84	-0.01	0.07
A_95_P264156	Not assigned	zinc finger MYM-type protein 1-like	-1.18	-0.40	0.63	0.00	-0.18
A_95_P003136	Not assigned	keratin-associated protein 21-1-like	-0.01	-1.22	0.26	-0.45	-0.07
A_95_P112057	Not assigned	photoassimilate-responsive protein-related	-0.04	-0.06	0.14	1.34	-0.04
A_95_P105012	Not assigned	putative ZIP protein	0.56	0.31	-1.03	0.25	0.12
A_95_P132842	Not assigned	RADIALIS-like 1	-0.20	-0.54	1.27	0.42	-0.60
A_95_P110392	Not assigned	Transcriptionally controlled tumor protein	-0.36	-1.09	0.04	-0.92	-0.22
A_95_P133212	Not assigned	two-component response regulator ARR6-like	-0.51	-1.03	0.51	0.15	-0.18
A_95_P032396	Not assigned	Uncharacterised	0.20	0.03	-1.79	-0.07	0.30
A_95_P000606	Not assigned	Uncharacterised ncRNA	0.16	0.66	-1.09	0.32	0.37
A_95_P292508	Not assigned	Uncharacterised ncRNA	1.04	-0.03	-0.64	0.33	0.45
A_95_P004706	Not assigned	unknown	-0.09	-1.47	-0.69	-0.67	-0.60
A_95_P163727	Not assigned	unknown	-0.54	-1.06	0.50	-0.17	-0.30
A_95_P111137	Not assigned	unknown	-0.12	-1.18	-0.62	-0.40	0.21
A_95_P004366	Not assigned	unknown	-0.58	-1.03	0.34	-0.06	-0.34
A_95_P257054	Not assigned	unknown	0.25	-0.54	-0.40	-0.51	1.08
A_95_P002836	Not assigned	unknown	0.65	-0.32	-1.15	0.32	-0.86
A_95_P271131	Not assigned	unknown	-0.51	-0.89	1.11	-0.92	-0.42
A_95_P210287	Not assigned	unknown	0.38	0.44	-1.22	0.19	-0.30
A_95_P016456	Not assigned	unknown	1.06	0.69	-0.94	0.90	0.80
A_95_P005781	Not assigned	unknown	-0.01	-1.29	0.67	-0.40	-0.30
A_95_P149882	Not assigned	unknown	-0.62	-1.40	0.93	0.10	-0.18
A_95_P264316	Not assigned	unknown	-0.58	-1.03	0.25	-0.60	-0.49
A_95_P013711	Not assigned	unknown	0.06	0.06	-0.58	0.29	2.05
A_95_P102472	Not assigned	unknown	0.00	-1.09	0.21	-0.01	-0.03
A_95_P113877	Not assigned	unknown	0.77	0.37	-1.06	0.16	-0.01
A_95_P147332	Not assigned	unknown	-0.04	1.03	-0.14	-0.62	0.57
A_95_P110052	Not assigned	unknown	-0.38	-1.15	0.19	-0.23	-0.32

Probe ID	Mapman annotation	Putative protein function	Δg0*	Δg12	Δg24	Δg36	Δg48
A_95_P017766	Not assigned	unknown	-0.30	-0.56	1.02	-0.36	-0.38
A_95_P246567	Not assigned	unknown	-0.45	-1.15	0.38	-0.17	-0.03
A_95_P112812	Not assigned	unknown	-0.22	-1.18	0.00	0.03	-0.09
A_95_P263506	Not assigned	unknown	-0.29	-1.29	0.12	0.07	-0.62
A_95_P086958	Not assigned	unknown	-0.74	-0.56	1.08	-0.36	-0.27
A_95_P250702	Not assigned	unknown	-0.22	-1.03	0.28	0.20	-0.15
A_95_P102582	Not assigned	unknown	0.86	-0.14	-1.09	-0.20	0.01
A_95_P203482	Not assigned	unknown	-1.56	-1.00	0.92	-0.76	-0.69
A_95_P120397	Not assigned	unknown	0.12	-1.40	0.43	0.14	-0.58
A_95_P032981	Not assigned	unknown	-0.79	-1.15	-0.10	-0.40	-0.22
A_95_P005681	Not assigned	unknown	0.95	0.06	-1.32	-0.01	-0.12
A_95_P074345	Not assigned	zinc finger MYM-type protein 1-like	-1.60	-0.49	0.97	-0.20	0.03
A_95_P221137	protein-degradation	zingipain-1-like	0.04	0.07	0.12	1.42	0.37
A_95_P239164	protein-degradation	arm repeat-containing protein	0.56	0.60	-0.89	0.39	1.16
A_95_P003966	protein-folding	peptidyl-prolyl cis-trans isomerase	2.00	0.52	-1.43	1.07	0.55
A_95_P148847	protein-synthesis	50S ribosomal protein L11, chloroplastic-like	-0.18	-0.69	0.45	-0.43	-1.18
A_95_P002906	PS-light reaction	chlorophyll a-b-binding protein	1.88	1.20	-2.56	0.12	0.19
A_95_P105332	light reaction	chlorophyll a-b binding protein 1	1.51	0.44	-2.12	0.06	-0.10
A_95_P006596	light reaction	chlorophyll a-b binding protein 2	1.23	0.51	-2.00	0.36	0.10
A_95_P003266	light reaction	chlorophyll a-b binding protein 21	1.14	0.50	-1.47	0.23	-0.10
A_95_P078000	light reaction	chlorophyll binding protein PSII type I	1.45	0.14	-1.69	-0.07	-0.06
A_95_P026346	light reaction	chlorophyll a-b binding protein 4	1.10	0.58	-1.51	0.32	0.04
A_95_P188122	light reaction	chlorophyll a-b binding protein 4	1.01	0.41	-1.12	0.46	0.03
A_95_P003231	light reaction	chlorophyll a-b binding protein 1	1.23	0.15	-1.51	0.21	0.01
A_95_P006166	light reaction	chlorophyll a-b binding protein 1	1.21	-0.23	-1.43	0.08	0.03
A_95_P177727	light reaction	chlorophyll a-b binding protein 37	1.11	0.52	-1.74	-0.17	-0.17
A_95_P009366	light reaction	chlorophyll binding protein 6	1.02	0.60	-1.84	0.30	0.08
A_95_P107827	light reaction	chlorophyll binding protein Lhcb2.4	1.47	0.39	-1.89	-0.09	-0.12
A_95_P176552	light reaction	chlorophyll binding protein PSII type I	1.83	0.61	-2.12	0.12	0.15
A_95_P108687	light reaction	photosystem II subunit T	0.40	0.48	-1.47	0.03	-0.71
A_95_P107847	light reaction	chlorophyll a-b binding protein 4	0.67	0.16	-1.29	-0.04	0.38
A_95_P111232	light reaction	chlorophyll a-b binding protein 4	0.91	-0.18	-1.32	0.07	0.11
A_95_P227104	light reaction	chlorophyll a-b binding protein 4	0.98	0.49	-1.22	0.20	0.01
A_95_P177967	light reaction	photosystem I light harvesting complex gene 2	0.71	0.61	-1.06	0.31	0.16
A_95_P012501	light reaction	PS I light harvesting complex	0.66	0.37	-1.25	0.23	0.36
A_95_P103872	light reaction	PS I reaction center subunit VI	0.49	0.54	-1.15	0.32	0.36
A_95_P005626	light reaction	PS I reaction center subunit VI-2	0.90	0.73	-1.18	0.23	0.26
A_95_P004106	light reaction	PS1 psaH	0.49	0.43	-1.06	0.28	0.31
A_95_P003241	light reaction	PSAO	0.51	0.12	-1.06	0.26	0.36
A_95_P110517	light reaction	PSAO	0.53	0.24	-1.12	0.20	0.29
A_95_P179537	light reaction	chlorophyll a-b binding protein 13	0.88	0.72	-1.84	0.36	0.07
A_95_P179542	light reaction	chlorophyll a-b binding protein 13	0.89	0.63	-1.84	0.31	0.03
A_95_P003321	light reaction	chlorophyll a-b binding protein 36	0.96	0.58	-2.12	0.37	-0.06
A_95_P247927	light reaction	chlorophyll a-b binding protein 36	0.95	0.30	-1.69	0.57	-0.18
A_95_P106952	light reaction	chlorophyll a-b binding protein 6A	0.82	0.44	-1.60	0.54	0.37
A_95_P247017	light reaction	chlorophyll a-b binding protein CP24 10A	0.42	0.65	-1.03	-0.07	0.11
A_95_P008206	light reaction	chlorophyll binding protein 3	0.95	0.62	-1.74	0.30	-0.10
A_95_P097848	redox-thioredoxin	protein disulfide isomerase-like	-0.56	-0.14	1.01	0.18	-0.34
A_95_P215277	RNA-processing	sm-like protein LSM8	-2.00	-1.69	1.79	-1.64	-1.64
A_95_P123237	RNA-processing	splicing factor U2af small subunit B-like	-1.43	-1.47	1.98	-1.18	-0.89
A_95_P215942	RNA-processing	tRNA (cytidine(34)-2'-O)-methyltransferase	0.46	1.04	-0.74	0.58	0.40
A_95_P160597	RNA-processing	zinc finger CCCH domain-containing protein 29-like	-0.12	-0.10	-1.06	-0.01	-0.01
A_95_P185012	RNA-processing	CCR4-associated factor 1	-0.23	-1.15	-0.69	-0.67	-0.32
A_95_P112417	RNA-regulation of transcription	Cys2-His2 type zinc finger	-0.14	-1.60	-0.43	-0.36	-0.43

Probe ID	Mapman annotation	Putative protein function	Δg0*	Δg12	Δg24	Δg36	Δg48
A_95_P102437	RNA-regulation of transcription	DC1 domain-containing protein	0.32	-1.09	0.08	-0.12	-0.36
A_95_P260116	RNA-regulation of transcription	WRKY 41	0.89	-0.45	-0.67	-0.18	1.11
A_95_P252864	RNA-regulation of transcription	WRKY3	-0.27	-0.32	-0.18	1.06	-0.09
A_95_P296123	RNA-RNA binding	RNA-binding protein 42-like	-1.18	-0.97	1.12	-0.10	-0.32
A_95_P097738	RNA-transcription	TATA box-binding protein-associated factor RNA polymerase I subunit B-like	-2.06	-1.40	2.41	-0.56	-0.64
A_95_P214537	RNA-transcription	RNA polymerase sigma factor sigA-like	0.62	0.88	-1.03	0.45	0.06
A_95_P003626	secondary metabolism-phenylpropanoids	lignin-forming anionic peroxidase-like	-0.45	-1.00	1.34	0.70	-0.56
A_95_P133452	secondary metabolism-isoprenoids-non-mevalonate pathway	geranylgeranyl diphosphate reductase	0.96	0.48	-1.36	0.51	-0.10
A_95_P250577	secondary metabolism-isoprenoids-non-mevalonate pathway	geranylgeranyl diphosphate reductase	0.85	0.58	-1.40	0.32	-0.49
A_95_P117317	secondary metabolism-isoprenoids-non-mevalonate pathway	GGPP reductase	0.84	0.37	-1.15	0.34	-0.17
A_95_P008966	secondary metabolism-phenylpropanoids	trans-resveratrol di-O-methyltransferase-like	-0.54	-0.97	1.61	-0.45	-1.32
A_95_P238364	signalling-calcium	Calmodulin 5	-2.12	-2.74	1.92	-1.43	-1.74
A_95_P139762	signalling-calcium	calcineurin B-like protein 7	-0.07	-0.34	1.08	-0.09	-0.27
A_95_P137067	signalling-calcium	calcium-binding protein PBP1-like	-0.38	-1.79	-0.47	0.11	-0.38
A_95_P008351	signalling-in sugar and nutrient physiology	phi-1	-0.12	-0.67	-0.22	0.12	-1.15
A_95_P001536	signalling-receptor kinases	Receptor-like protein kinase	-1.43	-0.76	0.55	-0.01	-0.34
A_95_P133932	signalling-receptor kinases	BRI1 kinase inhibitor 1-like	0.08	1.16	0.19	-0.54	0.20
A_95_P134327	signalling-receptor kinases	wound-induced protein 1-like	1.03	-0.20	-0.81	0.54	0.23
A_95_P004201	stress-abiotic	osmotin	-0.60	-1.12	1.36	-0.49	-1.29
A_95_P176202	stress-abiotic	osmotin	-0.45	-1.25	0.98	-0.10	-0.94
A_95_P184047	stress-abiotic	17.3 kDa class II heat shock protein	0.03	-0.07	-0.56	-1.69	0.25
A_95_P000306	stress-abiotic	heat shock cognate 70 kDa protein 2-like	0.29	0.07	-0.34	-0.27	1.08
A_95_P199882	stress-abiotic	heat shock cognate 70 kDa protein 3	0.14	0.07	-0.58	-0.22	1.37
A_95_P014536	stress-abiotic	heat shock protein 82	0.08	0.24	-0.14	-0.64	1.09
A_95_P195212	stress-abiotic	luminal binding protein	-0.71	-0.45	1.26	-0.38	-0.34
A_95_P113807	stress-abiotic	latex-like protein	1.13	0.00	-0.29	0.23	-0.22
A_95_P180582	stress-abiotic	osmotin-like	-0.25	-0.27	1.11	-0.01	-0.54
A_95_P004441	stress-biotic	SAR8.2n	-0.62	-1.00	0.58	-0.14	-0.36
A_95_P000196	stress-biotic	SAR8.2d	-0.58	-1.15	0.39	-0.06	-0.34
A_95_P007686	stress-biotic	acidic beta-1,3 glucanase	-1.12	-0.18	-0.25	0.56	-0.15
A_95_P103767	stress-biotic	acidic beta-1,3 glucanase	-1.00	-0.23	-0.20	0.58	-0.14
A_95_P159427	stress-biotic	acidic endochitinase precursor	-1.06	-0.49	-0.36	0.42	0.19
A_95_P005591	stress-biotic	Avr9/Cf-9 rapidly elicited protein 65	-0.22	-0.25	-1.36	-0.76	-0.40
A_95_P027946	stress-biotic	Avr9/Cf-9 rapidly elicited protein 76	-0.43	-1.22	-0.71	-0.03	-0.23
A_95_P021401	stress-biotic	PR-1a	0.01	-0.32	0.44	1.80	-0.03
A_95_P003871	stress-biotic	PR-1b	-0.15	-0.71	1.09	-0.03	-0.47
A_95_P018316	stress-biotic	PR-4A	-0.09	0.01	-0.29	1.14	0.44
A_95_P006336	stress-biotic	SAR8.2c	-0.56	-1.00	0.54	-0.18	-0.40
A_95_P180617	stress-biotic	SAR-related chitinase, basic	-1.12	-0.30	-0.25	0.59	-0.20
A_95_P185277	stress-biotic	trypsin and protease inhibitor family	-0.64	-0.62	-0.25	-0.01	-1.06
A_95_P178237	TCA / org- transformation	carbonic anhydrase	1.00	0.44	-1.69	0.81	0.07
A_95_P154167	TCA / org- transformation	carbonic anhydrase	0.84	0.08	-1.06	0.61	0.29
A_95_P249767	tetrapyrrole synthesis	Mg protoporphyrin IX chelatase	1.25	0.62	-1.47	0.62	-0.03
A_95_P026356	tetrapyrrole synthesis	ZIP	0.54	0.36	-1.03	0.23	0.10
A_95_P034683	tetrapyrrole synthesis	ZIP	0.51	0.26	-1.03	0.25	0.04
A_95_P295058	transport	Non-intrinsic ABC protein	0.01	-1.00	0.08	0.48	-0.27
A_95_P015251	transport	DELTA-TIP	1.02	0.00	0.04	-0.15	-0.01
A_95_P160277	transport	heavy metal-associated isoprenylated plant protein 3-like	-0.42	-1.09	-0.49	0.07	-0.03

Appendix C to Chapter 4

Histochemical staining for hydrogen peroxide

Diaminobenzidine (DAB) was used to detect hydrogen peroxide at the indicated sampling points (hours post infection: hpi). In some cases, infection did not occur (red background) and these leaf disks were omitted from further analyses. At 48 hpi, the majority of leaf disks were too fragile to stain.

15 hpi

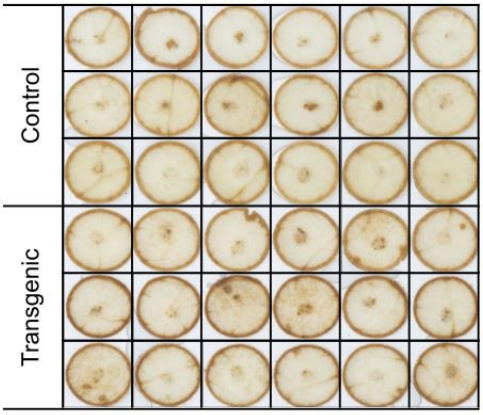

24 hpi

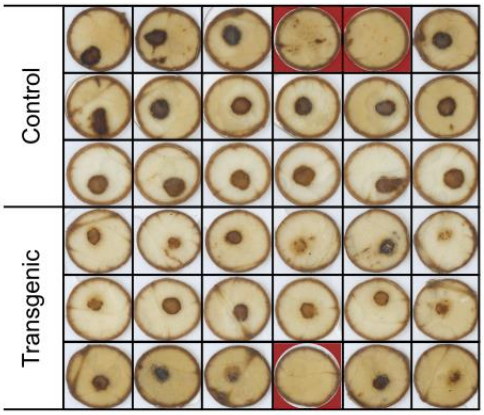

18 hpi

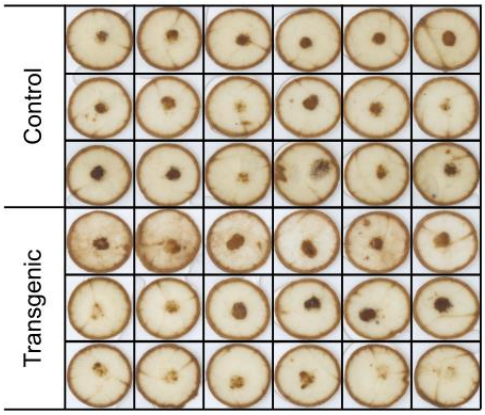

48 hpi

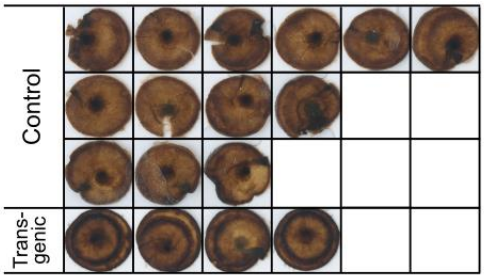

21 hpi

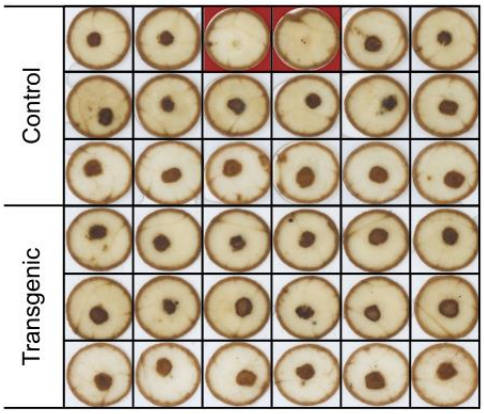

Appendix D to Chapter 4

Comparison of WT- and VviPGIP1-expressing tobacco at individual sampling points (distal expression profile)

Transcripts showing at least two-fold difference between WT and VviPGIP1-tobacco at one or more sampling points, with putative protein function, Mapman annotation and VviPGIP1 expression normalised to WT expression (per sampling point)

* Δg Fold-change data were expressed relative to the wild-type and log-scaled. Significant (fold change>2) induction and repression are highlighted in bold red/green respectively.

Probe ID	Mapman annotation	Putative protein function	Δg0*	Δg12	Δg24	Δg36	Δg48
A_95_P239420	amino acid metabolism-degradation	proline dehydrogenase 2, mitochondrial	0.03	-0.30	-0.51	-0.56	**-1.09**
A_95_P034139	cell wall-modification	Alpha-expansin A15	0.50	0.50	0.29	0.30	**1.24**
A_95_P223662	cell wall-modification	Expansin-related B1	-0.14	-0.09	**-1.00**	**-1.09**	-0.97
A_95_P180217	cell wall-modification	NtXTH23	-0.06	-0.45	-0.34	-0.30	**-1.00**
A_95_P010321	cell wall-modification	NtXTH2	0.30	-0.03	0.07	**-1.18**	-0.17
A_95_P186667	cell wall-pectin*esterases	pectin acetyl esterase	0.33	-0.06	0.46	0.43	**1.24**
A_95_P026141	cell-organisation	F-box protein PP2-B11	-0.58	-0.01	**1.20**	**-1.06**	**-1.40**
A_95_P008616	development	bidirectional sugar transporter N3	-0.34	-0.56	**-1.32**	-0.51	-0.64
A_95_P291973	development	protodermal factor 1	0.00	0.31	**2.24**	0.08	0.63
A_95_P033679	development	root phototropism protein 3	0.07	0.12	0.44	0.28	**1.04**
A_95_P002516	DNA-synthesis/chromatin structure	histone H2A.1	0.10	0.23	**1.20**	0.04	0.00
A_95_P201367	DNA-synthesis/chromatin structure	histone H2AX	0.15	0.42	**1.41**	-0.10	0.59
A_95_P033754	DNA-synthesis/chromatin structure	histone H2B.2	0.04	0.37	**1.33**	0.03	0.53
A_95_P030036	DNA-synthesis/chromatin structure	histone H2B.2	0.10	0.45	**1.27**	-0.01	0.59
A_95_P001101	DNA-synthesis/chromatin structure	histone H3.2	-0.01	0.44	**1.26**	0.10	0.39
A_95_P025316	DNA-synthesis/chromatin structure	histone H4	0.12	0.34	**1.32**	0.03	0.31
A_95_P140028	fermentation-aldehyde dehydrogenase	aldehyde dehydrogenase	0.66	0.56	**1.08**	**1.04**	**1.44**
A_95_P249012	gluconeogenese/ glyoxylate cycle	isocitrate lyase	0.00	0.04	-0.12	**-1.03**	-0.14
A_95_P183537	gluconeogenese/ glyoxylate cycle	isocitrate lyase	-0.09	0.07	-0.15	**-1.29**	-0.12
A_95_P202867	gluconeogenese/ glyoxylate cycle	malate synthase	-0.12	0.20	**-1.15**	**-1.22**	-0.51
A_95_P034768	hormone metabolism-ethylene	ethylene-responsive element binding protein 5	-0.30	-0.79	-0.43	-0.89	**-1.09**
A_95_P203507	hormone metabolism-ethylene	ethylene-responsive element binding protein 6	-0.09	-0.42	-0.60	-0.54	**-1.56**
A_95_P006976	hormone metabolism-ethylene	ethylene-responsive transcription factor 1	-0.34	-0.10	-0.84	-0.54	**-4.06**
A_95_P034798	hormone metabolism-ethylene	ethylene-responsive transcription factor 1B	-0.07	0.06	-0.84	-0.76	**-1.09**
A_95_P029636	hormone metabolism-jasmonate	LOX	0.21	0.42	0.83	**1.05**	-0.03
A_95_P015286	hormone metabolism-jasmonate	LOX homology domain	-0.34	0.04	**-1.12**	**-1.60**	-0.23
A_95_P197557	minor CHO metabolism	inositol 2-dehydrogenase	-0.25	-0.32	**-1.47**	-1.00	**-1.03**
A_95_P113847	misc-gluco-, galacto- and mannosidases	beta-galactosidase	-0.45	-0.15	**-1.06**	-0.79	-0.81
A_95_P154752	misc-gluco-, galacto- and mannosidases	beta-galactosidase 3	-0.29	-0.12	-0.69	**-1.40**	-0.36
A_95_P219462	misc-gluco-, galacto- and mannosidases	beta-galactosidase 3	-0.27	0.07	-0.56	**-1.29**	-0.15

Probe ID	Mapman annotation	Putative protein function	Δg0*	Δg12	Δg24	Δg36	Δg48
A_95_P205727	misc-gluco-, galacto- and mannosidases	beta-galactosidase	-0.43	0.01	-1.18	-0.79	-0.67
A_95_P009701	misc-invertase/pectin methylesterase inhibitor family protein	21 kDa protein	-0.45	-0.01	-0.29	-0.54	-1.06
A_95_P187637	misc-invertase/pectin methylesterase inhibitor family protein	invertase/pectin methylesterase inhibitor family	-0.15	-0.07	-1.06	-0.76	-0.86
A_95_P197852	misc-plastocyanin-like	early nodulin protein 1	0.32	-0.20	-0.10	1.23	1.34
A_95_P000776	misc-protease inhibitor...	microbial serine proteinase inhibitor	-0.45	-0.06	-1.51	-1.56	-0.92
A_95_P000771	misc-protease inhibitor...	microbial serine proteinase inhibitor	-0.54	0.20	-1.15	-0.86	-0.51
A_95_P301618	misc-protease inhibitor...	non-specific lipid-transfer protein 1	0.06	0.24	1.26	0.03	0.66
A_95_P238389	misc-protease inhibitor...	P-rich protein EIG-I30	-0.30	0.16	-1.09	-1.69	0.12
A_95_P000541	misc-protease inhibitor...	proline-rich protein DC2.15	0.46	0.08	-1.18	-0.18	-0.76
A_95_P103172	misc-protease inhibitor...	protease inhibitor/seed storage/LTP	0.12	0.01	-1.00	-0.07	-1.12
A_95_P019016	misc-protease inhibitor...	proteinase inhibitor type-2	-0.20	-0.10	-0.47	-1.74	-0.79
A_95_P185737	misc-protease inhibitor...	proteinase inhibitor type-2	-0.09	0.10	-0.36	-1.32	-0.43
A_95_P145647	Not assigned	ferrochelatase-2, chloroplastic	0.03	-0.60	0.11	0.15	1.06
A_95_P149777	Not assigned	inflorescence and root apices receptor kinase-interacting protein	-0.20	-0.34	-0.92	-0.76	-1.09
A_95_P260266	Not assigned	mitotic checkpoint serine/threonine-protein kinase BUB1	-0.43	-0.20	-1.60	-1.74	-1.47
A_95_P132842	Not assigned	RADIALIS 1	-0.10	-0.32	-1.06	0.08	-0.84
A_95_P205492	Not assigned	serine-rich protein-related	-0.14	-0.18	-1.12	-0.64	-1.15
A_95_P160902	Not assigned	S-locus lectin protein kinase family	-0.62	-0.43	-1.15	-0.84	-0.71
A_95_P118642	Not assigned	UBP1-associated protein 2B	-0.27	-0.36	-1.18	-1.36	-1.12
A_95_P000606	Not assigned	Uncharacterised ncRNA	-0.23	0.80	1.70	0.20	0.54
A_95_P292508	Not assigned	Uncharacterised ncRNA	0.06	-0.01	0.43	1.10	0.49
A_95_P154777	Not assigned	unknown	-0.43	-0.30	-1.32	-1.56	-1.40
A_95_P105277	Not assigned	unknown	-0.23	-0.22	-1.25	-1.69	-1.25
A_95_P203482	Not assigned	unknown	-0.60	-0.45	-1.18	-1.32	-1.47
A_95_P164077	Not assigned	unknown	-0.09	-0.20	-1.29	-0.56	-1.03
A_95_P234979	Not assigned	unknown	-0.20	-0.49	-1.06	-1.18	-0.76
A_95_P005781	Not assigned	unknown	-0.29	-0.32	-1.06	-1.18	-0.94
A_95_P264316	Not assigned	unknown	0.11	-1.12	-0.74	-0.92	-1.69
A_95_P201622	Not assigned	unknown	-0.81	-0.12	-1.09	-0.86	-1.03
A_95_P183012	Not assigned	unknown	0.08	-0.27	0.19	0.20	-1.03
A_95_P206357	Not assigned	unknown	-0.29	-0.14	-0.45	-0.22	-1.00
A_95_P299143	Not assigned	unknown	0.00	0.00	-0.89	-0.42	-2.32
A_95_P141517	Not assigned	unknown	-0.15	-0.25	-1.00	-0.47	-0.03
A_95_P104482	Not assigned	unknown	0.16	-0.27	-0.49	-0.01	-2.25
A_95_P003206	Not assigned	unknown	-0.23	0.04	-0.74	-0.47	-1.18
A_95_P216582	Not assigned	unknown	0.00	-0.30	-0.32	0.04	-1.51
A_95_P155492	Not assigned	unknown	-0.07	-0.25	-0.89	-1.22	-0.94
A_95_P030776	Not assigned	unknown	0.00	-0.17	-0.18	-1.12	-0.30
A_95_P218862	Not assigned	unknown	0.10	-0.07	-0.15	-0.03	-2.32
A_95_P021536	Not assigned	unknown	-0.04	-0.47	-0.54	-0.17	-1.84
A_95_P226469	Not assigned	unknown	-0.12	-0.14	-0.32	-0.10	-1.29
A_95_P218532	Not assigned	unknown	-0.14	-0.32	-0.23	0.07	-1.89
A_95_P123007	Not assigned	unknown	-0.14	-0.40	-1.29	-0.76	-0.64
A_95_P006051	Not assigned	unknown	0.16	-0.36	-0.49	-0.36	-2.56
A_95_P312788	Not assigned	unknown	-0.01	0.00	-0.22	-0.25	-1.47
A_95_P209062	Not assigned	unknown	-0.15	-0.51	0.49	0.25	1.20
A_95_P219932	Not assigned	unknown	-0.17	-0.10	-0.58	-1.09	-0.51
A_95_P001521	Not assigned	unknown	0.12	0.70	1.40	0.75	0.25
A_95_P303953	Not assigned	unknown	0.31	0.03	-0.32	-0.17	-1.29
A_95_P006266	Not assigned	unknown	0.31	-0.15	-0.15	-0.10	-2.84
A_95_P004706	Not assigned	unknown	0.20	-0.29	-0.23	-0.03	-1.47
A_95_P111137	Not assigned	unknown	0.10	-0.32	-0.03	-0.04	-1.22
A_95_P019226	Not assigned	unknown	-0.07	-0.10	-0.03	-0.07	-1.22
A_95_P180202	Not assigned	unknown	-0.23	0.01	-1.32	-0.62	-0.58

Probe ID	Mapman annotation	Putative protein function	Δg0*	Δg12	Δg24	Δg36	Δg48
A_95_P180197	Not assigned	unknown	-0.15	0.14	-1.36	-0.54	-0.81
A_95_P254394	Not assigned	unknown	0.30	-0.22	-0.20	0.07	-1.03
A_95_P093913	Not assigned	unknown	-0.18	-0.01	-0.79	-1.12	-0.92
A_95_P013711	Not assigned	unknown	0.19	0.19	0.24	0.19	3.09
A_95_P192252	Not assigned	unknown	-0.12	-1.15	-0.18	-0.03	-0.60
A_95_P246277	Not assigned	unknown	-0.14	0.07	-0.43	0.04	-1.32
A_95_P193178	Not assigned	unknown	0.08	0.38	1.02	0.10	0.33
A_95_P189942	Not assigned	unknown	-0.06	0.07	0.38	-0.23	1.18
A_95_P032981	Not assigned	unknown	0.39	-0.97	-0.38	-0.54	-2.12
A_95_P193567	Not assigned	unknown	0.06	-0.07	-0.34	-0.14	-1.09
A_95_P283578	Not assigned	unknown	-0.06	-0.49	0.00	-0.07	-1.51
A_95_P121687	protein-degradation	C3HC4-type RING finger	0.10	-0.34	-0.34	-0.04	-1.79
A_95_P139122	protein-degradation	E3 ubiquitin-protein ligase RING1	0.14	-0.23	-0.12	0.15	-1.06
A_95_P136387	protein-degradation	RING-H2 finger protein	-0.01	0.00	-0.23	0.07	-1.64
A_95_P003966	protein-folding	peptidyl-prolyl cis-trans isomerase	0.86	0.08	0.58	1.24	1.28
A_95_P134317	protein-posttranslational modification	CBL-interacting protein kinase	0.06	-0.17	0.21	0.31	1.14
A_95_P221647	protein-posttranslational modification	protein phosphatase	0.06	-0.04	0.24	0.18	1.20
A_95_P123972	protein-synthesis	60S acidic ribosomal protein P2-2	0.45	0.50	1.06	0.84	0.56
A_95_P005701	light reaction	photosystem I subunit O	0.10	-0.60	-0.06	-1.09	-0.14
A_95_P018826	redox-glutaredoxins	glutaredoxin	-0.29	-0.14	-1.12	-0.25	-0.89
A_95_P185012	RNA-processing	CCR4-associated factor 1	0.19	-0.60	-0.18	-0.25	-3.32
A_95_P123237	RNA-processing	splicing factor U2af small subunit B	-0.14	-0.29	-0.92	-1.09	-0.84
A_95_P112417	RNA-regulation of transcription	Cys2-His2 type zinc finger	-0.06	-0.43	-0.49	-0.47	-3.32
A_95_P162822	RNA-regulation of transcription	DC1 domain containing	0.10	-0.45	-0.45	-0.29	-1.18
A_95_P181572	RNA-regulation of transcription	DC1 domain-containing protein	-0.49	-0.27	-0.89	-1.00	-0.49
A_95_P195092	RNA-regulation of transcription	homeobox-leucine zipper protein	-0.06	0.10	0.16	-0.03	2.66
A_95_P101338	RNA-regulation of transcription	WRKY20	-0.07	-0.18	-0.30	-0.22	-1.03
A_95_P237924	RNA-regulation of transcription	WRKY3	0.23	-0.25	0.14	-0.06	-1.22
A_95_P097738	RNA-transcription	TATA box-binding protein-associated factor RNA polymerase I subunit B	-0.32	-0.17	-1.25	-0.38	-1.32
A_95_P001231	secondary metabolism-isoprenoids	5-epiaristolochene synthase (85%)	0.18	-0.14	-0.34	-0.01	-1.06
A_95_P124057	secondary metabolism-phenylpropanoids	uncharacterised acetyltransferase	-0.32	-0.03	-0.42	-0.18	-1.25
A_95_P135457	signalling-calcium	calcium-binding protein CML36	-0.10	-0.03	-0.76	-0.29	-1.47
A_95_P137067	signalling-calcium	calcium-binding protein PBP1	-0.23	-0.47	-0.74	-0.25	-2.56
A_95_P121297	signalling-calcium	calcium-binding protein PBP1	0.29	-0.17	-0.38	0.04	-1.51
A_95_P265181	signalling-calcium	calcium-transporting ATPase 7	-0.20	-0.22	-0.23	-0.42	-1.03
A_95_P238364	signalling-calcium	Calmodulin 5	-1.00	-0.62	-1.60	-1.64	-1.79
A_95_P194542	signalling-calcium	CaM-related	-0.17	-0.04	-0.23	-0.06	-2.47
A_95_P109997	signalling-calcium	Pinoid-binding protein 1, calcium ion binding	0.04	-0.29	-0.58	-0.14	-2.25
A_95_P003201	signalling-calcium	Regulator of gene silencing	-0.04	-0.10	0.18	0.08	-1.22
A_95_P023776	signalling-calcium	regulator of gene silencing	-0.07	-0.06	-0.12	0.10	-2.18
A_95_P008351	signalling-in sugar and nutrient physiology	phi-1	0.10	-0.34	-0.06	-0.27	-1.74
A_95_P026596	signalling-light	circadian clock coupling factor ZGT	0.07	0.03	0.65	0.04	1.44
A_95_P134327	signalling-receptor kinases	wound-induced protein 1	0.41	0.19	0.03	1.01	-0.32
A_95_P233289	stress-abiotic	15.4 kDa class V heat shock protein	-0.27	-0.17	-1.00	-0.38	-0.47
A_95_P189262	stress-abiotic	ABA receptor PYL4	-0.14	-0.04	-0.40	-0.17	-1.22
A_95_P120347	stress-abiotic	ABA receptor PYL4	0.07	0.03	-0.29	-0.09	-1.09
A_95_P003006	stress-abiotic	dehydration stress-induced protein	-0.34	-0.06	-0.92	-1.25	-0.60
A_95_P004201	stress-abiotic	osmotin	-0.49	-0.32	-1.03	-1.43	-0.81
A_95_P115287	stress-abiotic	osmotin	-0.40	-0.22	-1.18	-0.84	-0.34
A_95_P180582	stress-abiotic	osmotin	0.11	0.06	-0.60	-1.09	-0.60
A_95_P009846	stress-abiotic	SSUH2	0.00	-0.40	-1.22	-0.79	-0.51

Probe ID	Mapman annotation	Putative protein function	Δg0*	Δg12	Δg24	Δg36	Δg48
A_95_P005591	stress-biotic	Avr9/Cf-9 rapidly elicited protein 65	0.26	-0.04	-0.36	0.12	**-1.36**
A_95_P181542	stress-biotic	harpin inducing protein 18	-0.30	-0.15	-0.89	0.00	**-1.00**
A_95_P204522	stress-biotic	nematode resistance protein	0.19	-0.58	0.04	-0.36	**-1.43**
A_95_P108772	stress-biotic	PR-1b	-0.42	-0.03	-0.06	**-1.09**	-0.29
A_95_P003871	stress-biotic	PR-1b	-0.20	0.00	-0.23	**-1.32**	-0.79
A_95_P004306	stress-biotic	SAR8.2a	-0.74	-0.25	**-1.29**	-0.79	-0.86
A_95_P004321	stress-biotic	SAR8.2b	-0.67	-0.27	**-1.22**	-0.71	-0.74
A_95_P006336	stress-biotic	SAR8.2c	-0.36	-0.56	**-1.03**	-0.62	-0.71
A_95_P004441	stress-biotic	SAR8.2n	-0.47	-0.47	**-1.09**	-0.62	-0.79
A_95_P185277	stress-biotic	trypsin and protease inhibitor family	-0.22	-0.03	**1.94**	-0.34	**-1.32**
A_95_P299943	stress-biotic	virus-specific-signalling-pathway	0.03	0.04	-0.29	-0.14	**-1.09**
A_95_P249767	tetrapyrrole synthesis	Mg protoporphyrin IX chelatase	0.73	0.33	1.00	0.58	**1.32**
A_95_P248797	transport-Major Intrinsic Proteins	aquaporin PIP1-2	0.12	0.26	**1.01**	0.33	0.25
A_95_P012161	transport-Major Intrinsic Proteins	aquaporin TIP1-1	-0.01	0.04	-0.09	**-1.18**	-0.38
A_95_P122677	transport-sugars	PM-localised polyol/cyclitol/monosaccharide-H+-symporter	-0.18	**-1.09**	0.12	-0.09	0.36

Appendix E to Chapter 4

GO enrichment analysis of differentially expressed transcripts in tissue including the infection spot.

Transcripts with a minimum fold change of two were analysed using GOEAST. Only biological process ontologies are shown.

* Δt: Fold-change data are expressed relative to the earlier time point and log-scaled

GOID	Term	Induced in WT				Repressed in WT				Induced in VviPGIP1-line				Repressed in VviPGIP1-line			
		Δt0-12*	Δt12-24	Δt24-36	Δt36-48	Δt0-12	Δt12-24	Δt24-36	Δt36-48	Δt0-12	Δt12-24	Δt24-36	Δt36-48	Δt0-12	Δt12-24	Δt24-36	Δt36-48
GO:1901607	alpha-amino acid biosynthesis																2.E-04
GO:1901605	alpha-amino acid metabolism																2.E-05
GO:0043604	amide biosynthesis									2.E-09							
GO:0046348	amino sugar catabolism		1.E-02			7.E-02								8.E-02			9.E-07
GO:0006040	amino sugar metabolism		1.E-02			8.E-02								9.E-02			1.E-06
GO:0006026	aminoglycan catabolism		2.E-02			8.E-02								9.E-02			1.E-06
GO:0008150	biological_process	6.E-06	3.E-04		2.E-05		3.E-08	2.E-07	4.E-03	3.E-06	7.E-06				4.E-16	1.E-07	7.E-06
GO:0009058	biosynthesis									1.E-05							2.E-02
GO:1901136	carbohydrate derivative catabolism		6.E-02														1.E-05
GO:0005975	carbohydrate metabolism	6.E-02					3.E-02				2.E-04					3.E-02	
GO:0009056	catabolism	1.E-01		3.E-03					2.E-03		5.E-02						8.E-06
GO:0016998	cell wall macromolecule catabolism		1.E-01														4.E-05
GO:0044036	cell wall macromolecule metabolism																5.E-04
GO:0043603	cellular amide metabolism									4.E-09							
GO:0044249	cellular biosynthesis									7.E-06							4.E-03
GO:0044248	cellular catabolism			4.E-02					7.E-02								9.E-05
GO:0006073	cellular glucan metabolism	7.E-02					8.E-02	3.E-02							6.E-04	9.E-03	
GO:0034645	cellular macromolecule biosynthesis									5.E-08							
GO:0044237	cellular metabolism	2.E-02	1.E-01		4.E-05		3.E-02	3.E-04		1.E-04					7.E-08		9.E-06
GO:0044271	cellular nitrogen compound biosynthesis									1.E-05							
GO:0009987	cellular process	4.E-04	4.E-02		2.E-06		2.E-05	4.E-06	5.E-02	4.E-07	5.E-03				5.E-13	9.E-03	8.E-04
GO:0006032	chitin catabolism		1.E-02			7.E-02								8.E-02			9.E-07
GO:0006030	chitin metabolism		1.E-02			7.E-02								8.E-02			9.E-07
GO:0015995	chlorophyll biosynthesis							8.E-06							1.E-03	5.E-02	
GO:0015994	chlorophyll metabolism							8.E-05							8.E-03		
GO:0031497	chromatin assembly							1.E-03									
GO:0051188	cofactor biosynthesis				4.E-02			4.E-04									
GO:0009805	coumarin biosynthesis																6.E-07
GO:0009804	coumarin metabolism																6.E-07
GO:0006952	defense response	1.E-01	1.E-06		7.E-04	5.E-04	2.E-03	3.E-03		4.E-02				1.E-04	3.E-04		4.E-03
GO:0050832	defense response to fungus		2.E-06			1.E-03								3.E-05			
GO:0098542	defense response to other organism		6.E-06			7.E-03								3.E-03	2.E-02		
GO:0010467	gene expression									2.E-07							

GOID	Term	Induced in WT				Repressed in WT				Induced in VviPGIP1-line				Repressed in VviPGIP1-line			
		Δt0-12*	Δt12-24	Δt24-36	Δt36-48	Δt0-12	Δt12-24	Δt24-36	Δt36-48	Δt0-12	Δt12-24	Δt24-36	Δt36-48	Δt0-12	Δt12-24	Δt24-36	Δt36-48
GO:0006091	generation of precursor metabolites and energy	2.E-02	3.E-07		2.E-12	2.E-06	7.E-02	8.E-12		3.E-03	2.E-02			3.E-05	1.E-09		6.E-02
GO:0044042	glucan metabolism	7.E-02					8.E-02	3.E-02							6.E-04	9.E-03	
GO:1901072	glucosamine-containing compound catabolism		1.E-02			7.E-02								8.E-02			9.E-07
GO:1901071	glucosamine-containing compound metabolism		1.E-02			7.E-02								8.E-02			9.E-07
GO:0009059	macromolecule biosynthesis									6.E-08							
GO:0008152	metabolism	2.E-02			2.E-04		1.E-02	2.E-03	6.E-02	5.E-03	2.E-04				3.E-08	8.E-03	6.E-06
GO:0051704	multi-organism process		3.E-05		2.E-02	7.E-02	1.E-01	1.E-01			5.E-03			4.E-03	3.E-03		1.E-05
GO:0006807	nitrogen compound metabolism									3.E-06							6.E-02
GO:0006334	nucleosome assembly							1.E-03									
GO:0034728	nucleosome organization							1.E-03									
GO:0016053	organic acid biosynthesis																1.E-03
GO:1901576	organic substance biosynthesis									1.E-06							4.E-03
GO:1901575	organic substance catabolism	7.E-02							5.E-02								5.E-04
GO:1901566	organonitrogen compound biosynthesis									5.E-07							
GO:1901565	organonitrogen compound catabolism		1.E-02			8.E-02					2.E-02			3.E-02			2.E-04
GO:1901564	organonitrogen compound metabolism									3.E-07							6.E-04
GO:0055114	oxidation-reduction process	4.E-02						6.E-02		9.E-02	3.E-03				8.E-04		5.E-02
GO:0043043	peptide biosynthesis									2.E-09							
GO:0006518	peptide metabolism									3.E-09							
GO:0009699	phenylpropanoid biosynthesis																2.E-05
GO:0009698	phenylpropanoid metabolism																2.E-04
GO:0015979	photosynthesis		3.E-10		2.E-17	4.E-07		2.E-26						3.E-08	3.E-31	1.E-02	3.E-02
GO:0015979	photosynthesis		3.E-10		2.E-17	4.E-07		2.E-26						3.E-08	3.E-31	1.E-02	3.E-02
GO:0009765	photosynthesis, light harvesting		2.E-09		4.E-16	2.E-11		3.E-15						3.E-11	6.E-13		
GO:0019684	photosynthesis, light reaction		8.E-11		1.E-18	9.E-11		6.E-20						1.E-09	9.E-18		
GO:0046148	pigment biosynthesis		1.E-01		1.E-01			1.E-06							3.E-04		
GO:0042440	pigment metabolism		7.E-02					5.E-06							1.E-03		
GO:0006779	porphyrin-containing compound biosynthesis		5.E-02		6.E-02			2.E-07							5.E-04		
GO:0006778	porphyrin-containing compound metabolism		3.E-02		1.E-01			1.E-06							2.E-03		
GO:0006457	protein folding									3.E-03				9.E-02	2.E-05		
GO:0065004	protein-DNA complex assembly							1.E-03									
GO:0071824	protein-DNA complex subunit organization							1.E-03									
GO:0009628	response to abiotic stimulus	9.E-08	3.E-06	4.E-05	3.E-07		4.E-06	2.E-06	1.E-04	2.E-09	2.E-02			9.E-02	8.E-08	1.E-07	2.E-08
GO:0009607	response to biotic stimulus		7.E-07		2.E-03	5.E-03	3.E-02	6.E-03		9.E-02	9.E-03			1.E-04	8.E-05		1.E-06
GO:0009637	response to blue light		6.E-03		5.E-05	2.E-03		3.E-04						3.E-03	2.E-02		6.E-02
GO:0046686	response to cadmium ion	2.E-02		3.E-03			1.E-01		4.E-03	5.E-04	2.E-04						5.E-16
GO:0042221	response to chemical	2.E-03	3.E-05	2.E-04	8.E-03		1.E-01	9.E-03	1.E-06	6.E-03	3.E-03			3.E-03	2.E-04		3.E-17

GOID	Term	Induced in WT				Repressed in WT				Induced in VviPGIP1-line				Repressed in VviPGIP1-line			
		Δt0-12*	Δt12-24	Δt24-36	Δt36-48	Δt0-12	Δt12-24	Δt24-36	Δt36-48	Δt0-12	Δt12-24	Δt24-36	Δt36-48	Δt0-12	Δt12-24	Δt24-36	Δt36-48
GO:0009409	response to cold	6.E-07			1.E-02		5.E-04			3.E-07	1.E-02				2.E-02		9.E-02
GO:0009719	response to endogenous stimulus		9.E-04		6.E-03			9.E-03						2.E-03	5.E-02		
GO:0043207	response to external biotic stimulus		1.E-06		1.E-03	9.E-03	2.E-02	1.E-02		6.E-02	2.E-02			2.E-04	1.E-04		2.E-06
GO:0009605	response to external stimulus		1.E-06		7.E-04	4.E-04	1.E-01	6.E-02			1.E-02			1.E-05	8.E-04		4.E-05
GO:0010218	response to far red light		4.E-03		2.E-04	1.E-02		1.E-03						1.E-02	7.E-02		
GO:0009620	response to fungus		2.E-07		2.E-02	2.E-03								1.E-05	3.E-03		5.E-02
GO:0009408	response to heat				1.E-01					5.E-02							2.E-05
GO:0042542	response to hydrogen peroxide														7.E-02		4.E-04
GO:0010035	response to inorganic substance	3.E-04	3.E-03	3.E-03					1.E-05	1.E-04	3.E-05						4.E-18
GO:0009642	response to light intensity														4.E-05	1.E-01	
GO:0009416	response to light stimulus		4.E-03	2.E-03	1.E-03		3.E-03	3.E-05	8.E-03						5.E-08	2.E-07	1.E-02
GO:0010038	response to metal ion	4.E-03		3.E-03			1.E-01		1.E-03	1.E-04	2.E-04						5.E-16
GO:0010033	response to organic substance		9.E-05	3.E-02	1.E-03			2.E-02	8.E-03					2.E-04	1.E-04		3.E-02
GO:0006970	response to osmotic stress	1.E-01	6.E-02	4.E-03	2.E-03			2.E-03	7.E-02	8.E-04	3.E-02				5.E-02		5.E-06
GO:0051707	response to other organism		1.E-06		1.E-03	9.E-03	2.E-02	1.E-02		6.E-02	2.E-02			2.E-04	1.E-04		2.E-06
GO:0006979	response to oxidative stress		6.E-02		6.E-02					5.E-02	7.E-02						3.E-04
GO:1901700	response to oxygen-containing compound		6.E-03		1.E-03			9.E-03	8.E-03		6.E-02			3.E-03	6.E-06		1.E-04
GO:0009314	response to radiation		6.E-03	2.E-03	3.E-04		4.E-03	4.E-05	8.E-03						8.E-08	2.E-07	5.E-03
GO:0000302	response to reactive oxygen species																4.E-04
GO:0009651	response to salt stress		3.E-02	8.E-03	1.E-03			1.E-03		4.E-04					7.E-02		6.E-06
GO:0050896	response to stimulus	4.E-06	1.E-13	2.E-03	5.E-08	9.E-06	3.E-05	6.E-09	5.E-04	4.E-06	1.E-04			3.E-08	5.E-11	3.E-04	7.E-16
GO:0006950	response to stress	4.E-06	2.E-12		9.E-09	4.E-07	6.E-05	4.E-07		9.E-08	2.E-03	5.E-02		2.E-09	2.E-09		8.E-09
GO:0009266	response to temperature stimulus	2.E-06		9.E-02	7.E-03		4.E-04			4.E-09	2.E-02				2.E-02		5.E-05
GO:0009611	response to wounding		1.E-06			5.E-04		1.E-02				5.E-02		1.E-04	8.E-04		
GO:0022613	ribonucleoprotein complex biogenesis									2.E-04							
GO:0042254	ribosome biogenesis									1.E-04							
GO:0019748	secondary metabolism			3.E-03					7.E-02								3.E-06
GO:0044550	secondary metabolite biosynthesis																2.E-04
GO:0090487	secondary metabolite catabolism			9.E-05					1.E-02							1.E-02	1.E-02
GO:0044711	single-organism biosynthesis							9.E-02			1.E-02						1.E-07
GO:0044763	single-organism cellular process	2.E-02			1.E-02		2.E-03	3.E-02	1.E-02		1.E-05				2.E-02	5.E-02	2.E-07
GO:0044710	single-organism metabolism	5.E-02	2.E-02		1.E-02			4.E-02	2.E-02		6.E-06	7.E-02			6.E-04		1.E-07
GO:0044699	single-organism process	4.E-03	1.E-02		5.E-04		1.E-03	3.E-03	6.E-02	1.E-02	2.E-06				2.E-06	4.E-03	5.E-06
GO:0044281	small molecule metabolism	7.E-02					1.E-01		7.E-02		2.E-04						5.E-05
GO:0033014	tetrapyrrole biosynthesis		2.E-02		9.E-02			4.E-07							1.E-03		
GO:0033013	tetrapyrrole metabolism		1.E-02		1.E-01			2.E-06							4.E-03		
GO:0009407	toxin catabolism			9.E-05					1.E-02							1.E-02	1.E-02
GO:0009404	toxin metabolism			2.E-04					2.E-02							3.E-02	3.E-02
GO:0006412	translation									2.E-09							
GO:0055085	transmembrane transport										6.E-04						

Chapter 5

In silico analysis of the *XTH* gene family in tobacco

In silico analysis of the *XTH* gene family in tobacco

5.1 Introduction

Plant cells are encased in a fibrous wall primarily composed of complex polysaccharides (Cosgrove, 2005). Studies into cell wall structure have proposed a model where cellulose microfibrils are embedded in a matrix of complex polysaccharides, broadly classified as hemicelluloses and pectins. The exact details of how these three polymers interact *in muro* is still somewhat unclear, however, both the classical “tethered network” and the newer “biomechanical hotspots” models propose that hemicellulose creates bridges between cellulose microfibrils, likely providing higher tensile strength, while pectins limit friction between cellulose microfibrils (Cosgrove, 2014; Gao, 2016; Xiao and Anderson, 2016). Because this matrix of polymers is by nature somewhat inflexible, cell expansion requires that these polymers be modified/remodelled in order to allow polymer creep, an irreversible extension that increases the surface area of the cell wall (Cosgrove, 2005).

A key cell wall polymer necessary for cell wall extension is xyloglucan, the most common hemicellulose (Park and Cosgrove, 2012). Xyloglucan is a xylosylated glucan, present in cell walls of all land plants (Pauly and Keegstra, 2016). The linear β(1→4)-glucan backbone is substituted with α(1→6)-xylopyranosyl moieties at regular intervals, and these moieties can be further extended with other sugar moieties (Attia and Brumer, 2016). These substitutions and extensions make xyloglucan a highly-branched polymer, and its abundance has led to extensive research on its biosynthesis, *in muro* function, as well as degradation (Park and Cosgrove, 2012; Pauly and Keegstra, 2016; Rose et al., 2002; Xiao and Anderson, 2016).

In plants, the *in muro* degradation and rearrangement of xyloglucan is catalysed by representatives of the glycoside hydrolase 16 (GH16) family, collectively termed xyloglucan endotrans-glycosylase/hydrolases (XTHs; Eklöf and Brumer, 2010). Members of the XTH protein family can have one of two catalytic activities, one that shortens (cuts) xyloglucan, or remodels (cuts and pastes) the xyloglucan network. Xyloglucan endo-hydrolase (XEH) activity leads to irreversible chain-shortening, while xyloglucan endo-transglycosylase (XET) activity cleaves and ligates xyloglucan chains. The *Arabidopsis thaliana* genome contains 33 XTH genes that are all expressed during development (Becnel et al., 2006). XTH genes products have been grouped according to sequence similarity into four groups and previously characterised genes and proteins were renamed according to the groups they belong to (Rose et al., 2002). At-XTH1 to At-XTH11 belong to group I, At-XTH12 to At-XTH26 belong to group II, and At-XTH27 to At-XTH33 belong to group III (Eklöf and Brumer, 2010; Rose et al., 2002). Group III was subsequently divided into III-A (At-XTH31 and At-XTH32) and III-B (At-XTH27, At-XTH30, At-XTH33). Only XTHs from group III-A, the smallest group

in terms of numbers, have been demonstrated to have XEH activity, meaning that the majority of XTHs function in cell wall remodelling, rather than in cell wall degradation.

As with all members of the GH16 family, XTHs present a characteristic feature, the β-jellyroll fold, but display a major loop deletion in the negative subsite and a C-terminal extension in the positive subsite. These changes have been shown to widen the substrate-binding cleft to accommodate the highly branched xyloglucan substrates (Eklöf and Brumer, 2010). XTHs are furthermore defined by a catalytic domain motif (Figure 5.1) and highly conserved cysteine residues in the C-terminal extension. N-glycosylation sites define which group each XTH belongs to, with sites immediately adjacent to the catalytic site characteristic of groups I and II. Group III-B XTHs have N-glycosylation sites closer to the C-terminal, while group III-A members lack such sites.

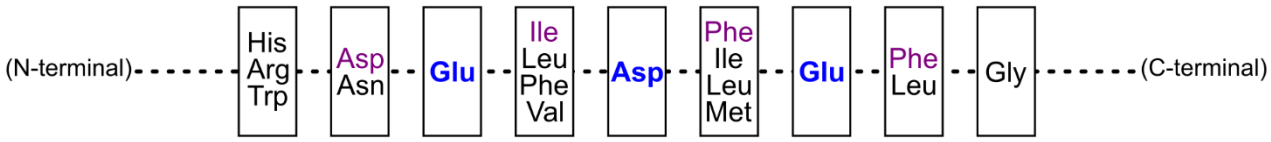

Figure 5.1 Catalytic domain of xyloglucan endotransglycosylase/hydrolases (Eklöf and Brumer, 2010). Each amino acid position is denoted within a block, with the amino acids residues found at that position. Catalytic residues are in blue, and the most commonly observed amino acids in purple.

As with many cell wall-related enzymes, the precise functions of XTHs are difficult to deduce from their sequences alone (Somerville et al., 2004). The use of expression profiling and mutant analysis has, however, provided some functional context for XTHs. The developmental expression patterns of *Arabidopsis* XTHs have been resolved using reporter gene expression driven by XTH regulatory elements combined with *in silico* gene expression analysis (Becnel et al., 2006). Four XTHs were particularly highly expressed in pollen and stamens. Organ-specific expression was observed in shoots (one *XTH*), seeds (two *XTH* genes), and roots/seedling radicles (five genes). Only two *XTHs* were detected in senescing tissues, with one being expressed at very high levels.

XTH activity and gene expression has also been studied in ripening tomato, apple and persimmon fruits, where some genes were shown to be expressed during fruit expansion and others during fruit softening (Han et al., 2015, 2016b; Miedes and Lorences, 2009; Muñoz-Bertomeu and Lorences, 2014). Induction of XTH gene expression has also been observed during abiotic stresses (Han et al., 2017; Iurlaro et al., 2016; Sasidharan et al., 2014) and metal toxicity (Han et al., 2014; Shi et al., 2015; Zhang et al., 2016).

Transgenic plants expressing specific XTHs have, unsurprisingly, showed changes in cell size and organization (Cho et al., 2006; Han et al., 2013, 2017; Ohba et al., 2011), and often enhanced tolerance for abiotic stresses due to the physical changes induced by overexpression. During *B. cinerea* infection, XTH repression is more common than induction (Birkenbihl et al., 2012; Coolen et al., 2016; Finiti et al., 2014; Mathys et al., 2012). Individual XTHs could, however, be induced during

infection even though most of the XTHs are repressed, as has been reported in apple fruit infected by *Penicillium expansum* (Muñoz-Bertomeu and Lorences, 2014).

The importance of XTHs in defence against *Botrytis cinerea*, a pathogen with a diverse arsenal of cell wall degrading enzymes (CWDE), has been studied in transgenic *Nicotiana tabacum* tobacco that constitutively expresses *VviPGIP1*, and is resistant to *B. cinerea* (Joubert et al., 2006). Microarray analysis of uninfected VviPGIP1-tobacco revealed that expression of a tobacco XTH, NtEXGT, was lower than in the (susceptible) wild-type (WT) tobacco (Alexandersson et al., 2011). The reduced expression level was confirmed using quantitative reverse-transcriptase PCR and enzyme activity assays. Cell wall profiling of VviPGIP1-tobacco revealed that transgenic plants displayed changes in cell wall architecture (Alexandersson et al., 2011; Nguema-Ona et al., 2013). These changes, along with altered hormone profiles and lignin deposition, suggested that VviPGIP1-tobacco displayed a primed defence phenotype that was partly realised by reducing the degradability of the cell wall by *B. cinerea*. Transcriptional profiling of WT and VviPGIP1-tobacco during infection (Chapter 3 and 4) revealed that several predicted *XTH* genes were transcriptionally regulated during infection, however, the lack of functional studies of tobacco XTHs prevented the interpretation of the diverse expression patterns observed. This prompted an *in silico* analysis of this gene/protein family in tobacco.

Functional studies of XTHs have been reported for many species, but in tobacco only two XTHs have been functionally characterised (Herbers et al., 2001; Kuluev et al., 2017); NtEXGT (GenBank ID AB017025.1) was found to be most highly expressed in the youngest aerial tissues, both in vegetative and reproductive organs, and was induced by application of the growth hormones, auxins, brassinosteroids, cytokinins and gibberellins, and by abiotic stresses (Kuluev et al., 2017). It was also found to be differentially responsive to abscisic acid (ABA), being induced by low concentrations and repressed by high concentrations and to cold, being induced by moderate cold (10°C) but repressed by freezing (0°C). Furthermore, constitutive overexpression of NtEXGT led to enhanced abiotic stress tolerance to salt-, frost- and heat-stress. *NtXET-1* (GenBank ID D86730, XTH-related) was highly expressed in floral tissues, stems and vascular tissue (Herbers et al., 2001). Antisense suppression of *NtXET-1* increased the molecular weight of xyloglucan in the cell walls of the central leaf veins.

Since the sequencing of the tobacco genome (Sierro et al., 2014), predicted XTH functions have been provided for a number of genes, but functional information is still lacking. The aim of this study was to use these sequences to describe the XTH gene/protein family in tobacco. By compiling a list of potential XTHs, and investigating their relationship/homology with XTHs of other species, current and future studies of tobacco cell wall metabolism could use this resource to better understand this large gene/protein family.

5.2 Materials and methods

5.2.1 Retrieval of XTH sequences

Since the genome sequences of *N. tabacum, N. sylvestris* (woodland tobacco) and *N. tomentosiformis* had been provisionally annotated by The NCBI Eukaryotic Genome Annotation Pipeline (https://www.ncbi.nlm.nih.gov/genome/annotation_euk/process), putative *XTH* genes were identified based on the RefSeq annotations. These genes appear to have been named using the *At-XTH* nomenclature described by Rose et al. (2002). Predicted XTH-like genes were excluded from the analysis, since preliminary sequence alignments revealed that they differed markedly from *XTH* genes.

Following literature searches for XTH homologs that had been functionally described, protein sequences were retrieved from persimmon (*Diospyros kaki*), apple (*Malus x domestica*), poplar (*Populus euphratica*) and pepper (*Capsicum annuum*). The classification of these XTHs does not follow the *At-XTH* nomenclature, but are numbered as new isoforms are described. The protein sequences of 12 tomato (Miedes and Lorences, 2009) and 33 *Arabidopsis* sequences (Rose et al., 2002) and the amino acid sequences linked to the predicted tobacco genes follow the *At-XTH* classification. The full list of XTH genes and proteins used in subsequent analyses is presented in Table 5.1 and Table 5.2 respectively.

Table 5.1 XTH nucleotide sequences retrieved from NCBI. Abbreviations are those used in the text.

Nicotiana tabacum		***Nicotiana tomentosiformis***		***Nicotiana sylvestris***	
Nt/N.ta EXGT	AB017025.1	N.to XTH	XM_009613022.2	N.sy XTH	XM_009790130.1
Nt/N.ta XTH related	D86730.1	N.to XTH-B	XM_009614131.2	N.sy XTH●	XM_009801634.1
Nt/N.ta XTH-B	XM_016632110.1	N.to XTH1	XM_009619020.2	N.sy XTH-B	XM_009773571.1
Nt/N.ta SEN4	NM_001325746.1	N.to XTH7	XM_009629819.2	N.sy XTH1	XM_009796203.1
Nt/N.ta XTH1	XM_016602857.1	N.to XTH8	XM_009591662.2	N.sy XTH1●	XM_009804253.1
Nt/N.ta XTH6	XM_016623416.1	N.to XTH8●	XM_009609037.2	N.sy XTH6	XM_009774799.1
Nt/N.ta XTH7	KJ730270.1	N.to XTH10	XM_009607403.2	N.sy XTH7	XM_009793982.1
Nt/N.ta XTH7●	XM_016616641.1	N.to XTH16	XM_009598734.2	N.sy XTH8	XM_009770972.1
Nt/N.ta XTH8♦	XM_016604292.1	N.to XTH23	XM_009610749.2	N.sy XTH8●	XM_009777210.1
Nt/N.ta XTH8	XM_016613738.1	N.to XTH23●	XM_009628368.2	N.sy XTH8♦	XM_009802222.1
Nt/N.ta XTH8●	XM_016641169.1	N.to XTH25	XM_009613111.2	N.sy XTH10	XM_009782048.1
Nt/N.ta XTH10	XM_016587509.1	N.to XTH26	XM_009623506.2	N.sy XTH15	XM_009760112.1
Nt/N.ta XTH10●	XM_016606450.1	N.to XTH26●	XM_009623507.2	N.sy XTH16	XM_009786746.1
Nt/N.ta XTH16	XM_016645272.1	N.to XTH26♦	XM_009626618.1	N.sy XTH23	XM_009762318.1
Nt/N.ta XTH16●	XM_016648508.1	N.to XTH27	XM_009623050.2	N.sy XTH23●	XM_009795558.1
Nt/N.ta XTH23	XM_016608389.1	N.to XTH30	XM_009610609.2	N.sy XTH25	XM_009799975.1
Nt/N.ta XTH23♦	XM_016639259.1	N.to XTH33	XM_009625603.2	N.sy XTH26	XM_009786544.1
Nt/N.ta XTH23●	XM_016616706.1			N.sy XTH26●	XM_009786545.1
Nt/N.ta XTH25	XM_016627766.1			N.sy XTH26♦	XM_009786546.1
Nt/N.ta XTH25●	XM_016648729.1			N.sy XTH27	XM_009779217.1
Nt/N.ta XTH26	XM_016604176.1			N.sy XTH30	XM_009766604.1
Nt/N.ta XTH26●	XM_016604177.1			N.sy XTH33	XM_009806028.1
Nt/N.ta XTH26♦	XM_016604179.1				
Nt/N.ta XTH26♣	XM_016629766.1				
Nt/N.ta XTH26♠	XM_016637442.1				
Nt/N.ta XTH27	XM_016610325.1				
Nt/N.ta XTH27●	XM_016640789.1				
Nt/N.ta XTH30	NM_001324753.1				
Nt/N.ta XTH33	XM_016600200.1				

♣ ● ♠ ♦ are used to distinguish between proteins with the same name, but different accession numbers

5.2.2 Sequence alignment

Sequences were imported into CLC Sequence Viewer (Qiagen Bioinformatics, Aarhus, Denmark). The "Alignments and Trees" tool was used to align sequences before generating an alignment tree. Bootstrap analysis was performed with 1000 replicates and the resulting trees were exported as cladograms. Tobacco amino acid sequence alignment was exported as a vector graphic and manually annotated.

Table 5.2 XTH amino acid sequences retrieved from NCBI. Abbreviations are those used in the text. The main source for non-tobacco sequences is given per species.

Arabidopsis thaliana **(Rose et al., 2002)**		***Nicotiana tabacum***		**Tomato: *Solanum lycopersicum*** **(Miedes and Lorences, 2009)**	
AtXTH1	OAP00587.1	NtEXGT	BAA32518.1	SlXTH1	BAA03923.1
AtXTH2	OAP01130.1	NtXTH-related	BAA13163.1	SlXTH2	AAG00902.1
AtXTH3	OAP02128.1	NtXTH-B	XP_016487596.1	SlXTH3	AAS46241.1
AtXTH4	AEC06021.1	NtSEN4	ADV41673.1	SlXTH4	AAG43444.1
AtXTH5	AED91952.1	NtXTH1	XP_016458343.1	SlXTH5	AAS46240.1
AtXTH6	AED98096.1	NtXTH2-like	XP_016453928.1	SlXTH6	AAS46242.1
AtXTH7	AEE86839.1	NtXTH6	XP_016478902.1	SlXTH7	AAS46243.1
AtXTH8	OAP11898.1	NtXTH7	AIE54304.1	SlXTH8	BAA88668.1
AtXTH9	AEE82292.1	NtXTH7●	XP_016472127.1	SlXTH9	AAS46244.1
AtXTH10	OAP08597.1	NtXTH7♦	XP_016507323.1	SlXTH10	CAA58002.1
AtXTH11	AEE78433.1	NtXTH8	XP_016469224.1	SlXTH11	CAA58003.1
AtXTH12	AED96911.1	NtXTH8●	XP_016496655.1	SlXTH12	AAF17600.1
AtXTH13	AED96913.1	NtXTH8♦	XP_016459778.1		
AtXTH14	AEE85118.1	NtXTH9-like	XP_016465066.1	**Apple: *Malus domestica***	
AtXTH15	AEE83378.1	NtXTH9-like●	XP_016478975.1	MdXTH1	ACD03226.1
AtXTH16	AEE76807.1	NtXTH10	XP_016442995.1	MdXTH2	ACD03227.1
AtXTH17	AEE34357.1	NtXTH10●	XP_016461936.1	MdXTH3	ACD03228.1
AtXTH18	AEE85746.1	NtXTH16	XP_016500758.1	MdXTH4	ACD03229.1
AtXTH19	AEE85747.1	NtXTH16●	XP_016503994.1	MdXTH5	ACD03230.1
AtXTH20	AED95616.1	NtXTH23	XP_016463875.1	MdXTH6	ACD03231.1
AtXTH21	AEC06809.1	NtXTH23●	XP_016472192.1	MdXTH7	ACD03232.1
AtXTH22	OAO96053.1	NtXTH23♦	XP_016494745.1	MdXTH8	ACD03233.1
AtXTH23	AEE85117.1	NtXTH25	XP_016483252.1	MdXTH9	ACD03234.1
AtXTH24	AEE85745.1	NtXTH25●	XP_016504215.1	MdXTH10	ACD03235.1
AtXTH25	AED96914.1	NtXTH26	XP_016459662.1	MdXTH11	ACD03225.1
AtXTH26	AEE85554.1	NtXTH26●	XP_016459663.1		
AtXTH27	AEC05508.1	NtXTH26♦	XP_016459665.1	**Persimmon: *Diospyros kaki*** **(Han et al., 2015)**	
AtXTH28	AEE29214.1	NtXTH26♣	XP_016485252.1	DkXTH1	AEQ37175.1
AtXTH29	AEE84120.1	NtXTH26♠	XP_016492928.1	DkXTH2	AEQ37176.1
AtXTH30	AEE31443.1	NtXTH27	XP_016465811.1	DkXTH3	AEQ37177.1
AtXTH31	AEE77976.1	NtXTH27●	XP_016496275.1	DkXTH4	AEQ37178.1
AtXTH32	AEC09308.1	NtXTH30	NP_001311682.1	DkXTH5	AGT29355.1
AtXTH33	AEE28593.1	NtXTH33	XP_016455686.1	DkXTH6	AGT29356.1
				DkXTH7	AGT29357.1
Pepper: *Capsicum annuum* **(Han et al., 2015)**		**Poplar: *Populus euphratica*** **(Han et al., 2015)**		DkXTH8	AHE13905.1
CaXTH1	ABD96607.1	PeXTH23	XP_011044000.1	DkXTH9	AHE13906.1
CaXTH2	ABD96608.1				
CaXTH3	ABD96609.1				

♣ ● ♠ ♦ are used to distinguish between proteins with the same name, but different accession numbers

5.2.3 Identification of expression patterns of XTH homologs

A literature survey was conducted to identify studies where XTH expression had been reported, particularly during biotic stresses. Expression data were available for selected XTHs from tomato (Asselbergh et al., 2007; Finiti et al., 2014; Vega et al., 2015), apple (Muñoz-Bertomeu and Lorences, 2014), persimmon (Han et al., 2015, 2016a, 2016b, 2017), pepper (Cho et al., 2006) and poplar (Han et al., 2014). In addition, untargeted transcriptome studies of *Botrytis*-infected *Arabidopsis* were used to source expression data for the 33 At-XTHs (Birkenbihl et al., 2012; Coolen et al., 2016; Mathys et al., 2012). XTH expression data of tobacco (WT and *VviPGIP1*-expressing) infected with *Botrytis* as presented in Chapters 3 and 4 of this thesis were also included. The Agilent Tobacco Gene Expression Microarray derived data deposited in ArrayExpress (Kolesnikov et al., 2015) and Gene Expression Omnibus (Edgar et al., 2002) were also retrieved. Normalised expression data for the putative XTH-targeting probes were extracted from GSM2433207-GSM2433213 (Zurbriggen et al., 2009) and E-MEXP-3934 (Jada et al., 2014). For expression analysis, data from Chapter 3 and 4 were normalised to uninfected (t=0) leaves. Data from Jada et al. (2014) were normalised to uninfected control plants and data from Zurbriggen et al. (2009) were normalised to mock-inoculated plants.

NtEXGT expression was verified using primers described by Alexandersson et al. (2011), namely forward 5'-AGTCCAAGTTTGTAACACC-3' and reverse 5'-TCTGTCCTTAGTGCATTCTG-3'. RNA extraction, cDNA synthesis and real-time PCR protocols were as described in section 3.2.4 of Chapter 3.

5.3 Results and Discussion

5.3.1 Tobacco XTH amino acid sequences analysis

Protein sequences from NCBI were aligned in CLC Sequence Viewer (Figure 5.2). All analysed sequences contained the conserved catalytic motif, with 18 having the most common amino acid sequence (HDEIDFEFLG). Twenty-six had an N-glycosylation binding motif immediately adjacent to the catalytic motif, while three did not have binding motifs between the catalytic domain and first pair of cysteine residues. All sequences had a conserved pair of cysteine residues near the C-terminal, with most sequences having 13 residues between them and a second pair of cysteine residues 35-40 residues nearer the catalytic site.

NtEXGT and NtXTH-related were nearly indistinguishable on amino acid level, with only four amino acid residues differing between them. All four amino acid substitutions are conservative mutations. Sequences of the N-terminal, catalytic motif, N-glycosylation sites and between the pairs of cysteine residues suggest that the predicted NtXTH6 may be an XTH7, or that NtXTH7 (GenBank ID KJ730270.1) was misidentified as an XTH7 and should be considered an XTH6.

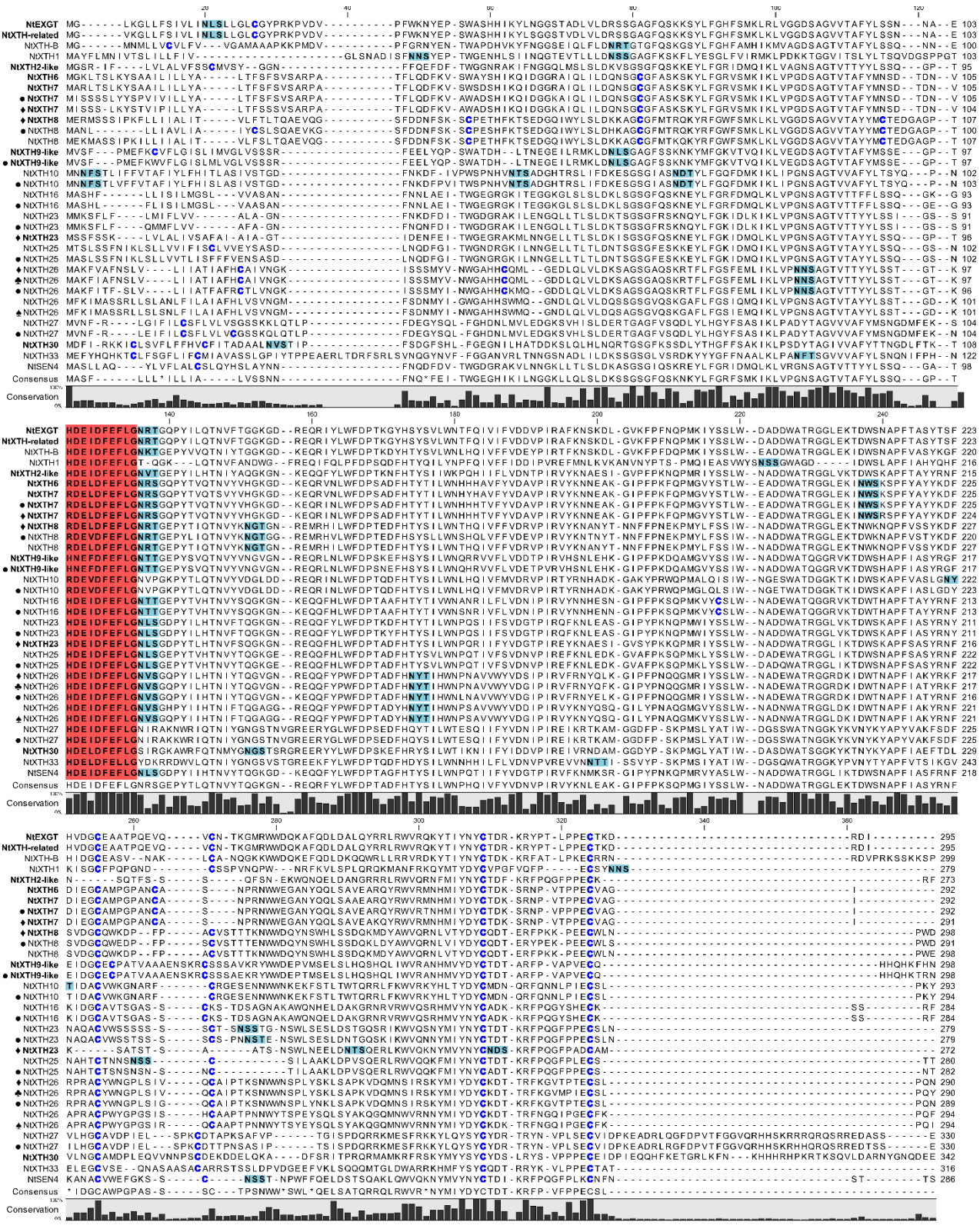

Figure 5.2 Amino acid sequence alignment of all putative XTH genes from tobacco. The catalytic motif is highlighted in red, all potential N-linked glycosylation sites (H-x-S/T) are highlighted in teal and all cysteine residues are highlighted in blue. Sequence conservation is shown as a bar graph, with the consensus sequence directly above it. Genes are sorted by name. Tobacco genes in bold are represented by probes on the Agilent tobacco gene expression microarray and were responsive to infection according to the statistical methods employed. ♣ ● ♠ ♦ are used to distinguish between proteins with the same name, but different accession numbers.

NtXTH10 and NtXTH27 do not have N-glycosylation sites, suggesting that they may belong to group III-A (Eklöf and Brumer, 2010). NtXTH1 and NtXTH33 have N-glycosylation sites towards the C-terminal, but at slightly different positions. They are therefore potentially representatives of group III-B, while the remainder of the XTH genes belong to group I/II. NtXTH2-like shares significant homology with NtXTH16, but is missing the first pair of cysteine residues, while NtXTH9-like is homologous to NtXTH7, with the addition of one cysteine residue between the first pair.

5.3.2 Tobacco XTH coding sequences in relation to parental species

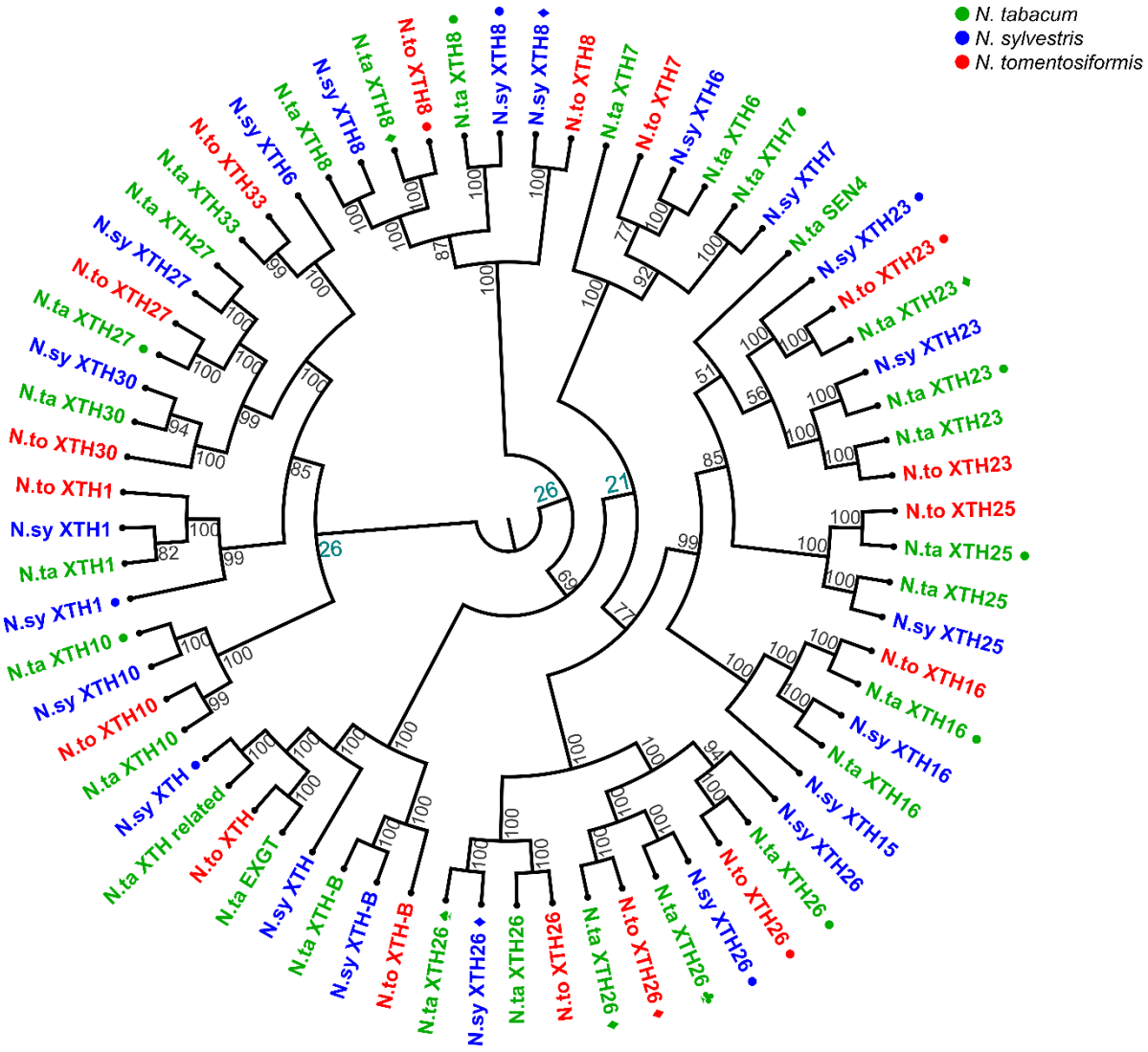

Figure 5.3 Alignment tree of XTH nucleotide sequences of three Nicotiana species. Bootstrap results are displayed for each branch and values below 50% highlighted in red. Genes are coloured according to species. ♣ ● ♠ ♦ are used to distinguish between proteins with the same name, but different accession numbers

Nucleotide sequences from *N. tabacum*, *N. sylvestris*, *N. tomentosiformis* were aligned and an cladogram generated (Figure 5.3). Bootstrapping analysis showed that sequences were not highly distinct (the first branch points had bootstrap values of 26%), however, XTHs were grouped according to RefSeq annotation (e.g. XTH25 sequences form a subgroup). Furthermore, since *N. sylvestris* and *N. tomentosiformis* are known to be the parental species for *N. tabacum* (Leitch et al., 2008), the sequence alignments provide indications that some XTHs were clearly derived from both

parents (XTH8, XTH10, XTH16, XTH23, XTH25, XTH26, XTH27). NtEXGT and XTH-related appear to derive from *N. tomentosiformis* and *N. sylvestris* respectively. NtSEN4 (GenBank ID HQ108341.1) falls in a grouping of XTH23, while NtXTH7 (GenBank ID KJ730270.1) grouped with other XTH7 sequences, but neither were closely aligned with sequences from parental species.

5.3.3 Expression patterns of XTHs

Unlike the previously reported VviPGIP1-expressing tobacco, where NtEXGT expression was significantly lower (Alexandersson et al., 2011), we observed a slight increase in expression, however the average fluorescence signal was relatively low (150 vs 242), and cross-hybridisation of NtEXGT and NtXTH-related may have occurred. Expression was therefore verified using qRT-PCR, and confirmed that NtEXGT expression was significantly lower in VviPGIP1-tobacco (Figure 5.4).

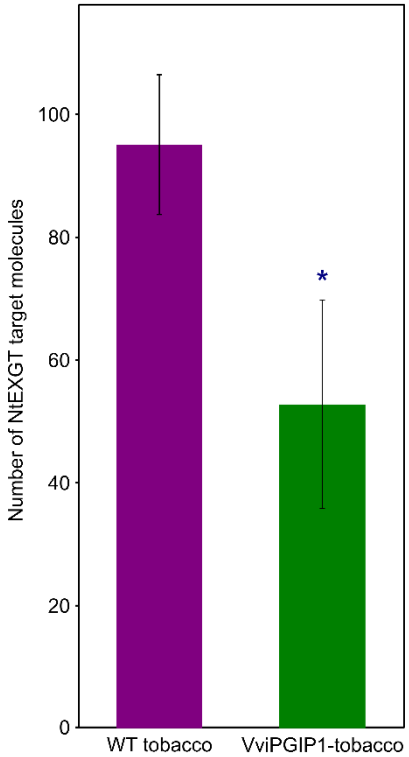

Figure 5.4 NtEXGT expression levels determined using quantitative PCR. Target molecules were quantified using linear regression of expression. Error bars represent standard deviation of technical repeats (n=2).

The expression analysis during *B. cinerea* (Chapter 3 and 4 of this dissertation), *Xanthomonas campestris* (Zurbriggen et al., 2009) and tobacco mosaic virus (Jada et al., 2014) infections of wild-type tobacco (Table 5.3) revealed only minimal changes in expression relative to uninfected tobacco. In contrast, the VviPGIP1-expressing tobacco line displayed substantial changes in XTH expression during infection, with the majority of *XTH* genes being repressed more than 2-fold 48 hours after infection. Only XTH30 was induced after infection.

Table 5.3 Relative expression of XTHs in tobacco infections with *Botrytis cinerea*, *Xanthomonas campestris* pv *vesicatoria (Xcv)* and tobacco mosaic virus (TMV)

		NtEXGT	NtXTH-related	NtXTH6	NtXTH7	NtXTH7	NtXTH7	NtXTH8	NtXTH9	NtXTH23	NtXTH30
		A_95_P178107	A_95_P000496	A_95_P177012	A_95_P015886	A_95_P177007	A_95_P293048	A_95_P093503	A_95_P018106	A_95_P180217	A_95_P009341
WT Local *B. cinerea* infection (vs 0 h)[1]	12 h	1.80	1.73	1.63	2.43	2.13	1.36	0.84	0.33	-0.81	-0.86
	24 h	0.70	0.31	0.41	0.73	0.35	0.49	-0.13	0.95	-0.53	-0.24
	36 h	-0.30	-1.03	-0.64	0.44	0.32	-0.51	-0.18	-1.06	-0.74	0.96
	48 h	-0.86	-1.53	-1.41	-1.13	-1.34	-1.67	-0.33	-1.33	-0.73	1.03
WT Distal *B. cinerea* infection (vs 0 h)[1]	12 h	0.46	0.49	0.39	1.08	1.09	0.34	1.09	-0.25	-0.69	-0.79
	24 h	0.67	0.47	-0.04	0.28	0.44	0.10	-0.14	-0.39	-0.11	0.47
	36 h	-0.38	-0.67	-0.56	0.40	-0.06	-1.09	0.26	-2.25	-1.89	2.25
	48 h	-0.08	-0.02	-0.51	-0.78	-0.86	-0.92	-0.38	-1.65	-0.73	1.52
VvPGIP1-tobacco Local *B. cinerea* infection (vs 0 h)[1]	12 h	0.71	0.78	0.52	1.55	1.32	0.11	0.63	0.63	-1.12	-0.58
	24 h	-0.20	-0.20	-0.62	-0.49	-0.20	-0.40	0.26	-1.29	-1.06	0.06
	36 h	-0.56	-0.97	-1.22	-0.30	-0.22	-1.51	0.30	-1.64	-0.94	1.20
	48 h	-1.22	-1.69	-2.12	-1.79	-1.89	-2.12	-0.01	-1.36	-1.15	1.14
VvPGIP1-tobacco Distal *B. cinerea* infection (vs 0 h)[1]	12 h	0.54	0.58	0.33	0.78	0.56	0.18	1.09	-0.14	-1.09	-0.67
	24 h	-0.07	0.03	-0.81	-0.15	-0.06	-0.51	-0.30	0.40	-0.38	0.33
	36 h	-0.69	-0.84	-0.86	-0.14	-0.71	-1.51	-0.15	-2.12	-2.12	2.12
	48 h	0.48	0.41	-0.40	-0.67	-1.03	-0.60	-0.45	-0.94	-1.69	1.49
TMV[2] (vs 0 h)	192 h	-0.91	-0.83	-0.15	0.42	0.63	0.60	0.86	0.14	0.67	-0.49
Xcv[3] (vs mock)	19 h	-1.67	-2.10	-2.27	-2.27	-2.20	-2.07	-0.89	-2.58	-0.49	4.36

[1]Chapter 3 and 4 (this dissertation) [2] tobacco mosaic virus (Jada et al., 2014) [3] *X. campestris* pv vesicatoria (Zurbriggen et al., 2009)
Fold change data are log scaled. Shading indicates level of induction (red) or repression (green)

5.3.4 Inferring function based on sequence similarity

Since tobacco datasets are poorly represented on Genevestigator (Zimmermann et al., 2004), co-expression analyses across species was performed thorough literature searches. The amino acid sequences of all 33 XTHs from tobacco were aligned with those for which some functional information was available. As was observed for the nucleotide alignments, bootstrap analysis revealed poor support for the division of the sequences into subgroups (Figure 5.5). Nonetheless, functional information was outlined for subgroups of the alignment tree that contained tobacco XTH gene products.

Since the focus of the analysis was inference of XTH function during infection, greatest emphasis was on studies where infection response was recorded (Asselbergh et al., 2007; Birkenbihl et al., 2012; Coolen et al., 2016; Finiti et al., 2014; Mathys et al., 2012; Muñoz-Bertomeu and Lorences, 2014; Vega et al., 2015). Three subgroups (5, 6 and 7) contained *Arabidopsis XTHs* that were induced during infection, while group 1 and 9 contained *XTHs* from apple fruit and tomato leaf respectively that were induced during infection. Response of *Arabidopsis XTH* genes to insect herbivory was generally activation, but again a few homologous genes were repressed. Drought induced and repressed *XTH* genes in *Arabidopsis*, and was also not predicted by sequence. Induced systemic resistance (ISR) repressed several *Arabidopsis XTHs* prior to infection (groups 3, 4, 9), but after *B. cinerea* infection, *At-XTH9* (group 4) was induced, while *At-XTH4* (group 9) was repressed. As sequence could not predict the expression patterns of XTH genes, the most likely alternative was

transcriptional regulation, and the differential regulation of *Arabidopsis* XTHs by WRKY33 appears to support this (Birkenbihl et al., 2012), but other forms of regulation cannot be ruled out. Intriguingly, several of the subgroups where *Arabidopsis* XTH genes were regulated by WRKY33 contain XTH genes that responded to *Botrytis* infection.

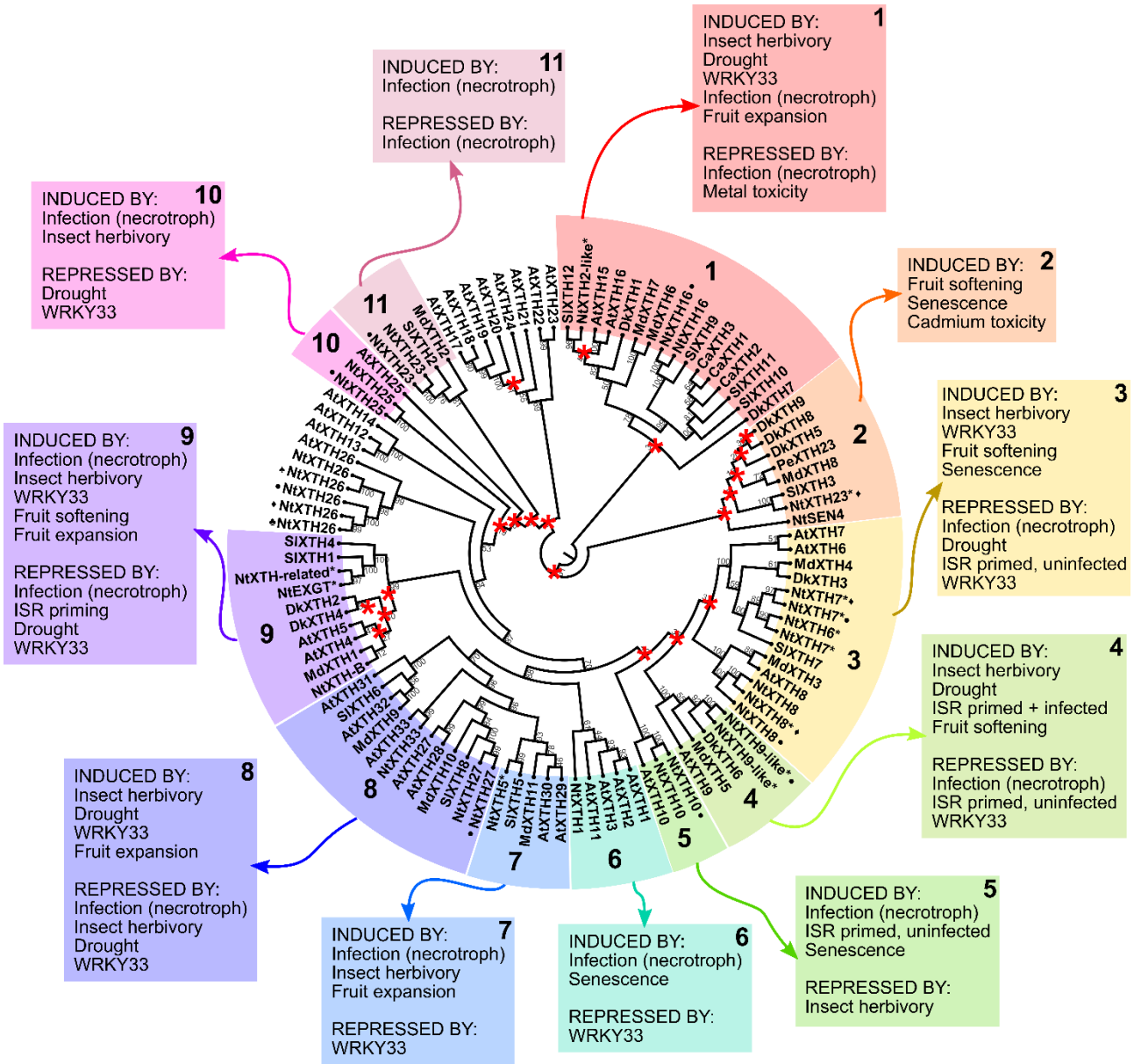

Figure 5.5 Alignment tree of amino acid sequences of tobacco (Nt), *Arabidopsis* (At), apple (Md), tomato (Sl), persimmon (Dk), pepper (Ca) and poplar (Pe). Tobacco genes with asterisks are represented by probes on the Agilent tobacco gene expression microarray and were responsive to infection according to the statistical methods employed. The proteins were grouped manually, according to the alignment tree. Branch points with a bootstrap value below 50% are marked with a red symbol. Expression data for several conditions (Asselbergh et al., 2007; Birkenbihl et al., 2012; Coolen et al., 2016; Finiti et al., 2014; Mathys et al., 2012; Muñoz-Bertomeu and Lorences, 2014; Vega et al., 2015) are summarised for each grouping, but do not represent expression patterns for all XTHs in the group. ♣ ● ♠ ♦ are used to distinguish between proteins with the same name, but different accession numbers

5.4 Conclusion

The aim of this study was to better describe the XTH family in tobacco and potentially infer functional information based on sequence similarity. Tobacco has an allotetraploid genome, derived from *N. sylvestris* and *N. tomentosiformis* (Leitch et al., 2008) and alignment of their *XTH* sequences suggest that tobacco *XTHs* originate from both genomes, with a few exceptions. The only two tobacco XTHs that have been functionally characterised (NtEXGT and XTH-related) are highly homologous, and displayed identical expression patterns during *B. cinerea* infection, which may be due to cross-hybridisation. In addition, the classification of the *XTH* gene currently described as XTH7 (KJ730270) may be incorrect, and could rather be considered an XTH6. Since XTH6 and XTH7 consistently grouped together in nucleotide and amino acid sequences irrespective of the species included, it is possible that they are minor variants/isoforms of the same enzyme, rather than distinct homologs.

The XTH gene family is large and highly homologous on the nucleotide and amino acid sequence levels, as evidenced by the low bootstrap values supporting the alignments generated during this study. For this reason, correlating sequence similarity with expression patterns could not provide robust relationships between sequence and potential functions, and XTHs with similar sequences occasionally displayed contradictory expression patterns. Consequently, one must conclude that XTH function correlates with regulatory features outside the open reading frame. Transcriptional regulation has been definitively shown during *B. cinerea* infection by WRKY33 (Birkenbihl et al., 2012), but expression of XTHs can also be influenced by other transcriptional regulatory mechanisms, such as histone methylation (Ndamukong et al., 2009) and auxin-regulated transcription (Osato et al., 2006).

This analysis has confirmed that the genes annotated by the NCBI genome annotation pipeline contained the catalytic domain required for XTH activity, disulphide bridges and (with two exceptions) N-glycosylation sites. As is the case with most other species (Eklöf and Brumer, 2010), the majority of putative XTHs in tobacco belong to group I/II, and two belong to group III-B, therefore most likely having XET activity. Two XTHs lack glycosylation sites, placing them in group III-A, and they may therefore have XEH activity. As has been reported for XTHs from other species, inferring XTH function (rather than catalytic activity) from gene/protein sequences is difficult due to the high homology within and between species. Transcriptomic analyses, combined with over-expression or gene silencing remains the most reliable avenue to study XTHs.

5.5 Literature cited

Alexandersson E, Becker JVW, Jacobson D, Nguema-Ona E, Steyn C, Denby KJ, Vivier MA (2011). Constitutive expression of a grapevine polygalacturonase-inhibiting protein affects gene expression and cell wall properties in uninfected tobacco. *BMC Res Notes* 4, 493. doi:10.1186/1756-0500-4-493.

Asselbergh B, Curvers K, França SC, Audenaert K, Vuylsteke M, Van Breusegem F, Höfte M (2007). Resistance to *Botrytis cinerea* in *sitiens*, an abscisic acid-deficient tomato mutant, involves timely production of hydrogen peroxide and cell wall modifications in the epidermis. *Plant Physiol* 144, 1863–1877. doi:10.1104/pp.107.099226.

Attia MA, Brumer H (2016). Recent structural insights into the enzymology of the ubiquitous plant cell wall glycan xyloglucan. *Curr Opin Struct Biol* 40, 43–53. doi:10.1016/j.sbi.2016.07.005.

Becnel J, Natarajan M, Kipp A, Braam J (2006). Developmental expression patterns of Arabidopsis XTH genes reported by transgenes and Genevestigator. *Plant Mol Biol* 61, 451–467. doi:10.1007/s11103-006-0021-z.

Birkenbihl RP, Diezel C, Somssich IE (2012). Arabidopsis WRKY33 is a key transcriptional regulator of hormonal and metabolic responses toward *Botrytis cinerea* infection. *Plant Physiol* 159, 266–285. doi:10.1104/pp.111.192641.

Cho SK, Kim JE, Park JA, Eom TJ, Kim WT (2006). Constitutive expression of abiotic stress-inducible hot pepper *CaXTH3*, which encodes a xyloglucan endotransglucosylase/hydrolase homolog, improves drought and salt tolerance in transgenic *Arabidopsis* plants. *FEBS Lett* 580, 3136–3144. doi:10.1016/j.febslet.2006.04.062.

Coolen S, Proietti S, Hickman R, Davila Olivas NH, Huang PP, Van Verk MC, Van Pelt JA, Wittenberg AHJ, De Vos M, Prins M, Van Loon JJA, Aarts MGM, Dicke M, Pieterse CMJ, Van Wees SCM (2016). Transcriptome dynamics of Arabidopsis during sequential biotic and abiotic stresses. *Plant J* 86, 249–267. doi:10.1111/tpj.13167.

Cosgrove DJ (2005). Growth of the plant cell wall. *Nat Rev* 6, 850–861. doi:10.1038/nrm1746.

Cosgrove DJ (2014). Re-constructing our models of cellulose and primary cell wall assembly. *Curr Opin Plant Biol* 22, 122–131. doi:10.1016/j.pbi.2014.11.001.

Edgar R, Domrachev M, Lash AE (2002). Gene Expression Omnibus: NCBI gene expression and hybridization array data repository. *Nucleic Acids Res* 30, 207–210. doi:10.1093/nar/30.1.207.

Eklöf JM, Brumer H (2010). The *XTH* gene family: An update on enzyme structure, function, and phylogeny in xyloglucan remodeling. *Plant Physiol* 153, 456–466. doi:10.1104/pp.110.156844.

Finiti I, De La O Leyva M, Vicedo B, Gómez-Pastor R, López-Cruz J, García-Agustín P, Real MD, González-Bosch C (2014). Hexanoic acid protects tomato plants against *Botrytis cinerea* by priming defence responses and reducing oxidative stress. *Mol Plant Pathol* 15, 550–562. doi:10.1111/mpp.12112.

Gao Y (2016). Parameters involved in the enzymatic deconstruction of the wine grape cell wall matrix during winemaking. *PhD dissertation*, Stellenbosch University, South Africa, 1–165.

Han Y, Sa G, Sun J, Shen Z, Zhao R, Ding M, Deng S, Lu Y, Zhang Y, Shen X, Chen S (2014). Overexpression of *Populus euphratica* xyloglucan endotransglucosylase/hydrolase gene confers enhanced cadmium tolerance by the restriction of root cadmium uptake in transgenic tobacco. *Environ Exp Bot* 100, 74–83. doi:10.1016/j.envexpbot.2013.12.021.

Han Y, Wang W, Sun J, Ding M, Zhao R, Deng S, Wang F, Hu Y, Wang Y, Lu Y, Du L, Hu Z, Diekmann H, Shen X, Polle A, Chen S (2013). *Populus euphratica* XTH overexpression enhances salinity tolerance by the development of leaf succulence in transgenic tobacco plants. *J Exp Bot* 64, 4225–4238. doi:10.1093/jxb/ert229.

Han Y, Ban Q, Hou Y, Meng K, Suo J (2016). Isolation and characterization of two persimmon xyloglucan endotransglycosylase/hydrolase (XTH) genes that have divergent functions in cell wall modification and fruit postharvest softening. *Front Plant Sci* 7, 624. doi:10.3389/fpls.2016.00624.

Han Y, Ban Q, Li H, Hou Y, Jin M, Han S, Rao J (2016). DkXTH8, a novel xyloglucan endotransglucosylase/hydrolase in persimmon, alters cell wall structure and promotes leaf senescence and fruit postharvest softening. *Sci Rep* 6, 39155. doi:10.1038/srep39155.

Han Y, Han S, Ban Q, He Y, Jin M, Rao J (2017). Overexpression of persimmon *DkXTH1* enhanced tolerance to abiotic stress and delayed fruit softening in transgenic plants. *Plant Cell Rep* 36, 583–596. doi:10.1007/s00299-017-2105-4.

Han Y, Zhu Q, Zhang Z, Meng K, Hou Y, Ban Q, Suo J, Rao J (2015). Analysis of xyloglucan endotransglycosylase/hydrolase (*XTH*) genes and diverse roles of isoenzymes during persimmon fruit development and postharvest softening. *PLoS ONE* 10, e0123668. doi:10.1371/journal.pone.0123668.

Herbers K, Lorences EP, Barrachina C, Sonnewald U (2001). Functional characterisation of *Nicotiana tabacum* xyloglucan endotransglycosylase (*Nt*XET-1): generation of transgenic tobacco plants and changes in cell wall xyloglucan. *Planta* 212, 279–287. doi:10.1007/s004250000393.

Iurlaro A, De Caroli M, Sabella E, De Pascali M, Rampino P, De Bellis L, Perrotta C, Dalessandro G, Piro G, Fry SC, Lenucci MS (2016). Drought and heat differentially affect XTH expression and XET activity and action in 3-day-old seedlings of durum wheat cultivars with different stress susceptibility. *Front Plant Sci* 7, 1686. doi:10.3389/fpls.2016.01686.

Jada B, Soitamo AJ, Siddiqui SA, Murukesan G, Aro E-M, Salakoski T, Lehto K (2014). Multiple different defense mechanisms are activated in the young transgenic tobacco plants which express the full length genome of the tobacco mosaic virus, and are resistant against this virus. *PLoS ONE* 9, e107778. doi:10.1371/journal.pone.0107778.

Joubert DA, Slaughter AR, Kemp G, Becker JVW, Krooshof GH, Bergmann CW, Benen JAE, Pretorius IS, Vivier MA (2006). The grapevine polygalacturonase-inhibiting protein (VvPGIP1) reduces *Botrytis cinerea* susceptibility

in transgenic tobacco and differentially inhibits fungal polygalacturonases. *Transgenic Res* 15, 687–702. doi:10.1007/s11248-006-9019-1.

Kolesnikov N, Hastings E, Keays M, Melnichuk O, Tang YA, Williams E, Dylag M, Kurbatova N, Brandizi M, Burdett T, Megy K, Pilicheva E, Rustici G, Tikhonov A, Parkinson H, Petryszak R, Sarkans U, Brazma A (2015). ArrayExpress update-simplifying data submissions. *Nucleic Acids Res* 43, D1113–D1116. doi:10.1093/nar/gku1057.

Kuluev B, Mikhaylova E, Berezhneva Z, Nikonorov Y, Postrigan B, Kudoyarova G, Chemeris A (2017). Expression profiles and hormonal regulation of tobacco *NtEXGT* gene and its involvement in abiotic stress response. *J Plant Physiol* 211, 203–215. doi:10.1016/j.jplph.2016.12.005.

Leitch IJ, Hanson L, Lim KY, Kovarik A, Chase MW, Clarkson JJ, Leitch AR (2008). The ups and downs of genome size evolution in polyploid species of *Nicotiana* (Solanaceae). *Ann Bot* 101, 805–814. doi:10.1093/aob/mcm326.

Mathys J, De Cremer K, Timmermans P, Van Kerckhove S, Lievens B, Vanhaecke M, Cammue BPA, De Coninck B (2012). Genome-wide characterization of ISR induced in *Arabidopsis thaliana* by *Trichoderma hamatum* T382 against *Botrytis cinerea* infection. *Front Plant Sci* 3, 108. doi:10.3389/fpls.2012.00108.

Miedes E, Lorences EP (2009). Xyloglucan endotransglucosylase/hydrolases (XTHs) during tomato fruit growth and ripening. *J Plant Physiol* 166, 489–498. doi:10.1016/j.jplph.2008.07.003.

Muñoz-Bertomeu J, Lorences EP (2014). Changes in xyloglucan endotransglucosylase/hydrolase (XTHs) expression and XET activity during apple fruit infection by *Penicillium expansum* Link. A. *Eur J Plant Pathol* 138, 273–282. doi:10.1007/s10658-013-0327-z.

Ndamukong I, Chetram A, Saleh A, Avramova Z (2009). Wall-modifying genes regulated by the Arabidopsis homolog of trithorax, ATX1: repression of the XTH33 gene as a test case. *Plant J* 58, 541–553. doi:10.1111/j.1365-313X.2009.03798.x.

Nguema-Ona E, Moore JP, Fagerström AD, Fangel JU, Willats WGT, Hugo A, Vivier MA (2013). Overexpression of the grapevine PGIP1 in tobacco results in compositional changes in the leaf arabinoxyloglucan network in the absence of fungal infection. *BMC Plant Biol* 13, 46. doi:10.1186/1471-2229-13-46.

Ohba T, Takahashi S, Asada K (2011). Alteration of fruit characteristics in transgenic tomatoes with modified expression of a xyloglucan endotransglucosylase/hydrolase gene. *Plant Biotechnol* 28, 25–32. doi:10.5511/plantbiotechnology.10.0922a.

Osato Y, Yokoyama R, Nishitani K (2006). A principal role for AtXTH18 in *Arabidopsis thaliana* root growth: A functional analysis using RNAi plants. *J Plant Res* 119, 153–162. doi:10.1007/s10265-006-0262-6.

Park YB, Cosgrove DJ (2012). Changes in cell wall biomechanical properties in the xyloglucan-deficient *xxt1/xxt2* mutant of Arabidopsis. *Plant Physiol* 158, 465–475. doi:10.1104/pp.111.189779.

Pauly M, Keegstra K (2016). Biosynthesis of the plant cell wall matrix polysaccharide xyloglucan. *Annu Rev Plant Biol* 67, 235–259. doi:10.1146/annurev-arplant-043015-112222.

Rose JKC, Braam J, Fry SC, Nishitani K (2002). The XTH family of enzymes involved in xyloglucan endotransglycosylation and endohydrolysis: Current perspectives and a new unifying nomenclature. *Plant Cell Physiol* 43, 1421–1435. doi:10.1093/pcp/pcf171.

Sasidharan R, Keuskamp DH, Kooke R, Voesenek LACJ, Pierik R (2014). Interactions between auxin, microtubules and XTHs mediate green shade- induced petiole elongation in Arabidopsis. *PLoS ONE* 9, e90587. doi:10.1371/journal.pone.0090587.

Shi YZ, Zhu XF, Miller JG, Gregson T, Zheng SJ, Fry SC (2015). Distinct catalytic capacities of two aluminium-repressed *Arabidopsis thaliana* xyloglucan endotransglucosylase/hydrolases, XTH15 and XTH31, heterologously produced in <i>Pichia</>. *Phytochemistry* 112, 160–169. doi:10.1016/j.phytochem.2014.09.020.

Sierro N, Battey JND, Ouadi S, Bakaher N, Bovet L, Willig A, Goepfert S, Peitsch MC, Ivanov N V (2014). The tobacco genome sequence and its comparison with those of tomato and potato. *Nat Commun* 5, 3833. doi:10.1038/ncomms4833.

Somerville C, Bauer S, Brininstool G, Facette M, Hamann T, Milne J, Osborne E, Paredez A, Persson S, Raab T, Vorwerk S, Youngs H (2004). Toward a systems approach to understanding plant cell walls. *Science* 306, 2206–2211. doi:10.1126/science.1102765.

Vega A, Canessa P, Hoppe G, Retamal I, Moyano TC, Canales J, Gutiérrez RA, Rubilar J (2015). Transcriptome analysis reveals regulatory networks underlying differential susceptibility to *Botrytis cinerea* in response to nitrogen availability in *Solanum lycopersicum*. *Front Plant Sci* 6, 911. doi:10.3389/fpls.2015.00911.

Xiao C, Anderson CT (2016). Interconnections between cell wall polymers, wall mechanics, and cortical microtubules: Teasing out causes and consequences. *Plant Signal Behav* 11, e1215396. doi:10.1080/15592324.2016.1215396.

Zhang M, Ma Y, Horst WJ, Yang ZB (2016). Spatial-temporal analysis of polyethylene glycol-reduced aluminium accumulation and xyloglucan endotransglucosylase action in root tips of common bean (*Phaseolus vulgaris*). *Ann Bot* 118, 1–9. doi:10.1093/aob/mcw062.

Zimmermann P, Hirsch-Hoffmann M, Henning L, Gruissem W (2004). GENEVESTIGATOR. Arabidopsis Microarray Database and Analysis Toolbox. *Plant Physiol* 136, 2621–2632. doi:10.1104/pp.104.046367.

Zurbriggen MD, Carrillo N, Tognetti VB, Melzer M, Peisker M, Hause B, Hajirezaei M-R (2009). Chloroplast-generated reactive oxygen species play a major role in localized cell death during the non-host interaction between tobacco and *Xanthomonas campestris* pv. *vesicatoria*. *Plant J* 60, 962–973. doi:10.1111/j.1365-313X.2009.04010.x.

Chapter 6

General discussion and conclusions

General discussion and conclusions

6.1 Introduction

Plants require a highly adaptable metabolism since they generally cannot move away from unfavourable situations to more beneficial ones. They are exposed to abiotic influences, for example changes in temperature or light; or biotic interactions, which involve encounters with other organisms, such as other plants, herbivores, viruses, bacteria and fungi. One of the most famous and far-reaching biotic interactions in human history is the Irish Potato Famine, caused by a *Phytophthora infestans* (potato late blight) epidemic that decimated the potato crop in Europe. While the effect of plant pathogens on food production since has not been so devastating, damage to crops by pathogens, and particularly fungal pathogens, continues to affect crop yields and quality, making the study of plant-pathogen interaction a key field of agricultural science (Dean et al., 2012; Strange and Scott, 2005).

If *P. infestans* holds the prize for causing the most historically famous plant disease, then *Botrytis cinerea*, the causal agent of grey mould rot, is certainly a contender for the most pervasive fungal disease. It infects over 500 genera, spanning the major dicotyledonous families and pectin-rich monocotyledonous families (Elad et al., 2016), of which a substantial number are commonly planted crops. It employs a battery of cell wall degrading enzymes (CWDE) to penetrate and macerate plant tissues (Amselem et al., 2011; Van Kan, 2006) and is not only resistant to the hypersensitive defence response most commonly used by plants, but actively induces it (Govrin and Levine, 2000; Shlezinger et al., 2011). Because of its robust infection strategy, ease of transformation and economic importance, *B. cinerea* has become a model for necrotrophic fungal pathogens (Amselem et al., 2011; Fillinger and Elad, 2016; Mbengue et al., 2016; Van Kan, 2006). The importance of CWDE enzymes in *B. cinerea* virulence has been emphasised by the discovery that two polygalacturonase (PG) isoforms, BcPG1 and BcPG2, are essential for full virulence (Kars et al., 2005; Ten Have et al., 1998). The importance of PGs for virulence is not unique to *B. cinerea*, with many other necrotrophic fungal pathogens reliant on PGs for successful infection (D'Ovidio et al., 2004). It is therefore not surprising that plants have developed mechanisms to counter PG-mediated cell wall degradation. The most specific of these are polygalacturonase-inhibiting proteins (PGIPs) that are found in plant cell walls (Albersheim and Anderson, 1971; Kalunke et al., 2015), while oligogalacturonides (OGs), products of PG-mediated cell wall degradation, act as elicitors for defence responses (Aziz et al., 2004; Brutus et al., 2010; Ferrari et al., 2013).

PGIPs are extracellular leucine-rich repeat (LRR) proteins, found in all plants tested to date (Kalunke et al., 2015). The LRR motif forms two β-sheets and contains residues critical for the PGIP-PG interaction (Di Matteo et al., 2003). PGIP encoding genes have been constitutively expressed in several hosts, and invariably induce resistance to fungal pathogens possessing PGs inhibited by

that particular PGIP, but not pathogens whose PGs were not inhibited (Kalunke et al., 2015). For this reason, the direct inhibition of PGs is considered the primary mode of action for PGIP. The enhanced defence is mediated through two mechanisms, namely the direct inhibition of fungal PG activity and the enhanced longevity of elicitor-active OGs, that trigger defence gene expression (Benedetti et al., 2015). There are, however, PGIPs that have no confirmed PG-inhibition activity and some that appear to have functions in growth and development (D'Ovidio et al., 2006; Kalunke et al., 2014, 2015; Kanai et al., 2010).

As part of an ongoing research focus on plant disease resistance, the Grapevine Molecular Biology Group at the Institute for Wine Biotechnology has identified and studied grapevine PGIPs using genetic engineering. *Vitis vinifera* polygalacturonase-inhibiting protein 1 (VviPGIP1), was isolated from *V. vinifera* cv Pinotage (De Ascensao, 2001) and was subsequently shown to inhibit BcPG1 and BcPG2 and reduce susceptibility of transgenic tobacco to *B. cinerea* (Joubert et al., 2006, 2007). Further analyses of transgenic tobacco led to the discovery that, prior to infection, plants displayed changes in gene expression, cell wall architecture and lignin deposition, and exhibited an accelerated induction of jasmonate accumulation during infection (Alexandersson et al., 2011; Nguema-Ona et al., 2013). These characteristics led to the formulation of a hypothesis that constitutive VviPGIP1 expression acted as a priming stimulus, that led to potentiated defence responses following infection by *B. cinerea*.

A microarray gene expression analysis was selected to study defence responses in the first 48 hours after infection, given that a primed defence response is characterised by a super-activation of defence (Martinez-Medina et al., 2016) and we therefore expected transgenic tobacco to show differential gene expression at this very early stage of the response. The time-course chosen for this study also represents a critical phase in the infection process of *B. cinerea*, where the fungal hyphae are most vulnerable to plant defence mechanisms (Shlezinger et al., 2011) and a sufficiently robust defence can halt the infection (Asselbergh et al., 2007; Smith et al., 2014). Gene expression in the leaves distal to the infection was also analysed to establish whether systemic differences would also be observed. The main findings of the study are presented below, in relation to the current information available in literature and potential avenues for future work are proposed.

6.2 Main findings of the study

The primary aim of this study was to characterise the response of a *VviPGIP1*-expressing tobacco line during a *B. cinerea* infection. However, despite its long history as a model host for the study of plant-pathogen interactions (Sierro et al., 2014), the transcriptional response of wild-type (WT) tobacco to *B. cinerea* had not been reported. The sequencing and provisional annotation of three tobacco cultivar genomes has provided valuable context for this study.

Although the microarray had been designed specifically for tobacco, the design of the microarray probes relied on three non-redundant databases as sources for EST sequences, one of which was no longer available when this study began. By mapping the microarray probes onto clusters of orthologous genes, and later aligning the probe sequences to the newly annotated genomes, we were able to obtain putative protein functions and gene ontology (GO) annotations for many genes that were temporally regulated. However, with newer technologies, such as *de novo* sequencing, it may be possible to identify more unique features of the response of tobacco to *B. cinerea* and the effect of *VviPGIP1*-expression on the transcriptome.

Tobacco displayed a classic local response to *B. cinerea*

This report represents the first untargeted transcriptome analysis of tobacco during *B. cinerea* infection. Since we had selected 12 h-intervals to profile responses, our sampling points encompassed two diurnal cycles. As the infection progressed, diurnal oscillations were either dampened, e.g. chlorophyll binding proteins, or amplified, e.g. enzymes producing reactive oxygen species (ROS). In future, the use of a mock infection control may help clarify the extent to which diurnal patterns were affected.

The similarity between tobacco transcriptional responses to *B. cinerea* and *Xanthomonas campestris* pv *vesicatoria*, both hypersensitive response (HR)-inducing pathogens in tobacco (Zurbriggen et al., 2009), supported the findings of this study. Transcriptional response of tobacco to *B. cinerea* was generally comparable to that in *Arabidopsis*, including the transition from source to sink metabolism, activation of antioxidant mechanisms, jasmonate/ethylene (JA/ET) signalling and secondary metabolism (Coolen et al., 2016; De Cremer et al., 2013; Mathys et al., 2012; Mulema and Denby, 2012; Windram et al., 2012), but there were genes that were regulated differently in the two species. Expression patterns of these genes in the tobacco response to *X. campestris* were, however, similar, suggesting that the tobacco “defence response toolbox” for HR-inducing pathogens differs slightly from that in *Arabidopsis*.

In WT tobacco, profiling the volatile organic compounds (VOC) revealed that, in addition to jasmonate and divinyl ether biosynthesis, the lipoxygenase (LOX) pathway activated biosynthesis of volatile lipid-derived compounds. Targeted transcript quantification, using the genome annotations to identify target LOX-pathway genes not represented on the microarray, could prove a promising avenue for further study. In addition, extending metabolite profiling to non-volatile secondary metabolites may reveal additional processes that are activated during localised defence.

B. cinerea lesion development primed a leaf distal to the infection for defence

Although our time-course was too short for systemic acquired resistance (SAR) to be activated (Frías et al., 2013), we observed a limited activation of defence pathways in leaves distal to the infection.

There was no dampening of the diurnal oscillations of photosynthetic and circadian clock transcripts, but several transcripts encoding fungitoxic proteins, such as SAR-related 8.2 isoforms and chitinases, and genes encoding enzymes that synthesise anti-fungal secondary metabolites were upregulated. Studying the antifungal potential of distal leaf extracts would clarify if these transcriptional changes do, in reality, contribute to a toxic environment for fungal pathogens.

Future studies into distal transcriptional regulation of tobacco to *B. cinerea* would benefit from an extended time-course, and secondary challenges with necrotrophic and biotrophic pathogens to establish the timing of *B. cinerea*-induced SAR in tobacco more precisely than has been reported (Frías et al., 2013). Since defence responses can be highly strain-specific, testing several *B. cinerea* strains would be advisable.

VvPGIP1 expression primed tobacco defence responses in tissue surrounding the lesion and in leaves distal to the infection

Although the time-course utilised in this study concluded before the onset of *B. cinerea*-induced SAR, which would be activated at a hitherto unspecified time point after 72 h (Frías et al., 2013), the priming effect of VviPGIP1-expression was proposed to be constitutive (Alexandersson et al., 2011). For this reason, the 48 h time-course was likely to capture some evidence of defence priming, particularly since this covers a critical phase of *B. cinerea* disease progression (Shlezinger et al., 2011).

As set out in the literature review (Chapter 2, Section 2.1.4), priming can be described by acceleration and/or enhanced activation of defence responses (Figure 2.4). Our experimental setup allowed us to evaluate both types of defence priming. We observed an accelerated shift from photosynthetic to glycolytic metabolism and earlier activation of lignin-forming peroxidase enzyme transcripts and several biotic- and abiotic-stress-related transcripts. In addition, we observed enhanced gene expression, particularly from 24 hours after infection onwards. Enhanced induction of PR proteins, along with *trans-resveratrol di-O-methyltransferase*, that codes for a pterostilbene-synthesising enzyme, confirmed that VviPGIP1-tobacco exhibited a potentiated defence response, as has been observed in several other primed pathosystems (Bruisson et al., 2016; Mahesh et al., 2017; Roylaway et al., 2015; Sun et al., 2017; Wang et al., 2015; Xue and Yi, 2018).

The enhanced activation of the two most prominent branches of the LOX pathway, synthesising divinyl ether and jasmonate oxylipins, is typical of primed defence against *B. cinerea* (Martínez-Hidalgo et al., 2015; Mehari et al., 2015; Nair et al., 2015; Van Wees et al., 1999). The suppression of most ethylene signalling components, though not its synthesis, presents an interesting situation. The only ethylene response factors (ERFs) to be enhanced in VviPGIP1-tobacco are belong to a subfamily of ERFs that inhibit the HR, but enhance necrosis (Fischer and Dröge-Laser, 2004; Ogata

et al., 2012). This may explain why the lesions of VviPGIP1-tobacco became dry and necrotic, rather than the wet, macerated lesions that developed on the WT.

In the resistant transgenic tobacco, many redox-related transcripts were differentially expressed. The transgenic line displayed reduced antioxidant capacity at 24 h after infection, a key phase in *B. cinerea* disease progression (Shlezinger et al., 2011). More diffuse *in situ* staining of hydrogen peroxide during a leaf disk assay suggested that VviPGIP1-tobacco was more efficient at detoxifying ROS, thereby reducing oxidative stress. This too is a feature of primed defence against *B. cinerea* (Finiti et al., 2014; Gong et al., 2015; Liu et al., 2016; Mathys et al., 2012).

In addition to the processes that displayed a primed defence phenotype, other processes were affected that may have contributed to resistance. A change in the expression patterns of two monolignol-synthesising enzyme transcripts (caffeic acid 3-O-methyltransferase and caffeoyl-CoA O-methyltransferase) suggests that monolignol composition may be affected. Furthermore, several defence genes encoding for antimicrobial proteins or phytoalexin-synthesising enzymes were specifically enhanced at 24 h after infection. It would appear that the resistant tobacco not only accelerates activation of hormone signalling and antioxidant mechanisms, but also activates anti-fungal mechanisms around the time that *B. cinerea* is most vulnerable to those mechanisms.

In this study, *B. cinerea* infection acts as a second priming treatment for distal leaves of transgenic plants, and, intriguingly, the VviPGIP1-tobacco distal response was similar to ISR induced by beneficent rhizobacteria in *Arabidopsis* (Mathys et al., 2012) and hexanoic acid-induced priming in tomato (Finiti et al., 2014). Enhanced accumulation of histone-encoding genes suggested that distal tissue was preparing to “store” the priming stimulus generated by distal *B. cinerea* infection (Conrath et al., 2015).

XTHs, a family of proteins where a single function fulfils diverse roles *in planta*

In characterising the protein sequences of putative XTH genes, it was clear that, like most XTH families, the majority of tobacco XTHs belong to groups I or II (Eklöf and Brumer, 2010). Comparison of tobacco XTHs with those from other species that had been functionally characterised revealed a high degree of sequence similarity, even between XTHs that respond differently to infection. Initial analyses of *VviPGIP1*-expressing tobacco highlighted reduced xyloglucan endotransglycosylase/ hydrolase (XTH) expression and activity prior to infection (Alexandersson et al., 2011). In contrast to the repression of XTH activity observed previously, our microarray analysis revealed that most detected XTH transcript levels were slightly higher prior to infection in both leaves analysed. The highly homologous nature of *XTH* sequences may have led to cross-hybridisation between different *XTH* genes, since expression analysis using NtEXGT-specific primers was able to confirm the prior findings.

Ontogenic response, biological variation, the photoperiod and expression profiling

In this study, we opted to profile, in a time-course, tissue from one leaf that represented the localised defence response and another that represented a leaf distal to the infection. The weakness of this approach was made clear by targeted expression analysis and VOC profiling. Both analyses revealed that a strong ontogenic effect influenced gene expression and volatile profile. Therefore, the local expression profiles and VOC profiles reported in this study should be defined according to the specific leaf age, since the older leaves respond slightly differently to infection. For the same reason, the local and distal expression profiles may differ, not only because of a treatment effect, but because leaves of different ages are not biological replicates of one another. In addition, because we did not include a mock inoculation, it was impossible to precisely determine the impact of *B. cinerea* infection on the diurnal cycle of gene expression, and we may have over- or underestimated the impact of infection or VviPGIP1-expression.

In order to analyse gene expression and metabolite levels in the same sample, the four biological replicates were pooled. This means that we were unable to estimate biological variation for the transcriptional response. Although this is an important limitation, VOC analysis of an independent experiment revealed that, though there was clear experimental variation, differences between infected and uninfected tissue were still distinguishable. Despite these limitations, we could benchmark our results against those reported by others and are confident of the conclusions reported here.

6.3 Perspectives

Contribution to *B. cinerea* and tobacco research

This study has provided the first large-scale transcriptional analysis of the tobacco-*B. cinerea* pathosystem, and adds to the small number of such datasets in tobacco (Bozsó et al., 2016; Daurelio et al., 2011; Szatmári et al., 2014), a scientifically important model plant. The preliminary study of VOC emphasised the role of these compounds in plant-necrotroph interactions. This dataset provides an important resource for studies of pathogen response in tobacco, and for studies of *B. cinerea* responses. Multiple layers of cross-comparison are possible, since the transcriptional profiling was performed in a time-course, in locally infected and systemically responding tissue, in susceptible and resistant plants. The advent of RNA sequencing technologies has made it possible to analyse the transcriptome in an even more untargeted way, and this large-scale dataset provides important context in deciding the experimental design required to provide the most robust conclusions with the least costly input.

VviPGIP1 and the PGIP mode-of-action model

According to the current model (Kalunke et al., 2015), PGIPs induce resistance through the inhibition of PG activity and the production of elicitor-active OGs following defence. An elegant series of

experiments has been carried out to support this model, where chimeric constructs of *Phaseolus vulgaris* PGIP2 (PvPGIP2) and *Fusarium phyllophilum* PG were expressed using pathogen- or elicitor-induced promoters (Benedetti et al., 2015). PvPGIP2 can be considered the “iconic” PGIP, showing inhibitory activity against a wide range of PGs, and is the only PGIP known to inhibit FpPG (D’Ovidio et al., 2004). These transgenic lines, when gene expression was activated, produced OGs and displayed typical features of activated defence, including salicylic acid (SA) accumulation, callose deposition, chlorosis and growth defects (Benedetti et al., 2015). As expected, they were more resistant to *B. cinerea*, *Pectobacterium carotovorum* (necrotrophic bacterium) and *Pseudomonas syringae* pv. tomato (hemibiotrophic bacterium).

The role of SA in PGIP-induced resistance has recently also been reported for a cotton PGIP (GhPGIP1) expressed in *Arabidopsis* (Liu et al., 2017), suggesting that the PGIP-OG mechanism may be functional in those plants as well. In contrast to the SA-mediated *in planta* roles of PvPGIP2 and GhPGIP1, VviPGIP1 did not induce enhanced SA accumulation in transgenic tobacco infected with *B. cinerea*, but rather potentiated JA accumulation (Alexandersson et al., 2011). The possibility exists that effective defence mechanisms differ in *Arabidopsis* and tobacco, especially since SA signalling is not required by tobacco for resistance to *B. cinerea* (Achuo et al., 2004), and that the PGIP-OG mechanism triggers irrespective of the hormone signalling network used to regulate defence. Since there are several transgenic tobacco lines expressing PGIPs from diverse sources, including apple (MdPGIP1; Oelofse et al., 2006), bean (PvPGIP2; Borras-Hidalgo et al., 2012; Manfredini et al., 2005), oilseed rape (BnPGIP2; HuangFu et al., 2013; Hwang et al., 2010), pepper (CaPGIP1; Wang et al., 2013) and wild grapevines (Moyo, 2011), more detailed characterisation of these lines in response to *B. cinerea* and other pathogens may clarify whether the difference in hormone regulation originates from the host plant or the PGIP transgene.

On the other hand, VviPGIP1 may activate defence metabolism through a different mechanism regardless of the plant species. Transgenic *Arabidopsis* expressing a sorghum simple LRR protein displayed enhanced resistance to necrotrophic pathogens, attributed to enhanced jasmonate content and responses (Zhu et al., 2015). LRR proteins feature prominently in defence responses (Jones and Jones, 1997). An *Arabidopsis* LRR receptor-like protein, RESPONSIVENESS TO *BOTRYTIS* POLYGALACTURONASES1 (RBPG1), activated defence responses after binding to *B. cinerea* PGs (Zhang et al., 2014). It is possible that VviPGIP1 acts both as an inhibitor of and a receptor for fungal PGs, and is able to signal the presence of *B. cinerea* before or alongside OGs generated by cell wall degradation. In this way, it may provide a dual surveillance system, where the OG receptor WALL ASSOCIATED KINASE 1 (WAK1) senses the OGs generated by VviPGIP1-PG inhibition (Brutus et al., 2010) and VviPGIP1 perceives the PGs and directly, or with the aid of “surveillance resistance proteins”, activates defence signalling. Hypothetically, a transmembrane

protein, or complex of proteins would detect the PGIP-PG interaction, and transmit a signal to the nucleus.

In conclusion, the role of VviPGIP1 during infection clearly extends further than its undisputed ability to inhibit cell wall degradation and indirectly activate OG-induced defence responses. The majority of PGIP transgenic lines have, at best, been tested for their resistance to pathogens, with little or no reports on the mechanics of their phenotypes (Kalunke et al., 2015). Perhaps there are different mechanisms at play in these resistance responses, with PvPGIP2 and GhPGIP1 representing one (possibly dominant) mechanism, while VviPGIP1 represents another. Alternatively, the priming role of VviPGIP1 may extend to other PGIPs, since their effect is rarely tested in uninfected plants. The extensive supply of plant lines expressing a wide diversity of PGIPs may not only provide the agricultural industry with potential sources of resistance to necrotrophic fungi, but provides a comprehensive population to study plant defence across multiple species and against multiple pathogens.

6.4 Literature cited

Achuo EA, Audenaert K, Meziane H, Höfte M (2004). The salicylic acid-dependent defence pathway is effective against different pathogens in tomato and tobacco. *Plant Pathol* 53, 65–72. doi:10.1046/j.1365-3059.2003.00947.x.

Albersheim P, Anderson AJ (1971). Proteins from plant cell walls inhibit polygalacturonases secreted by plant pathogens. *PNAS* 68, 1815–1819.

Alexandersson E, Becker JVW, Jacobson D, Nguema-Ona E, Steyn C, Denby KJ, Vivier MA (2011). Constitutive expression of a grapevine polygalacturonase-inhibiting protein affects gene expression and cell wall properties in uninfected tobacco. *BMC Res Notes* 4, 493. doi:10.1186/1756-0500-4-493.

Amselem J, Cuomo CA, Van Kan JAL, Viaud M, Benito EP, Couloux A, Coutinho PM, De Vries RP, Dyer PS, Fillinger S, Gout L, Hahn M, Kohn L, Lapalu N, Plummer KM, Sharon A, Simon A, Ten Have A, Que E, et al. (2011). Genomic analysis of the necrotrophic fungal pathogens *Sclerotinia sclerotiorum* and *Botrytis cinerea*. *PLoS Genet* 7, e1002230. doi:10.1371/journal.pgen.1002230.

Aziz A, Heyraud A, Lambert B (2004). Oligogalacturonide signal transduction, induction of defense-related responses and protection of grapevine against *Botrytis cinerea*. *Planta* 218, 767–774. doi:10.1007/s00425-003-1153-x.

Benedetti M, Pontiggia D, Raggi S, Cheng Z, Scaloni F, Ferrari S, Ausubel FM, Cervone F, De Lorenzo G (2015). Plant immunity triggered by engineered in vivo release of oligogalacturonides, damage-associated molecular patterns. *PNAS* 112, 5533–5538. doi:10.1073/pnas.1504154112.

Borras-Hidalgo O, Caprari C, Hernandez-Estevez I, De Lorenzo G, Cervone F (2012). A gene for plant protection: expression of a bean polygalacturonase inhibitor in tobacco confers a strong resistance against *Rhizoctonia solani* and two oomycetes. *Front Plant Sci* 3, 268. doi:10.3389/fpls.2012.00268.

Bozsó Z, Ott PG, Kámán-Tóth E, Bognár GF, Pogány M, Szatmári Á (2016). Overlapping yet response-specific transcriptome alterations characterize the nature of tobacco-*Pseudomonas syringae* interactions. *Front Plant Sci* 7, 251. doi:10.3389/fpls.2016.00251.

Bruisson S, Maillot P, Schellenbaum P, Walter B, Gindro K, Deglène-Benbrahim L (2016). Arbuscular mycorrhizal symbiosis stimulates key genes of the phenylpropanoid biosynthesis and stilbenoid production in grapevine leaves in response to downy mildew and grey mould infection. *Phytochemistry* 131, 92–99. doi:10.1016/j.phytochem.2016.09.002.

Brutus A, Sicilia F, Macone A, Cervone F, De Lorenzo G (2010). A domain swap approach reveals a role of the plant wall-associated kinase 1 (WAK1) as a receptor of oligogalacturonides. *PNAS* 107, 9452–9457. doi:10.1073/pnas.1000675107.

Césari S, Kanzaki H, Fujiwara T, Bernoux M, Chalvon V, Kawano Y, Shimamoto K, Dodds P, Terauchi R, Kroj T (2014). The NB-LRR proteins RGA4 and RGA5 interact functionally and physically to confer disease resistance. *EMBO J* 33, 1941–1959. doi:10.15252/embj.201487923.

Chen S, Vaghchhipawala Z, Li W, Asard H, Dickman MB (2004). Tomato phospholipid hydroperoxide glutathione peroxidase inhibits cell death induced by Bax and oxidative stresses in yeast and plants. *Plant Physiol* 135, 1630–1641. doi:10.1104/pp.103.038091.

Conrath U, Beckers GJM, Langenbach CJG, Jaskiewicz MR (2015). Priming for enhanced defense. *Annu Rev Phytopathol* 53, 97–119. doi:10.1146/annurev-phyto-080614-120132.

Coolen S, Proietti S, Hickman R, Davila Olivas NH, Huang PP, Van Verk MC, Van Pelt JA, Wittenberg AHJ, De Vos M, Prins M, Van Loon JJA, Aarts MGM, Dicke M, Pieterse CMJ, Van Wees SCM (2016). Transcriptome dynamics of Arabidopsis during sequential biotic and abiotic stresses. *Plant J* 86, 249–267. doi:10.1111/tpj.13167.

Daurelio LD, Petrocelli S, Blanco F, Holuigue L, Ottado J, Orellano EG (2011). Transcriptome analysis reveals novel genes involved in nonhost response to bacterial infection in tobacco. *J Plant Physiol* 168, 382–391. doi:10.1016/j.jplph.2010.07.014.

De Ascensao A (2001). Isolation and characterisation of a polygalacturonase-inhibiting protein (PGIP) and its encoding gene from *Vitis vinifera* L. *PhD dissertation*, Stellenbosch University, South Africa, 1–106.

De Cremer K, Mathys J, Vos C, Froenicke L, Michelmore RW, Cammue BPA, De Coninck B (2013). RNAseq-based transcriptome analysis of *Lactuca sativa* infected by the fungal necrotroph *Botrytis cinerea*. *Plant, Cell Environ* 36, 1992–2007. doi:10.1111/pce.12106.

Dean R, Van Kan JAL, Pretorius ZA, Hammond-Kosack KE, Di Pietro A, Spanu PD, Rudd JJ, Dickman M, Kahmann R, Ellis J, Foster GD (2012). The Top 10 fungal pathogens in molecular plant pathology. *Mol Plant Pathol* 13, 414–430. doi:10.1111/j.1364-3703.2011.00783.x.

Di Matteo A, Federici L, Mattei B, Salvi G, Johnson KA, Savino C, De Lorenzo G, Tsernoglou D, Cervone F (2003). The crystal structure of polygalacturonase-inhibiting protein (PGIP), a leucine-rich repeat protein involved in plant defense. *PNAS* 100, 10124–10128. doi:10.1073/pnas.1733690100.

D'Ovidio R, Mattei B, Roberti S, Bellincampi D (2004). Polygalacturonases, polygalacturonase-inhibiting proteins and pectic oligomers in plant-pathogen interactions. *Biochim Biophys Acta* 1696, 237–244. doi:10.1016/j.bbapap.2003.08.012.

Eklöf JM, Brumer H (2010). The *XTH* gene family: An update on enzyme structure, function, and phylogeny in xyloglucan remodeling. *Plant Physiol* 153, 456–466. doi:10.1104/pp.110.156844.

Elad Y, Pertot I, Cotes Prado AM, Stewart A (2016). Plant hosts of Botrytis spp. In *Botrytis - the Fungus, the Pathogen and its Management in Agricultural Systems*, eds S Fillinger and Y Elad (Switzerland: Springer International Publishing), 413–486. doi:10.1007/978-3-319-23371-0_20.

Ferrari S, Savatin D V, Sicilia F, Gramegna G, Cervone F, De Lorenzo G (2013). Oligogalacturonides: plant damage-associated molecular patterns and regulators of growth and development. *Front Plant Sci* 4, 49. doi:10.3389/fpls.2013.00049.

Finiti I, De La O Leyva M, Vicedo B, Gómez-Pastor R, López-Cruz J, García-Agustín P, Real MD, González-Bosch C (2014). Hexanoic acid protects tomato plants against *Botrytis cinerea* by priming defence responses and reducing oxidative stress. *Mol Plant Pathol* 15, 550–562. doi:10.1111/mpp.12112.

Fischer U, Dröge-Laser W (2004). Overexpression of *Nt*ERF5, a new member of the tobacco ethylene response transcription factor family enhances resistance to *Tobacco mosaic virus*. *Mol Plant-Microbe Interact* 17, 1162–1171. doi:10.1094/MPMI.2004.17.10.1162.

Frías M, Brito N, González C (2013). The *Botrytis cinerea* cerato-platanin BcSpl1 is a potent inducer of systemic acquired resistance (SAR) in tobacco and generates a wave of salicylic acid expanding from the site of application. *Mol Plant Pathol* 14, 191–196. doi:10.1111/j.1364-3703.2012.00842.x.

Glazebrook J (2005). Contrasting mechanisms of defense against biotrophic and necrotrophic pathogens. *Annu Rev Phytopathol* 43, 205–227. doi:10.1146/annurev.phyto.43.040204.135923.

Gong S, Hao Z, Meng J, Liu D, Wei M, Tao J (2015). Digital gene expression analysis to screen disease resistance-relevant genes from leaves of herbaceous peony (*Paeonia lactiflora* Pall.) infected by *Botrytis cinerea*. *PLoS ONE* 10, e0133305. doi:10.1371/journal.pone.0133305.

Govrin EM, Levine A (2000). The hypersensitive response facilitates plant infection by the necrotrophic pathogen *Botrytis cinerea*. *Curr Biol* 10, 751–757. doi:10.1016/S0960-9822(00)00560-1.

HuangFu H, Guan C, Jin F, Yin C (2013). Prokaryotic expression and protein function of *Brassica napus* PGIP2 and its genetic transformation. *Plant Biotechnol Rep*, 1–11. doi:10.1007/s11816-013-0307-y.

Hwang BH, Bae H, Lim HS, Kim KB, Kim SJ, Im MH, Park BS, Kim DS, Kim J (2010). Overexpression of polygalacturonase-inhibiting protein 2 (*PGIP2*) of Chinese cabbage (*Brassica rapa* ssp. *pekinensis*) increased resistance to the bacterial pathogen *Pectobacterium carotovorum* ssp. *carotovorum*. *Plant Cell Tissue Organ Cult* 103, 293–305. doi:10.1007/s11240-010-9779-4.

Jones DA, Jones JDG (1997). “The role of leucine-rich repeat proteins in plant defences,” in *Advances in Botanical Research*, eds. J. H. Andrews, I. C. Tommerup, and J. A. Callow (Academic Press Inc. (London) Limited), 90–167. doi:10.1016/S0065-2296(08)60072-5.

Joubert DA, De Lorenzo G, Vivier MA (2013). Regulation of the grapevine polygalacturonase-inhibiting protein encoding gene: expression pattern, induction profile and promoter analysis. *J Plant Res* 126, 267–281. doi:10.1007/s10265-012-0515-5.

Joubert DA, Slaughter AR, Kemp G, Becker JVW, Krooshof GH, Bergmann CW, Benen JAE, Pretorius IS, Vivier MA (2006). The grapevine polygalacturonase-inhibiting protein (VvPGIP1) reduces *Botrytis cinerea* susceptibility in transgenic tobacco and differentially inhibits fungal polygalacturonases. *Transgenic Res* 15, 687–702. doi:10.1007/s11248-006-9019-1.

Kalunke RM, Cenci A, Volpi C, O’Sullivan DM, Sella L, Favaron F, Cervone F, De Lorenzo G, D’Ovidio R (2014). The pgip family in soybean and three other legume species: evidence for a birth-and-death model of evolution. *BMC Plant Biol* 14, 189. doi:10.1186/s12870-014-0189-3.

Kalunke RM, Tundo S, Benedetti M, Cervone F, De Lorenzo G, D’Ovidio R (2015). An update on polygalacturonase-inhibiting protein (PGIP), a leucine-rich repeat protein that protects crop plants against pathogens. *Front Plant Sci* 6, 146. doi:10.3389/fpls.2015.00146.

Kanai M, Nishimura M, Hayashi M (2010). A peroxisomal ABC transporter promotes seed germination by inducing pectin degradation under the control of *ABI5*. *Plant J* 62, 936–947. doi:10.1111/j.1365-313X.2010.04205.x.

Kars I, Krooshof GH, Wagemakers L, Joosten R, Benen JAE, Van Kan JAL (2005). Necrotizing activity of five *Botrytis cinerea* endopolygalacturonases produced in *Pichia pastoris*. *Plant J* 43, 213–225. doi:10.1111/j.1365-313X.2005.02436.x.

Liu N, Zhang X, Sun Y, Wang P, Li X, Pei Y, Li F, Hou Y (2017). Molecular evidence for the involvement of a polygalacturonase-inhibiting protein, GhPGIP1, in enhanced resistance to Verticillium and Fusarium wilts in cotton. *Sci Rep* 7, 39840. doi:10.1038/srep39840.

Liu Z, Luan Y, Li J, Yin Y (2016). Expression of a tomato MYB gene in transgenic tobacco increases resistance to *Fusarium oxysporum* and *Botrytis cinerea*. *Eur J Plant Pathol* 144, 607–617. doi:10.1007/s10658-015-0799-0.

Mahesh HM, Murali M, Anup Chandra Pal M, Melvin P, Sharada MS (2017). Salicylic acid seed priming instigates defense mechanism by inducing PR-Proteins in *Solanum melongena* L. upon infection with *Verticillium dahliae* Kleb. *Plant Physiol Biochem* 117, 12–23. doi:10.1016/j.plaphy.2017.05.012.

Manfredini C, Sicilia F, Ferrari S, Pontiggia D, Salvi G, Caprari C, Lorito M, De Lorenzo G (2005). Polygalacturonase-inhibiting protein 2 of *Phaseolus vulgaris* inhibits BcPG1, a polygalacturonase of *Botrytis cinerea* important for pathogenicity, and protects transgenic plants from infection. *Physiol Mol Plant Pathol* 67, 108–115. doi:10.1016/j.pmpp.2005.10.002.

Martínez-Hidalgo P, García JM, Pozo MJ (2015). Induced systemic resistance against *Botrytis cinerea* by *Micromonospora* strains isolated from root nodules. *Front Microbiol* 6, 922. doi:10.3389/fmicb.2015.00922.

Martinez-Medina A, Flors V, Heil M, Mauch-Mani B, Pieterse CMJ, Pozo MJ, Ton J, Van Dam NM, Conrath U (2016). Recognizing plant defense priming. *Trends Plant Sci* 21, 818–822. doi:10.1016/j.tplants.2016.07.009.

Mathys J, De Cremer K, Timmermans P, Van Kerckhove S, Lievens B, Vanhaecke M, Cammue BPA, De Coninck B (2012). Genome-wide characterization of ISR induced in *Arabidopsis thaliana* by *Trichoderma hamatum* T382 against *Botrytis cinerea* infection. *Front Plant Sci* 3, 108. doi:10.3389/fpls.2012.00108.

Mbengue M, Navaud O, Peyraud R, Barascud M, Badet T, Vincent R, Barbacci A, Raffaele S (2016). Emerging trends in molecular interactions between plants and the broad host range fungal pathogens *Botrytis cinerea* and *Sclerotinia sclerotiorum*. *Front Plant Sci* 7, 422. doi:10.3389/fpls.2016.00422.

Mehari ZH, Elad Y, Rav-David D, Graber ER, Meller Harel Y (2015). Induced systemic resistance in tomato (*Solanum lycopersicum*) against *Botrytis cinerea* by biochar amendment involves jasmonic acid signaling. *Plant Soil* 395, 31–44. doi:10.1007/s11104-015-2445-1.

Moyo M (2011). Molecular and phenotypic characterisation of grapevines expressing non-vinifera PGIP encoding genes. *MSc thesis*, Stellenbosch University, South Africa, 1–74.

Mulema JMK, Denby KJ (2012). Spatial and temporal transcriptomic analysis of the *Arabidopsis thaliana-Botrytis cinerea* interaction. *Mol Biol Rep* 39, 4039–4049. doi:10.1007/s11033-011-1185-4.

Nair A, Kolet SP, Thulasiram H V, Bhargava S (2015). Systemic jasmonic acid modulation in mycorrhizal tomato plants and its role in induced resistance against *Alternaria alternata*. *Plant Biol* 17, 625–631. doi:10.1111/plb.12277.

Nguema-Ona E, Moore JP, Fagerström AD, Fangel JU, Willats WGT, Hugo A, Vivier MA (2013). Overexpression of the grapevine PGIP1 in tobacco results in compositional changes in the leaf arabinoxyloglucan network in the absence of fungal infection. *BMC Plant Biol* 13, 46. doi:10.1186/1471-2229-13-46.

Oelofse D, Dubery IA, Meyer R, Arendse MS, Gazendam I, Berger DK (2006). Apple polygalacturonase inhibiting protein1 expressed in transgenic tobacco inhibits polygalacturonases from fungal pathogens of apple and the anthracnose pathogen of lupins. *Phytochemistry* 67, 255–263. doi:10.1016/j.phytochem.2005.10.029.

Ogata T, Kida Y, Arai T, Kishi Y, Manago Y, Murai M, Matsushita Y (2012). Overexpression of tobacco ethylene response factor *NtERF3* gene and its homologues from tobacco and rice induces hypersensitive response-like cell death in tobacco. *J Gen Plant Pathol* 78, 8–17. doi:10.1007/s10327-011-0355-5.

Rose JKC, Braam J, Fry SC, Nishitani K (2002). The XTH family of enzymes involved in xyloglucan endotransglycosylation and endohydrolysis: Current perspectives and a new unifying nomenclature. *Plant Cell Physiol* 43, 1421–1435. doi:10.1093/pcp/pcf171.

Roylawar P, Panda S, Kamble A (2015). Comparative analysis of BABA and *Piriformospora indica* mediated priming of defence-related genes in tomato against early blight. *Physiol Mol Plant Pathol* 91, 88–95. doi:10.1016/j.pmpp.2015.06.004.

Shlezinger N, Minz A, Gur Y, Hatam I, Dagdas YF, Talbot NJ, Sharon A (2011). Anti-apoptotic machinery protects the necrotrophic fungus *Botrytis cinerea* from host-induced apoptotic-like cell death during plant infection. *PLoS Pathog* 7, e1002185. doi:10.1371/journal.ppat.1002185.

Smith JE, Mengesha B, Tang H, Mengiste T, Bluhm BH (2014). Resistance to *Botrytis cinerea* in *Solanum lycopersicoides* involves widespread transcriptional reprogramming. *BMC Genomics* 15, 334. doi:10.1186/1471-2164-15-334.

Strange RN, Scott PR (2005). Plant disease: a threat to global food security. *Annu Rev Phytopathol* 43, 83–116. doi:10.1146/annurev.phyto.43.113004.133839.

Sun G, Wang H, Shi B, Shangguan N, Wang Y, Ma Q (2017). Control efficiency and expressions of resistance genes in tomato plants treated with ε-poly-L-lysine against *Botrytis cinerea*. *Pestic Biochem Physiol*. doi:10.1016/j.pestbp.2017.07.007.

Szatmári Á, Zvara Á, Móricz ÁM, Besenyei E, Szabó E, Ott PG, Puskás LG, Bozsó Z (2014). Pattern triggered immunity (PTI) in tobacco: Isolation of activated genes suggests role of the phenylpropanoid pathway in inhibition of bacterial pathogens. *PLoS ONE* 9, e102869. doi:10.1371/journal.pone.0102869.

Ten Have A, Mulder W, Visser J, Van Kan JAL (1998). The endopolygalacturonase gene *Bcpg1* is required for full virulence of *Botrytis cinerea*. *Mol Plant-Microbe Interact* 11, 1009–1016. doi:10.1094/MPMI.1998.11.10.1009.

Van Kan JAL (2006). Licensed to kill: the lifestyle of a necrotrophic plant pathogen. *Trends Plant Sci* 11, 247–253. doi:10.1016/j.tplants.2006.03.005.

Van Wees SCM, Luijendijk M, Smoorenburg I, Van Loon LC, Pieterse CMJ (1999). Rhizobacteria-mediated induced systemic resistance (ISR) in *Arabidopsis* is not associated with a direct effect on expression of known defense-related genes but stimulates the expression of the jasmonate-inducible gene Atvsp upon challenge. *Plant Mol Biol* 41, 537–549. doi:10.1023/A:1006319216982.

Wang L, Jin P, Wang J, Jiang L, Shan T, Zheng Y (2015). Methyl jasmonate primed defense responses against *Penicillium expansum* in sweet cherry fruit. *Plant Mol Biol Report* 33, 1464–1471. doi:10.1007/s11105-014-0844-8.

Wang X, Zhu X, Tooley P, Zhang X (2013). Cloning and functional analysis of three genes encoding polygalacturonase-inhibiting proteins from *Capsicum annuum* and transgenic CaPGIP1 in tobacco in relation to increased resistance to two fungal pathogens. *Plant Mol Biol* 81, 379–400. doi:10.1007/s11103-013-0007-6.

Wasternack C, Hause B (2013). Jasmonates: biosynthesis, perception, signal transduction and action in plant stress response, growth and development. An update to the 2007 review in Annals of Botany. *Ann Bot* 111, 1021–1058. doi:10.1093/aob/mct067.

Windram O, Madhou P, McHattie S, Hill C, Hickman R, Cooke E, Jenkins DJ, Penfold CA, Baxter L, Breeze E, Kiddle SJ, Rhodes J, Atwell S, Kliebenstein DJ, Kim Y, Stegle O, Borgwardt K, Zhang C, Tabrett A, et al. (2012). *Arabidopsis* defense against *Botrytis cinerea*: chronology and regulation deciphered by high-resolution temporal transcriptomic analysis. *Plant Cell* 24, 3530–3557. doi:10.1105/tpc.112.102046.

Xue M, Yi H (2018). Enhanced *Arabidopsis* disease resistance against *Botrytis cinerea* induced by sulfur dioxide. *Ecotoxicol Environ Saf* 147, 523–529. doi:10.1016/j.ecoenv.2017.09.011.

Zhang L, Kars I, Essenstam B, Liebrand TWH, Wagemakers L, Elberse J, Tagkalaki P, Tjoitang D, Van Den Ackerveken G, Van Kan JAL (2014). Fungal endopolygalacturonases are recognized as microbe-associated molecular patterns by the Arabidopsis receptor-like protein RESPONSIVENESS TO BOTRYTIS POLYGALACTURONASES1. *Plant Physiol* 164, 352–364. doi:10.1104/pp.113.230698.

Zhu F-Y, Li L, Zhang J, Lo C (2015). Transgenic expression of a sorghum gene (*SbLRR2*) encoding a simple extracellular leucine-rich protein enhances resistance against necrotrophic pathogens in *Arabidopsis*. *Physiol Mol Plant Pathol* 91, 31–37. doi:10.1016/j.pmpp.2015.05.004.